

UCLA

UCLA Electronic Theses and Dissertations

Title

Mild polymerization methods for the synthesis of modular fluoropolymers

Permalink

<https://escholarship.org/uc/item/95h49989>

Author

Jaye, Joseph Alan

Publication Date

2021

Peer reviewed|Thesis/dissertation

UNIVERSITY OF CALIFORNIA

Los Angeles

Mild polymerization methods for the synthesis of modular fluoropolymers

A dissertation submitted in partial satisfaction of the
requirements for the degree Doctor of Philosophy
in Chemistry

by

Joseph Alan Jaye

2021

© Copyright by
Joseph Alan Jaye
2021

ABSTRACT OF THE DISSERTATION

Mild polymerization methods for the synthesis of modular fluoropolymers

by

Joseph Alan Jaye

Doctor of Philosophy in Chemistry

University of California, Los Angeles, 2021

Professor Ellen May Sletten, Chair

Fluorinated polymers are an essential class of soft materials spanning multiple industrial markets. Poly(tetrafluoroethylene), better known as Teflon, as well as other commercial fluoropolymers, are found throughout everyday life in the form of electrical insulation, weatherable paints and coatings, medical tubing, or even dental floss. Although being an essential class of materials, fluorinated polymers are finding increased scrutiny in media as one of the main sources of fluorinated surfactant pollution, commonly referred to as per- and polyfluoroalkyl substances (PFAS). There are large concerns on the bioaccumulative and toxic nature of PFAS, but alternatives remain scarce due to their necessity in emulsion polymerization for molecular weight fluoropolymers. Furthermore, there are academic barriers towards the use of the tetrafluoroethylene monomer, a common component in commercial fluoropolymer derivatives, as it is highly explosive and toxic. These factors have slowed the development of novel fluorinated polymer scaffolds in academia. Throughout my graduate work, I have worked towards developing new methods to reach fluorinated polymers with modular backbones. In this dissertation, the

synthesis of modular fluoropolymer scaffolds is optimized and applied towards an array of post-polymerization modifications to provide a library of novel fluorinated polymers.

Chapter one is a short review on recent developments towards fluoropolymers, encompassing the post-polymerization modification of commodity polymers, as well as the polymerization of non-acrylate and non-styrene monomers towards fine architecture control in block copolymers.

Chapter two describes our newly developed initiation system for iodo-ene polymers. The polymerization is optimized towards large molecular weight polymers and an end-capping method is applied. Post-polymerization modifications are performed where click handles such as azides, thiols, and alkenes are appended to the polymer backbone. Finally, a novel photo cross-linking method is detailed.

Chapter three extends the optimized polymerization conditions from chapter two towards the diyne functionality to establish the iodo-yne polymerization. These iodo-yne polymers are fully characterized and the vinyl iodide is modified by transition-metal catalyzed cross couplings. The vinyl iodide was also eliminated to give an activated alkyne, which is further modified via alkyne-azide cycloaddition.

Chapter four discusses a metal-free method for the addition of primary amines to fluorinated vinyl iodides. A new method is established for small molecule models and is then applied to iodo-yne polymers. Highly fluoruous polymers are synthesized through the addition of fluorinated amines.

Chapter five details a small-molecule synthetic method towards the generation of fluorinated 1,3-eneynes. The original method discovered in chapter three is optimized and applied to an array of functionalities incorporated into small molecules.

This dissertation of Joseph Alan Jaye is approved.

Heather D. Maynard

Kendall N. Houk

Timothy J. Deming

Ellen May Sletten, Committee Chair

University of California, Los Angeles

2021

*This dissertation is dedicated to my fiancée Ashley, my parents, Jeff and Joan
and to my siblings, Laretta and Elliott*

TABLE OF CONTENTS

ABSTRACT OF THE DISSERTATION	ii
COMMITTEE PAGE	iv
DEDICATION PAGE	v
TABLE OF CONTENTS.....	vi
LIST OF FIGURES	xi
LIST OF SCHEMES.....	xiv
LIST OF TABLES	xv
ACKNOWLEDGEMENTS.....	xvi
BIOGRAPHICAL SKETCH	xxii
CHAPTER ONE: Recent advances in the preparation of semifluorinated polymers	1
1.1 Abstract.....	1
1.2 Introduction.....	1
1.3 Discussion.....	3
1.3.1 Post-polymerization fluorination of commodity polymers.....	3
1.3.2 Synthesis of fluorous polymers through fluorinated monomers.....	9
1.3.3 Synthesis of polymers with a fluorinated backbone	16
1.4 Conclusion	16
1.5 References.....	17

CHAPTER TWO: Modular and processable fluoropolymers prepared via a safe, mild, iodo-ene polymerization

2.1 Abstract.....	26
2.2 Introduction.....	26
2.3 Results and discussion.....	30
2.4 Conclusions.....	52
2.5 Experimental procedures	53
2.5.1 General experimental procedures	53
2.5.2 Procedures for synthesis of small molecules	57
2.5.3 General procedure for the polymerization of diiodoperfluoroalkanes and dienes	61
2.5.4 Procedures for post-polymerization modifications.....	65
2.5.5 ¹ H-NMR spectra.....	71
2.5.6 ¹⁹ F-NMR spectra.....	87
2.5.7 ¹³ C-NMR spectra	102
2.5.8 IR spectra	104
2.5.9 SEC spectra.....	109
2.5.10 TGA traces.....	124
2.5.11 DSC traces	127
2.6 References and notes.....	133

CHAPTER THREE: Vinyl iodide containing polymers directly prepared via an iodo-yne polymerization

.....	140
3.1 Abstract.....	140
3.2 Introduction.....	140
3.3 Results and discusion.....	143
3.4 Conclusions.....	157
3.5 Experimental procedures	158
3.5.1 General experimental procedures	158
3.5.2 Procedures for synthesis of small molecules	161
3.5.3 Polymer experimental procedures.....	164
3.5.4 Procedures for post-polymerization modifications.....	164
3.5.5 ¹ H-NMR spectra.....	170
3.5.6 ¹³ C-NMR spectra	183
3.5.7 ¹⁹ F-NMR spectra.....	186
3.5.8 IR spectra	199
3.5.9 SEC spectra.....	209
3.5.10 TGA traces	226
3.5.11 DSC traces	234
3.6 References and notes.....	240

CHAPTER FOUR: Vinylogous amidine-containing fluorinated iodo-yne polymers

.....	244
4.1 Abstract.....	244
4.2 Introduction.....	246
4.3 Results and discusion.....	246

4.4 Conclusions.....	257
4.5 Experimental procedures	257
4.5.1 General experimental procedures	257
4.5.2 Procedures for synthesis of small molecules	261
4.5.3 Polymer experimental procedures.....	264
4.5.4 ¹ H-NMR spectra.....	266
4.5.5 ¹³ C-NMR spectra	276
4.5.6 ¹⁹ F-NMR spectra.....	282
4.5.7 IR spectra	292
4.6 References and notes.....	299

CHAPTER FIVE: Simple synthesis of fluorinated ene-yne via *in-situ* generation of allenes

.....	305
5.1 Abstract.....	305
5.2 Introduction.....	305
5.3 Results and discussion.....	307
5.4 Conclusions.....	318
5.5 Experimental procedures	320
5.5.1 General experimental procedures	320
5.5.2 Synthesis of starting materials and ene-yne	320
5.5.3 ¹ H-NMR spectra.....	332
5.5.4 ¹³ C-NMR spectra	352
5.5.5 ¹⁹ F-NMR spectra.....	370
5.5.6 HRMS spectra.....	388

5.6 References and notes.....	394
-------------------------------	-----

LIST OF FIGURES

CHAPTER ONE

<i>Figure 1.1</i> Overview on development of fluoropolymers.....	3
<i>Figure 1.2</i> Trifluoromethylation of aromatic containing commercial polymers	5
<i>Figure 1.3</i> Post-polymerization fluorination of commodity polymers	7
<i>Figure 1.4</i> Polymerization of fluorinated alkenes	10
<i>Figure 1.5</i> Synthesis and self-assembly of polylactide copolymers	12
<i>Figure 1.6</i> Structure and polymerization of oxazoline monomers.....	14

CHAPTER TWO

<i>Figure 2.1</i> Common industrial fluoropolymers and iodo-ene polymers.....	27
<i>Figure 2.2</i> Iodo-ene reaction mechanism.....	31
<i>Figure 2.3</i> Vial image of iodo-ene polymer precipitate.....	31
<i>Figure 2.4</i> NMR comparison of iodo-ene polymers synthesized through different methods	33
<i>Figure 2.5</i> Thermal analysis of reduced iodo-ene polymers.....	33
<i>Figure 2.6</i> Comparison of crude and pure iodo-ene polymer via SEC analysis	34
<i>Figure 2.7</i> End-capping method and molecular weight analysis of iodo-ene polymers ..	35
<i>Figure 2.8</i> Reaction progress pictures of iodo-ene polymer derivatives.....	36
<i>Figure 2.9</i> Contact angle measurements of iodo-ene polymers	37
<i>Figure 2.10</i> Large scale polymerization.....	37
<i>Figure 2.11</i> Functional diene polymerizations and degradation	38
<i>Figure 2.12</i> Polymerization and analysis of fluorinated diene polymer	39
<i>Figure 2.13</i> Degradation of ester containing polymer monitored by SEC.....	40
<i>Figure 2.14</i> Elimination and reduction of iodide from polymer backbone.....	41

<i>Figure 2.15</i> Contact angles of modified polymers	41
<i>Figure 2.16</i> NMR stability assay of eliminated and reduced polymers	43
<i>Figure 2.17</i> Treatment of iodo-ene polymers in the solid state	44
<i>Figure 2.18</i> Modification of iodo-ene polymers with thiols or azides.....	45
<i>Figure 2.19</i> IR analysis of thioacetate polymer and cross-linked derivatives	46
<i>Figure 2.20</i> TGA analysis of ethanedithiol cross-linked polymer	46
<i>Figure 2.21</i> TGA and IR of azide containing polymer and cross-linked derivative.....	47
<i>Figure 2.22</i> Chemical structure of cyclooctyne fluorophore	47
<i>Figure 2.23</i> Addition of allyl groups and photo-crosslinking of polymer	48
<i>Figure 2.24</i> Inverted vial experiment of photo-crosslinked polymers	48
<i>Figure 2.25</i> NMR analysis of small molecule cross-linking model.....	50
<i>Figure 2.26</i> HRGC-MS analysis of small molecule cross-linking model.....	50
<i>Figure 2.27</i> DEPT-135 analysis of small molecule cross-linking model	51
<i>Figure 2.28</i> Crude GC-MS analysis of possible cross-linking adducts	51
<i>Figure 2.29</i> Cross-linked fluoropolymer gels	52
<i>Figure 2.30</i> TGA analysis of treated fluoropolymer gel.....	52
<i>Figure 2.31</i> Photochemistry assembly	57

CHAPTER THREE

<i>Figure 3.1</i> Methods to install vinyl iodide functionality in polymers.....	143
<i>Figure 3.2</i> Model small molecule iodo-yne reaction	144
<i>Figure 3.3</i> Time lapse pictures of large scale polymerization	146
<i>Figure 3.4</i> Comparison of iodo-yne polymer molecular weights through different SEC instruments	146

Figure 3.5 DSC analysis of iodo-yne polymer and soxhlet fractions	147
Figure 3.6 Stability of iodo-yne polymer as measured by NMR	148
Figure 3.7 Palladium catalyzed cross-linking of iodo-yne polymers	149
Figure 3.8 Workflow of polymer purification following modification	152
Figure 3.9 Small molecule analog of phenol coupling reaction	153
Figure 3.10 Elimination of iodide to give alkynes and alkyne-azide cycloaddition	154
Figure 3.11 Thermal analysis of vinyl iodide polymer and eliminated polymers	155
Figure 3.12 Isomerization of the vinyl iodide motif	156
Figure 3.13 <i>In-situ</i> isomerization and elimination of vinyl iodide	157
Figure 3.14 Photochemistry assembly	161

CHAPTER FOUR

Figure 4.1 Synthesis and modification of iodo-yne polymers	245
Figure 4.2 NMR of alkyne terminated polymers	249
Figure 4.3 Vinylogous amidine reaction on vinyl iodide polymer	249
Figure 4.4 Polymer backbone impurities	250
Figure 4.5 Scope of iodo-yne polymer derivatives	251
Figure 4.6 Comparison of small molecule analogs and polymers	251
Figure 4.7 Molecular weight determination of vinylogous amidine containing polymers	252
Figure 4.8 Static TGA analysis of vinylogous amidine polymers	253
Figure 4.9 Stability of vinylogous amidine polymers at 0 °C	253
Figure 4.10 Stability of vinylogous amidine polymers in acidic buffer	254
Figure 4.11 Hydrolysis of vinylogous amidine polymers in HCl/DMF	254

<i>Figure 4.12</i> Synthesis of fluorinated vinylogous amidine polymer	255
<i>Figure 4.13</i> Thermal analysis of fluorinated vinylogous amidine polymer	256
<i>Figure 4.14</i> Solubility comparison of vinyl iodide containing polymer and vinylogous amidine containing polymer	256
 CHAPTER FIVE	
<i>Figure 5.1</i> Different synthetic routes to fluorous ene-yne.....	307
<i>Figure 5.2</i> Sequential additions of MTBD to fluorous vinyl iodides.....	310
<i>Figure 5.3</i> Comparison of reaction condition GC trace with ene-yne standard.....	311
<i>Figure 5.4</i> Reactions of fluorinated allenes with base in polar and non-polar solvents	312
<i>Figure 5.5</i> Comparison of reaction conditions GC trace with allene standard	313
<i>Figure 5.6</i> Reaction progress of ene-yne formation with cesium carbonate analyzed via GC-MS	315
<i>Figure 5.7</i> Ene-yne forming reaction with ester containing vinyl iodides.....	319

LIST OF SCHEMES

CHAPTER TWO

<i>Scheme 2.1</i> Iodo-ene polymerization of 1,9-decadiene.....	30
<i>Scheme 2.2</i> Synthesis of fluorinated diene.....	38

CHAPTER THREE

<i>Scheme 3.1</i> Iodo-yne polymerization of 1,9-decadiyne	145
<i>Scheme 3.2</i> Thiol-yne capping of terminal alkynes of iodo-yne polymers	150
<i>Scheme 3.3</i> Post-polymerization modification of iodo-yne polymers	151

CHAPTER FOUR

<i>Scheme 4.1</i> Optimization of vinylogous amidine forming conditions	246
<i>Scheme 4.2</i> Synthesis and hydrolysis of vinylogous amidines	247
CHAPTER FIVE	
<i>Scheme 5.1</i> Transformation of vinyl iodide to ene-yne	307
<i>Scheme 5.2</i> Proposed reaction mechanism of ene-yne forming reaction.....	315
<i>Scheme 5.3</i> Synthesis of fluorinated vinyl iodide starting materials.....	316
<i>Scheme 5.4</i> Scope of ene-yne forming reaction	317

LIST OF TABLES

CHAPTER TWO	
<i>Table 2.1</i> Optimization of the iodo-ene polymerization.....	30
<i>Table 2.2</i> Thermal properties of polymers.	42
CHAPTER THREE	
<i>Table 3.1</i> Optimization of the iodo-yne polymerization.	145
<i>Table 3.2</i> Summary of modified polymer conditions and thermal properties.....	151
CHAPTER FOUR	
<i>Table 4.1</i> Optimization of vinylogous amidine forming conditions.....	247
<i>Table 4.2</i> Summary of polymer properties.	253
CHAPTER FIVE	
<i>Table 5.1</i> Optimization of ene-yne forming conditions.....	308
<i>Table 5.2</i> Substrate scope of the reaction of vinyl iodides to fluorous ene-yne.	317

ACKNOWLEDGEMENTS

Graduate school was a time like no other in my life. Encompassing five years, it was a time of substantial professional and personal growth. During this time, I experienced some of my greatest successes, along with substantial failures. Looking back, I don't think I knew, or could have known, what I was signing up for when I excitedly enrolled at UCLA for graduate school. That said, I couldn't imagine having spent the last five years any other way. Throughout all the highs and lows, I thoroughly enjoyed the work I was doing, made incredible memories exploring California, and met a group of wonderful people that I'm excited to remain in contact with for life.

Of course, I wouldn't be anywhere close to where I am today without the exceptional guidance of my advisor Ellen Sletten. I owe a huge thanks to Ellen for everything she has done for me over the years. I haven't quite wrapped my head around the fact that it's already been five years and I'm working on my thesis, but when reviewing some of my old work it's not hard to see the substantial effect Ellen's mentorship has had on me in that time. It was interesting joining a such a young lab, as at the time there was only one older student, Maly, who was in the class above us and on a completely different project. Although I owe Maly a large thanks for her general help throughout lab, it was Ellen who taught me nearly everything I know. I remember my original meeting with Ellen in the early Fall of 2016, discussing my interest in the lab and saying, "I think I'd like to work on polymers", despite having no experience whatsoever in polymer synthesis or characterization at the beginning of graduate school. With the added naivety of the difficulty of working with, or I should say characterizing, fluoropolymers, there was what seemed like an impossibly large area for growth. While still containing peaks and valleys, Ellen's guidance throughout the journey provided a much smoother transition than I thought possible into the realm of polymer synthesis and characterization. Again, it's not possible to overstate the effect Ellen has

had on my scientific growth as a polymer chemist, but perhaps even more significant was her effect on my ability to communicate science. I'll always remember the group meeting of my second summer where I prepared a less than engaging presentation. Afterwards, Ellen told me I was no longer a first-year graduate student, and it was time to dedicate significant time to crafting better slides and better presentations overall. Although being a bumpy road throughout, and a road I didn't always enjoy, I owe a massive debt to Ellen for her help in this process. In a similar manner, I'll also never forget my first experience writing a paper with Ellen. I remember thinking I had prepared a solid first draft and it shouldn't take too much editing. I believe we spent close to six hours in her office going through and re-writing close to every line in the manuscript. That also doesn't cover the complete revision of every figure draft I had prepared, while thinking Ellen was a magician for how nice her figure drafts looked in comparison to mine. We finally got to a great manuscript to be submitted, which was unfortunately desk rejected from our first-choice journal. Ellen was instrumental in bouncing back from this, providing support for rejection, and giving direction on how we can improve. Following some quick improvements, we resubmitted our work to a new journal which was then accepted for my first, first author paper in graduate school. Looking back, I'm glad my first paper was a difficult one, with a twisting and turning road towards publication, as it laid an important foundation that I relied on for all subsequent manuscript preparations. I could go on and on about all the learning moments Ellen provided for me throughout the years, all the good and bad journal clubs, mechanism work on the board, one-on-ones and team meetings, and group meetings, but it would take about five years to summarize. Throughout all the good and bad days, I just want to give a sincere and heartfelt thank you one more time. Of course, there were plenty of enjoyable moments outside of the lab and office settings. I'll always look back fondly on our lab Thanksgiving in the first year of graduate school,

Oktoberfest celebrations, manuscript/fellowship/orals success parties, Dodger's games, Super Bowl viewings, and group retreats. Thank you for assembling such a wonderful group of people in the lab and providing an opportunity for such memorable group events.

I am also grateful for the support of all my committee members. I have fond memories of taking classes instructed by Ken Houk and Heather Maynard prior to them agreeing to be members of my committee. I owe a large thank you to every committee member for their help in preparation of my qualifying exam. Every committee member was instrumental in my growth as a scientist, giving wonderful feedback to my qualifying exam materials, and giving direction and advice I'll always keep with me. I would also like to thank my committee for their assistance in the meeting prior to my final year, keeping me on track for graduation and giving advice for finishing graduate studies during a pandemic. Thank you again for all your help and guidance.

I owe a colossal thank you to all members of the Sletten lab, past and present, which have made graduate school such a special time. Without all the support, jokes, shared frustration on our different projects, and overall companionship from other lab members, there would be no chance I could have finished this degree. I owe a special thank you to all the postdocs in the lab who have acted as a mentor throughout graduate school. Wei, Shang, Heidi, and Jon have all acted as important sources of information whenever I was struggling with a certain technique or method. I would specifically like to thank Heidi for her help with polymer characterization and Jon for all the guidance he provided towards my work on small molecule synthesis as well as directing me outside of the lab towards wonderful sources and brands of scotch. I would also like to give a thank you to Maly, the only older student we had in the lab, who was influential towards all stages of graduate school. Thank you Maly for being the first in the lab to experience 2nd year talk, orals,

and thesis writing, giving me a wonderful outline of how to reach these milestones. I would also like to give a very special thank you to the fellow students in my graduating year in the Sletten lab. There are so many memories I have with all of you, and I couldn't imagine having been in a lab without any of you. Although I could describe for many pages all my favorite memories with my cohort, I'll try to keep it a little shorter. Anna, I'll always remember sitting next to you in the office and being next to each other in lab for our first couple years. Of course, there were all the pre-group meeting freakouts where all my slides were wrong, but also the slow days of just googling random places on google maps and talking about the world or babbling about nothing for a while. Dan, I was so happy to have someone else in the lab who was excited about football. I could always count on being able to talk about whatever craziness happened in the NFL over the weekend, or to talk playoffs/super bowl. Not only with sports, but it was always nice to have someone else on team polymer. Gina, thank you for always putting together fun dinners and events and taking charge at Korean BBQ. It always seemed like you were central to some of my favorite memories in our lab, and some of my favorite times on the 5th floor just venting to each other about everything. Margeaux, it was so great to have another mechanism nerd in the group. I could always come to you to get excited about some cool mechanism in a paper or at journal club. It was nice to talk about general synthetic methodology with someone, and of course all the other departmental gossip. Monica, I can't believe how fast time has gone since we both rotated in the Harran lab our first summer here. Thank you for everything over the last 5 years. Especially for dealing with me on the 5th floor office and sharing a lab space. There are so many fun memories I have with you of just talking about nothing, Panda and Pinches trips, complaining about having to be awake, and everything else. Rachael, it was awesome to have another Midwesterner in the lab. When no one else understood something from the Midwest, I could always count on you to understand. Thank

you to all the other students in the Sletten lab as well. Irene, you were a constant source of dry humor and I loved being able to talk Big Brother with you. Tony and Cesar, I'm not sure what grad school would have been like without Panda Thursdays and making absurd get rich quick schemes. Erika, Joseph, and Kelly, it was great to get to know all of you and I'm excited to see where your graduate school journey takes you. Caitlyn, Kait, Quintashia, and Rita, I'm sorry that COVID took away most of our opportunities to get to know each other outside of lab. I loved getting to meet you over Zoom, and our short amount of time being able to interact in lab together.

Finally, there's no way I could have possibly made it through graduate school without the constant support of my family and friends, both inside and outside California. The constant support of my friends back home and their trips out to LA to visit were constant highlights throughout my time here. It was so nice to be enrolled in a graduate program at the same time as my brother Elliott, even though our exact times and locations didn't overlap, it was enjoyable to be in the same boat as someone else in the family. Laretta, thank you for your constant support throughout my California journey. Some of my favorite weekends are when work brought you here and we got to try a fancy new restaurant. Thank you to both my parents, Joan and Jeff, for being so understanding in my choice to leave the state for five years, even if it wasn't where you wanted me to go. Thank you for all the help you provided in me being on my own for the first time. And last, but certainly not least, I couldn't possibly thank enough my fiancée Ashley. You have been my rock throughout my Ph. D. and have been an invaluable source of unconditional love and support. You inspire me every day to be the best version of myself, and to press on, even when things seem impossibly difficult. I can't imagine any version of graduate school that doesn't involve you in it. I love you and can't wait to start the next chapter of our lives together. Thank

you to all those who I haven't named in this acknowledgement who have aided in my graduate studies.

Chapter one is a version of an unpublished review Jaye, J. A.; Sletten, E. M. "Recent advances in the preparation of semifluorinated polymers" (*In preparation*). Jaye and Sletten contributed to writing.

Chapter two is a version of Jaye, J. A.; Sletten, E. M. "Modular and processable fluoropolymers prepared via a safe, mild iodo-ene polymerization." *ACS Cent. Sci.* **2019**, *5*, 982-99. Jaye contributed to experimental work. Jaye and Sletten contributed to writing.

Chapter three is a version of Jaye, J. A.; Sletten, E. M. "Vinyl iodide containing polymers directly prepared via an iodo-yne polymerization." *ACS Macro Lett.* **2020**, *9*, 410-415. Jaye contributed to experimental work. Jaye and Sletten contributed to writing.

Chapter four is a version of unpublished work Jaye, J. A.; Garcia, J. A.; Sletten, E. M. "Vinylogous amidine-containing fluorinated iodo-yne polymers" (*In preparation*). Jaye and Garcia contributed to experimental work. Jaye and Sletten contributed to writing.

Chapter five is a version of Jaye, J. A.; Sletten, E. M. "Simple synthesis of fluorinated ene-yne via *in-situ* generation of allenes." *Synthesis*. **2021**, Accepted, DOI: 10.1055/s-0037-1610774. Jaye contributed to experimental work. Jaye and Sletten contributed to writing.

Throughout these studies I was supported by NSF GRFP. Further funding was provided by NSF MRI, Sloan Research Foundation, and MRSEC program of NSF

BIOGRAPHICAL SKETCH

Education:

University of California, Los Angeles, Los Angeles, CA
MS in Chemistry, 2018

University of Saint Thomas, St. Paul, Minnesota
BS in Chemistry, 2016

Thesis title: A computational and experimental investigation of the electrocyclic ring closure of BN-Pyrene

Thesis advisor: Eric H. Fort

Professional and Academic Experience:

Graduate Research Assistant

University of California, Los Angeles, Department of Chemistry and Biochemistry, 2016–2021
Advisor: Prof. Ellen M. Sletten

- Synthesis and characterization of novel fluoropolymer scaffolds.
- Development and optimization of reactions containing fluorinated alkyl or vinyl iodides

Undergraduate Research Assistant

University of Saint Thomas, Department of Chemistry and Biochemistry, 2014-2016
Advisor: Prof. Eric H. Fort

- Synthesis of azaborine heterocycles and computational investigation of their physical properties

Honors and Awards:

Theodore A. Geissman Dissertation Award, 2021

UCLA Donald J. Cram Excellence in Research Award, 2020

ACS POLY Excellence in Graduate Polymer Research Symposium Invite and Award, 2020

UCLA Research Showcase Fellowship, 2019

NSF Graduate Research Fellowship, 2018-2021

University of Saint Thomas Most Outstanding Organic Chemist Award, 2016

University of Saint Thomas Excellence in Teaching Award, 2016

William Larson Scholarship (Most prestigious chemistry scholarship at UST), 2015

ACS Award for Excellence at Poster Presentation, 2014

UST Young Scholar Undergraduate Research Grant, 2014 & 2015

Publications:

8. **Jaye, J. A.**; Garcia, J. A.; Sletten, E. M. “Vinylogous amidine-containing fluorinated iodo-yne polymers” (*In preparation*)

7. **Jaye, J. A.**; Sletten, E. M. “Recent advances in the preparation of semifluorinated polymers” (*In preparation*)

6. **Jaye, J. A.**; Sletten, E. M. “Simple synthesis of fluorinated ene-yne via *in-situ* generation of allenes.” *Synthesis*. **2021**, Accepted, DOI: 10.1055/s-0037-1610774.

5. **Jaye, J. A.**; Sletten, E. M. “Vinyl iodide containing polymers directly prepared via an iodo-yne polymerization.” *ACS Macro Lett.* **2020**, 9, 410-415.
4. **Jaye, J. A.**; Sletten, E. M. “Modular and processable fluoropolymers prepared via a safe, mild iodo-ene polymerization.” *ACS Cent. Sci.* **2019**, 5, 982-991.
3. Berger, B. E.; McCormick, G. M.; **Jaye, J. A.**; Rozeske, C. M.; Fort, E. H. “Synthesis of acridines through alkyne addition to diarylamines.” *Molecules.* **2018**, 23, 2867-2874.
2. **Jaye, J. A.**; Gelinas, B. S.; McCormick G. M.; Fort E. H. “Implications of the final ring closure to 10b-aza-10c-borapyrene for aryl-alkyne ring-closing mechanisms.” *Can. J. Chem.* **2016**, 95, 357-362.
1. Gelinas, B. S.; **Jaye, J. A.**; Mattos, G. R.; Fort, E. H. “Rapid and efficient desilylation and deuteration of alkynylpyridines.” *Tetrahedron Lett.* **2015**, 56, 4232-4233.

Recent advances in the preparation of semifluorinated polymers

Adapted from Joseph A. Jaye and Ellen M. Sletten.* Recent advances in the preparation of semifluorinated polymers. *In preparation.*

1.1 Abstract

Synthesis of semi-fluorinated polymers containing fluorous groups on the backbone or as side chains is an increasingly popular field of research. Impartment of fluorine on polymers offers many potential benefits such as decreased surface energy, modification of thermal properties, and enhanced self-assembly. Preparation of novel semi-fluorinated polymers offers an interesting challenge, as fluorous monomers are less common, often need to be synthesized, and can have different reactivities than their hydrocarbon analogues. Alternatively, polymers can be fluorinated as a post-polymerization modification. Achieving a balance between fluorination and polymer degradation remains a hurdle in polymer chemistry. In this chapter I will highlight recent methods in the post-polymerization fluorination of commodity polymers, as well as the polymerization of less common fluorous monomers.

1.2 Introduction

Fluorinated polymers have widespread utility as a result of the high chemical and thermal stability imparted by the inert C-F bond.¹ In addition, C-F bonds bestow other beneficial properties on materials such as decreased surface energies and increased phase-separation in both solution and solid states. This can be observed with the comparison between high density polyethylene (HDPE, **1.1**), poly(vinylidene difluoride) (PVDF, **1.2**), and the most widely produced fluoropolymer, poly(tetrafluoroethylene, **1.3**), better known as Teflon™ (Figure 1.1A). With increasing weight percent fluorine, melting point and decomposition temperature are increased. The decreased contact angle of PVDF can be traced to the dipole generated through fluorinated methylene spacers. Fluorinated polymers have been incorporated into materials such as electronics, weatherable clothing, non-stick pans, dental floss, and insulators.²

Although an essential component to many modern-day devices, Teflon™ has some significant drawbacks. The high crystallinity of the polymer, coupled with its aversion to organic and fluoruous solvents, have made it difficult to process into advanced materials.³⁻⁵ Furthermore, its monomer, tetrafluoroethylene, is an explosive and toxic gas.⁶⁻⁸ Due to emulsion polymerization being standard for the production of fluoropolymers, fluorinated surfactants are required to achieve maximum molecular weight. These fluorinated surfactants have received intense scrutiny for their toxicity and bioaccumulation⁹⁻¹², leading to an expanding field of research in perfluoroalkylated substance (PFAS) remediation.¹³⁻¹⁵ The processability and safety challenges apparent with PTFE are also encountered in other commercial fluoropolymers with tetrafluoroethylene-derived monomers.^{16,17}

Alternative polymerization methods are necessary to overcome the long-standing issues in the preparation of fluorinated polymers. After tetrafluoroethylene, two common monomers to obtain (semi)fluorinated polymers are fluorinated acrylates^{18,19} and styrenes.²⁰⁻²² Other routes include polymerization of perfluorovinyl ethers to give poly(perfluorocyclobutyl) ethers or use of fluoruous diols to generate fluorinated polyurethanes. These methodologies have already been discussed in detail in recent reviews²³ and will not be covered here. Inorganic fluoropolymers such as those containing phosphorus and silicon have also been previously highlighted.^{24,25} In recent years, there have been multiple extensive reviews on perfluorinated and semi-fluorinated polymers for biomedical and commercial purposes, but all with a heavy emphasis on the polymerization of fluoruous olefins and a dearth of less commonly used monomers or other synthetic routes.^{16,26-29} Here we highlight two more recent approaches to the creation of semifluorinated polymers: post-polymerization fluorination of commodity polymers (Figure 1.1B) and new fluorinated monomers (Figure 1.1C). The first approach leverages new chemistries for installation of perfluorocarbons. Imparting unique, advanced properties into common industrial polymers has been termed “upcycling.” Upcycling has the advantage of widespread availability of polymer starting material but lacks homogeneity in the final materials. To create defined semifluorinated polymers, new fluorinated monomers with unique reactivity are necessary to overcome

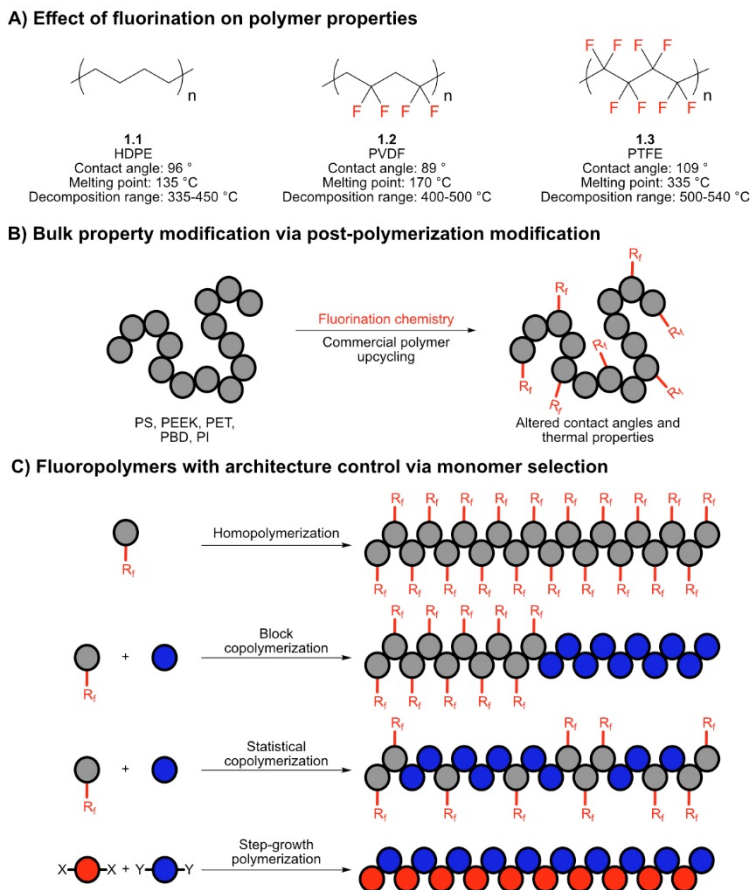


Figure 1.1: Overview of development of fluoropolymers. **A)** Comparison of thermal properties and surface energies of commercial polymers. **B)** Non-selective post-polymerization fluorination of polymers and the process of “upcycling” commercial polymers. **C)** Polymerization of fluorous monomers to give higher ordered polymer architectures.

the explosive nature of tetrafluoroethylene and complement fluorinated styrene , acrylate, and vinyl ether monomers. We cover the recent additions of fluorinated lactide, oxazoline, norbornene, and iodide monomers to create an array of semifluorinated polymers with both pendant perfluorinated chains and perfluorination installed directly in the backbone. The new monomers allow for more precise control of polymer physical properties and architectures with the trade-off of generally higher cost of synthesis.

1.3 Discussion

1.3.1 Post-polymerization fluorination of commodity polymers

Post-polymerization fluorination of aromatic containing polymers

Commercial polymers containing an aromatic ring, such as polystyrenes (**1.5a-1.5c**), numerous polycarbonates (**1.7**), and poly(ethylene terephthalate) (**1.9**) (Figure 1.2A-C), make up a significant

portion of plastics. The ability to tune the properties of these polymers is of great interest due to their overwhelming availability, either as freshly produced polymer or from recycling feedstocks. Specific interest is in increasing thermal stability, chemical resistance, water repulsion, and/or processability. Post-polymerization fluorination represents avenues to improve the properties, *i.e.* upcycle, commercial polymers.

The fluorination of polystyrene was originally studied by Margrave and Lagow in 1974, by exposure of finely powdered polystyrene to fluorine gas.³⁰ Through elemental analysis and IR spectroscopy of the resulting polymer, it was theorized that perfluorination had been achieved. The perfluorinated polystyrene was significantly more thermally stable than the parent polystyrene, with degradation temperature increasing to 175-250 °C from 120 °C in an atmosphere of air. Although fluorination could be achieved, highly toxic and corrosive fluorine gas was used as a fluorine source, and further characterization was limited, leaving questions regarding chain scission or crosslinking events. Following this report, perfluoroalkylation of the aromatic groups in poly(α -methyl styrene) and poly(phenyl methacrylate) were observed by Shuyama in 1985. Treatment of these aromatic polymers with (perfluoroalkyl)phenyliodinium trifluoromethylsulfonates allowed 14-74% of repeat units to be modified, with polymer scission also observed.³¹ This work was expanded by Zhao and coworkers in 1996 through the reaction of polystyrene with perfluorodiacyl peroxides.³² Finally, Sawada and coworkers studied the trifluoromethylation of polystyrene, poly(diphenylacetylene), and poly(2,6-dimethyl-*p*-phenylene oxide) utilizing similar chemistry in 2001.³³ Trifluoromethylation was successful on all polymers, with 16-100% of aromatic repeat units being modified. As previously observed, contact angle increased with higher levels of fluorination, but size exclusion chromatography (SEC) analysis showed increased dispersity of the polymers. After a modest gap in research, Leibfarth and coworkers have recently developed a photocatalytic method towards the fluorination of aromatic moieties in polymer chains (Figure 1.2A).³⁴ Through use of a ruthenium catalyst and pyridine-*N*-oxide oxidant, aromatic rings could be fluorinated via radicals generated from trifluoroacetic anhydride (**1.4a**), or other fluorous anhydrides for short fluorous chains. Fluorous acyl chloride (**1.4b**) could be used for C₇F₁₅ addition

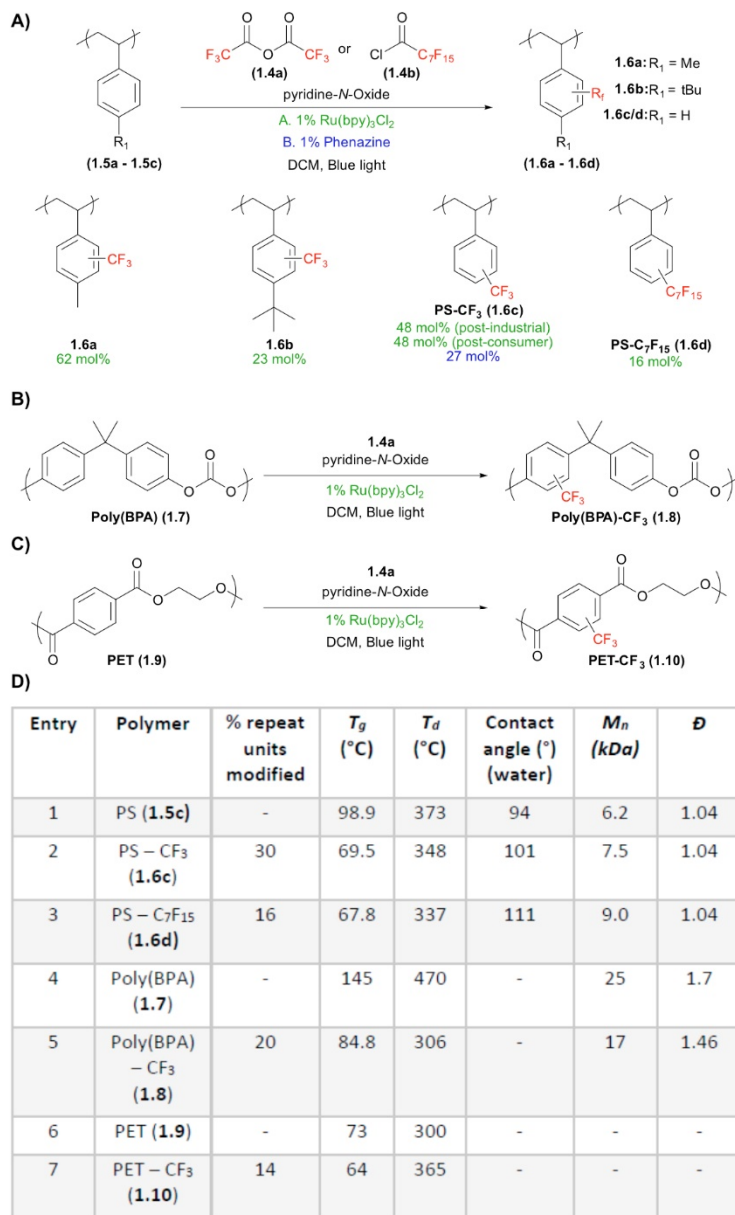


Figure 1.2: Trifluoromethylation of various aromatic containing commercial polymers and the resulting polymer properties. **A)** Fluorination of polystyrene and polystyrene derivatives (**1.5a-1.5c**) to give fluorinated styrenes (**1.6a-1.6d**). Trifluoromethylation via ruthenium catalyst (green text) was slightly more efficient than via phenazine organic photocatalyst (blue text). **B)** Fluorination of poly(BPA) (**7**) to give fluorinated poly(BPA) (**1.8**). **C)** Fluorination of poly(ethylene terephthalate) (**1.9**) to give fluorinated PET (**1.10**). **D)** A table summarizing thermal properties of polymers as well as surface energy through contact angle measurement against water.

(Figure 1.2A). The degree of fluorination could be controlled through the equivalents of fluorinating agent, with multiple polystyrene derivatives (**1.5a-c**, Figure 1.2A), poly(bisphenol A carbonate) (**1.7**, Figure 1.2B), and poly(ethylene terephthalate) (**1.9**, Figure 1.2C) all being successfully modified to give fluorinated analogues **1.6a-1.6d**, **1.8**, and **1.10**. Polystyrene could be modified with 20-110 fluorine groups per 100 styrene repeating units. In contrast to older reports, polymer dispersity was not significantly affected by fluorination. In most cases, degradation temperature (T_d) remained similar

between starting polymer and fluorinated polymer, with a lowering of the glass transition temperature (T_g) (Figure 1.2D, Table Entries 1-7). The introduction of fluorous character was assayed by the wettability of the polymer films. The authors found that the contact angle of water increased with increasing levels of fluorination and length of fluorous chain (Figure 1.2D, Table Entries 1-3). Soon after this report, a similar transformation was successful with a phenazine organic photocatalyst, albeit with a slightly lower fluorination efficiency (Figure 1.2A, blue text).³⁵

Post-polymerization fluorination of poly(ether ketones)

Semi-crystalline aromatic poly(ether ketones) are produced on an industrial scale as high-performance thermoplastics. Containing both aromatic rings and electrophilic carbonyls, these polymer scaffolds have attracted attention for post-polymerization modification in bulk and on surface level films.³⁶ Although the synthesis of fluorine containing poly(ether ketones) has been investigated^{37,38}, there are few cases of post-polymerization fluorination. In 1995, Badyal and Hopkins studied the fluorination of polyether ether ketone (PEEK) through the use of CF_4 plasma.³⁹ Elemental analysis provided evidence of high levels of fluorination, but further polymer analysis was not performed. Noiset and coworkers also reported surface level fluorination of PEEK through reduction of polymer ketones to alcohols with subsequent fluorination via diethylaminosulfur trifluoride in 1997.⁴⁰ Most recently, Liu and coworkers have developed methods for surface level fluorination of PEEK via activation with argon plasma, followed by treatment with aqueous HF.⁴¹ Fluorinated PEEK was shown to be a promising polymer for biomedical inserts.

Building from the work performed by the Liu group, Colquhoun and coworkers adapted small molecule chemistry for the trifluoromethylation of poly(ether ketone) **1.11** in solution phase (Figure 1.3A).^{42,43} Following generation of a trifluoromethyl anion, nucleophilic addition occurred quantitatively at the carbonyl sites in the polymer backbone. Subsequent alcohol deprotection gave quaternary carbons containing both the hydrophobic trifluoromethyl group and the hydrophilic alcohol on polymer **1.12**. Having amphiphilic functionality allowed for polymer dissolution in methanol and ethanol while retaining

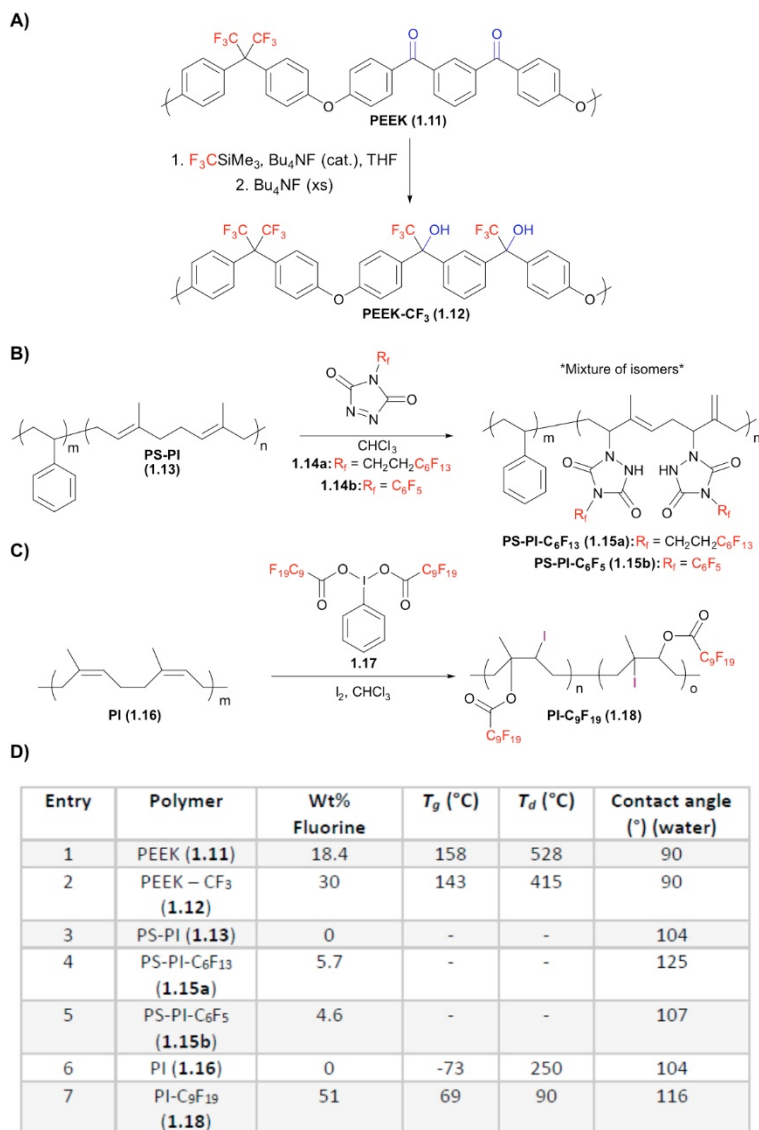


Figure 1.3: Post-polymerization modifications of commercial polymers. **A)** Synthetic scheme showing trifluoromethylation of the electrophilic ketone of a synthesized poly(ether ketone) (1.11), followed by desilylation of the resulting silyl ether to give the fluorinated polymer (1.12). **B)** Addition of fluorous groups to a statistical copolymer of polystyrene and polyisoprene (1.13) via triazolinediones (1.14a and 1.14b) giving a mixture of isomers on polymers 1.15a and 1.15b. **C)** Addition of a fluorinated ester 1.17 to polyisoprene 1.16 giving a mixture of regioisomers on fluorous polymer 1.18. **D)** A table summarizing thermal properties of polymers as well as surface energy through contact angle measurement against water.

similar physical and surface properties of the original THF-soluble polymer. Similar to the modification of polystyrene, the glass transition was lowered with trifluoromethylation (Figure 1.3D, Entries 1-2). The degradation temperature was also lowered, likely due to the presence of labile benzylic alcohol groups.

Polydienes represent another important class of commercial polymers, with polybutadiene and polyisoprene being the hallmark members of this family. The polydienes contain units of unsaturation in the polymer chain or incorporation of an allyl side group, which are convenient handles for direct functionalization of the polymer. Like polystyrene, original attempts of fluorination required fluorine gas. Two research groups used F₂ to fluorinate either polyisoprene or poly(sulfone-butadiene) copolymers in 1995, although further characterization of the polymers was limited.^{39,44} In 1998, Hillmyer and coworkers introduced a mild fluorination technique from a fluorous carbene generated through hexafluoropropylene oxide as a fluorine source.⁴⁵⁻⁴⁷ Quantitative fluorination could be achieved on polyisoprene, polybutadiene, and polydimethylbutadiene. In all cases, T_d was slightly lowered due to the incorporation of labile *gem*-difluorocyclopropane moiety, but T_g was significantly increased, as well as the water contact angle. Further work by the Hillmyer group in 2001 led to addition of a perfluoroalkyl iodide to polydienes⁴⁸, showing similar thermal and contact angle changes as their previous report. The addition of fluorous carbenes has also been applied to poly(1,3-cyclohexadiene) by Ways and coworkers in 2008.⁴⁹

Since these seminal reports, there has been a resurgence in the addition of fluorous groups to polydienes. Barner-Kowollik and coworkers applied multi-component reactions for the addition of bromide and an alcohol across the double bond of polydienes using *N*-bromosuccinimide (NBS) and a perfluoroaryl acid in THF.⁵⁰ Quantitative loss of olefin was reported, and further post-polymerization modifications could be performed on the alkyl bromide, such as displacement by sodium azide.

Du Prez and coworkers have also adapted a method for polydiene (**1.13**) functionalization via triazolinediones (Figure 1.3B).⁵¹ Fluorous triazolinediones (**1.14a**, **1.14b**) could be synthesized in three steps from an amine, and upon mixing with poly(styrene-isoprene-styrene) block copolymer, fluorination was achieved in as little as 10 minutes. When a long fluorous chain was used, **1.15a** was observed with 34% efficiency. In the case of a perfluorinated aryl moiety, **1.15b** was generated with 99% efficiency. The level of fluorination could be tuned through the weight percent of **1.14a** or **1.14b** in the reaction

mixture, and as seen with previous cases, fluorination of the polymer greatly increased the static contact angle against water (Figure 1.3D, Entries 3-5). In this study, the thermal properties were not recorded so comments cannot be made on the variance of T_d or T_g .

Most recently, Tsarevsky and coworkers have modified polyisoprene (**1.16**) through various techniques utilizing hypervalent iodine (Figure 1.3C).⁵² Fluoride atoms, trifluoromethyl groups, and fluorinated esters could be added concurrently with halides. Specifically, the addition of fluorous esters alpha to an alkyl iodide was accomplished through reaction of **1.16** with hypervalent iodine intermediate **1.17**. The fluorinated polymer (**1.18**) had significantly increased contact angle of water, but the electrophilic fluorous esters and alkyl iodide lowered the thermal stability of the polymer (Figure 1.3D, Entries 6 and 7).

1.3.2 Synthesis of fluorous polymers through fluorinated monomers

Uncontrolled polymerization of monomers with fluorous sidechains

While upcycling and post-polymerization fluorination approaches are able to alter the bulk properties of a material, fine control over the chemical composition remains poor. There is increased interest in the development of new fluoropolymer scaffolds, with control over the monomer composition for tuning of fluorination and bulk polymer properties. With PTFE and its derivative polymers being highly crystalline and insoluble, there has been development of alkenes containing longer fluoroalkyl chains. By the addition of bulky fluoroalkyl chains, crystallinity can be lowered giving a more easily processed polymer.¹⁷ In particular, perfluorohexylethylene (PFHE, **1.19b**, Figure 1.4A) is of interest due to the long hexyl chain. Although resistant to homopolymerization, PFHE was successfully copolymerized with non-fluorous olefins such as vinyl acetate (Vac, **1.19a**, Figure 1.4A) in 1985 giving polymer **1.20**. This copolymerization was further studied by Sen and Borkar via free and controlled radical polymerization, along with copolymerization of PFHE with methyl methacrylate via atom transfer radical polymerization (ATRP) in 2005.^{53,54} A patent was granted for the copolymerization of PFHE with

tetrafluoroethylene for the development of fluoruous membranes and films in 2009, a proposed alternative to Teflon-AF.⁵⁵

Most recently, Detrembleur and coworkers have optimized a cobalt mediated radical copolymerization of PFHE and VAc (Figure 1.4A, top).⁵⁶ PFHE could be incorporated into the copolymer in up to 49 mol% of the statistical mixture with low dispersity. As the ratio of PFHE monomer was increased there was also an increase in dispersity of the resultant polymer (Figure 1.4C, Table Entries 2

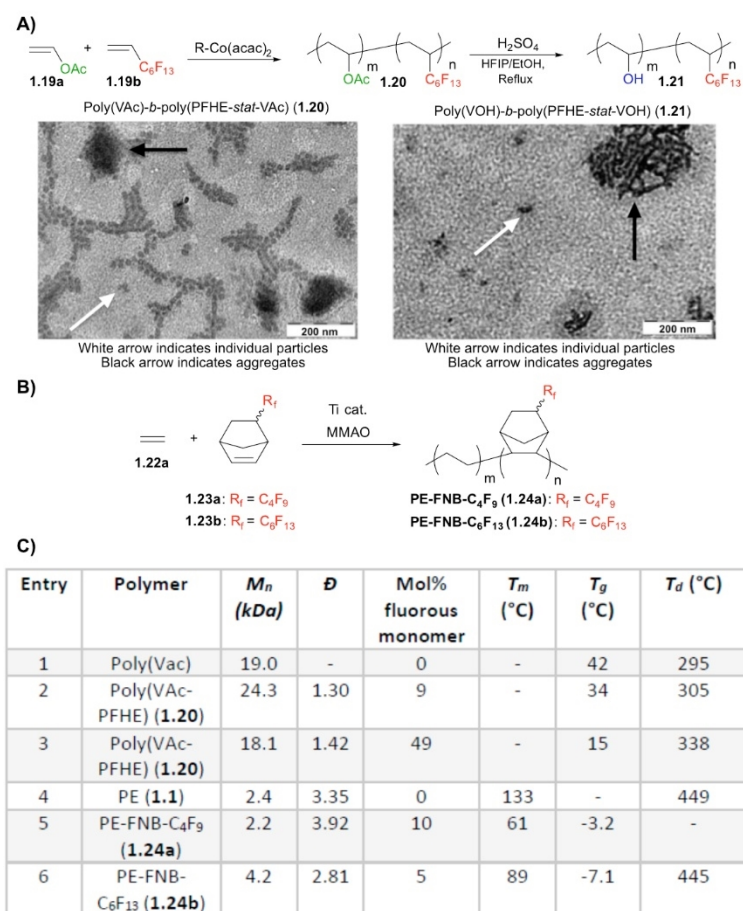


Figure 1.4: Use of fluoroalkyl alkenes to give semi-fluorinated polymers. **A)** Top: Copolymerization of perfluorohexylethylene (PFHE, **1.19a**) and vinyl acetate (VAc, **1.19b**) to give polymer **1.20** with subsequent hydrolysis of acetate giving polymer **1.21**. Bottom: TEM images of polymers **1.20** and **1.21** demonstrating increased polymer aggregation with generation of alcohol functionalities. Reproduced from Ref. 56 with permission from ACS Publications. **B)** Copolymerization of ethylene gas (**1.22a**) with fluorinated norbornenes (FNB, **1.23a** or **1.23b**) to give polymer **1.24a** or **1.24b**. **C)** Table of polymer properties comparing homopolymers to those containing fluoroalkyl side chains.

and 3). As predicted, increasing the fluoroalkyl monomer feed decreased the T_g of the polymer, but the thermal stability was improved (Figure 1.4C, Table Entries 1-3). Contact angles of the polymers were not measured in this study, but it had been previously observed that the incorporation of perfluorohexyl chain

in PVAc increased water contact angle to 104° ,⁵⁴ while perfluorooctyl and perfluorodecyl groups gave increases to 111° and 114° , respectively. The poly(PFHE-*stat*-VAc) copolymer, **1.20**, could be further modified through hydrolysis with a strong acid with full conversion from ester to alcohol giving poly(PFHE-*stat*-VA) copolymers, **1.21**. TEM images display increased aggregation of **1.21** when compared to **1.20**, likely due to the hydrogen bonding of the alcohol generated upon hydrolysis of the acetate groups (Figure 1.4A, bottom).

Another strategy for fluorine incorporation in polymers is the separation of the fluororous group from the propagating polymer site. The Cai and Tang groups have independently developed methods for the copolymerization of ethylene (**1.22a**) and fluorinated norbornenes (FNB) **1.23a** or **1.23b** as a statistical copolymer, **1.24a** or **1.24b**, respectively (Figure 1.4B).^{57,58} Both groups utilized titanium and MMAO catalysts, with reaction times between two and fifteen minutes. Fluororous norbornene incorporation could be varied between 1 and 5 mol%. In both reports, the degradation temperatures (T_d) of the copolymers were unchanged by fluororous chain addition (Figure 1.4C, Table Entries 4-6), while the melting points (T_m) were decreased with increasing fluororous chain incorporation. The Cai group demonstrated increased elongation at break with the addition of fluororous chains to the polymer.

Towards a new scaffold, a step-growth polymerization between dithiols and trifluoromethyl acetylenecarboxylates was presented by Durmaz and coworkers.⁵⁹ Trifluoromethyl containing polythioethers could be easily synthesized at room temperature with large molecular weight polymer being generated in as little as one minute. The thermal properties of these polymers could be readily modified through dithiol selection, although contact angle remained consistent due to preservation of the trifluoromethyl group.

Controlled polymerizations of monomers with fluororous side chains

While non-controlled polymerizations of fluorinated monomers are adequate at control over the total polymer composition and fluorine incorporation, fine control over the polymer architecture remains poor. In many instances, defined architectures that allow for self-assembled structures or uniform surface

coverage are desirable. For these applications, controlled polymerization are ideal. Controlled fluoropolymers can be prepared using fluorinated acrylate monomers followed by standard RAFT and ATRP polymerization. Fluorinated poly(acrylate)s have been reviewed previously^{18,19}, and here we highlight the controlled or living polymerization of other fluorous monomers, including lactides, oxazolines, and acetylenes.

Poly(lactides) can be formed through a controlled ring-opening polymerization from natural monomers. Their biocompatibility and biodegradability have rendered them popular biomaterials.⁶⁰ Methods to tune both the degradation properties as well as the glass transition temperature have prompted the introduction of fluorinated monomers.⁶¹ In 1998, McKie and coworkers prepared the first poly(trifluoromethyl lactic acid).⁶²

Twenty years later, Boydston and coworkers revisited trifluoromethylated poly(lactide) and prepared trifluoromethyl lactide monomer **1.25** (Figure 1.5A, top scheme).⁶³ Using a tin catalyst and

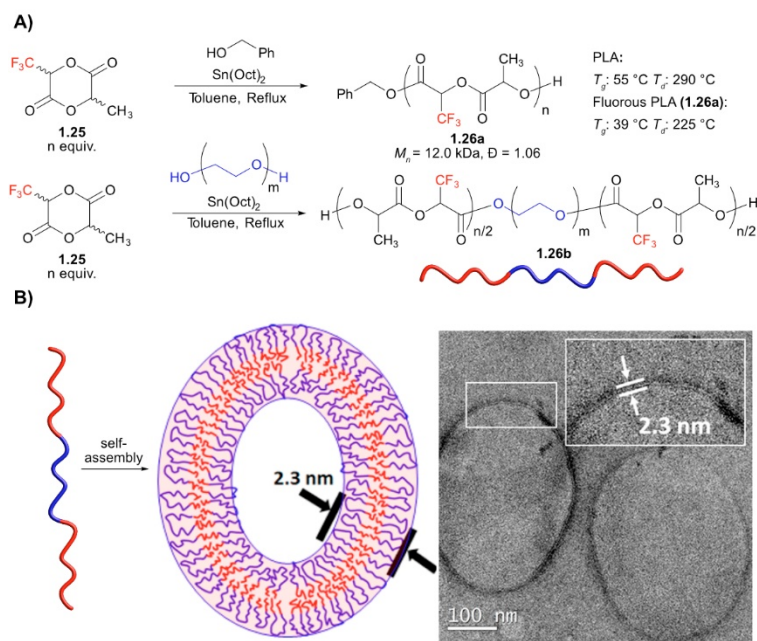


Figure 1.5: Synthesis and self-assembly of poly(lactide) copolymers. **A)** Top: Homopolymerization of trifluoromethyl lactide monomer **1.25** resulting in polymer **1.26a**. Bottom: Polymerization of trifluoromethyl lactide **1.25** with bifunctional polyethylene glycol (PEG) to give ABA block copolymer **1.26b**. **B)** Self-assembly of fluorous lactide ABA block copolymer **1.26b** in water. Reproduced from Ref. 63 with permission from ACS Publications.

benzyl alcohol as an initiator, a trifluoromethyl poly(lactic acid) (PLA) could be synthesized with excellent conversion and low dispersity (**1.26a**). Both the T_g and T_d were lowered by trifluoromethylation of lactide monomer, consistent with other fluorinated polymers. When poly(ethylene glycol) (PEG) was used as an initiator (Figure 1.5A, bottom scheme), triblock copolymer (**1.26b**) with controlled block lengths could be synthesized. In water, polymer **1.26b** self-assembled into vesicles with ~300 nm diameter with a 2.3 nm polymer shell (Figure 1.5B). The methods reported by Boydston and coworkers, to prepare fluorinated poly(lactic acid)s have been reproduced by others where contact angle and protein adsorption have been characterized.⁶⁴ The contact angle of fluorinated PLA **1.26a**, synthesized by Ratner and coworkers, was significantly increased to 88° in comparison to 70° from standard PLA. It was also demonstrated that fluorinated PLA has a higher rate of protein adsorption which is hypothesized to improve thromboresistance, a promising application of these materials.

Poly(oxazoline)s are another polymer scaffold with growing biomaterials interests that are obtained through a controlled ring opening polymerization. While it is poly(methyl-2-oxazoline) and poly(ethyl-2-oxazoline) that have garnered the most attention as poly(ethylene glycol) replacements, the polymerization of hydrophilic, hydrophobic and fluorinated oxazoline monomers (**1.27a-g**, Figure 1.6A) allows for the creation of amphiphiles and the tuning of the thermoresponsive behaviour. Although the polymerization of oxazolines has been known since 1966, incorporation of a fluorinated group on the oxazoline scaffold (**1.27c**) was not performed until 1988 by Saegusa and coworkers (Figure 1.6A).⁶⁵ In this study it was found that the electron withdrawing nature of fluorinated group greatly hampered polymerization kinetics, with most conditions only providing oligomeric **1.28a** (Figure 1.6B, top). Shortly after, Sogah and coworkers found that addition of an ethyl spacer between the oxazoline heterocycle and fluorinated group (**1.27e**) greatly improved polymerization giving **1.28b** (Figure 1.6B, bottom).⁶⁶ Building from this finding, Papadakis and coworkers synthesized the first hydrophilic/fluorinated block copolymers using oxazoline monomers **1.27a** and **1.27f** and observed micelle formation in an aqueous environment.⁶⁷ They found that the fluorinated core formed an elongated micelle in comparison to the spherical micelle formed from a lipophilic core (synthesized from **1.27a** and **1.27b**), demonstrating that incorporation of

fluorine has a unique effect on self-assembly due to the increased rigidity of perfluoroalkyl chains. To better understand the effect of fluorine on oxazoline polymerization, the Hoogenboom group has thoroughly studied the addition of alkyl spacers between the oxazoline heterocycle and fluorine group (Figure 1.6C, left).⁶⁸ The polymerization rates of 2-trifluoromethyl-2-oxazoline (**1.27c**), 2-(2,2,2-trifluoroethyl)-2-oxazoline (**1.27d**), and 2-(2,2,2-trifluoropropyl)-2-oxazoline monomers were compared

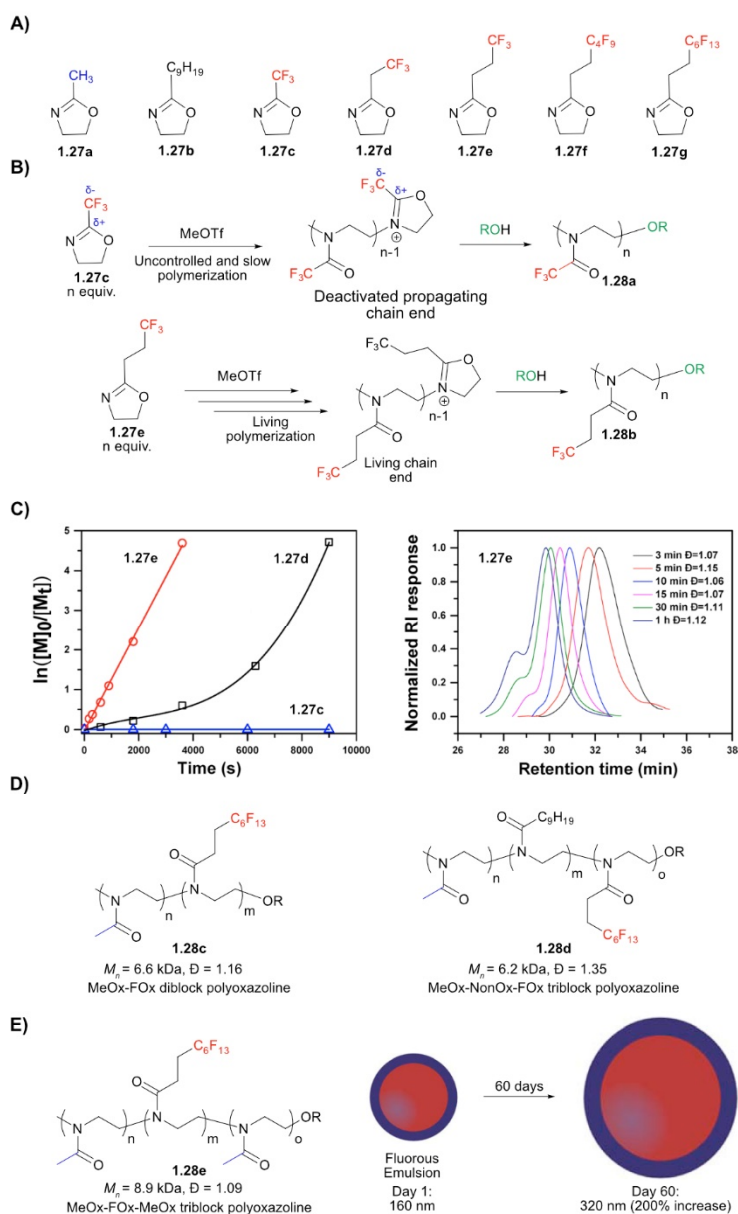


Figure 1.6: Structure of oxazoline monomers, kinetics of the polymerization of fluorous oxazolines, and the development of di and triblock fluorous polymers. **A)** Select hydrophilic, hydrophobic, and fluorophilic oxazoline monomers **1.27a-g**. **B)** Comparisons of the polymerization of oxazolines with fluorous groups directly attached to the oxazoline scaffold (**1.27c**) vs those with an ethyl spacer (**1.27e**). **C)** Left: Comparison of polymerization kinetics between oxazoline monomers containing different alkyl spacers between the fluorous group and oxazoline heterocycle (**1.27c-e**). Right: Size exclusion chromatography (SEC) traces of the **1.27e** homopolymer demonstrating low dispersity. Reproduced from Ref. 68 with permission from ACS Publications. **D)** Di and Triblock copolymers (**1.28c** and **1.28d**) synthesized from methyl, alkyl, or fluorous oxazoline monomers. **E)** Triblock polyoxazoline **1.28e** and the stability of the fluorous emulsions generated from it.

(**1.27e**). It was found that when 2-trifluoromethyl-2-oxazoline was used as a monomer, very little polymerization occurred (Figure 1.6C, left, blue line). Alternatively, the use of a methyl spacer allowed for polymerization, but the robust living kinetics of CROP were not observed (Figure 1.6C, left, black line). Extending to an ethyl spacer provided enough of a shield from the electron-withdrawing nature of the fluororous group that polymerization proceeded readily with living kinetics, yielding polymers with a dispersity under 1.2 (Figure 1.6C, left, red line, and Figure 1.6C, right). Hydrophilic-fluorophilic diblock and hydrophilic-lipophilic-fluorophilic triblock polymers could be polymerized, with morphology being observed via TEM. In efforts to increase the fluororous nature of the poly(2-oxazolines), the ethyl spacer has been retained but a longer perfluorohexyl group was appended in place of the trifluoromethyl group (oxazoline **1.27g**) to give polymers **1.28c** and **1.28d**.⁶⁹ Reaction kinetics were comparable for **1.27e** and **1.27g**, allowing highly fluorinated di and tri block copolymers to be prepared through similar methodology (Figure 1.6D). Notably, polymer **1.28d** was found to self-assemble in both water and DMSO, with DMSO self-assembly not occurring with the lipophilic comparison. We have employed a similar fluorinated oxazoline monomer to prepare custom, functionalizable amphiphiles for the stabilization of perfluorocarbon nanoemulsions (Figure 1.6E). The incorporation of fluororous character into the amphiphile (polymer **1.28e**) lead to more stable nanoemulsions over sixty days, as compared to a hydrocarbon variant.⁷⁰

Other controlled polymerizations to achieve polymers with pendant fluororous chains

Utilizing different scaffolds, Seki and coworkers have studied the self-assembly of low dispersity, unsymmetrical, alkyl-fluoroalkyl side chain containing polyacetylenes.⁷¹ Ihara and coworkers have recently developed a palladium initiated polymerization of fluoroalkyldiazo acetates.⁷² This polymerization led to poly(substituted methylene)s of modest molecular weight, which could be quantitatively modified through reactions with primary amines.

1.3.3 Synthesis of polymers with a fluorinated backbone

An important distinction of semi-fluorinated polymers is between those containing fluorinated side chains or fluorinated backbones. Thus far, we have highlighted incorporation of fluorinated character onto the side chains. While there are many commercial polymers with fluorine installed directly on the backbone, most are derived from fluorinated olefins which have significant safety concerns. Other approaches to incorporate fluorine directly into the backbone are the use of telechelic functional poly(perfluoroethers) or leveraging difunctional perfluorinated monomers. The former approach has been recently reviewed by Améduri and Friesen.²⁸ We will highlight the latter approach in chapters two and three.

1.4 Conclusion

In the last few years, new approaches to incorporate fluorine into polymers to achieve the advantageous stability and hydro/lipophobicity have been developed to complement the ubiquitous approaches of fluorinated acrylate or olefin monomers. The more modern methods to incorporate fluorine employ a variety of chemistries and starting materials. There is no single best approach and instead one should consider the needs of the material when choosing how to incorporate fluorine into a material. Starting from fluorinated monomers allows for more control over the polymer backbone, which is critical for self-assembly, or the ability to introduce co-monomers with additional functionality for polymer derivatization. Even inclusion of small amounts of fluorinated monomer in uncontrolled polymerizations can give polymers enhanced thermal stability, greater water repulsion, while increasing workability by lowering the glass transition or melting points. If cost and scale are a concern, post-polymerization fluorination methods are desirable as they can be performed on recycled commodity polymers. While these approaches provide heterogeneous samples, in many cases they improve thin film water contact angle while lowering the glass transition of rigid polymers.

Looking forward, there is much room for growth in fluoropolymer synthesis. Upcycling commodity polymers into fluoropolymers has only recently gained traction and there are many small molecule chemistry methodologies that can be applied to recycled materials. There is considerable room

for new fluorinated monomers for controlled polymerizations. An exciting development would be an approach that allows for fluorination installed directly in the backbone to be obtained with living reaction kinetics. Finally, we anticipate that the convergence of advances in functional, dynamic polymer materials to continue to merge with fluoropolymers to provide next-generation materials with enhanced stability and function.

1.5 References

- (1) Teng, H. Overview of the Development of the Fluoropolymer Industry. *Appl. Sci.* **2012**, *2*, 496–512.
- (2) Ebnesajjad, S. *Introduction to fluoropolymers*; William Andrew, Norwich, **2013**.
- (3) Tervoort, T.; Visjager, J.; Smith, P. Melt-processable Poly(tetrafluoroethylene)—Compounding, Fillers and Dyes. *J. Fluor. Chem.* **2002**, *114*, 133–137.
- (4) Li, M.; Zhang, W.; Wang, C.; Wang, H. Melt Processability of Polytetrafluoroethylene: Effect of Melt Treatment on Tensile Deformation Mechanism. *J Appl Polym Sci.* **2011**, *123*, 1667–1674.
- (5) Olabisi, O.; Adewale, K. *Handbook of thermoplastics*; CRC Press, Boca Raton, **2015**.
- (6) Hercules, D. A.; Parrish, C. A.; Saylor, T. S.; Tice, K. T.; Williams, S. M.; Lowery, L. E.; Brady, M. E.; Coward, R. B.; Murphy, J. A.; Hey, T. A.; et al. Preparation of Tetrafluoroethylene from the Pyrolysis of Pentafluoropropionate Salts. *J. Fluor. Chem.* **2017**, *196*, 107–116.
- (7) De Rademaeker, E.; Fabiano, B.; Buratti, S. S.; Ferrero, F.; Zeps, R.; Kluge, M.; Schröder, V.; Spoomaker, T. The Explosive Decomposition of Tetrafluoroethylene: Large Scale Tests and Simulations. *Chem. Eng. Trans.* **2013**, *13*, 817–822.
- (8) Hercules, D. A.; DesMarteau, D. D.; Fernandez, R. E.; Clark, J. L.; Thrasher, J. S. Evolution of Academic Barricades for the Use of Tetrafluoroethylene (TFE) in the Preparation of

Fluoropolymers. In *Handbook of Fluoropolymer Science and Technology*; John Wiley & Sons, Inc.: Hoboken, NJ, USA, 2014; pp 413–431.

- (9) Krafft, M. P.; Riess, J. G. Per- and Polyfluorinated Substances (PFASs): Environmental Challenges. *Curr. Opin. Colloid Interface Sci.* **2015**, *20*, 192–212.
- (10) Wang, P.; Lu, Y.; Wang, T.; Meng, J.; Li, Q.; Zhu, Z.; Sun, Y.; Wang, R.; Giesy, J. P. Shifts in Production of Perfluoroalkyl Acids Affect Emissions and Concentrations in the Environment of the Xiaoqing River Basin, China. *J. Hazard. Mater.* **2016**, *307*, 55–63.
- (11) Lau, C.; Butenhoff, J. L.; Rogers, J. M. The Developmental Toxicity of Perfluoroalkyl Acids and Their Derivatives. *Toxicol. Appl. Pharmacol.* **2004**, *198*, 231–241.
- (12) Kannan, K.; Corsolini, S.; Falandysz, J.; Fillmann, G.; Kumar, K.; Loganathan, B.; Mohd, M.; Olivero, J.; Wouwe, N.; Yang, J.; Aldous, K. Perfluorooctanesulfonate and related fluorochemicals in human blood from several countries. *Environ. Sci. Technol.* **2004**, *38*, 4489–4495.
- (13) Kumarasamy, E.; Manning, I. M.; Collins, L. B.; Coronell, O.; Leibfarth, F. A. Ionic Fluorogels for Remediation of Per- and Polyfluorinated Alkyl Substances from Water. *ACS Cent. Sci.* **2020**, *6*, 487–492.
- (14) Xiao, L.; Ling, Y.; Alsaiee, A.; Li, C.; Helbling, D. E.; Dichtel, W. R. β -Cyclodextrin Polymer Network Sequesters Perfluorooctanoic Acid at Environmentally Relevant Concentrations. *J. Am. Chem. Soc.* **2017**, *139*, 7689–7692.
- (15) Klemes, M. J.; Ling, Y.; Ching, C.; Wu, C.; Xiao, L.; Helbling, D. E.; Dichtel, W. R. Reduction of a Tetrafluoroterephthalonitrile- β -Cyclodextrin Polymer to Remove Anionic Micropollutants and Perfluorinated Alkyl Substances from Water. *Angew. Chemie Int. Ed.* **2019**, *58*, 12049–12053.
- (16) Améduri, B. The Promising Future of Fluoropolymers. *Macromol. Chem. Phys.* **2020**, *221*, 1900573.

- (17) Puts, G. J.; Crouse, P.; Ameduri, B. M. Polytetrafluoroethylene: Synthesis and Characterization of the Original Extreme Polymer. *Chem. Rev.* **2019**, *119*, 1763–1805.
- (18) Gong, H.; Gu, Y.; Chen, M. Controlled/Living Radical Polymerization of Semifluorinated (Meth)Acrylates. *Synlett* **2018**, *29*, 1543–1551.
- (19) Yao, W.; Li, Y.; Huang, X. Fluorinated Poly(Meth)Acrylate: Synthesis and Properties. *Polymer* **2014**, *55*, 6197–6211.
- (20) Borkar S.; Jankova, K.; Siesler, H. W.; Hvilsted, S. New Highly Fluorinated Styrene-Based Materials with Low Surface Energy Prepared by ATRP. *Macromolecules* **2004**, *37*, 788–794.
- (21) Wadekar, M. N.; Jager, W. F.; Sudhölter, E. J. R.; Picken, S. J. Synthesis of a Polymerizable Fluorosurfactant for the Construction of Stable Nanostructured Proton-Conducting Membranes. *J. Org. Chem.* **2010**, *75*, 6814–6819.
- (22) Audic, N.; Dyer, P. W.; Hope, E. G.; Stuart, A. M.; Suhard, S. Insoluble Perfluoroalkylated Polymers: New Solid Supports for Supported Fluorous Phase Catalysis. *Adv. Synth. Catal.* **2010**, *352*, 2241–2250.
- (23) Zhou, J.; Tao, Y.; Chen, X.; Chen, X.; Fang, L.; Wang, Y.; Sun, J.; Fang, Q. Perfluorocyclobutyl-Based Polymers for Functional Materials. *Mater. Chem. Front.* **2019**, *3*, 1280–1301.
- (24) Peng, H. Synthesis and Application of Fluorine-Containing Polymers with Low Surface Energy. *Polym. Rev.* **2019**, *59*, 739–757.
- (25) Wehbi, M.; Mehdi, A.; Negrell, C.; David, G.; Alaaeddine, A.; Améduri, B. Phosphorus-Containing Fluoropolymers: State of the Art and Applications. *ACS Appl. Mater. Interfaces.* **2020**, *12*, 38–59.

- (26) Mohammad, S. A.; Shingdilwar, S.; Banerjee, S.; Ameduri, B. Macromolecular Engineering Approach for the Preparation of New Architectures from Fluorinated Olefins and Their Applications. *Prog. Polym. Sci.* **2020**, *106*, 101255.
- (27) Ameduri, B. Fluoropolymers: The Right Material for the Right Applications. *Chem. - A Eur. J.* **2018**, *24*, 18830–18841.
- (28) Friesen, C. M.; Améduri, B. Outstanding Telechelic Perfluoropolyalkylethers and Applications Therefrom. *Progress in Polymer Science*, **2018**, *81*, 238–280.
- (29) Cardoso, V. F.; Correia, D. M.; Ribeiro, C.; Fernandes, M. M.; Lanceros-Méndez, S. Fluorinated Polymers as Smart Materials for Advanced Biomedical Applications. *Polymers*, **2018**, *10*, 161–187.
- (30) Lagow, R. J.; Margrave, J. L. The Controlled Reaction of Hydrocarbon Polymers with Elemental Fluorine. *J. Polym. Sci. Polym. Lett. Ed.* **1974**, *12*, 177–184.
- (31) Shuyama, H. Perfluoroalkylation of Poly(α -Methylstyrene) and Poly(Phenyl Methacrylate). *J. Fluor. Chem.* **1985**, *29*, 467–470.
- (32) Zhou, Z. Bin; He, H. Y.; Weng, Z. Y.; Qu, Y. L.; Zhao, C. X. Modification of Polystyrene via Aromatic per(Poly)Fluoroalkylation by per(Poly)Fluorodiacyl Peroxides. *J. Fluor. Chem.* **1996**, *79*, 1–5.
- (33) Hayakawa, Y.; Terasawa, N.; Sawada, H. Trifluoromethylation by Bis(Trifluoroacetyl) Peroxide of Polymers Bearing Benzene Rings. *Polymer*. **2001**, *42*, 4081–4086.
- (34) Lewis, S. E.; Wilhelmy, B. E.; Leibfarth, F. A. Upcycling Aromatic Polymers through C-H Fluoroalkylation. *Chem. Sci.* **2019**, *10*, 6270–6277.
- (35) Lewis, S. E.; Wilhelmy, B. E.; Leibfarth, F. A. Organocatalytic C–H Fluoroalkylation of Commodity Polymers. *Polym. Chem.* **2020**, *11*, 4914–4919.

- (36) Shukla, D.; Negi, Y. S.; Uppadhyaya, J. Sen; Kumar, V. Synthesis and Modification of Poly(Ether Ether Ketone) and Their Properties: A Review. *Polym. Rev.* **2012**, *52*, 189–228.
- (37) Goodwin, A. A.; Mercer, F. W.; McKenzie, M. T. Thermal Behavior of Fluorinated Aromatic Polyethers and Poly(Ether Ketone)s. *Macromolecules* **1997**, *30*, 2767–2774.
- (38) Asghar, H.; Ilyas, A.; Tahir, Z.; Li, X.; Khan, A. L. Fluorinated and Sulfonated Poly (Ether Ether Ketone) and Matrimid Blend Membranes for CO₂ Separation. *Sep. Purif. Technol.* **2018**, *203*, 233–241.
- (39) Hopkins, J.; Badyal, J. P. S. Nonequilibrium Glow Discharge Fluorination of Polymer Surfaces. *J. Phys. Chem.* **1995**, *99*, 4261–4264..
- (40) Marchand-Brynaert, J.; Pantano, G.; Noiset, O. Surface Fluorination of PEEK Film by Selective Wet-Chemistry. *Polymer.* **1997**, *38*, 1387–1394.
- (41) Chen, M.; Ouyang, L.; Lu, T.; Wang, H.; Meng, F.; Yang, Y.; Ning, C.; Ma, J.; Liu, X. Enhanced Bioactivity and Bacteriostasis of Surface Fluorinated Polyetheretherketone. *ACS Appl. Mater. Interfaces* **2017**, *9*, 16824–16833.
- (42) Leroux, F.; Bennett, R. A.; Lewis, D. F.; Colquhoun, H. M. Trifluoromethylation of Carbonyl Groups in Aromatic Poly(Ether Ketone)s: Formation of Strongly Polar yet Surface-Hydrophobic Poly(Arylenecarbinol)s. *Macromolecules* **2018**, *51*, 3415–3422.
- (43) Oladoyinbo, F. O.; Lewis, D. F.; Blundell, D. J.; Colquhoun, H. M. A Thermotropic Poly(Ether Ketone) Based on the: P-Quaterphenyl Unit: Evidence for a Smectic C Phase. *Polym. Chem.* **2019**, *11*, 75–83.
- (44) Ozerin, A. N.; Rebrov, A. V.; Feldman, V. I.; Krykin, M. A.; Storjuk, I. P.; Kotenko, A. A.; Tul'skii, M. N. Structural and Chemical Transformations in Statistical Multiblock-Copolymers with Soft and Rigid Blocks upon Fluorine Treatment. *React. Funct. Polym.* **1995**, *26*, 167–175.

- (45) Ren, Y.; Lodge, T. P.; Hillmyer, M. A. A New Class of Fluorinated Polymers by a Mild, Selective, and Quantitative Fluorination. *J. Am. Chem. Soc.* **1998**, *120*, 6830–6831.
- (46) Ren, Y.; Lodge, T. P.; Hillmyer, M. A. Synthesis, Characterization, and Interaction Strengths of Difluorocarbene-Modified Polystyrene-Polyisoprene Block Copolymers. *Macromolecules* **2000**, *33*, 866–876.
- (47) Davidock, D. A.; Hillmyer, M. A.; Lodge, T. P. Persistence of the Gyroid Morphology at Strong Segregation in Diblock Copolymers. *Macromolecules* **2003**, *36*, 4682–4685.
- (48) Ren, Y.; Lodge, T. P.; Hillmyer, M. A. A Simple and Mild Route to Highly Fluorinated Model Polymers. *Macromolecules* **2001**, *34*, 4780–4787.
- (49) Huang, T.; Messman, J. M.; Mays, J. W. A New Fluorinated Polymer Having Two Connected Rings in the Main Chain: Synthesis and Characterization of Fluorinated Poly(1,3-Cyclohexadiene). *Macromolecules* **2008**, *41*, 266–268.
- (50) Geiselhart, C. M.; Offenloch, J. T.; Mutlu, H.; Barner-Kowollik, C. Polybutadiene Functionalization via an Efficient Avenue. *ACS Macro Lett.* **2016**, *5*, 1146–1151.
- (51) De Bruycker, K.; Delahaye, M.; Cools, P.; Winne, J.; Prez, F. E. Du. Covalent Fluorination Strategies for the Surface Modification of Polydienes. *Macromol. Rapid Commun.* **2017**, *38*, 1700122.
- (52) Cao, Y.; Sayala, K. D.; Gamage, P. L.; Kumar, R.; Tsarevsky, N. V. Synthesis of Fluorine-Containing Polymers by Functionalization of Cis-1,4-Polyisoprene with Hypervalent Iodine Compounds. *Macromolecules* **2020**, *53*, 8020–8031.
- (53) Borkar, S.; Sen, A. Novel Fluoroalkene-Methyl Acrylate Copolymers by Atom Transfer Radical Polymerization. *Macromolecules* **2005**, *38*, 3029–3032.

- (54) Borkar, S.; Sen, A. Controlled Copolymerization of Vinyl Acetate with 1-Alkenes and Their Fluoro Derivatives by Degenerative Transfer. *J. Polym. Sci. Part A Polym. Chem.* **2005**, *43*, 3728–3736.
- (55) Sabol, E.; Baillie, R. Copolymers of Tetrafluoroethylene. US7531611B2, 2009.
- (56) Demarteau, J.; Améduri, B.; Ladmiral, V.; Mees, M. A.; Hoogenboom, R.; Debuigne, A.; Detrembleur, C. Controlled Synthesis of Fluorinated Copolymers via Cobalt-Mediated Radical Copolymerization of Perfluorohexylethylene and Vinyl Acetate. *Macromolecules* **2017**, *50*, 3750–3760.
- (57) Sun, Y.; Wang, C.; Tanaka, R.; Shiono, T.; Cai, Z. Copolymerization of Ethylene and Fluoroalkylnorbornene Using Highly Active *Ansa*- (Fluorenyl)(Amido)Titanium-Based Catalysts. *Macromol. Chem. Phys.* **2019**, *220*, 1900306.
- (58) Ji, L.; Liu, J.-S.; Wang, X.-Y.; Li, J.-F.; Chen, Z.; Liao, S.; Sun, X.-L.; Tang, Y. An Efficient and Mild Route to Highly Fluorinated Polyolefins via Copolymerization of Ethylene and 5-Perfluoroalkylnorbornenes. *Polym. Chem.* **2019**, *10*, 3604–3609.
- (59) Daglar, O.; Cakmakci, E.; Gunay, U. S.; Hizal, G.; Tunca, U.; Durmaz, H. A Straightforward Method for Fluorinated Polythioether Synthesis. *Macromolecules* **2020**, *53*, 2965–2975.
- (60) Mehta, R.; Kumar, V.; Bhunia, H.; Upadhyay, S. N. Synthesis of Poly(Lactic Acid): A Review. *J. Macromol. Sci. Part C Polym. Rev.* **2005**, *45*, 325–349.
- (61) Bhardwaj, R.; Mohanty, A. K. Modification of Brittle Polylactide by Novel Hyperbranched Polymer-Based Nanostructures. *Biomacromolecules* **2007**, *8*, 2476–2484.
- (62) McKie, D. B.; Lepeniotis, S. Optimization Techniques for Carbodiimide Activated Synthesis of Poly((RS)-3,3,3-Trifluorolactic Acid); Statistically Designed Experiments to Optimize Polymerization Conditions. In *Chemometrics and Intelligent Laboratory Systems*; Elsevier, 1998; Vol. 41, pp 105–113.

- (63) Lee, C. U.; Khalifehzadeh, R.; Ratner, B.; Boydston, A. J. Facile Synthesis of Fluorine-Substituted Polylactides and Their Amphiphilic Block Copolymers. *Macromolecules* **2018**, *51*, 1280–1289.
- (64) Khalifehzadeh, R.; Ratner, B. D. Trifluoromethyl-Functionalized Poly(Lactic Acid): A Fluoropolyester Designed for Blood Contact Applications. *Biomater. Sci.* **2019**, *7*, 3764–3778.
- (65) Miyamoto, M.; Aoi, K.; Saegusa, T. Mechanisms of Ring-Opening Polymerization of 2-(Perfluoroalkyl)-2-Oxazolines Initiated by Sulfonates: A Novel Covalent-Type Electrophilic Polymerization. *Macromolecules* **1988**, *21*, 1880–1883.
- (66) Rodríguez-Parada, J. M. R. P.; Kaku, M.; Sogah, D. Y. Monolayers and Langmuir-Blodgett Films of Poly(N-Acylethylenimines) with Hydrocarbon and Fluorocarbon Side Chains. *Macromolecules* **1994**, *27*, 1571–1577.
- (67) Ivanova, R.; Komenda, T.; Bonné, T. B.; Lüdtke, K.; Mortensen, K.; Pranzas, P. K.; Jordan, R.; Papadakis, C. M. Micellar Structures of Hydrophilic/Lipophilic and Hydrophilic/Fluorophilic Poly(2-Oxazoline) Diblock Copolymers in Water. *Macromol. Chem. Phys.* **2008**, *209*, 2248–2258.
- (68) Kaberov, L. I.; Verbraeken, B.; Riabtseva, A.; Brus, J.; Talmon, Y.; Stepanek, P.; Hoogenboom, R.; Filippov, S. K. Fluorinated 2-Alkyl-2-Oxazolines of High Reactivity: Spacer-Length-Induced Acceleration for Cationic Ring-Opening Polymerization As a Basis for Triphilic Block Copolymer Synthesis. *ACS Macro. Lett.* **2018**, *7*, 7–10.
- (69) Kaberov, L. I.; Verbraeken, B.; Riabtseva, A.; Brus, J.; Radulescu, A.; Talmon, Y.; Stepanek, P.; Hoogenboom, R.; Filippov, S. K. Fluorophilic-Lipophilic-Hydrophilic Poly(2-Oxazoline) Block Copolymers as MRI Contrast Agents: From Synthesis to Self-Assembly. *Macromolecules* **2018**, *51*, 6047–6056.
- (70) Estabrook, D. A.; Ennis, A. F.; Day, R. A.; Sletten, E. M. Controlling Nanoemulsion Surface Chemistry with Poly(2-Oxazoline) Amphiphiles. *Chem. Sci.* **2019**, *10*, 3994–4003.

- (71) Motomura, Y.; Hattori, Y.; Sakurai, T.; Ghosh, S.; Seki, S. Impact of Unsymmetrical Alkyl–Fluoroalkyl Side Chains over Coil-to-Rod Transition of Soluble Polyacetylenes: Modulation of Electronic Conjugation of Isolated Chains and Their Self-Assembly. *Macromolecules* **2019**, *52*, 4916–4925.
- (72) Shimomoto, H.; Kudo, T.; Tsunematsu, S.; Itoh, T.; Ihara, E. Fluorinated Poly(Substituted Methylene)s Prepared by Pd-Initiated Polymerization of Fluorine-Containing Alkyl and Phenyl Diazoacetates: Their Unique Solubility and Postpolymerization Modification. *Macromolecules* **2018**, *51*, 328–335.

CHAPTER TWO

Modular and Processable Fluoropolymers Prepared via a Safe, Mild, Iodo–Ene Polymerization

Adapted from Joseph A. Jaye and Ellen M. Sletten.* Modular and Processable Fluoropolymers Prepared via a Safe, Mild, Iodo–Ene Polymerization. *ACS Cent. Sci.* **2019**, 5, 982-991. DOI: 10.1021/acscentsci.9b00128

2.1 Abstract

Fluoropolymers have infiltrated society as coatings and insulators. However, low processability, few opportunities for polymer functionalization, and explosive monomers hampering academic investigation of these materials have precluded the extension of the unique properties of perfluorocarbons to the cutting edge of material science. Here, we present semifluorinated iodo-ene polymers as a scaffold to overcome fluoropolymer limitations. A sodium dithionate initiated polymerization of perfluorodiiodides and dienes allows for high molecular weight polymers (>100 kDa) to be prepared in the presence of oxygen and water with up to 59 wt% fluorine content. These conditions are sufficiently mild to enable the polymerization of functional dienes, leading to biodegradable fluoropolymers. The iodo-ene polymerization results in the addition of polarizable iodine atoms, which improve polymer processability, yet these atoms can be removed after processing for enhanced stability. Displacement of the iodine atoms with thiols or azides facilitates covalent surface modification and crosslinking. Finally, the low bond dissociation energy of the C-I bond allows allyl group addition as well as photocrosslinking. Collectively, the simple synthesis and modular nature of the semifluorinated iodo-ene polymers will enable the convergence of perfluorocarbons and advanced materials.

2.2 Introduction

Since the accidental discovery of poly(tetrafluoroethylene) (PTFE, **2.1**, Figure 2.1A) in 1938, fluoropolymers have found widespread utility due to the high chemical and thermal stability of the C-F bond and non-polarizability of perfluorocarbons.¹ PTFE, commonly known as TeflonTM, is fully integrated into modern society and can be found in everyday materials such as non-stick pans, weather-proof clothing, dental floss, and insulators for electronics.² Despite the success of PTFE, it has significant

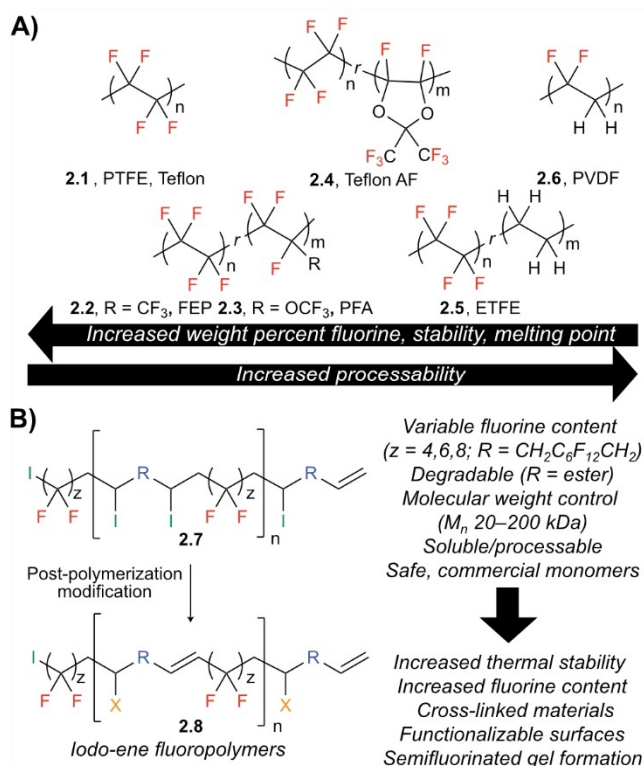


Figure 2.1: A. Common industrial fluoropolymers prepared with decreasing fluorine content. Generally, stability and melting points correlate with increased weight percent fluorine, while there is an inverse relationship with processability. B. Iodo-ene fluoropolymers reported herein that are processable, tunable, simple to prepare, and can be readily modified through post-polymerization modification to improve stability or functionality mechanical, chemical, and safety limitations,³⁻⁷ which have prevented the advancement of fluorinated polymers into sophisticated, multifunctional, dynamic materials.

The primary mechanical challenges of PTFE are its high crystallinity and poor solubility, which prohibit facile melt processing and solution casting techniques commonly employed for thermoplastics.⁸ To overcome the processability challenges of PTFE, numerous other fluoropolymers have been manufactured including: fluorinated ethylene propylene (FEP, **2.2**), poly(tetrafluoroethylene-*co*-perfluoropropylvinylether) (PFA, **2.3**), Teflon AFTM (**2.4**), poly(ethylene-*co*-tetrafluoroethylene) (ETFE, **2.5**), and poly(vinylidene difluoride) (PVDF, **2.6**).^{9,10} By drastically lowering the weight percent fluorine, PVDF can be easily melt-processed and dissolved in select organic solvents. This allows for manipulation into plastics and films, but at the cost of significantly lower thermal and chemical resistance.¹¹⁻¹³ FEP and PFA retain high weight percent fluorine, but lower crystallinity through the addition of bulkier substituents, allowing these polymers to be melt-processed into bulk materials with advantageous thermal and chemical resistance. However, FEP and PFA remain insoluble in organic or fluorine solvent, and maintain high melt viscosity.¹⁴ Teflon-AFTM's amorphous nature leads to it being one of the most

processable commercial fluoropolymers, even displaying some solubility in fluoruous solvents,¹⁵ while retaining similar thermal and chemical stability as PTFE.¹⁶ Although displaying advantageous properties, the widespread use of Teflon-AFTM has been limited by its costly preparation.¹⁷

While the inertness of the C-F bond is a hallmark of perfluorocarbons, it hinders the diversification of fluorinated materials. The covalent functionalization of fluoropolymers is desirable for crosslinking, surface modification, and for the creation of advanced fluoruous materials. Crosslinking is a common approach to reduce creep, the deformation of materials under stress, which is a common problem for PTFE.^{5,6} Current methods for crosslinking PTFE require extreme conditions (ionizing radiation and high temperature), preventing their widespread use.¹⁸ High energy methods such as ionizing radiation and plasma treatment have also been utilized to functionalize PTFE films, allowing for covalent attachment of small molecules and polymers to surfaces.¹⁹⁻²¹ Other fluoropolymers have been functionalized by fluoride elimination (PVDF, **2.6**), reduction (FEP, **2.2**)²², or photocrosslinking fluorinated polyethers with activated acrylate end-groups.²³ Taken together, these harsh conditions highlight the difficulty in advancing the applications of fluoropolymers.

A final challenge of fluoropolymer research is the safety of the fluorinated ethylene monomers. Tetrafluoroethylene is explosive on contact with organic compounds,²⁴ limiting its academic use,²⁵⁻²⁷ and making co-polymers such as ETFE (**2.5**) especially dangerous to produce. Additionally, many of the fluoropolymers are prepared via emulsion polymerization, which require fluorosurfactants that are prone to bioaccumulation.^{7,28,29} Methods to prepare fluoropolymers that do not require explosive monomers or persistent surfactants will make these materials more accessible and expand both the academic and industrial applications.

Here we report the preparation of semifluorinated polymers under mild conditions with safe, commercially available monomers and no need for surfactant. We employ a step-growth iodo-ene polymerization, which results in two iodine atoms installed within the backbone of every repeat unit (**2.7**, Figure 2.1B). The large, polarizable iodine atoms enhance the processability, yet can be easily removed

after processing to result in thermally stable fluoropolymers. Furthermore, the iodine atoms provide a functional handle for post-polymerization modification and crosslinking (**2.8**) via S_N2 displacement or homolytic cleavage of the C-I bond. The fluorine content can be tuned by varying the monomers (z and R in **2.7**). Additionally, other functionality can be installed into the backbone of the polymer by diene selection (R in **2.7**). Through these strategies, we are able to prepare fluoropolymers that: 1) are soluble in organic solvent, 2) are treatable with heat and base into thermally stable films, 3) are readily covalently modified or crosslinked with a variety of chemistries, and 4) are photocured into gels. Notably, the fluorine content within these polymers is on the backbone making them distinct from existing approaches to impart standard polymers (*e.g.* acrylates, styrenes) with fluorous character,³⁰⁻³⁴ or through fluorination reactions as a post-polymerization modification.³⁵⁻³⁶

The addition of perfluoroalkyl iodides into alkenes, the iodo-ene reaction (Figure 2.2), is an established method to install perfluorinated chains onto a molecule.³⁷⁻⁴² It was first explored as a polymerization method using diiodoperfluorohexane and 1,9-decadiene in 1993 by Wilson and Griffin who employed heat and azobisisobutyronitrile (AIBN) to access short semifluorinated polymers.⁴³ A few years later, Percec and coworkers employed Pd(PPh₃)₄ at room temperature to afford similar polymers.⁴⁴ Zhu and coworkers have recently revisited this polymerization using a tris(bipyridine)ruthenium(II) chloride (Ru(bpy)₃Cl₂) catalyst and blue light to obtain polymers with *M_n* up to 30 kDa.^{45,46} While the photoinitiated polymerization is an improvement, we looked to establish a simpler, greener method that did not require deoxygenation and produced high molecular weight semifluorinated polymers. Upon method development, we demonstrate the utility and versatility of these unique fluoropolymers.

2.3 Results and discussion

Scheme 2.1: Iodo-ene polymerization of 1,9-decadiene (**2.9**) and diiodoperfluoroalkyl iodides (**2.10a-c**) to yield fluorinated polymers (**2.11a-d**) with varying fluorous blocks

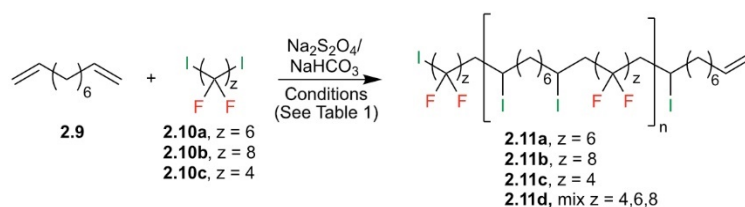


Table 2.1: Optimization of polymerization conditions

Entry #	Polymer	z	Solvent	Energy Input	Time (Hours)	M_n (kDa)	n	\bar{D}
1	2.11a	6	MeCN:DMC:H ₂ O	Sonication	0.5	25.0 ^b	35	2.07
2	2.11a	6	Neat plus AIBN ^a	Heat	4	10 ^b	14	1.65
3	2.11a	6	MeCN:DMC:H ₂ O	Sonication	0.5	67.9	98	1.88
4	2.11a	6	Neat plus AIBN ^a	Heat	4	57.3	83	1.38
5	2.11a	6	MeCN:DMC:H ₂ O	Sonication	8	101	147	1.88
6	2.11a	6	MeCN:DMC:H ₂ O	Sonication	14	128	184	1.28
7	2.11a	6	MeCN:DMC:H ₂ O	Heating	14	198	286	1.43
8	2.11a	6	MeCN:DMC:H ₂ O	365 nm UV	14	112 ^c	161	1.31
9	2.11a	6	DMSO	Stirring	48	36	65	1.80
10	2.11a	6	MeCN:H ₂ O	Sonication	14	187 ^c	270	1.27
11	2.11a	6	H ₂ O	Sonication	14	25.9	37	1.53
12	2.11b	8	MeCN:DMC:H ₂ O	Sonication	14	192	277	1.30
13	2.11c	4	MeCN:DMC:H ₂ O	Sonication	14	86.5 ^c	125	1.52
14	2.11d	4, 6, 8	MeCN:DMC:H ₂ O	Sonication	14	83.7 ^c	121	1.67

^a AIBN employed instead of Na₂S₂O₄/NaHCO₃. ^b SEC analysis performed in THF at 40 °C at a flow rate of 0.7 mL/min. M_n and \bar{D} calculated through calibration with poly(styrene) standards. In all other cases, SEC analysis performed in DMSO at 65 °C at a flow rate of 0.35 mL·min⁻¹. M_n and \bar{D} calculated through calibration with poly(methyl methacrylate) standards. ^c Bimodal distribution in SEC is likely due to early termination.

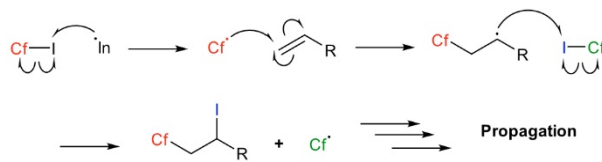


Figure 2.2: General reaction mechanism of the iodo-ene reaction on a small molecule alkene.

Inspired by reports of sodium dithionate ($\text{Na}_2\text{S}_2\text{O}_4$) initiated addition of perfluoroalkyl iodides into alkenes,⁴⁷ we looked to employ these conditions for the polymerization of diiodoperfluoroalkanes and dienes. We were particularly interested in the brief communication by Tong and Keese who demonstrated that sonication of perfluorobutyl iodide and 1-hexene in acetonitrile and water gave high yields of iodo-ene product in one hour.⁴⁸ We envisioned that these rapid and mild reaction conditions would enable high molecular weight polymers and expand the scope of monomers compatible with the iodo-ene polymerization. Our optimization of the sodium dithionate initiated iodo-ene polymerization began with monomers 1,9-decadiene (**2.9**) and diiodoperfluorohexane (**2.10a**) to produce semifluorinated polymer **2.11a** (Scheme 2.1).

Dimethyl carbonate (DMC) was employed as a co-solvent, due to its precedent for increasing reaction rates and decreasing chain transfer.⁴⁹ Within 30 minutes of sonicating **2.9** and **2.10a** under these conditions, precipitate was evident, suggesting polymer formation (Figure 2.3). Isolation of the precipitate and nuclear magnetic resonance (NMR) analysis indicated polymer **2.11a** (Table 2.1, Entry 1), which was compared to a standard prepared *via* AIBN initiation. $^1\text{H-NMR}$, $^{19}\text{F-}$

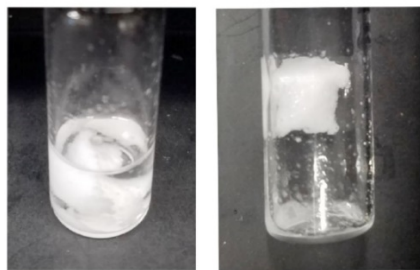


Figure 2.3: Polymer precipitation in standard reaction conditions of sulfinate dehalogenation polymerization. Polymer precipitation following 30 minutes of polymerization in a sonication bath, front view (left), vial laid on side (right).

NMR (Figure 2.4), thermal gravimetric analysis (TGA), and differential scanning calorimetry (DSC) analysis (Figure 2.5) all indicate that both sodium dithionate and AIBN initiation produce **2.11a**. While the repeat units of these polymers are identical, the molecular weights are significantly different. After only 30 minutes at room temperature, the dithionate initiation yielded a 25 kDa polymer. In comparison, slow ramping of heat from 80 °C to 160 °C over a period of 4 hours with sequential addition of AIBN every 10 minutes, a previously optimized method, gave 10 kDa polymers (Table 2.1, Entries 1 vs. 2).⁵⁰ These molecular weight data were obtained with size exclusion chromatography (SEC) in tetrahydrofuran (THF), as was previously reported.⁴⁴ We noted that the dithionate initiated polymer **2.11a** gave very broad peaks on the THF SEC, suggesting aggregation of higher molecular weight polymer. In efforts to gain accurate M_n and M_w data for the iodo-ene polymers, we resorted to SEC in 65 °C dimethyl sulfoxide (DMSO) using an Agilent Mixed-B column, emulating conditions that were previously reported for PVDF analysis.⁵¹ SEC analysis of **2.11a** in DMSO corroborated that the sodium dithionate conditions yielded higher molecular weight polymer (Table 2.1, Entries 3 and 4), yet did not match the THF SEC data (discussed in further detail below). Using SEC in DMSO, further investigation of polymer **2.11a** prepared via sonication in the presence of sodium dithionate was performed. Analysis at multiple time points demonstrated that although the polymer quickly precipitates, the reaction requires 14 hours to reach the maximum size of 128 kDa. At both 30 minutes and 8 hours (Table 2.1, Entries 3 and 5), the polymer dispersity remains the same although the SEC trace indicates further conversion. At the 14-hour time point, dispersity drops significantly while the molecular weight grows. This is likely due to the lower solubility of high molecular weight polymer

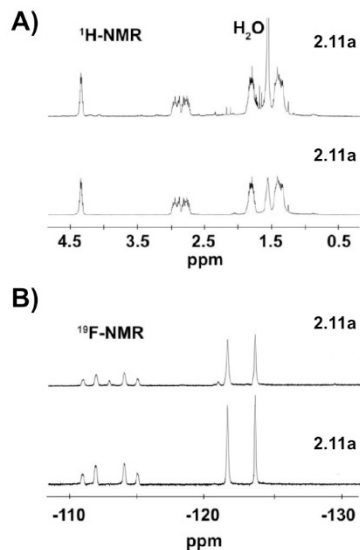


Figure 2.4: NMR comparison of polymer **2.11a** prepared by AIBN (known) and sulfinate dehalogenation (reported herein). **A.** $^1\text{H-NMR}$ of iodo-ene polymer through AIBN polymerization (top) and through sulfinate dehalogenation conditions in MeCN/H₂O/DMC with sonication as energy source (bottom). **B.** $^{19}\text{F-NMR}$ of iodo-ene polymer through AIBN polymerization (top) and through sulfinate dehalogenation conditions in MeCN/H₂O/DMC with sonication as the energy source (bottom). Additional peaks in the AIBN polymerization belong to polymer end-group. The reduction of these peaks in the sulfinate dehalogenation polymerization is consistent with the increased molecular weights of polymers prepared under these conditions.

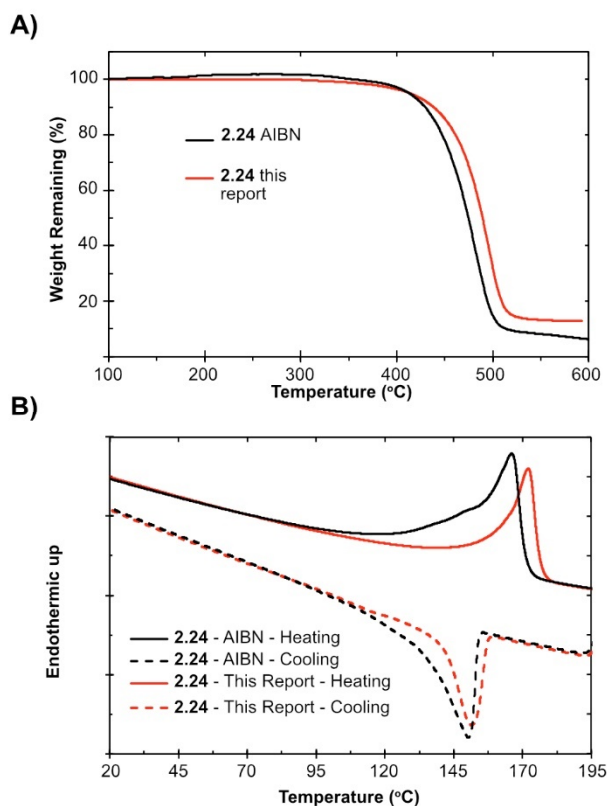


Figure 2.5: Thermal analysis of reduced polymer **2.24**. **A.** Thermal gravimetric analysis (TGA) comparison of polymer **2.24** prepared by AIBN (known, black) and sulfinate dehalogenation (reported herein, red). **B.** Overlaid differential scanning calorimetry (DSC) curves of polymer **2.24** (15 mg of polymer, 2nd cycle) heating rate of 20 °C/min and cooling rate of 15 °C/min (Heating cycle solid line, cooling cycle dotted line). Average apex melting point of **2.24** prepared by AIBN (black, 3 trials): 165.1 +/- 1.32 °C. Average apex melting point of **2.24** prepared by sulfinate dehalogenation (red, 3 trials): 170.3 +/- 2.07 °C.

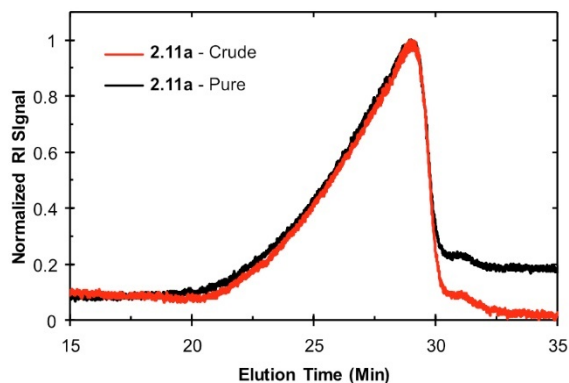


Figure 2.6: An overlay of SEC data showing size difference in pure and crude polymer **2.11a**. Crude polymer **2.11a** (red line, 76.9 kDa, $\bar{D} = 1.50$). Pure polymer **2.11a** (black line, 78.2 kDa, $\bar{D} = 1.48$). SEC analysis performed with 10 mM LiBr solution in DMF at 40 °C at a flow rate of 1.0 mL/min on a Jasco system equipped with a refractive index detector, a UV detector, a Waters Styragel guard column, and four Waters HR Styragel 5 μ m columns (100-5K, 500-30K, 50-100K, and 5- 600K). M_n and \bar{D} calculated through calibration with polystyrene standards from Jordi Laboratories.

resulting in precipitation and a kinetic molecular weight distribution. Analysis of the polymer precipitate before and after washing showed nearly identical molecular weights (Figure 2.6).⁵² Further exploring the scope of the polymerization, we found that the iodo-ene reaction initiated with sodium dithionite readily proceeded with traditional heating or 365 nm light as energy inputs (Table 2.1, Entries 7–8). Polymer **2.11a** could also be obtained without the use of the dimethyl carbonate additive, or with solely DMSO or water as the solvent (Table 2.1, Entries 9–11).

Next, we further explored the discrepancies between the molecular weight data obtained *via* SEC in THF and DMSO. To gain confidence in the DMSO SEC data, we developed an end-capping method such that M_n could be determined by NMR analysis. We prepared alkene **2.12** that contains a dimethylamino group with ¹H-NMR chemical shifts distinct from the polymer backbone. Four different polymers were prepared by sonication of **2.9**, **2.10a**, and differing amounts of **2.12** (4.3, 1.7, 1.1, 0 wt%) in a MeCN/DMC/H₂O solution with a sodium dithionite initiator (Figure 2.7).

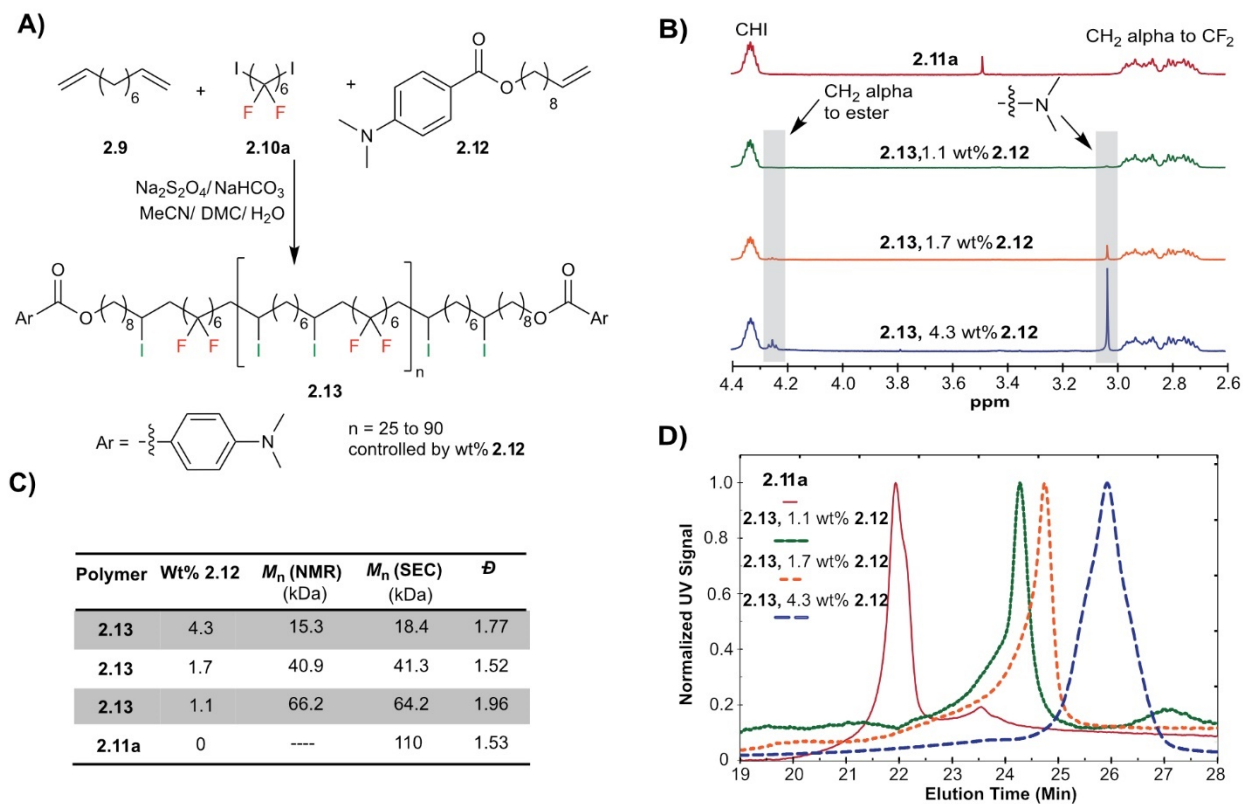


Figure 2.7: **A.** The preparation of end-capped iodo-ene fluoropolymers using alkene **2.12**. **B.** Stacked $^1\text{H-NMR}$ spectra of end-capped polymers **2.13** compared to **2.11a** (red, top). $^1\text{H-NMR}$ signals from the end-cap are highlighted in gray. **C.** Table of weight percent end-cap employed in the polymerization and the resulting molecular weight determined through NMR and SEC. **D.** SEC traces for polymer **2.11a** (red, solid) compared to **2.13** with varied weight percent **2.12** (green, orange, blue, dashed). SEC traces were obtained from 3 mg/mL solutions of fluoropolymers in DMSO and analyzed on an Agilent Mixed-B column with DMSO eluent at 65 °C.

The M_n calculated via NMR for polymers end-capped with **2.12** were 15.3 kDa (4.3 wt%), 40.9 kDa (1.7 wt%), and 66.2 kDa (1.1 wt%). These data matched the M_n obtained by the SEC in DMSO well (Figure 2.7B–D), validating the use of DMSO SEC for iodo-ene fluoropolymers, and providing confidence in M_n values in Table 2.1.⁵³ The end-capping approach also allows for the molecular weight of the semifluorinated polymers to be controlled, a feat that has not been achieved with chain growth methods industrially employed for fluoropolymer synthesis. Current methods to obtain 10–100 kDa PTFE include fragmenting larger PTFE with ionizing radiation or through polymerization of TFE in supercritical CO_2 or fluoroform.^{54–56} We found that the polymerization proceeded readily with C4, C6, and C8 diiodoperfluoroalkanes **2.10a–c** to yield polymers **2.11a–c** (Figure 2.8). Thin films of polymers **2.11a–c** were prepared by drop-casting from THF, dimethylformamide (DMF), or DMSO solutions and contact angles of water were measured to gain insight on the fluorous character of the respective polymers, as

compared to PVDF films⁵⁷ (Figures 2.9). Despite having lower weight percent fluorine than PVDF, polymers **2.11a–c** all have larger contact angles, suggesting that consecutive CF₂ groups enhance fluorous character. This is also supported through ETFE's significantly higher contact angle than PVDF.⁵⁷ The similarity between the contact angle measurements of **2.11a–c** prompted the synthesis of polymer **2.11d**, which employs monomers **2.10a–c** in a ratio representative of crude perfluoroalkyldiiodide.⁵⁸ Thus, polymer **2.11d** represents a low-cost iodo-ene polymer, providing opportunities for large scale synthesis. To date, we have scaled the polymerization up to four grams (Figure 2.10). Further characterization of polymers **2.11a–d** by TGA show similar 10% mass loss temperatures of 290 °C due to the loss of iodine. DSC indicates that the glass transition temperature (T_g) of these materials is heavily dependent on the length of the fluorous block (Table 2.2).

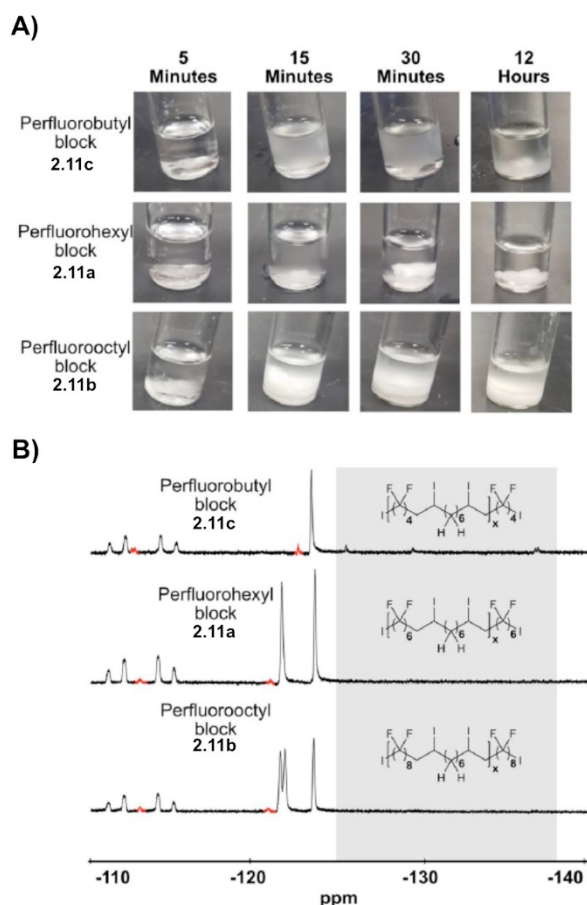


Figure 2.8: **A.** Pictures of standard sulfinatodehalogenation polymerization precipitate formation of polymer **2.11a**, **2.11b**, and **2.11c** at 5, 15, 30 minutes and 12 hours of sonication. **B.** Stacked ¹⁹F-NMR of polymers **2.11a**, **2.11b**, and **2.11c** after 12 hours of sonication. Peaks highlighted in red indicate end-groups of polymer chain. Gray box indicating peaks due to termination through hydrogen abstraction. Hydrogen abstraction is more pronounced with the shorter, less reactive diiodoperfluorobutane monomer.

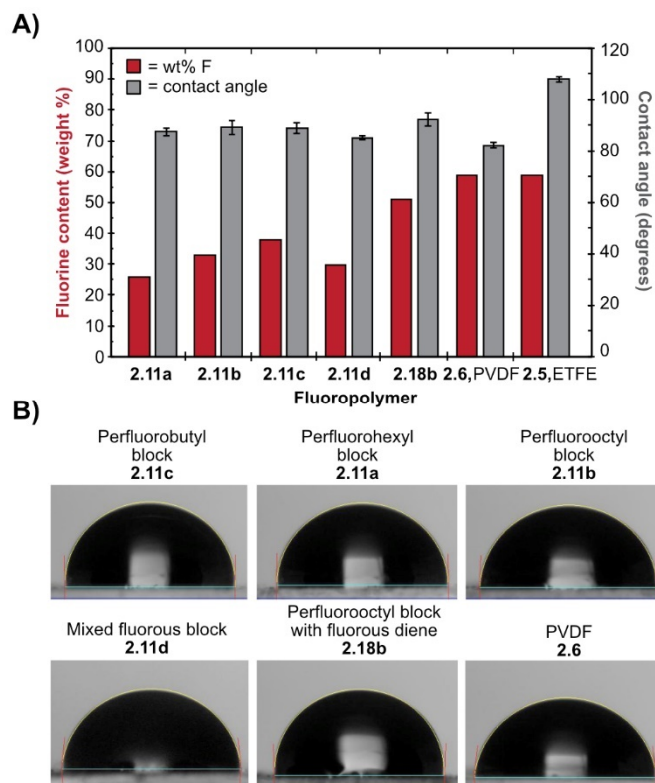


Figure 2.9: Contact angle measurements of polymers **2.11a–d**, **2.18b**, in comparison to PVDF (**2.6**) and ETFE (**2.5**). **A.** Comparison of contact angle of water on fluorinated thin films (gray) and the fluorine content (red) of the polymers. **B.** Images of water droplets on thin films. Thin films were prepared by dropcasting a 5 mg/mL polymer solution in THF, DMF, or DMSO onto a slide and annealed at 80 °C. Contact angle measurements were obtained by slow dropping of water. Contact angles were measured with a 5 second delay from initial contact of water with the polymer surface. The reported values are the average of at least three independent droplets per sample.

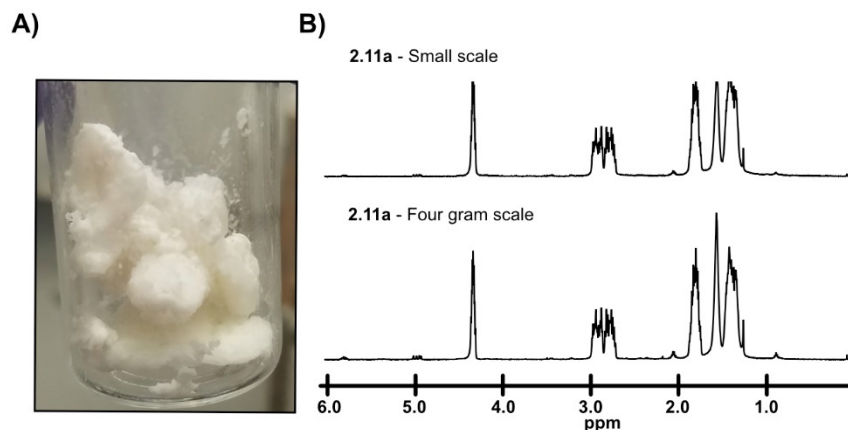
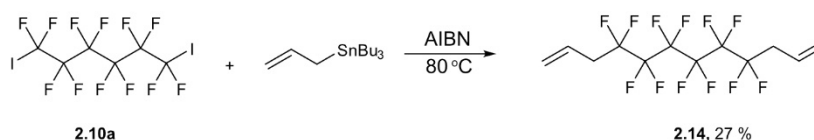


Figure 2.10: Iodo-ene polymerization run on a four-gram scale after precipitation and washing. **A.** Picture of scintillation vial containing four grams of iodo-ene polymer. **B.** Stacked NMR spectra of polymer **2.11a** synthesized through sulfinate dehalogenation with sonication as energy input on a 0.1-gram scale (top, M_n – 128 kDa) and on a 4.0 gram scale (bottom, M_n – 110 kDa).

Having established that the semifluorinated iodo-ene polymers are sufficiently fluororous, we looked to leverage the iodine installed within the backbone and the diene composition to increase the wt%

fluorine, biocompatibility, processability, as well as install functional handles for grafting and crosslinking. Chemical modifications to the diene monomer provide an avenue to further increase the fluorine content or incorporate additional functional groups. To create additional fluorinated polymers using the iodo-ene polymerization, we prepared fluorinated diene **2.14** (Scheme 2.2) and polymerized **2.14** with diiodoperfluorooctane **2.10b** to result in polymer **2.18b** (Figure 2.11A), increasing the wt% fluorine by 1.5x and achieving a structure just three CF₂ units from Teflon™ (Figure 2.12). We also explored the addition of more hydrophilic functionality and found that ether and ester-containing dienes (**2.15–2.17**) both afforded semifluorinated polymers of significant molecular weight (Figure 2.11B).



Scheme 2.2: Synthesis of fluorinated diene **2.14**.

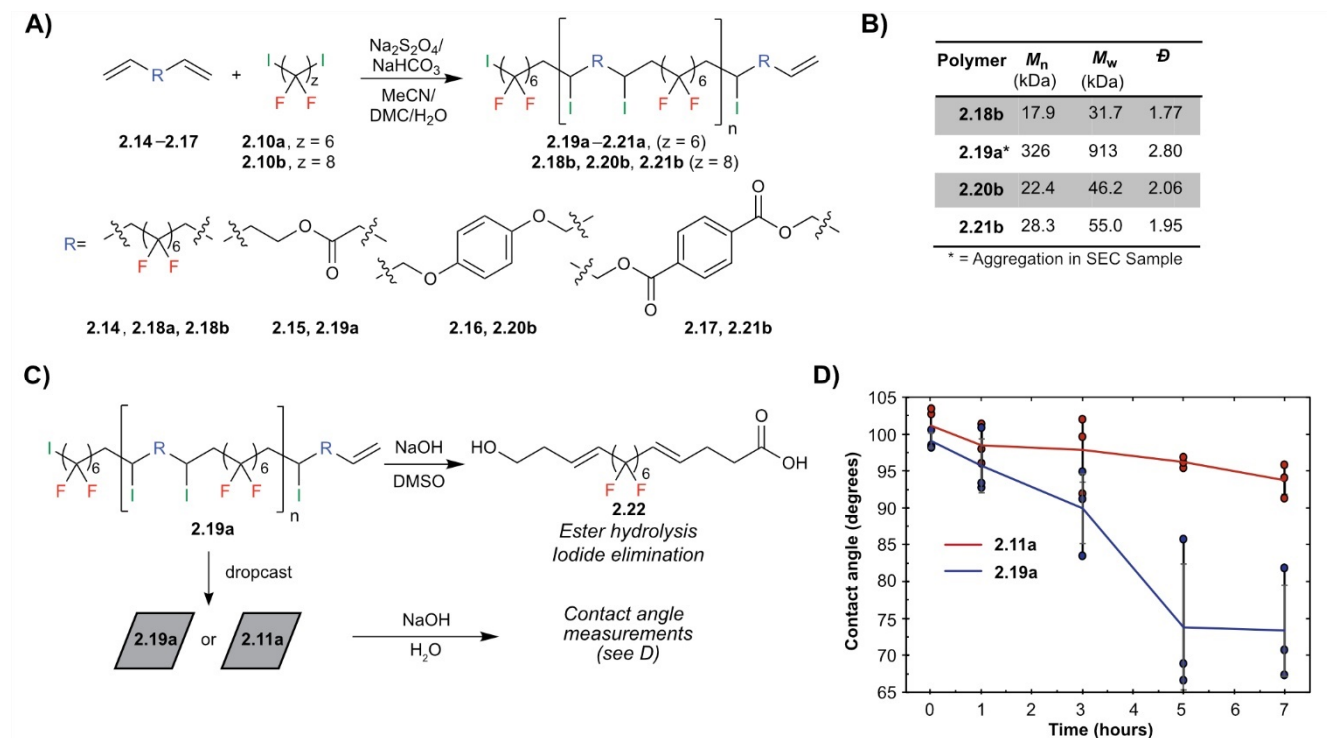


Figure 2.11. Diene scope of sulfinatodehalogenation iodo-ene polymerization. **B.** Molecular weight data for the functionalized fluoropolymers as determined by SEC in DMSO. **C.** Hydrolysis of ester-containing polymer with sodium hydroxide, which proceeds in solution as confirmed by SEC (see Figure 2.13) and thin films as confirmed by contact angle. **D.** Contact angle measurements of slides containing films of polymers **2.11a** and **2.19a** treated in aqueous sodium hydroxide over time. Circles representing the average of triplicate contact angle measurements on individual thin-films and the solid line representing the average of contact angle measurements across three films. Error bars denote standard deviation of contact angle measurements across three films.

The sonication method proved particularly important for **2.20b** as diene **2.16** undergoes Cope rearrangement at elevated temperatures.⁵⁹ Ester-containing semifluorinated polymer **2.19a** is of particular interest as it can undergo degradation into **2.22**, which contains only C₆F₁₂ units that do not bioaccumulate.⁷ We demonstrated the degradation of **2.19a** under basic conditions in solution and on surfaces. After 5 hours in basic conditions, ester-containing polymer **19a** had significantly

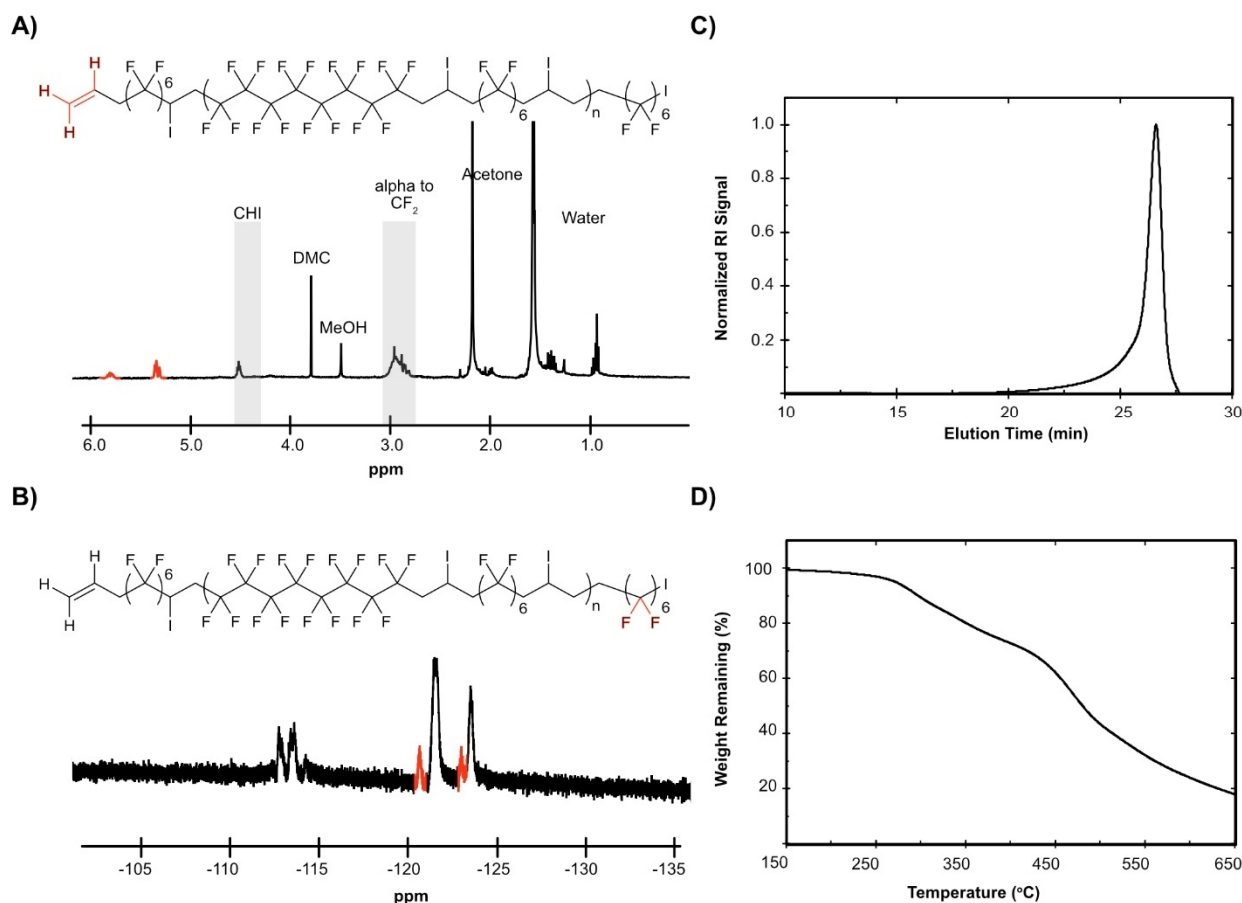


Figure 2.12: Analysis of 1-perfluorohexyl-2,11-diiodo-4,4,5,5,6,6,7,7,8,8,9,9 dodecafluorohexyl dodecane block polymer **2.18b**. **A.** ¹H-NMR spectra in CDCl₃ providing evidence of the desired repeat unit. Peaks highlighted in red are polymer end groups. **B.** ¹⁹F-NMR spectra demonstrating fluorine repeat unit. Peaks highlighted in red are polymer end groups. **A./B.** Poor solubility of polymer due to high fluorine content only allows oligomers to be analyzed in the NMR. **C.** SEC analysis of polymer **2.18b** run in DMSO at 65 °C. **D.** Thermal gravimetric analysis of polymer **2.18b** showing loss of iodine beginning at 280 °C.

smaller M_n (Figure 2.13) and the contact angle of surfaces coated with **2.19a** had decreased, suggesting the presence of polar carboxylic acids (Figure 2.11C,D). In contrast, semifluorinated polymer **2.11a** only showed minor changes in molecular weight and contact angle, consistent with elimination of iodide but not scission of the polymer backbone (Figures 2.11D, 2.13).

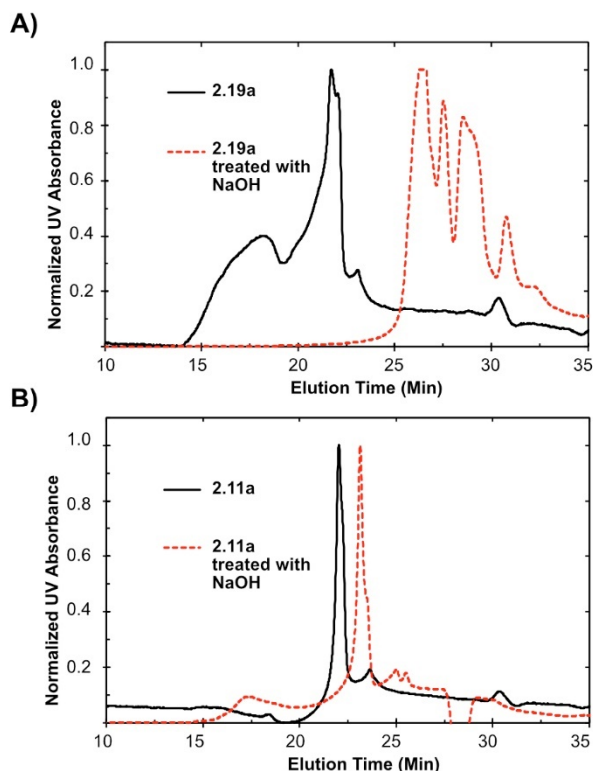


Figure 2.13: SEC analysis of the degradation of **2.11a** vs. **2.19a** upon treatment with base. **A.** DMSO SEC trace of ester-containing polymer **2.19a** before (black, solid) and after (red, dashed) treatment with 1M NaOH in DMSO at rt for 6 hours. **B.** DMSO SEC trace of polymer **2.11a** (black, solid) and after (red, dashed) treatment with 1M NaOH in DMSO at rt for 6 hours.

Iodide elimination represents another avenue for increasing the wt% fluorine as well as the thermal stability of the semifluorinated polymers. We found that quantitative elimination of iodide could be obtained by treatment with 1,8-diazabicyclo[5.4.0]undec-7-ene (DBU, Figure 2.14A). As previously reported, we could also remove the iodine atoms by treatment with AIBN and tributyltin hydride (HSnBu_3).⁴³ We compared the properties of the eliminated polymer **2.23** and reduced polymer **2.24** to the initial iodo-ene product **2.11a**. Interestingly, the contact angles did not undergo significant change in the eliminated product, but were significantly increased in the reduced product (Figure 2.15). Both polymers **2.23** and **2.24** displayed superior thermal stability when compared to iodine-containing polymer **2.11a**. TGA indicates that **2.11a** undergoes loss of iodine at 300 °C. In contrast, the semifluorinated polymers without iodine display excellent thermal

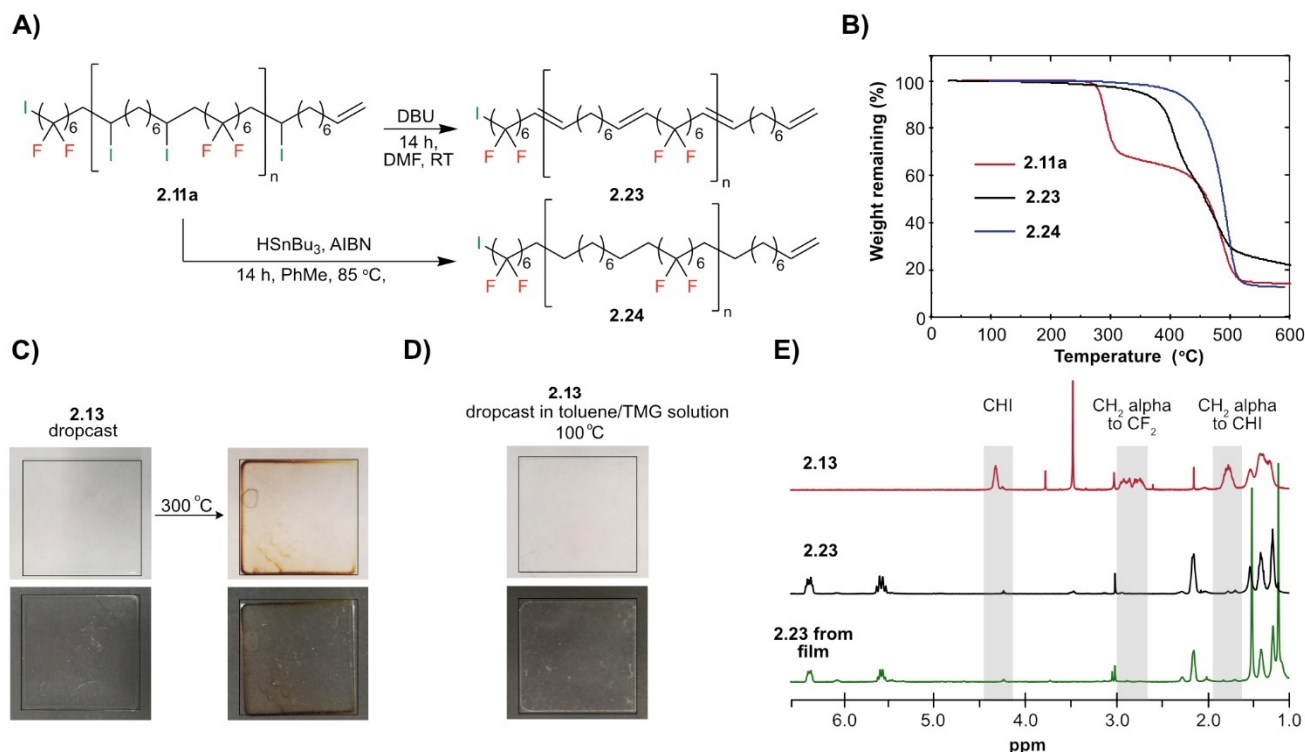


Figure 2.14. Removal of the iodine atoms by elimination with 1,8-Diazabicyclo[5.4.0]undec-7-ene (DBU) or reduction with tributyltin hydride (HSnBu_3). **B.** TGA data for polymers **2.11a** (red), **2.23** (black), and **2.24** (blue). **C.** Workflow for preparation of stable films of iodo-ene fluoropolymers. A 5 mg/mL solution of **2.13** was prepared in toluene, dropcast onto films, and annealed at 300 °C. **D.** A 5 mg/mL solution of **2.13** was prepared and quickly diluted with 15% tetramethylguanidine (TMG) and then dropcast onto a glass slide and annealed at 100 °C. **E.** $^1\text{H-NMR}$ spectra of **2.13** (red) in comparison with polymer **2.23** prepared through solution phase elimination (black) and polymer **2.23** generated from thin-film elimination (green).

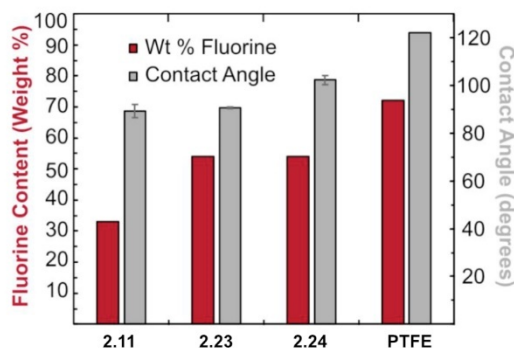


Figure 2.15: Contact angle (gray) and weight percent fluorine (red) of iodo-ene polymers when iodine is eliminated (polymer **2.23**) or reduced (polymer **2.24**) from the backbone of the polymer. Contact angle measurements were collected by single drop onto glass slide followed by 5 second wait time.

stability with degradation temperatures approaching 430 °C (Figure 2.14B, Table 2.2), rivaling that of PTFE.⁶⁰ The chemical stability of polymers **2.23** and **2.24** are also excellent, showing no loss of fluorine upon treatment with acid, base, amine, or thiol (Figure 2.16).

Table 2.2: Thermal properties of polymers

Polymer	T _g (°C)	Melting Point Onset (°C)	10% Mass loss (°C)
2.11a	-0.7	n/a	286
2.11a^a	-6.2	n/a	286
2.11b	75	88.6, 97.0	300
2.11c	-11.1	n/a	282
2.11d	-6.0	n/a	292
2.23	24.7	51.5	383
2.24	124	140.7	430
2.26	-9.8	n/a	282
2.28	134	n/a	364
2.29	101	n/a	280
2.30	144	n/a	331
2.32	n/a	n/a	220
2.33	n/a	n/a	332

a. AIBN used as an initiator.

While the fluororous content and stability of the semifluorinated polymers **2.23** and **2.24** are desirable, a drop in processability is observed when iodine is removed. Since the iodine is facile to remove *via* heat or base, we proposed coating surfaces with **2.13** and then removing the iodine after processing (Figure 2.17A). Toward this end, we prepared thin films of **2.13** and subjected them to 300 °C for 30 minutes (Figure 2.14C), which resulted in quantitative removal of iodine as determined by TGA (Figure 2.17). We also prepared films of **2.13** with 15 vol% tetramethyl guanidine (TMG) in toluene. The films were annealed at 100 °C for 10 minutes, resulting in elimination of the iodine (Figure 2.14D) as observed by ¹H-NMR (Figure 2.14E) and TGA (Figure 2.17). We also found that elimination was successful on the

bulk polymer (Figure 2.17B). In all cases, TGA data indicate improved thermal stability of surfaces and materials treated with heat or base.

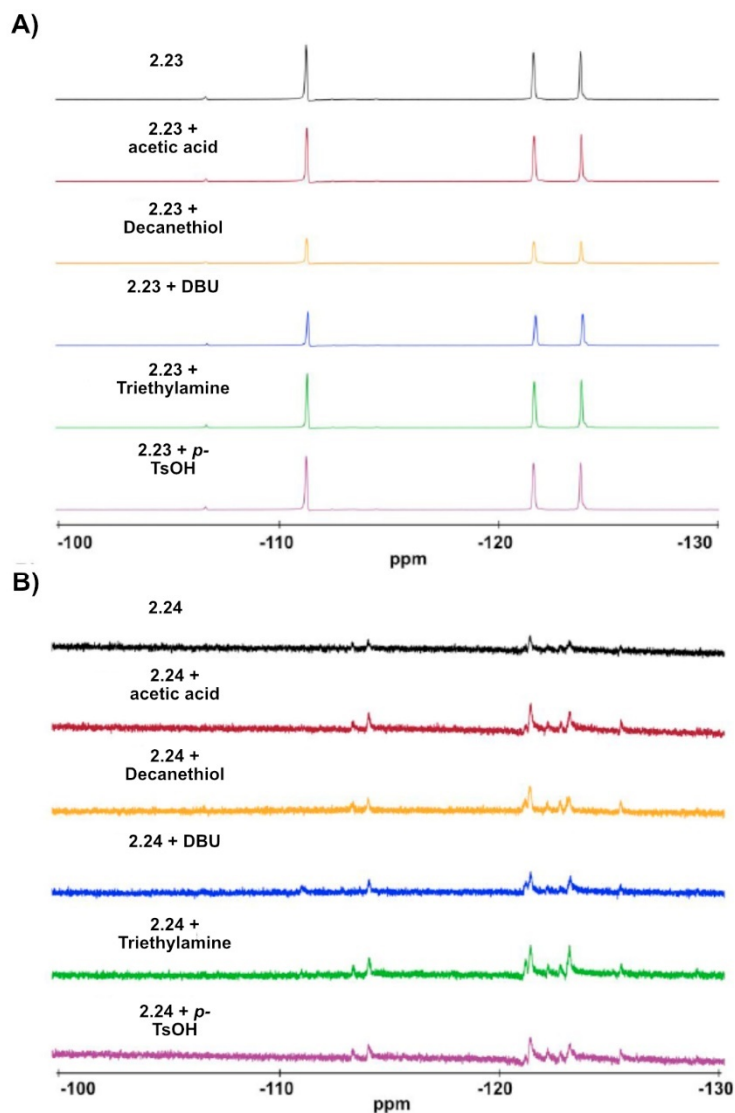


Figure 2.16: Chemical stability of polymers **2.23** and **2.24**. A 8 mg/mL solution of **2.23** (A) or **2.24** (B) was combined with 0.2 mmol of acetic acid (red), decanethiol (orange), DBU (blue), triethylamine (green), or toluene sulfonic acid (purple) in an NMR tube. The mixtures were monitored over 2 days. Shown are the ^{19}F -NMR spectra taken 48 hours after initial solution preparation.

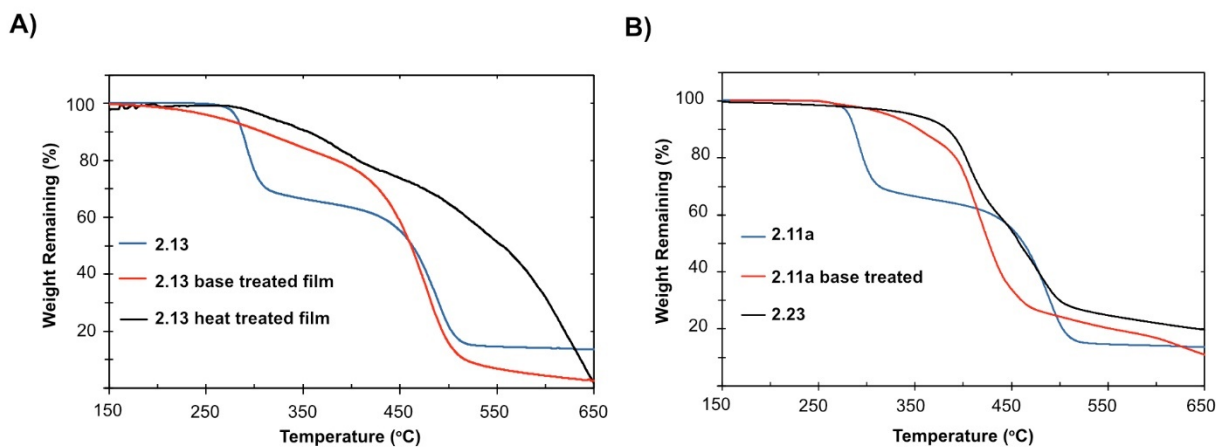


Figure 2.17: Treatment of polymer thin films of **2.13**. **A.** Thermal gravimetric analysis of a polymer **2.13** (blue), **2.13** following dropcasting a 5 mg/mL solution in toluene and annealing at 300 °C for 30 minutes (black), and **2.13** following dropcasting a 5 mg/mL solution in toluene with 15 vol% tetramethyl guanidine base and annealing at 100 °C (red). **B.** Comparison of thermal stability of polymer **2.11a**, polymer **2.11a** with iodine eliminated in the solid phase, and polymer **2.23** prepared in solution. Thermal gravimetric analysis showing degradation temperature of starting polymer **2.11a** (blue), and polymer that had been treated via submersion in DBU for 5 minutes (red), and eliminated polymer **2.23** (black)

The iodine atoms incorporated into the backbone of the iodo-ene polymers are not only a handle for increasing the processability; they also offer avenues to add chemical functionality for post-polymerization functionalization, covalent modification of surfaces, and crosslinking. Iodine can be efficiently displaced with thioacetate (**2.25**) to give polymer **2.26** (Figure 2.18A). Removal of the acetate groups yielded thiol containing polymer **2.27**, that could undergo Michael addition with acrylamide to produce **2.31** or oxidation to give crosslinked network **2.28**. Crosslinked polymer **2.28** represents a redox-active material, providing opportunities for responsive, dynamic fluoros scaffolds. Irreversibly crosslinked materials could also be prepared by treatment of **2.11a** with ethanedithiol or photocrosslinking **2.26** *via* thiol-ene chemistry with 1,9-decadiene (**2.9**) to give polymers **2.29** and **2.30**, respectively. Permanently crosslinked fluoros materials are advantageous for reducing creep.⁶ All polymer crosslinks were confirmed by TGA, DSC, and infrared (IR) spectroscopy (Figures 2.18B, 2.18C, 2.19, 2.20, Table 2.2, respectively).

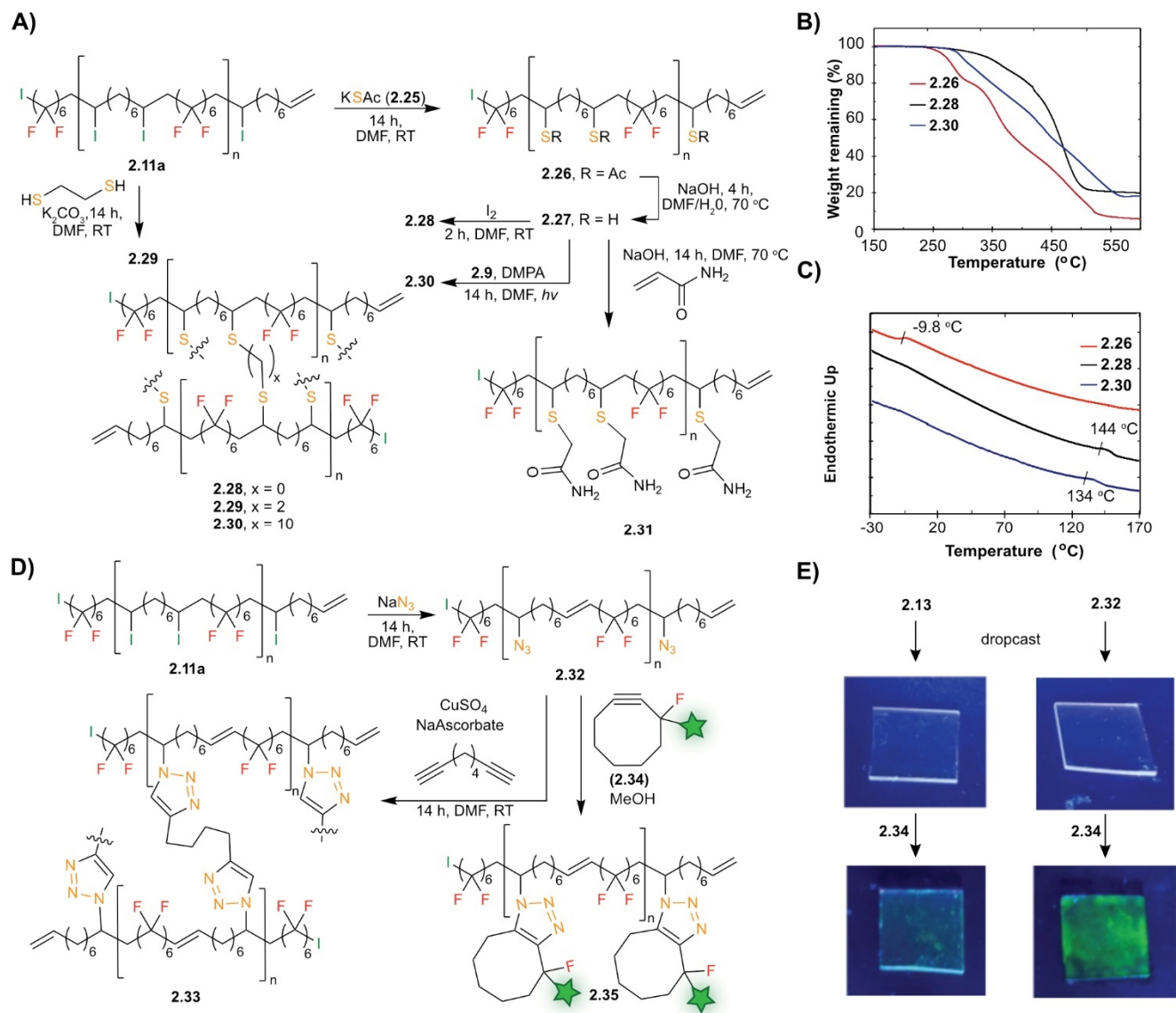


Figure 2.18. Functionalization and cross-linking methods using thiols. **B.** TGA analysis of thioacetate polymer **2.26** and crosslinked polymers **2.28** and **2.30**. **C.** Differential scanning calorimetry of thioacetate polymer **2.26** and cross-linked polymers **2.28** and **2.30** with T_g onset midpoints indicated. **D.** The addition of azide to the polymer backbone and reaction with alkynes to yield cross-linked or fluorescent polymers (See Figure S19 for complete structure of cyclooctyne fluorophore). **E.** Dropcast films of **2.11a** and **2.32** before and after treatment with cyclooctyne **2.34**. Films were prepared by dropcasting 5 mg/mL polymer solutions in THF and annealing at 85 °C for 10 minutes. Films of **2.11a** and **2.32** were placed in a 0.6 mg/mL solution of **2.34** in methanol for 14 hours. Films were then sequentially washed with water and methanol to remove excess **2.34** and then placed under 365 nm light for photographs.

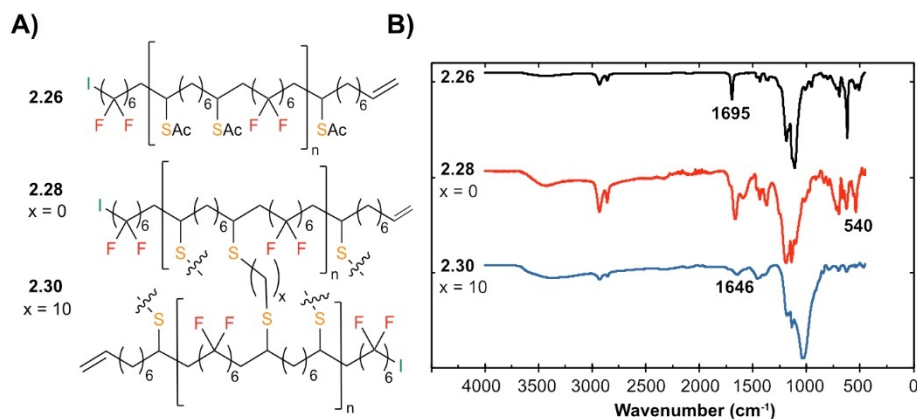


Figure 2.19: A. Structures of thiol-modified polymers and materials. B. Stacked IR spectra of thioacetate polymer **2.26** and cross-linked polymers **2.28** and **2.30**. Thioacetate polymer **2.26** (black) with a carbonyl peak located at 1699 cm^{-1} . Oxidized polymer **2.28** (red) showing growth of disulfide IR peaks at 540 cm^{-1} . Thiol-ene cross linked polymer **2.30** (blue) with decadiene, showing loss of peak 1699 cm^{-1} corresponding to thioester. The peak at 1646 cm^{-1} is attributed to residual decadiene from incomplete crosslinking.⁶⁴

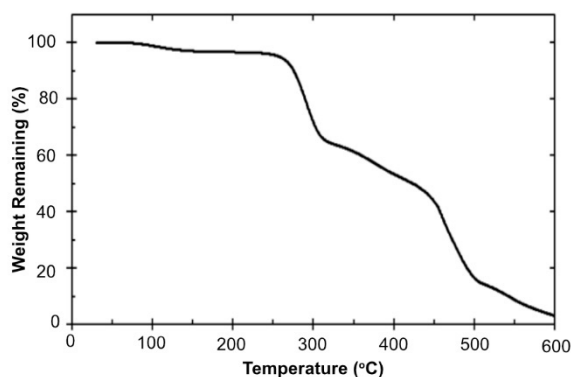


Figure 2.20: Thermal gravimetric analysis (TGA) of polymer **2.29**, synthesized through the chemical cross-linking of polymer **2.11a** with ethanedithiol.

Thiols are not the only nucleophile which can displace the iodine atoms on the polymer backbone. We found that azide groups could also be appended to the fluoropolymers to yield polymer **2.32** (Figure 2.18D). In this instance, competing elimination was observed, resulting in 50% of iodine being replaced with an azide. The azide incorporation allowed for crosslinking of the polymers *via* Cu-catalyzed azide alkyne cycloaddition (**2.33**, Figure 2.18D, Figure 2.21). The azide also represents an opportunity to covalently conjugate to surfaces coated with the semifluorinated polymers, as demonstrated through the attachment of monofluorinated cyclooctyne⁶¹ **2.34** (Figure 2.22) to films of **2.32** to yield fluorescent polymer **2.35** (Figure 2.18E).

Finally, we looked to exploit the homolytic reactivity of the C-I bond for post-polymerization modification and crosslinking. By treatment of **2.11a** with AIBN and allyl ethyl sulfone (**2.36**), we were able to install allyl functionality onto the polymer backbone with a 45% conversion (Figure 2.23A), producing polymer **2.37**. This unique post-polymerization modification opens many avenues for further modification and crosslinking.

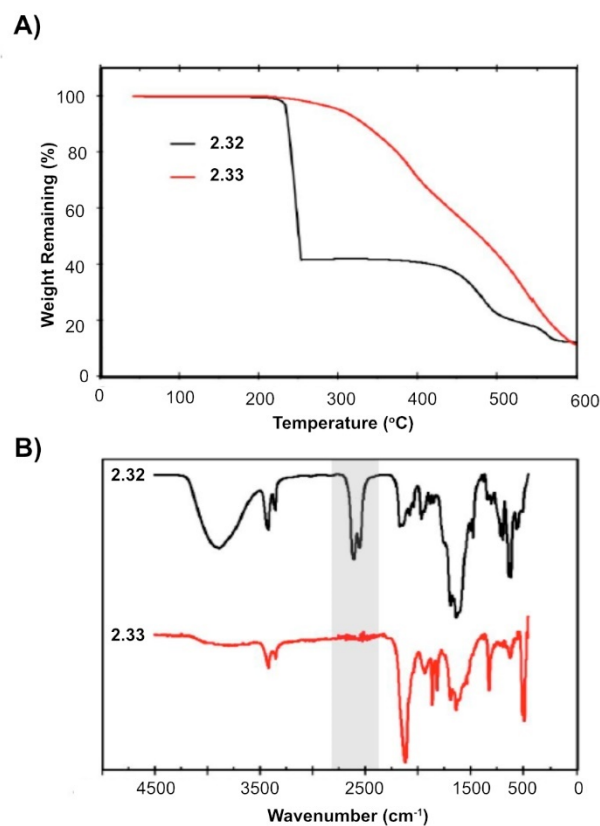


Figure 2.21: Comparison of azide-containing polymer **2.32** before and after crosslinking with Cu-catalyzed azide alkyne cycloaddition. **A.** Thermal gravimetric analysis (TGA) of azide containing polymer **2.32** (black) and cross-linked azide-alkyne polymer **2.33** (red) showing improved stability through removal of heat labile azide functionality. **B.** FT-IR of polymers **2.32** (black) and **2.33** (red) with the gray box indicating the wavenumber that azide functional groups absorb at.

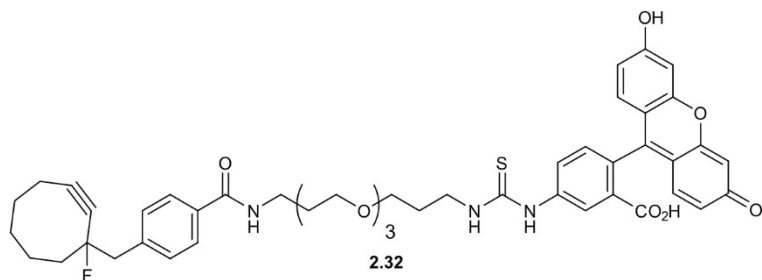


Figure 2.22: Full structure of **2.32**.

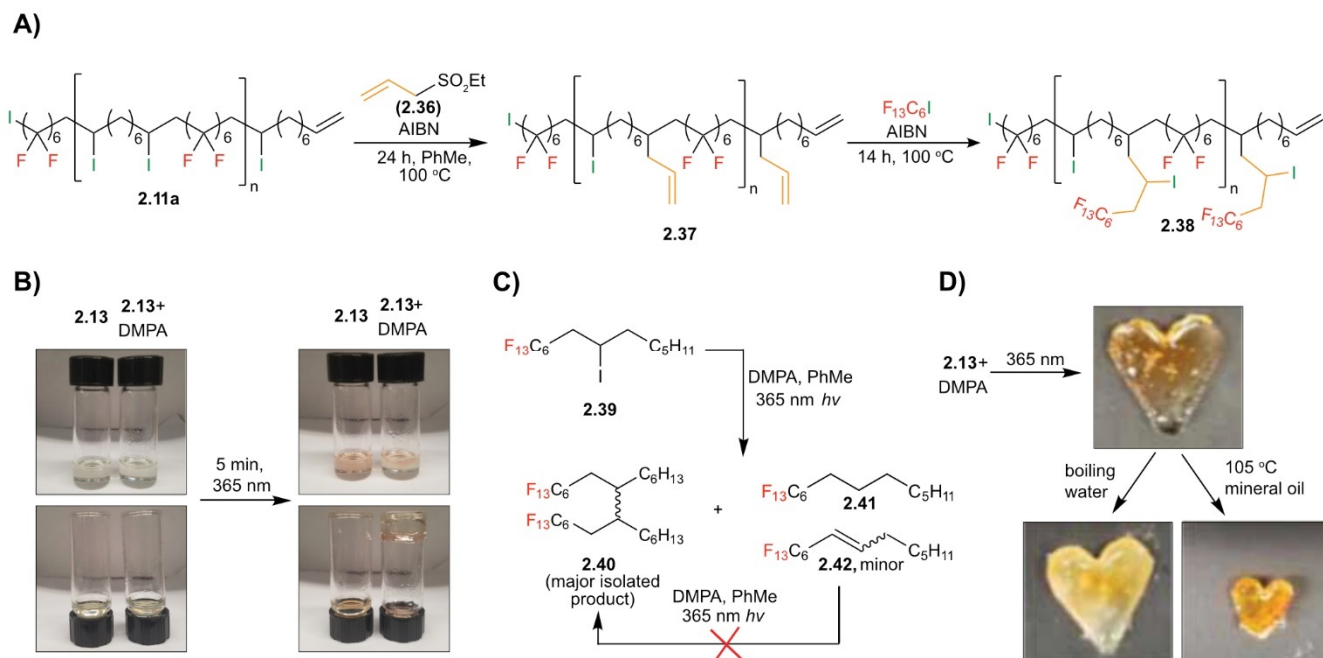


Figure 2.23. **A.** Addition of allyl groups to the polymer backbone and subsequent iodo-ene reaction with perfluorohexyliodide. **B.** Gelation of **2.13** in the presence of 2,2-dimethoxy-2-phenylacetophenone (DMPA). Two solutions of **2.13** in toluene (20 mg/mL) were prepared, 15% DMPA was added to the solution on the right. Both solutions were irradiated with 365 nm light for 5 min. Pictures were taken before and after irradiation. **C.** Model compound **2.39** to probe the crosslinking mechanism of **2.13** with DMPA. **D.** Molding and photo-curing of polymer **2.13** into a heart. A solution of compound **2.13** (100 mg/mL) and DMPA (15%) was placed in a heart mold and irradiated with 365 nm light for 5 min. The resulting gel was removed from the mold, treated with boiling water or 105 °C mineral oil without loss of the heart shape.

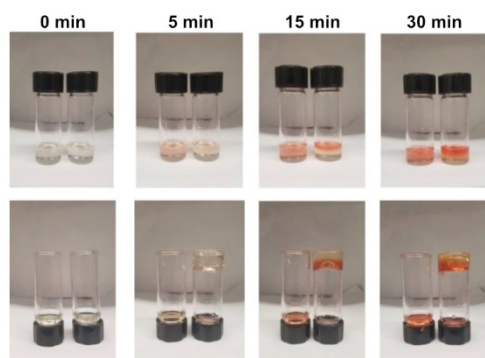


Figure 2.24: UV curing of polymer **2.13** in toluene. Two solutions of **2.13** in toluene (20 mg/mL) were prepared, 15 wt% DMPA was added to the solution on the right. Both solutions were irradiated with 365 nm light for differing amounts of time. Pictures were taken before and after irradiation, **2.13** without DMPA (left) and with DMPA (right). The red color that increases over time is attributed to iodine formation.

We demonstrated the introduction of additional fluororous character by performing another iodo-ene reaction on **2.37** to produce **2.38**. Next, we exploited the homolytic reactivity of the C-I bond for direct photocrosslinking of the iodo-ene polymers. We prepared 20 mg/mL samples of polymer **2.13** in toluene with or without 15 wt% photoinitiator 2,2-dimethoxy-2-phenylacetophenone (DMPA). The solutions were placed under a 365 nm UV lamp and gelation began within 5 minutes if DMPA was present (Figure 2.23B). After 30 minutes had passed, no gelation was evident in the DMPA-free control (Figure 2.24). Thus, we are able to photocrosslink the iodo-ene polymers in a DMPA-dependent manner. To determine the cause of gelation, small molecule **2.39** was synthesized and submitted to light and DMPA (Figure 2.23C). ¹H-NMR and ¹⁹F-NMR supported that the reaction proceeded to complete loss of iodine in 10 minutes with 2 equiv. DMPA (Figure 2.25). High resolution gas chromatography-mass spectrometry (HR-GCMS) provided evidence of dimerization to compound **2.39** (Figure 2.26), which was further supported by DEPT135 ¹³C-NMR (Figure 2.27). An authentic HR-GCMS standard of **2.40** was prepared by oxidative coupling chemistry of **2.39**⁶² and confirmed the presence of **2.40** in the photocrosslinking conditions. On inspection of the crude reaction mixture, we also observed minor amounts of reduced product **2.41**, eliminated iodine product **2.42**, and DMPA-adducts (Figure 2.28); however, subjecting **2.42** to photocrosslinking conditions did not yield any dimer formation. Based on these data, we hypothesize covalent crosslinking is achieved via recombination of radicals generated after homolytic cleavage of the C-I bond. Interestingly, similar radicals are generated throughout the polymerization mechanism, yet we do not detect crosslinked polymer. This may be due to differences in the lifetime/concentration of the radicals during the polymerization and the photocrosslinking.⁶³

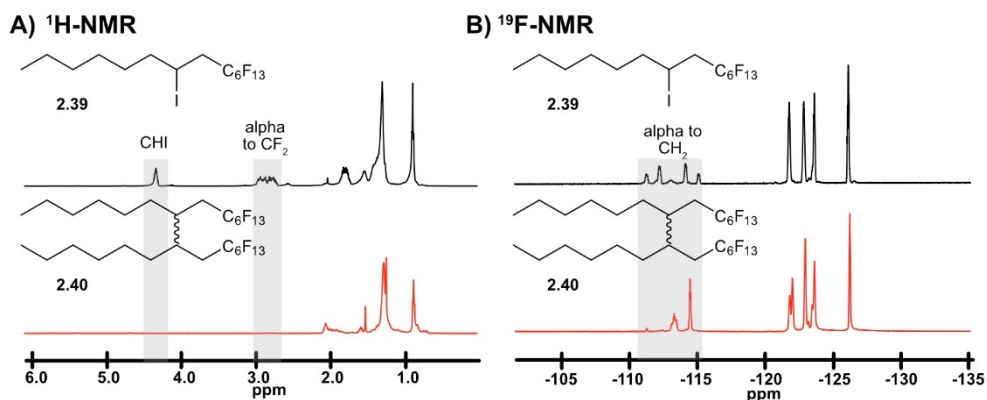


Figure 2.25: NMR spectra showing the loss of iodine in the photodimerization reaction of **2.39** to form **2.40**. A) $^1\text{H-NMR}$ spectra of **2.39** (black) and **2.40** (red) gray boxes showing loss of peaks related to CHI hydrogen and CH_2 α to CF_2 . B) $^{19}\text{F-NMR}$ spectra of **2.39** (black) and **2.40** (red) with gray boxes showing loss of peaks related to C-F bonds α to CH_2 .

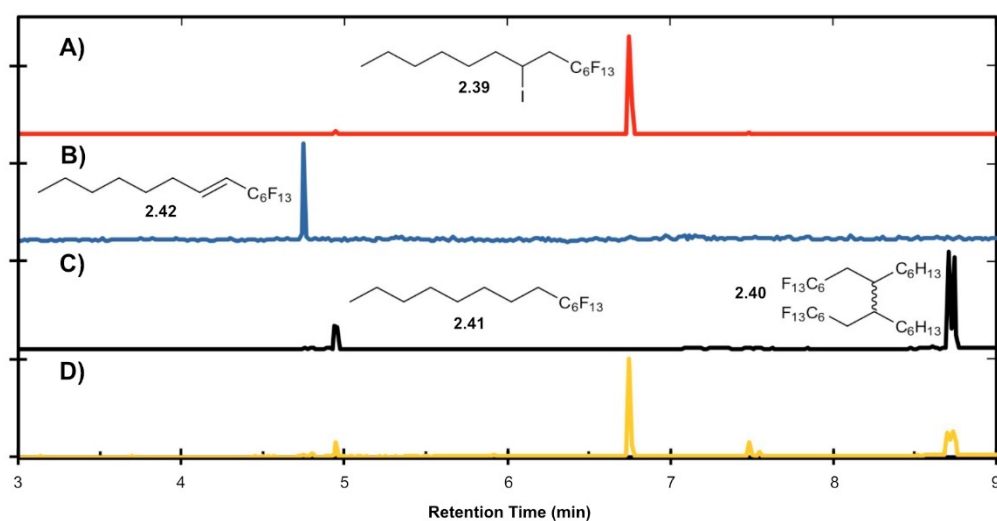


Figure 2.26: Small molecule model system to study the photocrosslinking of **2.11a**. HR-GCMS data of **A**. Starting material **2.39** prepared through sulfinate dehalogenation coupling of 1-octene and perfluorohexyl iodide. **B**. Prepared standard **2.42** from the elimination of iodine from small molecule **2.39**. **C**. Products obtained through DMPA initiated dimerization of **2.39** under 365 nm UV light following purification through silica plug. **D**. Products obtained through copper and manganese catalyzed oxidative coupling of **2.39**⁶²

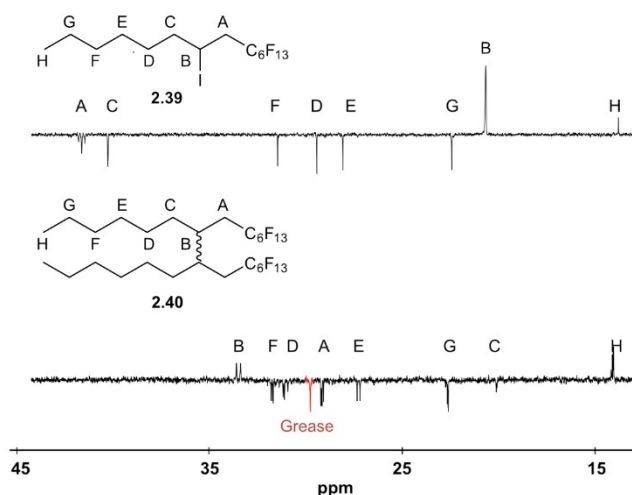


Figure 2.27: DEPT-135 ^{13}C -NMR of starting material **2.39** (top) and dimerized product **2.40** (bottom) purified from treatment of **2.39** with 2 equivalents of DMPA and 365 nm light for 1 hour. Complete loss of iodine can be observed through loss of peak A, B, and C (top) and growth of peaks A, B, and C (bottom).

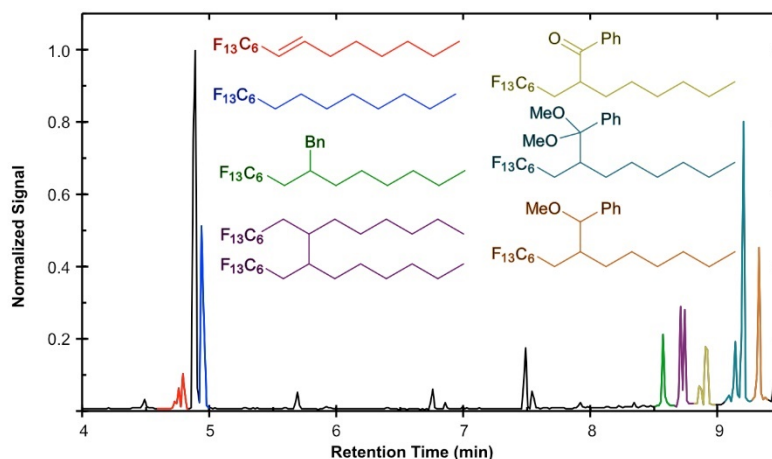


Figure 2.28: Crude HR-GCMS spectra showing desired products and DMPA adducts by color. Elimination (red), reduction (blue), toluene addition (green), dimerization product **2.40** (purple), phenyl acetone addition (yellow), α,α -dimethoxytoluene addition (teal), α -methoxytoluene addition (orange). Other DMPA degradation products and unidentified products in black. Structural assignments made using HR-GCMS. Note that 2 equivalents of DMPA rather than 15 wt% DMPA was employed in the small molecule studies, resulting in significant DMPA adducts in the GCMS trace.

The direct photocrosslinking of the iodo-ene polymers allow opportunities to fabricate organo- and fluorogels. We prepared a 100 mg/mL solution of **2.13** in toluene and placed it into a heart mold. After 5 minutes of irradiation, the crosslinked gel was removed from the mold and retained the heart shape (Figure 2.23D). We found that the gel withstood hot mineral oil and boiling water without shape deformation, although it became smaller in mineral oil due to leaching of the toluene. The mineral oil treated gel could be readily re-swollen in toluene or semifluorinated solvents such as trifluorotoluene (Figure 2.29A). As with surfaces containing **2.13**, the stability of the fluoropolymers is much lower when

the iodine atoms are present. We were able to increase the thermal stability of the gel by treatment with DBU in toluene for 5 minutes with no loss of the gel shape (Figures 2.29B, 2.30). Thus, we are able to obtain bulk, thermally stable fluororous materials through a combined photo and chemical treatment process.

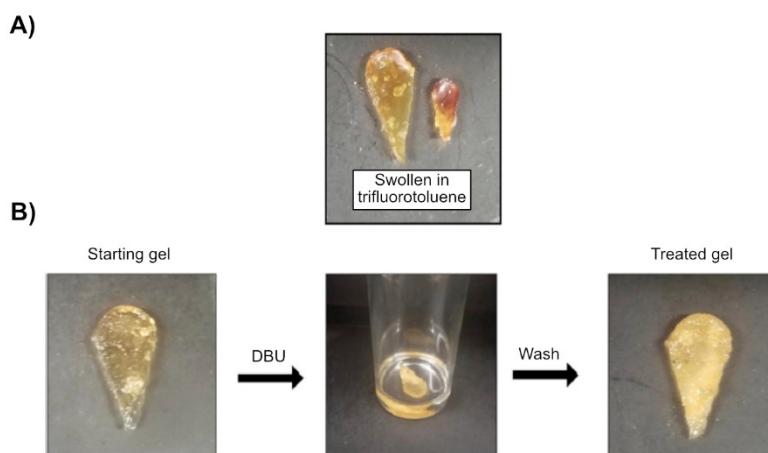


Figure 2.29: Swelling of crosslinked semifluorinated gel. **A.** Semi-fluorinated gel after submersion in trifluorotoluene for 15 minutes (left) in comparison to semi-fluorinated gel that had solvent removed (right). **B.** Elimination of iodine from crosslinked polymer gel in DBU. Starting fluoropolymer gel (left) submersion in DBU for 5 minutes (center), followed by purification by washing with water and toluene (right).

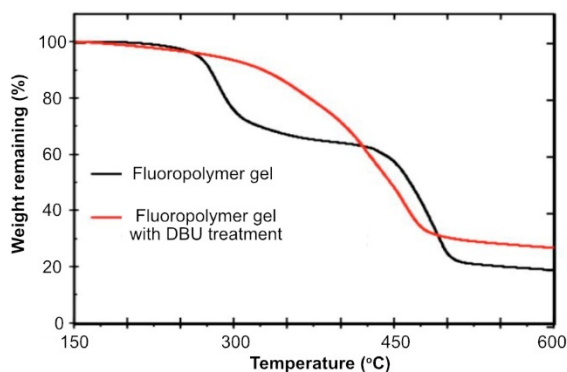


Figure 2.30: Thermal gravimetric analysis of base treated fluoropolymer gel. The fluoropolymer gel was prepared by subjecting 20 mg/mL **2.13** in THF with 15 wt% DMPA to 365 nm light. Fluoropolymer gel before submersion in DBU (black, see Figure 2.30) and after of submersion in DBU for 5 minutes (red).

2.4 Conclusion

We have developed a facile polymerization of dienes and diiodoperfluoroalkanes that allows access to an array of fluorinated polymers up to 128 kDa. Further size control can be performed through

the addition of end-caps. The fluororous nature of the polymer can be easily tuned through strategic selection of monomers and post-polymerization modifications. The mild polymerization conditions enable sensitive monomers to be polymerized and yields fluorinated polymers that degrade into segments that do not bioaccumulate. Iodine incorporation along the polymer backbone gives an exquisite handle for modification, shown through addition of azides, thiols, and allyl groups. These functional handles expedite surface modification and crosslinking *via* click chemistries, a stark contrast to ionizing radiation necessary to modify and crosslink PTFE. The polarizable iodine atoms also facilitate processing into thin-films that can be cured to remove iodine and increase their thermal stability. Additionally, fluoropolymers can be directly photocrosslinked through the use of a photo-initiator, providing opportunities for photopatterning and 3D printing. Taken together, we have addressed the main limitations of PTFE, setting the stage for the unique properties of perfluorocarbons to be employed at the forefront of material science.

2.5 Experimental procedures

2.5.1 General experimental procedures:

Chemical reagents were purchased from Sigma-Aldrich, Alfa Aesar, Fisher Scientific, or Acros Organics and used without purification unless noted otherwise. No unexpected or unusually high safety hazards were encountered. Anhydrous and deoxygenated solvents toluene (PhMe), tetrahydrofuran (THF), dichloromethane (DCM), acetonitrile (MeCN), and dimethylformamide (DMF) were dispensed from a Grubb's-type Phoenix Solvent Drying System. Thin layer chromatography was performed using Silica Gel 60 F254 (EMD Millipore) plates. Flash chromatography was executed with technical grade silica gel with 60 Å pores and 40–63 µm mesh particle size (Sorbtech Technologies). Solvent was removed under reduced pressure with a Büchi Rotovapor with a Welch self-cleaning dry vacuum pump and further dried with a Welch DuoSeal pump. Bath sonication was performed using a Branson 3800 ultrasonic cleaner. Nuclear magnetic resonance (¹H-NMR, ¹³C-NMR, and ¹⁹F-NMR) spectra were taken on Bruker Avance 500 (¹H-NMR and ¹³C-NMR) or AV-300 (¹⁹F-NMR) instruments and processed with MestReNova software. All ¹H, ¹³C, and ¹⁹F NMR spectra are reported in ppm and relative to residual solvent signals

(^1H and ^{13}C). Size exclusion chromatography (SEC), unless otherwise noted, was conducted on a Shimadzu prominence-I LC-2030C high performance liquid chromatography (HPLC) system with a UV detector and connected to a Wyatt Dawn Heleos-II light scattering detector and Wyatt Optilab T-rEX refractive index detector, one Agilent PLgel guard column D, and an Agilent PLgel 10 μm mixed B columns. Eluent was DMSO at 65 $^\circ\text{C}$ (flow rate: 0.35 mL/ min). Calibration was performed using near monodisperse poly(methyl-methacrylate) PMMA standards from Polymer Laboratories. Differential scanning calorimetry measurements were taken on a PerkinElmer DSC. Thermal gravimetric analysis was performed on a PerkinElmer Pyris Diamond TG/DTA Thermogravimetric/Differential Thermal Analyzer. Mass spectra (Electron impact (EI) or electrospray ionization (ESI)) were collected on an Agilent 7890B-7520 Quadrupole Time-of-Flight GC/MS and Thermo Scientific Q ExtractiveTMPlus Hybrid Quadrupole-OrbitrapTM. Irradiation with light was performed with BI365 nm Inspection UV LED lamp, purchased from Risk reactor (Output power density $>5000\mu\text{W}/\text{cm}^2$ at 15" (38 cm), voltage range 90-265V ac, output power: 3*325 mW at 365 nm peak). Centrifugation was performed on a Thermo Scientific Sorvall ST 16 Centrifuge. All sonication was done in a Branson M-Series Model 3800 120V bath sonicator.

Abbreviations: AIBN = azobisisobutyronitrile; DBU = 1,8-Diazabicyclo[5.4.0]undec-7-ene; DCM = dichloromethane; DMF = dimethylformamide; DMPA = 2,2-dimethoxy-2-phenylacetophenone; DMSO = dimethylsulfoxide; DSC = differential scanning calorimetry; Et₂O = diethyl ether; MeCN = acetonitrile ; MeOH = methanol; PhMe = toluene; SEC = size exclusion chromatography; TGA = thermal gravimetric analysis; THF = tetrahydrofuran

SEC prep/procedures: Polymers were dissolved in a 3 mg/mL solution of DMSO through sonication for 60 minutes, or by stirring at 125 $^\circ\text{C}$ for 15 minutes. Stirring at high temperature was necessary for longer polymers due to solubility issues. Sonication or stirring at high temperature for extended times lead to polymer degradation through elimination or displacement of iodine by DMSO. Polymer solutions were filtered and 50 μL were then run through one Agilent PLgel guard column D, and a Polymer Laboratories

PLgel 10 μm mixed B columns at 65 $^{\circ}\text{C}$ with an eluent rate of 0.35 mL/min. Unless otherwise noted, UV absorption was used for molecular weight determination. We found sample preparation to be critical to the success of SEC analysis of the iodo-ene polymers.

TGA prep/procedures: Polymer sample (5–10 mg) were placed in a calibrated ceramic container and the temperature was raised to 100 $^{\circ}\text{C}$. After a delay of 1 minute to remove residual solvent, the weight of the sample was re-recorded, and the temperature was raised to 650 $^{\circ}\text{C}$ at a rate of 20 $^{\circ}\text{C}/\text{min}$. The resulting data were then normalized to % weight loss of sample.

DSC prep/procedures: Polymer sample (10–20 mg) were placed in an aluminum pan and cooled to -50 $^{\circ}\text{C}$ and equilibrated for 2 minutes. For unmodified polymers, the samples were then heated to 150 $^{\circ}\text{C}$ at a rate of 20 $^{\circ}\text{C}/\text{min}$ with a 2-minute pause at 150 $^{\circ}\text{C}$. Samples were then cooled back down to -50 $^{\circ}\text{C}$ at a rate of 15 $^{\circ}\text{C}/\text{min}$ with a 2-minute pause at -50 $^{\circ}\text{C}$. This cycle was then repeated two additional times. All other polymers were analyzed in a similar manner, but with heating until 200 $^{\circ}\text{C}$ at the same rate.

Thin film preparation: Polymer (5 mg) was dissolved in solvent (1mL, DMF, toluene, DMSO, or THF) at 85 $^{\circ}\text{C}$. The polymer solution (0.5 mL) was then drop cast onto a glass slide and allowed to evaporate at room temperature (THF or toluene) or heated at 80 $^{\circ}\text{C}$ to remove solvent (DMSO or DMF). Following solvent evaporation, the thin films were annealed further at 85 $^{\circ}\text{C}$.

Contact angle measurements: Thin films were prepared in the same manner as previously described. Contact angles were measured with a slowly dispensed drop of water at a height where the drop immediately contacts film. Contact angles were measured with a 5 second delay from initial contact of water with the polymer surface. The reported values are the average of at least three independent droplets per sample.

Ester hydrolysis procedures on films and in solution: Thin films were prepared in the same manner as previously described. Three thin films of the ester containing polymer **2.19a** and hydrocarbon polymer **2.11a** were formed on glass slides and placed in a 2M solution of aqueous sodium hydroxide. Each film was removed from solution, washed with water, and dried under N₂ gas at the 1, 3, 5, and 7-hour time points and contact angles were measured in triplicate for each film.

For solution phase hydrolysis, 5 mg/mL solutions of polymers (5 mg/mL in DMSO) were prepared and analyzed via SEC. Aqueous sodium hydroxide (10 M) was added dropwise until a final concentration of 1M NaOH was reached. The resulting solution was stirred at room temperature for 8 hours. Following hydrolysis, polymer solutions were filtered and analyzed via SEC.

Processability of films, heat treated: Films of polymer **2.13** were prepared in a similar manner as previously described. Films of polymer **2.13** on glass slides were placed in an oven at 300 °C for 30 minutes. Following heat treatment and cooling, the remaining polymer was removed from the glass slide and analyzed via TGA.

Processability of films and polymer in bulk, base treated: Polymer **2.13** (5 mg) was dissolved in toluene (1 mL) at 85 °C and cooled to room temperature. Tetramethyl guanidine (0.15 mL) was quickly added and 0.5 mL of the resulting solution was dropped on a glass slide to be annealed at 100 °C. Following removal of solvent, the glass slide was washed with water and further annealed at 100 °C for 5 minutes. Following cooling to room temperature, the polymer was removed from the glass slide and analyzed via TGA. Bulk polymers were cured via submersion in neat DBU for 5 minutes. Following submersion, the polymers were washed methanol (3 x 10 mL). Polymers were dried on high vac and analyzed via TGA.

Click chemistry on surfaces: Thin films of polymers **2.11a** and **2.32** were prepared in a similar manner as previously described. Films of **2.11a** and **2.32** were placed in a solution of **2.34** (0.6 mg/mL in MeOH) for 14 hours. Films were then sequentially washed with water (3 x 20 mL) and MeOH (3 x 20 mL) to

remove excess **2.34** and then placed under 365 nm light for photographs. For photographs, the thin-films were dunked in a methanol solution and quickly irradiated with a 365 nm light to keep the fluorescein in the open, fluorescent form.

Photochemistry assembly: Our homemade photobox was assembled to the shape of the UV light source using cardboard and black tape. The interior was then coated with aluminum foil and holes were cut on the top sample placement.

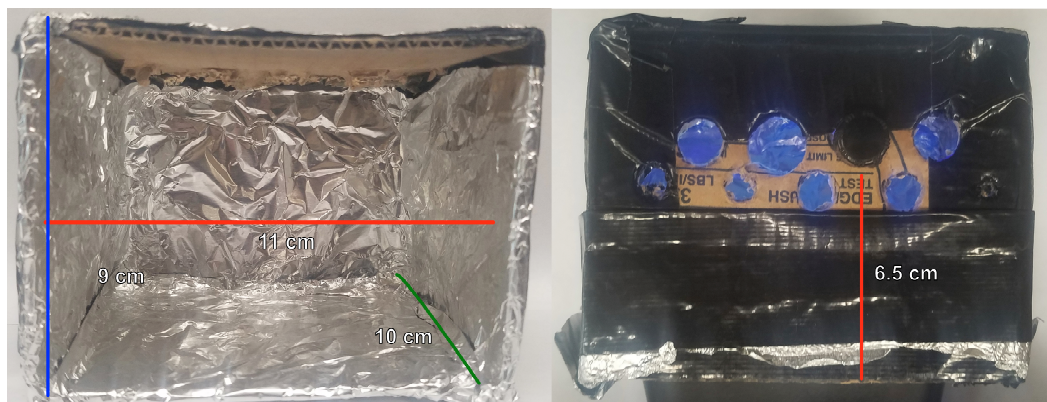


Figure 2.31: Photobox assembly for UV irradiation of polymers and small molecules.

2.5.2 Procedures for synthesis of small molecules:

2.12, dec-9-en-1-yl 4-(dimethylamino)benzoate end-cap:

Dimethylaminobenzoyl chloride (0.55 g, 3.0 mmol, 1.0 eq) was dissolved in DCM (12 mL, anhydrous). Pyridine (0.28 g, 3.3 mmol, 1.1 eq) was added dropwise, followed by dropwise addition of 9-decen-1-ol (0.47 g, 3.3 mmol, 1.1 eq). The solution was stirred for 16 hours at room temperature, at which point it was diluted with saturated ammonium chloride (10 mL) and further washed with saturated ammonium chloride (2 x 10 mL). The organic layer was collected and dried under reduced pressure to give a crude oil. The oil was purified by flash chromatography (20% EtOAc/Hexanes) to give the pure product **2.12** as a white crystalline solid (0.32 g, 1.05 mmol, 35 %). ¹H NMR (CDCl₃, 500 MHz): δ 7.91 (d, J = 9.1 Hz, 2H), 6.64 (d, J = 9.1 Hz, 2H), 5.81 (m, 1H), 4.95 (m, 2H), 4.25 (t, J = 6.7 Hz, 2H), 3.03 (s, 6H),

2.03 (m, 2H), 1.73 (m, 2H), 1.36 (m, 10H). ¹³C NMR (CDCl₃, 126 MHz), δ ppm: 167.1, 153.2, 139.2, 131.3, 117.4, 114.1, 110.7, 64.3, 40.1, 33.8, 29.39, 29.28, 29.07, 28.91, 28.88, 26.1. HRGC-MS (EI): Calculated for C₁₉H₂₉O₂H⁺ [M⁺]: 303.2198; found 303.2184.

2.17, 4,4,5,5,6,6,7,7,8,8,9,9-dodecafluorododeca-1,11-diene:

Diiodoperfluorohexane (1.0 g, 1.8 mmol, 1.0 eq), allyltributyltin (1.2 g, 3.6 mmol, 2.0 eq), and azoisobutyronitrile (AIBN) (0.03 g, 0.2 mmol, 0.1 eq) were added to a flame dried round bottom flask and stirred at 80 °C for 16 hours, at which point **2.17** was distilled out under reduced pressure (67-70 °C/4 torr) to yield **2.17**, as a clear oil (0.321 g, 0.49 mmol, 27%). ¹H-NMR (CDCl₃, 500 MHz), δ: 5.85 (m, 2H), 5.38 (m, 4H), 2.89 (m, 4H). ¹⁹F-NMR (CDCl₃, 282 MHz), δ: -113 (s, 4F), -122 (s, 4F), -123 (s, 4F). NMR spectra matched literature reference.⁶⁵

2.18, but-3-en-1-yl pent-4-enoate:

4-pentenoic acid (0.6 g, 6 mmol, 1 eq) and thionyl chloride (0.71 g, 6.0 mmol, 1.0 eq) were added to a flame dried round bottom flask equipped with condenser and refluxed for 1 hour. Excess thionyl chloride was removed under reduced pressure via rotary evaporator and the remaining oil was re-dissolved in DCM (8 mL, anhydrous). Pyridine (0.47 g, 6.6 mmol, 1.1 eq) was then added dropwise to the solution, followed by dropwise addition of 3-buten-1-ol (0.51 g, 6.6 mmol, 1.1 eq). The solution was stirred 16 hours at room temperature, at which point the solution was diluted with saturated ammonium chloride (20 mL) and washed (2 x 10 mL) with saturated ammonium chloride. The organic layer was collected and dried with MgSO₄, filtered, and concentrated under reduced pressure. Flash chromatography (20% EtOAc/Hexanes) yielded **2.18** as a clear oil, (0.44 g, 2.8 mmol, 47%). ¹H NMR (CDCl₃, 500 MHz), δ: 5.83 (m, 2H), 5.10 (m, 4H), 4.17 (t, *J* = 6.7 Hz, 2H), 2.42 (m, 6H). NMR spectra matched literature reference.⁶⁶

2.19, 1,4-bis(allyloxy)benzene:

Hydroquinone (1.0 g, 9.1 mmol, 1.0 eq), allyl bromide (2.75 g, 22.7 mmol, 2.5 eq), and potassium carbonate (3.1 g, 23 mmol, 2.5 eq) were added to MeCN (10 mL, anhydrous) and refluxed for 24 hours, at which point the salts were filtered and the resulting organic layer was concentrated under reduced pressure. The crude oil was purified through flash chromatography (10% EtOAc/Hexanes) to yield **2.19** as a crystalline solid (1.14 g, 6.0 mmol, 66 %). ¹H NMR (CDCl₃, 500 MHz), δ: 6.89 (s, 4H), 6.09 (m, 2H), 5.39 (m, 4H), 4.53 (dt, *J* = 5.3, 1.5 Hz, 4H). NMR spectra matched literature reference.⁶⁷

2.39, 1,1,1,2,2,3,3,4,4,5,5,6,6-tridecafluoro-8-iodotetradecane:

AIBN Method:

1-Octene (0.143 g, 1.28 mmol, 1.00 eq), perfluorohexyl iodide (0.577 g, 1.28 mmol, 1.00 eq), and AIBN (0.02 g, 0.13 mmol, 0.10 eq) were added to an oven dried scintillation vial under an N₂. The reaction mixture was stirred at 85 °C for 16 hours. The crude oil was flushed through a silica plug with hexanes as the eluent to yield **2.39** as a colorless oil (571 mg, 1.0 mmol, 80 %) ¹H NMR (CDCl₃, 500 MHz), δ: 4.34 (tt, *J* = 8.8, 4.7 Hz, 1H), 2.85 (m, 2H), 1.88 (m, 2H), 1.32 (m, 8H), 0.9 (t, *J* = 8 Hz, 3H) ¹³C NMR (CDCl₃, 126 MHz), δ ppm: 119.8-115.9, (m 6C), 41.6 (t, *J* = 20.9 Hz, 1C), 40.2, 31.4, 29.4, 28.0, 22.4, 20.6, 13.8. ¹⁹F NMR (CDCl₃, 282 MHz), δ ppm: -80.78 (s, 3F), -114.07 (m, 2F), -121 (s, 2F), -122.81 (s, 2F), -123.63 (s, 2f), -126.05 (s, 2F). HRMS (EI) Calculated for C₁₄H₁₆F₁₃I [M-I⁻]: 431.1044, found: 430.1021. Spectral analysis was in agreement with literature values.³⁷

Sulfinatodehalogenation method:

1-Octene (0.30 g, 2.7 mmol, 1.0 eq), perfluorohexyl iodide (1.19 g, 2.67 mmol, 1.0 eq), sodium bicarbonate (0.34 g, 4.0 mmol, 1.5 eq), and sodium dithionite (0.70 g, 4.0 mmol, 1.5 eq) were added to a solution of MeCN (16 mL), dimethyl carbonate (10 mL), and water (7.0 mL). The resulting slurry was then placed in a sonication bath for 14 hours. The reaction mixture was concentrated under reduced

pressure and then washed with diethyl ether (3 x 15 mL) and the organic layer was dried and concentrated. The crude oil was then flushed through a silica plug with hexanes as the eluent to yield **2.39** as a colorless oil. (1100 mg, 2.0 mmol, 73%).

DMSO method:

1-Octene (0.056 g, 0.5 mmol, 1.0 eq), perfluorohexyl iodide (0.222 g, 0.5 mmol, 1.0 eq), sodium bicarbonate (0.063 g, 0.75 mmol, 1.5 eq), and sodium dithionite (0.130 g, 0.75 mmol, 1.5 eq) were added to a solution of DMSO (6 mL). The resulting slurry was then placed in a sonication bath for 14 hours. The reaction mixture was diluted with 15 mL water and then washed with diethyl ether (3 x 15 mL) and the organic layer was dried and concentrated. The crude oil was then flushed through a silica plug with hexanes as the eluent to yield **2.39** as a colorless oil. (150 mg, 0.27 mmol, 54%)

2.40, 1,1,1,2,2,3,3,4,4,5,5,6,6,11,11,12,12,13,13,14,14,15,15,16,16,16-hexacosafluoro-8,9-dihexylhexadecane by treatment with light and DMPA:

Compound **2.38** (0.4 g, 0.7 mmol, 1 eq) was dissolved in toluene (16 mL) and 2,2-dimethoxy-2-phenylacetophenone (DMPA) (0.37 g, 1.4 mmol, 2.0 eq) was added. The solution was placed under 365 nm UV light for 1 hour, at which point the toluene was removed under reduced pressure and the resulting crude oil purified by flash chromatography (100% hexanes) to give a mixture of products **2.39**, **2.40**, and **2.41** in 85.5:13:1.5 ratio 0.111 g total. 0.118 mmol of **2.39** (16%, HRMS (EI) calculated for $C_{28}H_{32}F_{26}$ [M/2]: 431.1044; found: 431.1021); 0.018 mmol **2.40** (3% HRMS (EI) calculated for $C_{14}H_{16}F_{13}$ [M-C₂H₅]: 403.0731; found: 403.0716); 0.0021 mmol **2.41** (0.3%, HRMS (EI) calculated for $C_{14}H_{15}F_{13}$ [M]: 430.0966; found: 430.0944)

2.40, 1,1,1,2,2,3,3,4,4,5,5,6,6,11,11,12,12,13,13,14,14,15,15,16,16,16-hexacosafluoro-8,9-dihexylhexadecane by oxidative coupling⁶²:

Compound **2.38** (0.22 g, 0.39 mmol, 1.0 eq) was added to water (1 mL), along with manganese mesh (0.063 g, 1.2 mmol, 3.0 eq) and copper chloride (0.007 g, 0.04 mmol, 0.1 eq). The resulting slurry was stirred at reflux for 16 hours. The solution was then diluted with diethyl ether (20 mL) and filtered. The

aqueous layer was washed with diethyl ether (2 x 5 mL). The organic layer was then dried with MgSO₄, filtered, and concentrated under reduced pressure. The crude oil was purified by flash chromatography (100% hexanes) to give a mixture of starting material **2.38** and products **2.39**, and **2.40** in 47:32.5:7.5 ratio, 0.114 g total. 0.094 mmol **2.38** (24%, HRMS (EI) Calculated for C₁₄H₁₆F₁₃I [M-I]: 431.1044, found: 430.1021); 0.064 mmol **2.39** (16%, HRMS (EI) calculated for C₂₈H₃₂F₂₆ [M/2]: 431.1044; found: 431.1021); 0.014 mmol **2.40** (4%, HRMS (EI) calculated for C₁₄H₁₆F₁₃ [M-C₂H₅]: 403.0731; found: 430.0716)

2.42, (E)-1,1,1,2,2,3,3,4,4,5,5,6,6-tridecafluorotetradec-7-ene:

Compound **2.39** (0.73 g, 1.3 mmol, 1.0 eq) was dissolved in DMF (3 mL). DBU (0.41 g, 2.7 mmol, 2.1 eq) was slowly added and the solution was stirred for 5 hours at room temperature, at which point the mixture was diluted with DCM (15 mL) and washed with saturated sodium bicarbonate solution (3 x 5 mL). The organic layer was collected, dried with MgSO₄, decanted and concentrated under reduced pressure. The resulting crude oil was then flushed through a silica plug with hexanes to yield **2.40** as a colorless oil in 83:17 ratio of E:Z (0.301 g, 0.70 mmol, 54%). ¹H NMR (CDCl₃, 500 MHz), δ: 6.40 (m, 1H), 5.59 (m, 1H), 2.19 (m, 2H), 1.44 (m, 2H), 1.30 (m, 6H), 0.88 (t, *J* = 8 Hz, 3H). ¹³C NMR (CDCl₃, 126 MHz), δ: -143.4, 118.5-107.9 (m, 6C), 116.7 (t, *J* = 22.8 Hz, 1C), 32.2, 31.5, 28.6, 27.9, 22.5, 13.9. ¹⁹F NMR (CDCl₃, 282 MHz), δ: -80.8 (s, 3F), -111.1 (s, 2F), -121.6 (s, 2F), -122.9 (s, 2F), -123.6 (s, 2F), -126.1 (s, 2F). HRMS (EI) calculated for C₁₄H₁₅F₁₃ [M]: 430.0966; found: 430.0944

2.5.3 General procedure for the polymerization of diiodoperfluoroalkanes and dienes:

Diiodoperfluoroalkane (0.1 mmol, 1 eq) was dissolved in acetonitrile (0.6 mL), dimethyl carbonate (0.5 mL), and water (0.3 mL). 1,9-Decadiene (0.0138 g, 0.100 mmol, 1 eq) was added to the solution. Na₂S₂O₄ (0.032 g, 0.15 mmol, 1.5 eq) and NaHCO₃ (0.012 g, 0.15 mmol, 1.5 eq) were added and the

vial was placed in a sonication bath for 6-14 hours, unless otherwise indicated in the reaction conditions. Following polymerization, the resulting polymer was precipitated from cold methanol (50 mL) and further washed with water (50 mL) and methanol (50 mL). Precipitate was centrifuged at 2500 X g for 5 minutes, and the resulting pellet was dried with high vacuum.

2.11a, 1-perfluorohexyl-2,9-diiododecyl block polymer:

White powder, 57.0 mg, 0.083 mmol, 83 %. ¹H NMR (CDCl₃, 500 MHz), δ: 4.33 (tt, *J* = 9.0, 5.2 Hz, 2H), 2.83 (m, 4H), 1.80 (m, 4H), 1.38 (m, 8H). ¹⁹F NMR (CDCl₃, 282 MHz), δ: -113.4 (m, 4F), -121.6 (s, 4F), -123.6 (s, 4F). SEC, DMSO: *M_n*: 128 kDa, *M_w*: 164 kDa, *Đ*: 1.29. TGA: 10% mass loss at 286 °C. *T_g* (DSC): -0.7 °C

2.11b, 1-perfluorooctyl-2,9-diiododecyl block polymer:

White powder, 73.6 mg, 0.093 mmol, 93%. ¹H NMR (CDCl₃, 500 MHz), δ: 4.33 (tt, *J* = 9.0, 5.2 Hz, 2H), 2.83 (m, 4H), 1.80 (m, 4H), 1.38 (m, 8H). ¹⁹F NMR (CDCl₃, 282 MHz), δ ppm: -113.4 (m, 4F), -121.6 (s, 4F), -121.9 (s, 4F), -123.6 (s, 4F). SEC, DMSO: *M_n*: 192 kDa, *M_w*: 245 kDa, *Đ*: 1.30. TGA: 10% mass loss at 300 °C. *T_g* (DSC): 75 °C

2.11c, 1-perfluorobutyl-2,9-diiododecyl block polymer:

White powder, 45.0 mg, 0.076 mmol, 76 %. ¹H NMR (CDCl₃, 500 MHz), δ ppm: 4.33 (tt, *J* = 9.0, 5.2 Hz, 2H), 2.81 (m, 4H), 1.80 (m, 4H), 1.36 (m, 8H). ¹⁹F NMR (CDCl₃, 282 MHz), δ ppm: -113.4 (m, 4F), -123.4 (s, 4F). SEC, DMSO: *M_n*: 86.5 kDa, *M_w*: 131 kDa, *Đ*: 1.53. TGA: 10% mass loss at 282 °C. *T_g* (DSC): -11.1 °C

2.11d, 1-(perfluorobutyl- perfluorohexyl- perfluorooctyl)-2,9-diiododecyl block polymer:

White powder, 53.0 mg, 0.081 mmol, 81 %. ¹H NMR (CDCl₃, 500 MHz), δ ppm: 4.33 (tt, *J* = 9.0, 5.2 Hz, 2H), 2.83 (m, 4H), 1.80 (m, 4H), 1.38 (m, 8H). ¹⁹F NMR (CDCl₃, 282 MHz), δ ppm: -113.4 (m,

8F), -121.6 (m, 2F), -121.8 (m, 1F), 123.4 (m, 2F), 123.6 (m, 2F). SEC, DMSO: M_n : 83.7 kDa, M_w : 140 kDa, \bar{D} : 1.67. TGA: 10% mass loss at 292 °C. T_g (DSC): -6.0 °C

Alternative polymerization method to form polymer 2.11a, DMSO:

Diiodoperfluorohexane (0.055 g, 0.100 mmol, 1 eq) and 1,9-Decadiene (0.0138 g, 0.100 mmol, 1 eq) were dissolved in dimethylsulfoxide (1.5 mL). $\text{Na}_2\text{S}_2\text{O}_4$ (0.032 g, 0.15 mmol, 1.5 eq) and NaHCO_3 (0.012 g, 1.5 mmol, 1.5 eq) were added and the solution slowly turned bright yellow. The reaction was then stirred at room temperature for 48 hours. The resulting polymer was precipitated from water (25 mL) followed by methanol (25 mL) and the precipitate was centrifuged at 2500 X g for 5 minutes to yield a white solid, (35 mg, 51%). ^1H NMR (CDCl_3 , 500 MHz), δ : 4.33 (tt, $J = 9.0, 5.2$ Hz, 2H), 2.83 (m, 4H), 1.80 (m, 4H), 1.38 (m, 8H). ^{19}F NMR (CDCl_3 , 282 MHz), δ : -113.4 (m, 4F), -121.6 (s, 4F), -123.6 (s, 4F). SEC, DMSO: M_n : 36.0 kDa, M_w : 65.0 kDa, \bar{D} : 1.80. TGA: 10% mass loss at 286 °C.

Alternative polymerization method to form polymer 2.11a, AIBN:

The neat polymerization method described by Wilson and coworkers was followed.⁴³

Alternative polymerization method to form polymer 2.11a, ACHN:

Diiodoperfluorohexane (0.100g, 0.181 mmol, 1 eq) and 1,9-Decadiene (0.025g, 0.181 mmol, 1 eq) were placed in a two-neck flask under N_2 . 1,1'-Azobis(cyclohexanecarbonitrile (ACHN, 0.003g, 0.012 mmol, 0.067 eq) was added to the flask and the solution was raised to 80 °C. ACHN (0.003g, 0.012 mmol, 0.067 eq) was added to the reaction mixture every 10 minutes for the remainder of the reaction. The reaction was allowed to stir for 2 hours and then the solution was raised to 100 °C, 120 °C, and 140 °C over the course of an hour to maintain stirring. The polymer mixture was then cooled to 90 °C and dissolved in 1 mL of toluene. The resulting polymer solution was then precipitated from cold methanol (50 mL). Precipitate was centrifuged at 2500 X g for 5 minutes, and the resulting pellet was dried with high vacuum. White powder, 33.6 mg, 0.048 mmol, 26.7%. ^1H NMR (CDCl_3 , 500 MHz), δ : 4.33 (tt, $J =$

9.0, 5.2 Hz, 2H), 2.83 (m, 4H), 1.80 (m, 4H), 1.38 (m, 8H). ^{19}F NMR (CDCl_3 , 282 MHz), δ : -113.4 (m, 4F), -121.6 (s, 4F), -123.6 (s, 4F). SEC, THF: M_n : 5.25 kDa, M_w : 8.33 kDa, D : 1.59.

Procedure for the synthesis of end-capped polymers, 2.13

Diiodoperfluoroalkane (0.055 g, 0.1 mmol, 1 eq) was dissolved in acetonitrile (0.6 mL), dimethyl carbonate (0.5 mL), and water (0.3 mL). 1,9-Decadiene (0.014 g, 0.10 mmol, 1 eq) and **2.12** (0.003 g, 0.01 mmol, 0.01 eq) was added to the solution. $\text{Na}_2\text{S}_2\text{O}_4$ (0.032 g, 0.15 mmol, 1.5 eq) and NaHCO_3 (0.012 g, 0.15 mmol, 1.5 eq) were added and the vial was placed in a sonication bath for 6–14 hours, unless otherwise indicated in the reaction conditions. Following polymerization, the resulting polymer was precipitated from cold methanol (50 mL). Precipitate was centrifuged at 2500 X g for 5 minutes, and the resulting pellet was dried with high vacuum. Yellow powder, 58.0 mg, 0.084 mmol, 84%. ^1H NMR (CDCl_3 , 500 MHz), δ : 4.33 (tt, $J = 9.0, 5.2$ Hz, 2H), 2.83 (m, 4H), 1.80 (m, 4H), 1.38 (m, 8H). ^{19}F NMR (CDCl_3 , 282 MHz), δ : -113.4 (m, 4F), -121.6 (s, 4F), -123.6 (s, 4F). SEC, DMSO: M_n : 41.3 kDa, M_w : 62.7 kDa, D : 1.52. TGA: 10% mass loss at 286 °C.

Procedure for the polymerization of functionalized dienes 2.14–2.17:

Same general procedure as described above, but with the addition of functionalized diene in place of a hydrocarbon diene. **2.14**: (0.038 g, 0.1 mmol, 1 eq), **2.15**: (0.015 g, 0.1 mmol, 1 eq), **2.16**: (0.019 g, 0.1 mmol, 1 eq), **2.17**: (0.017 g, 0.1 mmol, 1 eq).

2.18b, 1-perfluorohexyl-2,11-diiodo-4,4,5,5,6,6,7,7,8,8,9,9 dodecafluorohexyl dodecane block polymer

White powder, 57 mg, 0.061 mmol, 61%. ^1H NMR (CDCl_3 , 500 MHz), δ : 4.52 (m, 1H), 2.92 (m, 4H). ^{19}F NMR (CDCl_3 , 282 MHz), δ ppm: -113.4 (m, 8F), -121.6 (s, 14F), -123.3 (s, 6F). SEC, DMSO: M_n : 17.9 kDa, M_w : 31.7 kDa, D : 1.77.

2.19a, 1-perfluorohexyl-2-iodo-butyl-pentan-4-iodo-ate:

White powder, 38 mg, 0.055 mmol, 55%. ^1H NMR (CDCl_3 , 500 MHz), δ ppm: 4.36 (m, 3H), 4.20 (m, 1H), 2.90 (m, 4H), 2.53 (m, 2H), 2.10 (m, 4H). ^{19}F NMR (CDCl_3 , 282 MHz), δ ppm: -113.4 (m, 4F), -121.7 (s, 4F), -123.6 (s, 4F). SEC, DMSO: M_n : 326 kDa, M_w : 913 kDa, D : 2.80.

2.20b, 1,4-bis(2-iodopropyl-1-perfluorooctyl)benzene block polymer

White powder, 59 mg, 0.080 mmol, 80%. ^1H NMR (CDCl_3 , 500 MHz), δ ppm: 6.86 (s, 4H), 4.49 (s, 2H), 4.16 (m, 4H), 2.97 (m, 4H). ^{19}F NMR (CDCl_3 , 282 MHz), δ ppm: -113.4 (m, 4F), -121.5 (s, 4F), -121.8 (s, 4F), -123.5 (s, 4F). SEC, DMSO: M_n : 22.4, M_w : 46.2, D : 2.06

2.21b, 1,4-bis(2-iodopropyl-1-perfluorooctyl) terephthaloyl ester block polymer

White powder, 60.8 mg, 0.068 mmol, 68%. ^1H NMR (CDCl_3 , 500 MHz), δ ppm: 8.16 (s, 4H), 4.60-4.40 (m, 6H), 2.94 (m, 4H). ^{19}F NMR (CDCl_3 , 282 MHz), δ ppm: -113.1 (m, 2F), -121.5 (s, 2F), -121.8 (s, 2F), -123.4 (s, 2F). SEC, DMSO: M_n : 28.3 kDa, M_w : 55.0 kDa, D : 1.95.

2.5.4 Procedures for post-polymerization modifications:

2.23, elimination of iodine from polymer 2.11a:

Polymer **2.11a** (0.05 g, 0.07 mmol, 1 eq) was swollen in dimethylformamide (1.5 mL). 1,8-diazabicyclo(5.4.0)undec-7-ene (DBU) (0.065 g, 0.43 mmol, 6.0 eq) was added dropwise and stirred overnight at room temperature. The resulting polymer was precipitated from cold methanol (50 mL). Precipitate was centrifuged at 2500 X g for 5 minutes, and the resulting pellet was dried with high vacuum to yield a white powder (30 mg, 0.07 mmol, 100%). ^1H NMR (CDCl_3 , 500 MHz), δ : 6.37 (m, 2H), 5.58 (q, $J = 13.0$ Hz, 2H), 2.19 (s, 4H), 1.44 (s, 4H), 1.31 (s, 4H). ^{19}F NMR (CDCl_3 , 282 MHz), δ : -111.2 (s, 4F), -121.6 (s, 4F), -123.8 (s, 4F). TGA: 10% mass loss at 383 °C. T_g (DSC): 24.7 °C.

2.24, reduction of iodine from polymer 2.11a:

Polymer **2.11a** (0.05 g, 0.07 mmol, 1 eq), tributyltin hydride (0.052 g, 0.18 mmol, 2.5 eq) and AIBN (0.001 g, 0.007 mmol, 0.1 eq) and toluene (1.5 mL) were placed in a dram vial and freeze-pump-thawed three times. The vial was capped and stirred overnight at 85 °C. The resulting polymer was precipitated from cold methanol (50 mL) and washed with methanol (2 x 50 mL) to remove tin impurities. The precipitate was centrifuged at 2500 X g for 5 minutes, and the resulting pellet was dried with high vacuum to yield a white powder (28 mg, 0.063 mmol, 90%). TGA: 10% mass loss at 430 °C. T_g (DSC): 127 °C. Matched literature reference.⁴⁶

2.26, addition of potassium thioacetate to polymer 2.11a:

Polymer **2.11a** (0.05g, 0.072 mmol, 1 eq) was swollen in dimethylformamide (1 mL). Potassium thioacetate (0.098 g, 0.43 mmol, 6.0 eq) was added and stirred overnight at room temperature. The resulting polymer was precipitated from cold methanol (50 mL). The precipitate was centrifuged at 2500 X g for 5 minutes, and the resulting pellet was dried with high vacuum to yield a white powder (33 mg, 0.059 mmol, 83 %). ¹H NMR (CDCl₃, 500 MHz), δ : 3.86 (s, 2H), 2.33 (m, 10H), 1.76 (m, 4H), 1.36 (m, 8H). ¹⁹F NMR (CDCl₃, 282 MHz), δ : -112.7 (m, 4F), -121.6 (s, 4F), -123.7 (s, 4F). FT-IR: 2932 (C-H str) (w), 1695 (C=O) thioester (s), 1100-1200 (C-F bend) (vs). TGA: 10% mass loss at 282 °C. T_g (DSC): -9.8 °C

2.28, deprotection of polymer 2.26 and oxidative crosslinking through disulfide formation:

Thioacetate containing polymer **2.28** (0.024 g, 0.040 mmol, 1.0 eq) was swollen in a mixture of dimethylformamide and water (1.8 mL, 8:1 v/v%). Sodium hydroxide (0.10 g, 0.32 mmol, 8.0 eq) was added and stirred at 70 °C for 4 hours, at which point the reaction was cooled to room temperature and neutralized with glacial acetic acid. Catalytic iodine (2 mg, 0.007 mmol, 0.2 equiv.) was then added and stirred for an additional two hours. The resulting slurry was precipitated from water (25 mL) followed

by methanol (25 mL) and the precipitate was centrifuged at 2500 X *g* for 5 minutes to yield an orange solid (18 mg, 0.035 mmol, 89%). FT-IR: 2930 (C-H stretch) (weak), 1630 (C=O stretch) (strong), 1100-1200 (C-F bend) (very strong), 540 (S-S bend) (weak). TGA: 10% mass loss at 364 °C. *T_g* (DSC): 151 °C

2.29, crosslinking of polymer 2.11a through displacement of iodine with ethanedithiol:

Polymer **2.11a** (0.022 g, 0.032 mmol, 1.0 eq) was swollen in dimethylformamide (1 mL). Ethylene thiol (0.004 g, 0.04 mmol, 1.0 eq) and potassium carbonate (0.006 g, 0.04 mmol, 1 eq) were added to the solution and stirred overnight at room temperature. The resulting slurry was precipitated from water (25 mL) followed by methanol (25 mL) and the precipitate was centrifuged at 2500 X *g* for 5 minutes to give a white solid (19 mg, 0.032 mmol, 99%) FT-IR: 2932 (C-H stretch) (weak), 1100-1200 (C-F bend) (very strong). TGA: 10% mass loss at 280 °C. *T_g* (DSC): 101 °C

2.30, deprotection of polymer 2.26 and crosslinking through thiol-ene chemistry:

Thioacetate containing polymer **2.28** (0.024 g, 0.040 mmol, 1.0 eq) was swollen in a mixture of dimethylformamide and water (1.8 mL, 8:1 v/v%). Sodium hydroxide (0.100 g, 0.32 mmol, 8 eq) was added and stirred at 70 °C for 4 hours. The solution was cooled to room temperature and 1,9-decadiene (0.007g, 0.05 mmol, 1.2 eq) and dimethoxyphenylacetophenone (DMPA) (0.0015 g, 0.005 mmol, 0.012 eq) were added and then irradiated under 365 nm light for 14 hours. The resulting slurry was precipitated from water (25 mL) followed by methanol (25 mL) and the precipitate was centrifuged at 2500 X *g* for 5 minutes to give an orange solid, (10 mg, 0.014 mmol, 35%. FT-IR: 2925 (C-H stretch) (weak), 1646 (C=C stretch) (weak), 1100-1200 (C-F bend) (very strong). TGA: 10% mass loss at 331 °C. *T_g* (DSC): 141 °C

2.31, deprotection of polymer 2.26 followed by Michael addition into acrylamide:

Thioacetate containing polymer **2.28** (0.024 g, 0.040 mmol, 1.0 eq) was swollen in a mixture of dimethylformamide and water (1.8 mL, 8:1 v/v%). Sodium hydroxide (0.10 g, 0.32 mmol, 8.0 eq) was added and was freeze-pump-thawed for 3 cycles. The solution was then stirred at 70 °C for 4 hours, at which point acrylamide (0.06 g, 0.8 mmol, 20 eq) was added and stirred for 14 hours. The solution was then precipitated from 50 mL of water and washed with an additional 50 mL of methanol and the precipitate was centrifuged at 2500 X g for 5 minutes to give an orange solid (12 mg, 0.017 mmol, 43 %.) Not soluble for NMR analysis. FT-IR: 2932 (C-H stretch) (weak), 1713 (C=O amide stretch) (strong), 1100-1200 (C-F bend) (very strong).

2.32, addition of sodium azide to polymer 2.11a:

Polymer **2.11a** (0.05 g, 0.07 mmol, 1 eq) was swollen in DMF (1 mL). Sodium azide (0.028 g, 0.43 mmol, 6.0 eq) was added and stirred overnight at room temperature. The resulting polymer was precipitated from cold methanol (50 mL). Precipitate was centrifuged at 2500 X g for 5 minutes, and the resulting pellet was dried with high vacuum to give a white powder (24 mg, 0.52 mmol, 72% isolated yield, 53% azide incorporation, 47% eliminated iodine). ¹H NMR (CDCl₃, 500 MHz), δ ppm: 6.38 (m, 1H), 5.58 (q, *J* = 13.9 Hz, 1H), 3.74 (m, 1.1H), 2.2 (m 4H), 1.61 (m, 2H), 1.4 (m, 8H). ¹⁹F NMR (CDCl₃, 282 MHz), δ ppm: -111.2 (s, 2F), -113.2 (s, 2F), -121.6 (s, 4F), -123.7 (s, 4F). FT-IR: 2917 (C-H str) (weak), 2107 -N=N=N (stretch) (strong), 1672 (C=C stretch) (strong), 1100-1200 (C-F bend) (very strong). TGA: 10% mass loss at 220 °C.

2.33, copper catalyzed alkyne-azide crosslinking of polymer 2.32:

Azide containing polymer **2.34** (0.08 g, 0.16 mmol, 1 eq) and 1,7-octadiyne (0.017 g, 0.16 mmol, 1 eq) were dissolved in dimethylformamide (2 mL). Copper sulfate (0.003 g, 0.016 mmol, 0.1 eq) and sodium ascorbate (0.006 g, 0.032 mmol, 0.2 eq) were pre-dissolved in 0.1 mL of water and added to the

solution. The solution was then stirred overnight at room temperature. The resulting slurry was precipitated from water (25 mL) followed by methanol (25 mL) and the precipitate was centrifuged at 2500 X g for 5 minutes. Black solid, quantitative. (0.092 g, 0.16 mmol, 100%) FT-IR: 2917 (C-H stretch) (weak), 1614 C=C (stretch) (very strong), 1100-1200 (C-F bend) (strong) TGA: 10% mass loss at 332 °C.

2.37, free radical displacement of iodine on polymer 2.11a and addition of allyl group:

Polymer **2.11a** (0.1 g, 0.1 mmol, 1 eq), allyl ethyl sulfone (0.133 g, 1.15 mmol, 8.00 eq), AIBN (0.005 g, 0.03 mmol, 0.2 eq) and toluene (6 mL) were added to a two-neck round bottom flask and freeze-pump-thawed three times. Solution was then heated to 100 °C for 24 hours with AIBN being added over the course of the reaction. The solution was then cooled to room temperature and the resulting polymer was precipitated from hexanes. Precipitate was centrifuged at 2500 X g for 5 minutes, and the resulting pellet was dried with high vacuum to give white powder, (42 mg, 0.069 mmol, 48% isolated yield, 45% allyl incorporation, 55% remaining iodine. ¹H NMR (CDCl₃, 500 MHz), δ ppm: 5.72 (m, 1H), 5.06 (m, 2H), 4.33 (t, *J* = 9.0, 5.2 Hz, 1.2H), 2.8 (m, 2.4H), 2.08 (m, 5H), 1.80 (m, 2.4H), 1.58 (m, 4H), 1.32 (m, 6H). ¹⁹F NMR (CDCl₃, 282 MHz), δ ppm: -112.7 (s, 2F), -113.4 (m, 2F), -122 (s, 4F), -124 (s, 4F). FT-IR: 2920 (C-H stretch) (weak), 1643 C=C (stretch) (weak), 1100-1200 (C-F bend) (strong).

2.38, iodo-ene addition of perfluorohexyl iodide into polymer 2.37:

Polymer **2.36** (25 % allyl) (0.018 g, 0.03 mmol, 1 eq) was mixed with perfluorohexyl iodide (0.267 g, 0.60 mmol, 20 eq) and AIBN (0.005 g, 0.03 mmol 1 eq) and freeze-pump-thawed (3X). While under N₂, the solution was raised in temperature to 100 °C for 18 hours. The resulting solid was then centrifuged at washed with methanol (1 x 50 mL) followed by hexanes (2 x 50 mL) and centrifuged 2500 X g for 5 minutes. The resulting pellet was dried with high vacuum to give a brown solid (0.021 g, 0.021 mmol, 71% yield, 25% fluorous branch). ¹H NMR (CDCl₃, 500 MHz), δ ppm: 4.33 (tt, *J* = 9.0, 5.2 Hz, 2H), 2.8 (m, 4H), 2.08 (m, 1.5H), 1.80 (m, 2H), 1.40 (m, 12.5H). ¹⁹F NMR (CDCl₃, 282 MHz, Signal to

noise too low for integration), δ ppm: -80.7 (s), -113.4 (m), -121.6 (s), -122.8 (s), -123.7 (s), -126.1 (s).

FT-IR: 2924 (C-H stretch) (weak), 1100-1200 (C-F bend) (strong)

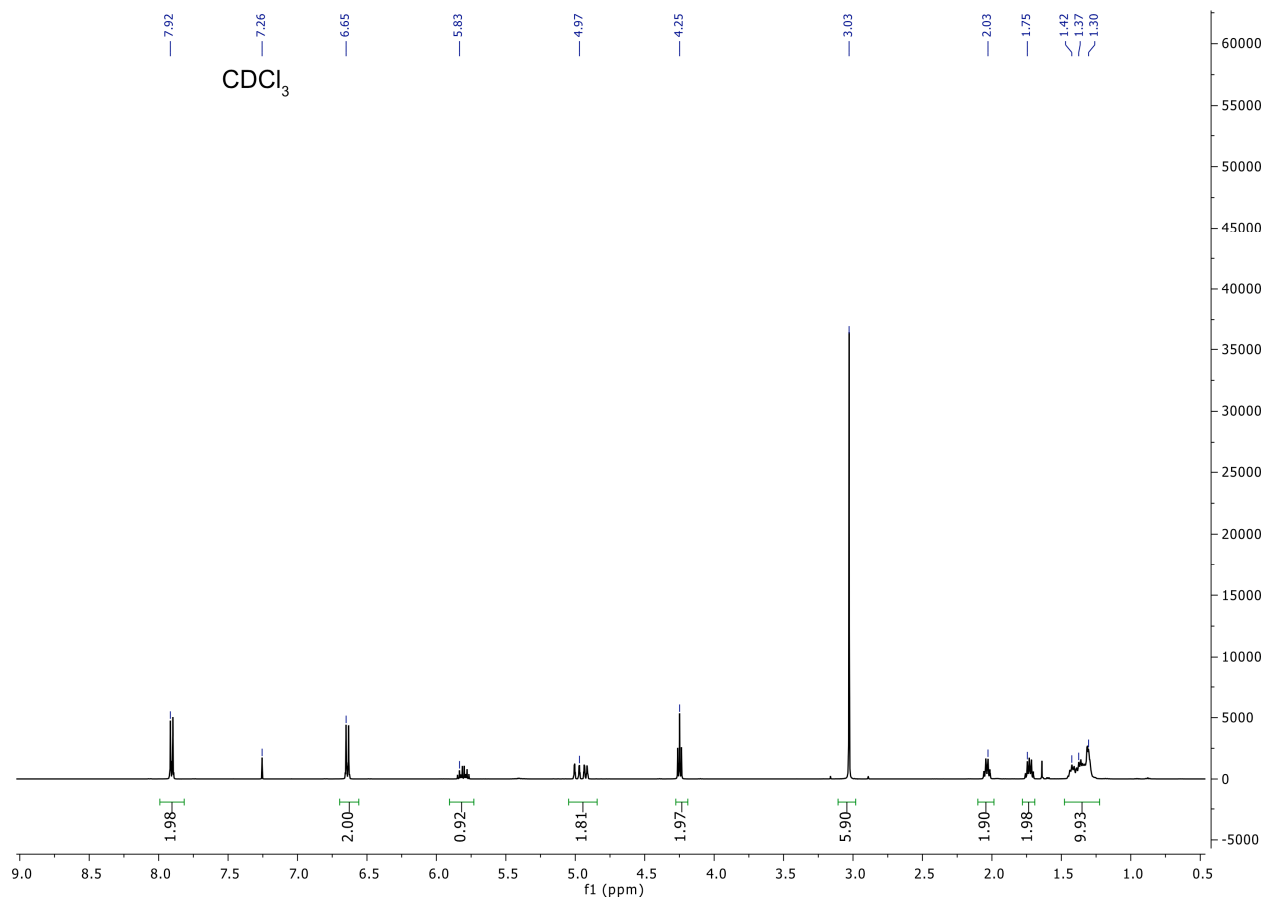
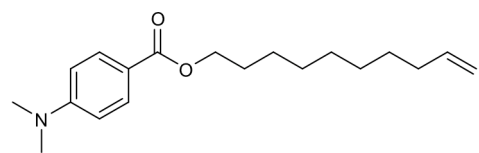
Procedure for photo crosslinking polymer 2.13 with DMPA as an initiator:

Polymer **2.13** (0.05 g, 0.07 mmol, 1 eq) and 15 wt. % 2,2-dimethoxy-2-phenylacetophenone (DMPA) (0.0075g, 0.029 mmol, 0.4 eq) were dissolved in toluene (2.5 mL) at 80 °C and then cooled to room temperature. The resulting yellow solution was then placed under 365 nm light for 5 minutes at which point the yellow solution formed a yellow-orange gel. Excess toluene was removed via decanting and the polymer was reswollen and decanted 2X to remove DMPA. The newly formed gel was then dried on high vacuum to remove toluene. Rubbery orange solid, (0.048 g, 0.071 mmol, 98%). TGA: 10% mass loss at 286 °C.

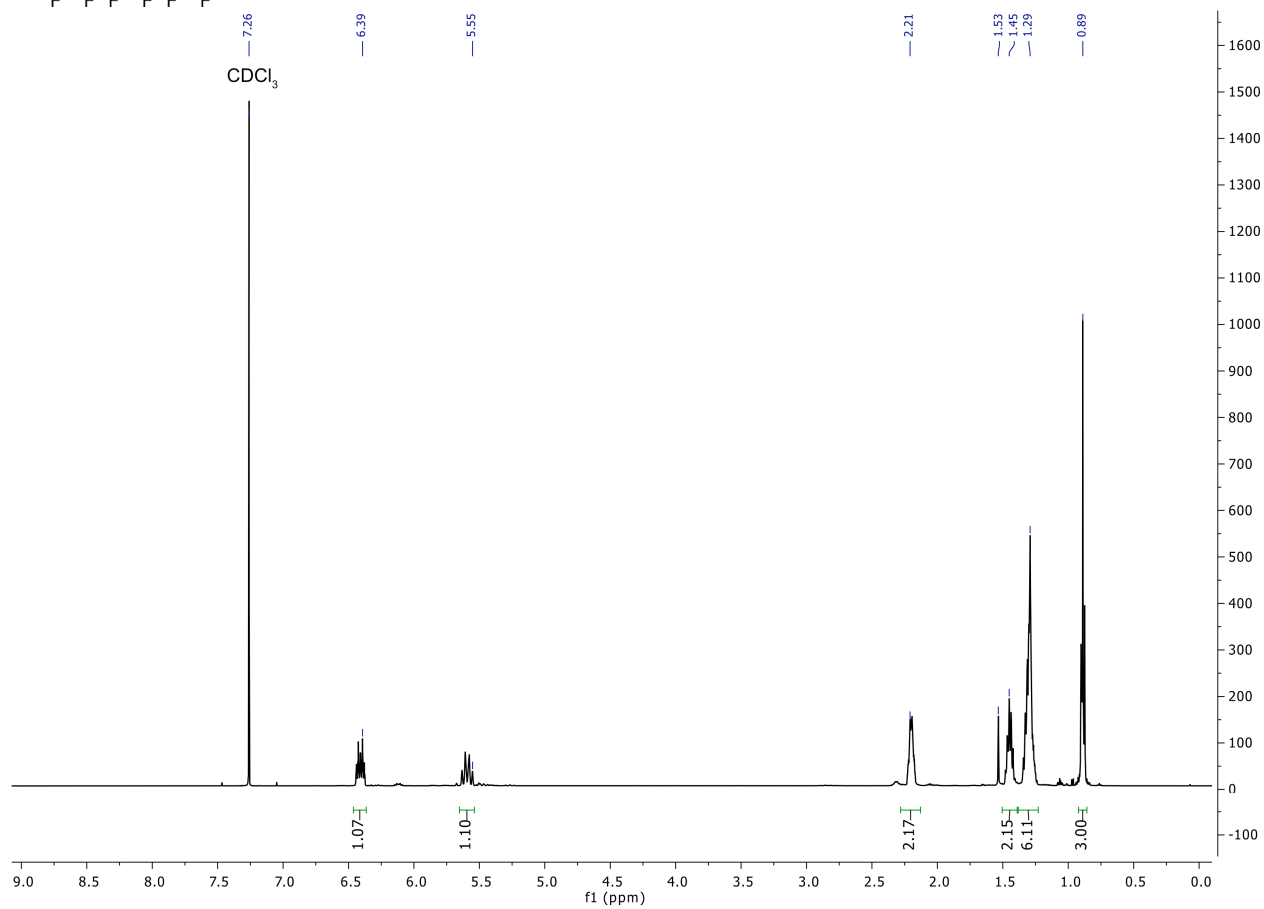
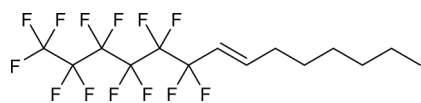
Photocrosslinking in mold: Polymer **2.13** (0.10 g, 0.14 mmol, 1 eq) and 15 wt. % 2,2-dimethoxy-2-phenylacetophenone (DMPA) (0.015 g, 0.06 mmol, 0.4 eq) were dissolved in toluene (2.5 mL) at 80 °C and then cooled to room temperature. The resulting yellow solution was then placed in a heart mold and 365 nm light was irradiated on face of the mold for 2.5 minutes, at which point the yellow solution formed a yellow-orange gel. Excess toluene was removed via decanting and the polymer was reswollen and decanted (2 x 15 mL) to remove DMPA. The newly formed gel was then dried on high vacuum to remove toluene.

2.5.5 $^1\text{H-NMR}$ spectra:

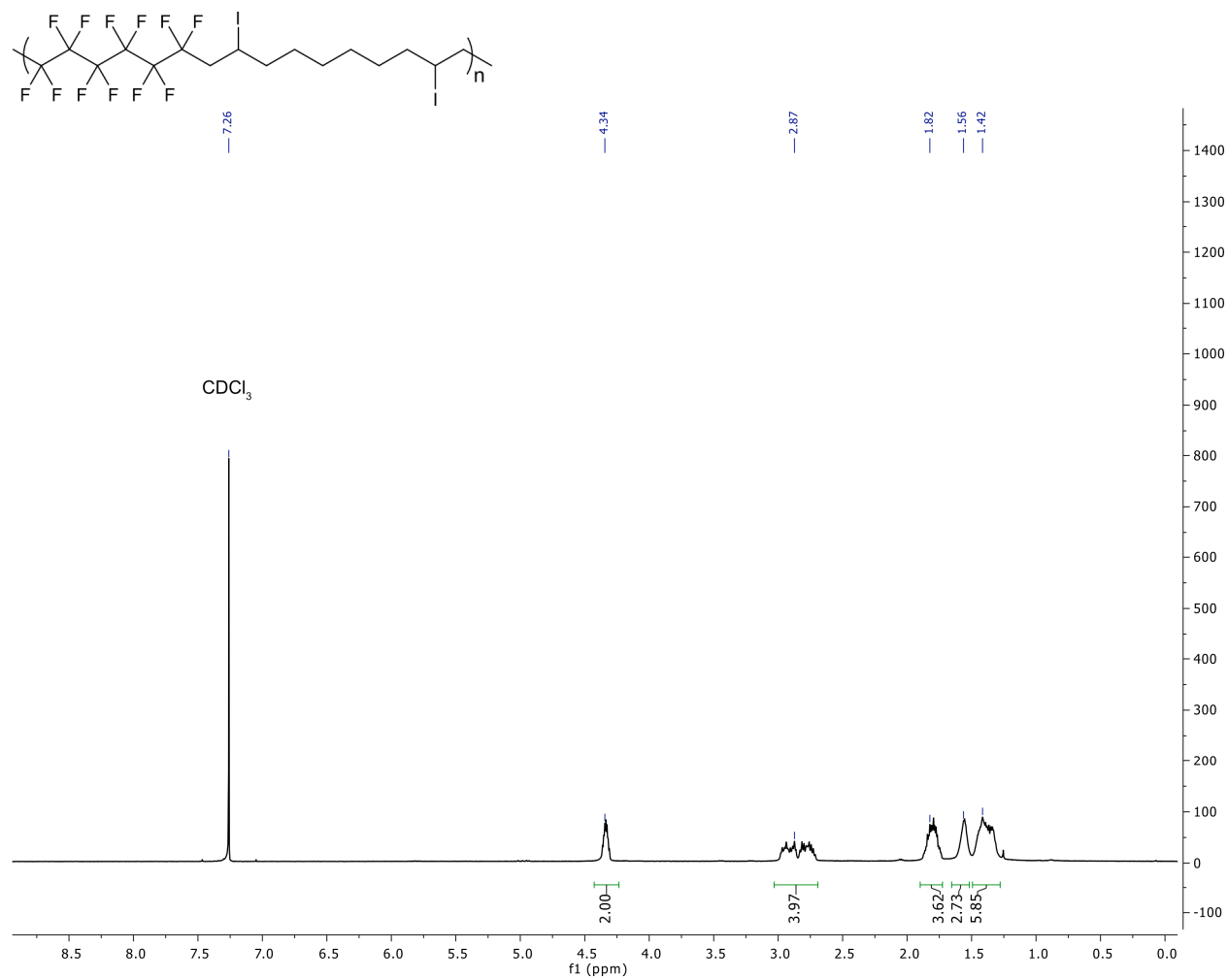
2.12, dec-9-en-1-yl 4-(dimethylamino)benzoate end-cap:



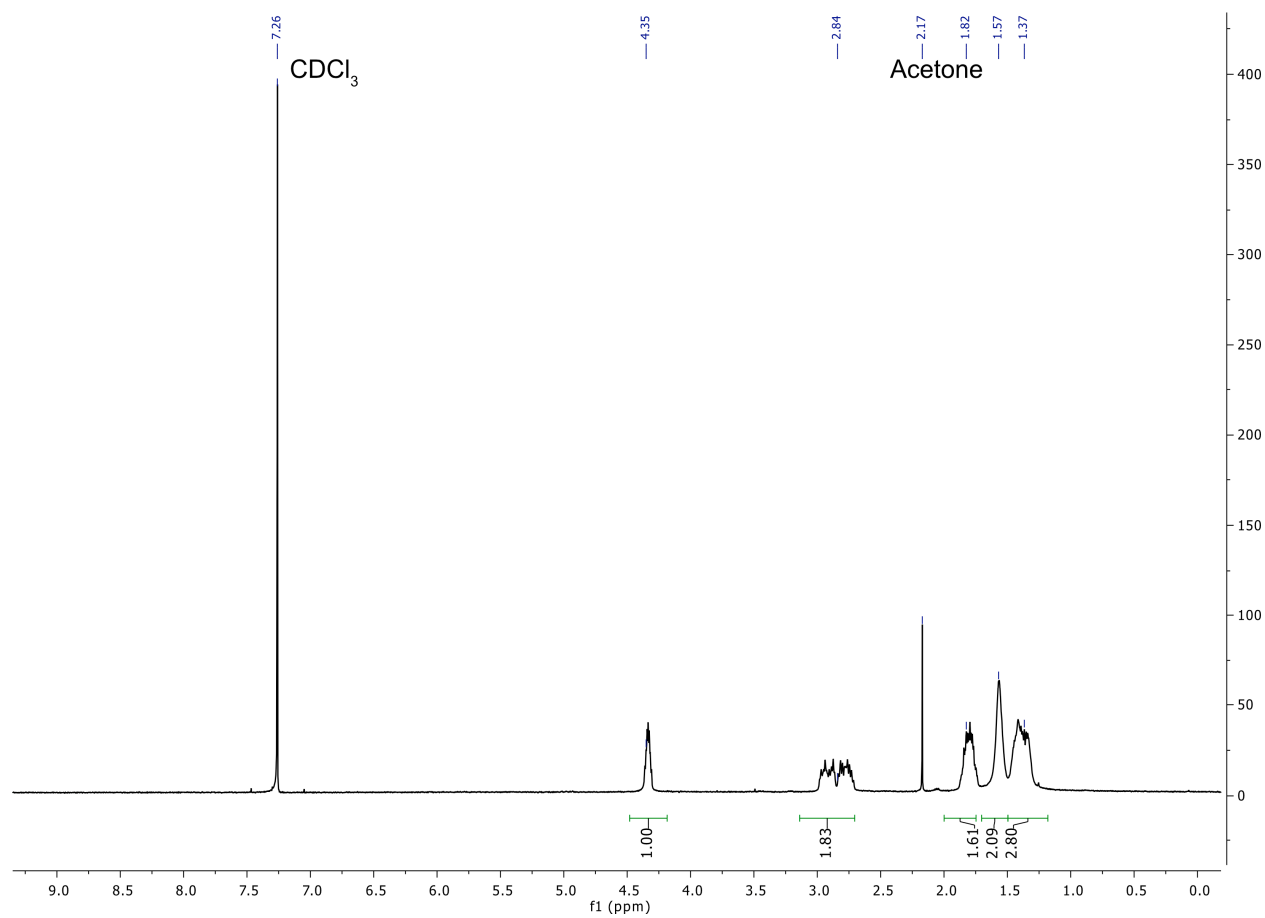
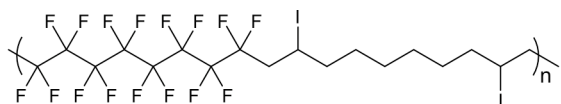
2.40, (E)-1,1,1,2,2,3,3,4,4,5,5,6,6-tridecafluorotetradec-7-ene



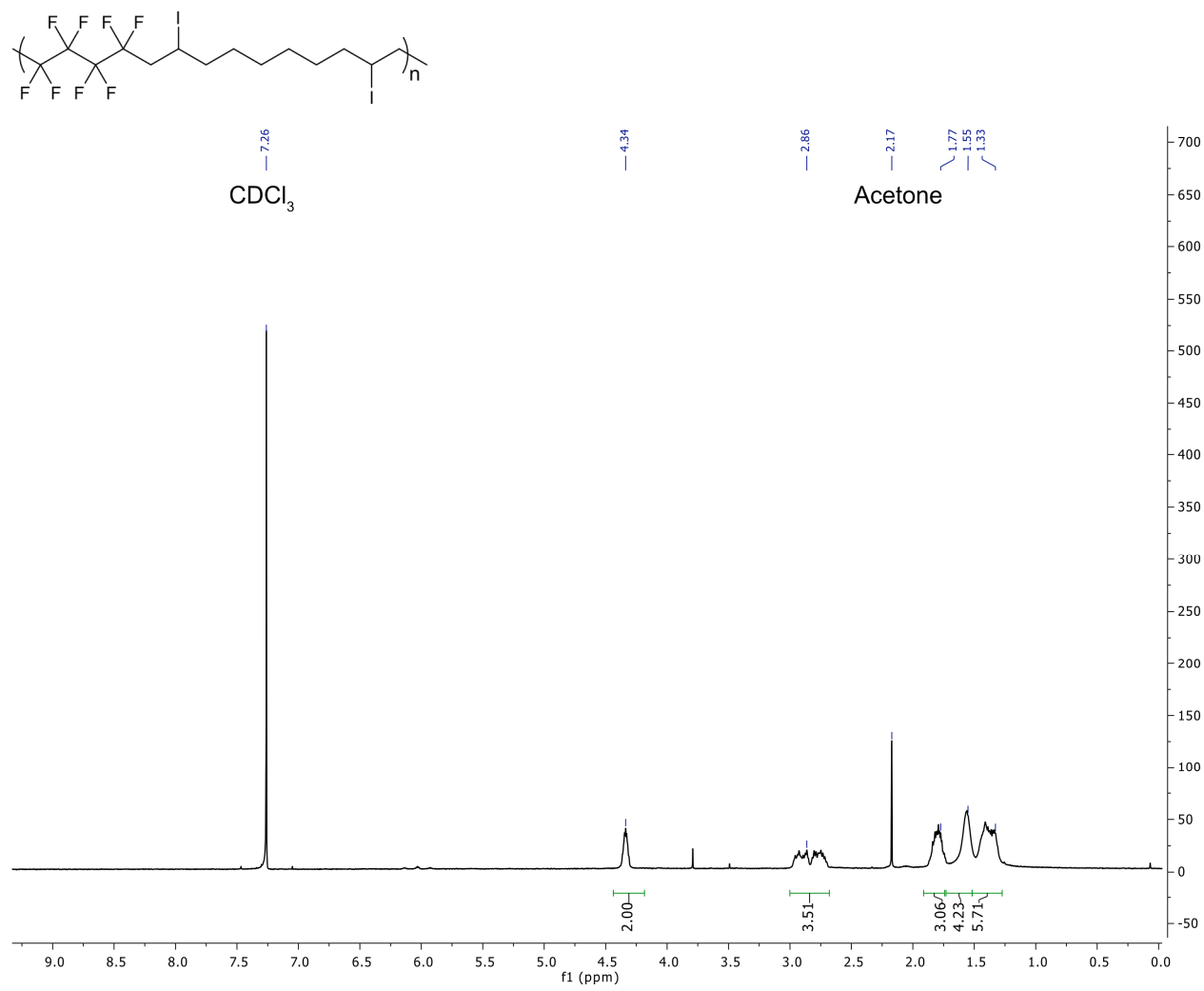
2.11a, 1-perfluorohexyl-2,9-diiododecyl block polymer:



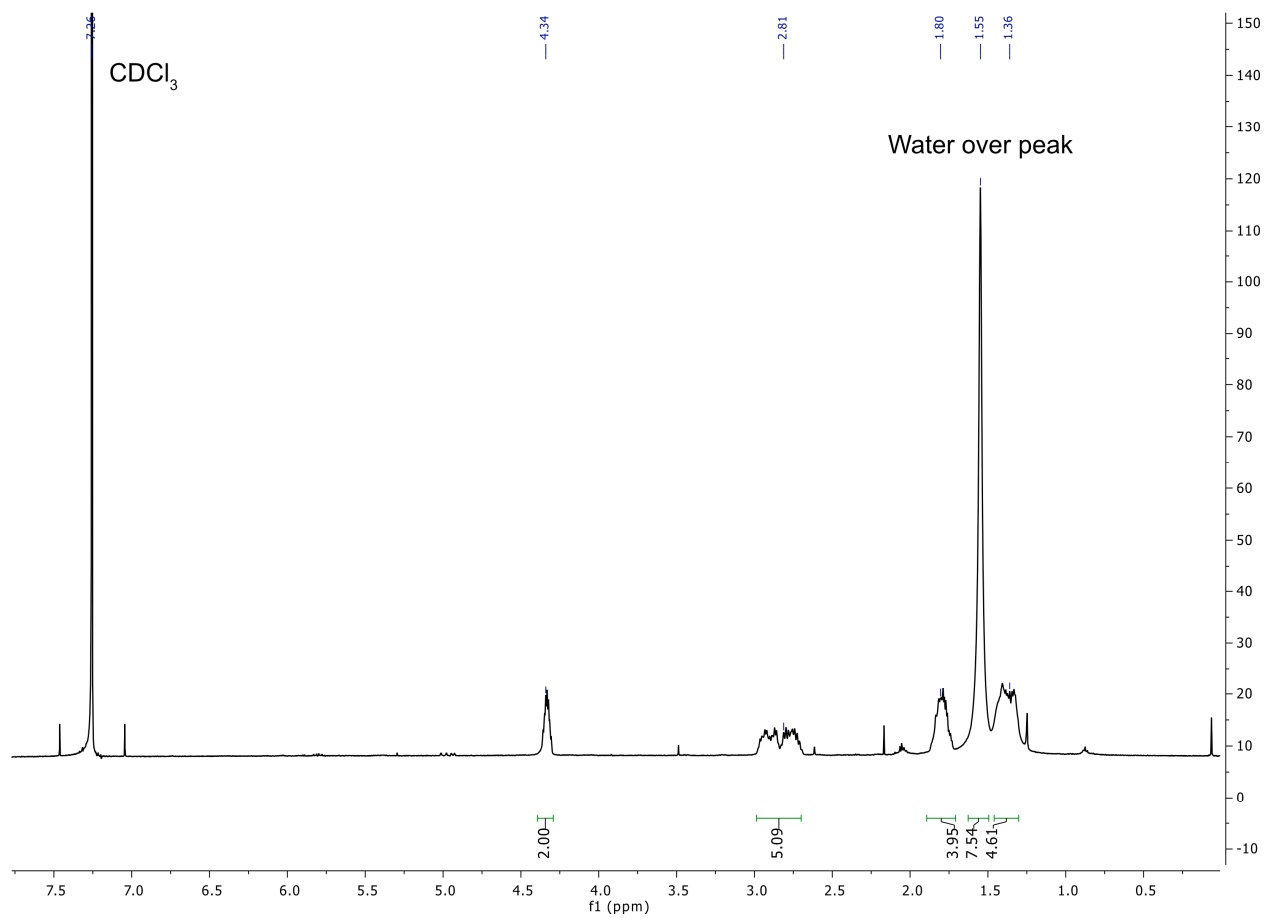
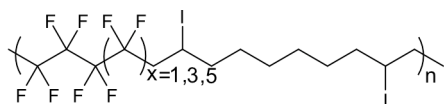
2.11b, 1-perfluorooctyl-2,9-diiododecyl block polymer:



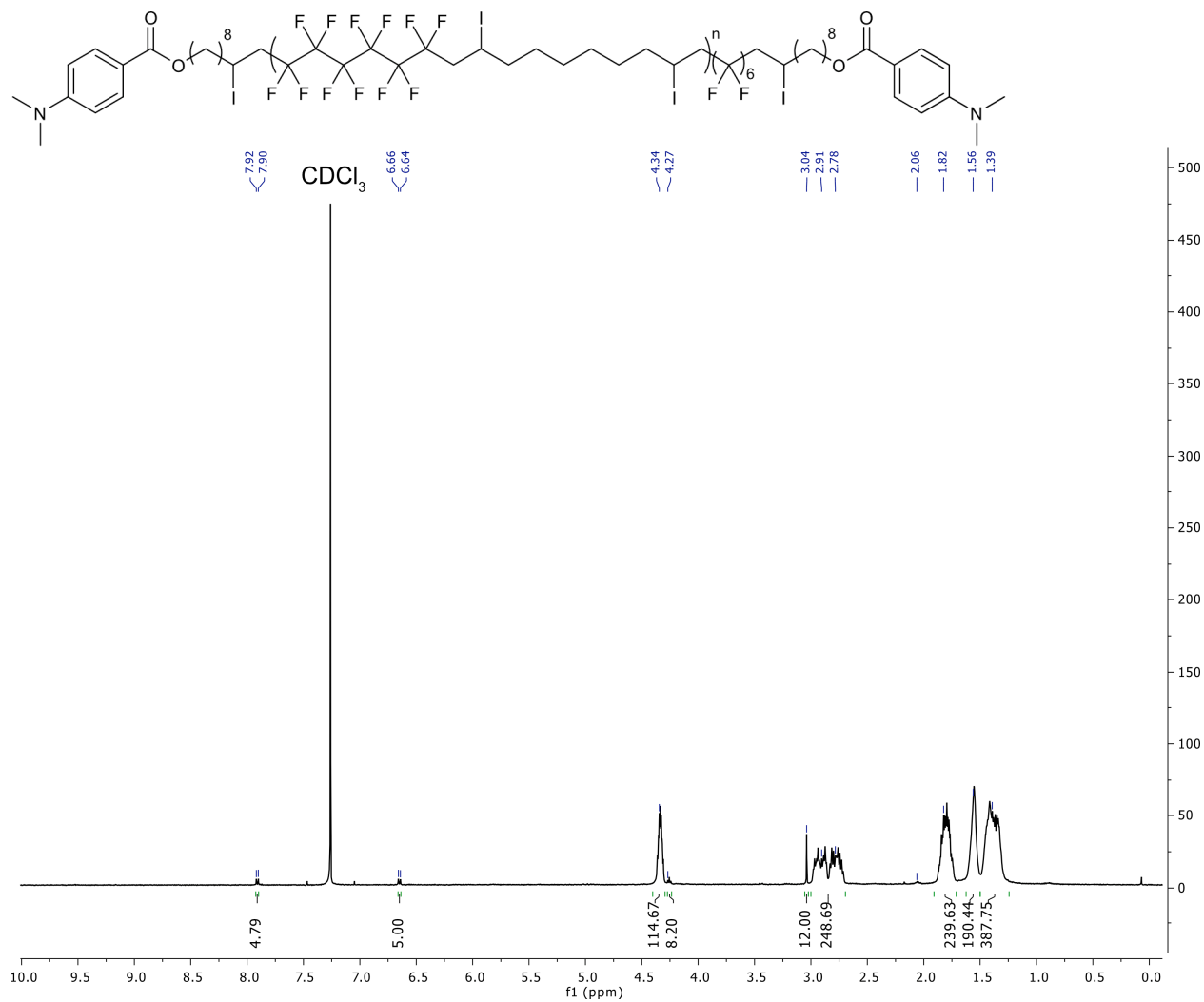
2.11c, 1-perfluorobutyl-2,9-diiododecyl block polymer:



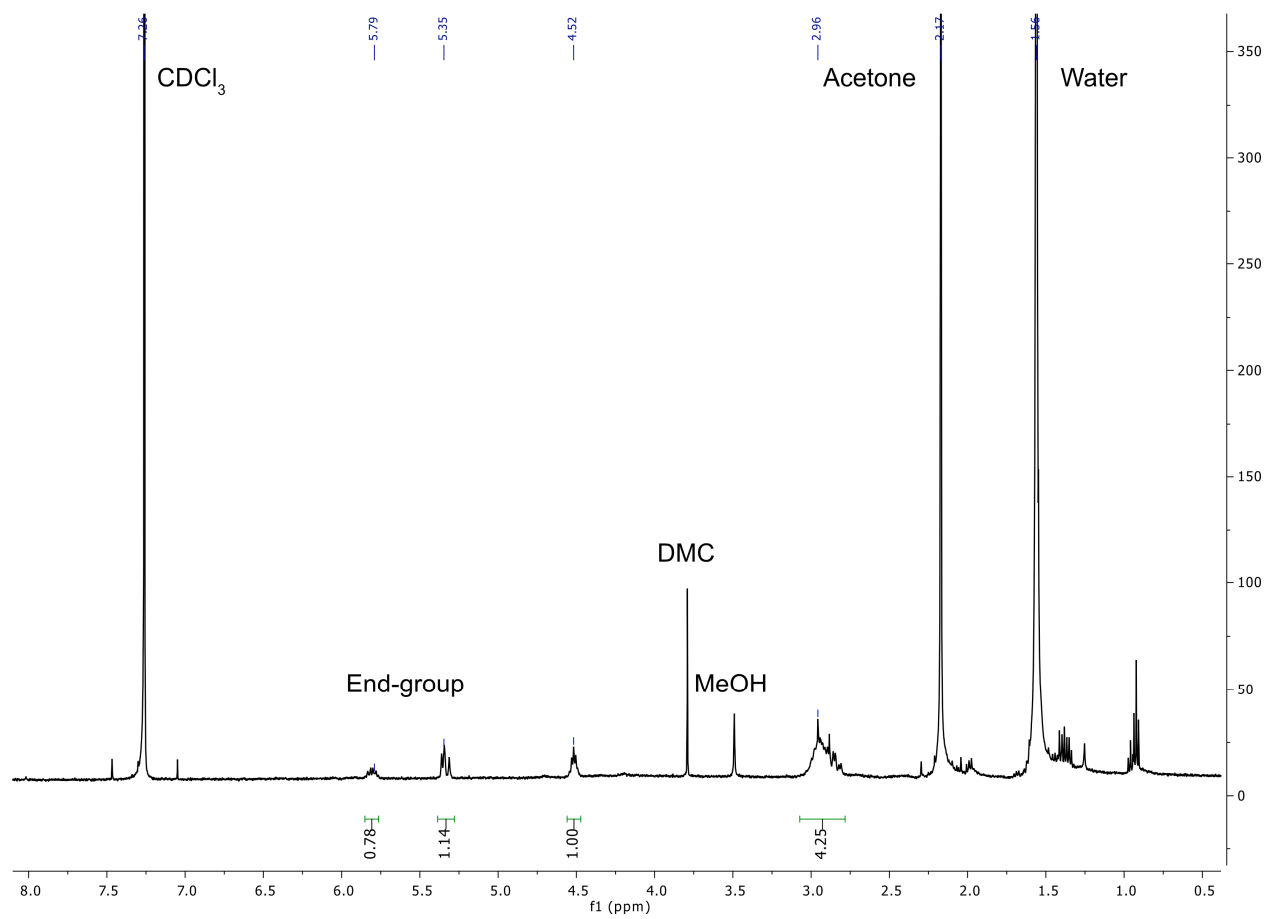
2.11d, 1-(perfluorobutyl- perfluorohexyl- perfluorooctyl)-2,9-diiododecyl block polymer:



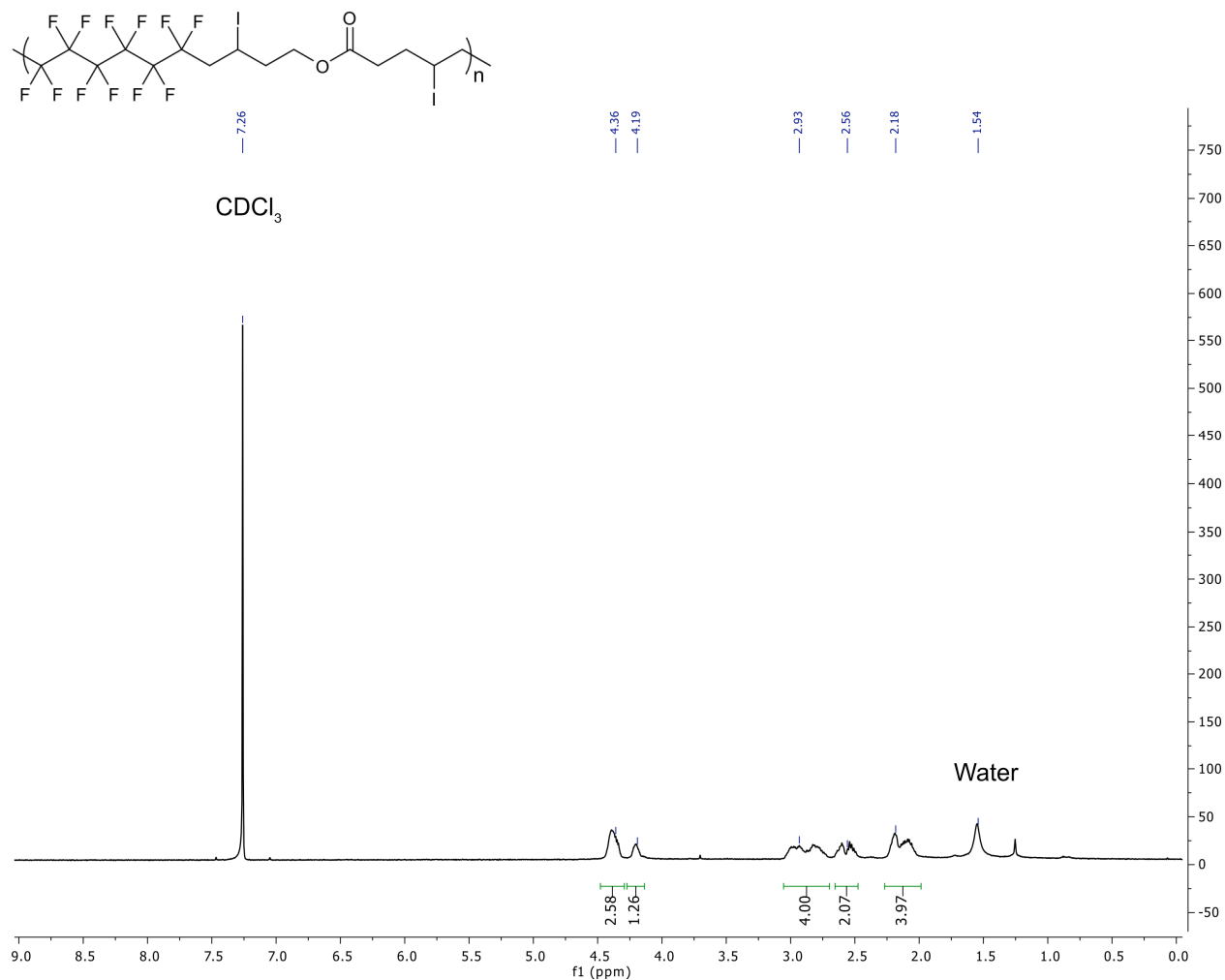
2.13, end-capped perfluorohexyl-1,8-diiododecyl block polymer:



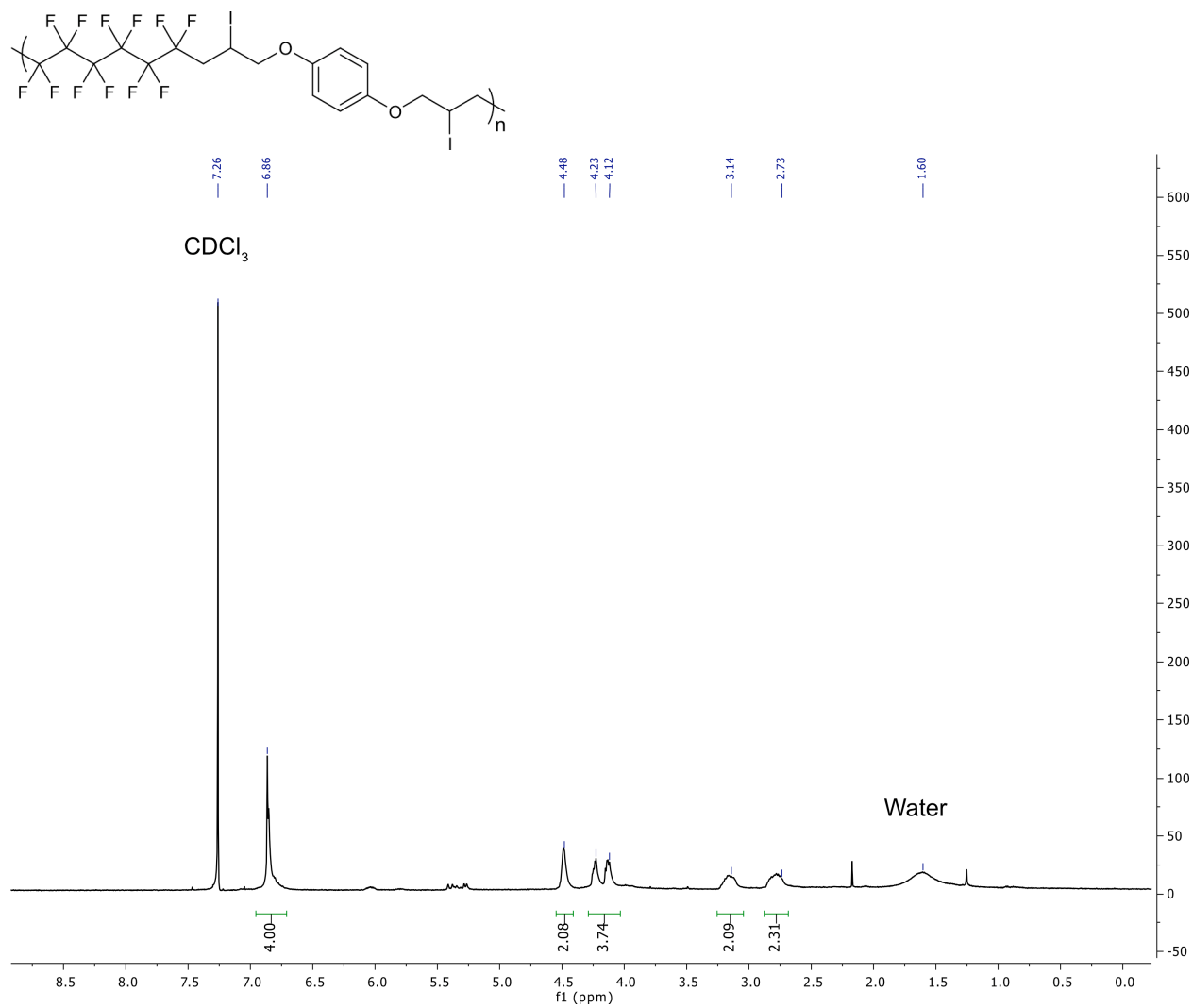
2.18b, 1-perfluorohexyl-2,11-diiodo-4,4,5,5,6,6,7,7,8,8,9,9 dodecafluorohexyl dodecane block polymer:



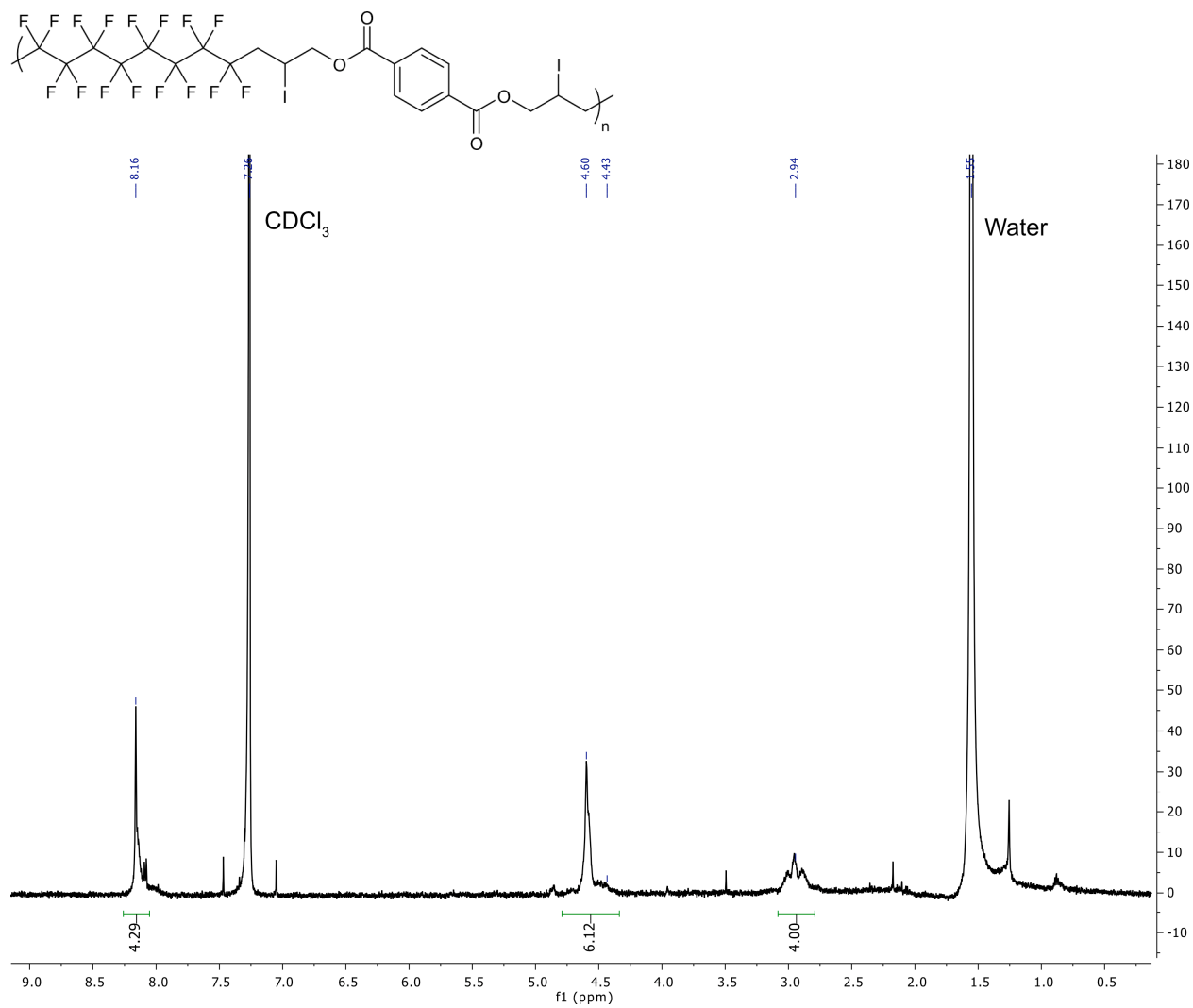
2.19a, 1-perfluorohexyl-2-iodo-butyl-pentan-4-iodo-ate:



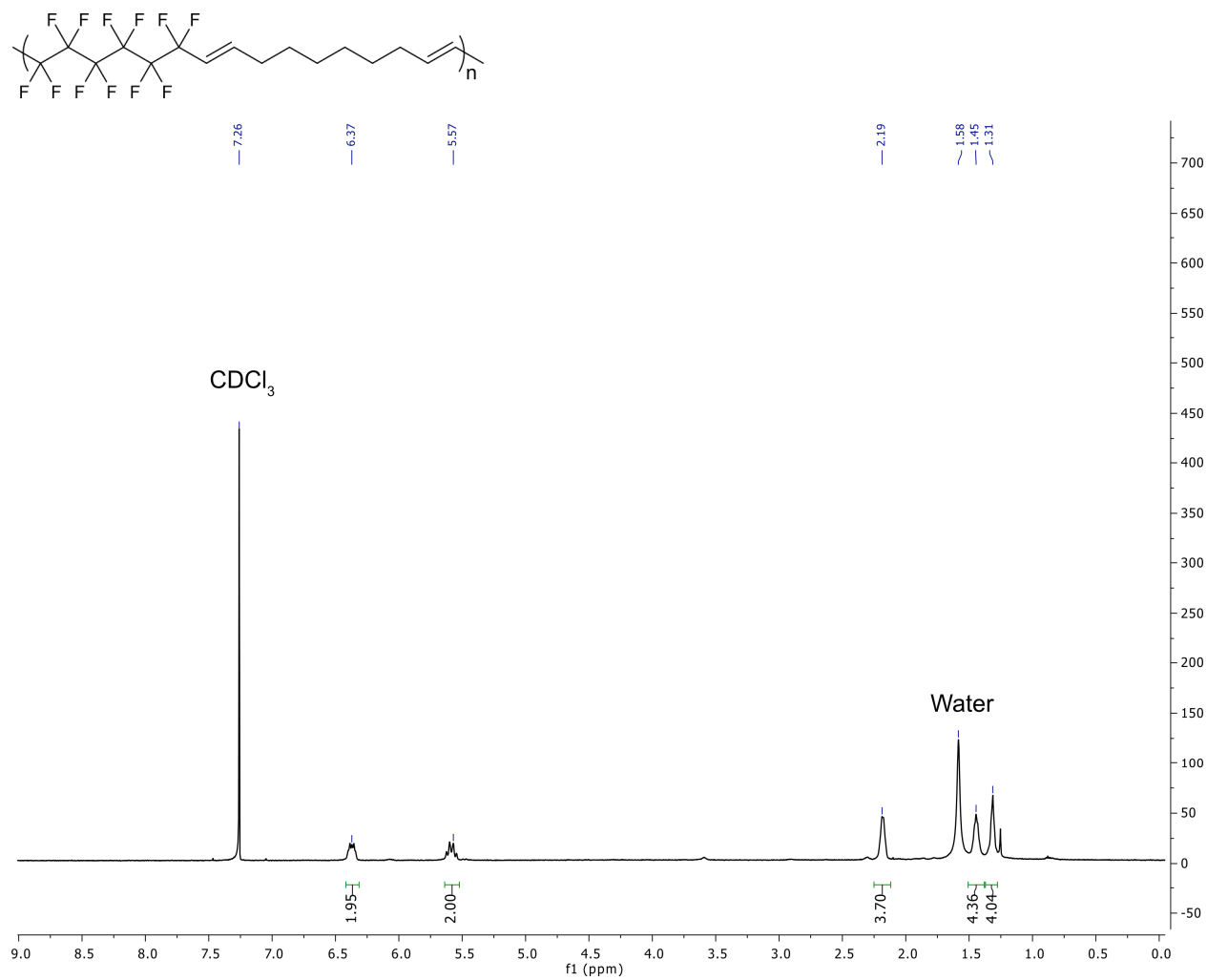
2.20b, 1,4-bis(2-iodopropyl-1-perfluorooctyl)benzene block polymer:



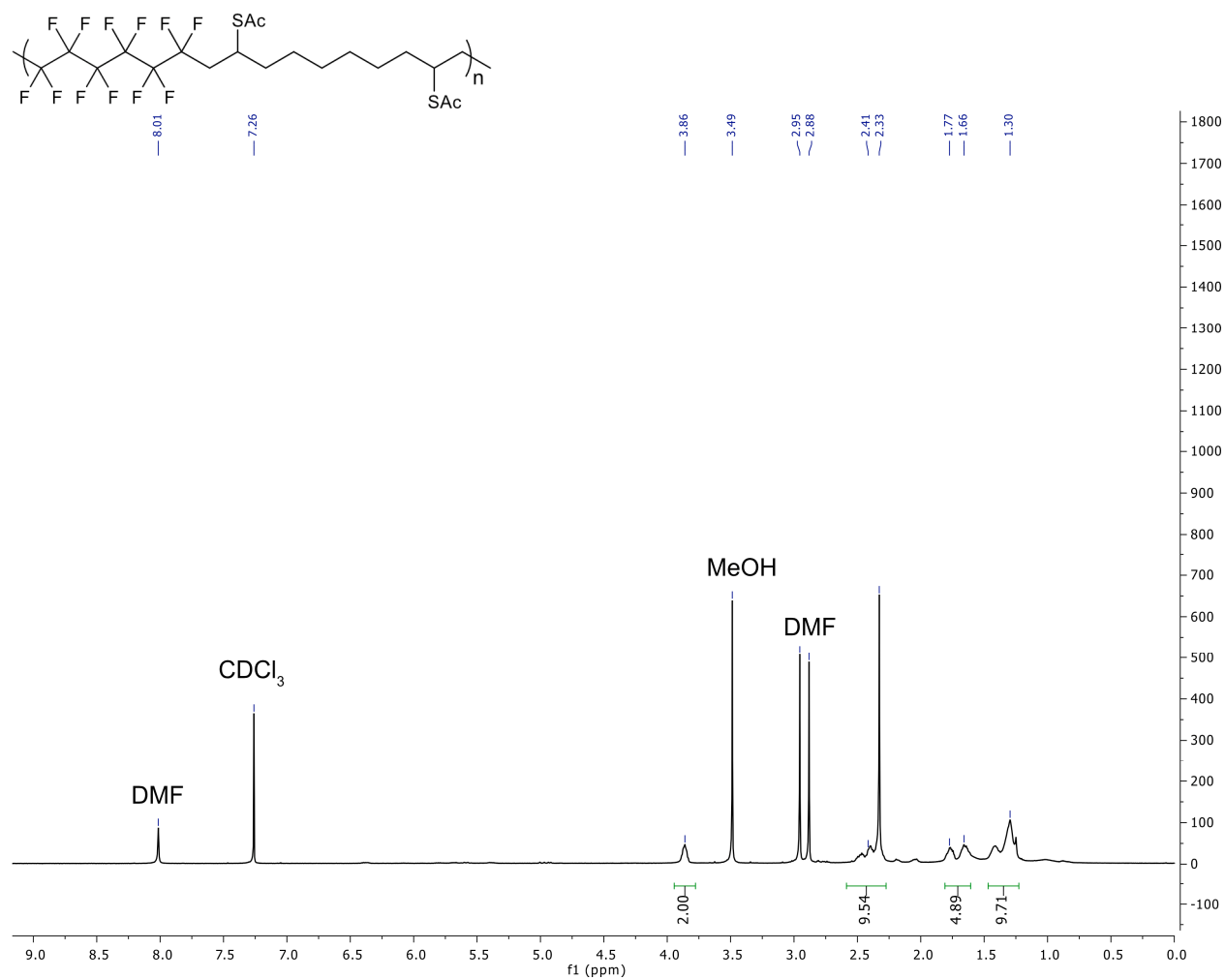
2.21b, 1,4-bis(2-iodopropyl-1-perfluorooctyl) terephthaloyl ester block polymer:



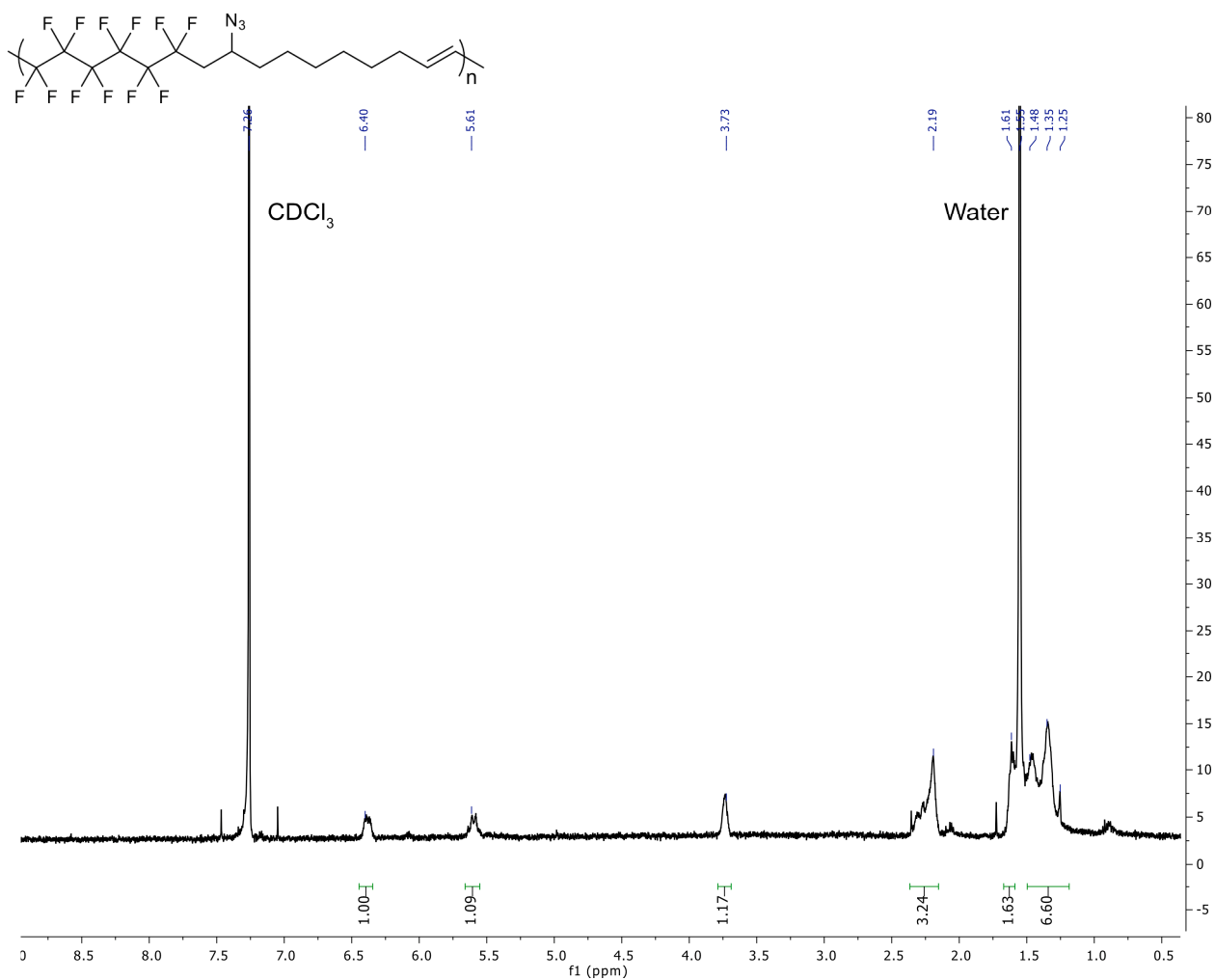
2.23, elimination of iodine from polymer 2.11a:



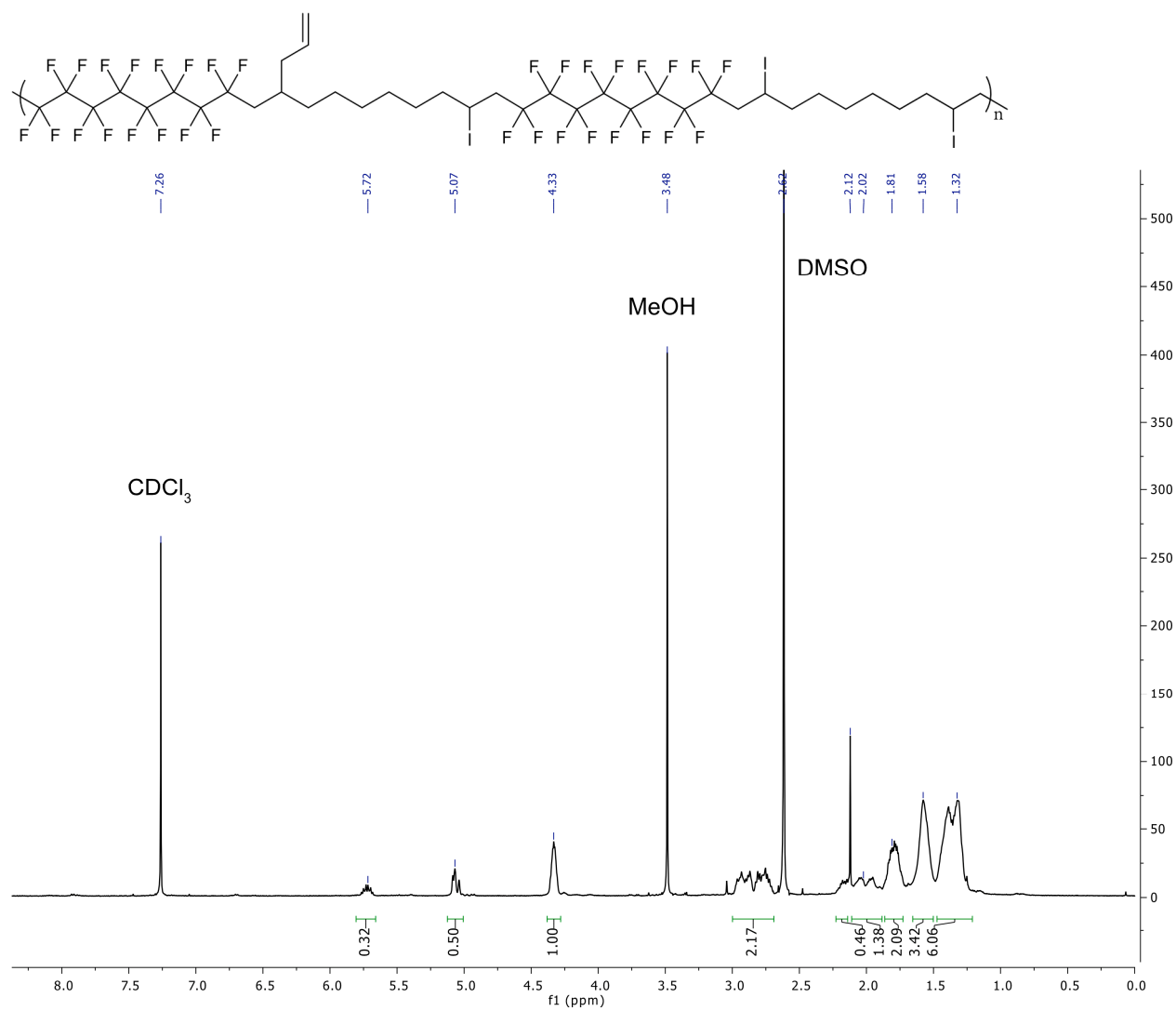
2.26, addition of potassium thioacetate to polymer 2.11a:



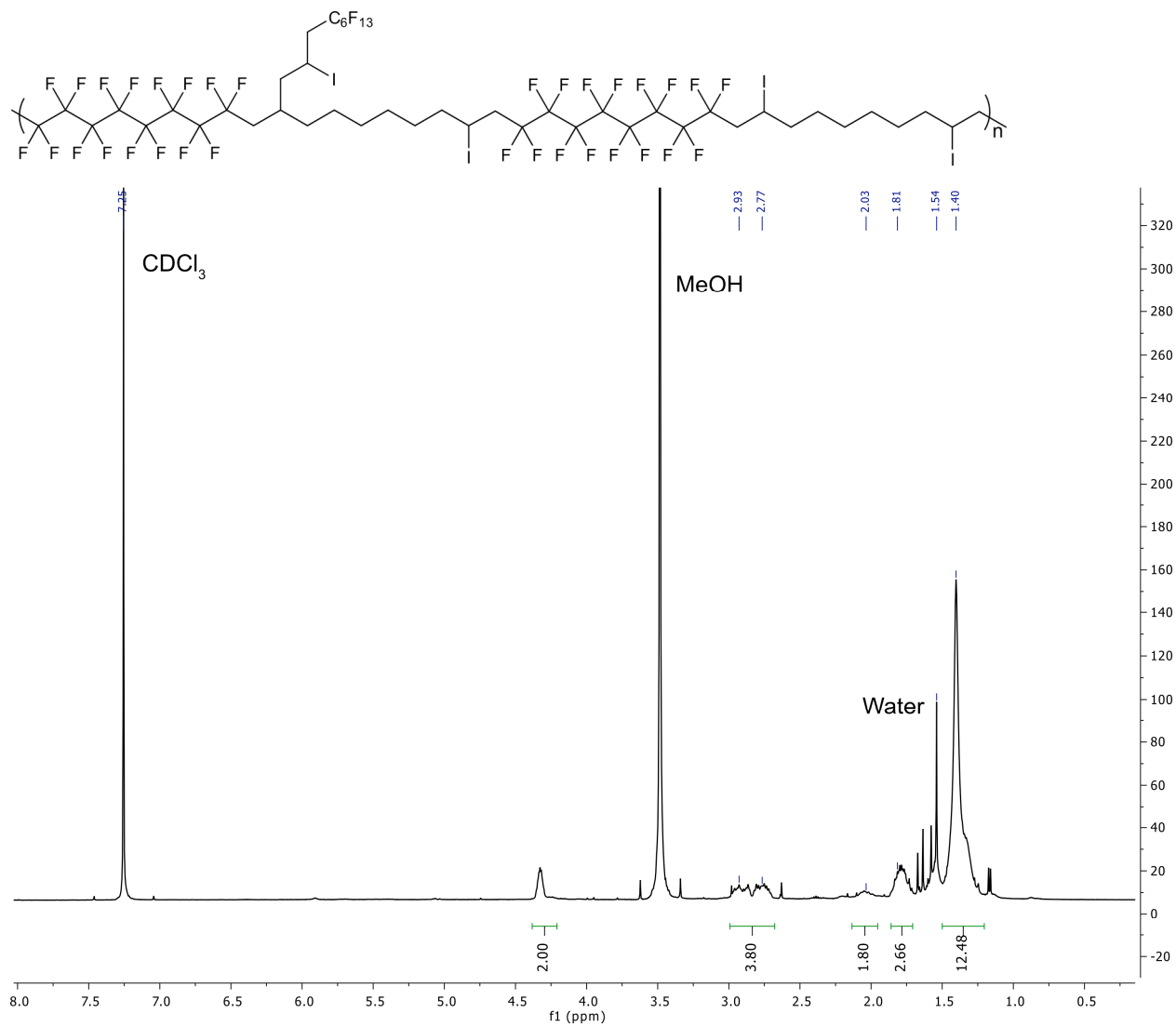
2.32, addition of sodium azide to polymer 2.11a:



2.37, free radical displacement of iodine on polymer 2.11a and addition of allyl group, 25 % incorporation:

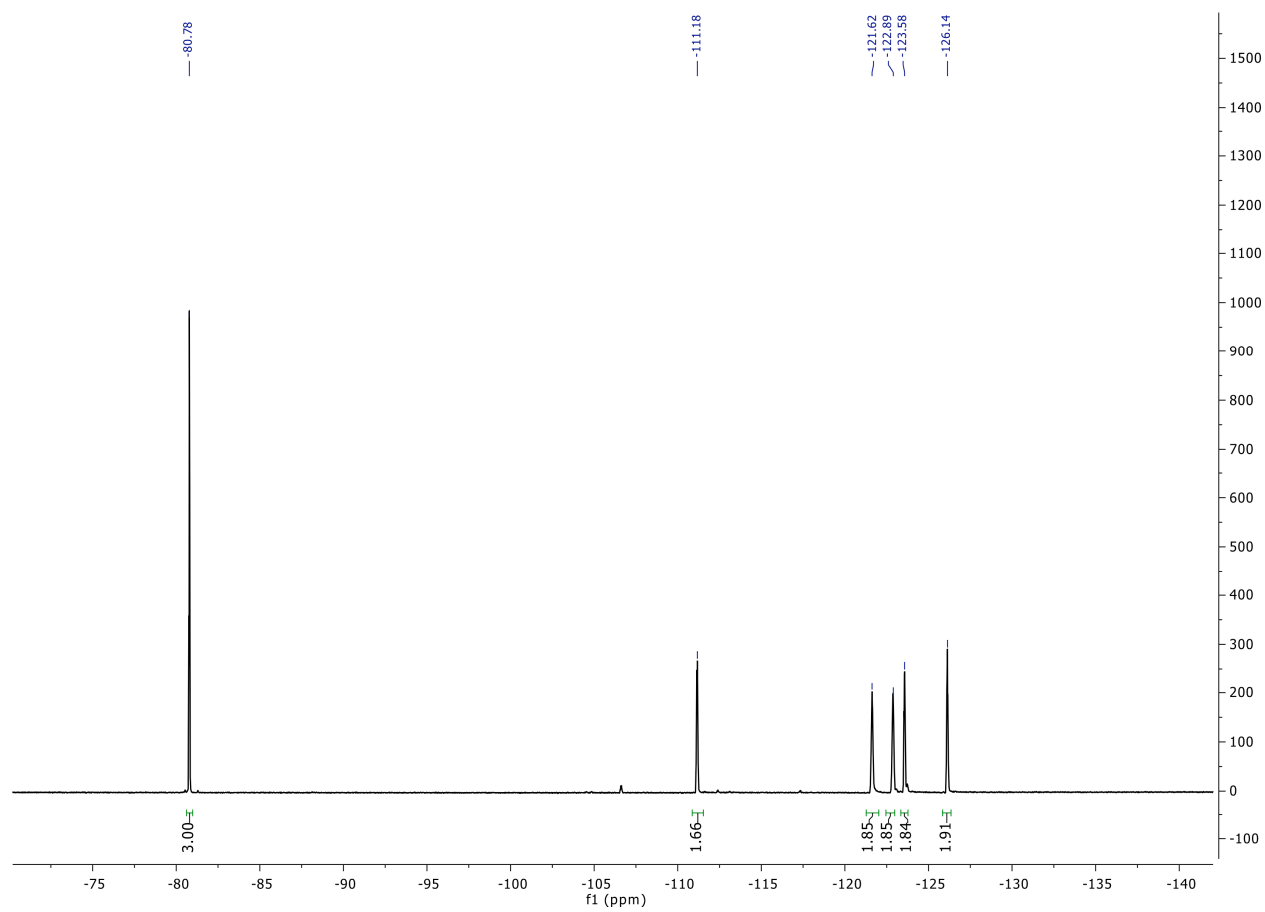
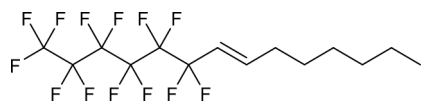


2.38, iodo-ene addition of perfluorohexyl iodide into polymer 2.36:

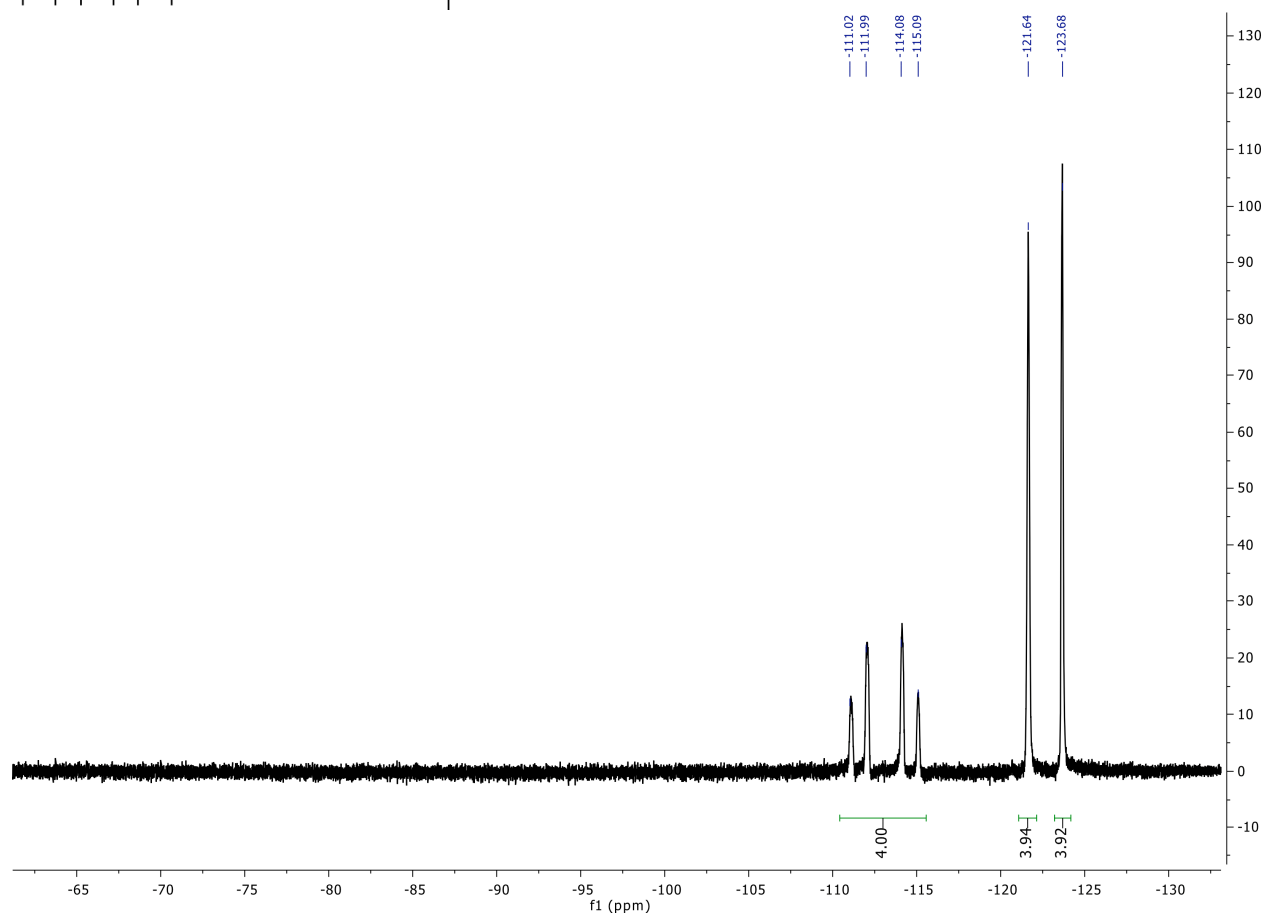
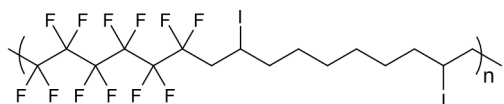


2.5.6 ^{19}F -NMR spectra:

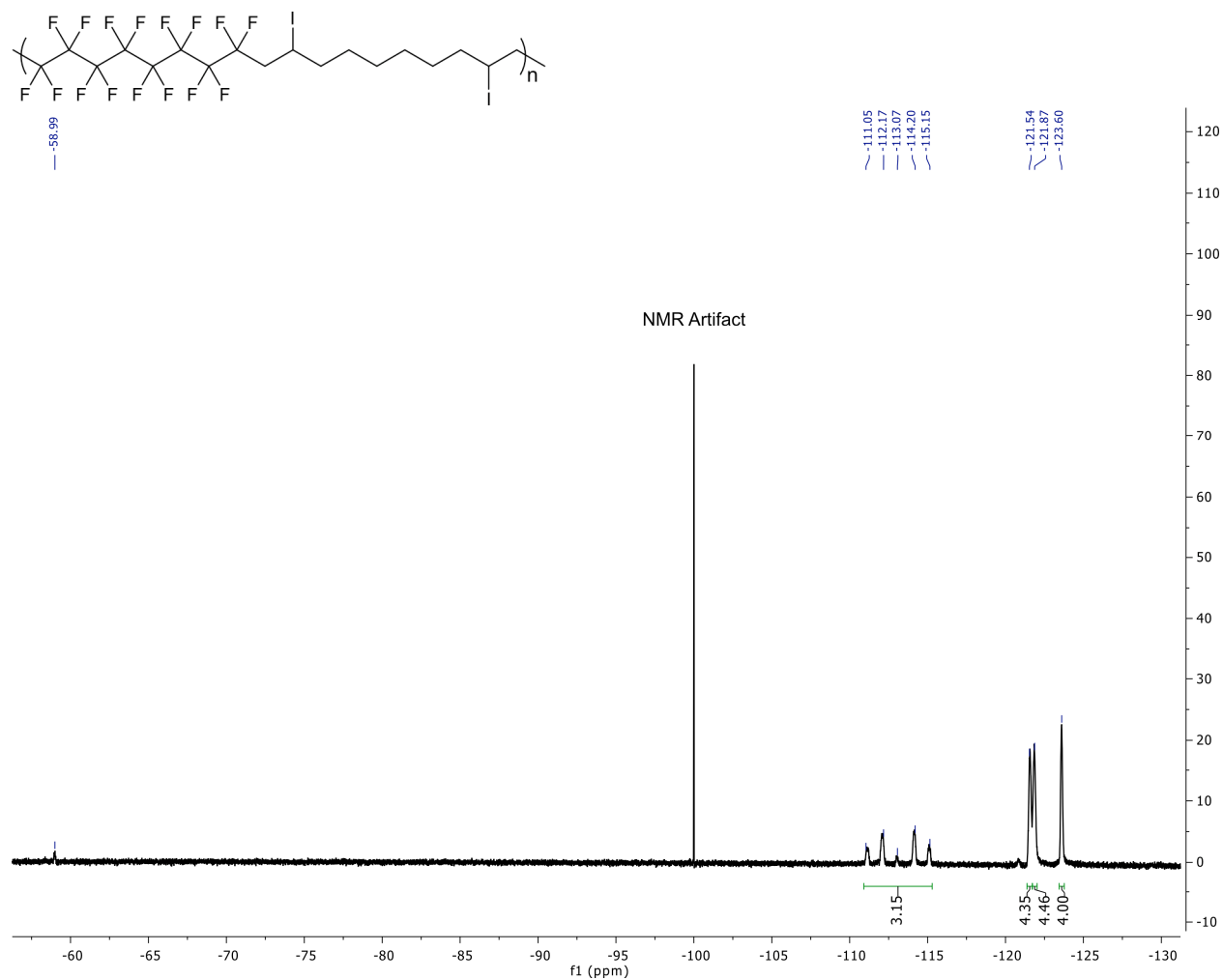
2.40, (E)-1,1,1,2,2,3,3,4,4,5,5,6,6-tridecafluorotetradec-7-ene



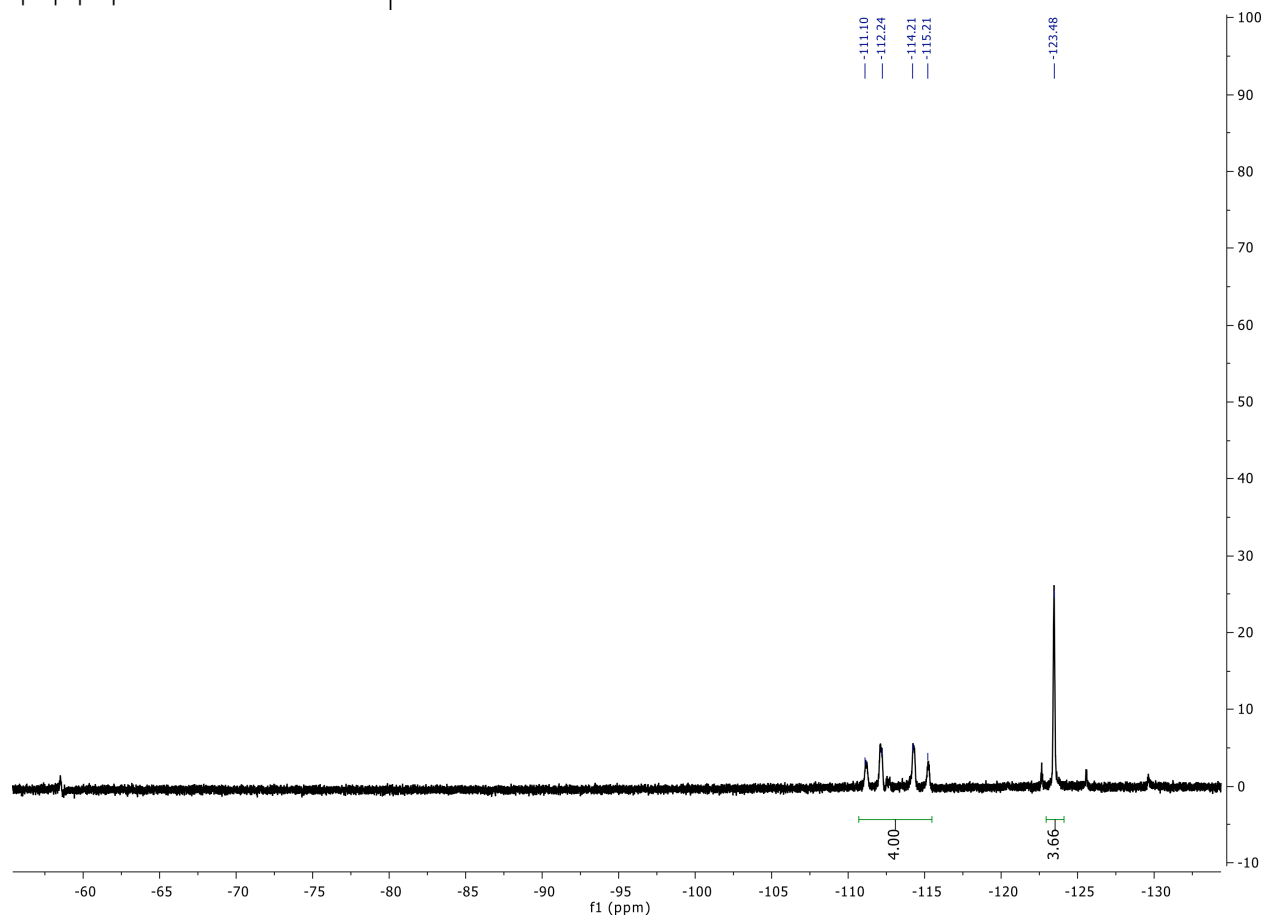
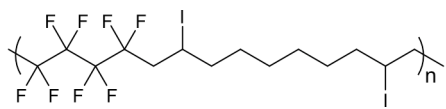
2.11a, 1-perfluorohexyl-2,9-diiododecyl block polymer:



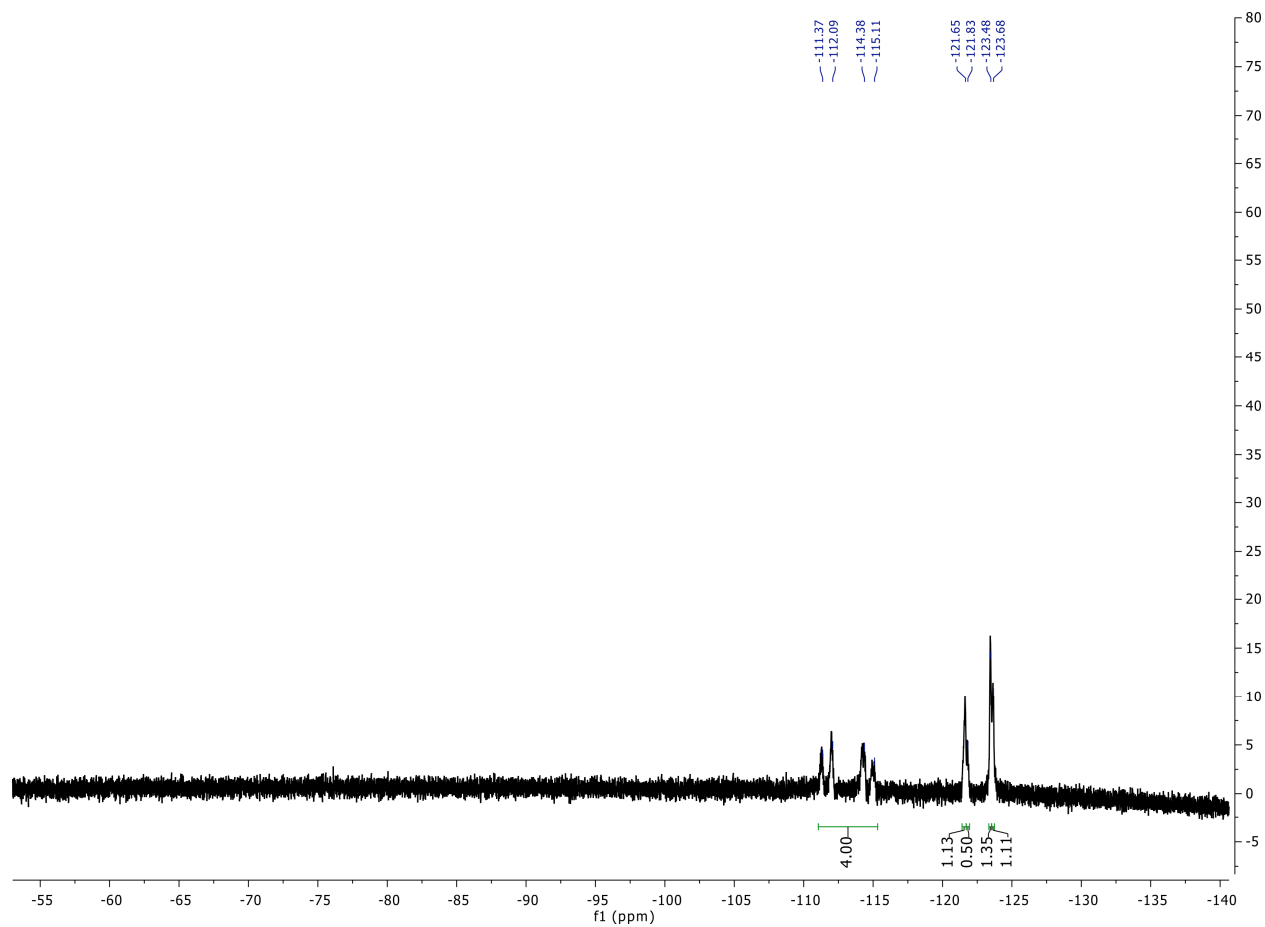
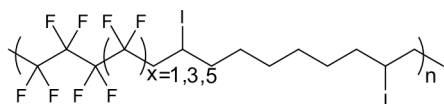
2.11b, 1-perfluorooctyl-2,9-diiododecyl block polymer:



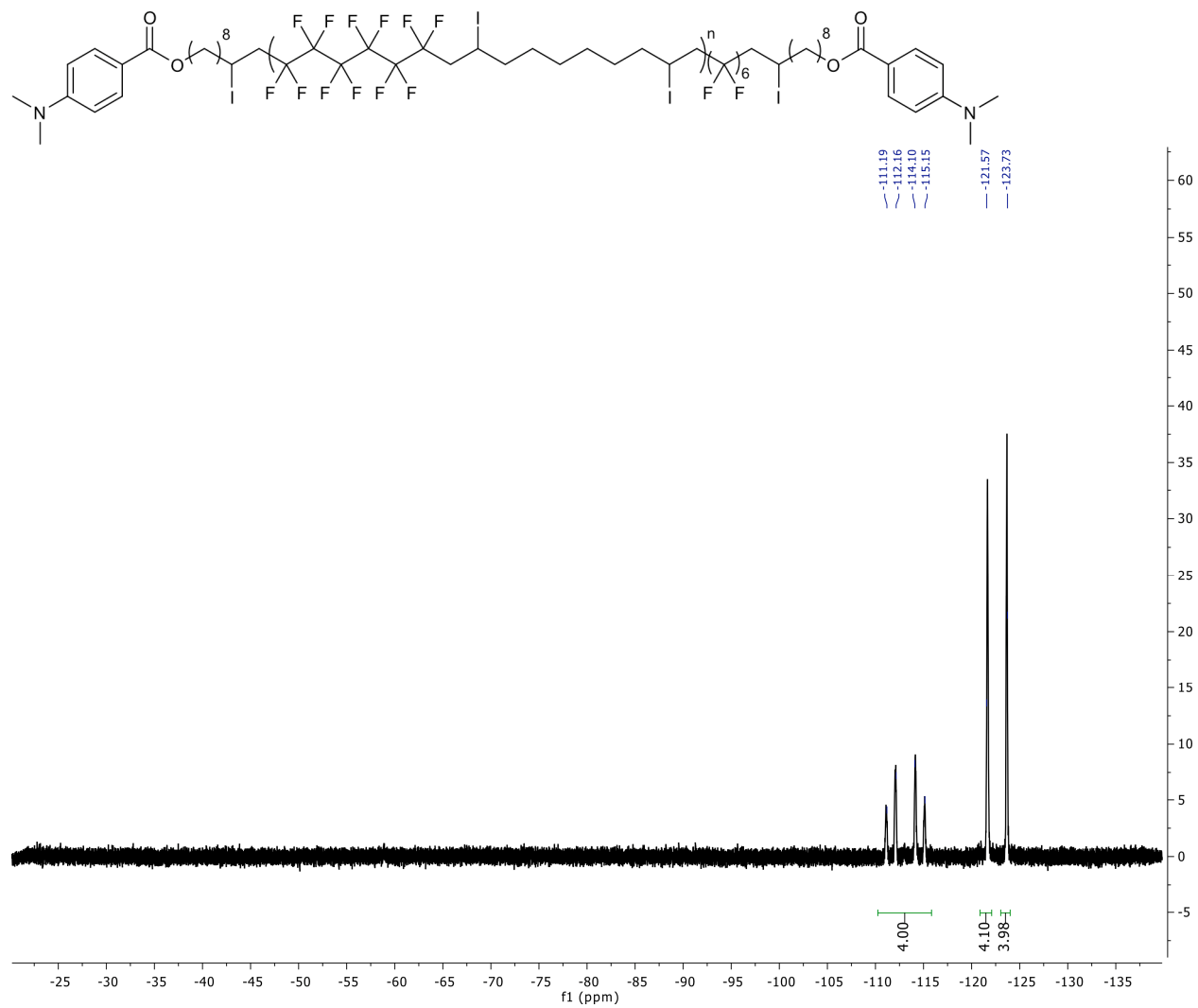
2.11c, 1-perfluorobutyl-2,9-diiododecyl block polymer:



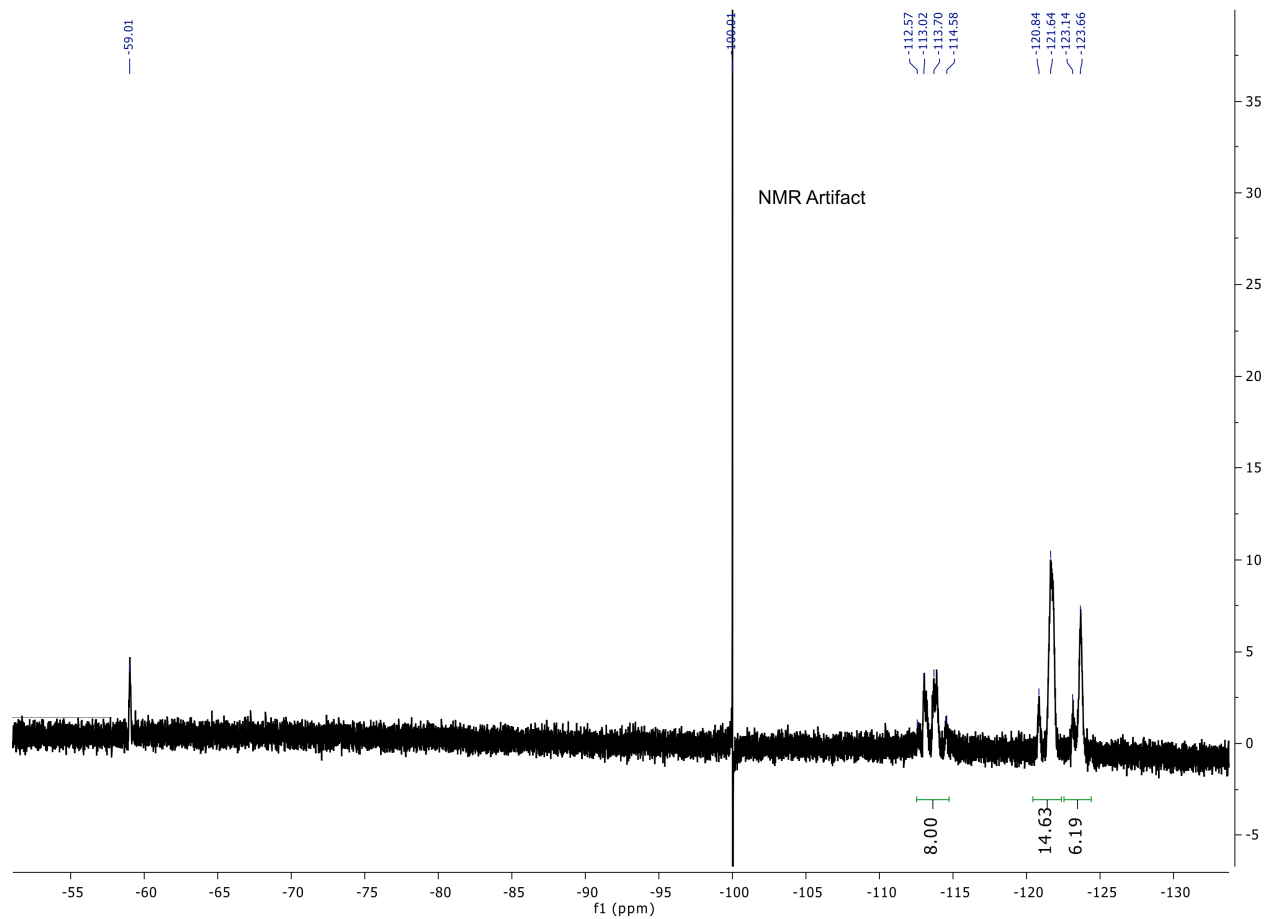
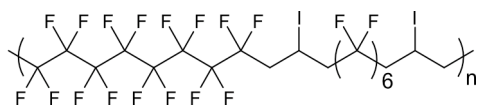
2.11d, 1-(perfluorobutyl- perfluorohexyl- perfluorooctyl)-2,9-diiododecyl block polymer:



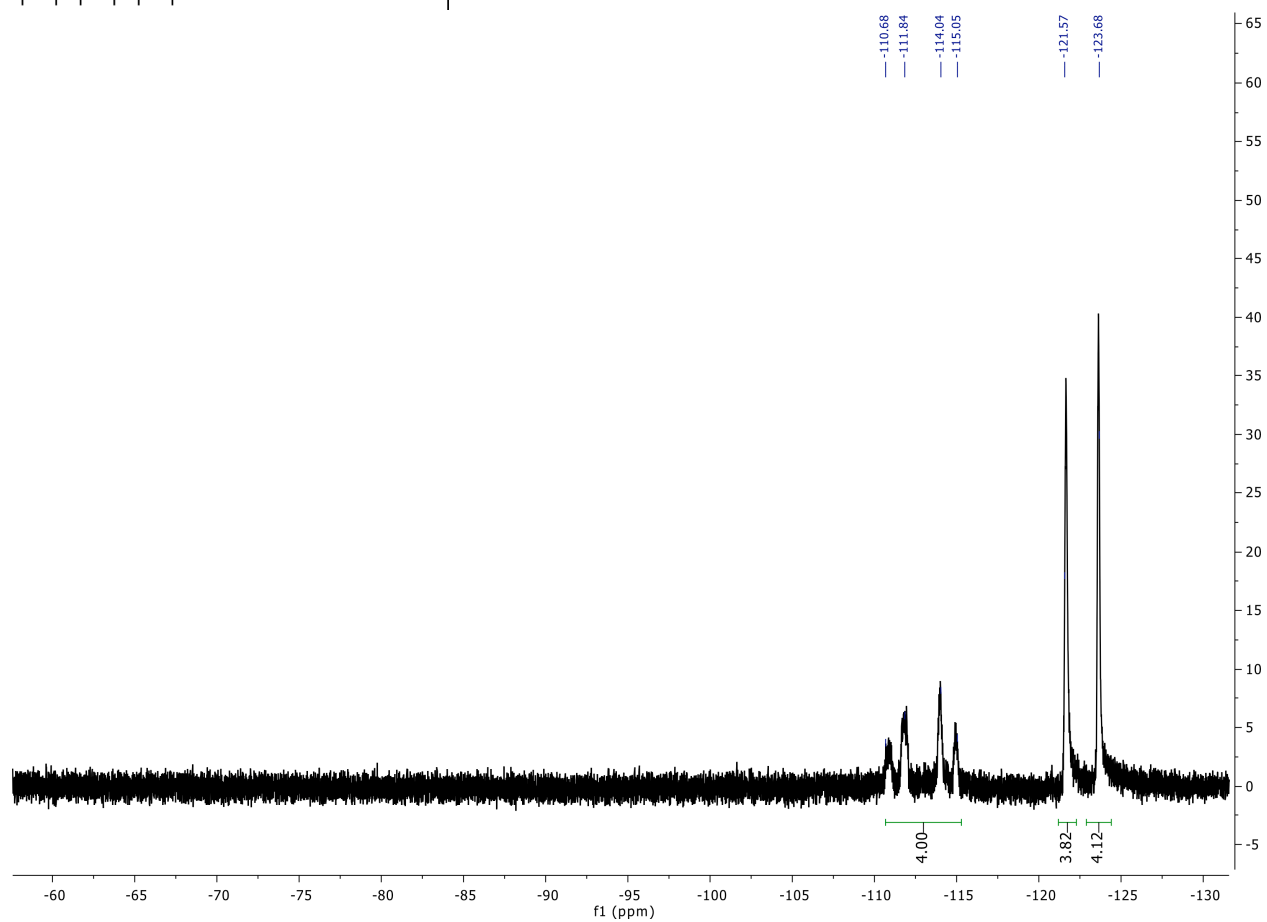
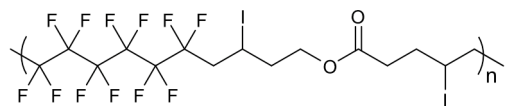
2.13, end-capped perfluorohexyl-1,8-diiododecyl block polymer:



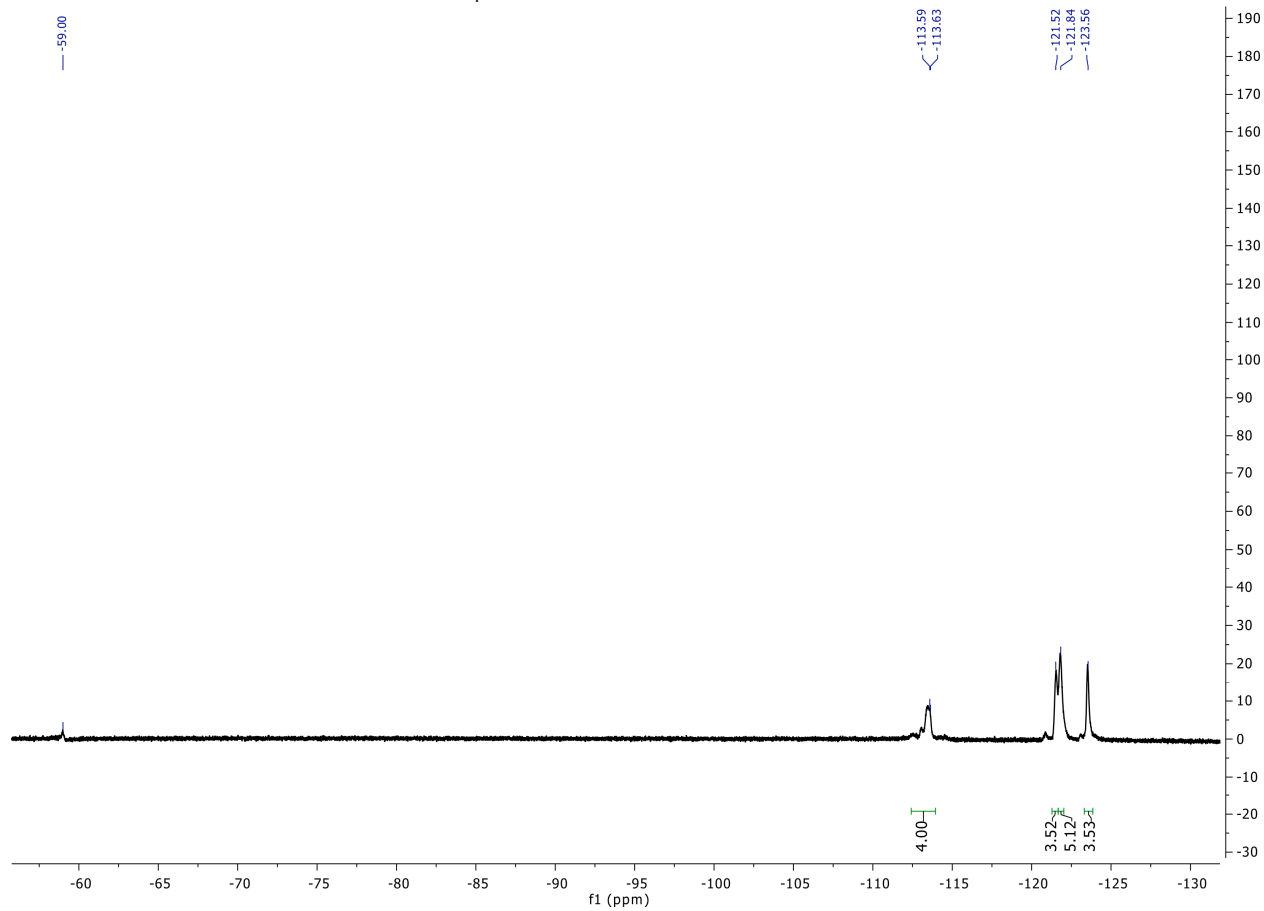
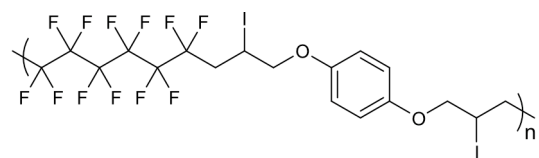
2.18b, 1-perfluorohexyl-2,11-diiodo-4,4,5,5,6,6,7,7,8,8,9,9 dodecafluorohexyl dodecane block polymer:



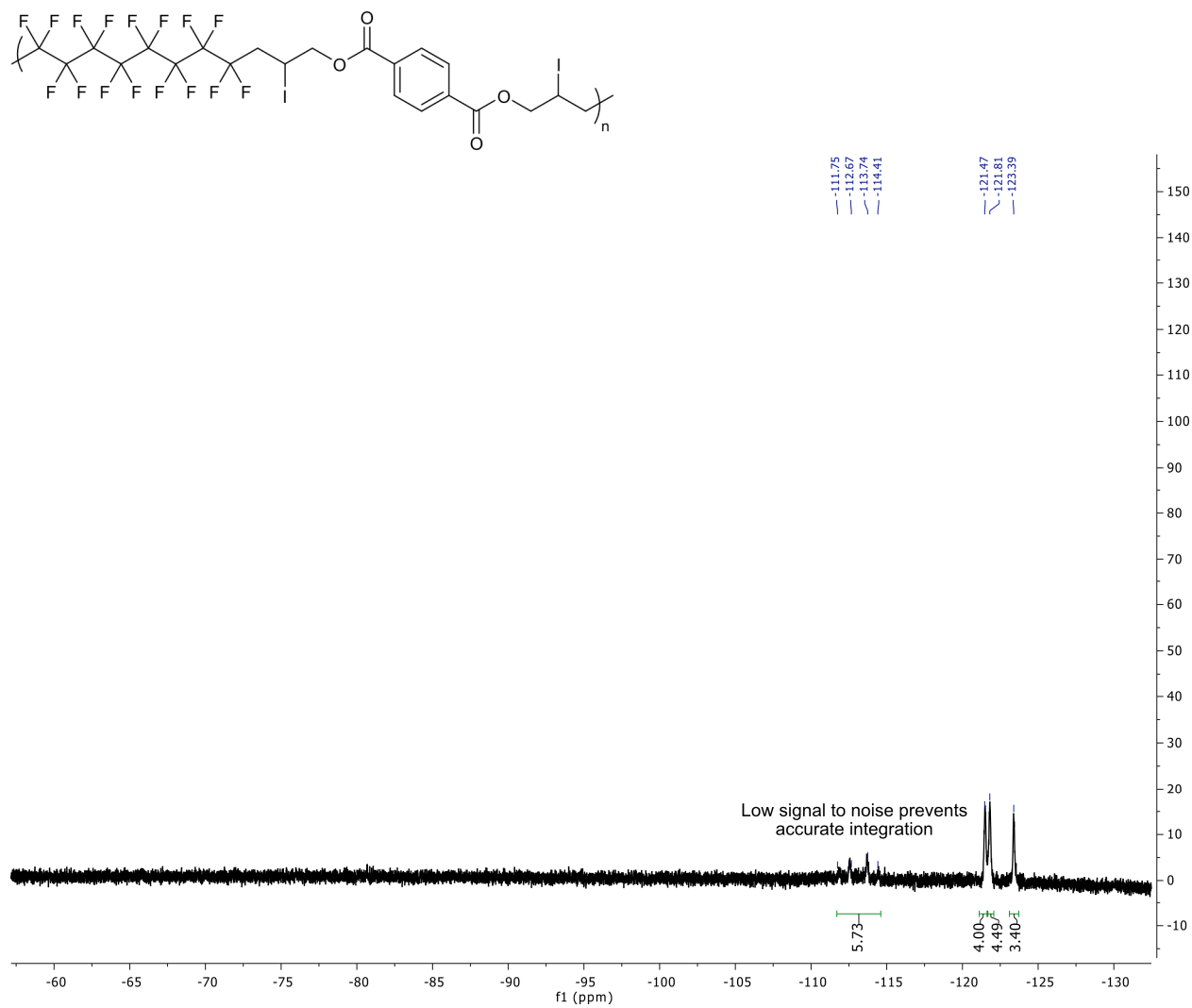
2.19a, 1-perfluorohexyl-2-iodo-butyl-pentan-4-iodo-ate:



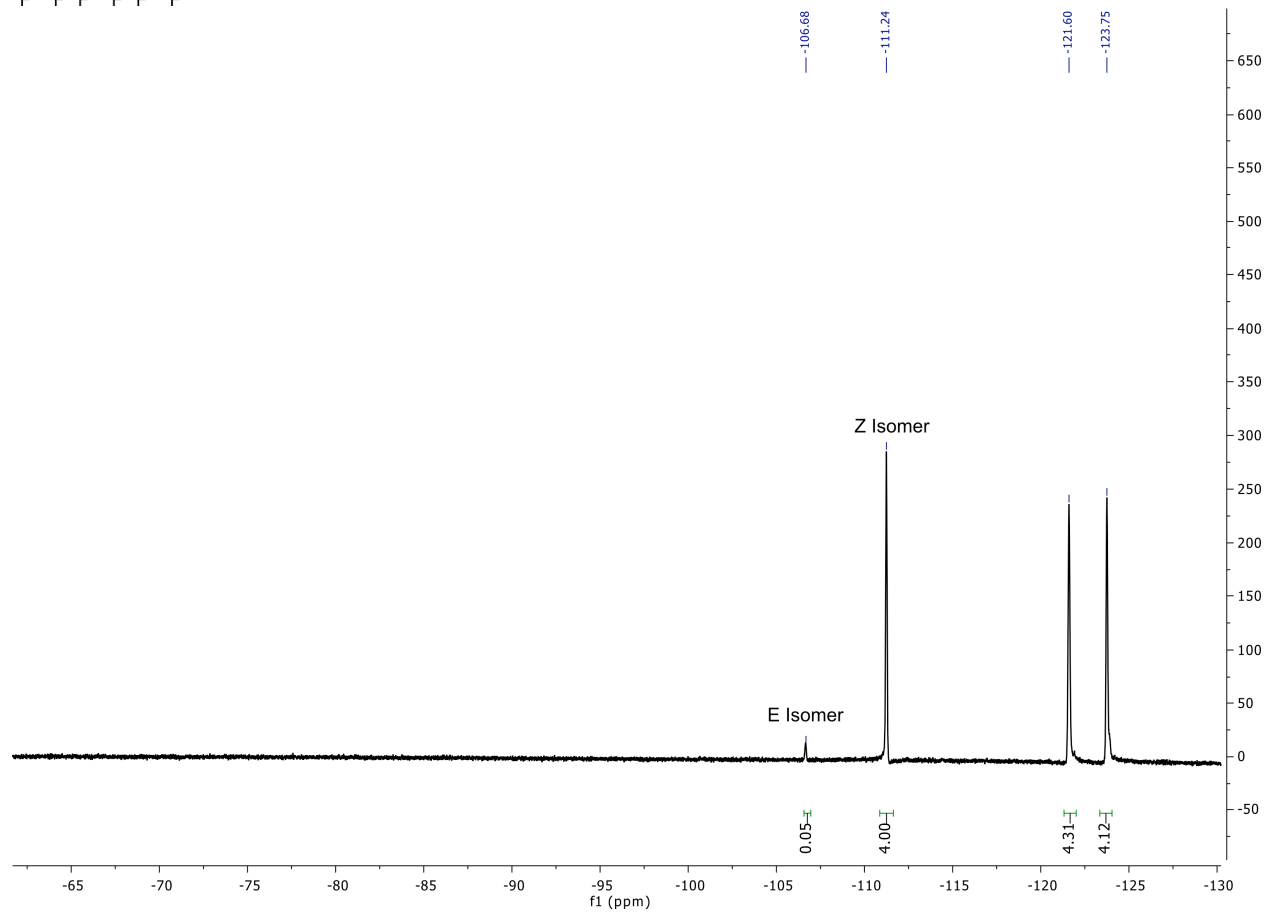
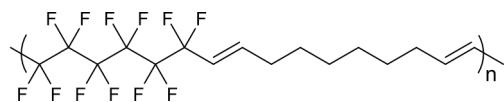
2.20b, 1,4-bis(2-iodopropyl-1-perfluorooctyl)benzene block polymer:



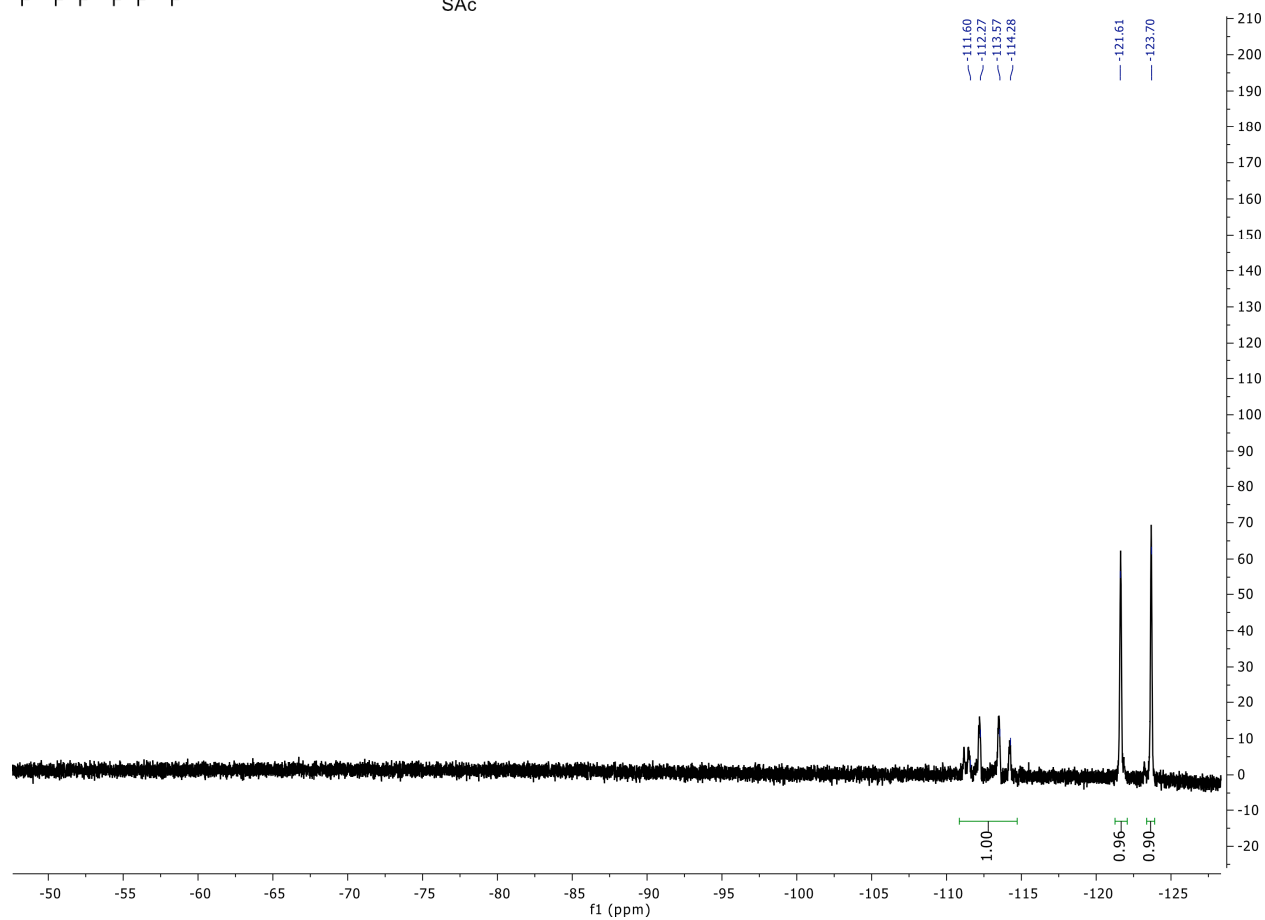
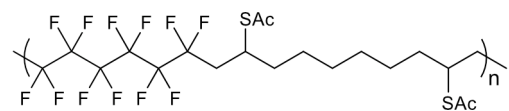
2.21b, 1,4-bis(2-iodopropyl-1-perfluorooctyl) terephthaloyl ester block polymer:



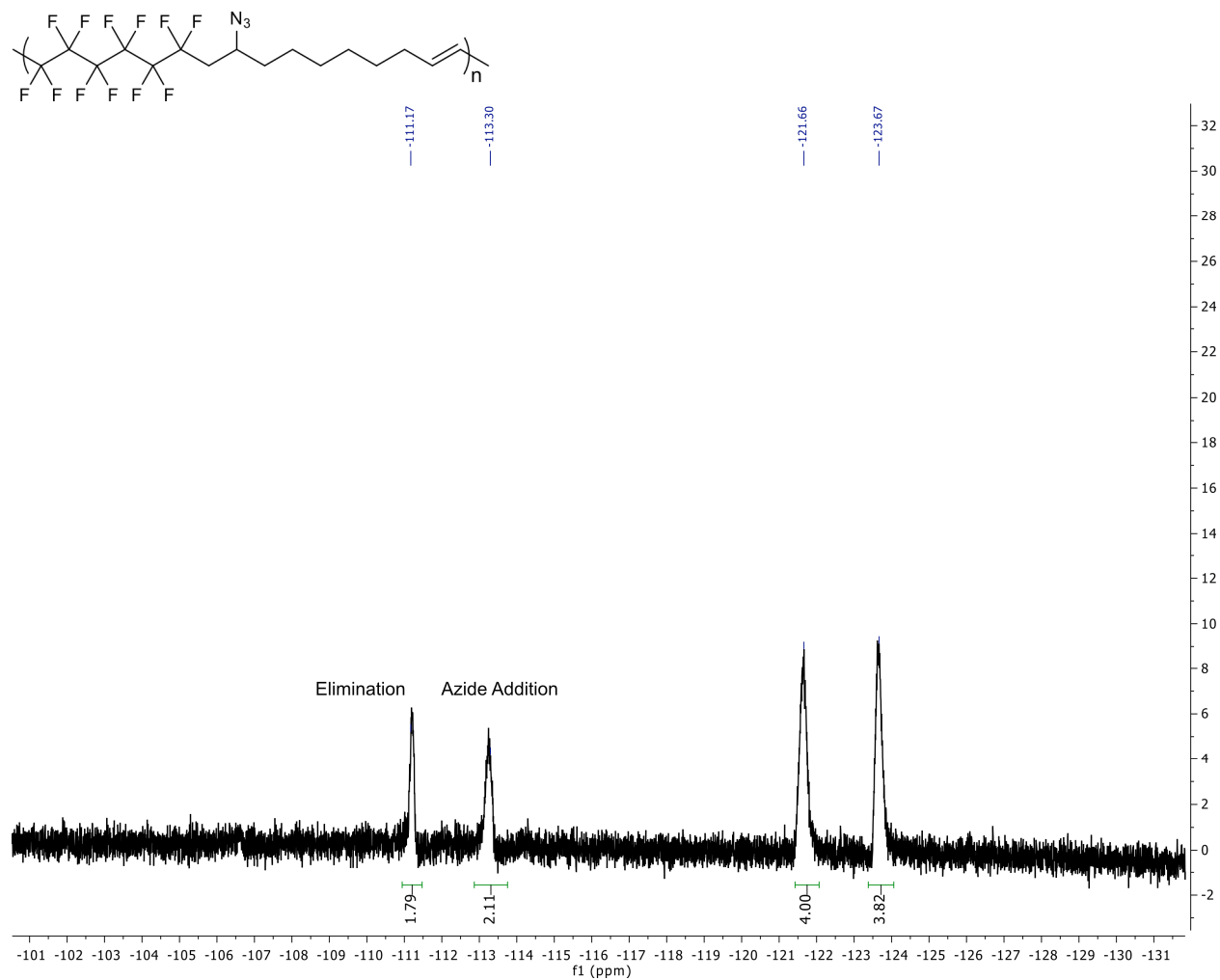
2.23, elimination of iodine from polymer 2.11a:



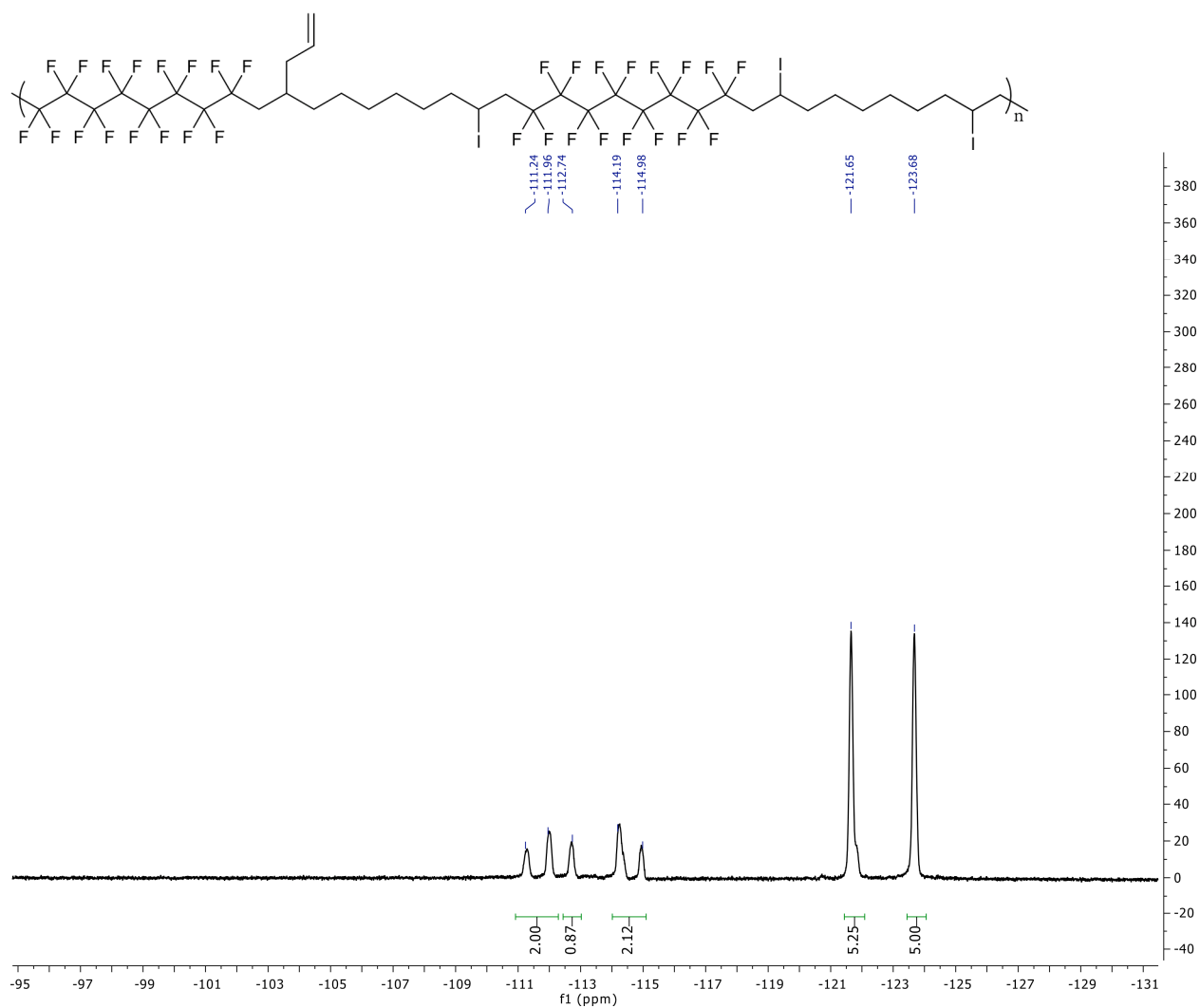
2.26, addition of potassium thioacetate to polymer 2.11a:



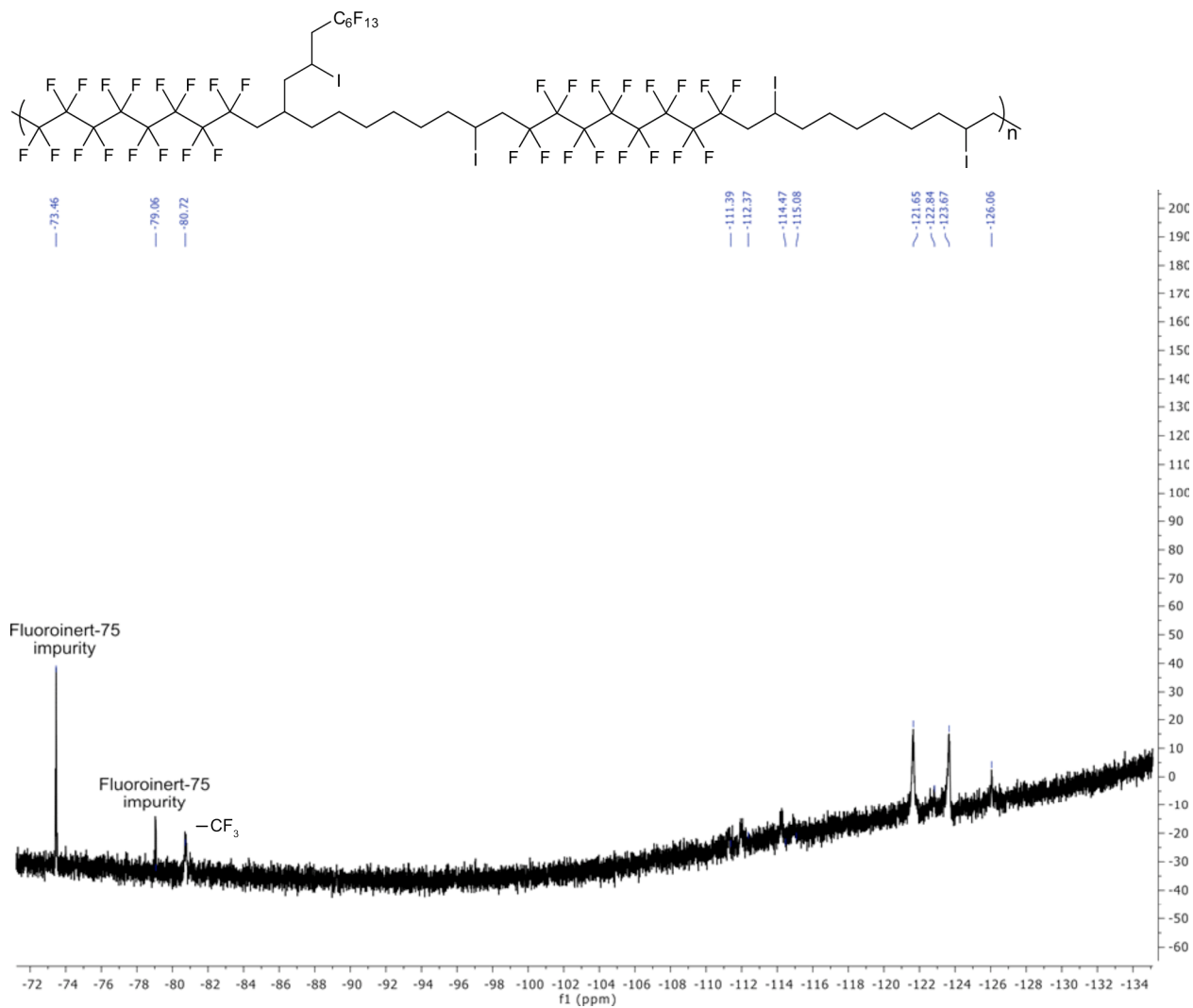
2.32, addition of sodium azide to polymer 2.11a:



2.37, free radical displacement of iodine on polymer 2.11a and addition of allyl group:

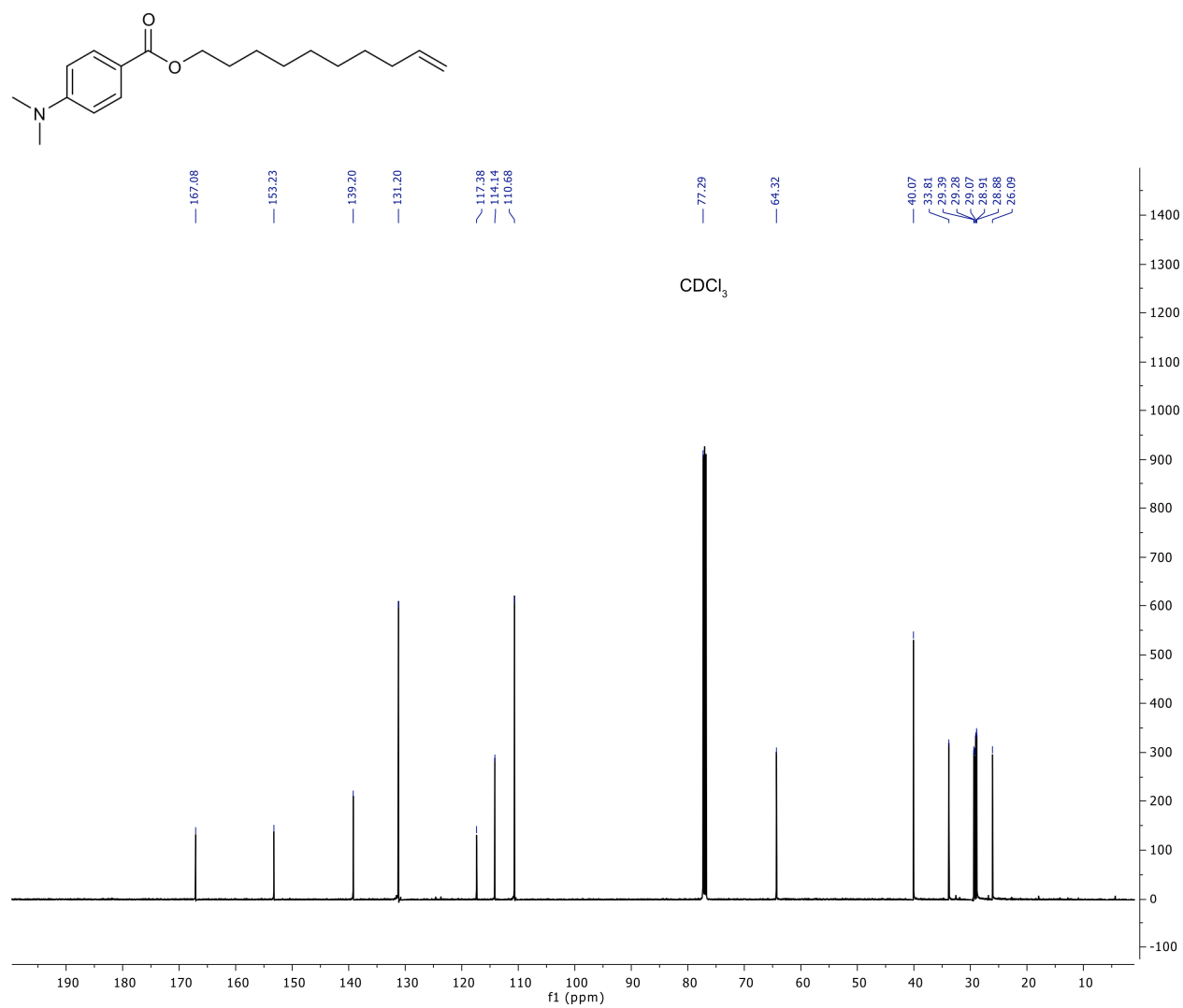


2.38, iodo-ene addition of perfluorohexyl iodide into polymer 2.36:

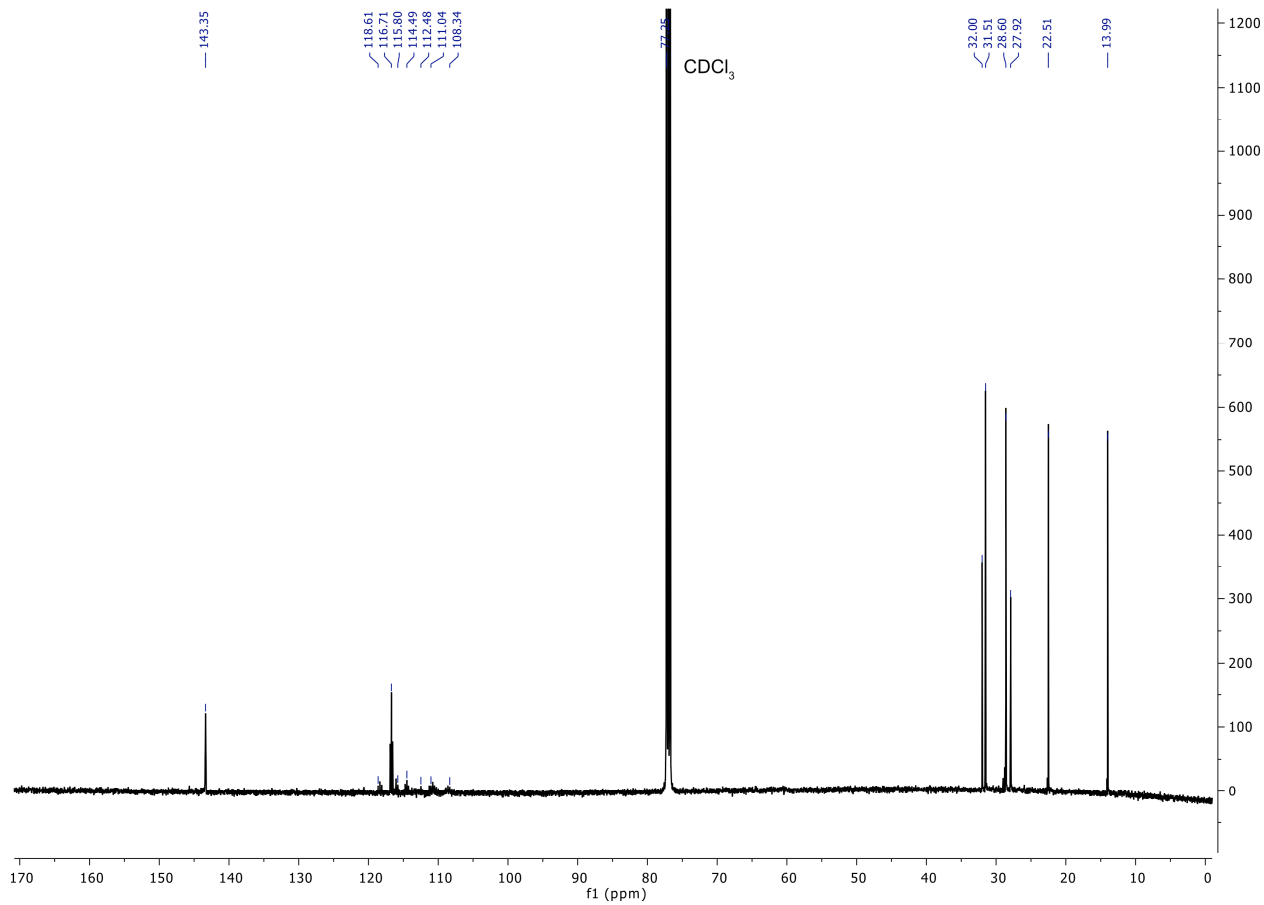
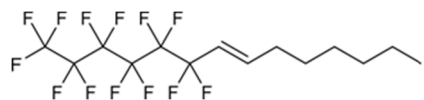


2.5.7 ^{13}C -NMR spectra:

2.12, dec-9-en-1-yl 4-(dimethylamino)benzoate end-cap:

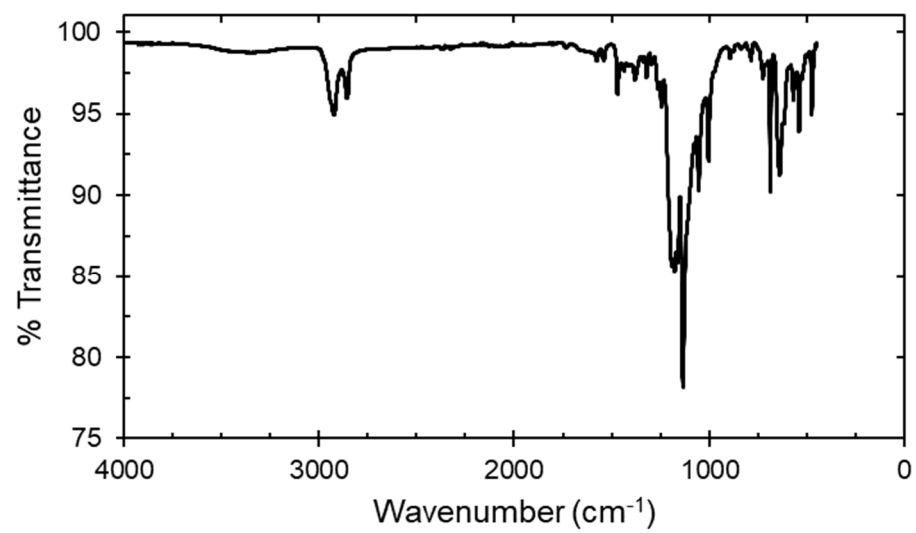


2.40, (E)-1,1,1,2,2,3,3,4,4,5,5,6,6-tridecafluorotetradec-7-ene:

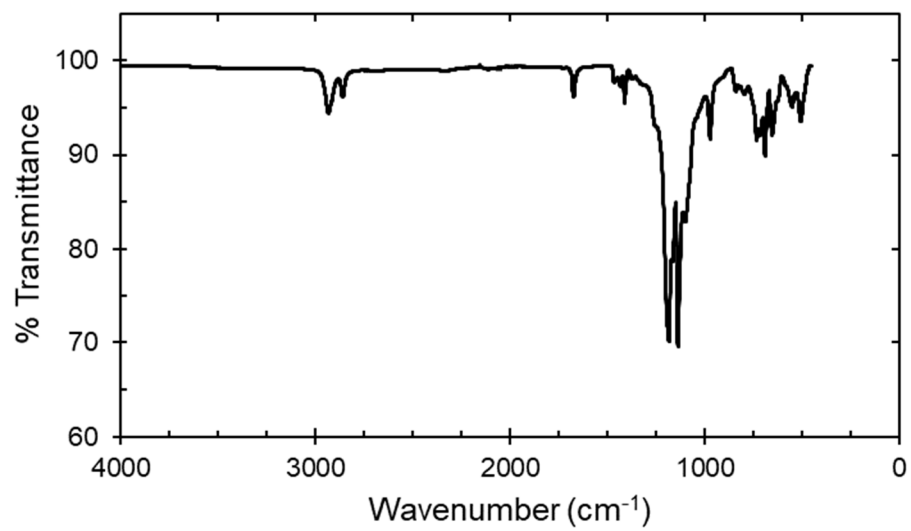


2.5.8 IR spectra:

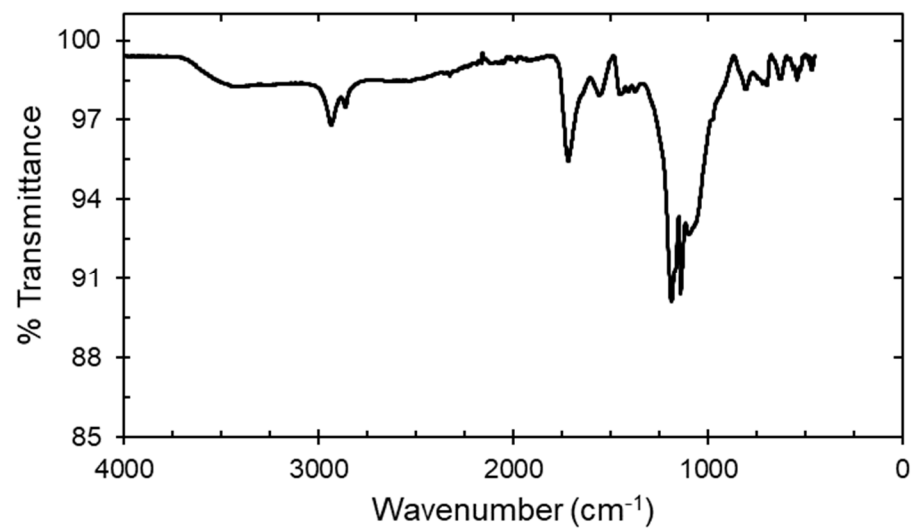
2.24, reduction of iodine from polymer 2.11a:



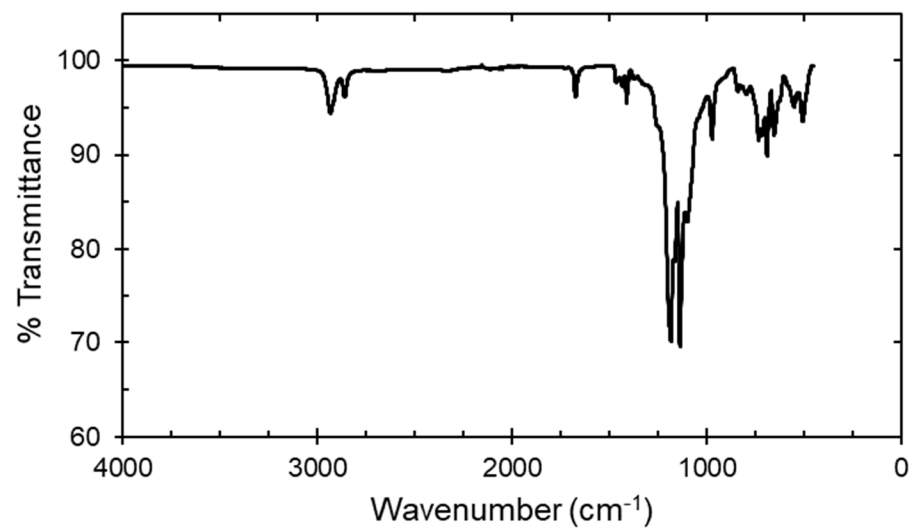
2.29, crosslinking of polymer 2.11a through displacement of iodine with ethanedithiol:



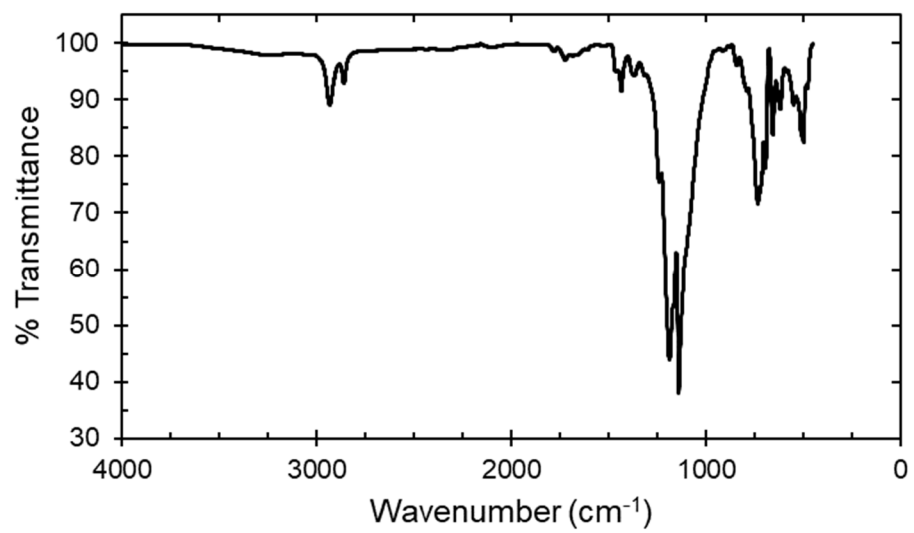
2.31, deprotection of polymer 2.26 followed by Michael addition into acrylamide:



2.37, free radical displacement of iodine on polymer 2.11a and addition of allyl group:

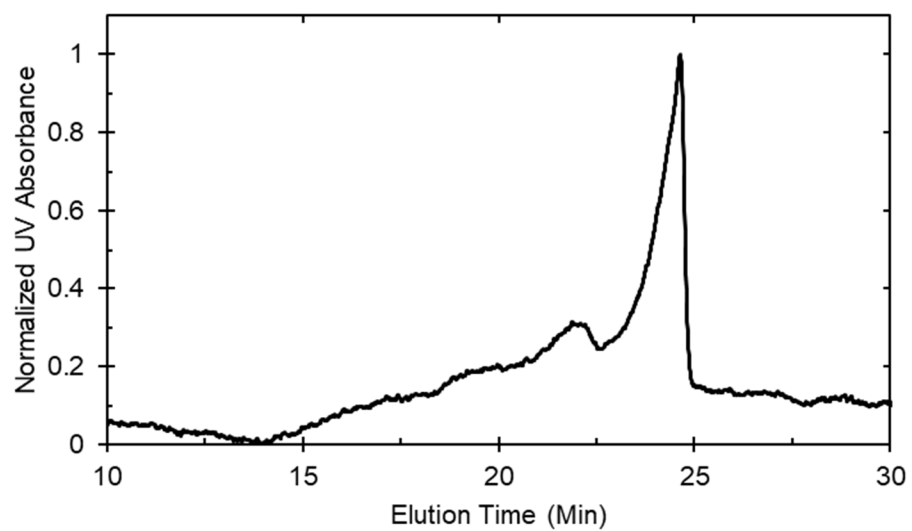


2.38, iodo-ene addition of perfluorohexyl iodide into polymer 2.36:

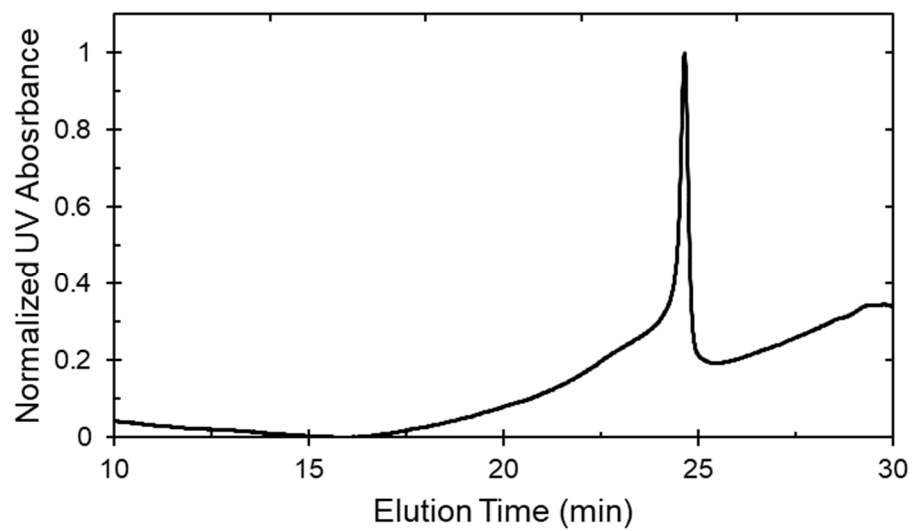


2.5.9 SEC spectra:

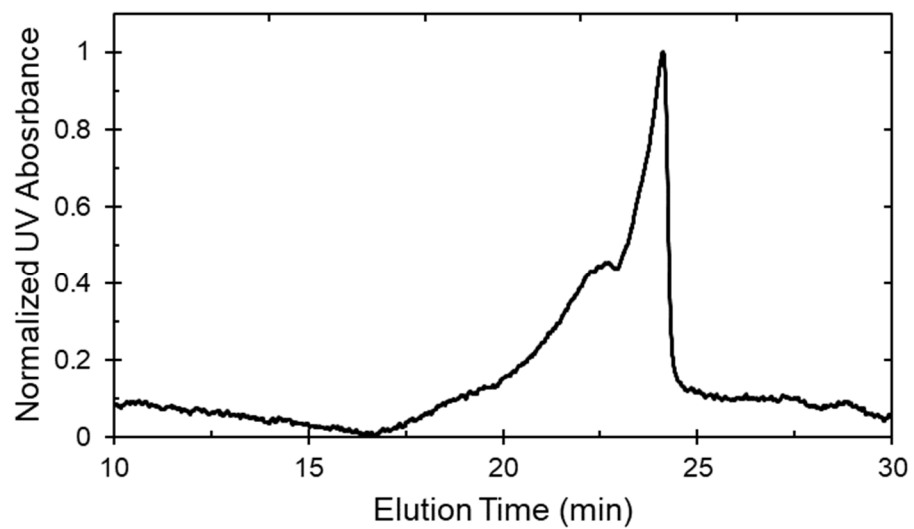
2.11a, 1-perfluorohexyl-2,9-diiododecyl block polymer, Table 1, Entry 3, 30 min reaction:



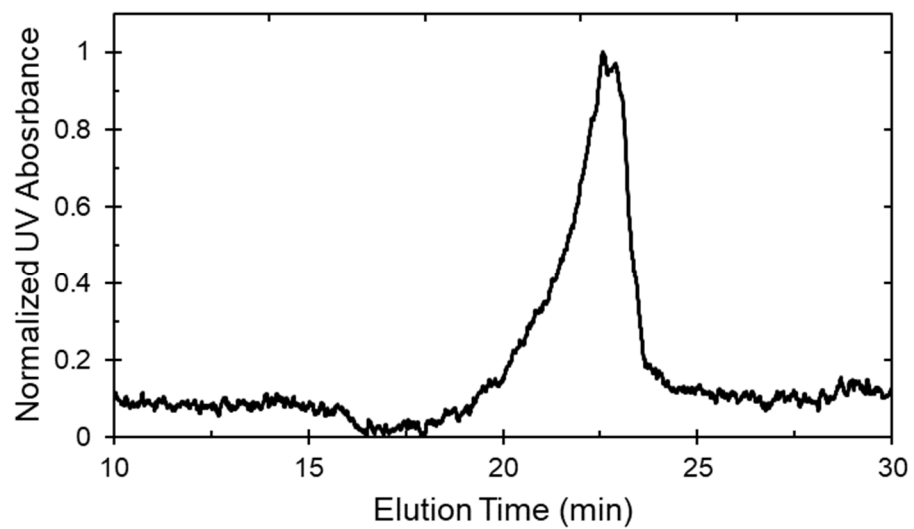
2.11a, 1-perfluorohexyl-2,9-diiododecyl block polymer, Table 1, Entry 4:



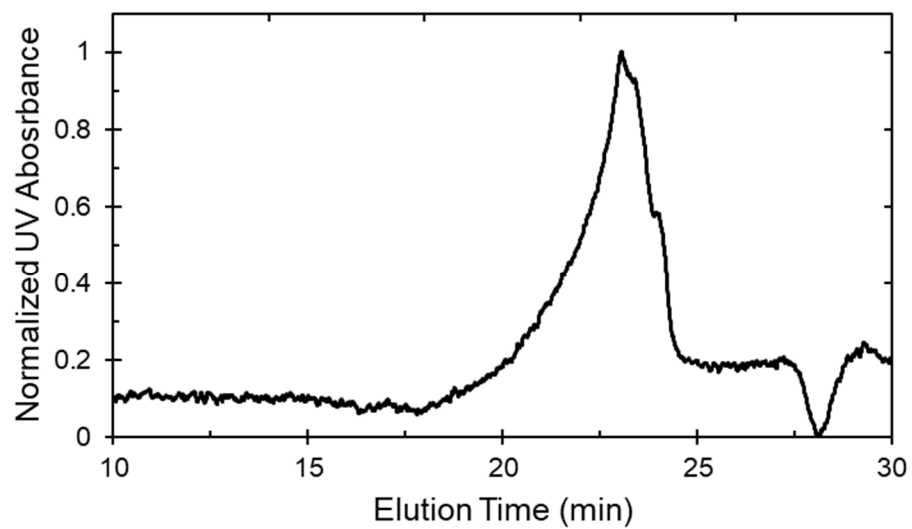
2.11a, 1-perfluorohexyl-2,9-diiododecyl block polymer, Table 1 Entry 5:



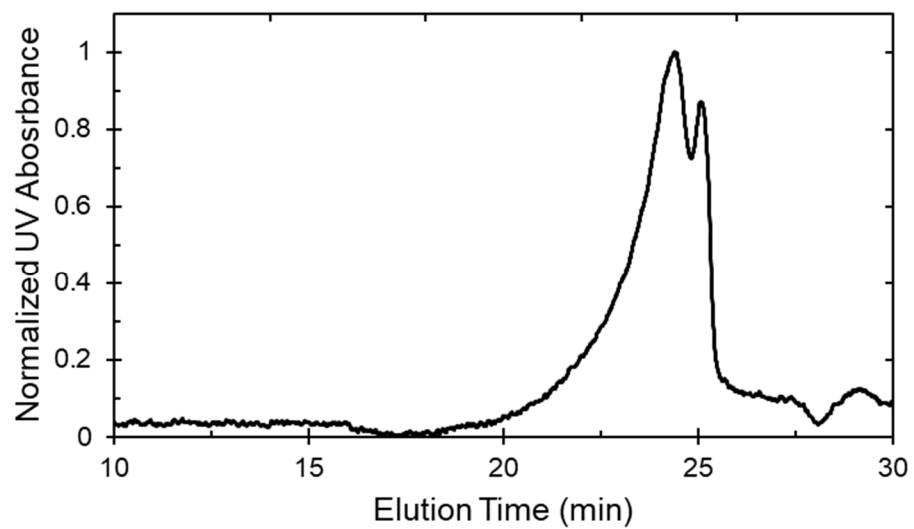
2.11a, 1-perfluorohexyl-2,9-diiododecyl block polymer, Table 1, Entry 6:



2.11a, 1-perfluorohexyl-2,9-diiododecyl block polymer, Table 1, Entry 7:

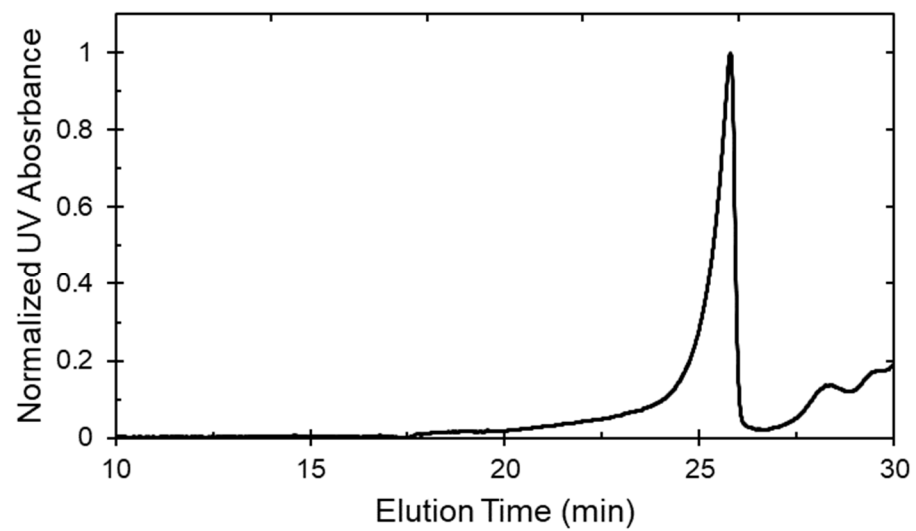


2.11a, 1-perfluorohexyl-2,9-diiododecyl block polymer, Table 1, Entry 8:

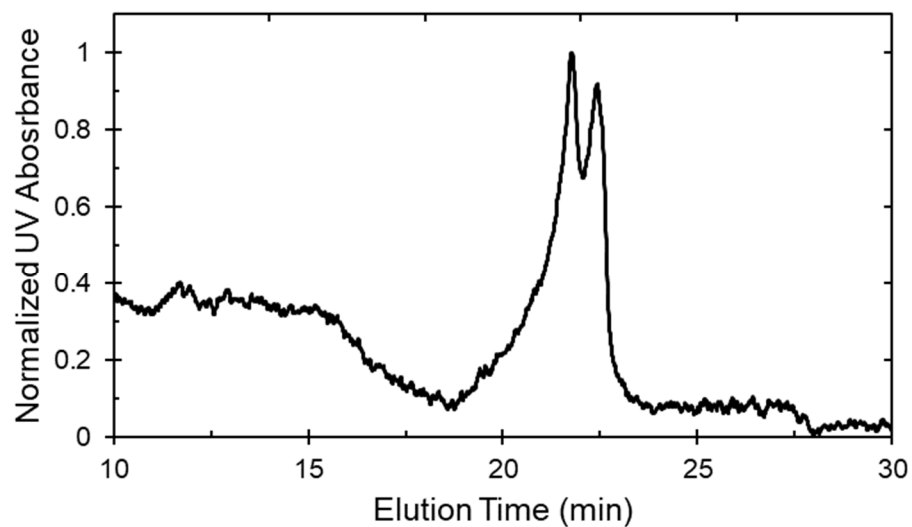


Note: Lower molecular weight shoulder could be due to enhanced radical abstraction under UV conditions

2.11a, 1-perfluorohexyl-2,9-diiododecyl block polymer, Table 1 Entry 9:

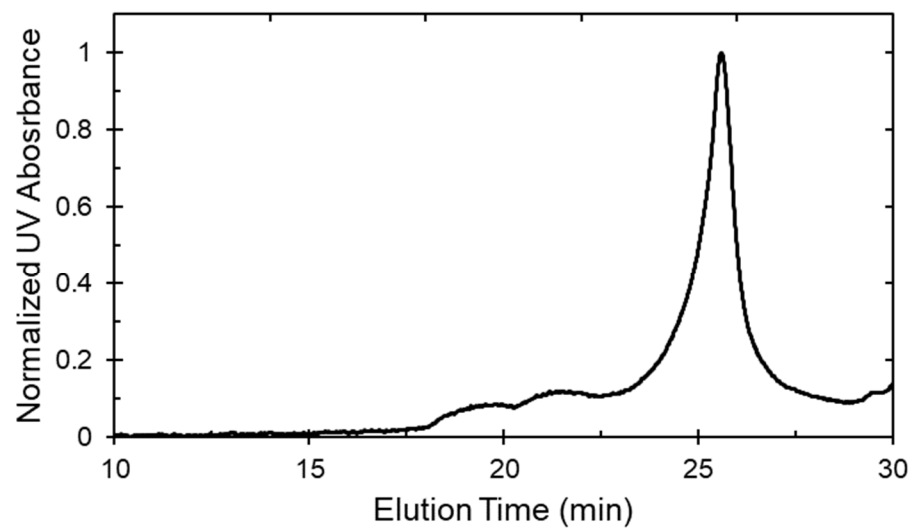


2.11a, 1-perfluorohexyl-2,9-diiododecyl block polymer, Table 1 Entry 10:

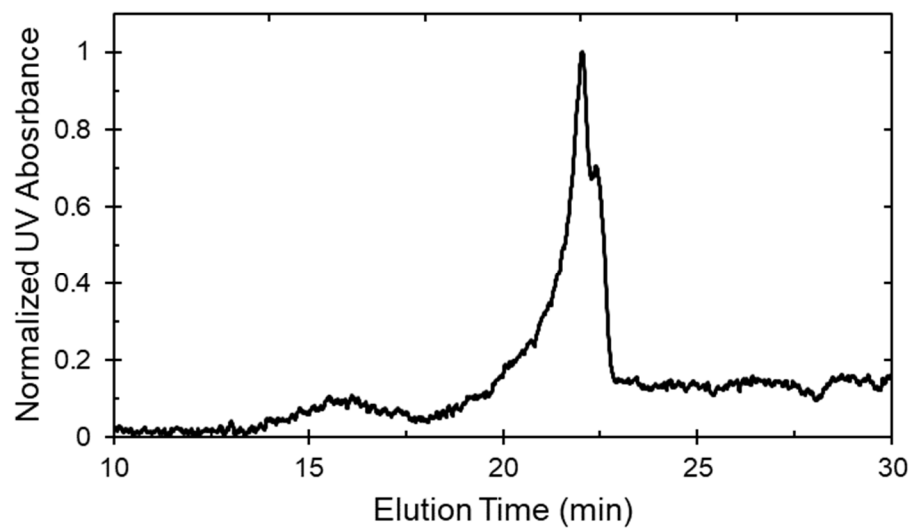


Note: Smaller peak due to early termination due to hydrogen abstraction. This is theorized due to a lack of dimethyl carbonate in the reaction mixture, which has been shown to lower the rate of chain transfer.¹⁰

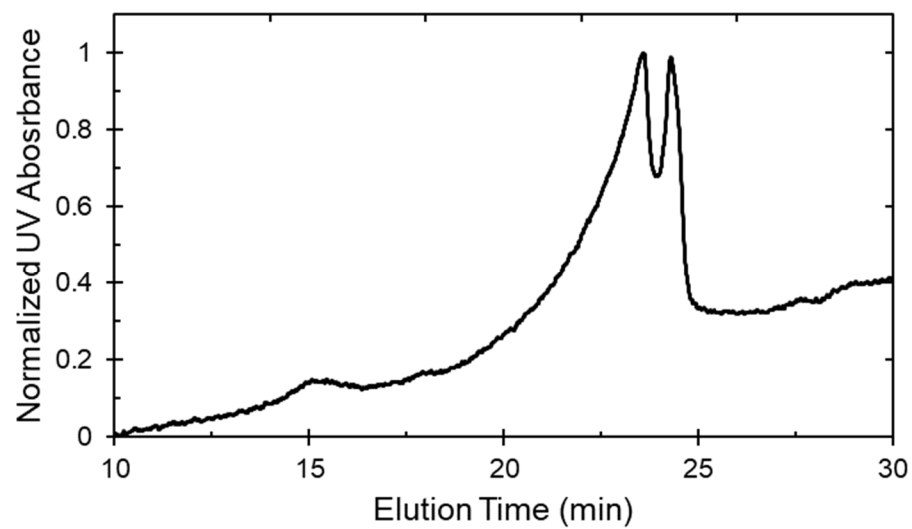
2.11a, 1-perfluorohexyl-2,9-diiododecyl block polymer, Table 1, Entry 11:



2.11b, 1-perfluorooctyl-2,9-diiododecyl block polymer, Table 1, Entry 12:

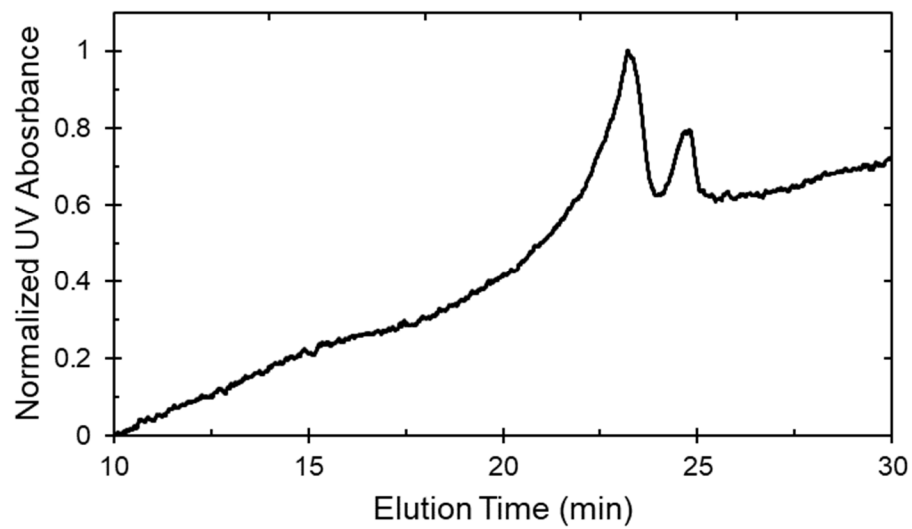


2.11c, 1-perfluorobutyl-2,9-diiododecyl block polymer, Table 1, Entry 13:



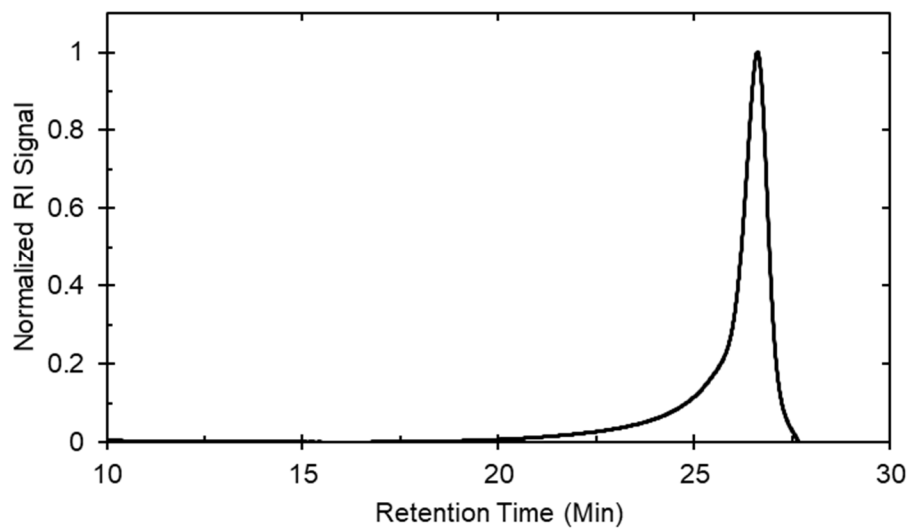
Note: Bimodal character likely due to early termination, which is consistent with hydrogen abstraction in the NMR spectra (Figure S5)

2.11d, 1-(perfluorobutyl- perfluorohexyl- perfluorooctyl)-2,9-diiododecyl block polymer, Table 1, Entry 14:

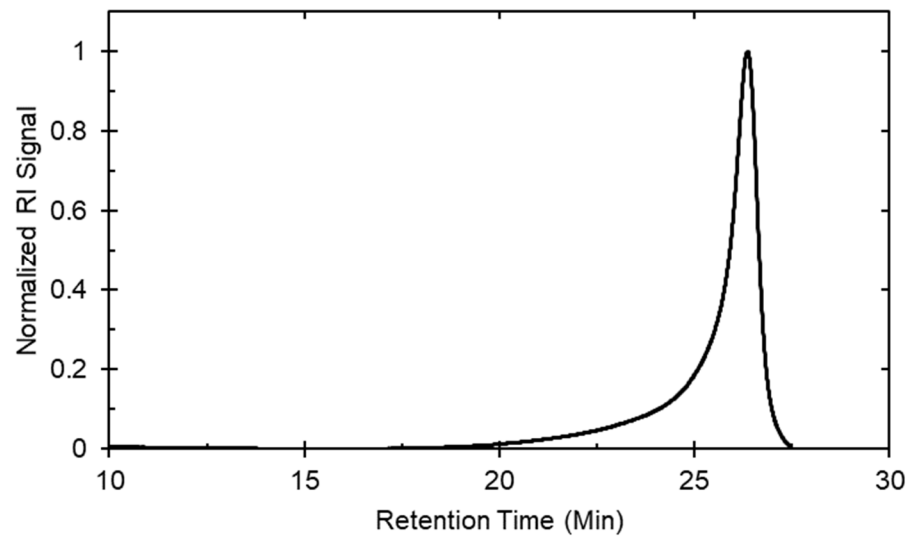


Note: Bimodal character likely due to early termination, due to presence of diiodoperfluorobutane monomer.

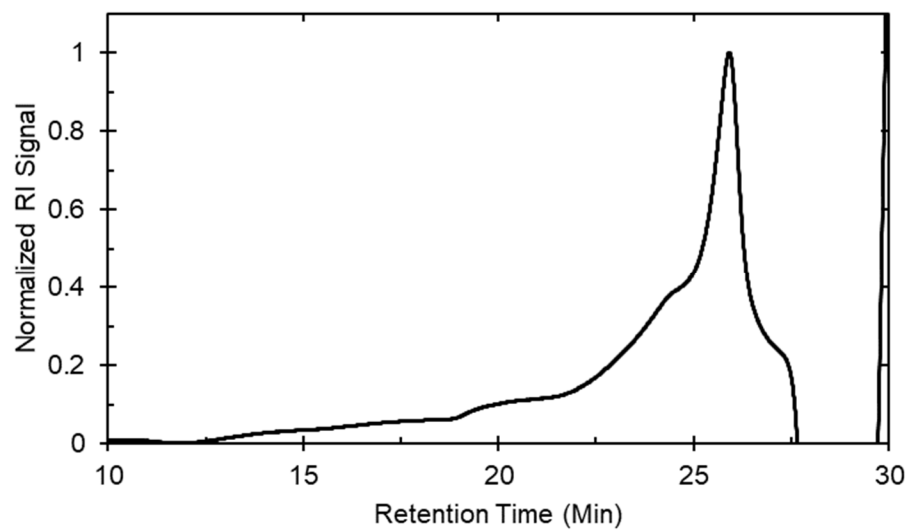
2.18b, 1-perfluorohexyl-2,11-diiodo-4,4,5,5,6,6,7,7,8,8,9,9 dodecafluorohexyl dodecane block polymer:



2.20b, 1,4-bis(2-iodopropyl-1-perfluorooctyl)benzene block polymer:

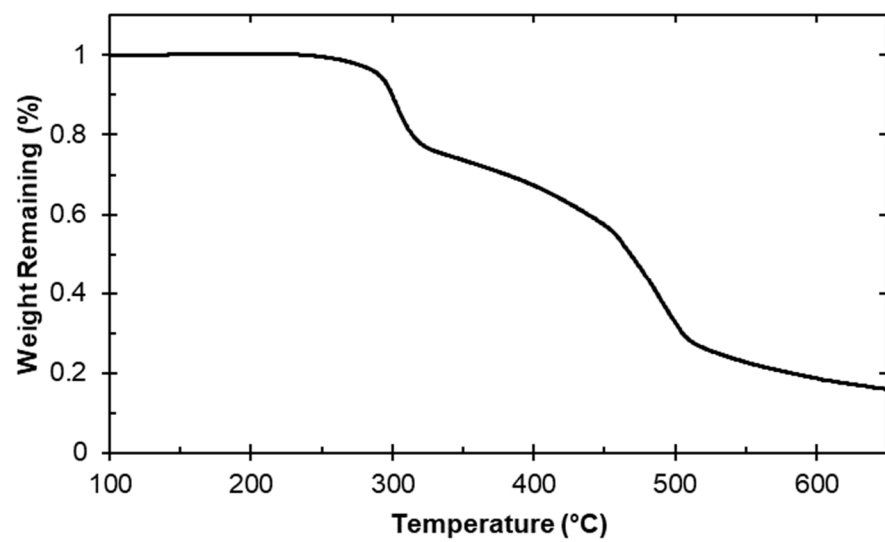


2.21b, 1,4-bis(2-iodopropyl-1-perfluorooctyl) terephthaloyl ester block polymer:

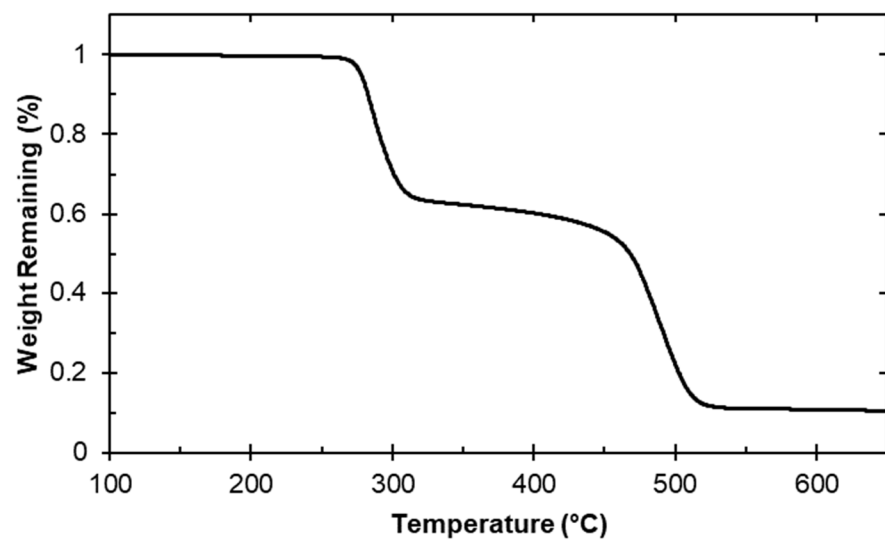


2.5.10 TGA traces:

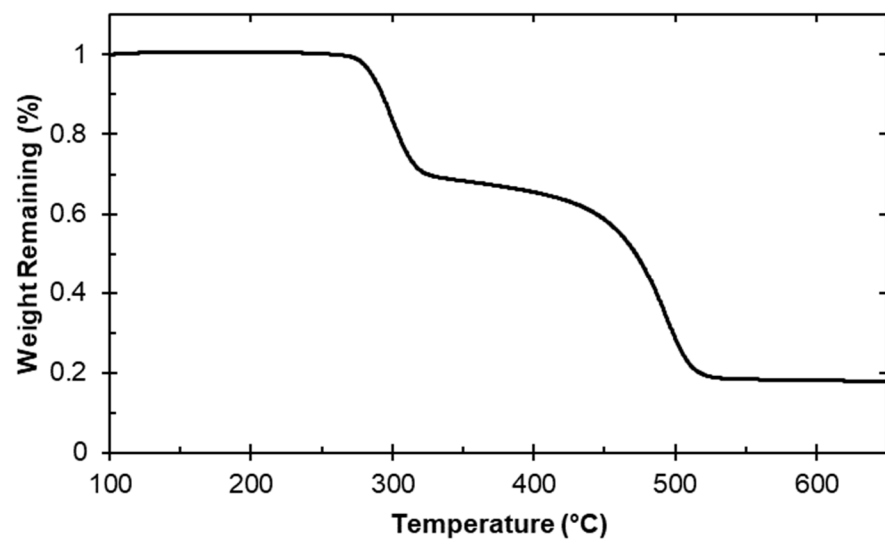
2.11a, 1-perfluorohexyl-2,9-diiododecyl block polymer:



2.11c, 1-perfluorobutyl-2,9-diiododecyl block polymer:

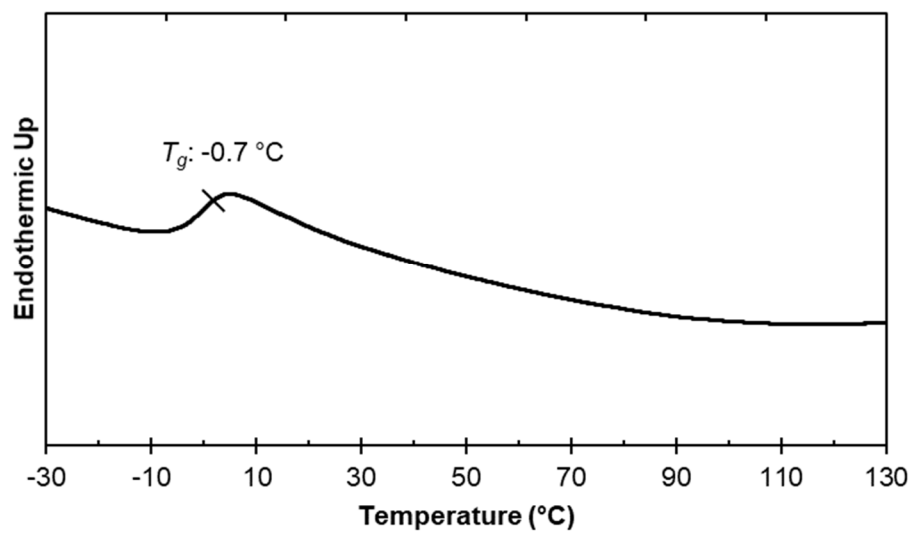


2. 11d, 1-(perfluorobutyl- perfluorohexyl- perfluorooctyl)-2,9-diiododecyl block polymer:

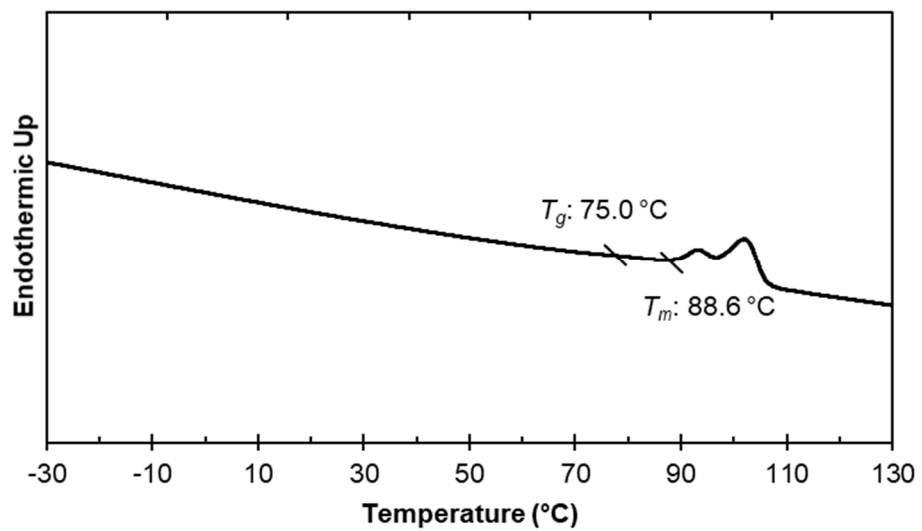


2.5.11 DSC traces:

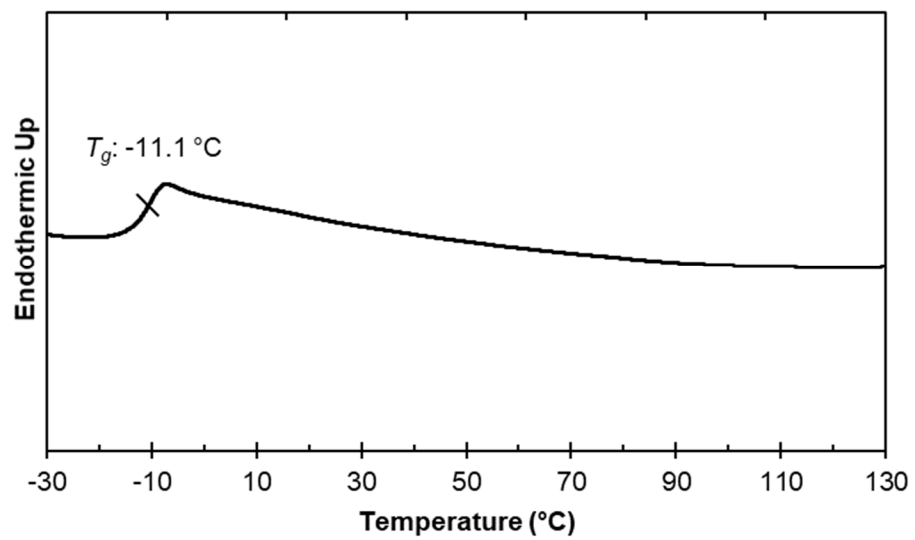
2.11a, 1-perfluorohexyl-2,9-diiododecyl block polymer:



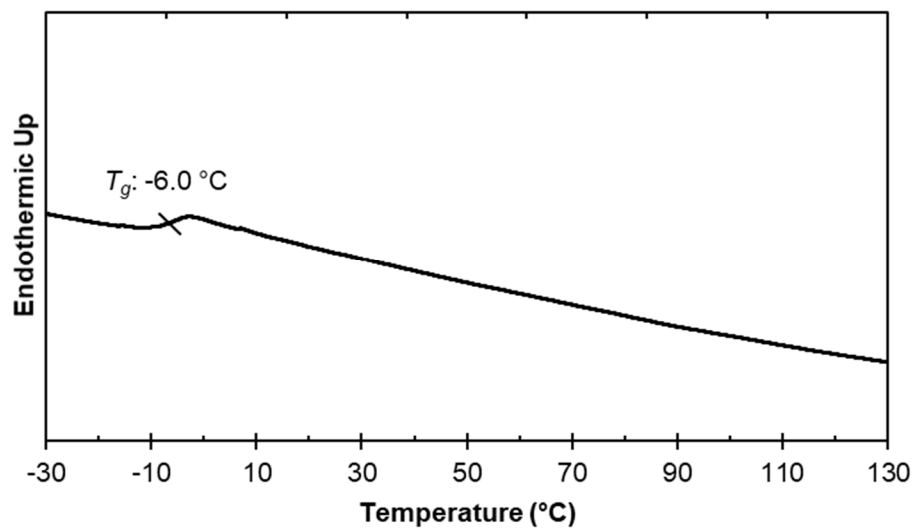
2.11b, 1-perfluorooctyl-2,9-diiododecyl block polymer:



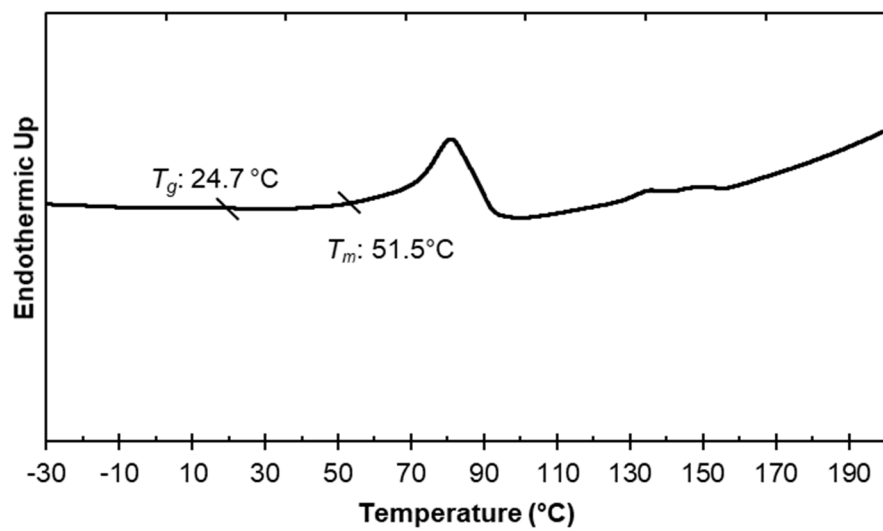
2.11c, 1-perfluorobutyl-2,9-diiododecyl block polymer:



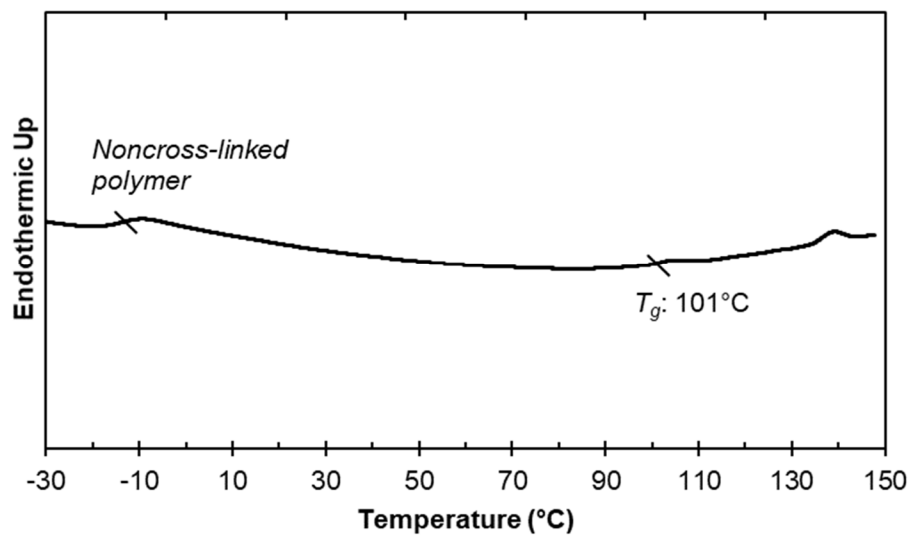
2.11d, 1-(perfluorobutyl- perfluorohexyl- perfluorooctyl)-2,9-diiododecyl block polymer:



2.23, elimination of iodine from polymer 2.11a:



2.29, crosslinking of polymer 2.11a through displacement of iodine with ethanedithiol:



2.6 References and notes

1. Teng, H. Overview of the development of the fluoropolymer industry. *Appl. Sci.* **2012**, *2*, 496–512.
2. Ebnesajjad, S. *Introduction to fluoropolymers*; William Andrew, Norwich, 2013.
3. Li, M.; Zhang, W.; Wang, C.; Wang, H. Melt processability of polytetrafluoroethylene: Effect of melt treatment on tensile deformation mechanism. *J. Appl. Polym. Sci.* **2011**, *123*, 1667–1674.
4. Olabisi, O.; Adewale, K. *Handbook of thermoplastics*; CRC Press, Boca Raton, 2015.
5. Shi, X.; Wu, C.; Rong, M.; Czigany, T.; Ruan, W.; Zhang, M. Improvement of creep resistance of polytetrafluoroethylene films by nano-inclusions. *Chinese J. Polym. Sci.* **2013**, *31*, 377–387.
6. Sun, H.; Cooke, S.; Bates, D.; Wynne, J. Supercritical CO₂ processing and annealing of polytetrafluoroethylene (PTFE) and modified PTFE for enhancement of crystallinity and creep resistance. *Polymer*, **2005**, *46*, 8872–8882.
7. Krafft, M.; Riess, J. Per- and polyfluorinated substances (PFASs): Environmental challenges. *Curr. Opin. Colloid Interface Sci.* **2015**, *20*, 192–212.
8. Tervoort, T.; Visjager, J.; Smith, P. Melt-processable poly(tetrafluoroethylene)—compounding, fillers and dyes. *J. Fluor. Chem.* **2002**, *114*, 133–137.
9. Platzer, N. *Encyclopedia of polymer science and engineering, second edition, volume 6*; Interscience, New York, 1986.
10. Schué, F. *Modern fluoropolymers*; John Wiley & Sons, Chichester, 1997.
11. Inderherbergh, J. Polyvinylidene fluoride (PVDF) appearance, general properties and processing. *Ferroelectrics*, **1991**, *115*, 295–302.

12. Asandei, A. Photomediated controlled radical polymerization and block copolymerization of vinylidene fluoride. *Chem. Rev.* **2016**, *116*, 2244–2274.
13. Ameduri, B. From vinylidene fluoride (VDF) to the applications of VDF-containing polymers and copolymers: Recent developments and future trends. *Chem. Rev.* **2009**, *109*, 6632–6686.
14. Hintzer, K.; Carlson, D.; Schmiegel, W. *Ullmann's encyclopedia of industrial chemistry (Organic Fluoropolymers)*; Wiley-VCH, Weinheim, 2002.
15. Zhao, H.; Zhang, J.; Wu, N.; Zhang, Wu.; Crowley, K.; Weber, S. Transport of organic solutes through amorphous teflon-AF films. *J. Am. Chem. Soc.* **2005**, *127*, 15112–15111.
16. Hung, M. The chemistry of fluorinated dioxoles and dioxolanes. 5. Structure-property relationship of fluorinated dioxole polymers. *Macromolecules*, **1993**, *26*, 5829-5834.
17. See Chemours website for pricing details.
(https://www.chemours.com/Teflon_Industrial/en_US/products/index.html)
18. Oshima, A.; Washio, M. Chemical and radiation cross-linking of polytetrafluoroethylene by containing fluorinated compound. In *Polymer Durability and Radiation Effects*. ACS Symposium Series. **2007**, pp 204–217.
19. Kang, E.; Zhang, Y. Surface modification of fluoropolymers via molecular design. *Adv. Mater.* **2000**, *12*, 1481–1494.
20. Kang, E.; Tan, K.; Kato, K.; Uyama, Y.; Ikada, Y. Surface modification and functionalization of polytetrafluoroethylene films. *Macromolecules*, **1996**, *29*, 6872–6879.
21. Tan, K.; Woon, L.; Wong, K.; Kang, E.; Neoh, K. Surface modification of plasma-pretreated poly(tetrafluoroethylene) films by graft copolymerization. *Macromolecules*, **1993**, *26*, 2832–2836.

22. Shoichet, M.; McCarthy, T. Convenient syntheses of carboxylic acid functionalized fluoropolymer surfaces. *Macromolecules*, **1991**, *24*, 982–986.
23. Hu, Z.; Finlay, J.; Chen, L.; Betts, D.; Hillmyer, M.; Callow, M.; Callow, J.; DeSimone, J. Photochemically cross-linked perfluoropolyether-based elastomers: Synthesis, physical characterization, and biofouling evaluation. *Macromolecules*, **2009**, *42*, 6999–7007.
24. Gozzo, F.; Camaggi, G. Oxidation reactions of tetrafluoroethylene and their products—I: Auto-oxidation. *Tetrahedron* **1996**, *22*, 1765–1770.
25. Hercules, D.; DesMarteau, D.; Fernandez, R.; Clark, J.; Thrasher, J. Evolution of academic barricades for the use of tetrafluoroethylene (TFE) in the preparation of fluoropolymers. in *Handbook of Fluoropolymer Science and Technology*; John Wiley & Sons, Inc., Hoboken, **2014**; pp 413–431.
26. Li, L.; Ni, C.; Xie, Q.; Hu, M.; Wang, F.; Hu, J. TMSCF₃ as a convenient source of CF₂=CF₂ for pentafluoroethylation, (aryloxy)tetrafluoroethylation, and tetrafluoroethylation. *Angew. Chemie Int. Ed.* **2017**, *56*, 9971–9975.
27. Hercules, D.; Parrish, C.; Sayler, T.; Tice, K.; Williams, S.; Lowery, L.; Brady, M.; Coward, R.; Murphy, J.; Hey, T.; Scavuzzo, A.; Rummeler, L.; Burns, E.; Matsnev, A.; Fernandez, R.; MicMillen, C.; Thrasher, J. Preparation of tetrafluoroethylene from the pyrolysis of pentafluoropropionate salts. *J. Fluor. Chem.* **2017**, *196*, 107–116.
28. Kannan, K.; Corsolini, S.; Falandysz, J.; Fillmann, G.; Kumar, K.; Loganathan, B.; Mohd, M.; Olivero, J.; Wouwe, N.; Yang, J.; Aldous, K. Perfluorooctanesulfonate and related fluorochemicals in human blood from several countries. *Environ. Sci. Technol.* **2004**, *38*, 4489–4495.
29. Lau, C.; Butenhoff, J.; Rogers, J. The developmental toxicity of perfluoroalkyl acids and their derivatives. *Toxicol. Appl. Pharmacol.* **2004**, *198*, 231–241.

30. Samanta, S.; Cai, R.; Percec, V. A rational approach to activated polyacrylates and polymethacrylates by using a combination of model reactions and SET-LRP of hexafluoroisopropyl acrylate and methacrylate. *Polym. Chem.* **2015**, *6*, 3259–3270.
31. Lee, C., Khalifehzadeh, R., Ratner, B. & Boydston, A. Facile synthesis of fluorine-substituted polylactides and their amphiphilic block copolymers. *Macromolecules*, **2018**, *51*, 1280–1289.
32. Samanta, S., Cai, R. & Percec, V. SET-LRP of semifluorinated acrylates and methacrylates. *Polym. Chem.* **2014**, *5*, 5479–5491.
33. Borkar, S.; Jankova, K.; Siesler, H.; Hvilsted, S. New highly fluorinated styrene-based materials with low surface energy prepared by ATRP. *Macromolecules*, **2004**, *37*, 788–794.
34. Discekici, E.; Anastasaki, A.; Kaminker, R.; Willenbacher, J.; Truong, N.; Fleischmann, C.; Oschmann, B.; Lunn, D.; Alaniz, J.; Davis, P.; Bates, C.; Hawker, C. Light-mediated atom transfer radical polymerization of semi-fluorinated (meth)acrylates: Facile access to functional materials. *J. Am. Chem. Soc.* **2017**, *139*, 5939–5945.
35. Ren, Y.; Lodge, T.; Hillmyer, M. A new class of fluorinated polymers by a mild, selective, and quantitative fluorination. *J. Am. Chem. Soc.* **1998**, *120*, 6830–6831.
36. Ren, Y.; Lodge, T.; Hillmyer, M. A Simple and mild route to highly fluorinated model polymers. *Macromolecules*, **2001**, *34*, 4780–4787.
37. Davis, C.; Burton, D.; Yang, Z. Titanium-catalyzed addition of perfluoroalkyl iodides to alkenes. *J. Fluor. Chem.* **1995**, *70*, 135–140.
38. Iqbal, N.; Choi, S.; Kim, E.; Cho, E. Trifluoromethylation of alkenes by visible light photoredox catalysis. *J. Org. Chem.* **2012**, *77*, 11383–11387.

39. Xu, T.; Cheung, C.; Hu, X. Iron-catalyzed 1,2-addition of perfluoroalkyl iodides to alkynes and alkenes. *Angew. Chemie Int. Ed.* **2014**, *53*, 4910–4914.
40. Urata, H.; Kinoshita, Y.; Asanuma, T.; Kosukegawa, O.; Fuchikami, T. A facile synthesis of alpha,omega-dicarboxylic acids containing perfluoroalkylene groups. *J. Org. Chem.* **1991**, *56*, 4996–4999.
41. Edwards, H.; Nagappayya, S.; Pohl, N. Probing the limitations of the fluorine content for tag-mediated microarray formation. *Chem. Commun.* **2012**, *48*, 510–512.
42. Scott, T.; Furgal, J.; Kloxin, C. Expanding the alternating propagation-chain transfer-based polymerization toolkit: The iodo-ene reaction. *ACS Macro Lett.* **2015**, *4*, 1404–1409.
43. Wilson, L.; Griffin, A. Liquid-crystalline fluorocarbon—hydrocarbon microblock polymers. *Macromolecules*, **1993**, *26*, 6312–6314.
44. Percec, V.; Schlueter, D.; Ungar, G. Rational design of a hexagonal columnar mesophase in telechelic alternating multicomponent semifluorinated polyethylene oligomers. *Macromolecules*. **1997**, *30*, 645–648.
45. Xu, T.; Zhang, L.; Cheng, Z.; Zhu, X. The positive effect of water on photo-induced step transfer-addition; radical-termination (START) polymerization. *RSC Adv.* **2017**, *7*, 17988–17996.
46. Xu, T.; Zhang, L.; Cheng, Z.; Zhu, X. Insight into the polymerization mechanism of photoinduced step transfer-addition & radical-termination (START) polymerizations. *Polym. Chem.* **2017**, *8*, 3910–3920.
47. Zhang, C.; Chen, Q.; Guo, Y.; Xiao, J.; Gu, Y.. Progress in fluoroalkylation of organic compounds via sulfinate dehalogenation initiation systems. *Chem. Soc. Rev.* **2012**, *41*, 4536–4559.

48. Rong, G.; Keese, R. The addition of perfluorobutyl iodide to carbon-carbon multiple bonds and the preparation of perfluorobutylalkenes. *Tet. Lett.* **1990**, *31*, 5615–5616.
49. Simpson, C.; Adebolu, O.; Kim, J.; Vasu, V.; Asandei, A. Metal and ligand effects of photoactive transition metal carbonyls in the iodine degenerative transfer controlled radical polymerization and block copolymerization of vinylidene fluoride. *Macromolecules*, **2015**, *48*, 6404–6420.
50. 1,1'-Azobis(cyclohexanecarbonitrile) (ACHN) was also used as an initiator due to increased thermal stability. ACHN initiated polymerization gave low molecular weight polymer with low yield (26.7 %). SEC, THF (polystyrene standards) : M_n : 5.25 kDa, M_w : 8.33 kDa, D : 1.59.
51. Agilent Technologies application note, Cleaver, G.
(<https://www.agilent.com/cs/library/applications/5990-8328EN.pdf>)
52. Tuminello, W. Solubility of Poly(Tetrafluoroethylene) and its Copolymers in *Fluoropolymers 2: Properties*; Springer, US, **1999**; pp 137-143.
53. MALS analysis was available for SEC molecular weight determination, but light scattering signal for these polymers was very low. For these reasons, UV detection was utilized for a majority of SEC analysis.
54. Kudoh, H., Sasuga, T. & Seguchi, T. High-energy ion irradiation effects on polymer materials. *ACS Symposium Series 2–10* (**1996**).
55. Mori, T.; Tsuchiya, Y.; Okahata, Y. Polymerizations of tetrafluoroethylene in homogeneous supercritical fluoroform and in detergent-free heterogeneous emulsion of supercritical fluoroform/water. *Macromolecules*, **2006**, *39*, 604–608.
56. Xu, A.; Yuan, W.; Zhang, H.; Wang, L.; Li, H.; Zhang, Y. Low-molecular-weight polytetrafluoroethylene bearing thermally stable perfluoroalkyl end-groups prepared in supercritical carbon dioxide. *Polym. Int.* **2012**, *61*, 901–908.

57. Lee, S.; Park, J.; Lee, T. The Wettability of fluoropolymer surfaces: Influence of surface dipoles. *Langmuir*, **2008**, *24*, 4817–4826.
58. Hung, M. Process for manufacturing diidooeperfluoroalkanes. European Patent 1422211, May 26th, 2004.
59. Hoang, G.; Walsh, D.; McGarry, K.; Anderson, C.; Douglas, C. Development and mechanistic study of quinoline-directed acyl C–O bond activation and alkene oxyacylation reactions. *J. Org. Chem.* **2017**, *82*, 2972–2983.
60. Conesa, J.; Font, R. Polytetrafluoroethylene decomposition in air and nitrogen. *Polym. Eng. Sci.* **2001**, *41*, 2137–2147.
61. Agard N. J.; Baskin J. M.; Prescher J. A.; Lo A.; Bertozzi C. R. A Comparative Study of Bioorthogonal Reactions with Azides. *ACS Chem. Biol.* **2006**, *1*, 644–648.
62. Ma, J.; Chan, T. Organometallic-type reactions in aqueous media. Wurtz-coupling of alkyl halides with manganese/cupric chloride. *Tet. Lett.* **2008**, *39*, 2499-2502.
63. Fischer, H.; Baer, R.; Hany, R.; Verhoolen, I.; Walbiner, M. 2,2-Dimethoxy-2-phenylacetophenone: photochemistry and free radical photofragmentation. *J. Chem. Soc., Perkin. Trans. 2* 1990, *0*, 787-798.
64. Lee, M.; Enders, D.; Nagao, T.; Ariga, K. Characteristic IR C=C stretch enhancement in monolayers by nonconjugated, noncumulated unsaturated bonds. *Langmuir*, **2010**, *26*, 4594–4597.
65. Yamamoto, Y.; Saito, K. Synthesis of olefins by the reaction of β -((trimethylsilyl)oxy)alkyl iodides with zinc. *Organometallics*, **1997**, *16*, 2207-2208.
66. Conrad, J.; Eelman, M.; Silva, J.; Monfette, S.; Parans, H.; Snelgrove, J.; Fogg, D. Oligomers as intermediates in ring-closing metathesis. *J. Am. Chem. Soc.*, **2007**, *129*, 1024–1025.
67. Ma, J.; Shi, F.; Tian, D.; Li, H. Macroscopic responsive liquid quantum dots constructed via pillar[5]arene-based host-guest interactions. *Chem. Eur. J.* **2016**, *22*, 13805–13809.

Vinyl iodide containing polymers directly prepared via an iodo-yne polymerization

Adapted from Joseph A. Jaye and Ellen M. Sletten.* Vinyl Iodide Containing Polymers Directly Prepared Via An Iodo-Yne Polymerization. *ACS Macro Letters* **2020**, *9*, 410-415. DOI: 10.1021/acsmacrolett.9b00979

3.1 Abstract

Post-polymerization modifications are a prominent route for tuning polymer properties and diversifying materials. Thus, polymers containing robust chemical handles are desirable. Vinyl iodide functionality is commonly enlisted for selective transformations on small molecules but these chemistries, while efficient enough for post-polymerization modifications, are less frequently performed on macromolecules due to limited methods to install vinyl iodide groups into polymers. Here, we present an iodo-yne polymerization involving diynes and diiodoperfluoroalkanes to facilitate give semifluorinated polymers with vinyl iodide groups throughout the polymer chain. The iodo-yne polymerization yields polymers of at least 6 kDa while open to air in aqueous solvent. We demonstrate that the iodo-yne polymers can be modified at the vinyl iodide functionality via a variety of metal-catalyzed cross-coupling reactions. Additionally, the iodide can be eliminated to give electronically activated alkynes that can undergo cycloaddition with azides. Taken together, this work will push the current boundaries of functional polymers and assist in the development of modernized, smart materials.

3.2 Introduction

The 21st century has seen a rise in functional materials with highly customized and dynamic behaviors^{1,2}. As the demands on material properties and applications increase, the toolbox of chemistries must also expand. Polymers are the foundation of many materials spanning from robust polyolefins^{3,4} to responsive, custom hydrogels.⁵⁻⁷ A fruitful avenue to tune the properties of a polymer is to incorporate unique functional groups into the backbone, which can undergo post-polymerization modification. Thus,

polymerization methods that introduce selectively reactive, chemical functionality into the repeating unit are an advantageous route to a diverse array of materials.

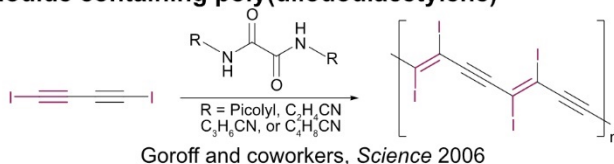
Here, we take advantage of the unique reactivity of perfluoriodo compounds with alkynes to directly yield polymers with vinyl iodide functionality in the backbone. Vinyl iodide groups are particularly promising functional handles as they can be elaborated via an array of cross-coupling chemistries.⁸ The only existing method to directly produce vinyl iodide functionality in the backbone of a polymer is the topochemical polymerization of iodo-alkynes (Figure 3.1A).^{9,10} This polymerization is limited in scope and requires careful preorganization of iodo-alkyne and halogen bond acceptor monomers in the crystalline state to produce poly(diiododiacetylene). Poly(diiododiacetylene) also has low thermal stability due to facile loss of iodide. A more indirect route to install vinyl iodide groups into the polymer backbone is through post-polymerization treatment of an activated functionality pre-installed throughout the polymer. Examples of these functionalities are vinylstannanes or zirconacyclopentadienes, which can be treated with elemental iodine to give displaced or ring-opened product. (Figure 3.1B).^{11,12} Although useful, this indirect route requires multiple post-polymerization modifications to give functional products. (Hetero)aryl iodides, which can undergo similar cross-coupling chemistries, can be introduced into the polymer backbone through click chemistry of azides and iodo-alkynes or through the synthesis of conjugated polymers.^{13,14} All of these methods either require custom, sensitive, iodo-alkyne starting materials and/or multiple steps to arrive at the vinyl iodide functionality. Other polymerizations of alkyne containing monomers have been developed leading to olefinic or aromatic backbones, but without vinyl halide functionality.¹⁵⁻²⁰

Interested in the tunability of vinyl iodide containing polymers, we looked to explore new methods to produce this unique functionality in a simple, efficient reaction. Learning from the work by Goroff and Fokin^{9,14}, it is most efficient to have an activated iodide atom already present on the monomer. Previous work from our group and others²¹⁻²⁴ have exploited the easily activated perfluorocarbon-iodide bond to

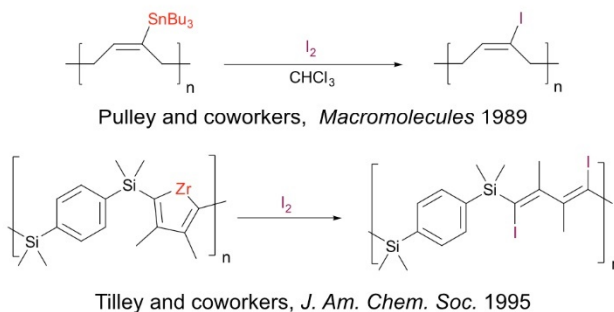
prepare semifluorinated polymers from perfluorodiiodide and diene monomers in an iodo-ene polymerization. Mild, green polymerization conditions were employed to yield iodo-ene polymers containing sp^3 C–I moieties in the backbone. We envisioned that similar chemistries could be extended to the polymerization of diyne monomers to fashion an iodo-yne polymerization. Mechanistically, this polymerization would provide polymers containing sp^2 C–I functionality within the backbone (Figure 3.1C). In contrast to existing methods⁹⁻¹⁴, the iodo-yne polymerization would directly and simply yield vinyl iodide containing polymers from readily available, stable monomers.

Drawing from the synthetic and fluorine chemistry communities, the addition of perfluoroalkyl iodides into small molecule alkynes has been established using sodium dithionite, UV irradiation, iron or zinc.²⁵⁻²⁹ Due to our previous investigation of the iodo-ene polymerization¹⁵, we were particularly interested in $Na_2S_2O_4$ as a free radical initiator, as it is bench stable and only requires water and sonication for activation. Initial reports regarding the use of $Na_2S_2O_4$ to perform the addition of iodoperfluoroalkanes into alkynes required excess fluorine reagent, which is not viable for step-growth polymerizations. Thus, optimization was required to furnish iodo-yne polymers.

A) Topochemical polymerization to give vinyl iodide containing poly(diiododiacetylene)



B) Installment of vinyl iodide groups through post-polymerization modification



C) Work presented herein. Direct installation of vinyl iodide groups into the polymer backbone

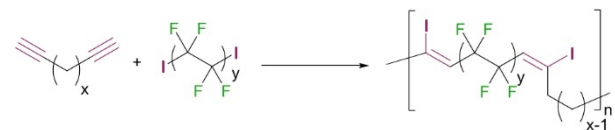
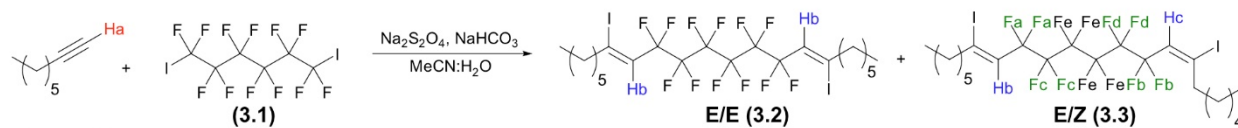


Figure 3.1. Methods to install vinyl iodide functionality within a polymer backbone. **A)** Topochemical polymerization to give the conductive, vinyl iodide containing poly(diiododiacetylene). **B)** Post-polymerization modifications to yield vinyl iodide containing polymers. **C)** Work presented herein where direct installation of vinyl iodide groups is achieved via iodo-yne polymerization.

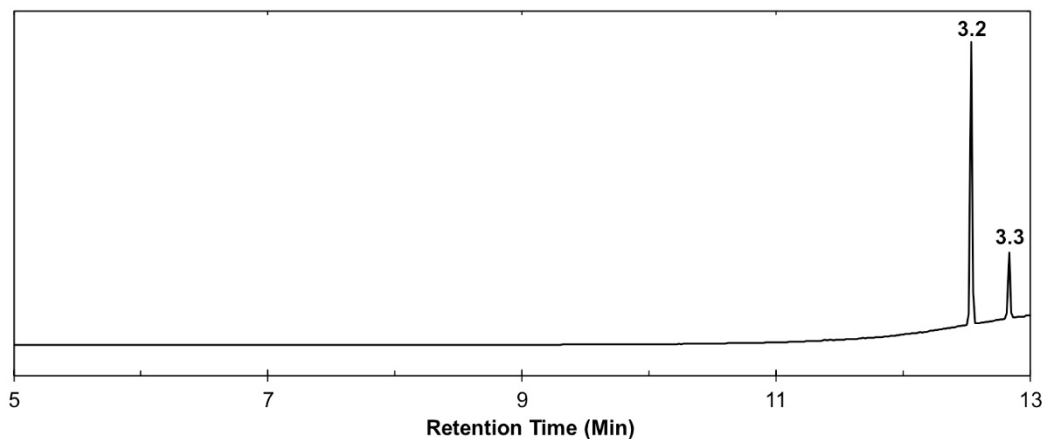
3.3 Results and discussion

To identify reaction conditions for the iodo-yne polymerization, we first investigated the model system of diiodoperfluorohexane (**3.1**) and 1-octyne. We determined that the reaction required two or more equivalents of initiator in a combination of acetonitrile/water to yield complete addition of 1-octyne into diiodoperfluorohexane to provide the desired vinyl iodide containing adducts **3.2** and **3.3** (Figure 3.2). Gratifyingly, we found that the conditions optimized for the monomer readily translated to the polymerization of 1,9-decadiyne (**3.4**) and diiodoperfluorohexane (**3.1**) to give iodo-yne polymer **3.5** (Scheme 3.1).³⁰ Notably, the polymerization is performed in a sonication bath open to air. Polymer **3.5** was endowed with repeating vinyl iodide groups on the backbone with a 3:1 E/Z ratio (Table 3.1). Further exploration of polymerization conditions indicated that a change in the concentration of the

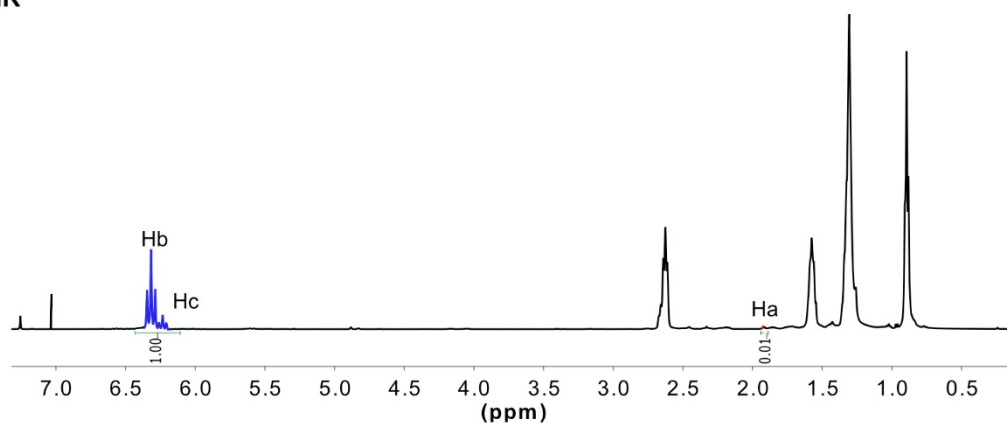
A) Model reaction of 1-octyne and diiodoperfluorohexane



B) HR GC-MS



C) $^1\text{H-NMR}$



D) $^{19}\text{F-NMR}$

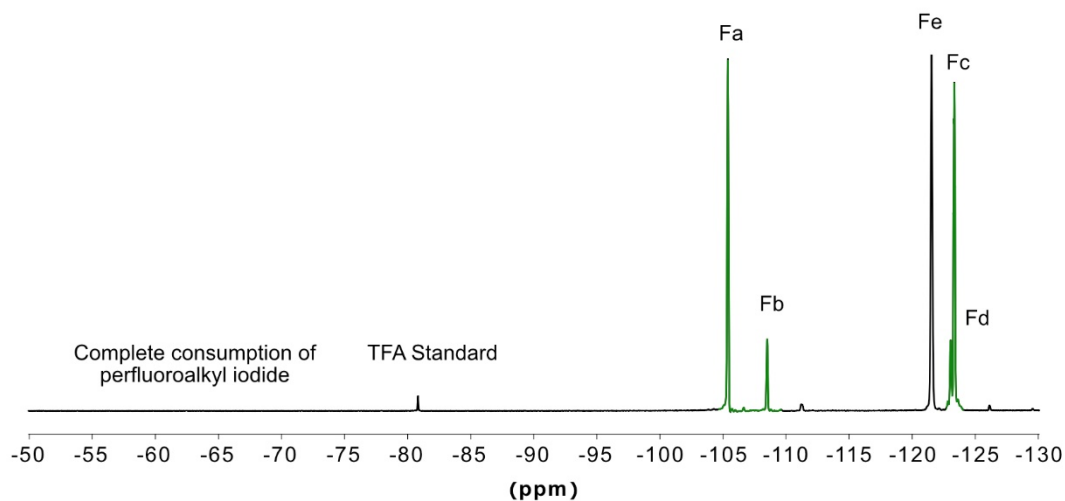


Figure 3.2: Diiodoperfluorohexane and 1-Octyne model system for polymerization. **A)** Reaction scheme of model system that gives a mix of diastereomers. **B)** High resolution GCMS of diastereomers. **C)** $^1\text{H-NMR}$ demonstrating nearly quantitative conversion of 1-octyne and diiodoperfluorohexane. **D)** $^{19}\text{F-NMR}$ demonstrating nearly quantitative conversion of 1-octyne and diiodoperfluorohexane.

Scheme 3.1: Polymerization of 1,9-Decadiyne (**3.4**) and diiodoperfluorohexane (**3.1**) to yield iodo-yne polymer **3.5**.

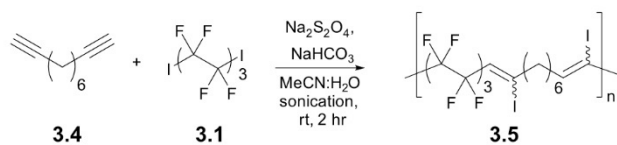


Table 3.1: Optimization of polymerization conditions

Entry (#)	Monomer ratio (3.1:3.4)	Concentration (M)	Sonication source	Yield ^c (%)	E:Z ratio	M_n^b (kDa)	\mathcal{D}^b
1	1:1	0.13	Bath	52	74:26	5.13	1.47
2	1:1	0.25	Bath	78 (94)	73:27	6.88	1.49
3	1:1	0.50	Bath	79	73:27	6.25	1.50
4	1.05:1	0.25	Bath	81	77:23	6.27	1.44
5 ^a	1:1	0.25	Bath	93	77:23	7.57	1.50
6	1:1	0.25	Probe (20 %) ^d	63	75:25	9.02	1.56
7	1:1	0.25	Probe (40 %) ^d	71	73:27	8.77	1.59
8	1:1	0.25	Probe (60 %) ^{d,e}	73	74:26	8.32	1.52

a. Reaction was performed with sonication at 0 °C through the use of an ice filled sonication bath. **b.** Molecular weight determined through SEC analysis with low dispersity polystyrene standards using an ultra-high performance liquid chromatography instrument. Incomplete dissolution of polymer samples led to minimum molecular weight value (See Figures 3.4, 3.5). **c.** Yields for entries 1 to 6 correspond to an average of two measurements on a 0.1 mmol scale. For entry 2, a 2.3 gram scale reaction gave 94% yield. **d.** Number in parentheses corresponds to amplitude. **e.** Pulsed sonication (10 second cycle).

polymerization reactants had only minor effects on the polymer yield (Table 3.1, entries 1–3), and no significant effect on the E/Z ratio. Conversely, changing the amount of initiator to one equivalent gave trace amounts of polymer. Interested in altering the E/Z ratio, we performed the polymerization at 0 °C which gave a slight increase in yield but no change in E/Z ratio (Table 3.1, entry 5), we performed the polymerization with a probe sonicator at different amplitudes and observed a slight decrease in yield with constant E/Z ratio (Table 3.1, entries 6–8). Using optimized polymerization conditions of 0.25 M $\text{Na}_2\text{S}_2\text{O}_4$ and a 1:1 ratio of **3.1** and **3.4** in the bath sonicator, we were able to scale up the iodo-yne polymerization to yield 2.3 g of product (94% yield, Figure 3.3) in 120 minutes. Due to solubility challenges with the iodo-yne polymers, an accurate determination of the molecular weight and dispersity of the products was troublesome. We attempted characterization with different SEC instruments and conditions giving inconsistent results (Figure 3.4).

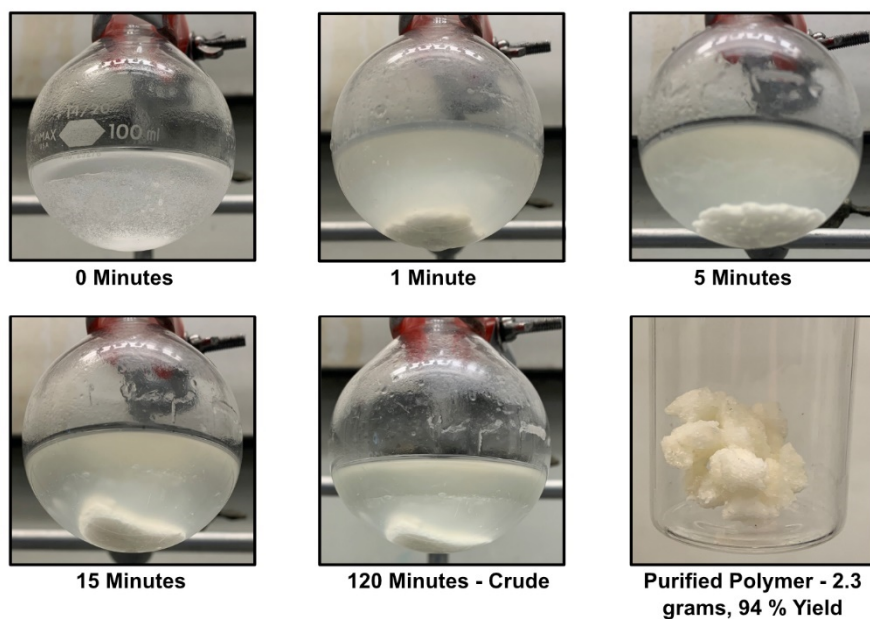


Figure 3.3: Time lapse of large scale polymerization of diiodoperfluorohexane and 1,9-decadiyne. Purified polymer yielded 2.3 grams, a 94% yield

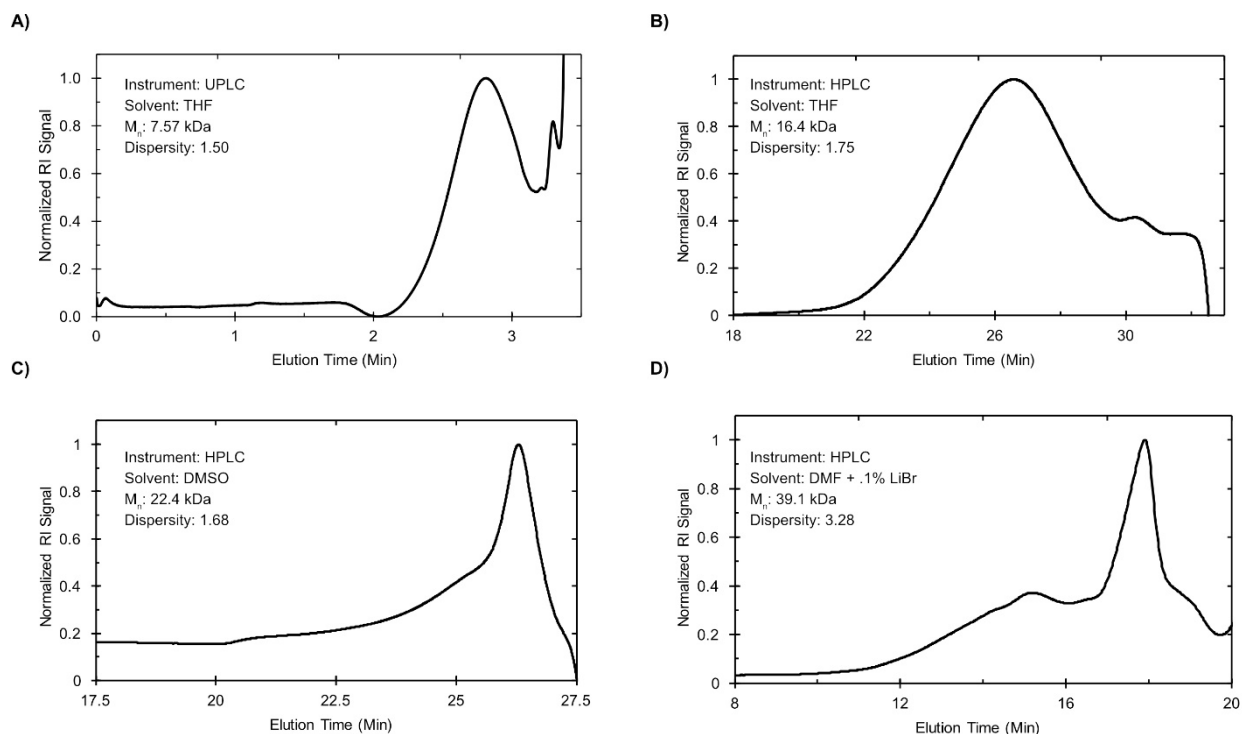
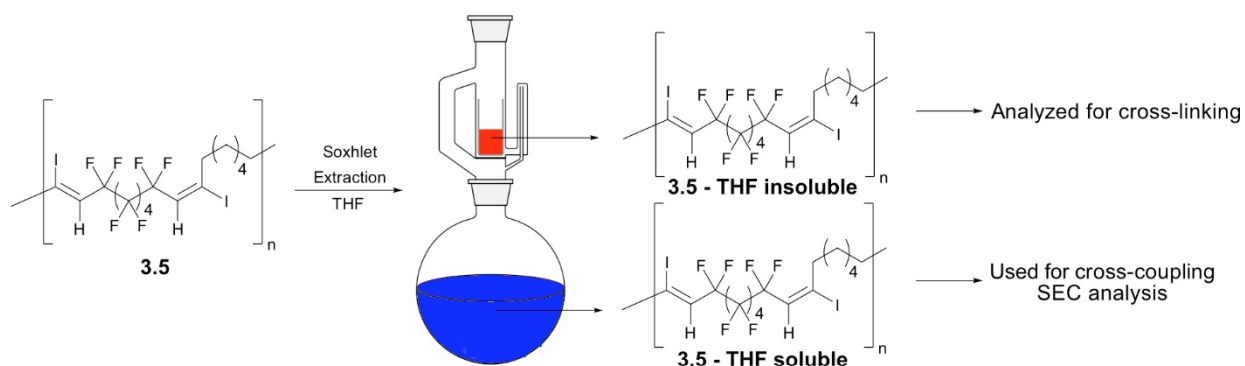


Figure 3.4: Comparison of iodo-yne polymer molecular weight calculation through different SEC analysis conditions. All molecular weight data was calculated through refractive index signal. **A)** SEC performed with THF as an eluent at 39 °C with a flowrate of 0.9 mL/min at 6900 PSI. The instrument was calibrated with a set of low dispersity polystyrene standards. **B)** SEC performed with THF as eluent at 50 °C with a flowrate of 0.7 mL/min. The instrument was calibrated with a set of low dispersity polystyrene standards. **C)** SEC performed with DMSO as eluent at 65 °C with a flowrate of 0.3 mL/min. The instrument was calibrated with a set of low dispersity poly(methyl methacrylate) standards. **D)** SEC performed with DMF + 0.1% LiBr as eluent at 50 °C with a flowrate of 1.0 mL/min. The instrument was calibrated with a set of low dispersity polystyrene standards.

Data obtained on a THF SEC utilizing ultra-high pressure liquid chromatography instrumentation calibrated to low dispersity polystyrene samples are shown in Table 3.1 and indicate approximately 6 kDa polymer, which we believe represents the minimum molecular weight. M_n values as high as 39 kDa have been obtained using DMF as an eluent, but there was significant bimodal character (Figure 3.4D). We confirmed that the higher molecular weight shoulder was not cross-linked via differential scanning calorimetry (Figure 3.5).

A)



B)

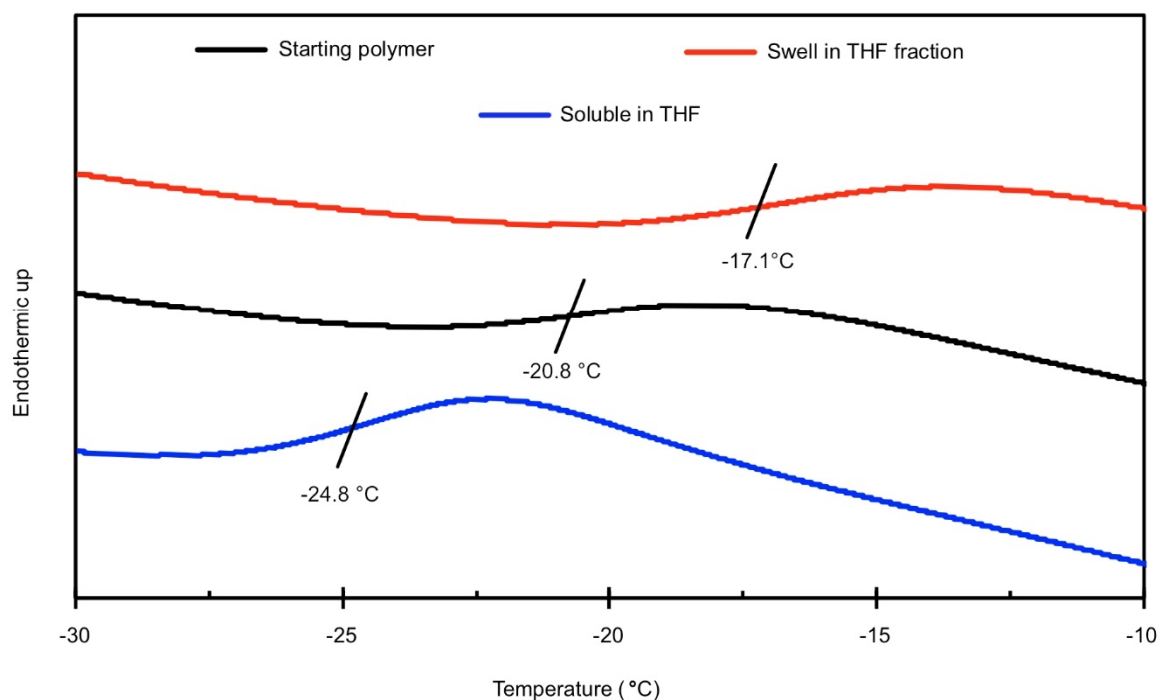


Figure 3.5: Soxhlet fractionation of polymer **3.5** and analysis via differential scanning calorimetry. **A)** Scheme representing Soxhlet extraction of THF soluble polymer **3.5**. **B)** Differential scanning calorimetry comparison of iodo-yne polymer **3.5** before and after Soxhlet purification in THF. Polymer **3.5** before Soxhlet purification (middle, black), the THF soluble fraction of polymer **3.5** (bottom, blue) and the THF insoluble fraction of polymer **3.5** (top, red).

Stability experiments on polymer **3.5** indicate that the vinyl iodide containing polymers were stable to either 110 °C heating or UV irradiation for 18 hours in the solid state. Polymer **3.5** was also stored under ambient conditions over six months with no detectable degradation (Figure 3.6).

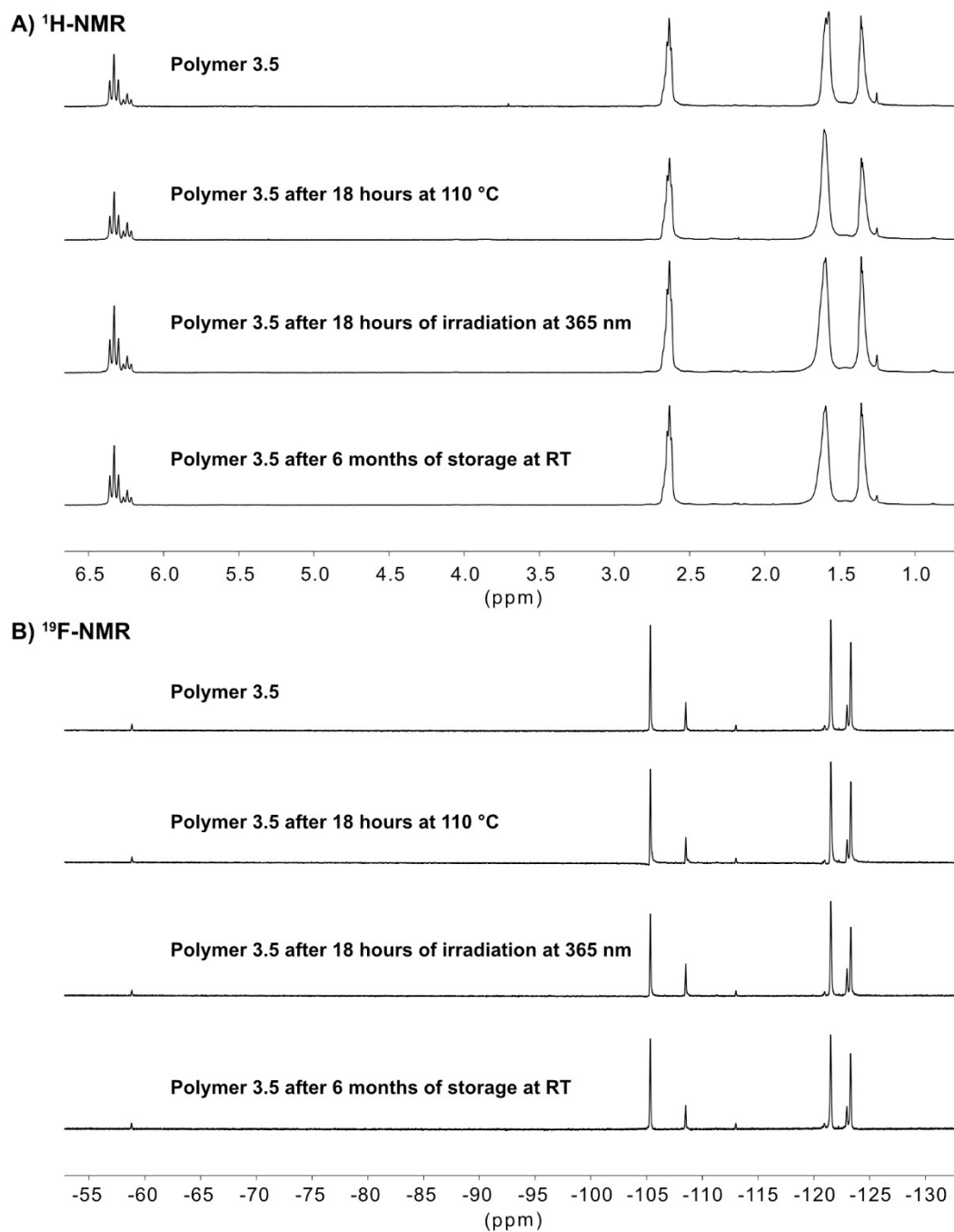


Figure 3.6: NMR analysis of polymer **3.5** following exposure to heat, light, or prolonged shelf life. **A)** $^1\text{H-NMR}$. **B)** $^{19}\text{F-NMR}$.

With polymers containing vinyl iodide functionality readily synthesized, we looked to validate an array of cross-coupling chemistries on the semifluorinated polymers. Vinyl halide couplings are well preceded on small molecules, but there have been few opportunities for these transformations on polymeric backbones. Initially, Sonogashira coupling was attempted on polymer **3.5** with 1-octyne, but only insoluble polymer was observed, which we believe to be a result of reactivity of the terminal alkynes. A control experiment with polymer **3.5**, Pd(PPh₃)₄ and base supported this hypothesis (Figure 3.7).

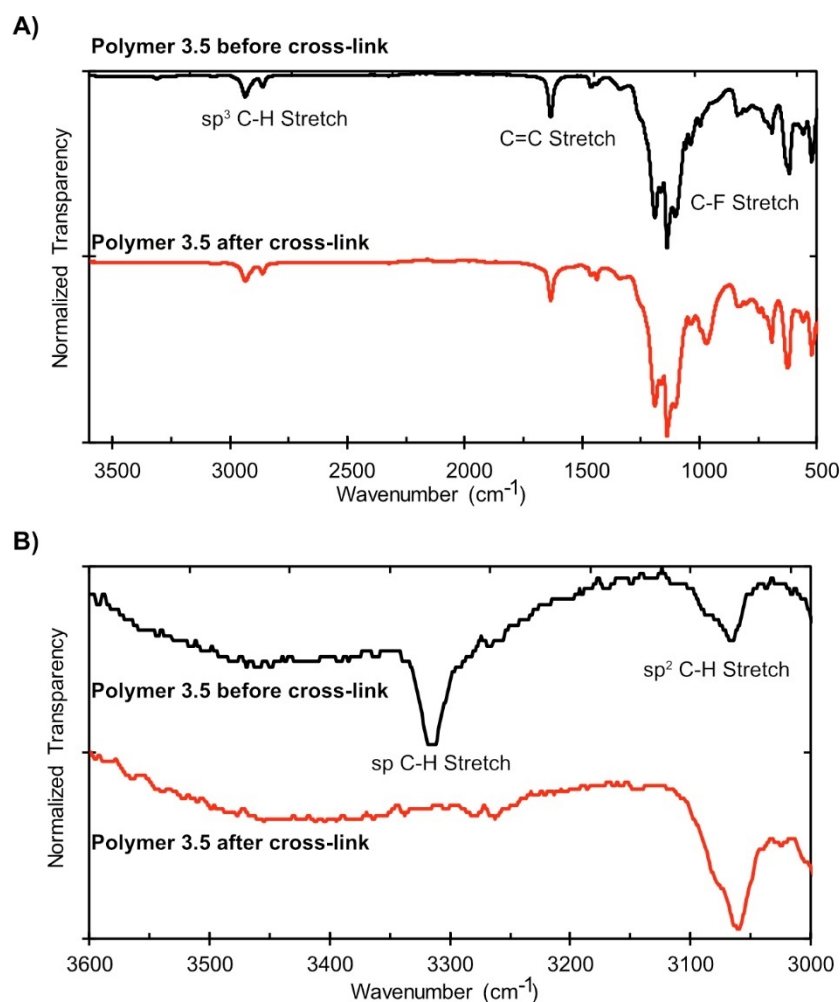
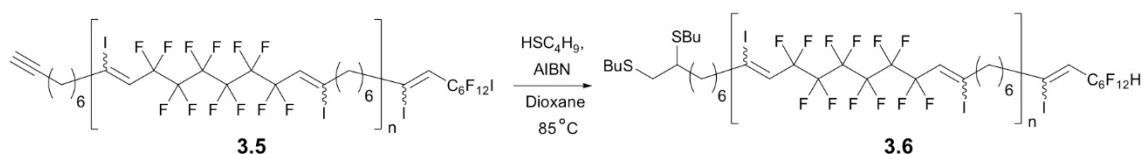


Figure 3.7: Characterization of polymer **3.5** treated with Pd(PPh₃)₄. **A)** Infrared spectroscopy (IR) spectra of polymer **3.5** before (black, top) and after (red, bottom) treatment. **B)** Enhanced region of the identical infrared spectroscopy (IR) spectra in **A**, revealing complete loss of terminal alkyne C-H stretch due to reaction between vinyl iodide groups and terminal alkyne groups.

Scheme 3.2: Reaction scheme of AIBN initiated thiol-yne addition of butanethiol to polymer **3.5** to give polymer **3.6**



To prevent cross-coupling between the vinyl iodide group and terminal alkynes, polymer **3.5** was capped with butane thiol to give polymer **3.6** (Scheme 3.2, Scheme 3.3). Polymer **3.6** successfully underwent Sonogashira coupling with 1-octyne in 100% conversion to give **3.7** in a 51% isolated yield using standard methanol precipitation conditions (Table 3.2, Entry 1). The yield could be further improved to 74% via optimization of isolation conditions (Figure 3.8). Other standard palladium cross-coupling chemistries were also efficient methods of post-polymerization modification with Stille and Suzuki couplings giving greater than 90% conversion, to yield **3.8** and **3.9** with 57% and 74% isolated yield, respectively (Table 3.2, Entries 2 and 3). It should be noted that due to the excess K₂CO₃ and high temperature of the Stille coupling, a small amount (7%) of iodide elimination to yield alkynes was observed. Looking to other metal catalyzed transformations, we found that copper(I) iodide could catalyze the addition of phenols and thiophenols. Interestingly, phenol coupling gave complete conversion at the E-isomer but underwent a series of eliminations and rearrangements on the Z-isomer to yield polymer **3.10** containing both phenol and ene-yne functionality in 88% isolated yield. Final polymer **3.10** represented 65% of vinyl iodide groups being converted to vinyl ethers functionality and 35% being converted to the ene-yne product. (Table 3.2, Entry 4). A small molecule model was used to confirm the identity of the ene-yne product through analysis via GCMS and NMR (Figure 3.9). In contrast to the results with phenol, cross-coupling with thiophenol gave 100% conversion to thioether product **3.11** in 79% yield (Table 3.2, Entry 5). Lastly, iron could be utilized as a catalyst to promote a Kumada coupling between an alkyl Grignard and the vinyl iodide moieties in polymer **3.5** to yield polymer **3.12** (Table 3.2, Entry 6), with competing iodide reduction occurring at 30% of the vinyl iodide sites, giving polymer **3.12**

Scheme 3.3: Reaction scheme of AIBN initiated thiol-yne addition of butanethiol to polymer 3.5 to give polymer 3.6 and the following polymer modifications

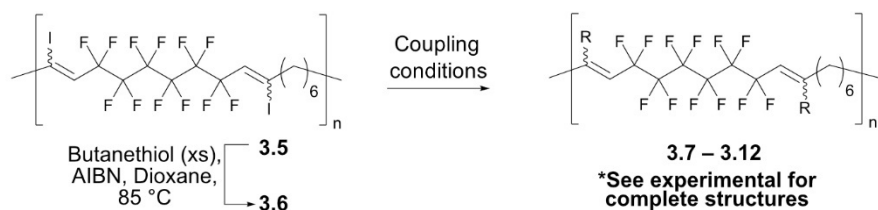
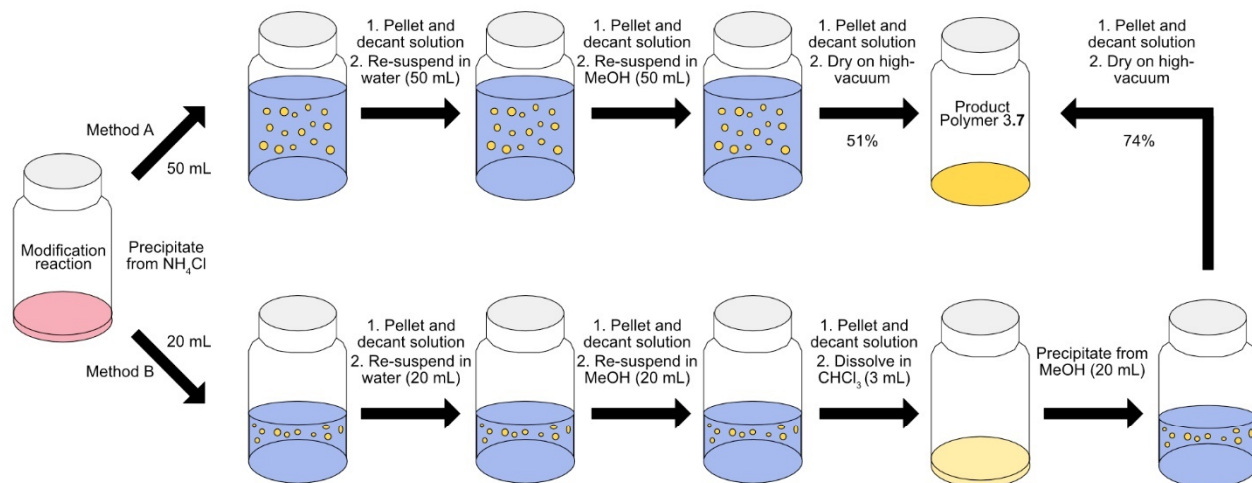


Table 3.2: Scope of cross couplings on vinyl iodide containing polymers

Entry #	Starting polymer	Product	Reagent	R	Catalyst	Solvent	Iodide conversion ^{a,b} (NMR)	M _n ^{c,d}	<i>D</i>	T _g (°C)	T _d (°C)
1	3.6	3.7			Pd(PPh ₃) ₄ / CuI (10 %)	DIPA	100%	20.4	1.8	-25	245
2	3.6	3.8			Pd(PPh ₃) ₄ (10 %)	Toluene	100%	18.7	2.3	-7	266
3	3.6	3.9			Pd(PPh ₃) ₄ (10 %)	DMF	93% coupled to heptene 7% eliminated to give alkynes	12.2	1.9	-37	333
4	3.6	3.10			CuI (20 %)	Dioxane	65% coupled to phenol 35% eliminated and rearranged to ene-yne product	14.2	3.1	-10	329
5	3.6	3.11			CuI (20 %)	Toluene	100%	17.0	2.4	-6	370
6	3.5	3.12	H ₃ C–MgBr		Fe(acac) ₃ (50 %)	THF	70% coupled to methyl group 30% reduced to give alkenes	15.2	2.6	-43	373

a. Calculated as conversion from vinyl iodide to desired functionality. In all reactions, no vinyl iodide was left remaining. The remaining percentage can be attributed to side-reactions indicated in the table. **b.** See experimental for complete representation of polymer structures **c.** THF soluble fraction of polymer 3.5 after Soxhlet extraction was used as a starting material for molecular weight determination, with a starting molecular weight 12.6 kDa and a dispersity of 2.25. **d.** Molecular weight calculated through calibration of low dispersity poly(styrene) standards with THF as an eluent using a standard high performance liquid chromatography instrument. These values differed from those obtained on a ultrahigh pressure THF SEC. See Figure 3.

A) Workflow of polymer purification



B) Stacked $^1\text{H-NMR}$ of pure Polymer 3.7 and the concentrated work-up solution

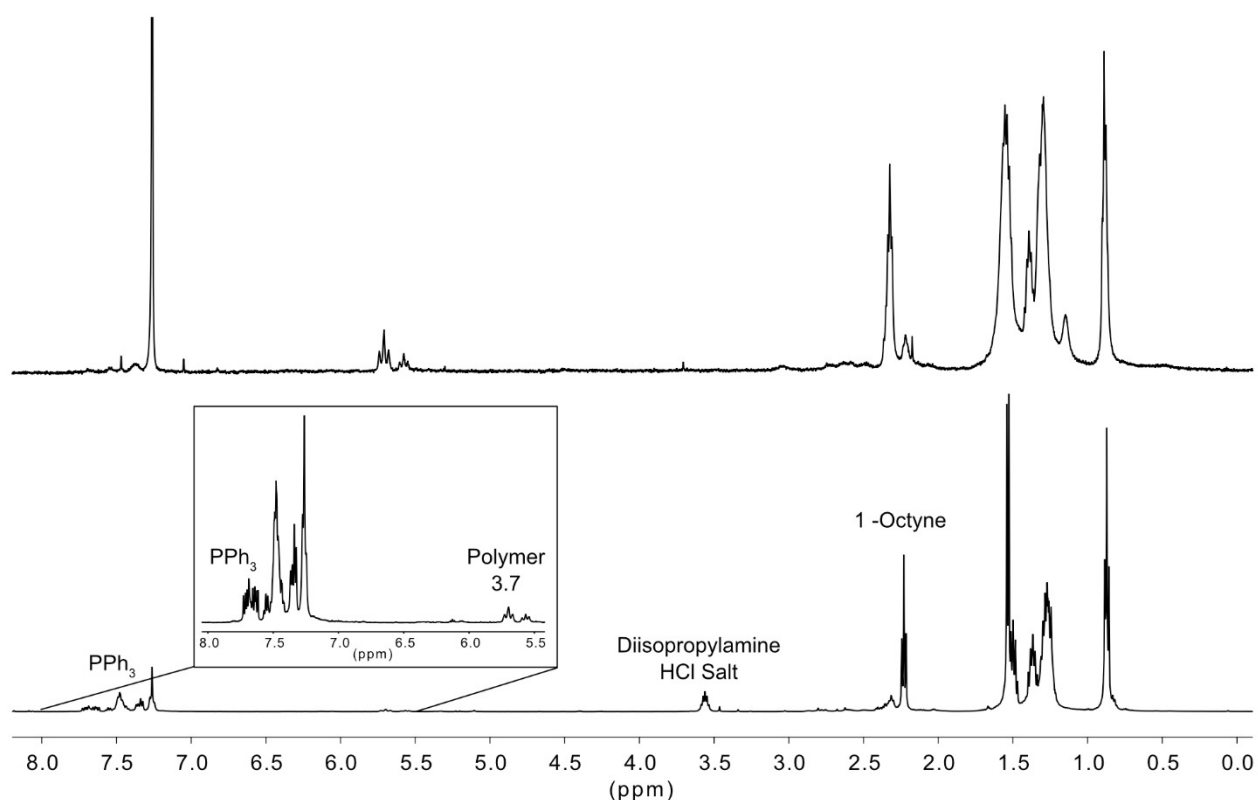


Figure 3.8: Optimization of purification conditions of the Sonogashira coupling to give polymer **3.7**. **A)** Unoptimized purification conditions to give polymer **3.7** in 51% yield (top, method A) and the optimized conditions which gave polymer **3.7** in 74% yield (bottom, method B). **B)** Stacked $^1\text{H-NMR}$ of the purified polymer **3.7** (top) and the concentrated methanol work-up containing 1-octyne, triphenylphosphine, diisopropylammonium chloride, and extracted polymer **3.7** (bottom).

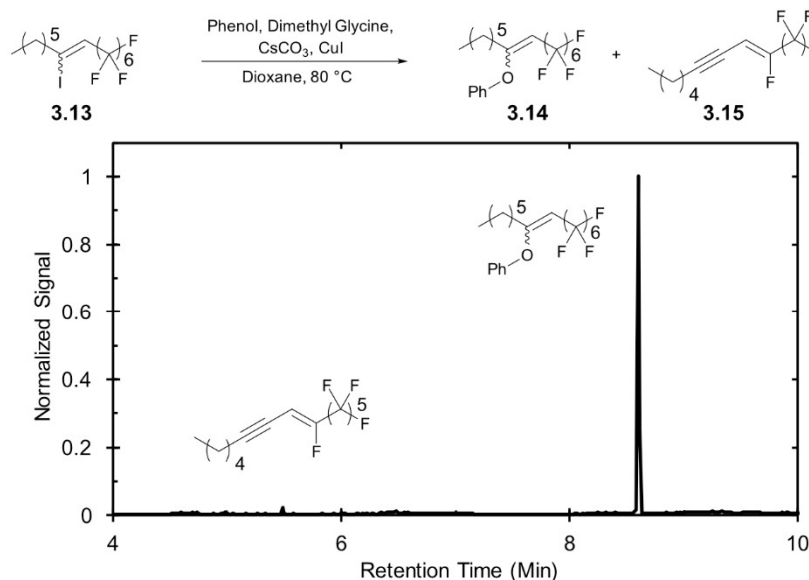


Figure 3.9: Small molecule analog to investigate the phenol coupling. Small molecule **3.13** when reacted with phenol and copper iodide employing dimethylglycine as the ligand to give the phenol coupled product **3.14** as the major product, with a small amount of ene-yne **3.15** formed as a by-product.

in 87% yield. Representative structures of polymers containing significant side reactions (**3.9**, **3.10**, and **3.12**) can be found in the experimental procedures. The vinyl iodide couplings were all performed on THF soluble **3.5**, obtained via Soxhlet extraction (Figure 3.5), such that SEC analysis could be performed. Molecular weight data suggest no scission of the polymer backbone. Note that unlike in methods optimization, standard high performance liquid chromatography instrumentation was used for SEC analysis, leading to discrepancies in M_n between Tables 3.1 and 3.2 (Figure 3.4). Thermal characterization of polymers **3.7–3.12** demonstrates that the T_g could successfully be varied between -6 °C and -43 °C through post-polymerization cross-coupling. With all starting polymers and modifications, 10% mass loss temperatures were 245 °C or above, in contrast to the more thermally labile poly(diiododiacetylenes).

Not only are vinyl halides efficient cross-coupling partners, they can also be eliminated to provide alkynes. We investigated if the vinyl iodide groups could be transformed into activated alkynes across the polymer backbone. The iodo-yne polymerization naturally installs electron withdrawing perfluorinated groups, which have been shown to activate alkynes toward cycloadditions.³¹ Thus, eliminated iodo-yne polymers provide another intriguing functionality for post-polymerization modification. Initial attempts

at iodide elimination from polymer **3.5**, employing KOH, KO t Bu, or tetramethylguanidine (TMG) as a base produced polymer **3.16**, with Z but not E vinyl iodide groups transformed to alkynes (Figure 3.10A).

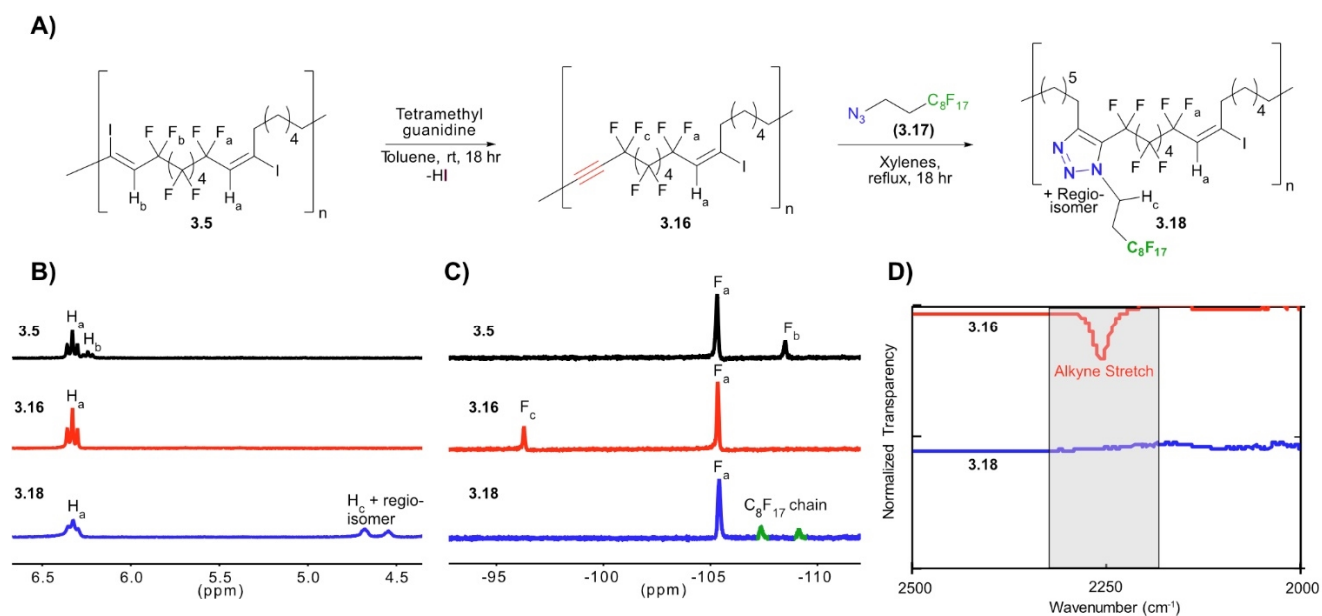


Figure 3.10. A) Elimination of iodide with tetramethyl guanidine to yield activated alkynes that undergo cycloaddition with azides. B) Portion of ¹H-NMR of polymer **3.5** (top, black), polymer **3.16** (middle, red), and polymer **3.18** (bottom, blue). C) Portion of ¹⁹F-NMR of polymer **3.5** (top, black), polymer **3.16** (middle, red), polymer **3.18** (bottom, blue). D) Portion of infrared spectroscopy (IR) depicting the alkyne stretch for polymer **3.16** (top, red) and cycloadduct **3.18** (bottom, blue). Full NMR and IR spectra can be found in the supporting information.

Any attempts with stronger bases and higher temperatures yielded significant degradation. Elimination of iodide from the polymer backbone provided increased thermal stability while maintaining a similar glass transition temperature (Figure 3.11). To enhance the yield of elimination, olefin isomerization to increase the amount of easily eliminated Z vinyl iodide was pursued using 365 nm light. When a solution of **3.5** was irradiated in toluene for 16 hours, the E:Z ratio could be converted from 3:1 to 6:5 (Figure 3.12), an interesting contrast to UV irradiation in the solid state. By dual treatment with 365 nm light and TMG in toluene, 50% elimination could be obtained (Figure 3.13). Next, we aimed to perform cycloaddition chemistries on the alkynes installed in the backbone. Polymer **3.16** was treated with fluororous azide **3.17** and upon heating, triazole formation was observed to give polymer **3.18**, as a mixture of regio-isomers. This simple post-polymerization modification opens many possibilities for further attachment of side chains, such as a fluorophores or biomolecules, as well as potential for cross-linked materials.

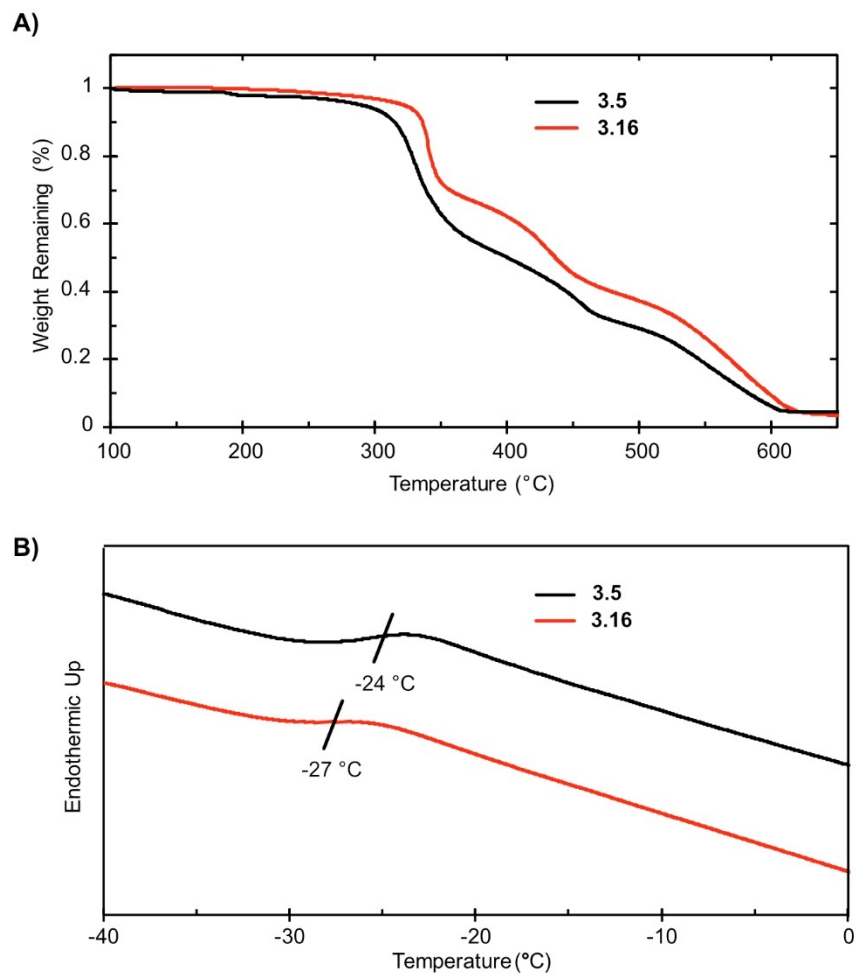
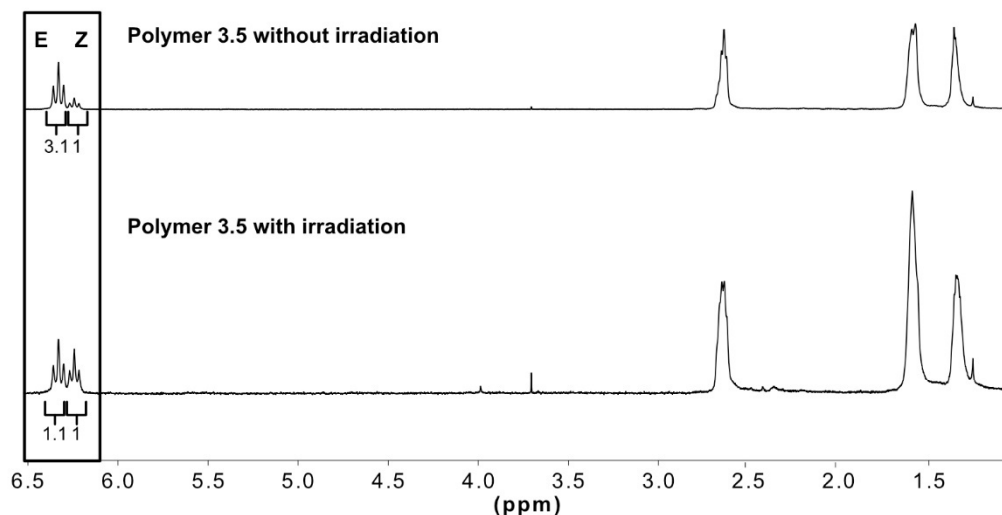


Figure 3.11: Thermal analysis of polymers **3.5** and **3.16**. **A)** Thermal gravimetric analysis (TGA) of polymers **3.5** (black) and **3.16** (red) under oxygen, showing an increase in thermal stability following elimination of the iodide with tetramethyl guanidine. **B)** Differential scanning calorimetry (DSC) of polymers **3.5** (black) and **3.16** (red) indicating a minor change in the glass transition temperature (T_g).

A) $^1\text{H-NMR}$



B) $^{19}\text{F-NMR}$

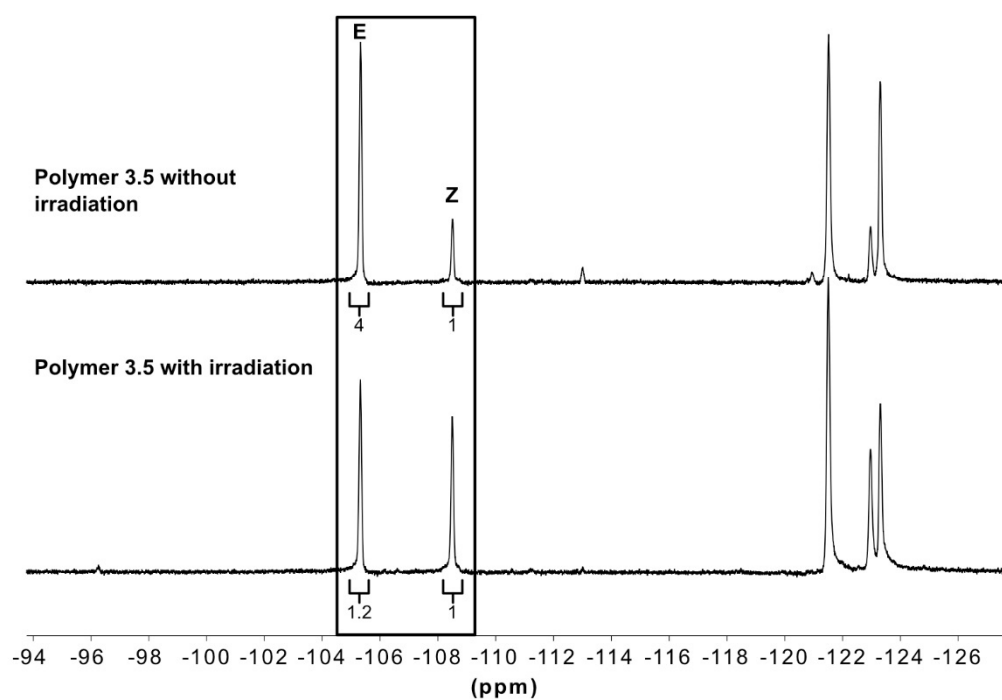


Figure 3.12: Use of 365 nm light to isomerize the olefin generated via iodo-yne polymerization. Polymer sample was irradiated while swollen in toluene solution at a concentration of 100 mg/mL. **A)** $^1\text{H-NMR}$ comparing polymer **3.5** that had not been irradiated with light (top) and polymer **3.5** that had been irradiated with light (bottom). **B)** $^{19}\text{F-NMR}$ comparing polymer **3.5** that had not been irradiated with light (top) and polymer **3.5** that had been irradiated with light (bottom).

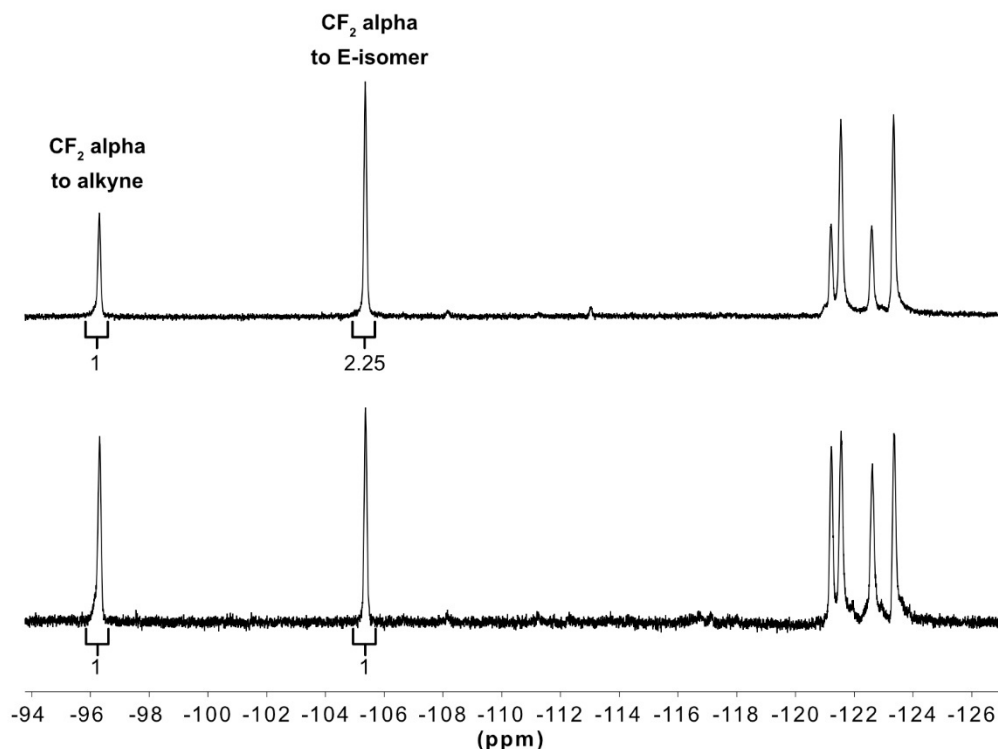


Figure 3.13: Overlaid ^{19}F -NMR spectra comparing the elimination of vinyl iodide with and without irradiation of 365 nm light. ^{19}F -NMR of polymer **3.16** that was synthesized with tetramethyl guanidine as a base, without 365 nm light (top) and ^{19}F -NMR of polymer **3.16** that was synthesized with tetramethyl guanidine as a base, with illumination via 365 nm light throughout the reaction (bottom).

3.4 Conclusion

In summary, a simple polymerization method of diynes and diiodoperfluoroalkanes was developed to facilitate the production of vinyl iodide containing semifluorinated polymers. Vinyl iodide functionality on the backbone is scarce in the polymer literature, making this method an important addition to the toolbox for the preparation of functional materials. We demonstrated that the vinyl iodide group is a versatile handle for post-polymerization modification through cross-coupling chemistries. Additionally, varying levels of elimination can be achieved through isomerization of the olefin bond with 365 nm light followed by elimination. The resulting polymers containing activated alkynes can be further modified through cycloaddition chemistries. These methods have demonstrated a high level of tunability in iodo-yne polymers, paving the way for future smart materials.

3.5 Experimental procedures

3.5.1 General experimental procedures:

Chemical reagents were purchased from Sigma-Aldrich, Alfa Aesar, Fisher Scientific, or Acros Organics and used without purification unless noted otherwise. No unexpected or unusually high safety hazards were encountered. Anhydrous and deoxygenated solvents toluene (PhMe), tetrahydrofuran (THF), dichloromethane (DCM), acetonitrile (MeCN), and dimethylformamide (DMF) were dispensed from a Grubb's-type Phoenix Solvent Drying System.³² Thin layer chromatography was performed using Silica Gel 60 F254 (EMD Millipore) plates. Flash chromatography was executed with technical grade silica gel with 60 Å pores and 40–63 µm mesh particle size (Sorbtech Technologies). Solvent was removed under reduced pressure with a Büchi Rotovapor with a Welch self-cleaning dry vacuum pump and further dried with a Welch DuoSeal pump. Bath sonication was performed using a Branson 3800 ultrasonic cleaner. Nuclear magnetic resonance (¹H-NMR, ¹³C-NMR, and ¹⁹F-NMR) spectra were taken on Bruker Avance 500 (¹H-NMR and ¹³C-NMR) or AV-300 (¹⁹F-NMR) instruments and processed with MestReNova software. All ¹H, ¹³C, and ¹⁹F NMR spectra are reported in ppm and relative to residual solvent signals (¹H, ¹³C). Fluorine NMR were reported with trifluoroacetic acid as the reference peak as an external standard. Size exclusion chromatography (SEC), unless otherwise noted, was conducted on a Shimadzu prominence-I LC-2030C high performance liquid chromatography (HPLC) system with a UV detector and connected to a Wyatt Dawn Heleos-II light scattering detector and Wyatt Optilab T-rEX refractive index detector, one MZ Analysentechnik GPC-Precolumn 50 x 8.0 mm MZ-Gel SDplus Linear LS 5µm pore, and two MZ Analysentechnik GPC-column 300 x 8.0 mm MZ-Gel SDplus Linear LS 5µm pore. Eluent was THF at 50 °C (flow rate: 0.70 mL/ min). Calibration was performed using near monodisperse polystyrene PS standards from Polymer Laboratories. Differential scanning calorimetry measurements were taken on a PerkinElmer DSC. Thermal gravimetric analysis was performed on a PerkinElmer Pyris Diamond TG/DTA Thermogravimetric/Differential Thermal Analyzer. Mass spectra (Electron impact (EI)) were collected on an Agilent 7890B-7520 Quadrupole Time-of-Flight GC/MS. Irradiation with light was performed with BI365 nm Inspection UV LED lamp, purchased from Risk reactor (Output power

density $>5000\mu\text{W}/\text{cm}^2$ at 15" (38 cm), voltage range 90-265V ac, output power: 3*325 mW at 365 nm peak). Centrifugation was performed on a Thermo Scientific Sorvall ST 16 Centrifuge. All sonication was done in a Branson M-Series Model 3800 120V bath sonicator. For probe sonication, a QSonica (Q125) sonicator was used.

Abbreviations: AIBN = azoisobutyronitrile; DBU = 1,8-Diazabicyclo[5.4.0]undec-7-ene; DCM = dichloromethane; DMF = dimethylformamide; DMSO = dimethylsulfoxide; DSC = differential scanning calorimetry; Et₂O = diethyl ether; MeCN = acetonitrile ; MeOH = methanol; PhMe = toluene; SEC = size exclusion chromatography; TGA = thermal gravimetric analysis; THF = tetrahydrofuran; TMG = tetramethylguanidine

SEC prep/procedures:

THF HPLC instrument: Size exclusion chromatography (SEC) was conducted on a Shimadzu prominence-I LC-2030C high performance liquid chromatography (HPLC) system with a UV detector and connected to a Wyatt Dawn Heleos-II light scattering detector and Wyatt Optilab T-rEX refractive index detector. Calibration was performed using near monodisperse polystyrene standards from Polymer Laboratories. Polymer samples were dissolved in THF (5 mg/mL) and stirred at 50 °C for 1 hour. Polymer solutions were filtered through 0.2 micron PTFE filter and 50 μL were then run through one MZ Analysentechnik GPC-Precolumn 50 x 8.0 mm MZ-Gel SDplus Linear LS 5 μm pore, and two MZ Analysentechnik GPC-column 300 x 8.0 mm MZ-Gel SDplus Linear LS 5 μm pore columns at 50 °C with an eluent rate of 0.7mL/min. Unless otherwise noted, UV absorbance was used for molecular weight determination.

DMSO HPLC instrument: Size exclusion chromatography (SEC) was conducted on a Shimadzu prominence-I LC-2030C high performance liquid chromatography (HPLC) system with a UV detector and connected to a Wyatt Dawn Heleos-II light scattering detector and Wyatt Optilab T-rEX refractive index detector. Calibration was performed using near monodisperse poly(methyl-methacrylate) PMMA standards from Polymer Laboratories. Polymer samples were dissolved in DMSO (5 mg/mL) and stirred

at 100 °C for 1 hour. Polymer solutions were filtered through 0.2 micron PTFE filter and 50 µL were then run through one Agilent PLgel guard column D, and an Agilent PLgel 10 µm mixed B columns at 65 °C with a flow rate at 0.35 mL/min. Unless otherwise noted, RI signal was used for molecular weight determination.

DMF HPLC instrument: Size exclusion chromatography (SEC) was conducted on a Waters Alliance HPLC System, 2695 Separation Module high performance liquid chromatography (HPLC) system with a Waters 2414 Differential Refractometer (RI) and Waters 2998 Photodiode Array Detector (PDA). Calibration was performed using near monodisperse polystyrene standards from Polymer Laboratories. Polymer samples were dissolved in DMF (5 mg/mL) and stirred at 85 °C for 1 hour. Polymer solutions were filtered through 0.2 micron PTFE filter and 40 µL were then run through 2 Tosoh TSKgel Super HM-M columns at 50 °C with a flow rate at 0.30 mL/min. Unless otherwise noted, RI signal was used for molecular weight determination.

THF UPLC instrument: Size exclusion chromatography (SEC) was conducted on a Waters Acquity APC ultra-high performance liquid chromatography (UPLC) system with an ACQUITY UPLC PDA Detector and an ACQUITY UPLC Refractive Index Detector. Calibration was performed using near monodisperse polystyrene standards from Polymer Laboratories. Polymer samples were dissolved in THF (5 mg/mL) and stirred at 50 °C for 1 hour. Polymer solutions were filtered through 0.2 micron PTFE filter and 25 µL were then run through Three Acquity APC XT Columns (45 + 200 + 450 pore sizes) at 39 °C with a flow rate at 0.9 mL/min with a column pressure of 6900 PSI. Unless otherwise noted, RI signal was used for molecular weight determination.

TGA prep/procedures: Polymer samples (5–10 mg) were placed in a calibrated ceramic container and the temperature was raised to 100 °C. After a delay of 1 minute to remove residual solvent, the weight of the sample was re-recorded, and the temperature was raised to 650 °C at a rate of 20 °C/min. The resulting

data were then normalized to % weight loss of sample. Unless otherwise noted all samples were run under nitrogen atmosphere.

DSC prep/procedures: Polymer sample (10–20 mg) were placed in an aluminum pan and cooled to -50 °C and equilibrated for 2 minutes. The samples were then heated to 100 °C at a rate of 20 °C/min with a 2-minute pause at 100 °C. Samples were then cooled back down to -50 °C at a rate of 15 °C/min with a 2-minute pause at -50 °C. This cycle was then repeated two additional times.

Photochemistry assembly: Our homemade photobox was assembled to the shape of the UV light source (Risk reactor (Output power density $>5000\mu\text{W}/\text{cm}^2$ at 15" (38 cm), voltage range 90-265V ac, output power: 3*325 mW at 365 nm peak)) using cardboard and black tape. The interior was then coated with aluminum foil and holes were cut on the top sample placement.

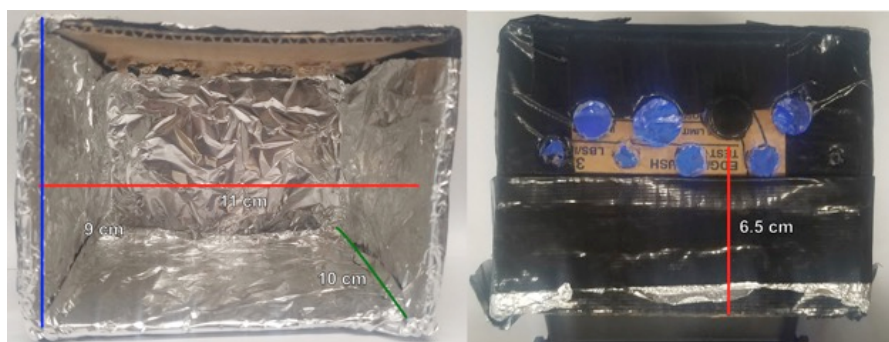


Figure 3.14: Photochemistry assembly for all reactions and isomerizations.

3.5.2 Procedures for the synthesis of small molecules:

9,9,10,10,11,11,12,12,13,13,14,14-dodecafluoro-7,16-diiododocosa-7,15-diene, 3.2 (E,E) and 3.3 (E,Z):

Diiodoperfluorohexane (1.1 g, 2.0 mmol, 1.0 eq) was dissolved in acetonitrile (8 mL) and water (6 mL). 1-Octyne (0.451 g, 4.09 mmol, 2.1 eq) was added, followed by sodium bicarbonate (0.39 g, 4.6 mmol, 2.3 eq). Sodium dithionite (0.80 g, 4.6 mmol, 2.3 eq) was then added and the solution was placed in a sonication bath for 2 hours. The reaction mixture was diluted with brine (10 mL) and extracted with EtOAc (3 x 15 mL). The organic layer was dried with MgSO_4 , decanted, and concentrated to give crude

oil. Purification through silica plug with hexanes as the eluent yielded the product as a clear oil and mix of isomers (0.83 g, 1.3 mmol, 65%). ¹H NMR (CDCl₃, 500 MHz), δ ppm: 6.31 (t, *J* = 12 Hz, 1.6H), 6.23 (t, *J* = 12 Hz, 0.4H), 2.62 (m, 4H), 1.57 (m, 4H), 1.30 (m, 12H), 0.9 (t, *J* = 8 Hz, 6H). ¹³C NMR (CDCl₃, 126 MHz), δ ppm: 126.7 (t, *J* = 25.2 Hz), 122.8 (t, *J* = 6.3 Hz), 121.8 (t, *J* = 25.2 Hz), 117.0-107.0, (m, 7C), 41.1, 31.5, 30.0, 29.0, 28.1, 27.6, 22.5, 14.0. ¹⁹F NMR (CDCl₃, 376 MHz), δ ppm: -105.35 (s, 4F), -108.46 (s, 0.8F), -121.51 (s, 4.8F), -123.00 (s, 0.8F), -123.29 (s, 4F). HRMS (EI) Calculated for C₂₂H₂₈F₁₂I₂ [M-I]: 774.0089, found: 774.0069.

1,1,1,2,2,3,3,4,4,5,5,6,6-tridecafluoro-8-iodotetradec-7-ene, 3.13:

Iodoperfluorohexane (1.5 g, 3.3 mmol, 1.1 eq) was dissolved in acetonitrile (6 mL) and water (4.5 mL). 1-Octyne (0.33 g, 3.0 mmol, 1.0 eq) was added followed by sodium bicarbonate (0.32 g, 3.8 mmol, 1.2 eq). Sodium dithionite (0.66 g, 3.8 mmol, 1.2 eq) was then added and the solution was placed in a sonication bath for 2 hours. The reaction mixture diluted with brine (10 mL) and extracted with EtOAc (3 x 15 mL). The organic layer was dried with MgSO₄, decanted, and concentrated to give crude oil. Purification through a silica plug with hexanes as the eluent gave pure product as a clear oil (1.38 g, 2.71 mmol, 82%). NMR data matched known compound.³³

((9,9,10,10,11,11,12,12,13,13,14,14,14-tridecafluorotetradec-7-en-7-yl)oxy)benzene, 3.14:

Compound **3.13** (0.52 g, 0.93 mmol, 1.0 eq) was dissolved in dioxane (6.5 mL). Phenol (0.350 g, 3.92 mmol, 4.0 eq) and dimethyl glycine (0.028 g, 0.28 mmol, 0.30 eq) were then added. The solution was degassed via freeze-pump-thaw (x3). Cesium carbonate (0.636 g, 1.81 mmol, 2.0 eq) and copper iodide (0.017 g, 0.093 mmol, 0.10 eq) were then added and the reaction was set to 90 °C for 16 hours. The reaction was cooled to room temperature, concentrated and run through a silica column with hexanes as the eluent to give a mixture of compounds **3.14** and **3.15** in a 4:1 ratio as a clear oil (0.210 g, 0.402 mmol, 43%). This mixture was further separated by preparatory TLC. ¹H NMR (CDCl₃, 500 MHz), δ ppm: 7.40 (t, *J* = 8.0 Hz, 2H), 7.23 (t, *J* = 7.4 Hz, 1H), 7.01 (d, *J* = 7.5 Hz, 2H), 4.41 (t, *J* = 14.9 Hz, 1H), 2.52 (t, *J* = 7.7 Hz, 2H), 1.72 (p, *J* = 7.6 Hz, 2H), 1.49 – 1.28 (m, 6H), 0.91 (t, *J* = 8.3, 7.5 Hz, 3H). ¹³C NMR

(CDCl₃, 126 MHz), δ ppm: 170.1, 153.5, 130.1, 125.6, 121.4, 119.4 – 107.2 (m, 6C), 92.1 (t, J = 25.2 Hz), 31.5, 31.4 (t, J = 2.5 Hz), 28.9, 27.4, 22.5, 14.0. ¹⁹F NMR (CDCl₃, 376 MHz), δ ppm: δ -80.81 (t, J = 9.9 Hz, 3F), -102.56 (q, J = 13.6 Hz, 2F), -121.67 (m, 2F), -122.86 (m, 2F), -123.38 (m, 2F), -126.14 (m, 2F). HRMS (EI) Calculated for C₂₀H₁₉F₁₃O [M-HOC₆H₅]: 428.0810, found: 428.0633.

1,1,1,2,2,3,3,4,4,5,5,6-dodecafluorotetradec-6-en-8-yne, 3.15:

Compound **3.13** (0.42 g, 0.75 mmol, 1.0 eq) was dissolved in dioxane (4.2 mL). Phenol (0.28 g, 3.0 mmol, 4.0 eq) and 3,4,7,8-tetramethyl phenanthroline (0.053 g, 0.23 mmol, 0.30 eq) were then added. The solution was sparged under nitrogen gas for 20 minutes. Cesium carbonate (0.53 g, 1.5 mmol, 2.0 eq) and copper iodide (0.014 g, 0.075 mmol, 0.10 eq) were then added and the reaction was set to 90 °C for 16 hours. The reaction was cooled to room temperature, concentrated and run through a long silica column with hexanes as the eluent to give a mixture of compounds with predominately the en-yne rearrangement product **s5** as a 3:1 ratio of E/Z isomers, but with a small fraction of starting material and phenol coupled product which couldn't be removed (0.080 g, 0.20 mmol, 26%). ¹H NMR (CDCl₃, 500 MHz), δ ppm: δ 6.09 – 5.99 (m, 0.25H), 5.71 (dt, J = 29.3, 2.1 Hz, 0.75H), 2.39 (t, J = 6.7 Hz, 1.5H), 2.33 (t, J = 6.9 Hz, 0.5H), 1.61 – 1.54 (m, 2H), 1.43 – 1.22 (m, 4H), 0.91 (t, J = 7.2 Hz, 3H). ¹³C NMR (CDCl₃, 126 MHz), δ ppm: 152.2 (dt, J = 272.3, 28.3 Hz), 119.6 – 107.3 (m, 6C), 103.4 (d, J = 6.7 Hz), 98.2 (q, J = 6.4 Hz), 69.3, 31.0, 27.9, 22.1, 19.7, 13.9. ¹⁹F NMR (CDCl₃, 376 MHz), δ ppm: -80.83 (s, 3F), -115.91 – -116.87 (m, 0.5F), -118.02 (q, J = 13.8 Hz, 1.5F), -118.42 – -119.16 (m, 0.75F), -120.12 – -120.91 (m, 0.25F), -122.47 – -123.73 (m, 4F), -126.23 (2F). Calculated for C₁₄H₁₂F₁₂ [M]: 408.0747, found: 408.0577.

3.5.3 Polymer experimental procedures:

1-perfluorohexyl-2,9-diiodo-1,9-decadiene block polymer, 3.5:

Diiodoperfluorohexane (2.0 g, 3.6 mmol, 1.0 eq) was dissolved in acetonitrile (14.4 mL) and water (11.0 mL). 1,9-Decadiyne (0.48 g, 3.6 mmol, 1.0 eq) was added, followed by sodium bicarbonate (0.70 g, 8.3 mmol, 2.3 eq). Sodium dithionite (1.44 g, 8.27 mmol, 2.3 eq) was added and the solution was placed in a sonication bath for 2 hours. The reaction mixture was then precipitated from water (100 mL) and washed

with methanol (2 x 100 mL). The precipitate was centrifuged at 2500 X g for 5 minutes, and the resulting pellet was dried under high vacuum at 60 °C to yield a white solid (2.33 g, 3.38 mmol, 94%). ¹H NMR (CDCl₃, 500 MHz), δ ppm: 6.33 (t, *J* = 14.4 Hz, 1.5H), 6.24 (t, *J* = 13.0 Hz, 0.5H), 2.65 (m, 4H), 1.59 (m, 4H), 1.45 – 1.27 (m, 4H). ¹⁹F NMR (CDCl₃, 376 MHz), δ ppm: -105.35 (s, 3F), -108.53 (s, 1F), -121.52 (s, 4F), -122.91 (s, 1F), -123.27(s, 3F). FT-IR: 2932 (C-H str) (w), 1635 (C=C) Vinyl iodide (s), 1100-1200 (C-F bend) (vs). TGA: 10% mass loss at 330 °C. *T_g* (DSC): -24.0 °C

Fractionation between THF soluble and insoluble polymer 3.5:

Polymer **3.5** (0.176 g, 0.254 mmol, repeat unit eq) was placed in a Soxhlet extraction apparatus lined with a cellulose thimble connected to a round bottom flask charged with THF without inhibitor (100 mL). THF was then brought to reflux for 16 hours. The THF layer was concentrated and dried under high vacuum to give THF soluble polymer **3** (0.105 g, 0.152 mmol, 60%). Polymer **3.5** remaining in the cellulose thimble was removed and dried under high vacuum for 16 hours to give THF insoluble polymer **3.5** (0.071g, 0.102 mmol, 40%).

3.5.4 Procedures for post-polymerization modifications:

Thiol capping of polymer 3.5, 3.6:

Polymer **3.5** (0.80 g, 1.2 mmol, repeat unit eq) was swollen in dioxane (8 mL). Butanethiol (1.05 g, 11.2 mmol, 10 eq) was added, followed by AIBN (0.095 g, 0.58 mmol, 0.50 eq). The reaction mixture was then heated to 90 °C for fourteen hours. The following morning the mixture was precipitated from ice water (100 mL). The precipitate was then washed with cold methanol (2 x 100 mL). The precipitate was centrifuged at 2500 X g for 5 minutes, and the resulting pellet was dried with high vacuum at 60 °C to yield an orange solid (0.712 g, 1.03 mmol, 89%). ¹H NMR (CDCl₃, 500 MHz), δ ppm: 6.33 (t, *J* = 14.4 Hz, 1.5H), 6.24 (t, *J* = 13.0 Hz, 0.5H), 2.65 (m, 4H), 1.59 (m, 4H), 1.45 – 1.27 (m, 4H). ¹⁹F NMR (CDCl₃, 376 MHz), δ ppm: -105.35 (s, 3F), -108.53 (s, 1F), -121.52 (s, 4F), -122.91 (s, 1F), -123.27(s, 3F). FT-IR: 2932 (C-H str) (w), 1635 (C=C str) (s), 1100-1200 (C-F bend) (vs).

Sonogashira coupling of polymer 3.6, 3.7:

Polymer **3.6** (0.100 g, 0.145 mmol, repeat unit eq) was swollen in diisopropylamine (1 mL). 1-Octyne (0.095 g, 0.87 mmol, 6.0 eq) was added. The solution was degassed via freeze-pump-thaw (x3). Copper iodide (0.0015 g, 0.0070 mmol, 0.05 eq) and tetrakis(triphenylphosphine) palladium (0.008 g, 0.007 mmol, 0.05 eq) were added. The reaction mixture was then heated to 50 °C for fourteen hours. The following morning the mixture was precipitated from saturated ammonium chloride (50 mL), followed by washing with water (50 mL) and methanol (50 mL). The precipitate was centrifuged at 2500 X *g* for 5 minutes, and the resulting pellet was dried under high vacuum to yield a light brown solid (0.048 g, 0.074 mmol, 74%). ¹H NMR (CDCl₃, 500 MHz), δ ppm: 5.71 (t, *J* = 16.2 Hz, 1.4H), 5.57 (t, *J* = 11.3 Hz, 0.7H), 2.40 – 2.27 (m, 5.4H), 2.27 – 2.18 (m, 1.3H), 1.64 – 1.47 (m, 10H), 1.47 – 1.18 (m, 16H), 0.89 (t, *J* = 6.7 Hz, 6H). ¹⁹F NMR (CDCl₃, 376 MHz), δ ppm: -105.47 (m, 3F), -108.31 (m, 1F), -121.93 (m, 4F), -123.81 (m, 4F). FT-IR: 2932 (C-H str) (w), 2222 (C≡C str) (w), 1630 (C=C str) (s), 1100-1200 (C-F bend) (vs). TGA: 10% mass loss at 245 °C. *T_g* (DSC): -25.0 °C

Stille coupling of polymer 3.6, 3.8:

Polymer **3.6** (0.100 g, 0.145 mmol, repeat unit eq) was swollen in toluene (1 mL). 2-(tributyltin) furan (0.30 g, 0.87 mmol, 6.0 eq) was added. The solution was degassed via freeze-pump-thaw (x3). Tetrakis(triphenylphosphine) palladium (0.008 g, 0.007 mmol, 0.05 eq) was then added and capped. The reaction mixture was heated to 60 °C for fourteen hours. The following morning the mixture was precipitated from cold methanol (50 mL), followed by washing with methanol two times (50 mL). The precipitate was centrifuged at 2500 X *g* for 5 minutes, and the resulting pellet was dried with high vacuum to yield a light orange solid (0.046 g, 0.082 mmol, 57%). ¹H NMR (CDCl₃, 500 MHz), δ ppm: 7.45 (s, 0.6H), 7.41 (s, 1.4H), 6.66 (s, 0.6H), 6.53 (s, 1.4H), 6.42 (s, 2H), 6.04 (t, *J* = 16.2 Hz, 1.4H), 5.46 (t, *J* = 16.2 Hz, 0.6H), 2.61 – 2.44 (m, 4H), 1.66 – 1.52 (m, 2H), 1.49 – 1.27 (m, 6H). ¹⁹F NMR (CDCl₃, 376 MHz), δ ppm: -104.52 (s, 3F), -104.87 (s, 1F), -121.39 (s, 4F), -122.54 – -124.29 (m, 4F). FT-IR: 2932

(C-H str) (w), 1707 (C=C str) furan (s), 1635 (C=C str) alkene (s), 1100-1200 (C-F bend) (vs). TGA: 10% mass loss at 266 °C. T_g (DSC): 17.0 °C

Suzuki coupling of polymer 3.6, 3.9:

Polymer **3.6** (0.100 g, 0.145 mmol, repeat unit eq) was swollen in dimethylformamide (2 mL). 7-heptenyl boronic acid (0.082 g, 0.58 mmol, 4.0 eq) was added. The solution was degassed via freeze-pump-thaw (x3). Potassium carbonate (0.12 g, 0.87 mmol, 6.0 eq) and tetrakis(triphenylphosphine) palladium (0.008 g, 0.007 mmol, 0.05 eq) were then added. The reaction mixture was heated to 85 °C for fourteen hours. The following morning the mixture was precipitated from saturated sodium bicarbonate (50 mL), followed by washing with water (50 mL) and methanol (2 x 50 mL). The precipitate was centrifuged at 2500 X g for 5 minutes, and the resulting pellet was dried under high vacuum to yield a light brown solid (0.066 g, 0.11 mmol, 74%) that included 93% alkene addition and 7% iodide elimination. ^1H NMR (CDCl_3 , 500 MHz), δ ppm: 6.50 (d, $J = 16.2$ Hz, 1H), 5.96 (s, 3H), 5.41 – 5.30 (m, 1H), 5.29 – 5.20 (m, 1H), 2.52 – 2.03 (m, 8H), 1.65 – 1.15 (m, 20H), 0.89 (s, 6H). ^{19}F NMR (CDCl_3 , 376 MHz), δ ppm: -102.92 (s, 1F), -104.38 (s, 3F), -121.44 (s, 4F), -123.01 – -123.80 (m, 4F). FT-IR: 2932 (C-H str) (w), 1646 (C=C str) diene (s), 1100-1200 (C-F bend) (vs). TGA: 10% mass loss at 333 °C. T_g (DSC): -37 °C

Phenol coupling of polymer 3.6, 3.10:

Polymer **3.6** (0.100 g, 0.145 mmol, repeat unit eq) was swollen in dioxane (1 mL). Phenol (0.110 g, 1.16 mmol, 8.00 eq) and dimethyl glycine (0.009 g, 0.09 mmol, 0.6 eq) were added. The solution was degassed via freeze-pump-thaw (x3). Cesium carbonate (0.204 g, 0.580 mmol, 4.00 eq) and copper iodide (0.005 g, 0.03 mmol, 0.2 eq) were then added and the reaction was set to 90 °C for 16 hours. The following morning the mixture was precipitated from saturated sodium bicarbonate (50 mL), followed by washing with water (50 mL) and methanol (2 x 50 mL). The precipitate was centrifuged at 2500 X g for 5 minutes, and the resulting pellet was dried under high vacuum to yield a light yellow solid (0.069 g, 0.10 mmol, 88%) that included 65% phenol addition and 35% en-yne rearrangement. ^1H NMR (CDCl_3 , 500 MHz), δ ppm: 7.37 (s, 2.6H), 7.20 (s, 1.3H), 6.98 (s, 2.6H), 5.67 (d, $J = 38.6$ Hz, 0.7H), 4.43 (t, $J = 15.2$ Hz, 1.3H),

2.52 (s, 2.6H), 2.42 (s, 1.3), 1.74 (s, 2.6H), 1.62 (s, 1.3), 1.57 (s, 1.3H), 1.47 (s, 2.6H). ^{19}F NMR (CDCl_3 , 376 MHz), δ ppm: -102.62 (s, 2.75F), -117.95 (1.85F), -121.55 (s, 2.75F), -122.99 (s, 1.25F), -123.51 (4F). FT-IR: 2932 (C-H str) (w), 2230 ($\text{C}\equiv\text{C}$ str) (w), 1660 ($\text{C}=\text{C}$ str) alkene (s), 1590 ($\text{C}=\text{C}$ str) aromatic (s), 1490 ($\text{C}=\text{C}$ bend) aromatic (s), 1100-1200 (C-F bend) (vs). TGA: 10% mass loss at 329 °C. T_g (DSC): -10 °C.

Thiophenol coupling of polymer 3.6, 3.11:

Polymer **3.6** (0.100 g, 0.145 mmol, repeat unit eq) was swollen in toluene (2 mL). Thiophenol (0.127 g, 1.16 mmol, 8.00 eq), 1,10-phenanthroline (0.010 g, 0.056 mmol, 0.40 eq), and triphenylphosphine (0.030 g, 0.11 mmol, 0.80 eq) were added. The solution was degassed via freeze-pump-thaw (x3). Potassium phosphate (0.121 g, 0.560 mmol, 4.00 eq) and copper iodide (0.010 g, 0.058 mmol, 0.4 eq) were then added and the reaction was set to 90 °C for 16 hours. The following morning the mixture was precipitated from saturated sodium bicarbonate (50 mL), followed by washing with water (50 mL) and methanol (2 x 50 mL). The precipitate was centrifuged at 2500 X *g* for 5 minutes, and the resulting pellet was dried under high vacuum to yield a light orange solid (0.065 g, 0.10 mmol, 79%). ^1H NMR (CDCl_3 , 500 MHz), δ ppm: 7.53 – 7.31 (m, 10H), 5.73 – 5.47 (m, 0.5H), 4.95 – 4.72 (m, 1.5H), 2.56 – 2.36 (m, 3H), 2.07 (m, 1H), 1.78 – 1.26 (m, 8H). ^{19}F NMR (CDCl_3 , 376 MHz), δ ppm: -103.75 (s, 3F), -104.44 (s, 1F), -121.57 (s, 4F), -123.02 (s, 1F), -123.55 (s, 3F). FT-IR: 2932 (C-H str) (w), 1626 ($\text{C}=\text{C}$ str) alkene (s), 1583 ($\text{C}=\text{C}$ str) aromatic (s), 1477 ($\text{C}=\text{C}$ bend) aromatic (s), 1100-1200 (C-F bend) (vs). TGA: 10% mass loss at 370 °C. T_g (DSC): -6 °C.

Kumada coupling of polymer 3.5, 3.12:

Polymer **3.5** (0.200 g, 0.290 mmol, repeat unit eq) was swollen in THF (4 mL). Iron (III) acetylacetonate (0.050 g, 0.15 mmol, 0.50 eq) was added under nitrogen. Methyl magnesium bromide (1M) (1.8 mL, 1.8 mmol, 6.0 eq) was then added dropwise over an hour at room temperature. After complete addition of methyl magnesium bromide, methanol (1 mL) was slowly added to quench the remaining reagents. The solution was precipitated from water (50 mL), followed by washing with methanol (2 x 50 mL). The

precipitate was centrifuged at 2500 X *g* for 5 minutes, and the resulting pellet was dried under high vacuum to yield a brown solid (0.115 g, 0.220 mmol, 87%) as 70% methyl addition and 30% iodide reduction by proton NMR. ¹H NMR (CDCl₃, 500 MHz), δ ppm: 6.44 – 6.30 (m, 0.25H), 6.12 – 6.00 (m, 0.25H), 5.68 – 5.54 (m, 0.25H), 5.54 – 5.45 (m, 0.25H), 5.31 (t, *J* = 16.7 Hz, 1.5H), 2.24 (s, 3H), 2.19 – 2.03 (m, 1H), 1.87 (s, 4.5H), 1.55 (s, 1H), 1.45 (s, 3H), 1.38 – 1.11 (m, 4H). ¹⁹F NMR (CDCl₃, 376 MHz), δ ppm: -104.76 (s, 3F), -105.37(s, 0.35F), -106.65 (s, 0.17F), -111.27 (s, 0.37F), -121.58 (s, 4F), -123.23 – -124.66 (m, 4F). FT-IR: 2932 (C-H str) (w), 1667 (C=C str) (s), 1100-1200 (C-F bend) (vs). TGA: 10% mass loss at 373 °C. *T_g* (DSC): -39 °C

Elimination of iodide from polymer 3.5, 3.16:

Polymer **3.5** (0.200 g, 0.290 mmol, repeat unit eq) was swollen in toluene (4 mL). Tetramethylguanidine (0.33 g, 2.9 mmol, 10 eq) was added dropwise and the solution was allowed to stir for 16 hours. The following morning the reaction mixture was precipitated from cold methanol (50 mL) and additionally washed with saturated ammonium chloride (50 mL), followed by an additional wash of methanol (50 mL). The precipitate was centrifuged at 2500 X *g* for 5 minutes, and the resulting pellet was dried under high vacuum to yield a brown solid (0.090 g, 0.14 mmol, 49%) as polymer with all Z-Isomer iodide eliminated. ¹H NMR (CDCl₃, 500 MHz), δ ppm: 6.33 (t, *J* = 14.6 Hz, 1.5H), 2.69 – 2.53 (m, 3H), 2.36 (t, *J* = 5.5 Hz, 1H), 1.60 (s, 4H), 1.47 – 1.31 (m, 4H). ¹⁹F NMR (CDCl₃, 376 MHz), δ ppm: -96.31 (s, 1F), -105.37 (s, 3F), -121.19 (s, 1F), -121.53 (s, 3F), -122.61 (s, 1F), -123.36 (s, 3F). FT-IR: 2932 (C-H str) (w), 2260 (C≡C str) (w), 1635 (C=C str) (s), 1100-1200 (C-F bend) (vs). TGA: 10% mass loss at 347 °C. *T_g* (DSC): -27 °C

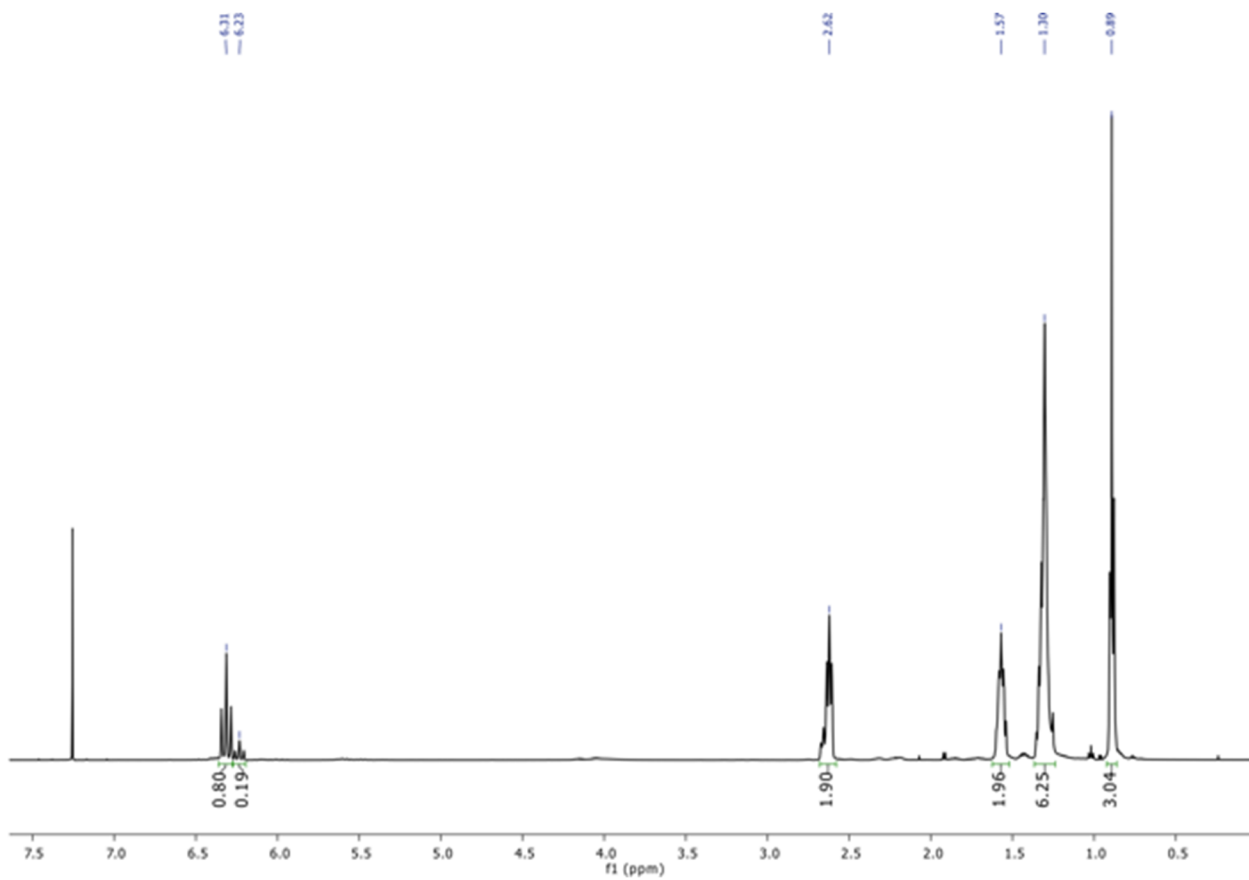
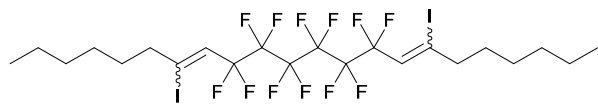
Alkyne-azide coupling of polymer 3.16, 3.18:

Polymer **3.16** (0.010 g, 0.018 mmol, repeat unit eq) was dissolved in xylenes (0.25 mL). 2-azidoethyl perfluorooctane (0.030 g, 0.073 mmol, 4.0 eq) was then added and refluxed for 18 hours. The following morning the reaction mixture was precipitated from methanol (10 mL) and washed with methanol (2 x 10 mL). The precipitate was centrifuged at 2500 X *g* for 5 minutes, and the resulting pellet was dried under

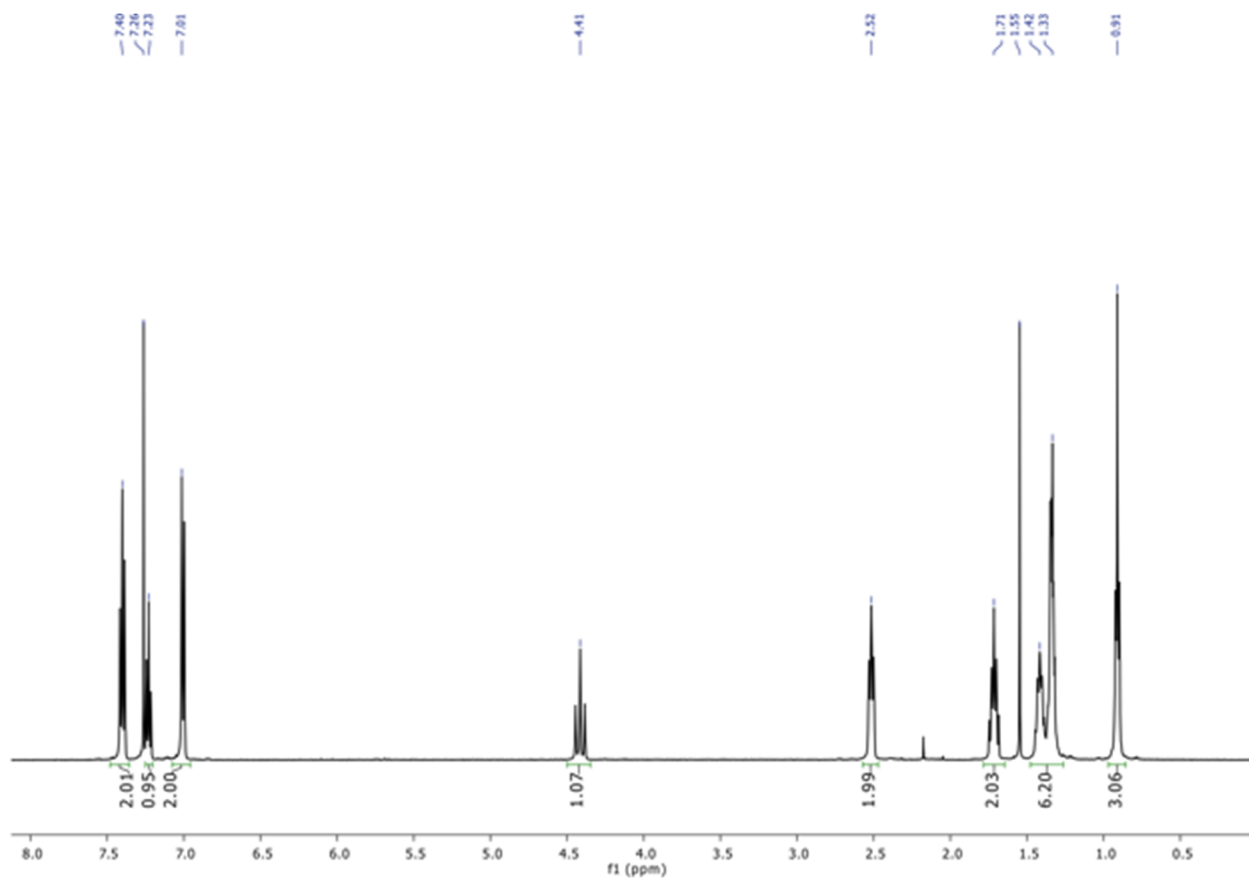
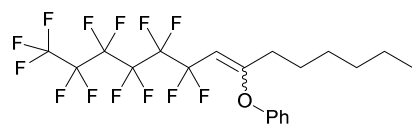
high vacuum to yield a brown solid (0.013 g, 0.014 mmol, 80%). ^1H NMR (CDCl_3 , 500 MHz), δ ppm: 6.32 (t, $J = 15.0$ Hz, 1H), 4.68 (s, 0.5H), 4.53 (s, 0.5H), 3.05 – 2.72 (m, 2H), 2.63 (s, 3H), 1.88 – 1.30 (m, 8H). ^{19}F NMR (CDCl_3 , 376 MHz), δ ppm: -80.89 (s, 1.5F), -105.37 (s, 3F), -107.42 (s, 0.6F), -109.17 (s, 0.4F), -114.35 (s, 1F), -121.07 – -122.62 (m, 7F), -122.88 (s, 1F), -123.46 (s, 5F), -126.25 (s, 1F). FT-IR: 2932 (C-H str) (w), 1632 (C=C str) alkene + aromatic (s), 1458 (C=C bend) aromatic 1100-1200 (C-F bend) (vs).

3.5.5 $^1\text{H-NMR}$ spectra:

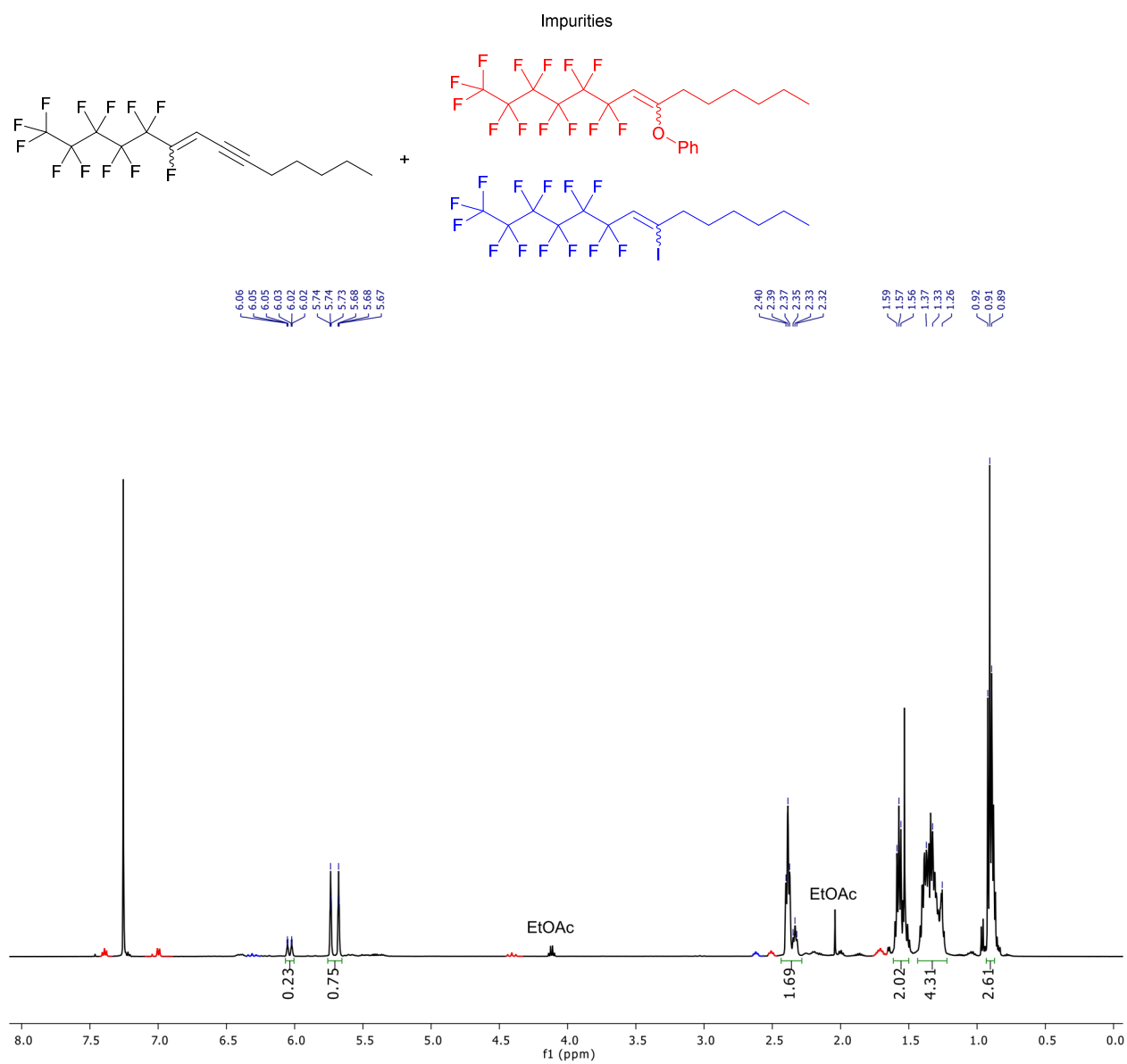
9,9,10,10,11,11,12,12,13,13,14,14-dodecafluoro-7,16-diiododocosa-7,15-diene, 3,3, 3.4:



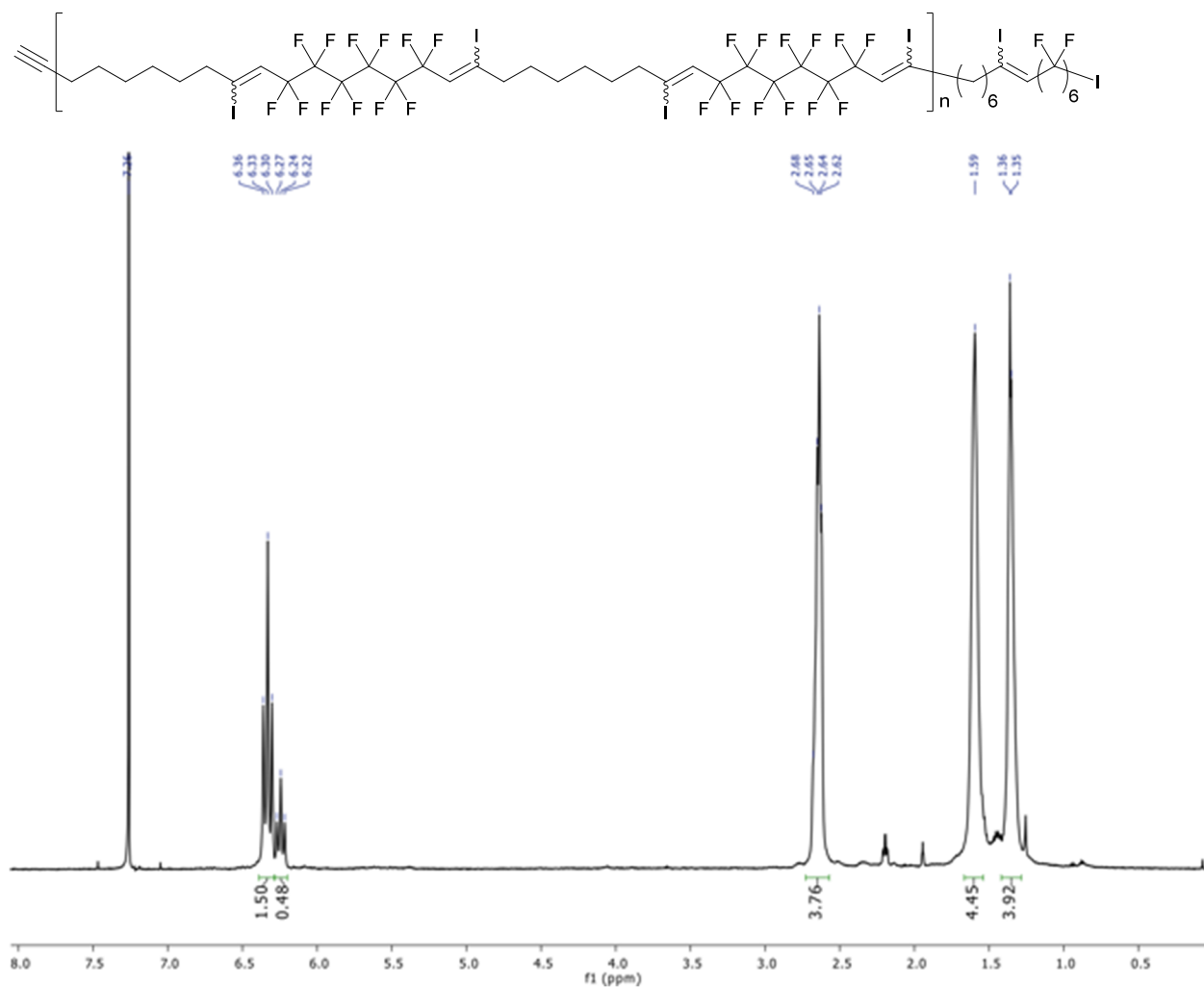
((9,9,10,10,11,11,12,12,13,13,14,14,14-tridecafluorotetradec-7-en-7-yl)oxy)benzene, 3.14:



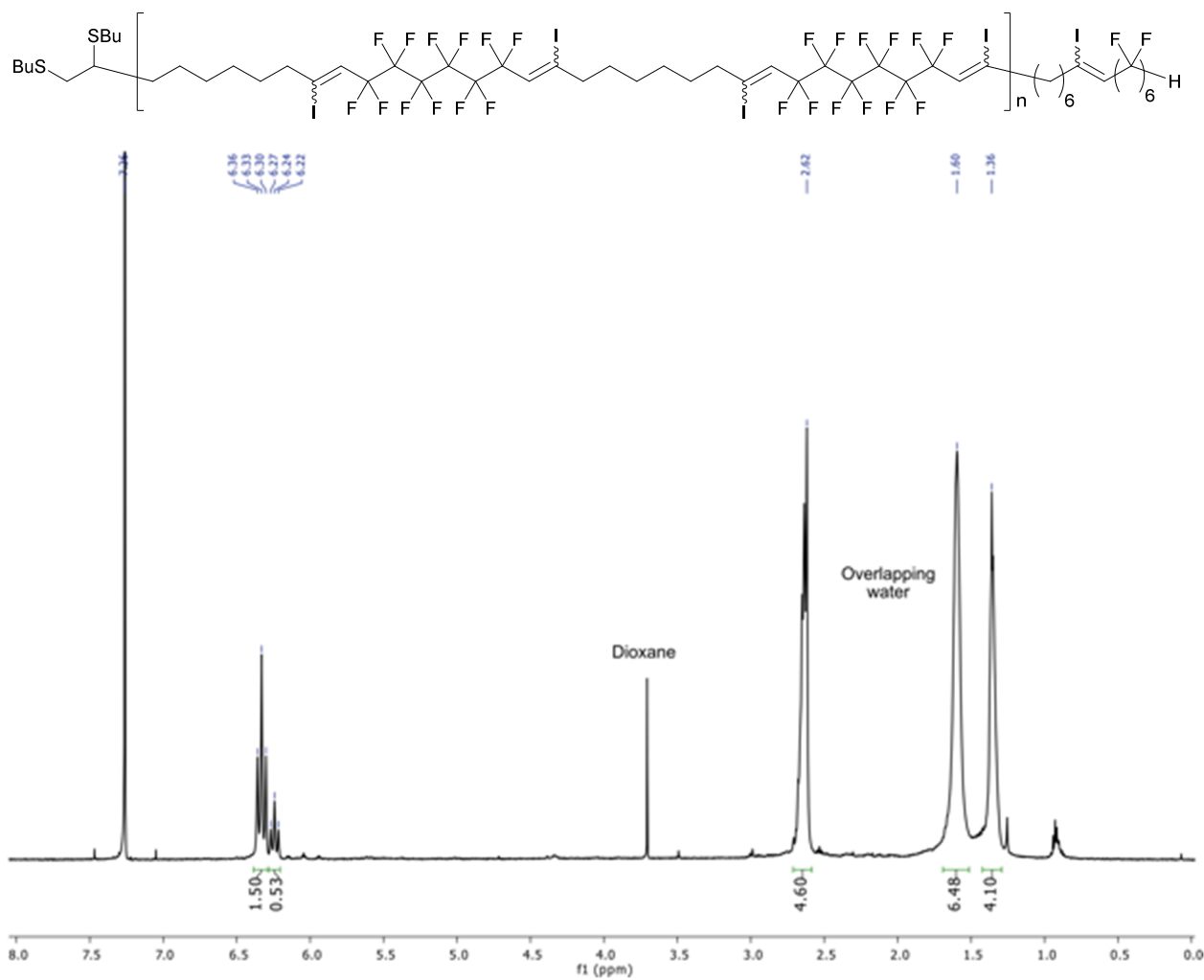
1,1,1,2,3,3,4,4,5,5,6-dodecafluorotetradec-6-en-8-yne, 3.15:



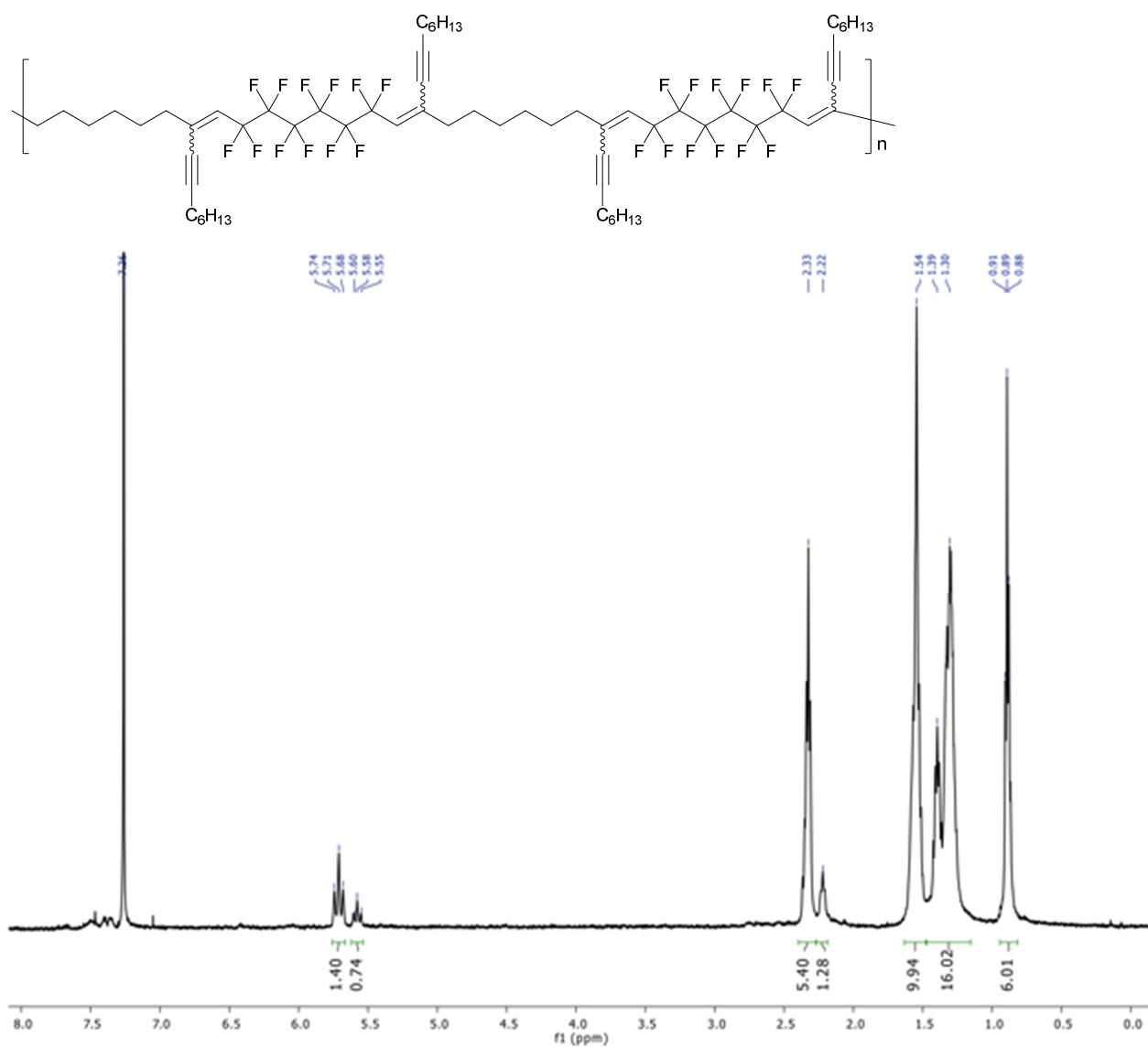
1-perfluorohexyl-2,9-diiodo-1,9-decadiene block polymer, 3.5:



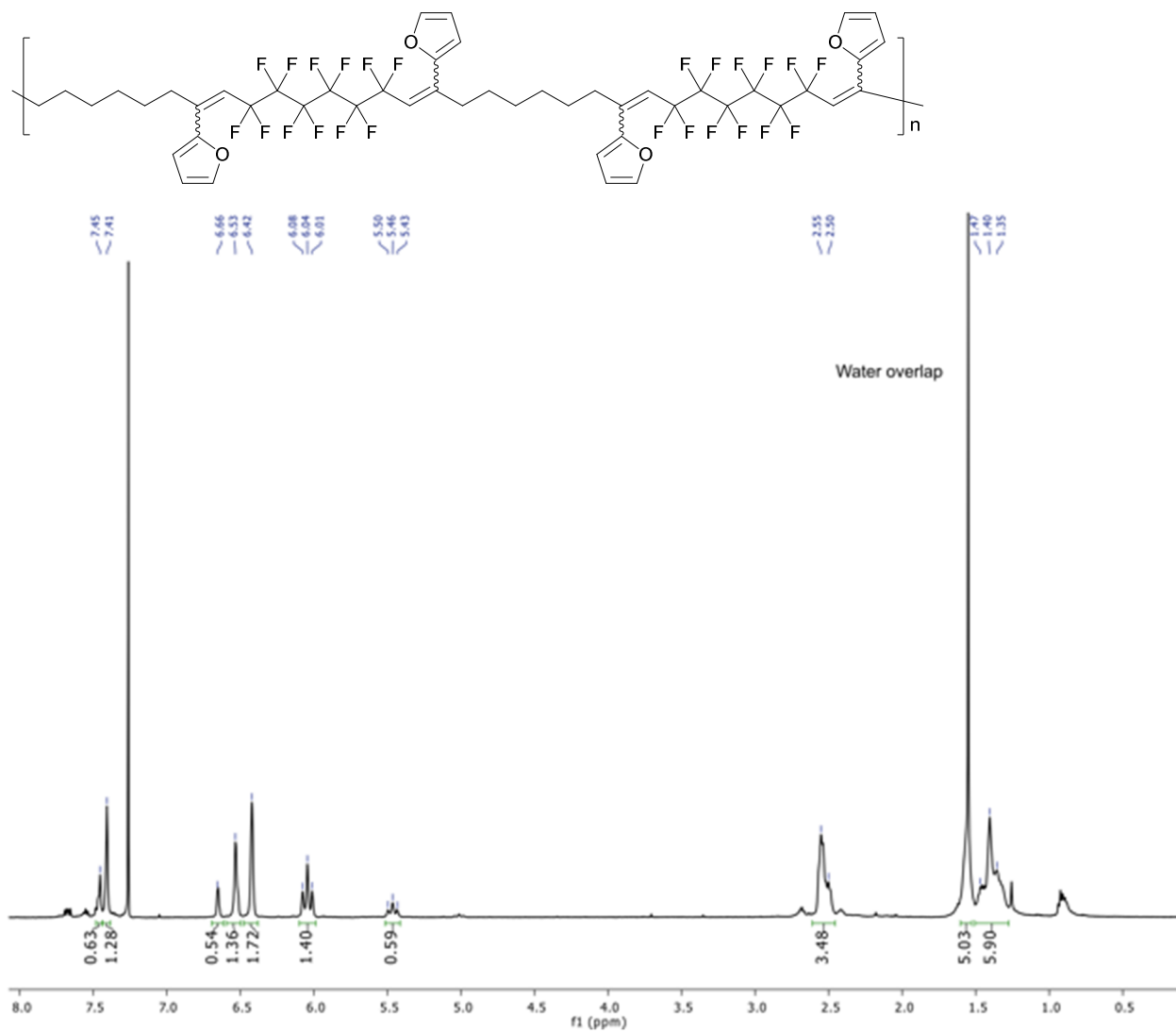
Thiol capping of polymer 3.5, 3.6:



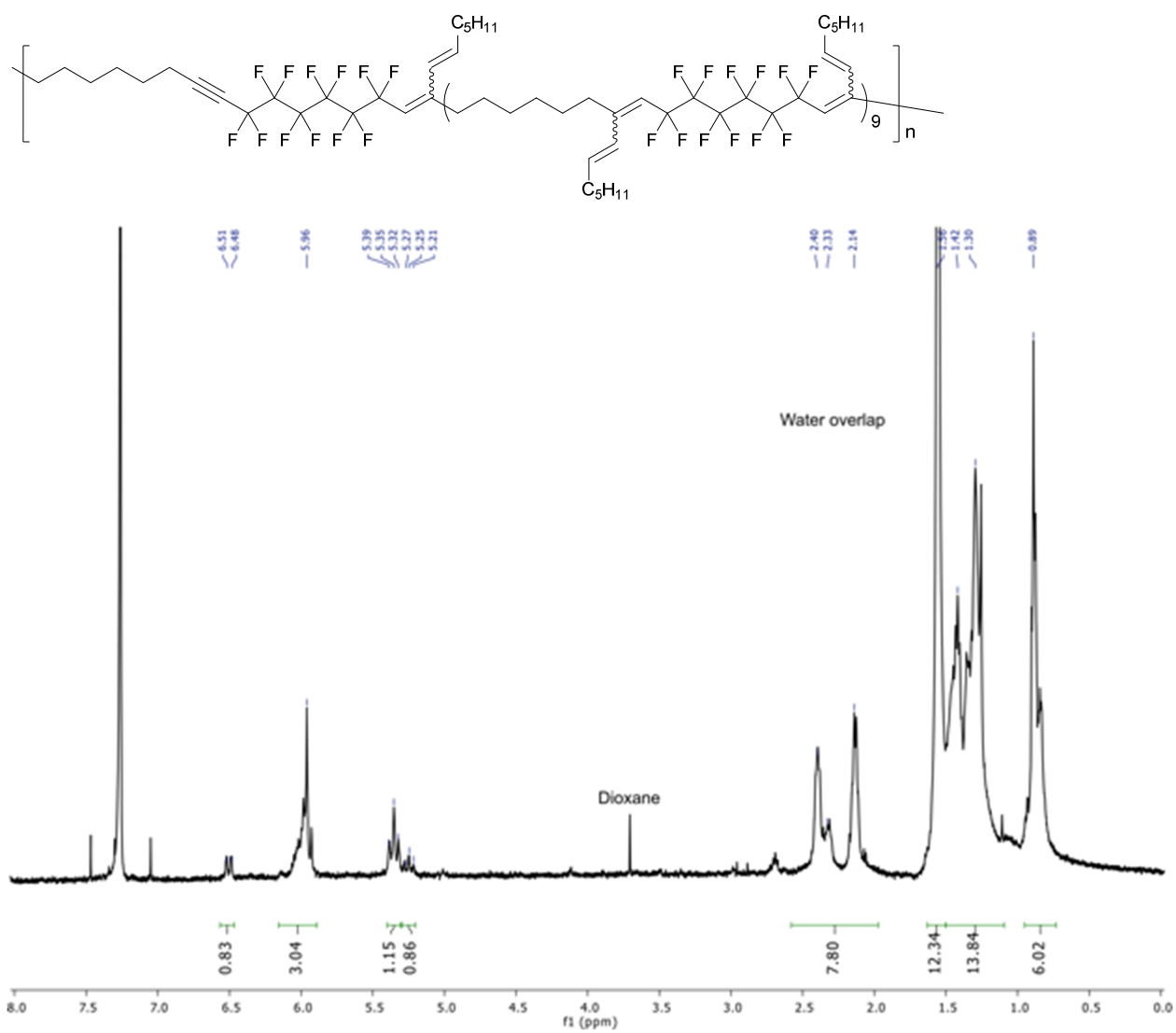
Sonogashira coupling of polymer 3.6, 3.7:



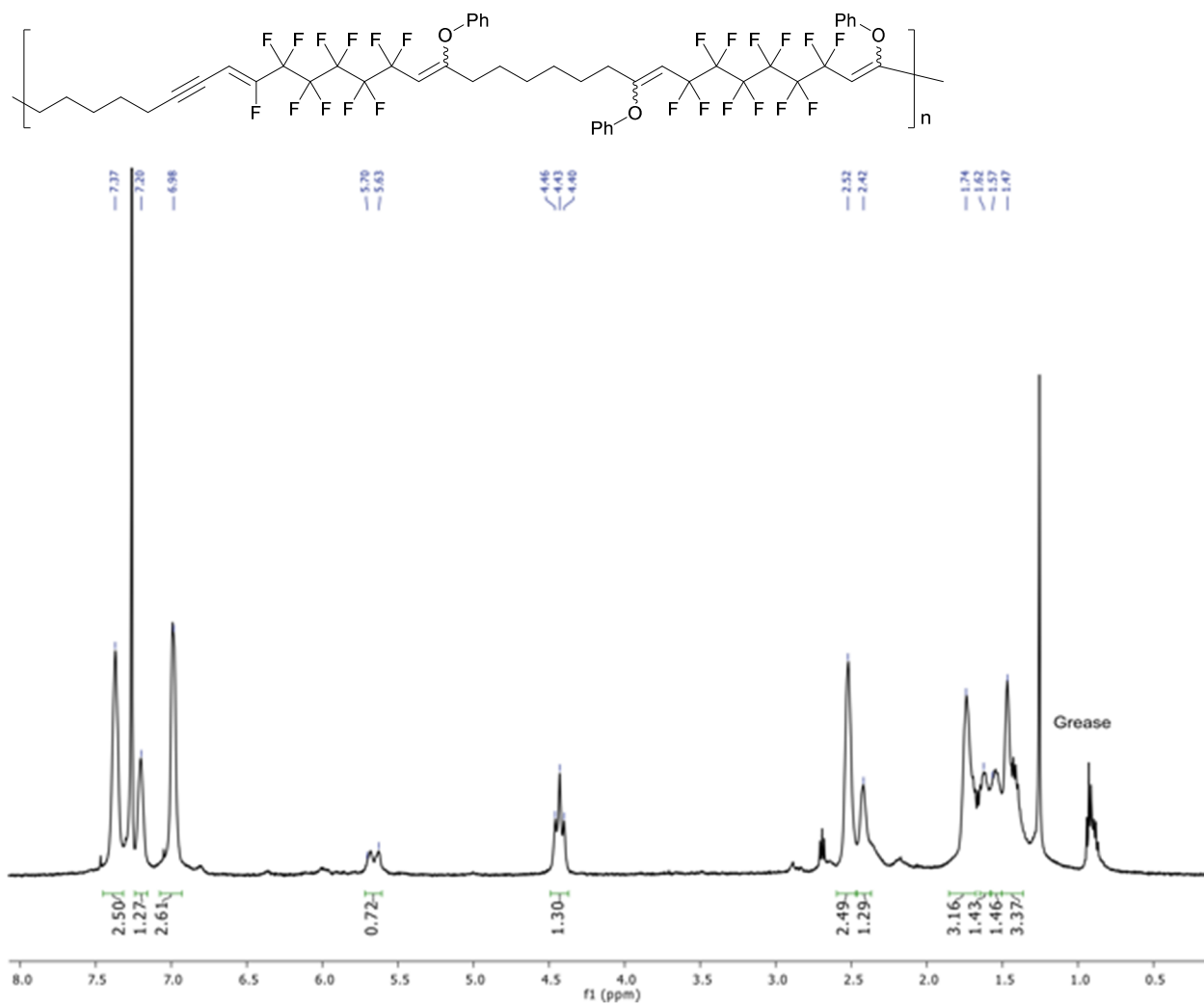
Stille coupling of polymer 3.6, 3.8:



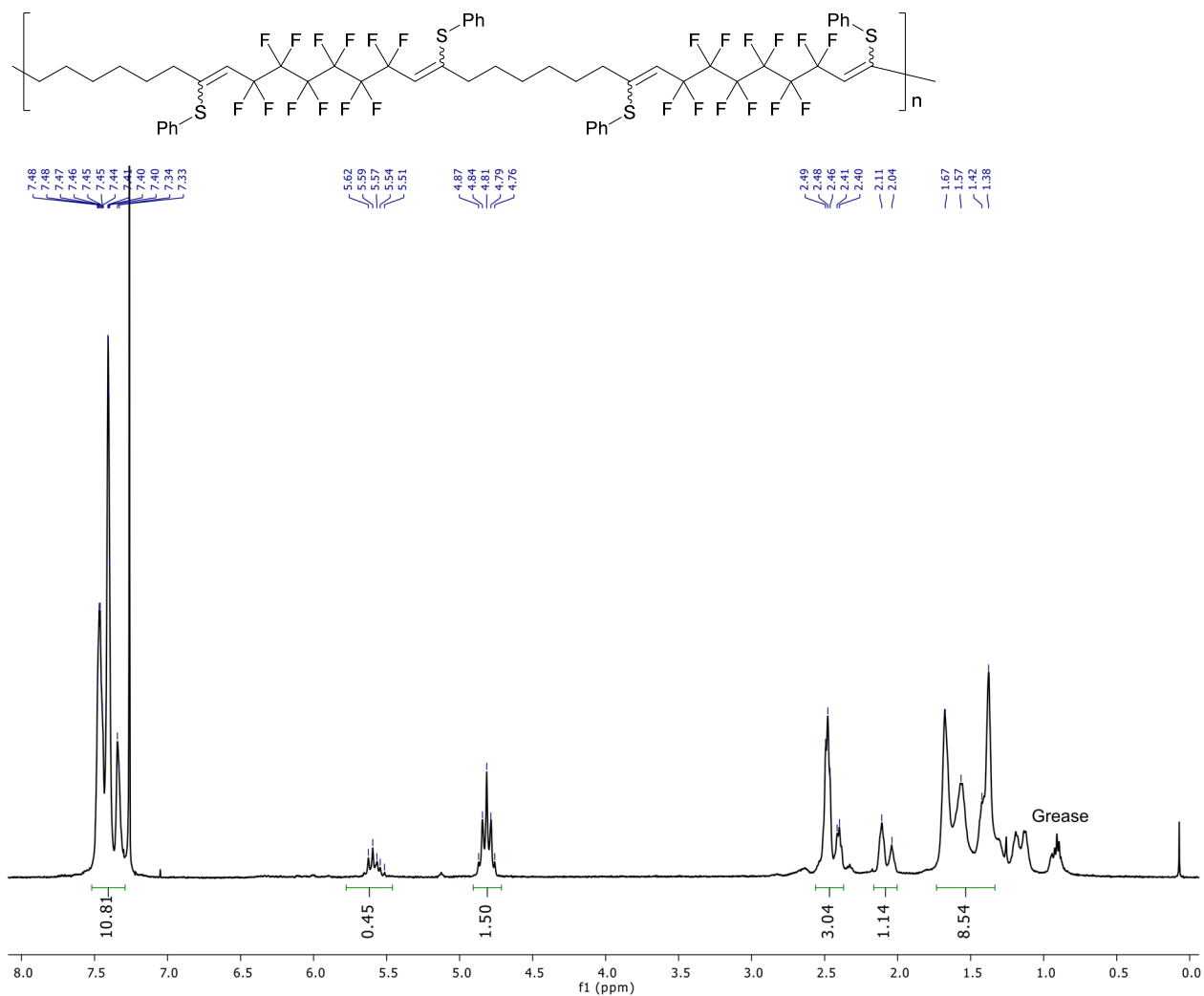
Suzuki coupling of polymer 3.6, 3.9:



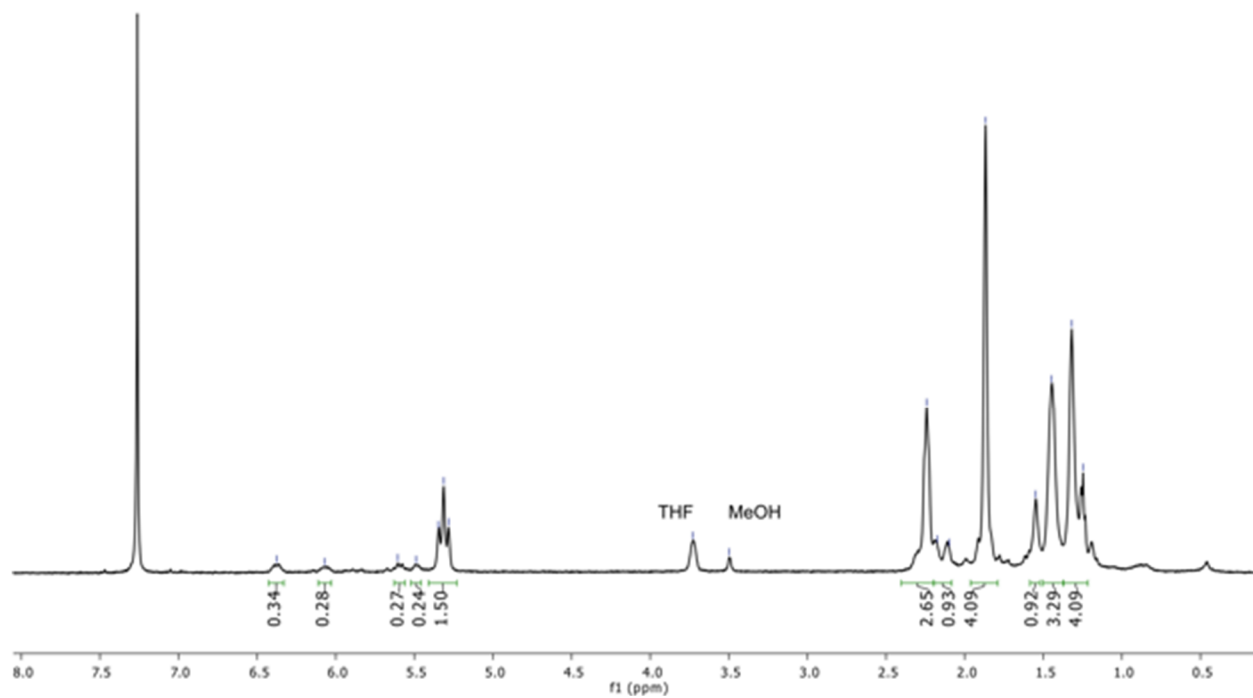
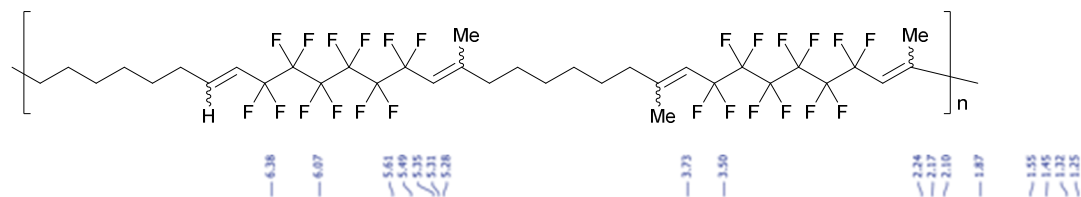
Phenol coupling of polymer 3.6, 3.10:



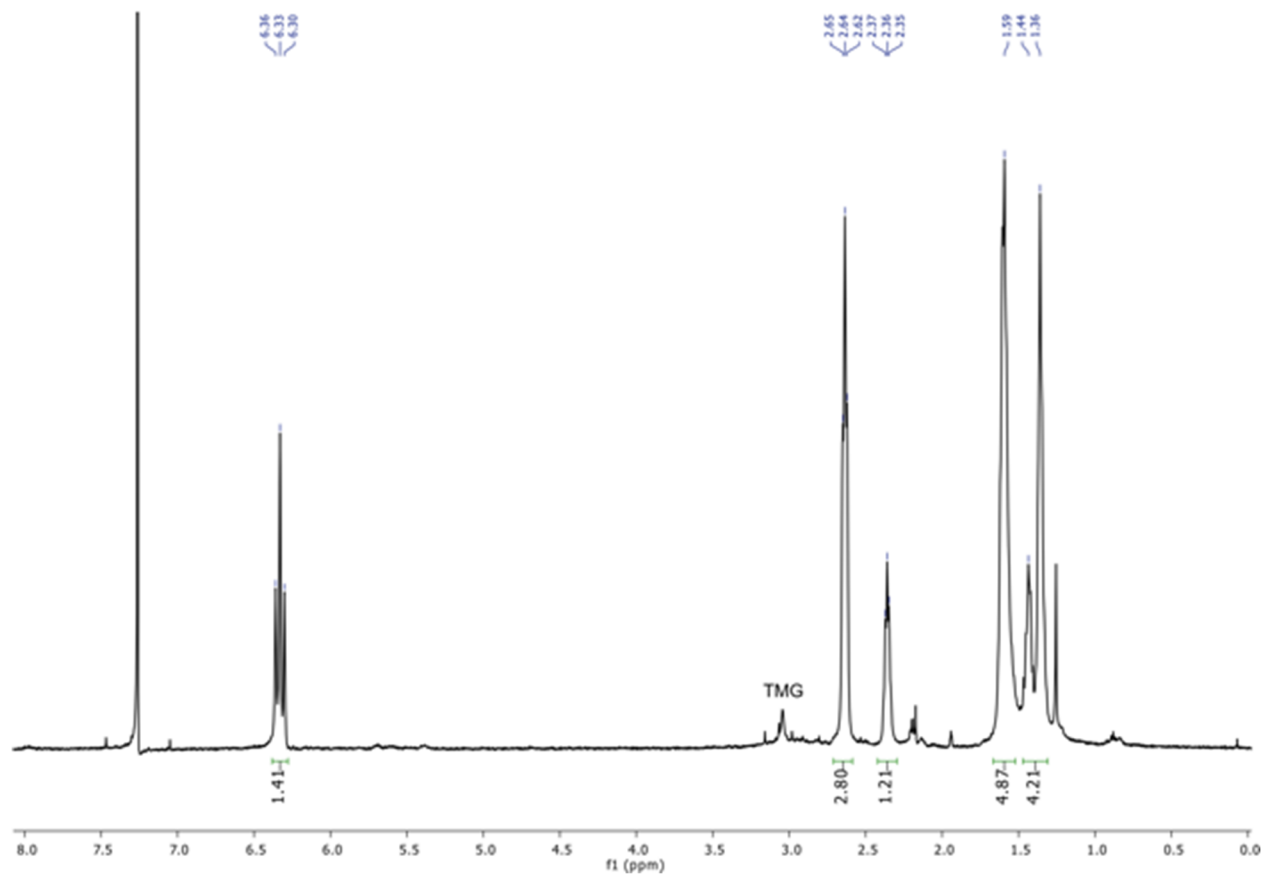
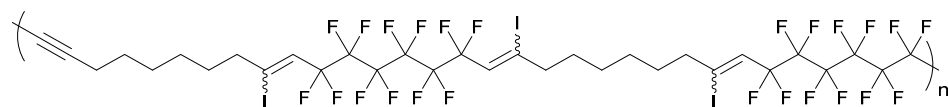
Thiophenol coupling of polymer 3.6, 3.11:



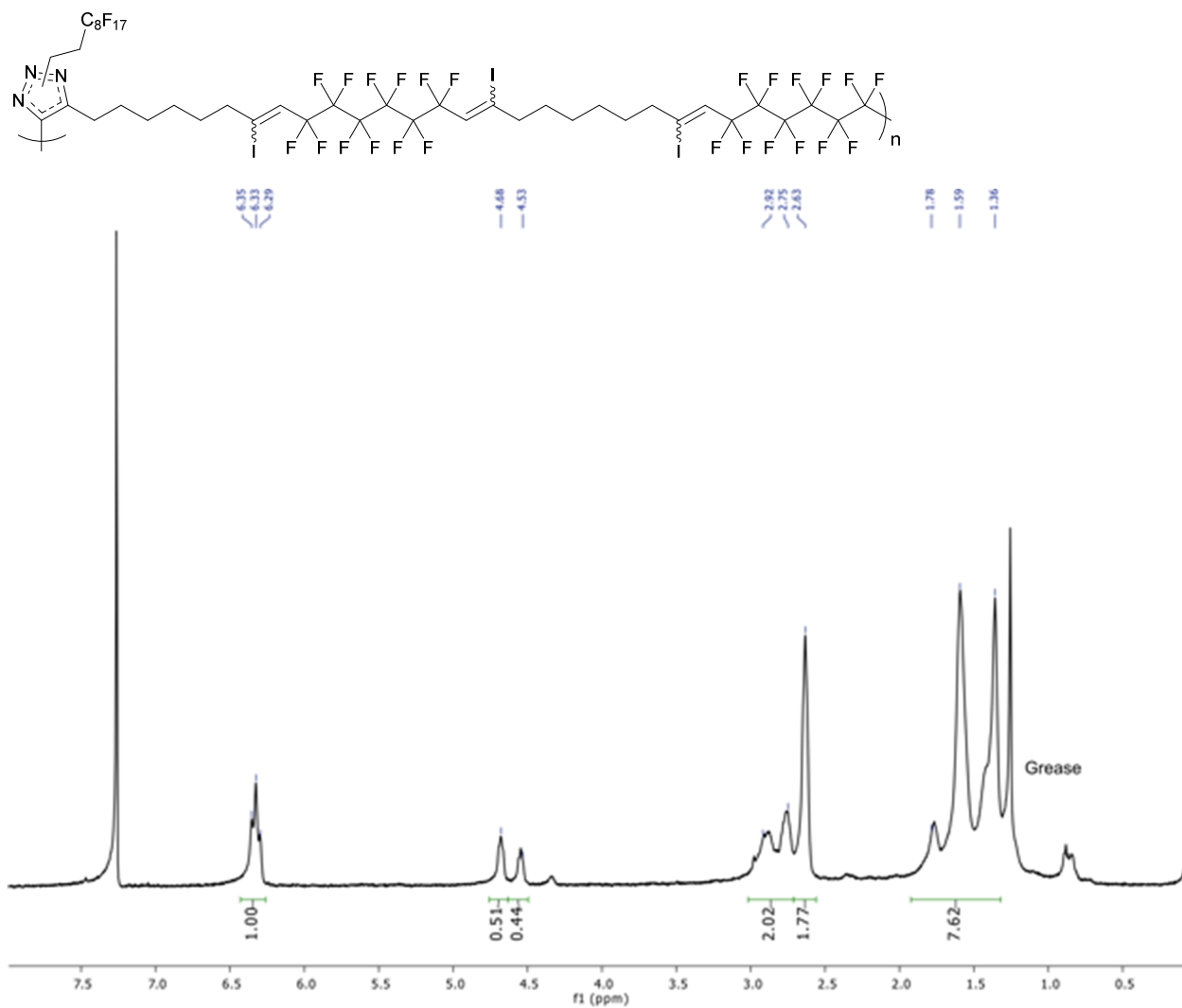
Kumada coupling of polymer 3.5, 3.12:



Elimination of iodide from polymer 3.5, 3.16:

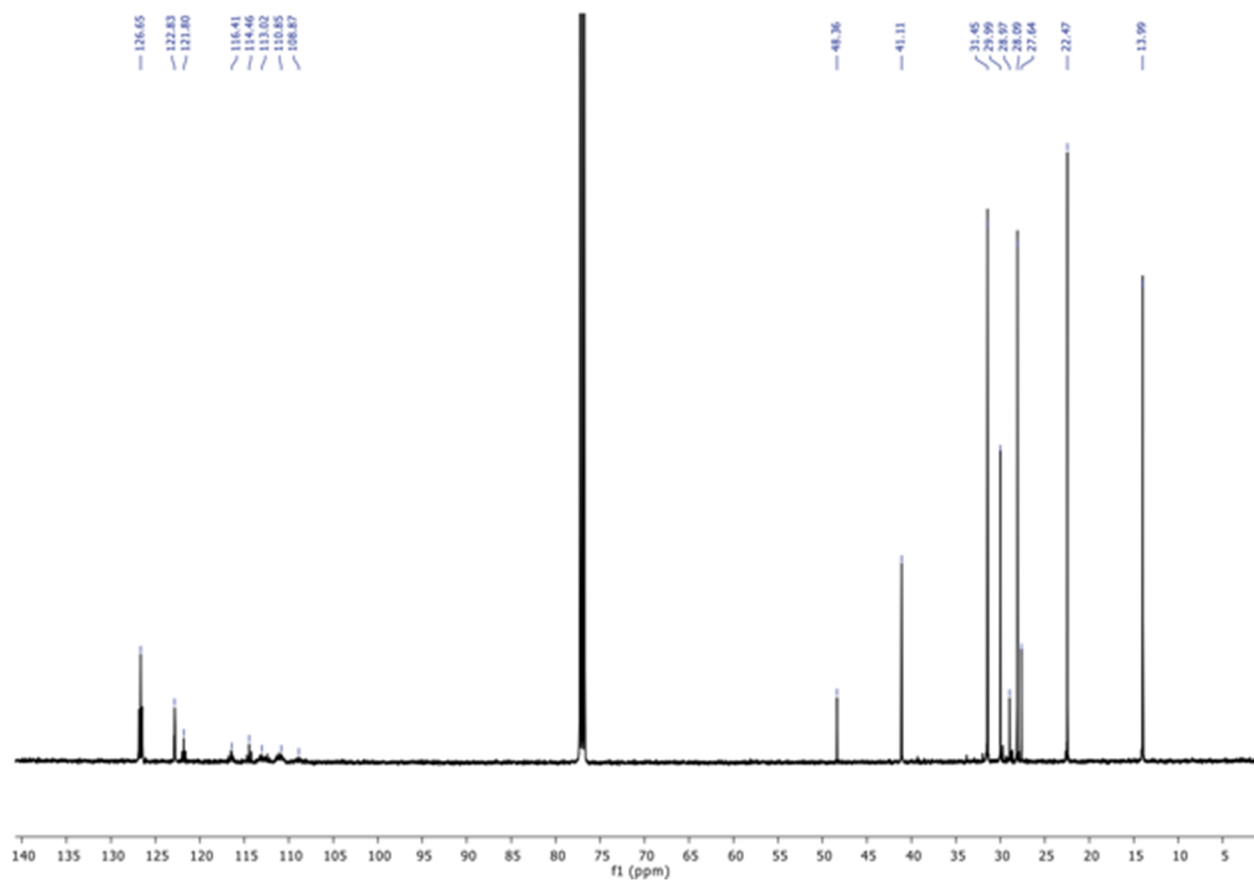
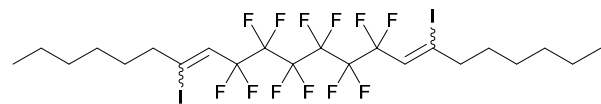


Alkyne-azide coupling of polymer 3.16, 3.18:

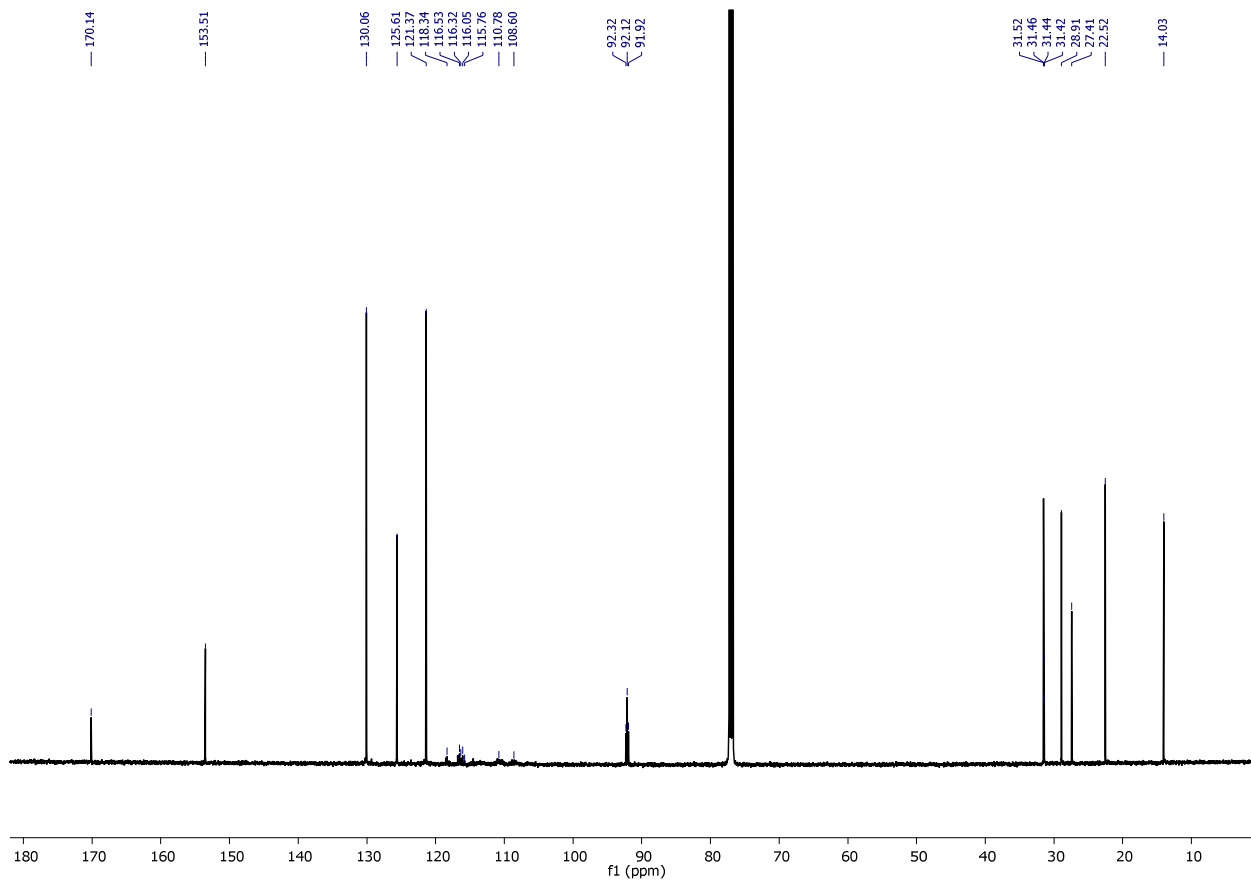
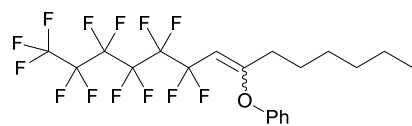


3.5.6 ^{13}C -NMR spectra:

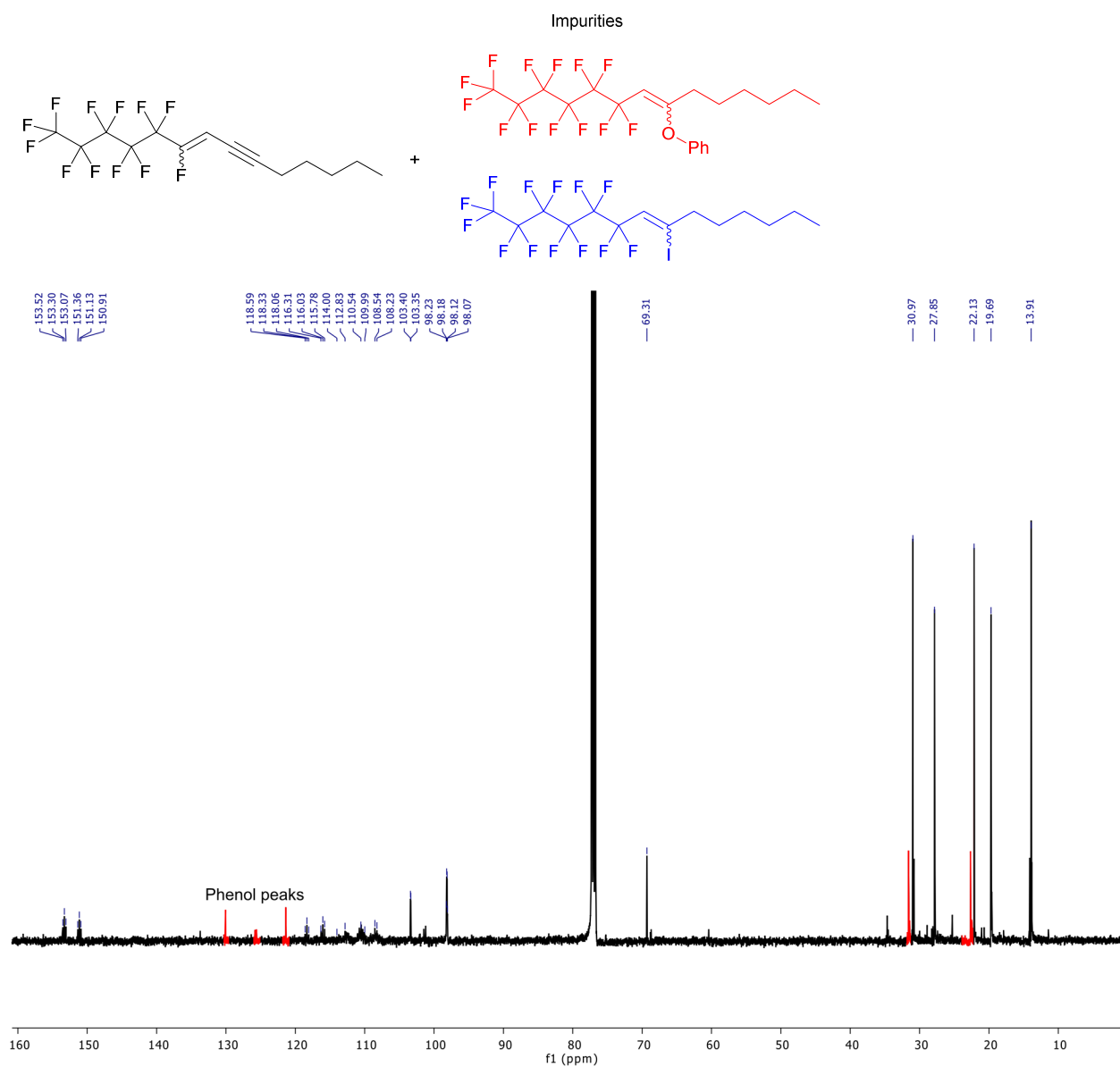
9,9,10,10,11,11,12,12,13,13,14,14-dodecafluoro-7,16-diiododocosa-7,15-diene, 3.3, 3.4:



((9,9,10,10,11,11,12,12,13,13,14,14,14-tridecafluorotetradec-7-en-7-yl)oxy)benzene, 3.14:

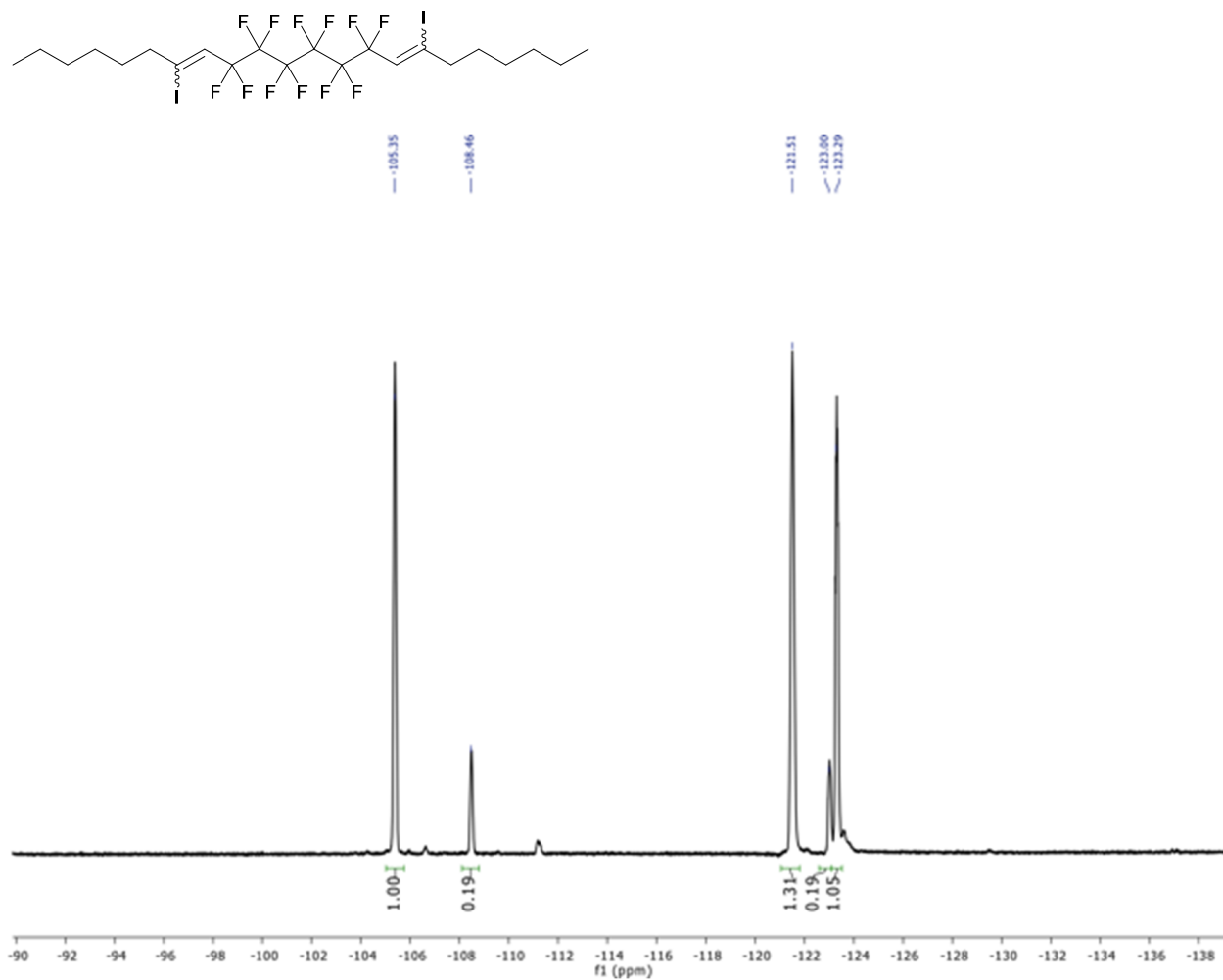


1,1,1,2,2,3,3,4,4,5,5,6-dodecafluorotetradec-6-en-8-yne, 3.15:

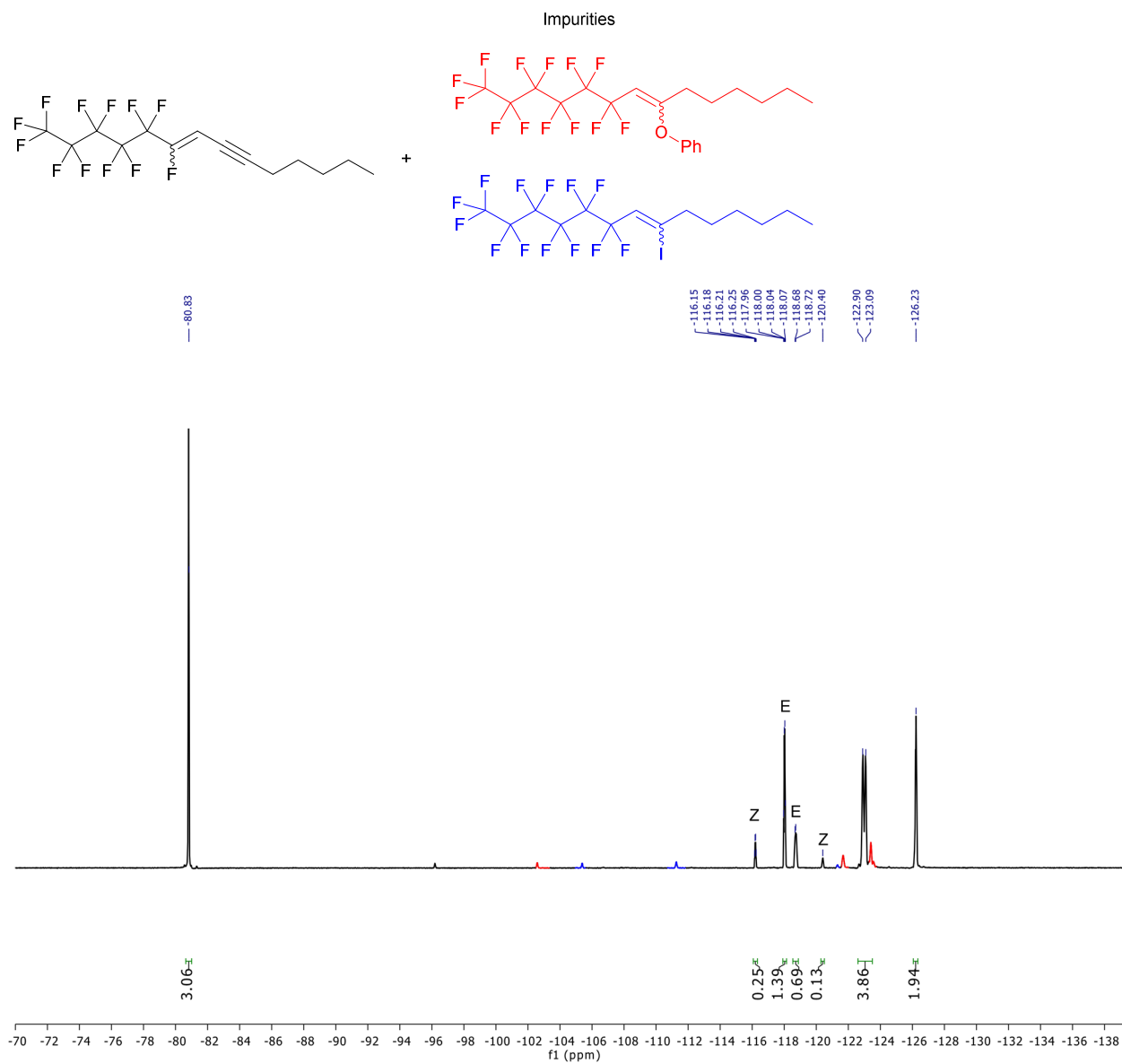


3.5.7 ^{19}F -NMR spectra

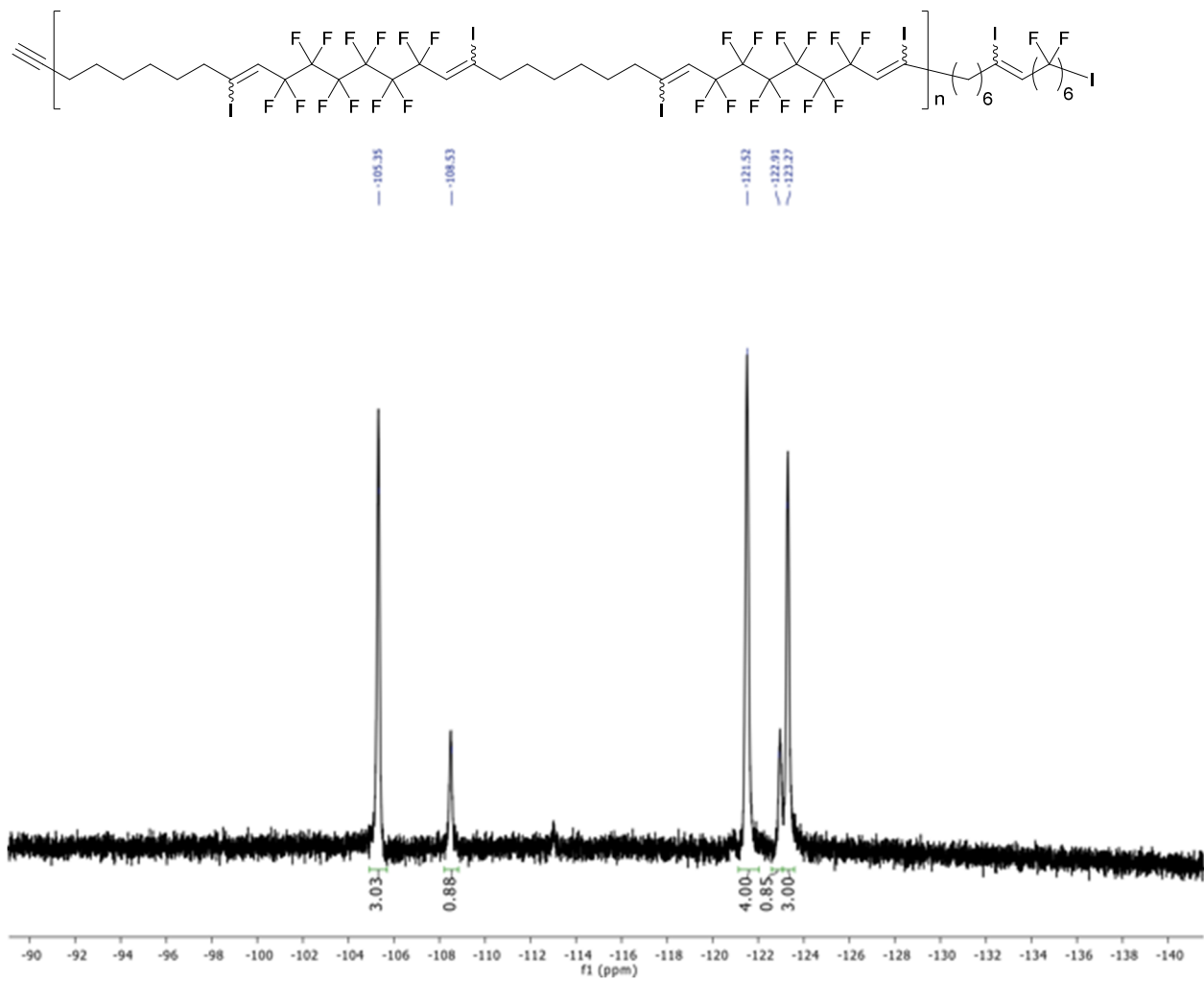
9,9,10,10,11,11,12,12,13,13,14,14-dodecafluoro-7,16-diiododocosa-7,15-diene, 3.3, 3.4:



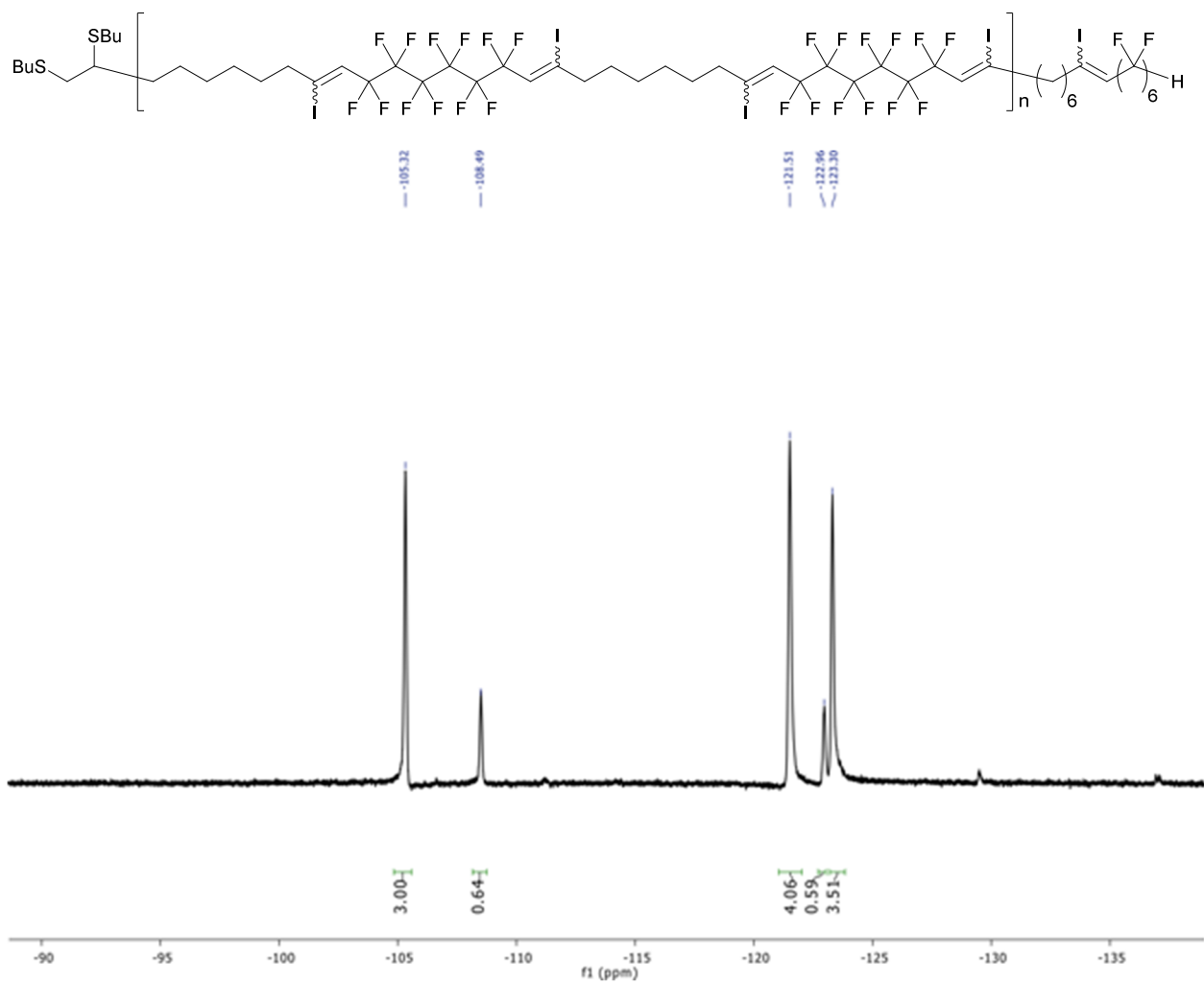
1,1,1,2,2,3,3,4,4,5,5,6-dodecafluorotetradec-6-en-8-yne, 3.15:



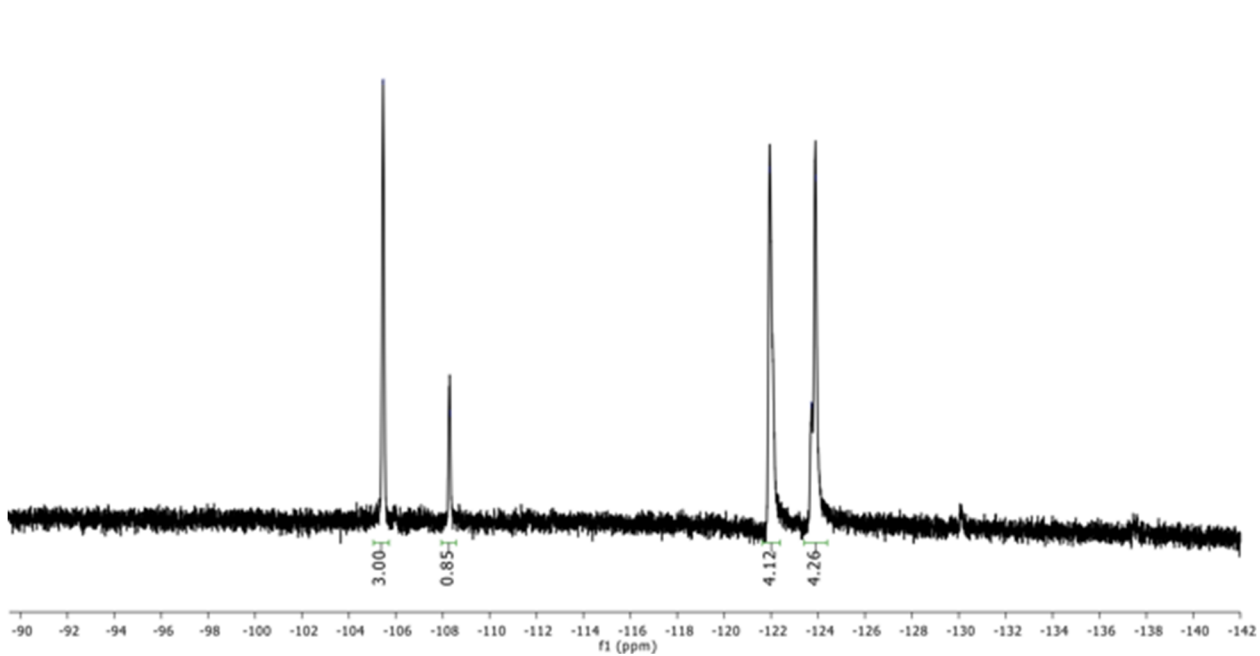
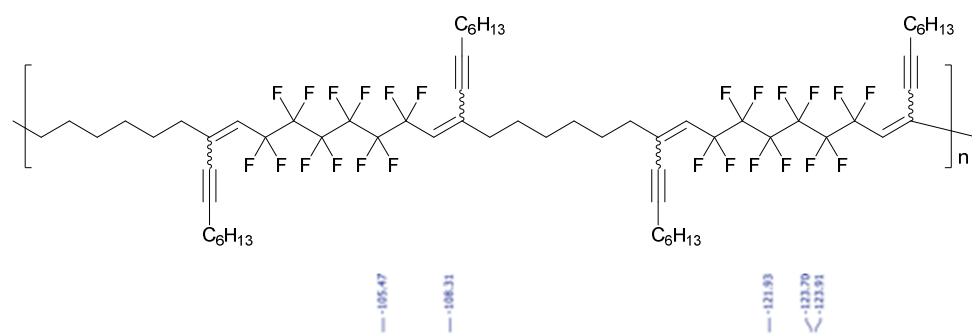
1-perfluorohexyl-2,9-diiodo-1,9-decadiene block polymer, 3.5:



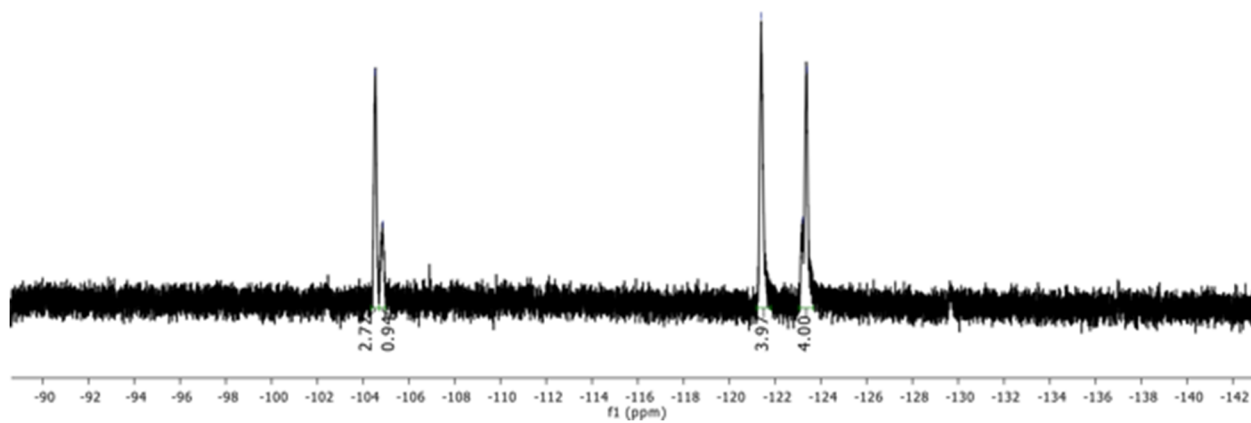
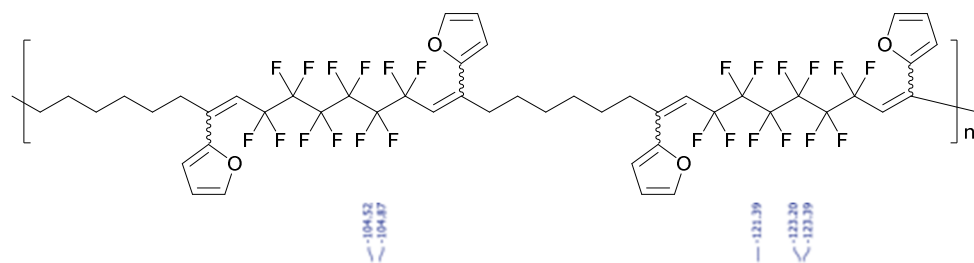
Thiol capping of polymer 3.5, 3.6:



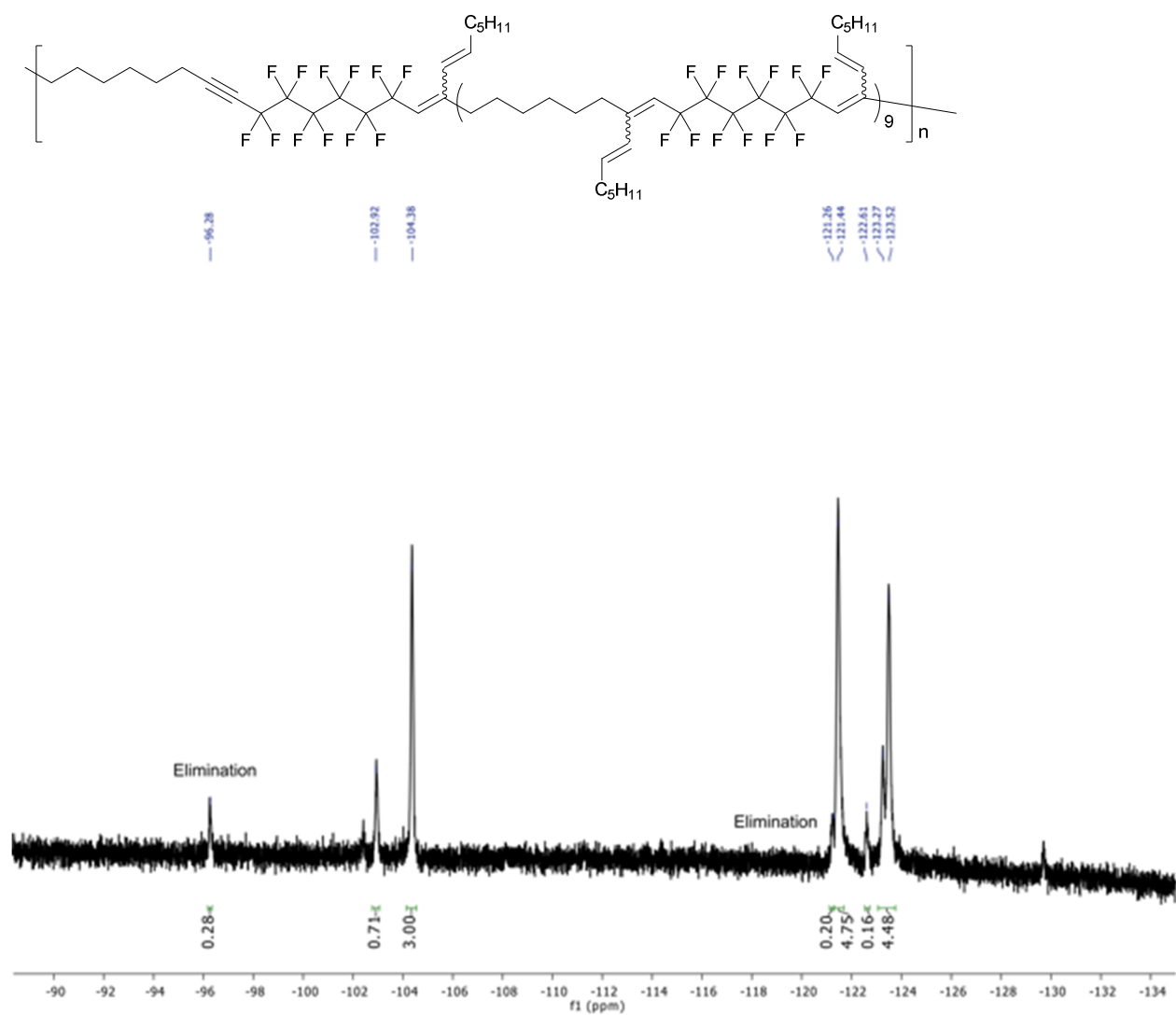
Sonogashira coupling of polymer 3.6, 3.7:



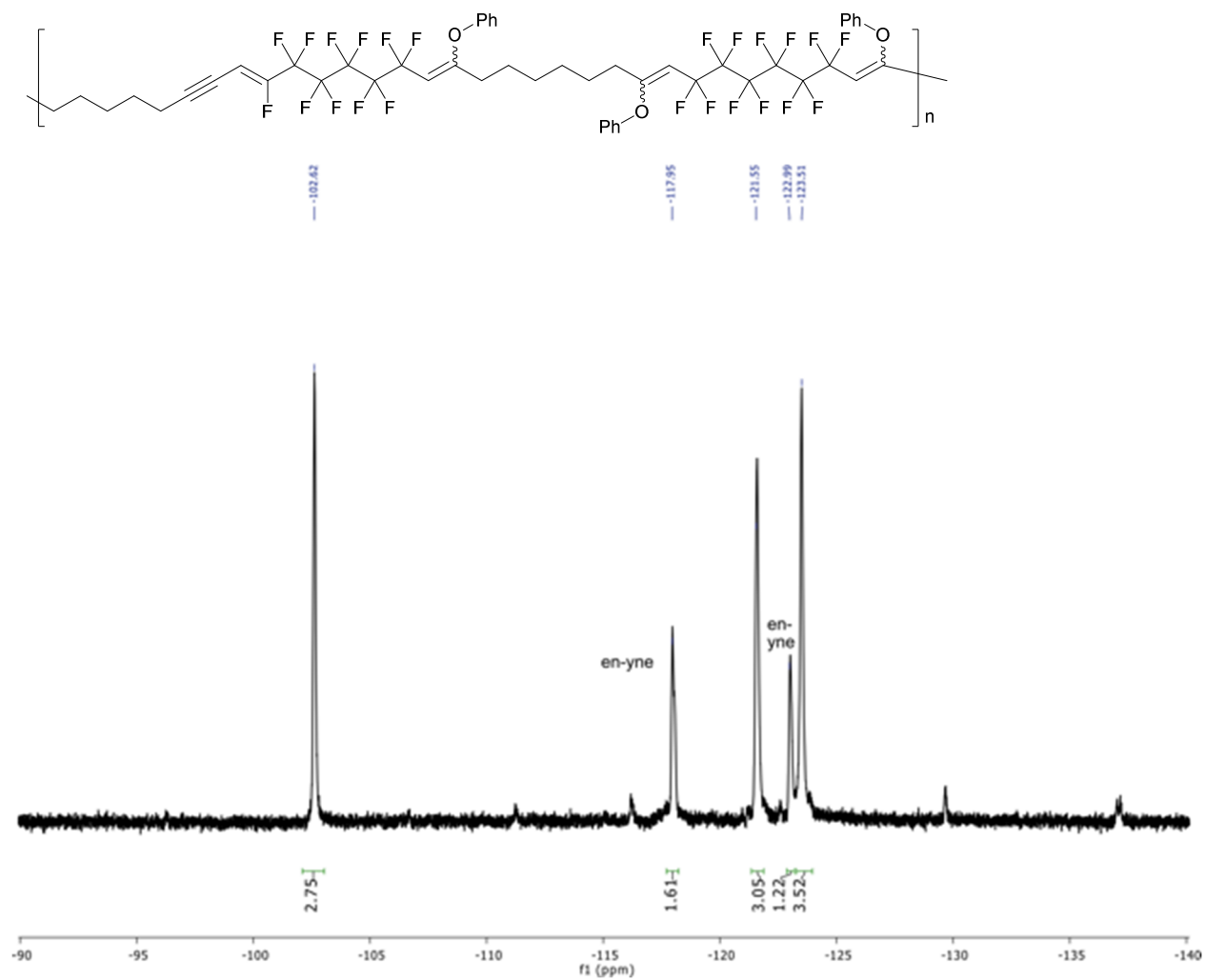
Stille coupling of polymer 3.6, 3.8:



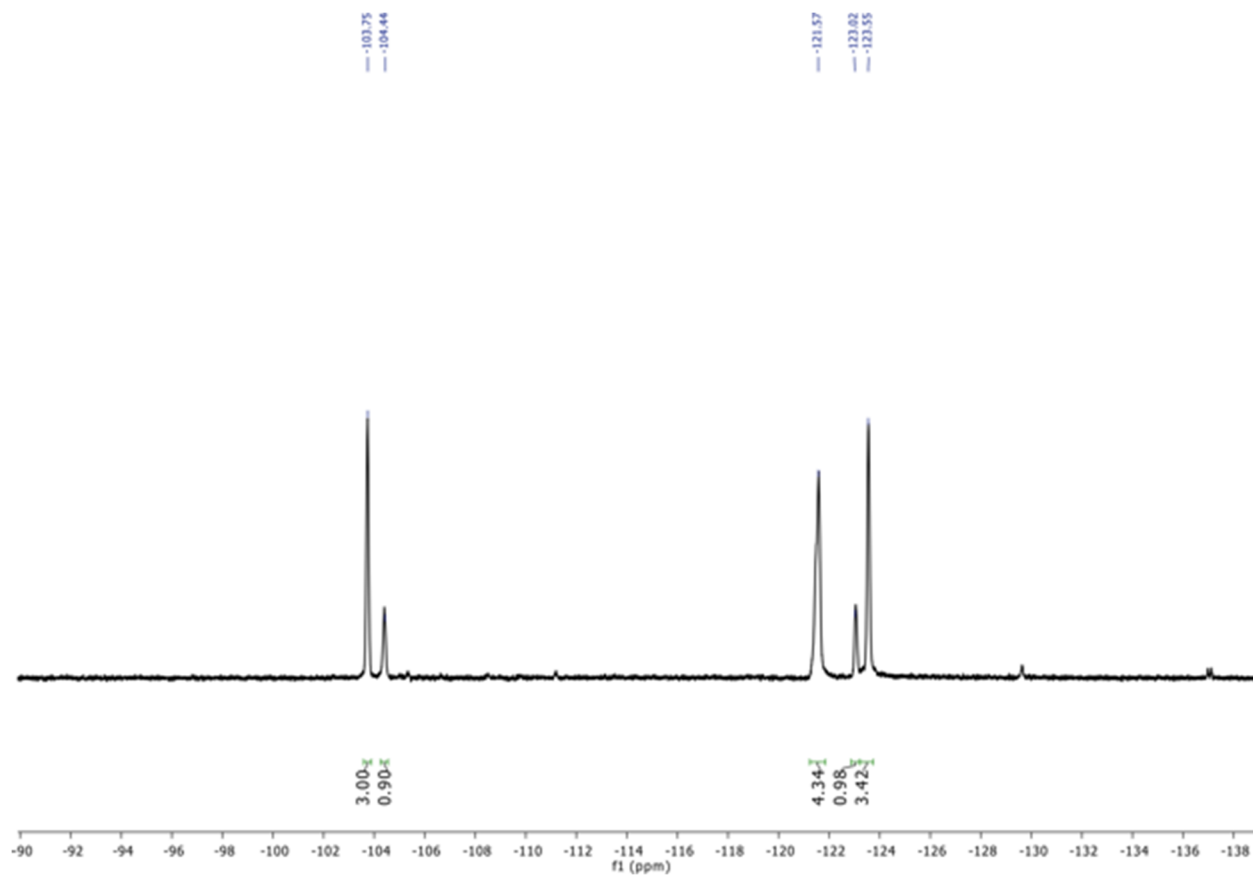
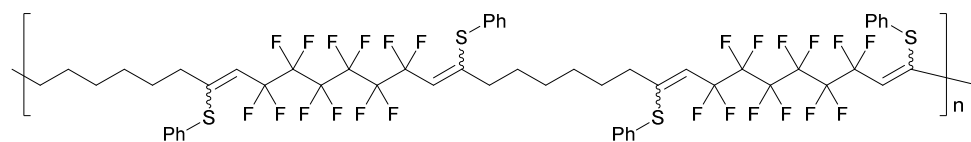
Suzuki coupling of polymer 3.6, 3.9:



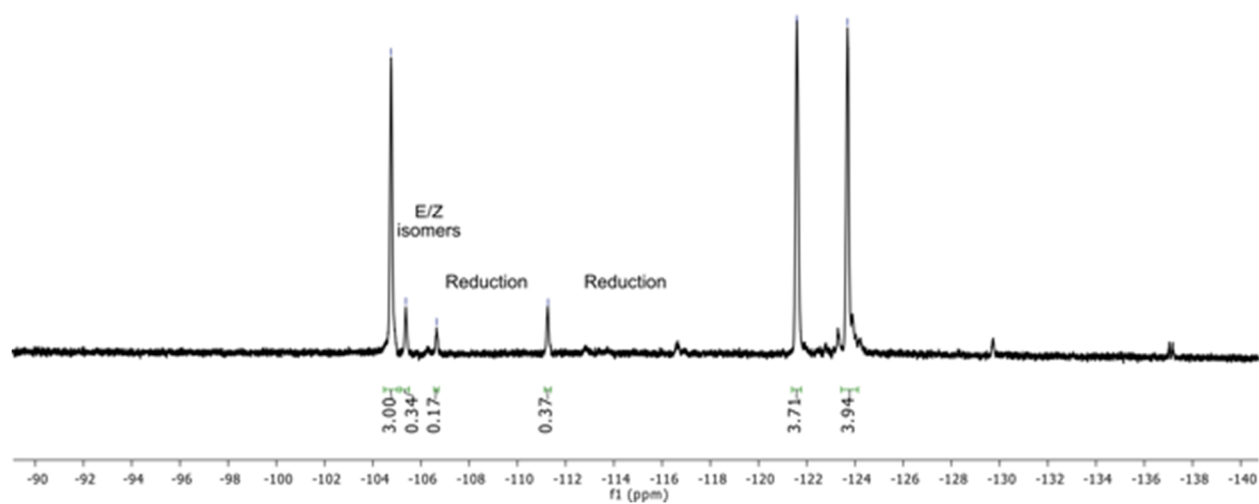
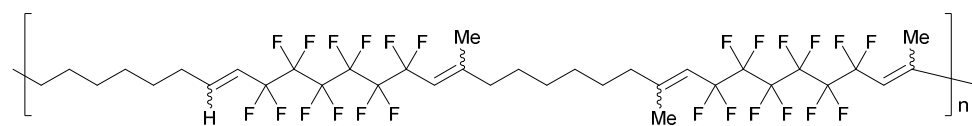
Phenol coupling of polymer 3.6, 3.10:



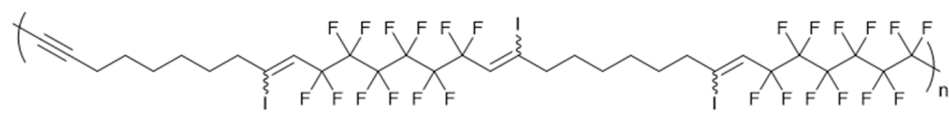
Thiophenol coupling of polymer 3.6, 3.11:



Kumada coupling of polymer 3.5, 3.12:



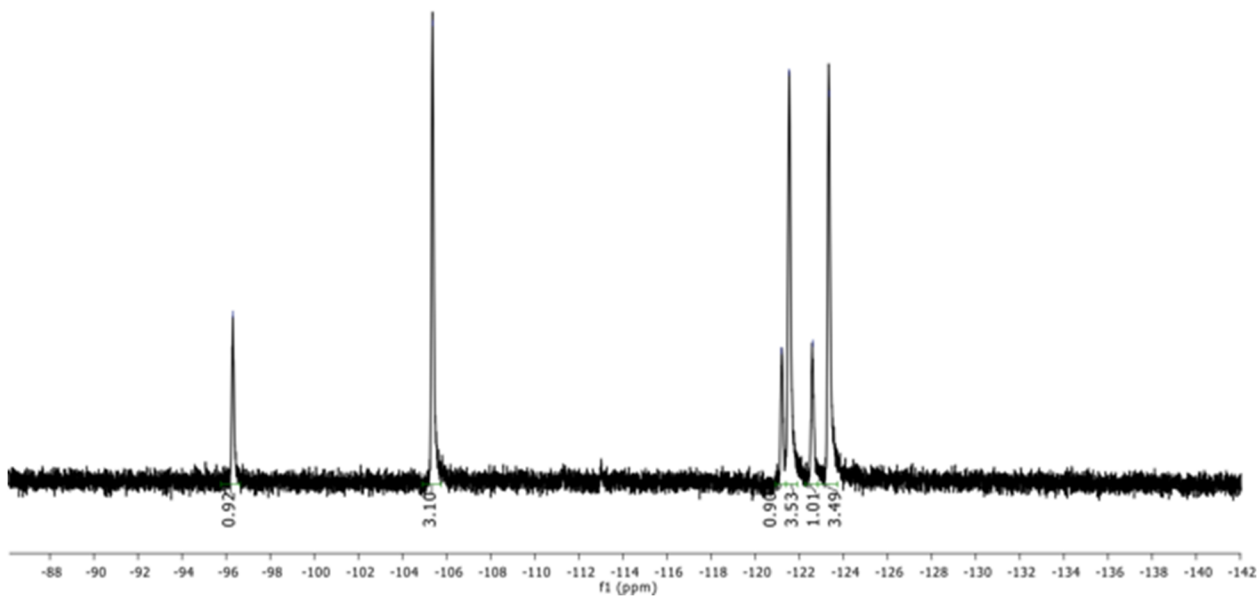
Elimination of iodide from polymer 3.5, 3.16:



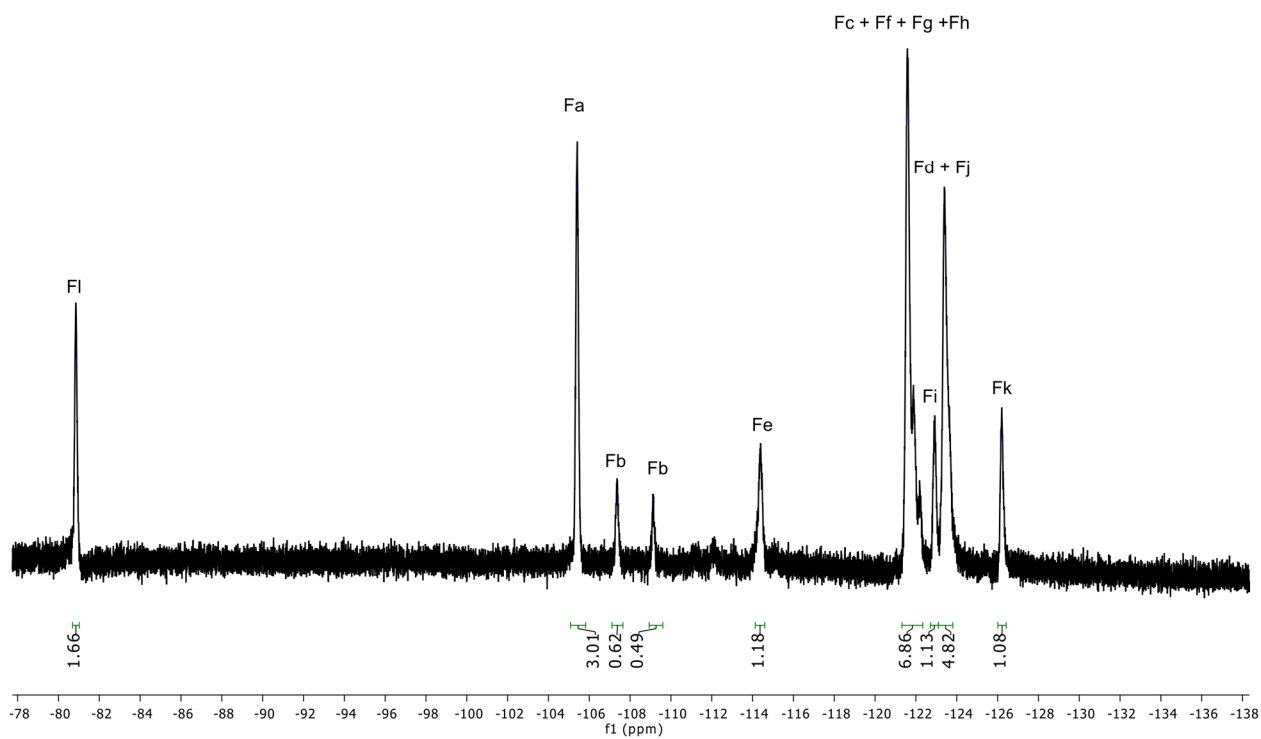
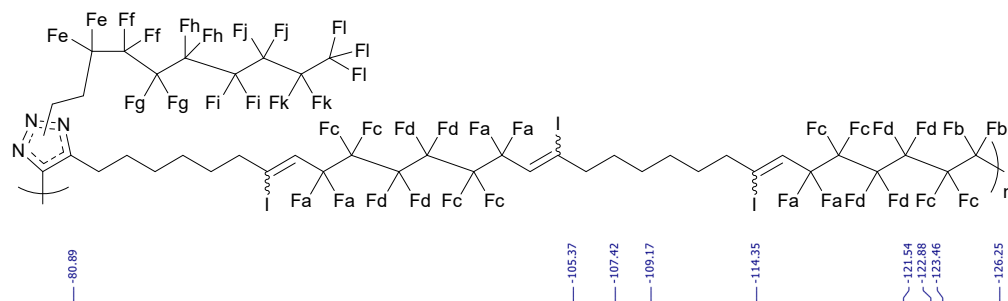
-96.31

-105.37

-121.19
-121.53
-122.61
-123.36

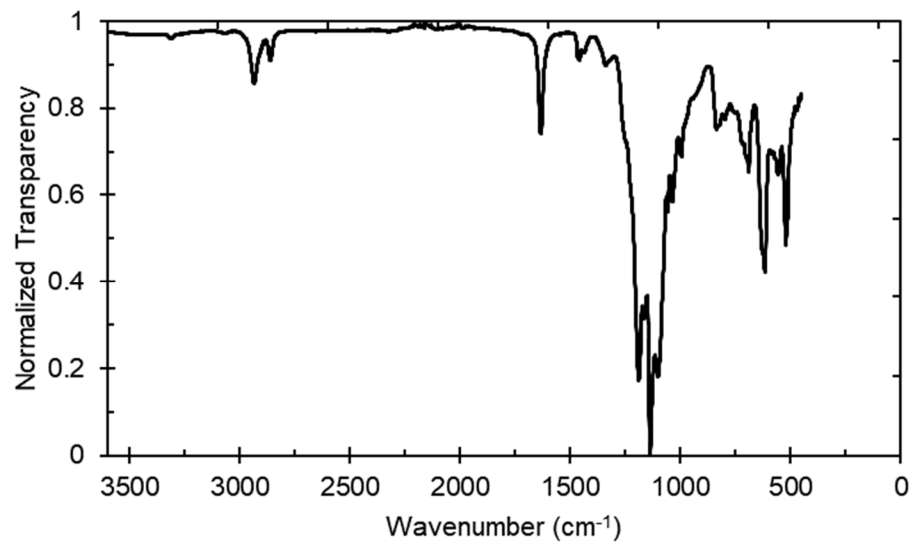
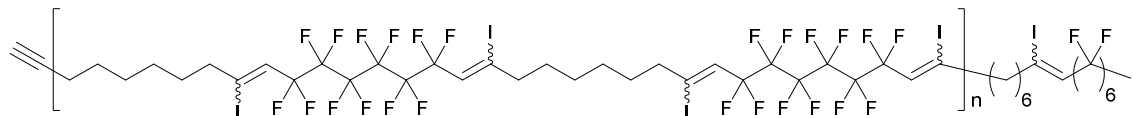


Alkyne-azide coupling of polymer 3.16, 3.18:

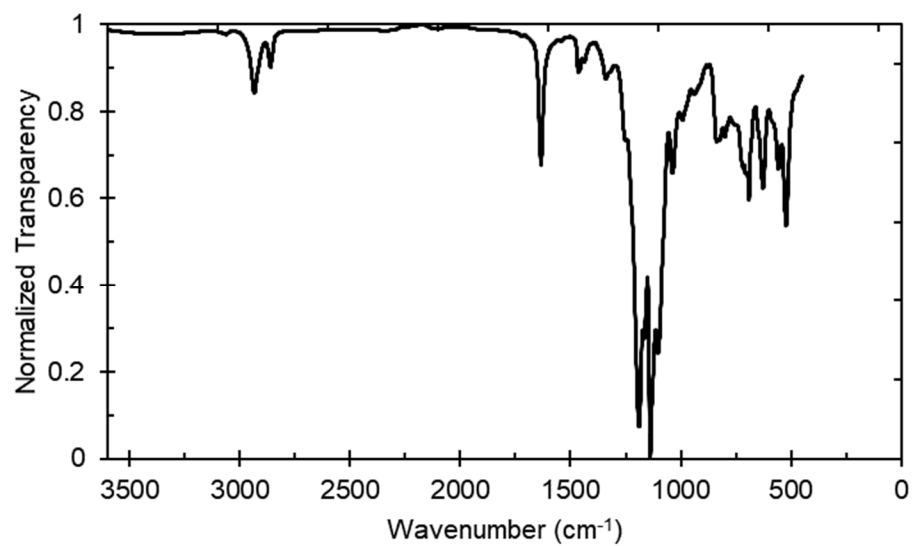
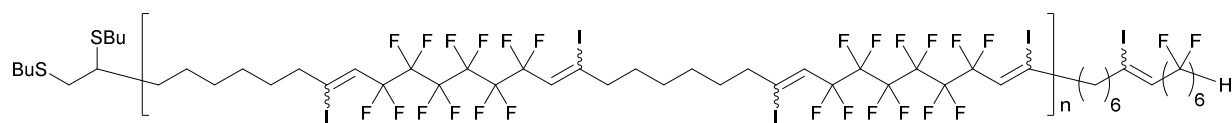


3.5.8 IR spectra

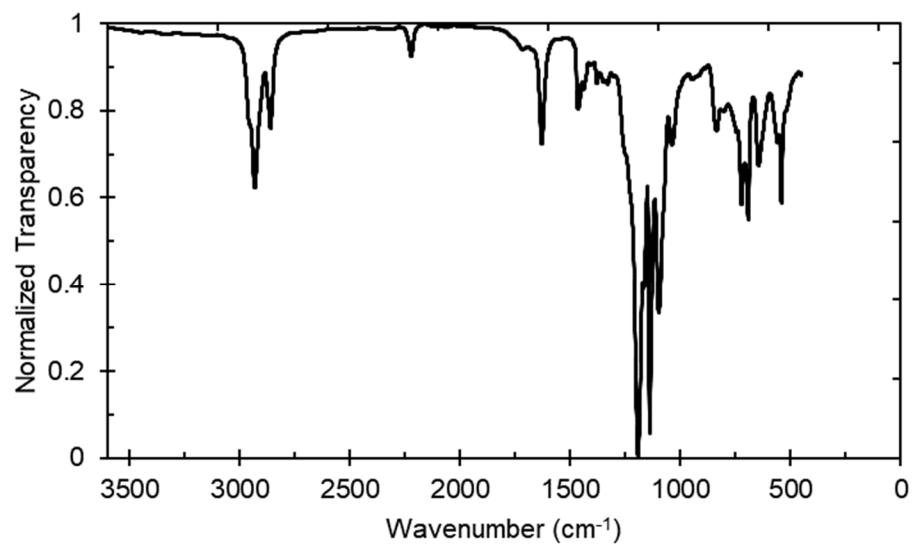
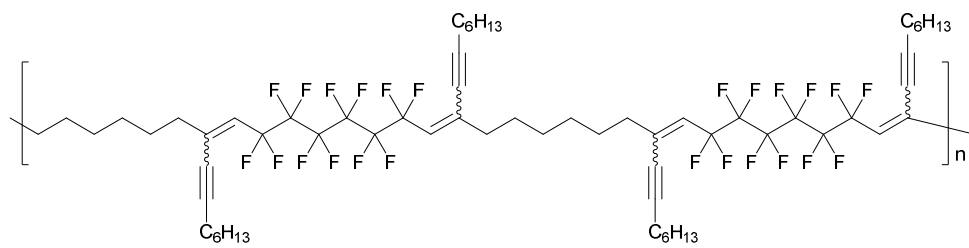
1-perfluorohexyl-2,9-diiodo-1,9-decadiene block polymer, 3.5:



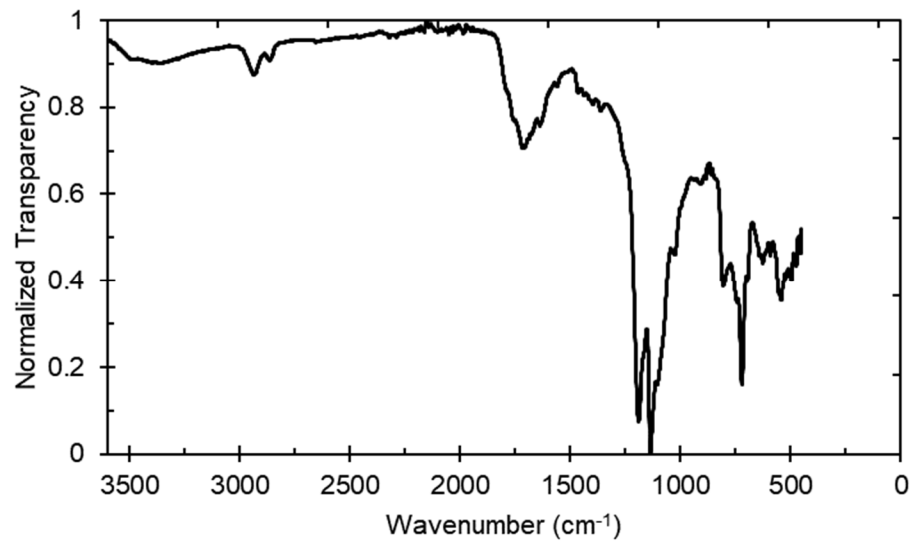
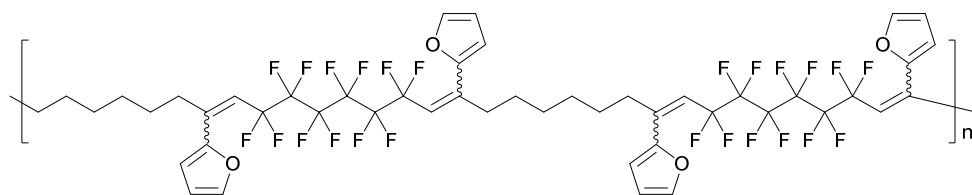
Thiol capping of polymer 3.5, 3.6:



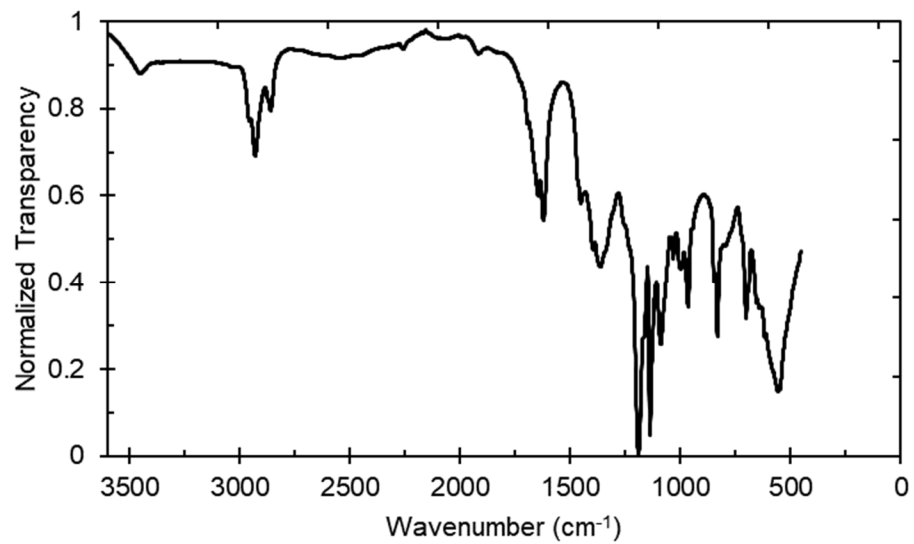
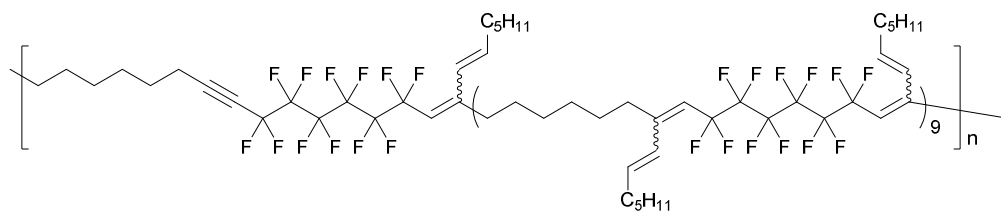
Sonogashira coupling of polymer 3.6, 3.7:



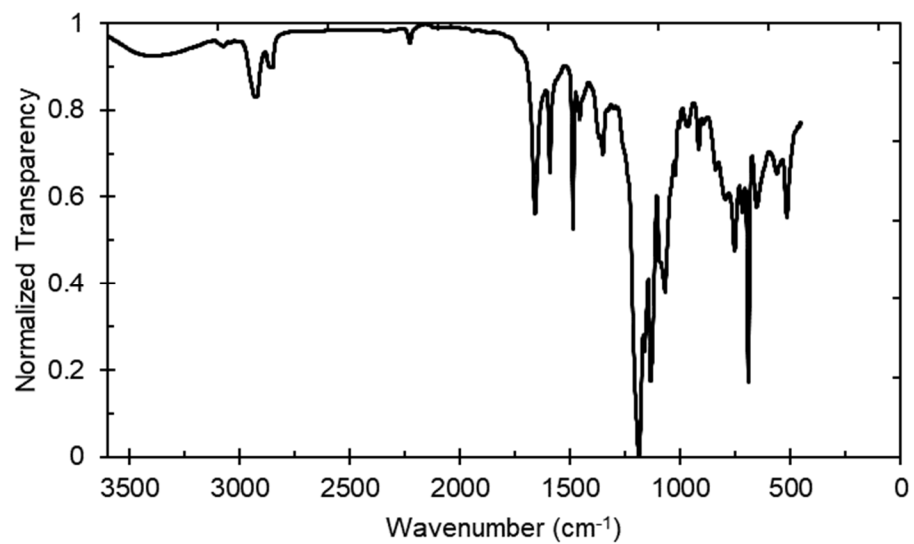
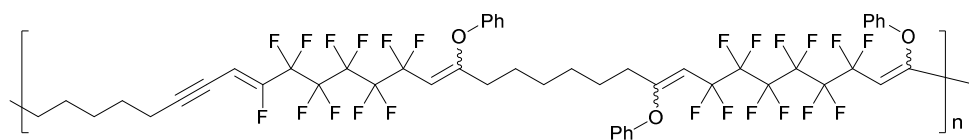
Stille coupling of polymer 3.6, 3.8:



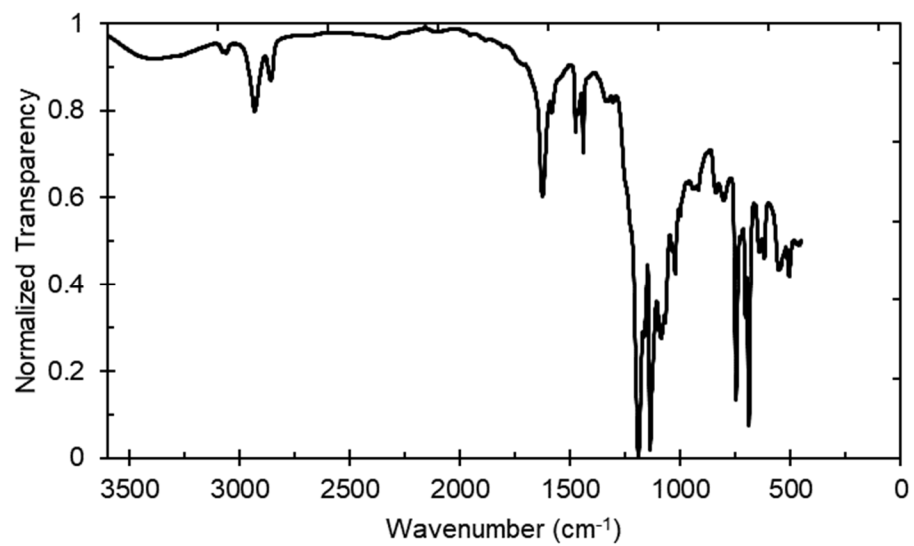
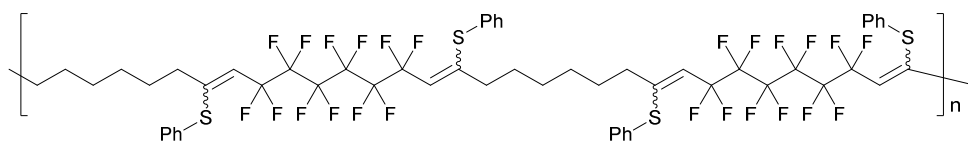
Suzuki coupling of polymer 3.6, 3.9:



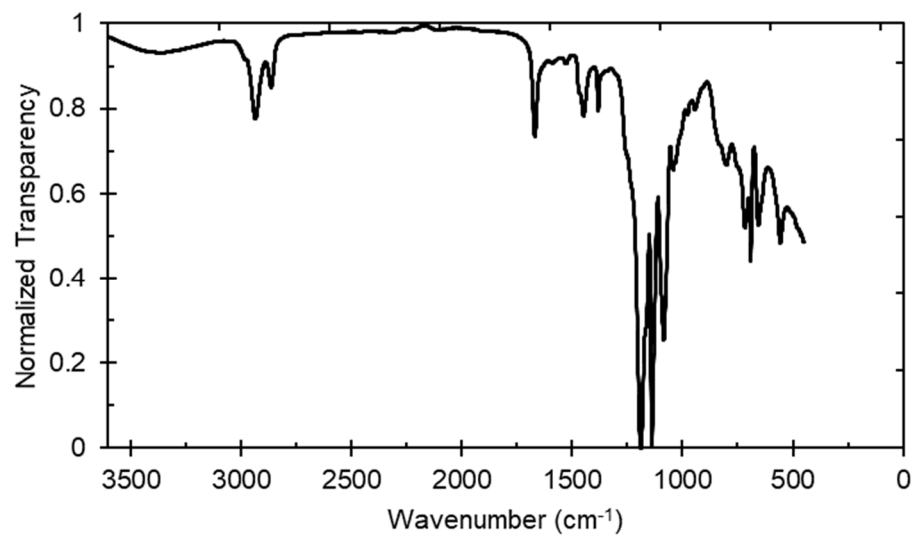
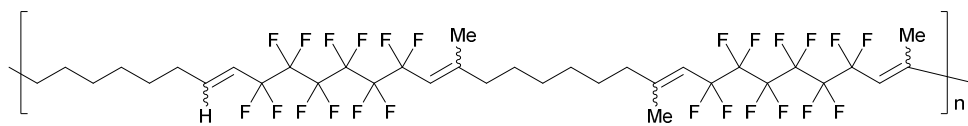
Phenol coupling of polymer 3.6, 3.10:



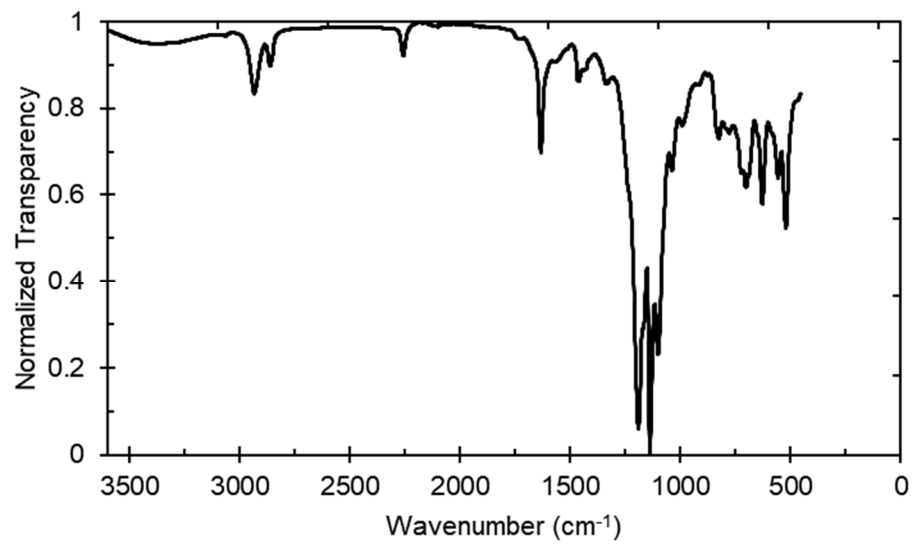
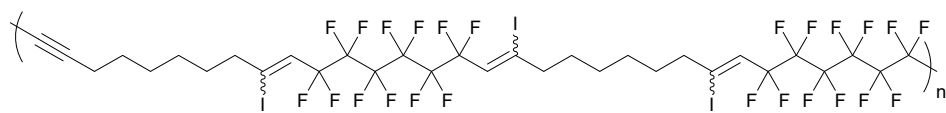
Thiophenol coupling of polymer 3.6, 3.11:



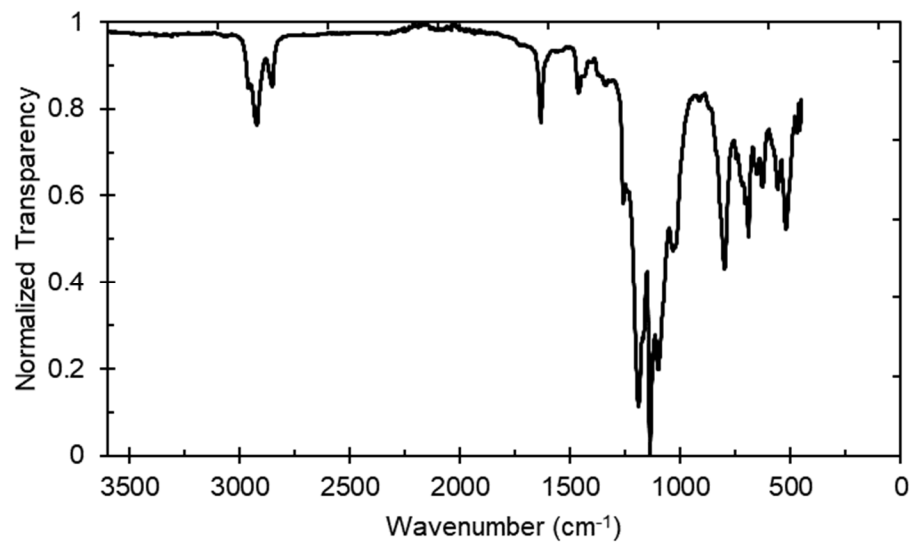
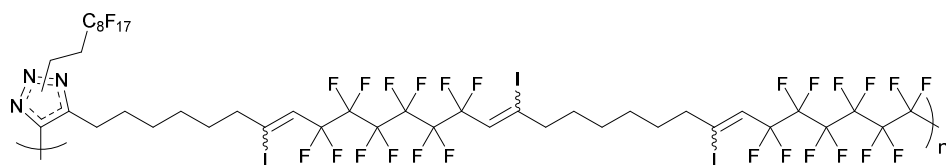
Kumada coupling of polymer 3.5, 3.12:



Elimination of iodide from polymer 3.5, 3.16:

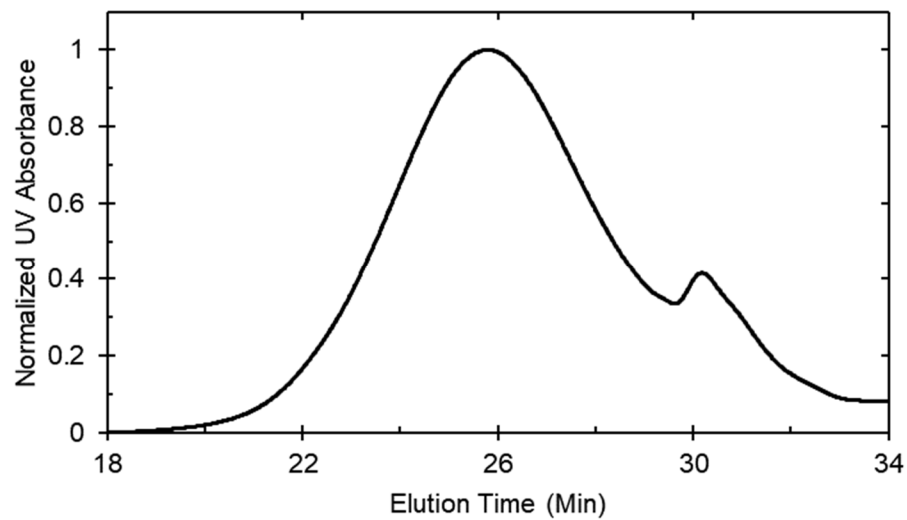
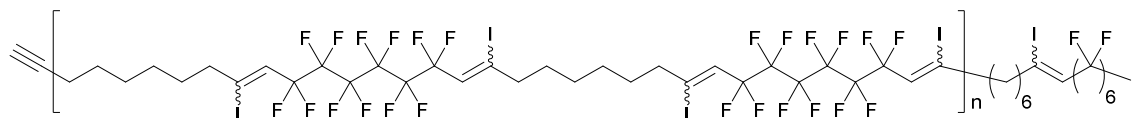


Alkyne-azide coupling of polymer 3.16, 3.18:



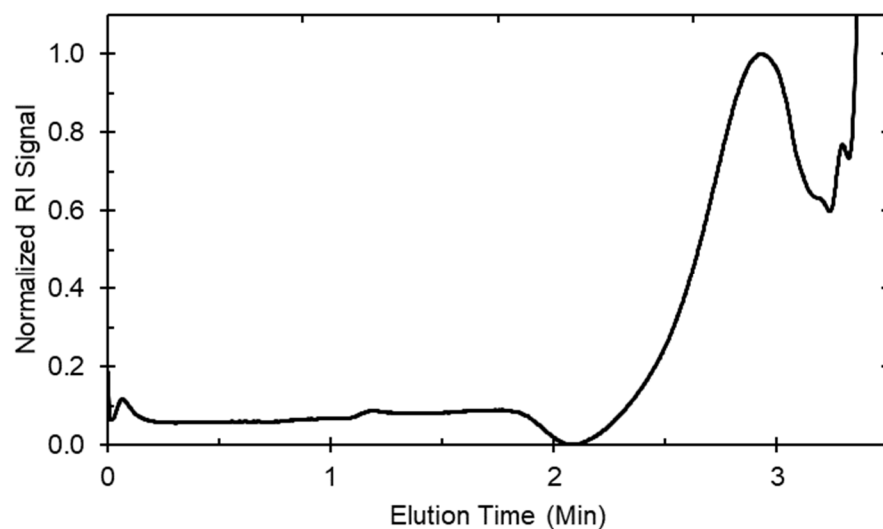
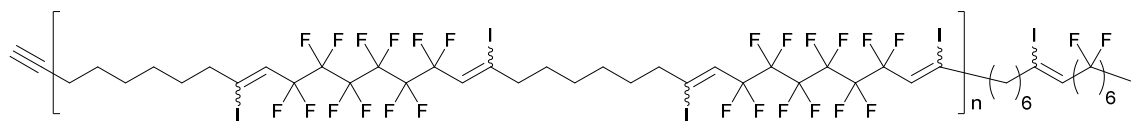
3.5.9 SEC traces

1-perfluorohexyl-2,9-diiodo-1,9-decadiene block polymer, 3.5, HPLC SEC:



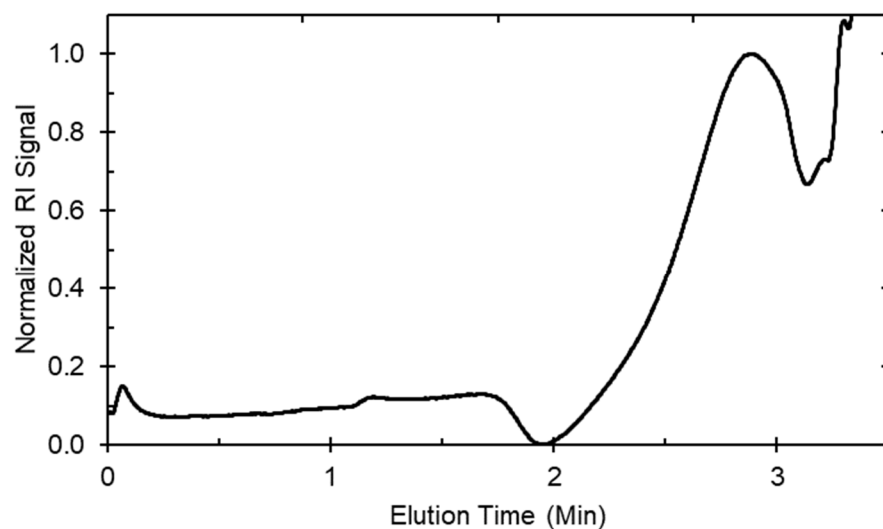
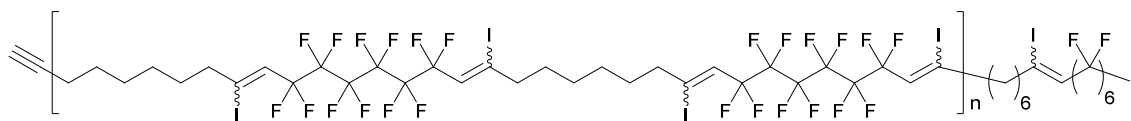
*We hypothesize that the low molecular shoulder is due to a small amount of oligomer or cyclic product that couldn't be removed by precipitation.

1-perfluorohexyl-2,9-diiodo-1,9-decadiene block polymer, 3.5, UHPLC SEC, Table 1, Entry 1:



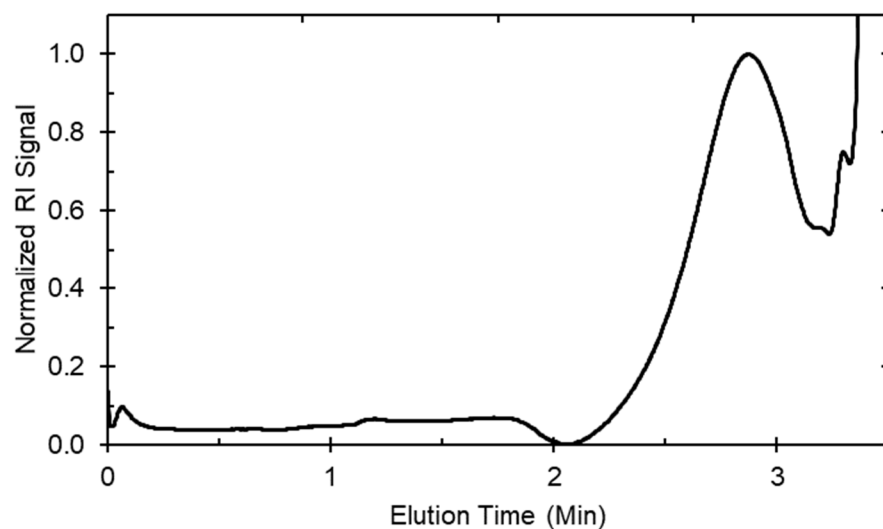
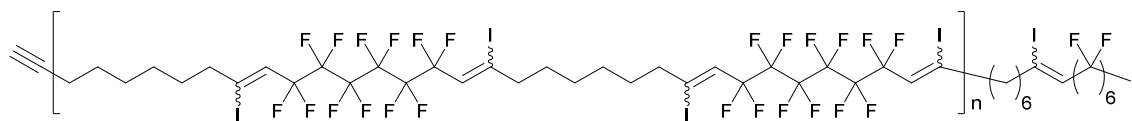
*Peak following 3.1 minutes belongs to solvent delay.

1-perfluorohexyl-2,9-diiodo-1,9-decadiene block polymer, 3.5, UHPLC SEC, Table 1, Entry 2



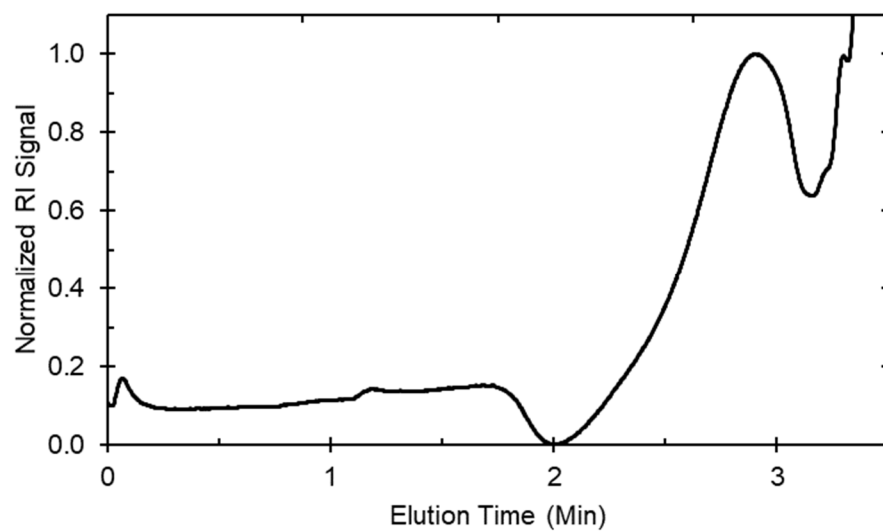
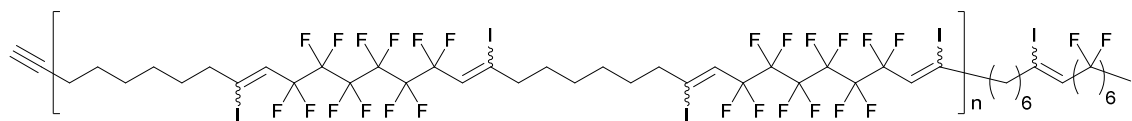
*Peak following 3.1 minutes belongs to solvent delay.

1-perfluorohexyl-2,9-diiodo-1,9-decadiene block polymer, 3.5, UHPLC SEC, Table 1, Entry 3:



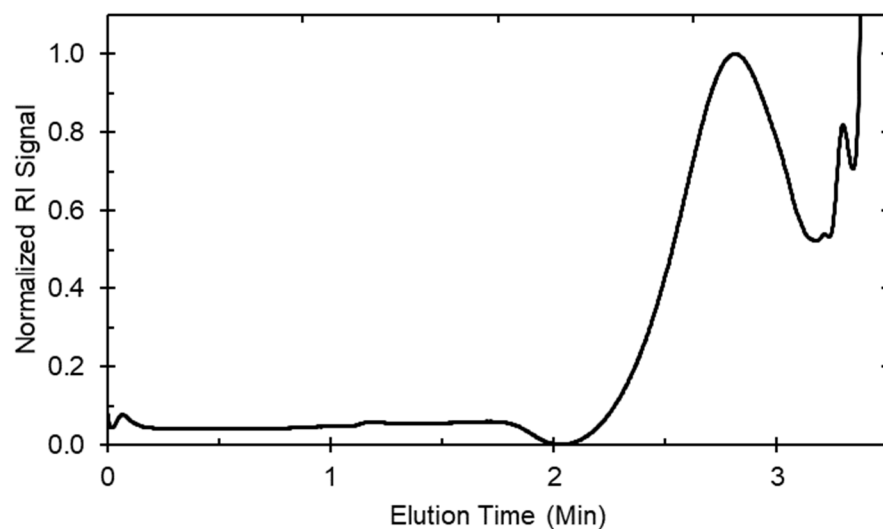
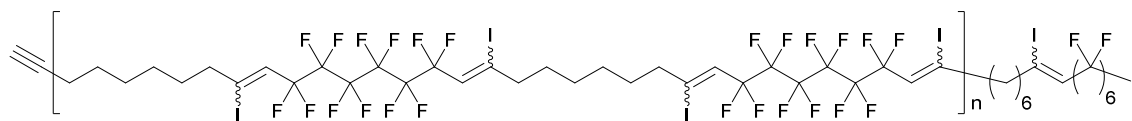
*Peak following 3.1 minutes belongs to solvent delay.

1-perfluorohexyl-2,9-diiodo-1,9-decadiene block polymer, 3.5, UHPLC SEC, Table 1, Entry 4:



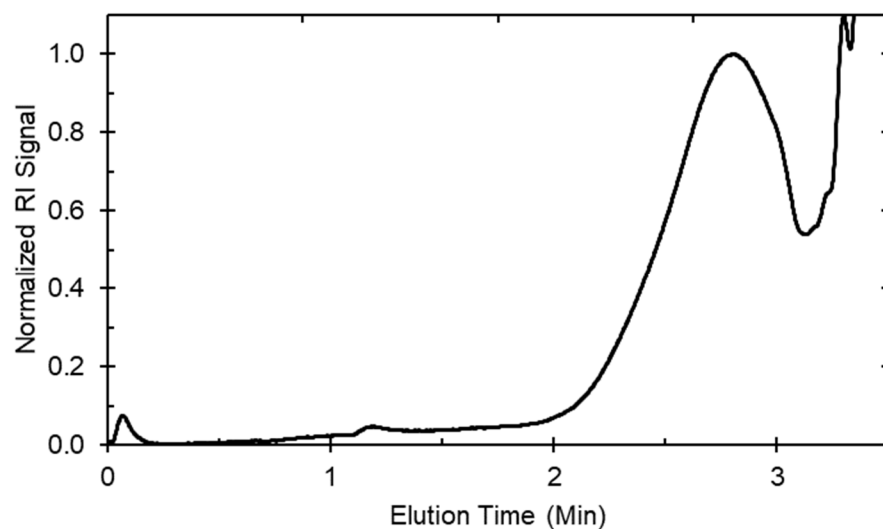
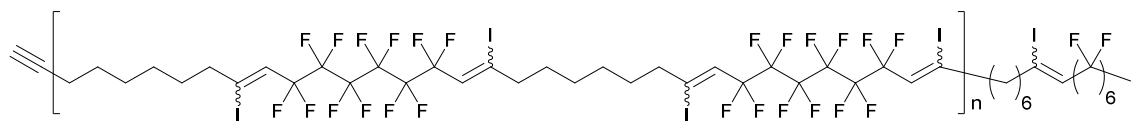
*Peak following 3.1 minutes belongs to solvent delay.

1-perfluorohexyl-2,9-diiodo-1,9-decadiene block polymer, 3.5, UHPLC SEC, Table 1, Entry 5:



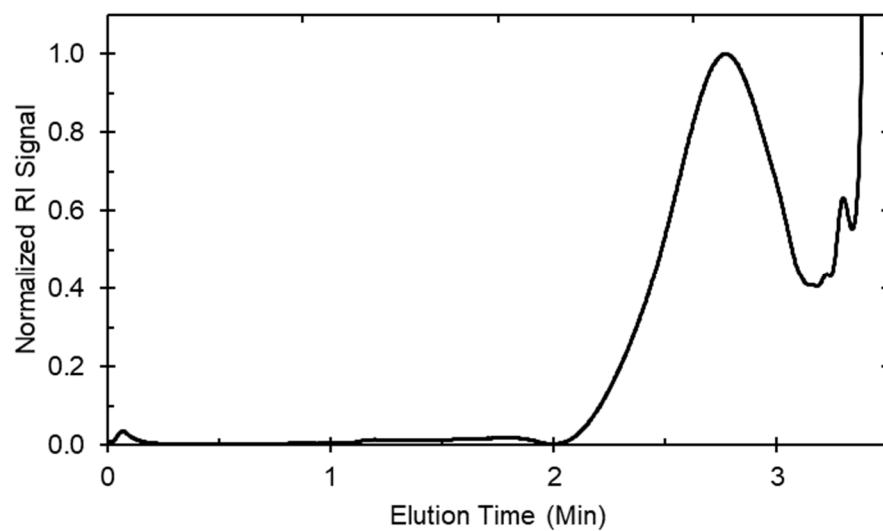
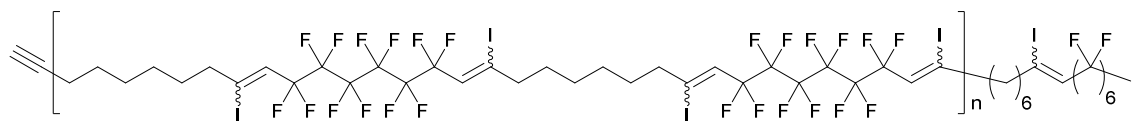
*Peak following 3.1 minutes belongs to solvent delay.

1-perfluorohexyl-2,9-diiodo-1,9-decadiene block polymer, 3.5, UHPLC SEC, Table 1, Entry 6:



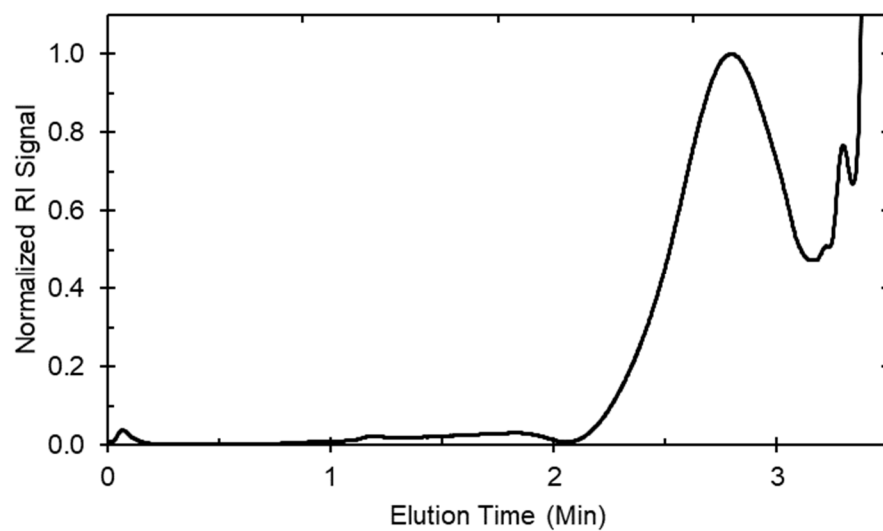
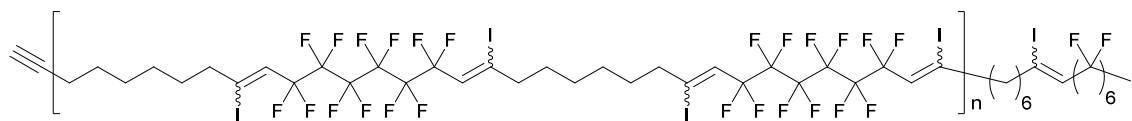
*Peak following 3.1 minutes belongs to solvent delay.

1-perfluorohexyl-2,9-diiodo-1,9-decadiene block polymer, 3.5, UHPLC SEC, Table 1, Entry 7:



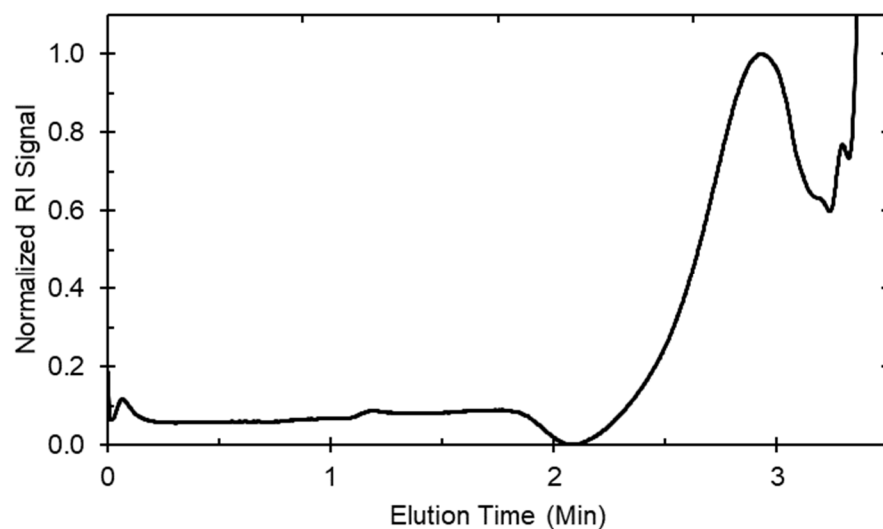
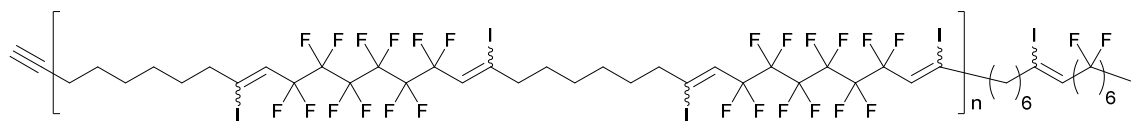
*Peak following 3.1 minutes belongs to solvent delay.

1-perfluorohexyl-2,9-diiodo-1,9-decadiene block polymer, 3.5, UHPLC SEC, Table 1, Entry 8:



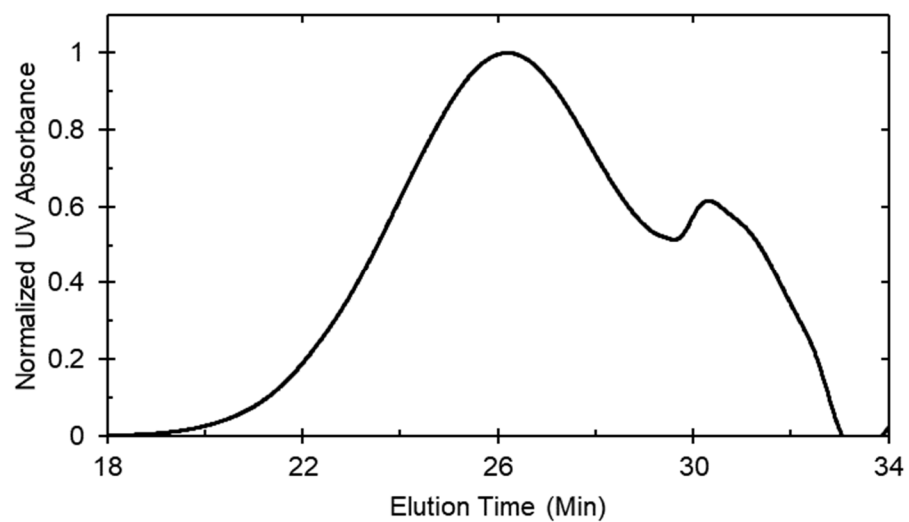
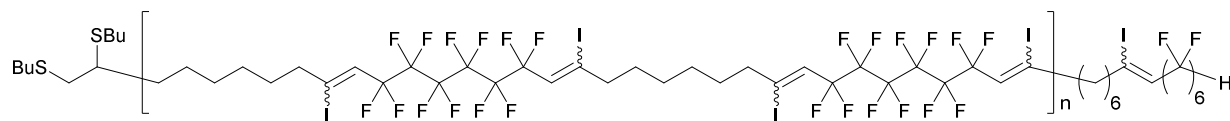
*Peak following 3.1 minutes belongs to solvent delay.

1-perfluorohexyl-2,9-diiodo-1,9-decadiene block polymer, 3.5, UHPLC SEC, Table 1, Entry 1:

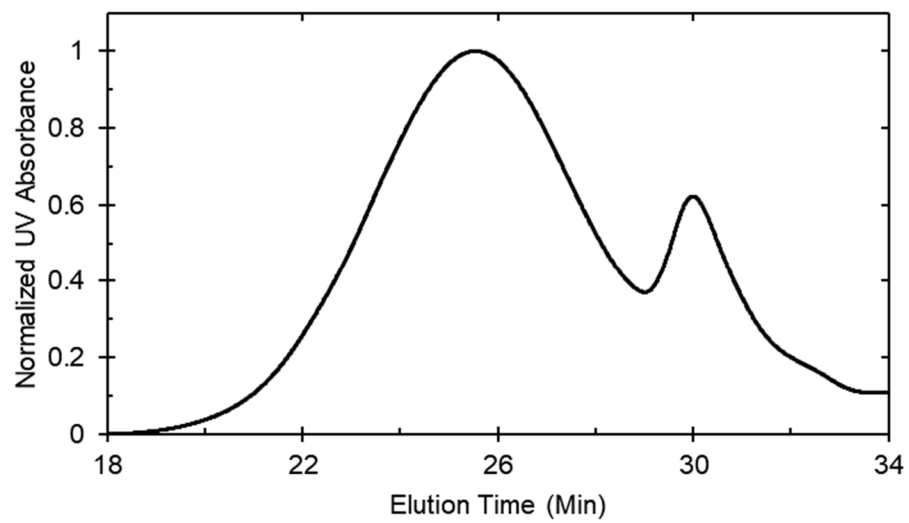
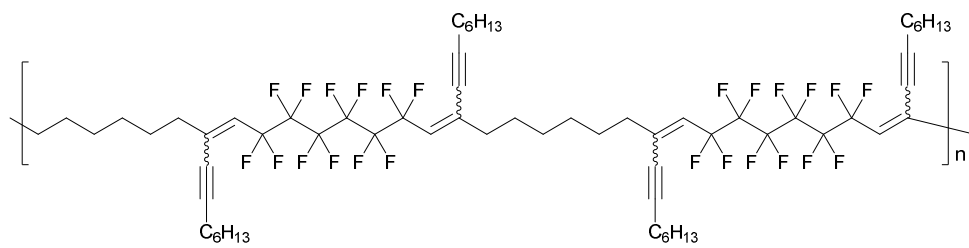


*Peak following 3.1 minutes belongs to solvent delay.

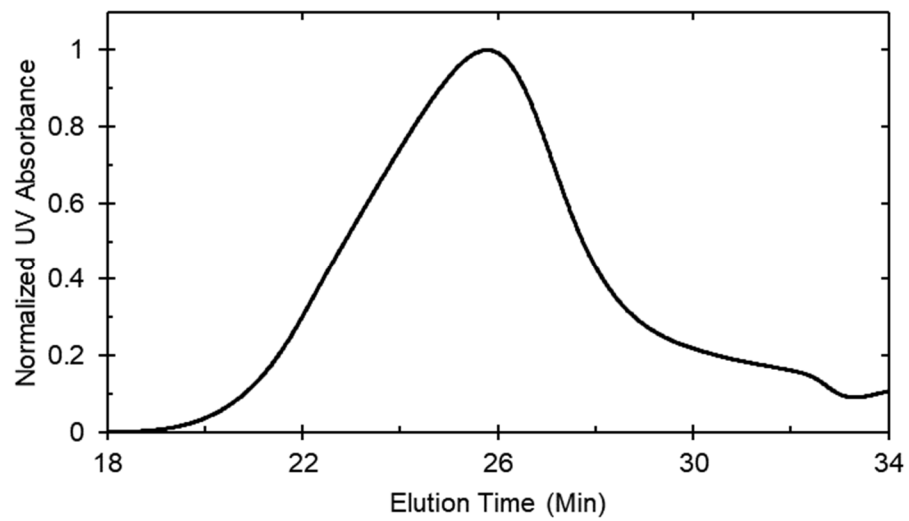
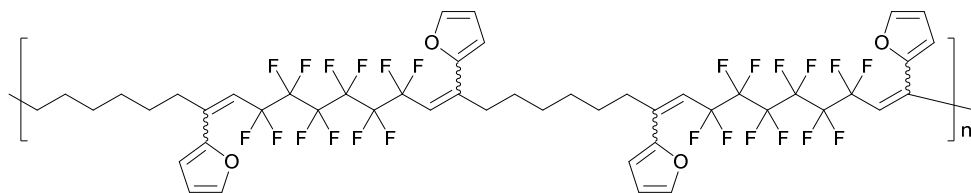
Thiol capping of polymer 3.5, 3.6:



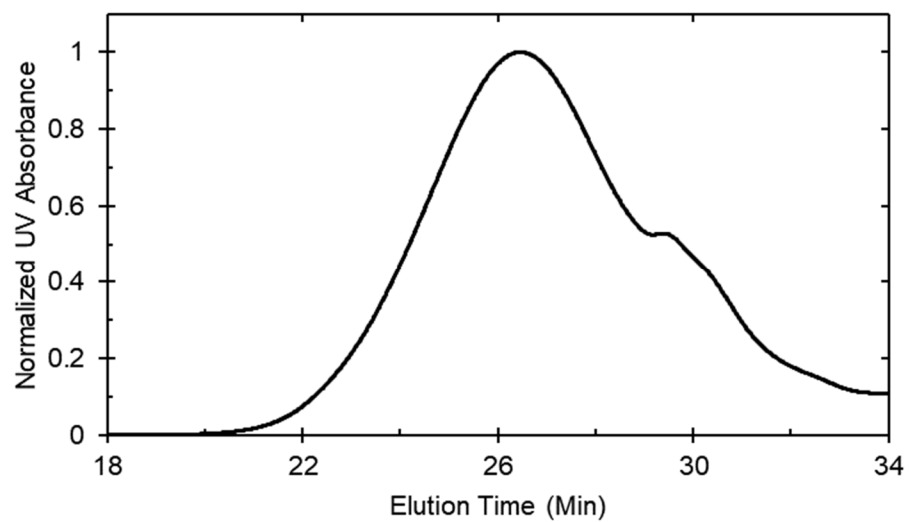
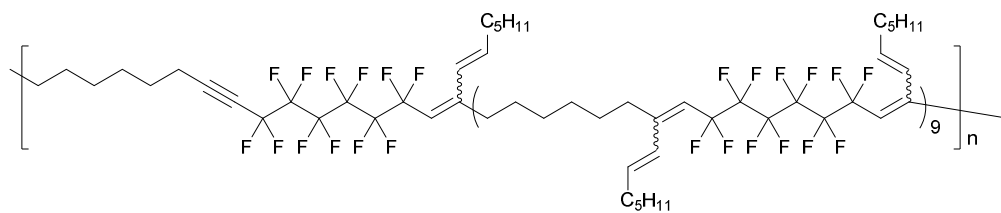
Sonogashira coupling of polymer 3.6, 3.7:



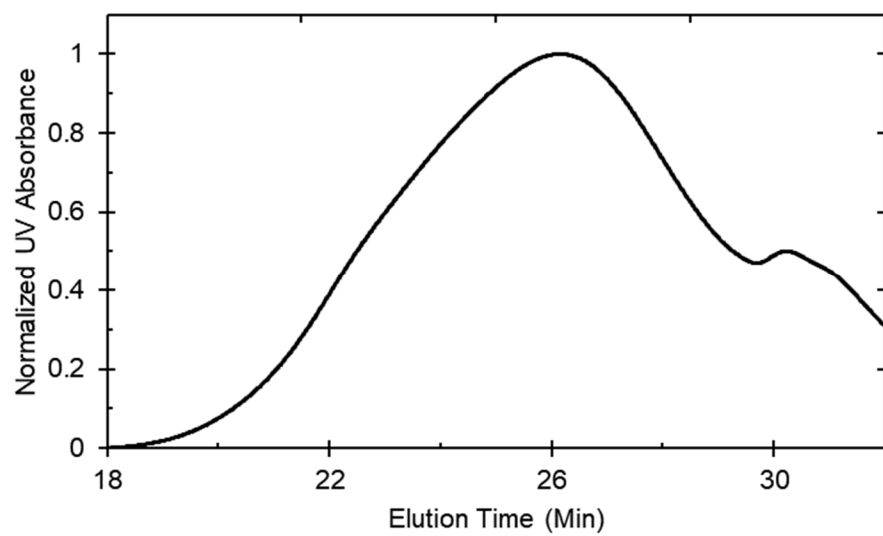
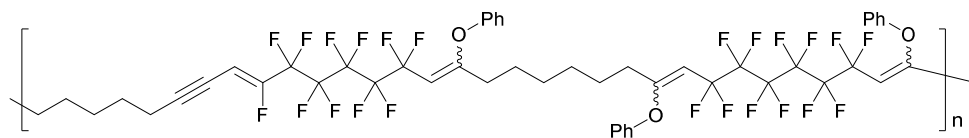
Stille coupling of polymer 3.6, 3.8:



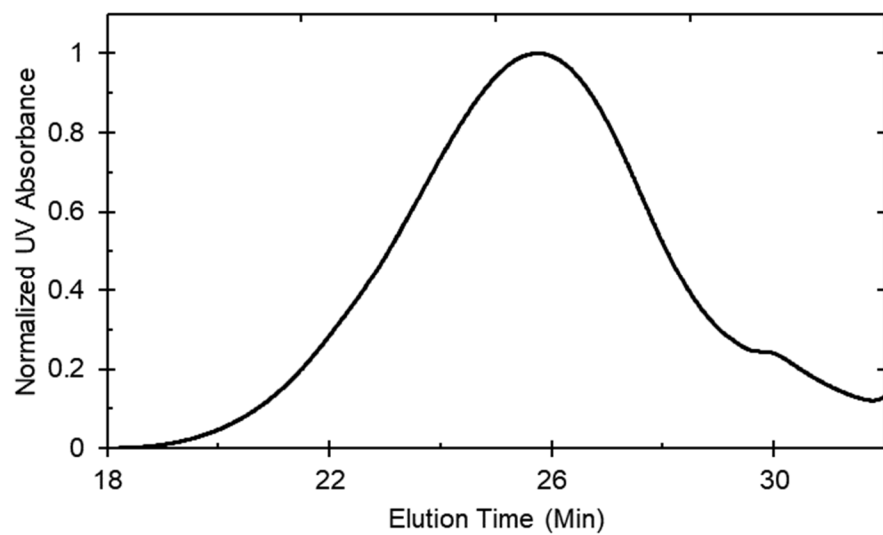
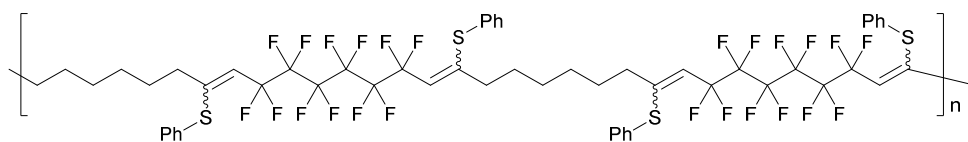
Suzuki coupling of polymer 3.6, 3.9:



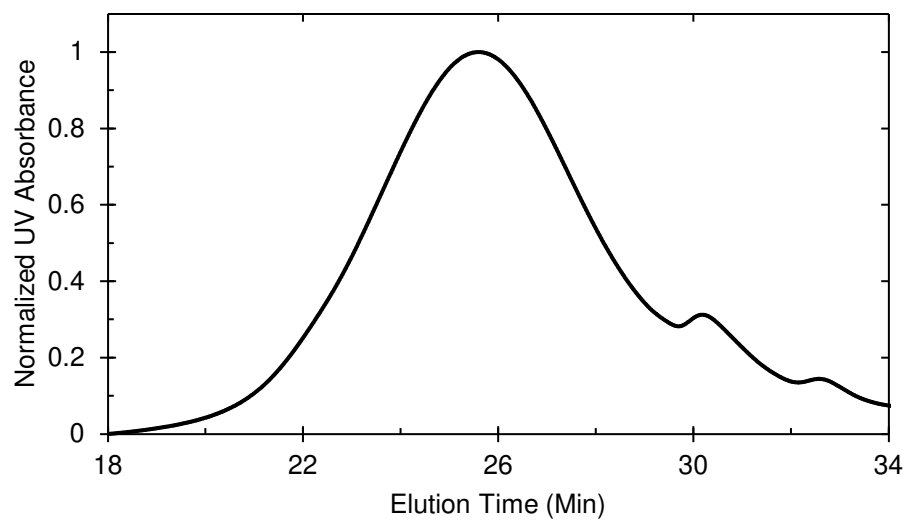
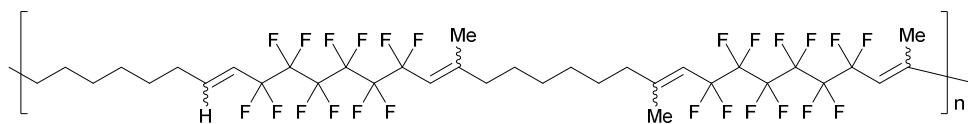
Phenol coupling of polymer 3.6, 3.10:



Thiophenol coupling of polymer 3.6, 3.11:

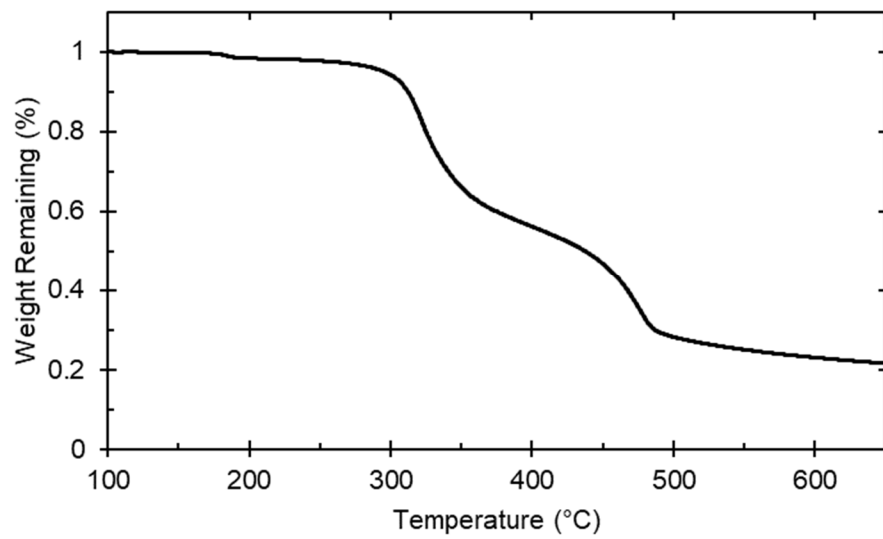
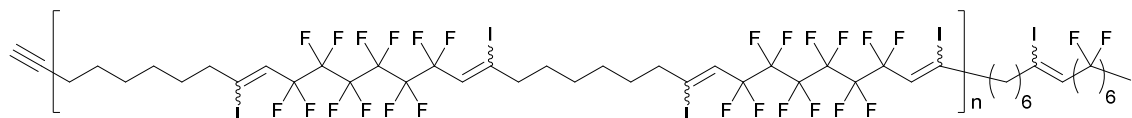


Kumada coupling of polymer 3.5, 3.12:

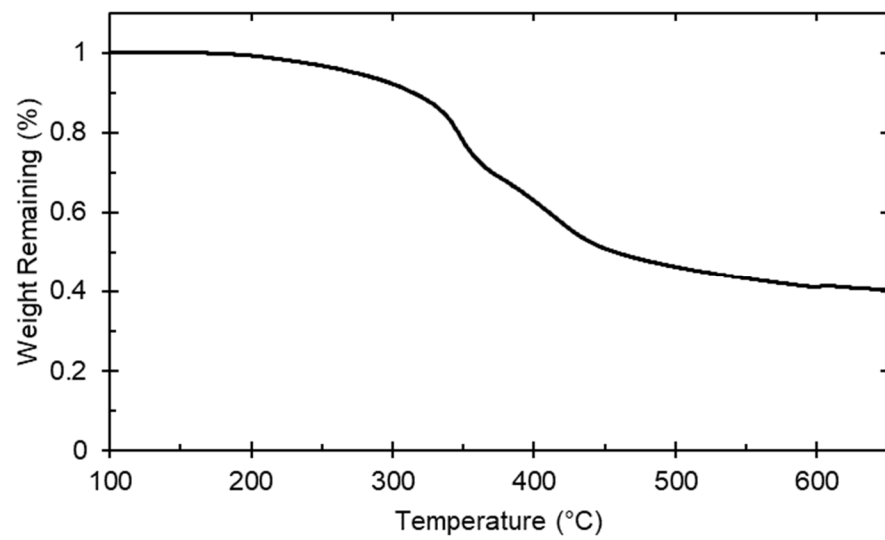
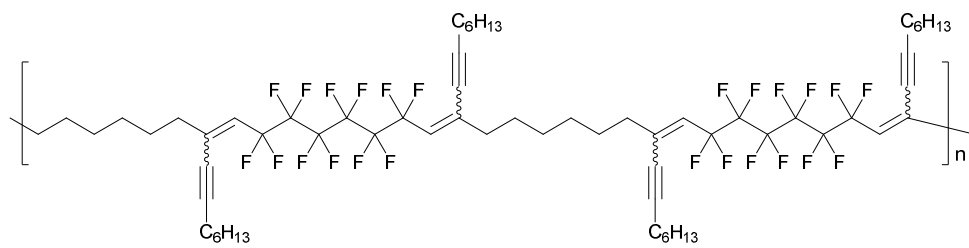


3.5.10 TGA traces

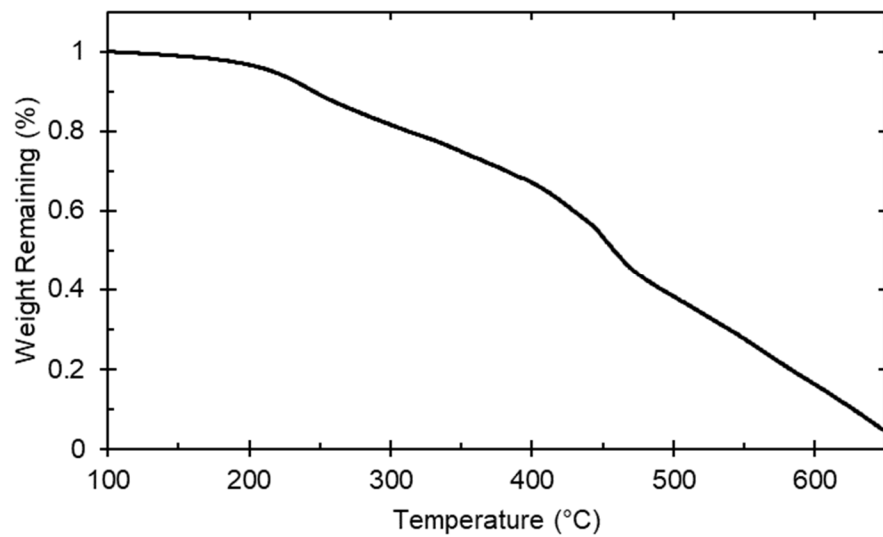
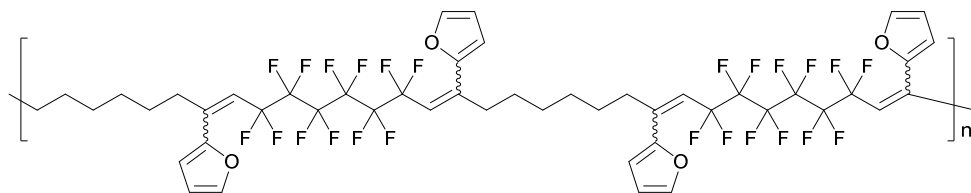
1-perfluorohexyl-2,9-diiodo-1,9-decadiene block polymer, 3.5:



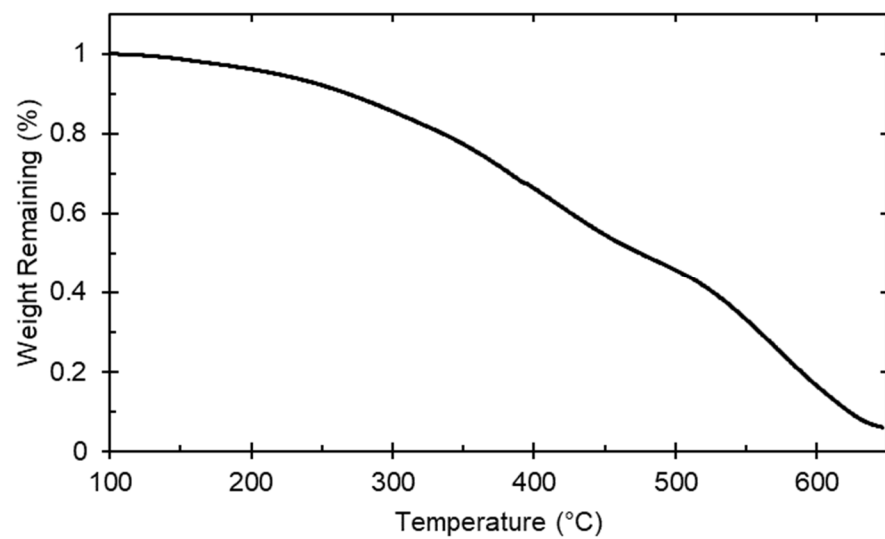
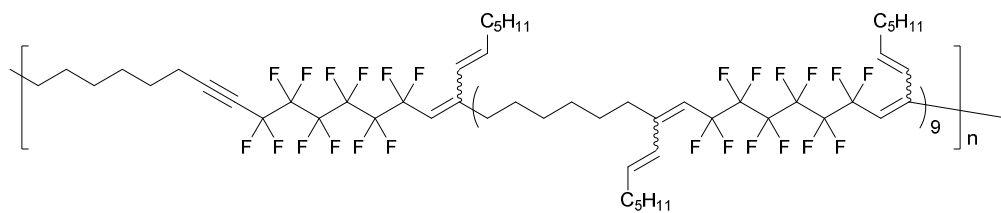
Sonogashira coupling of polymer 3.6, 3.7:



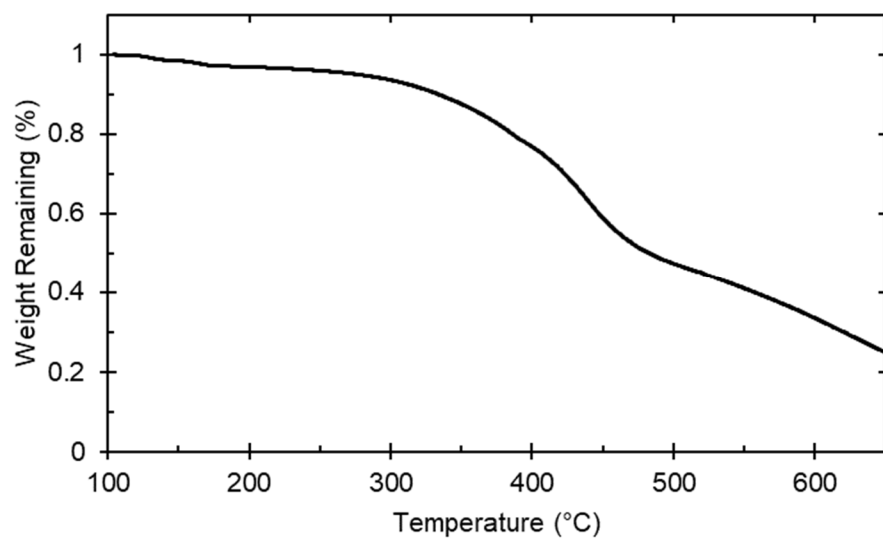
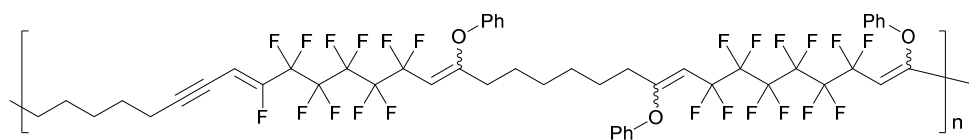
Stille coupling of polymer 3.6, 3.8:



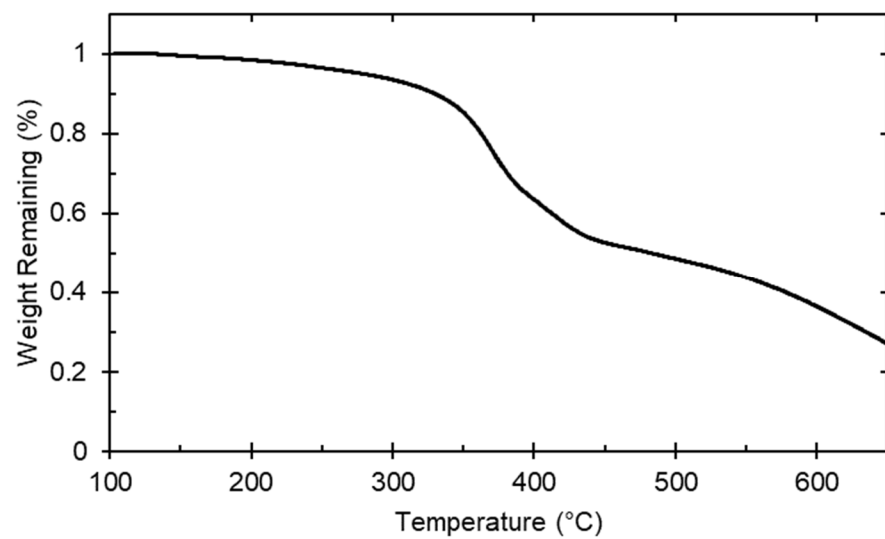
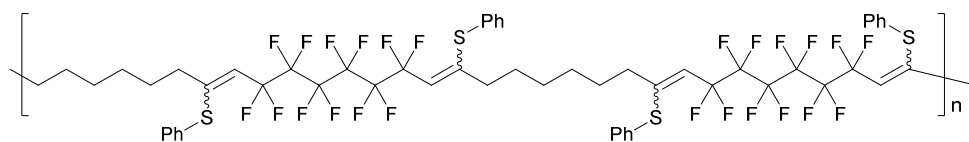
Suzuki coupling of polymer 3.6, 3.9:



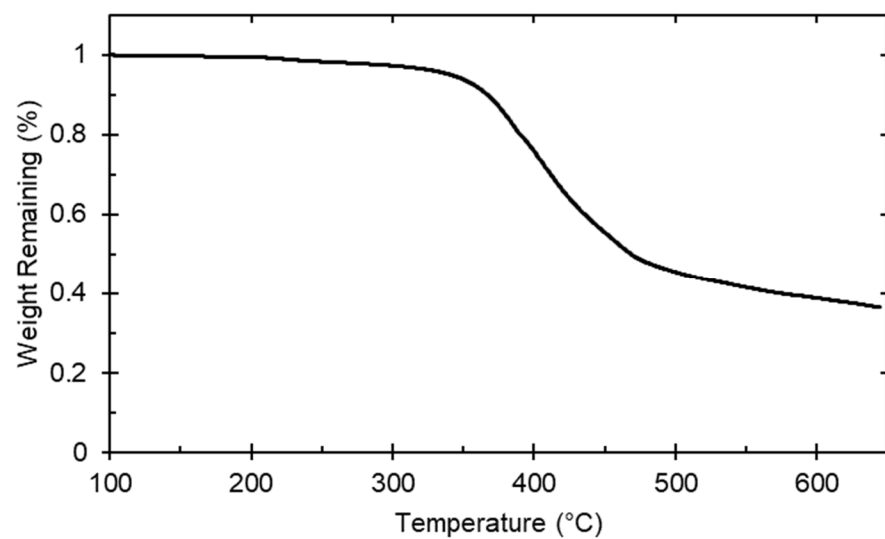
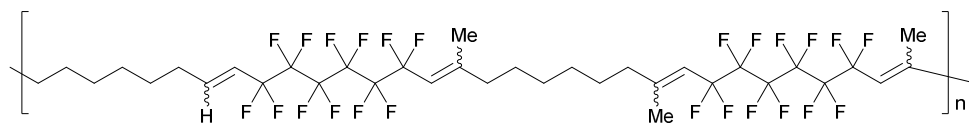
Phenol coupling of polymer 3.6, 3,10:



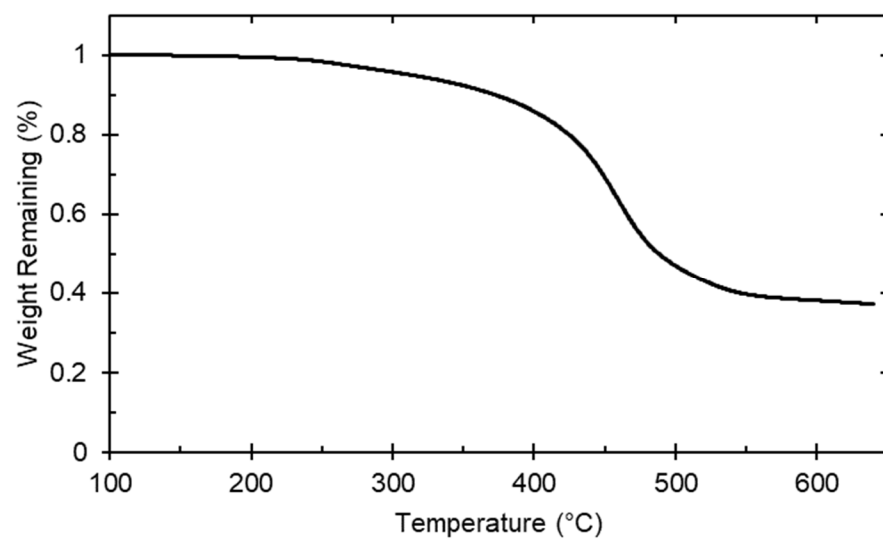
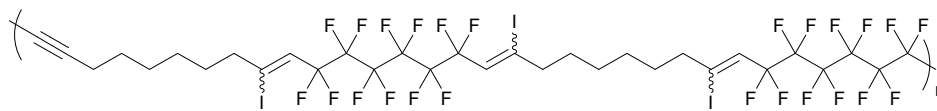
Thiophenol coupling of polymer 3.6, 3.11:



Kumada coupling of polymer 3.5, 12:

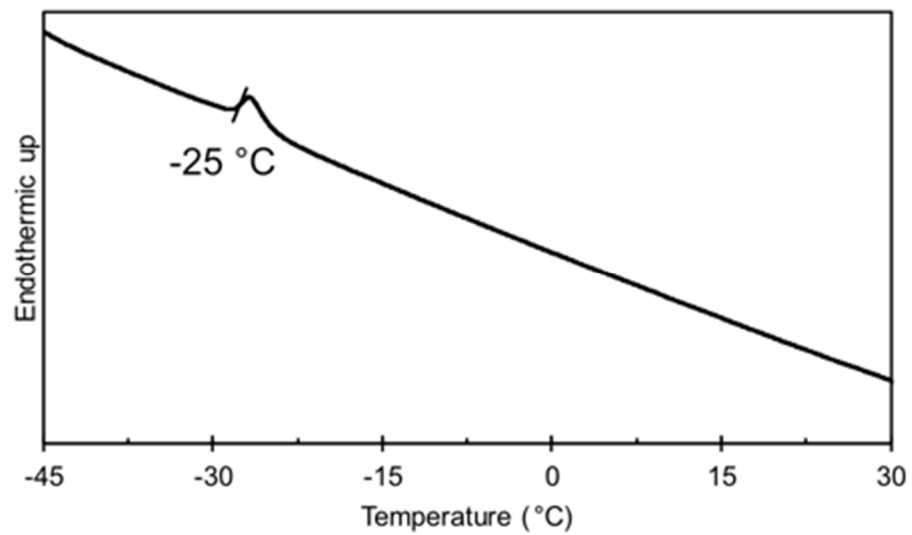
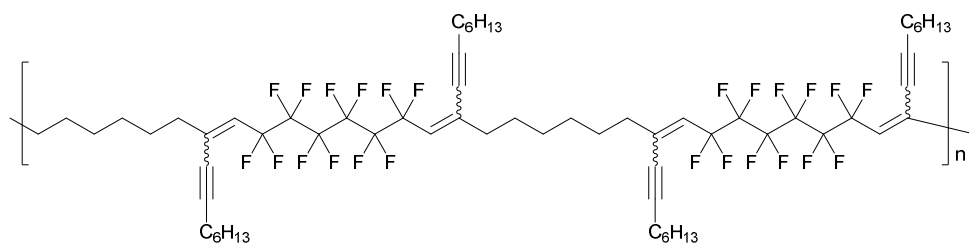


Elimination of iodide from polymer 3.5, 3.16:

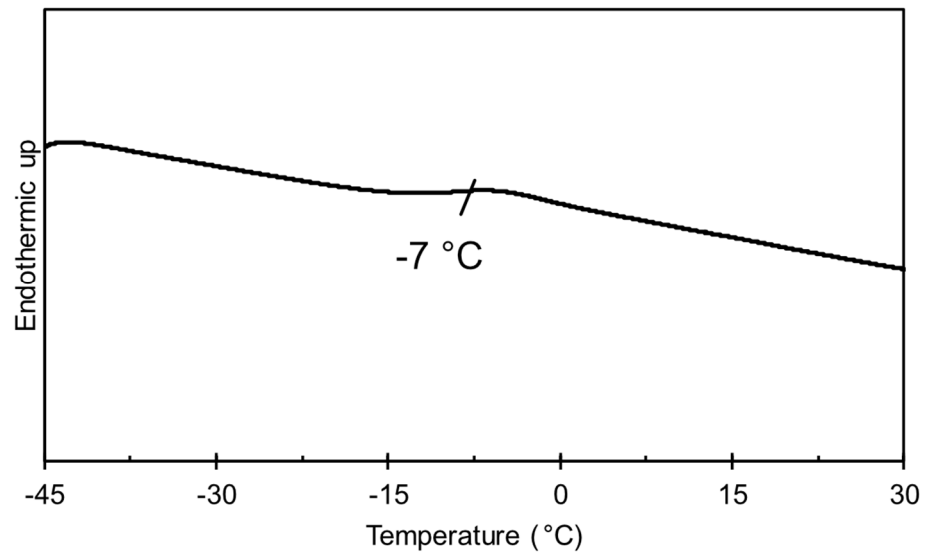
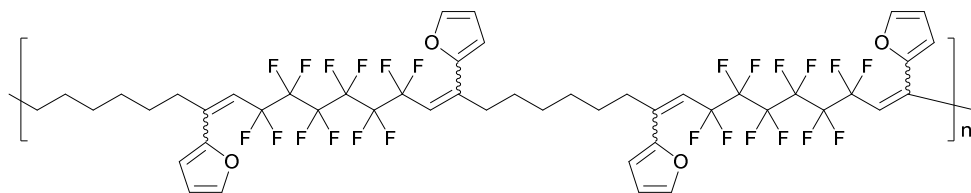


3.5.11 DSC traces

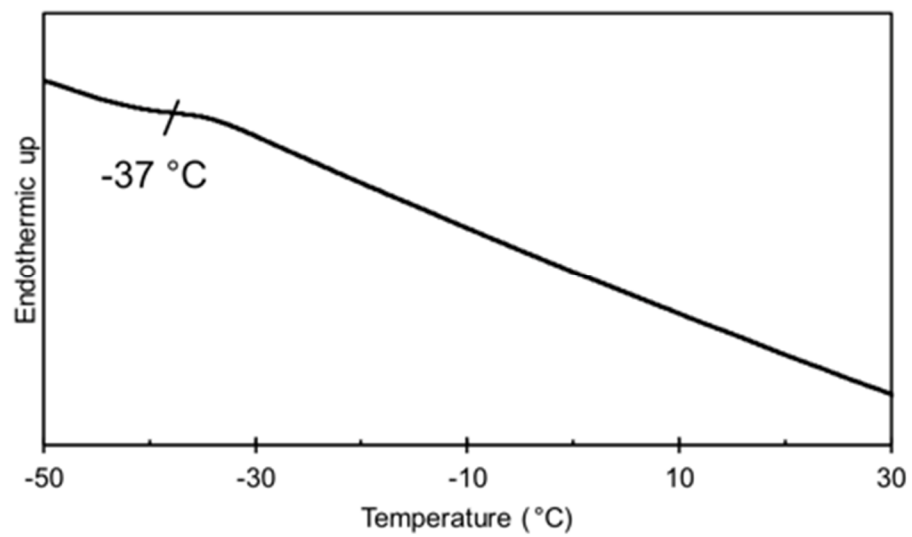
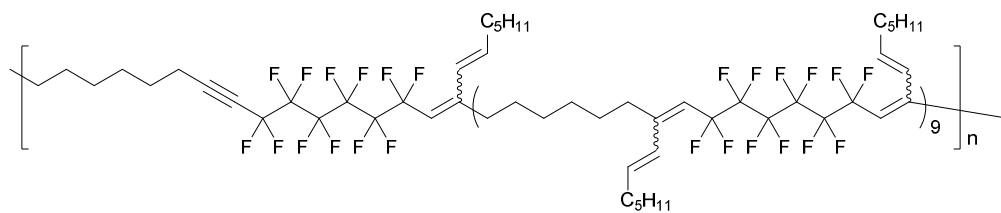
Sonogashira coupling of polymer 3.6, 3.7:



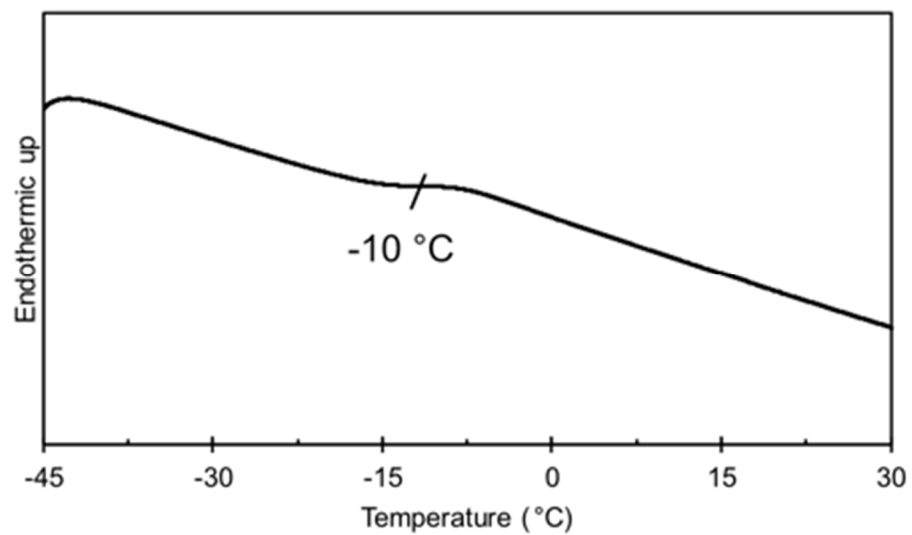
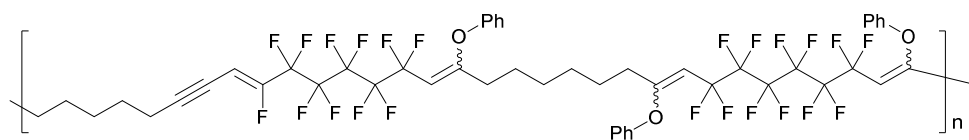
Stille coupling of polymer 3.6, 3.8:



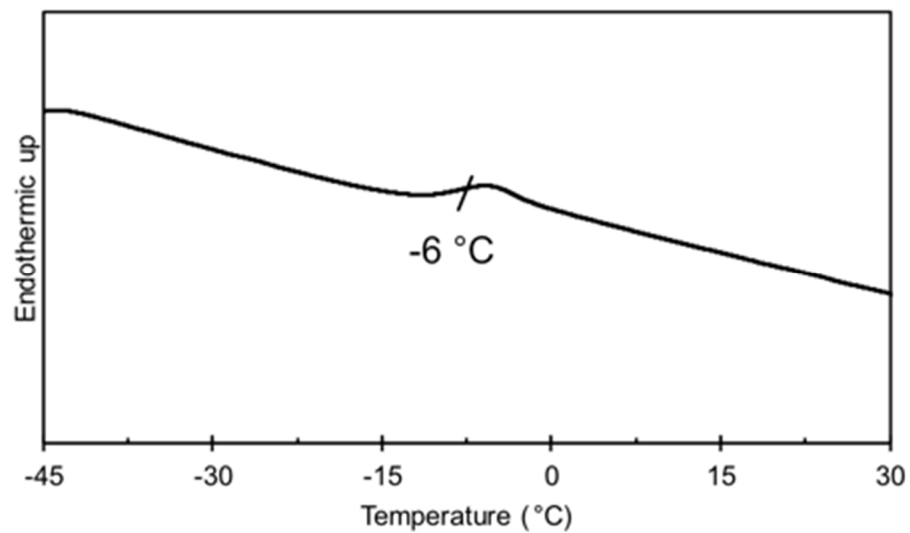
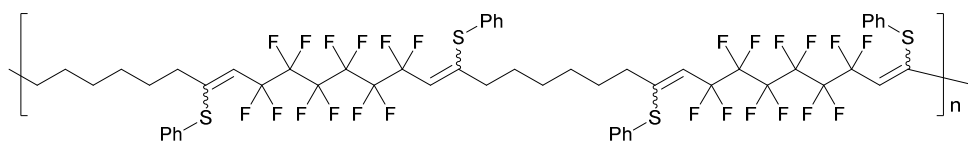
Suzuki coupling of polymer 3.6, 3.9:



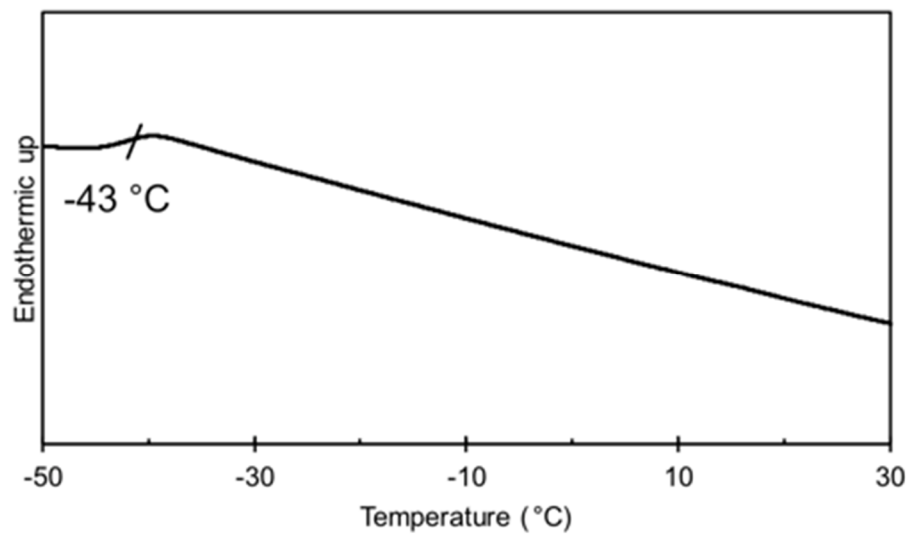
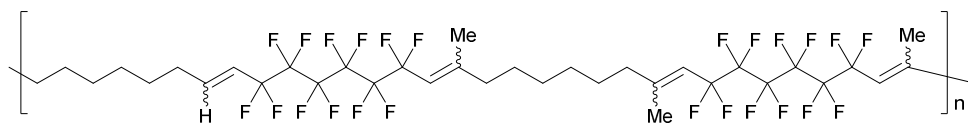
Phenol coupling of polymer 3.6, 3.10:



Thiophenol coupling of polymer 3.6, 3.11:



Kumada coupling of polymer 3.5, 3.12:



3.6 References and notes

- (1) Liu, F. Recent Advances and Challenges in Designing Stimuli-Responsive Polymers. *Prog. Polym. Sci.* **2010**, *35*, 3–23.
- (2) Yang, Y.; Urban, M. W. Self-Healing Polymeric Materials. *Chem. Soc. Rev.* **2013**, *42*, 7446–7467.
- (3) Qiao, J.; Guo, M.; Wang, L.; Liu, D.; Zhang, X.; Yu, L.; Song, W.; Liu, Y. Recent Advances in Polyolefin Technology. *Polym. Chem.* **2011**, *2*, 1611–1623.
- (4) Galli, P.; Vecellio, G. Technology: Driving Force behind Innovation and Growth of Polyolefins. *Prog. Polym. Sci.* **2001**, *26*, 1287–1336.
- (5) Mohammed, J. S.; Murphy, W. L. Bioinspired Design of Dynamic Materials. *Adv. Mater.* **2009**, *21*, 2361–2374.
- (6) Tokarev, I.; Minko, S. Stimuli-Responsive Hydrogel Thin Films. *Soft Matter* **2009**, *5*, 511–524.
- (7) Gil, E. S.; Hudson, S. M. Stimuli-Responsive Polymers and Their Bioconjugates. *Prog. Polym. Sci.* **2004**, *29*, 1173–1222.
- (8) Ma, D.; Cai, Q. Copper/Amino Acid Catalyzed Cross-Couplings of Aryl and Vinyl Halides with Nucleophiles. *Acc. Chem. Res.* **2008**, *41*, 1450–1460.
- (9) Sun, A.; Lauher, J. W.; Goroff, N. S. Preparation of Poly(Diiododiacetylene), an Ordered Conjugated Polymer of Carbon and Iodine. *Science* **2006**, *312*, 1030–1034.
- (10) Jin, H.; Young, C. N.; Halada, G. P.; Phillips, B. L.; Goroff, N. S. Synthesis of the Stable Ordered Conjugated Polymer Poly(Dibromodiacetylene) from an Explosive Monomer. *Angew. Chemie Int. Ed.* **2015**, *54*, 14690–14695.
- (11) Wright, M. E.; Pulley, S. R. Transition-Metal-Catalyzed Modification of Polymer Backbones. 1. Palladium-Catalyzed Cross-Coupling Reactions of Copolymers Containing Vinyltributylstannane and Vinyl Iodide Groups. *Macromolecules* **1989**, *22*, 2542–2544.
- (12) Mao, S. S. H.; Tilley, T. D. New Route to Unsaturated Organosilicon Polymers and Macrocycles Based on Zirconocene Coupling of 1,4-MeC≡C(Me₂Si)C₆H₄(SiMe₂)C≡CMe. *J. Am. Chem.*

Soc. **1995**, *117*, 5365–5366.

- (13) Zhang, Z.; Qin, Y. Structurally Diverse Poly(Thienylene Vinylene)s (PTVs) with Systematically Tunable Properties through Acyclic Diene Metathesis (ADMET) and Postpolymerization Modification. *Macromolecules* **2016**, *49*, 3318–3327.
- (14) Schwartz, E.; Breitenkamp, K.; Fokin, V. V. Synthesis and Postpolymerization Functionalization of Poly(5-Iodo-1,2,3-Triazole)S. *Macromolecules* **2011**, *44*, 4735–4741.
- (15) He, B.; Su, H.; Bai, T.; Wu, Y.; Li, S.; Gao, M.; Hu, R.; Zhao, Z.; Qin, A.; Ling, J.; Tang, B. Z. Spontaneous Amino-Yne Click Polymerization: A Powerful Tool toward Regio- and Stereospecific Poly(β -Aminoacrylate)S. *J. Am. Chem. Soc* **2017**, *139*, 5437–5443.
- (16) Binauld, S.; Damiron, D.; Hamaide, T.; Pascault, J.-P.; Fleury, E.; Drockenmuller, E. Click Chemistry Step Growth Polymerization of Novel α -Azide- ω -Alkyne Monomers. *Chem. Commun.* **2008**, *35*, 4138–4140.
- (17) Li, H.; Wang, J.; Sun, J. Z.; Hu, R.; Qin, A.; Tang, B. Z. Metal-Free Click Polymerization of Propiolates and Azides: Facile Synthesis of Functional Poly(Aroxycarbonyltriazole)s. *Polym. Chem.* **2012**, *3*, 1075–1083.
- (18) Wei, B.; Li, W.; Zhao, Z.; Qin, A.; Hu, R.; Tang, B. Z. Metal-Free Multicomponent Tandem Polymerizations of Alkynes, Amines, and Formaldehyde toward Structure- and Sequence-Controlled Luminescent Polyheterocycles. *J. Am. Chem. Soc* **2017**, *139*, 5075–5084.
- (19) Han, T.; Zhao, Z.; Lam, J. W. Y.; Tang, B. Z. Monomer Stoichiometry Imbalance-Promoted Formation of Multisubstituted Polynaphthalenes by Palladium-Catalyzed Polycouplings of Aryl Iodides and Internal Diynes. *Polym. Chem.* **2018**, *9*, 885–893.
- (20) Liu, Y.; Roose, J.; Lam, J. W. Y.; Tang, B. Z. Multicomponent Polycoupling of Internal Diynes, Aryl Diiodides, and Boronic Acids to Functional Poly(Tetraarylethene)S. *Macromolecules* **2015**, *48*, 8098–8107.
- (21) Jaye, J. A.; Sletten, E. M. Modular and Processable Fluoropolymers Prepared via a Safe, Mild, Iodo–Ene Polymerization. *ACS Cent. Sci.* **2019**, *5*, 982–991.

- (22) Scott, T. F.; Furgal, J. C.; Kloxin, C. J. Expanding the Alternating Propagation-Chain Transfer-Based Polymerization Toolkit: The Iodo-Ene Reaction. *ACS Macro Lett.* **2015**, *4*, 1404–1409.
- (23) Wilson, L. M.; Griffin, A. C. Liquid-Crystalline Fluorocarbon—Hydrocarbon Microblock Polymers. *Macromolecules* **1993**, *26*, 6312–6314.
- (24) Xu, T.; Zhang, L.; Cheng, Z.; Zhu, X. Insight into the Polymerization Mechanism of Photoinduced Step Transfer-Addition & Radical-Termination (START) Polymerizations. *Polym. Chem.* **2017**, *8*, 3910–3920.
- (25) Slodowicz, M.; Barata-Vallejo, S.; Vázquez, A.; Nudelman, N. S.; Postigo, A. Light-Induced Iodoperfluoroalkylation Reactions of Carbon–Carbon Multiple Bonds in Water. *J. Fluor. Chem.* **2012**, *135*, 137–143.
- (26) Wei-Yuan, H.; Long, L.; Yuan-Fa, Z. Studies on Sulfinatodehalogenation: XVI. Sodium Dithionite-Initiated Addition of Perfluoroalkyl Iodides to Terminal Alkynes. *Chinese J. Chem.* **1990**, *8*, 350–354.
- (27) Konno, T.; Chae, J.; Kanda, M.; Nagai, G.; Tamura, K.; Ishihara, T.; Yamanaka, H. Facile Syntheses of Various Per- or Polyfluoroalkylated Internal Acetylene Derivatives. *Tetrahedron* **2003**, *59*, 7571–7580.
- (28) Abou-Ghazaleh, B.; Laurent, P.; Blancou, H.; Commeyras, A. Addition d'iodoperfluoroalcane RFI (C_nF_{2n+1} , $N=4, 6, 8$) Au 2-Méthyl-3-Butyn-2-OL Catalysée Par Le Zinc Dans Différent Solvants. Application à La Synthèse de l'acétylénique à Chaîne Perfluorée. *J. Fluor. Chem.* **1994**, *68*, 21–24.
- (29) Rong, G.; Keese, R. The Addition of Perfluorobutyl Iodide to Carbon-Carbon Multiple Bonds and the Preparation of Perfluorobutylalkenes. *Tetrahedron Lett.* **1990**, *31*, 5615–5616.
- (30) Other fluorous monomers were tested. When diiodoperfluorobutane was used as a monomer only trace polymer was isolated. Conversely, diiodoperfluorooctane could be polymerized with decadiyne to give polymer in 93% yield.
- (31) De Pasquale, R. J.; Padgett, C. D.; Rosser, R. W. Highly Fluorinated Acetylenes. Preparation

and Some Cyclization Reactions. *J. Org. Chem.* **1975**, *40*, 810–811.

- (32) Pangborn, A. B.; Giardello, M. A.; Grubbs, R. H.; Rosen, R. K.; Timmers, F. J. Safe and Convenient Procedure for Solvent Purification. *Organometallics* **1996**, *15* (5), 1518–1520.
- (33) Xu, T.; Cheung, C. W.; Hu, X. Iron-Catalyzed 1,2-Addition of Perfluoroalkyl Iodides to Alkynes and Alkenes. *Angew. Chemie Int. Ed.* **2014**, *53* (19), 4910–4914.

CHAPTER FOUR

Vinylogous amidine-containing fluorinated iodo-yne polymers

Adapted from Joseph A. Jaye, Joseph A. Garcia, and Ellen M. Sletten.* Vinylogous amidine-containing fluorinated iodo-yne polymers. *In preparation*.

4.1 Abstract

Fluorination of polymer backbones and sidechains is a key route towards altering thermal, physical, and self-assembly properties of the polymer. Herein, we present a novel post-polymerization modification of a fluorinated vinyl iodide polymer scaffold. Through mild reaction conditions, linear primary amines are appended to the polymer backbone in the form of the vinylogous amidine functionality. Alkyl, aromatic, ether, and fluorous chains were successfully added and analysed for change in polymer stability, thermal transitions, and wettability.

4.2 Introduction

The introduction of fluorine into a polymer scaffold is a well reported method to alter the physical and chemical properties of the polymer.¹ There are two main types of fluorinated polymers, those with fluorine on the backbone and those with fluorinated side chains. Although there are many routes towards the latter²⁻⁵, the former is heavily reliant on fluorinated olefin derivatives.⁶⁻⁹ While fluorinated olefins are produced on the industrial scale for the synthesis of commercial fluoropolymers such as poly(tetrafluoroethylene) (PTFE, Teflon) or poly(vinylidene fluoride) (PVDF), their safety concerns largely prohibit their use in an academic setting.¹⁰⁻¹² Furthermore, the polymerization of these fluorous olefins is dependent on the use of fluorous surfactants, which have received increasing scrutiny due to their toxicity and bioaccumulation.¹³⁻¹⁵

In the pursuit of new routes towards fluorinated polymers, there has been a rise in the use of telechelic fluorinated monomers to give step-growth polymers. While fluorous diols and perfluoropolyether (PFPE) derivatives have been implemented¹⁶⁻¹⁹, our group, as well as others, have

demonstrated the utility of diiodoperfluoroalkanes (DIPFAs) as a monomer towards iodo-ene or iodo-yne polymers (Figure 4.1A).^{20–25} Many initiator and diene combinations have been utilized towards iodo-ene polymers, but we recently developed the first method towards the polymerization of diynes and DIPFAs, named the iodo-yne polymerization.²¹ Although having a similar polymer architecture as the iodo-ene polymer, the iodo-yne polymer has a vinyl iodide functionality incorporated into the backbone, in place of the alkyl iodide observed with iodo-ene polymerization.

We found that through use of excess diyne monomer, alkyne end-groups could be placed at both termini of the polymer chain. This development allows for click modification of the end-groups as a means towards fluorinated triblock copolymers.^{18,26–28} The fluorinated block offers the advantage of increased hydrophobicity and rigidity for self-assembly, while retaining the orthogonal vinyl iodide motifs for modification. Previously, we have experimented with an array of transition-metal catalyzed post-polymerization modifications that were successful in appending aromatic, alkene, and alkyne functionalities to the polymer backbone (Figure 4.1B, left).

Aiming towards the use of the iodo-yne block for biological applications, it is desirable to find new modification techniques that avoid the use of toxic transition metals, such as copper or palladium, while retaining the high modification conversions that they provide. We became interested in the metal-free addition of amines to fluorinated vinyl iodides giving the vinylogous amidine functionality (Figure

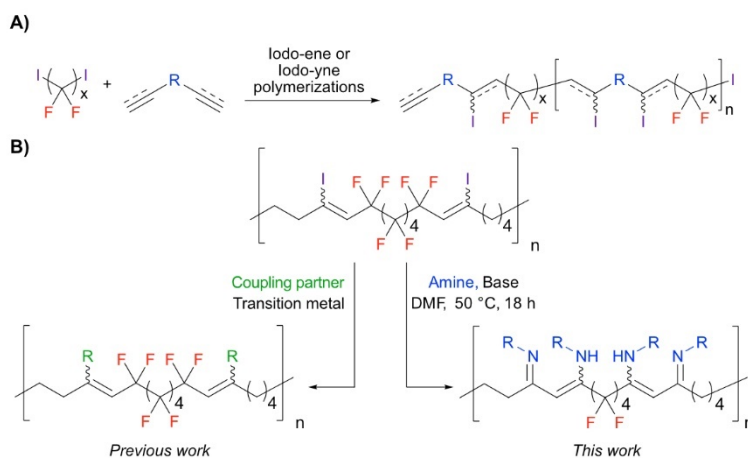


Figure 4.1: Synthesis and modification of iodo-yne polymers. **A)** Synthesis of iodo-ene or iodo-yne polymers from diiodoperfluoroalkanes and dienes or diynes. **B)** Post-polymerization modification of iodo-yne polymers via transition-metal catalyzed couplings (left) and through the metal-free reaction of amines with fluorinated vinyl iodides (right).

4.1B, right). This transformation has been observed by the Liu group, with both the addition of aromatic amines at high temperatures and the utilization of difunctional amines to provide cyclic vinylogous amidines.^{29,30} Notably, this transformation is unique to the fluorous vinyl iodide motif as it is reliant on the activation provided by the fluoroalkyl chain, in contrast to standard transition-metal catalyzed cross couplings of vinyl halides. We looked to further develop this method towards the addition of linear primary amines to fluorinated vinyl iodides as it provides an efficient and simple route towards a functionality that hasn't previously been observed in a polymer, the vinylogous amidine.

4.3 Results and discussion

We began our optimization on vinyl iodide containing small molecule **4.1** (Scheme 4.1A). We tested the optimized conditions developed by Liu and coworkers for the addition of linear primary amines towards acyclic amidine products, but lowered conversions were observed (Table 4.1). It is believed that the perfluoroalkyl group plays an important role in activating the vinyl iodide towards either an elimination/addition or addition/elimination pathway. We hypothesized a stronger base, in addition to the primary amine, would improve conversions. Through a brief condition screen (Table 4.1), we found that excess amine in the presence of either tetramethylguanidine or cesium carbonate gave 90%+ conversion to vinylogous amidine compounds **4.2a** (Scheme 4.1), with an ene-yne byproduct being observed as a competing pathway (Table 4.1).

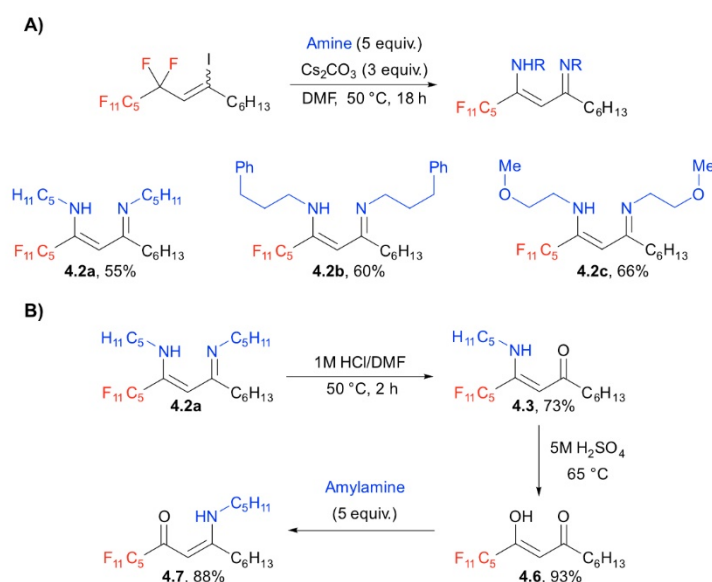
Scheme 4.1: Optimization of vinylogous amidine forming conditions



Table 4.1: Optimization of vinylogous amidine forming conditions

Entry	Amylamine (equiv.)	Base (equiv.)	Solvent	Temp (°C)	4.1 ^a (%)	4.2a ^a (%)	4.3 ^a (%)	4.4 ^a (%)	4.5 ^a (%)
1	8.0	none	Ethanol	reflux	45	51	0	3	1
2	6.0	none	Dioxane	60	93	7	0	0	0
3	6.0	DIPEA ^b (3.0)	Dioxane	60	95	5	0	0	0
4	3.0	DIPEA (6.0)	DMF	100	0	84	12	4	0
5	2.1	TEA ^c (4.0)	DMF	100	51	28	11	5	5
6	2.5	TMG ^d (3.0)	DMF	50	0	88	4	7	0
7	5.0	None	DMF	50	19	79	0	2	0
8	4.0	Cs ₂ CO ₃ (2.0)	DMF	50	12	85	0	3	0
9	6.0	Cs ₂ CO ₃ (2.5)	DMF	50	0	82	0	18	0
10	6.0	NaHCO ₃ (2.5)	DMF	50	18	80	0	2	0
11	2.0	TMG (4.0)	DMF	50	7	61	0	32	0
12	3.0	TMG (3.0)	DMF	50	0	87	0	12	1
13	4.0	TMG (2.0)	DMF	50	0	92	0	8	0
14	5.0	TMG (2.0)	DMF	50	0	93	0	7	0
15	5.0	TMG (2.0)	THF	50	27	59	0	3	11
16	5.0	TMG (1.0)	DMF	50	18	78	0	4	0
17	5.0	Cs ₂ CO ₃ (3.0)	DMF	50	0	91	0	9	0

a. Conversions determined by the integration of peaks in the gas chromatography trace. **b.** Diisopropylethylamine. **c.** Triethylamine. **d.** Tetramethylguanidine.



Scheme 4.2: Synthesis and hydrolysis of vinylogous amidines. **A)** The synthesis of small molecule fluorinated vinylogous amidines **4.2a-c** from a fluorinated vinyl iodide **4.1**. **B)** Stepwise hydrolysis of vinylogous amidine **4.2a** and the addition of amyamine to vinylogous acid **4.6**.

Importantly, this method was optimized to a mild temperature of 50 °C with no exclusion of water or air. We found that through our optimized conditions, model compounds containing alkyl (**4.2a**), phenyl (**4.2b**), or ether (**4.2c**) groups could all be prepared in good yields (Scheme 4.2A). It should be noted that this vinylogous amidine functionality was unstable to purification by either silica or alumina column chromatography conditions. Nevertheless, all compounds could be isolated with sufficient purity through extraction, demonstrating the high conversion of the optimized conditions. Furthermore, there is less concern for solid-phase stability on the desired polymers as they can be purified via precipitation. Due to its low stability on solid phase, we explored the hydrolysis of vinylogous amidine **4.2a** in aqueous media (Scheme 4.2B). In a mixture of 1M HCl and DMF, **4.2a** can be selectively hydrolyzed to vinylogous amide product **4.3**. This vinylogous amide could in turn be further hydrolyzed to vinylogous acid **4.6** through vigorous stirring in 5M H₂SO₄. We found that resubjecting **4.6** to excess amine gave quantitative conversion to the regioisomer of **4.3**, vinylogous amide **4.7**. The lability of the amidine functionality to acidic conditions, and the ability for re-addition of the amine functionality could have potential uses as a vitrimer scaffold. Vinylogous amides, urethanes, and esters are all common vitrimer components³¹⁻³⁴, but the vinylogous amidine functionality is notably missing.

With the small molecule reaction conditions optimized, we moved to begin modification of alkyne terminated polymer **4.8** (Figure 4.2). To our delight, the addition of octylamine to polymer **4.8** proceeded readily giving polymer **4.9** in excellent agreement with small molecule analog **4.2a** (Figure 4.3A) through analysis of nuclear magnetic resonance (NMR) and infrared spectroscopy (IR) spectra (Figure 4.3B, Figure 4.3C). We found that incomplete conversion gave low amounts of enamine functionality on the

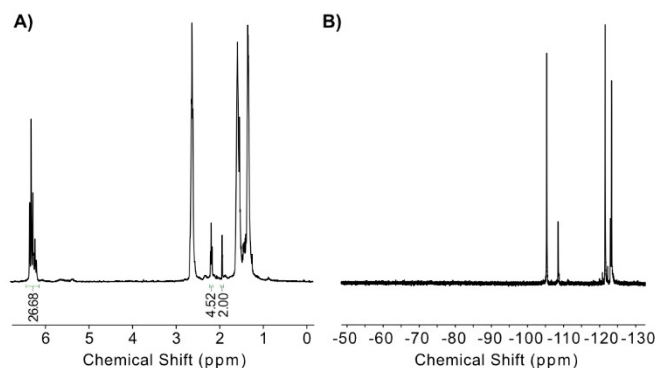


Figure 4.2: Nuclear magnetic resonance analysis (NMR) of alkyne terminated polymer **4.8**. **A)** ^1H -NMR of polymer **4.8** demonstrating a degree of polymerization of ~ 13 . **B)** ^{19}F -NMR demonstrating successful end-group capping due to missing CF_2I signal at -59 ppm.

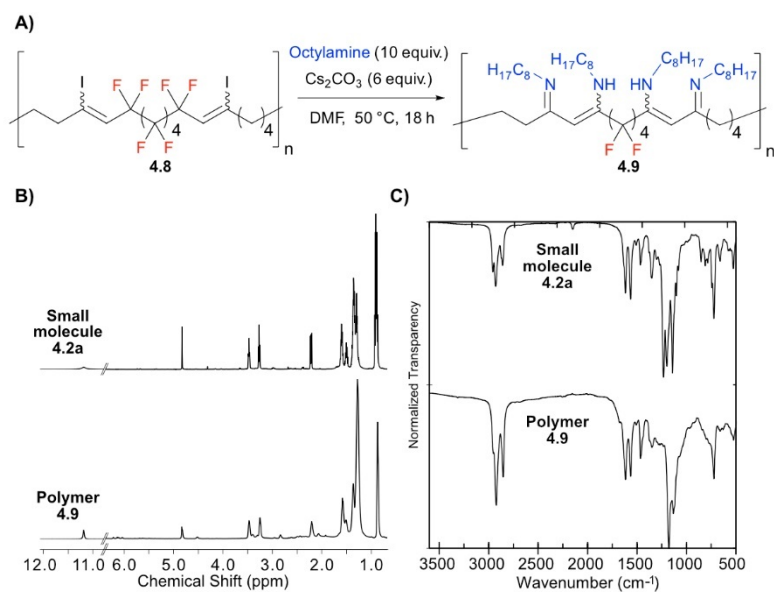


Figure 4.3: Optimized vinylogous amidine forming conditions on polymer **4.8**. **A)** Reaction scheme of the synthesis of polymer **4.9**. **B)** Stacked ^1H NMR spectra comparing small molecule model **4.2a** with desired polymer **4.9**. **C)** Stacked IR spectra comparing small molecule model **4.2a** with desired polymer **4.9**.

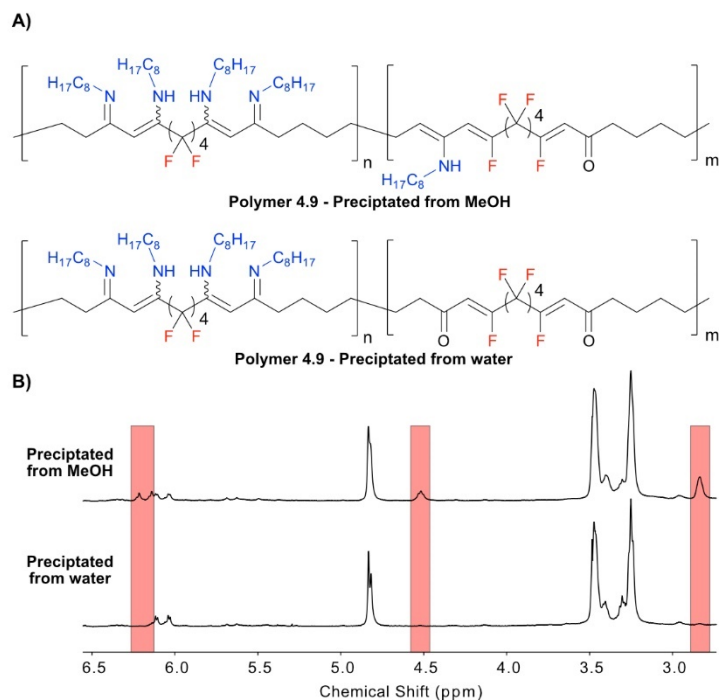


Figure 4.4: Polymer backbone impurities that are dependent on precipitation conditions. **A)** Structures of polymers when precipitated from MeOH (top) or water (bottom) demonstrating the presence of an enamine functionality or conjugated vinyl fluoride, respectively. **B)** $^1\text{H-NMR}$ demonstrating the loss of enamine peaks (highlighted in red) when polymer **4.9** is precipitated from water in place of MeOH.

backbone, which could be hydrolyzed to the respective ketone upon precipitation from water in place of methanol (Figure 4.4).

Gratifyingly, we found that polymer **4.10** could also be synthesized readily through the reaction of vinyl iodide containing polymer **4.8** with 3-phenyl-1-propyl amine (Figure 4.5, blue polymer). As with alkyl containing polymer **4.9**, NMR analysis indicated phenyl containing polymer **4.10** was in good agreement with its small molecule model (**4.2b**) (Figure 4.6A). Following the addition of both alkyl and phenyl groups, the addition of the more polar 2-methoxyethyl amine was attempted on polymer **4.8**. Although giving close resemblance to small molecule analog **4.2c**, there was a significant unknown peak from 3.10-3.35 ppm observed through $^1\text{H NMR}$ analysis (Figure 4.6B). Hypothesizing that the proximity of the electron withdrawing methoxy group was the cause for polymer degradation, we increased the number of methylene spacers from 2 to 3. We found the change to 3-methoxypropyl amine gave good conversion to polymer **4.11** (Figure 4.5A, green polymer) with no observable degradation peaks.

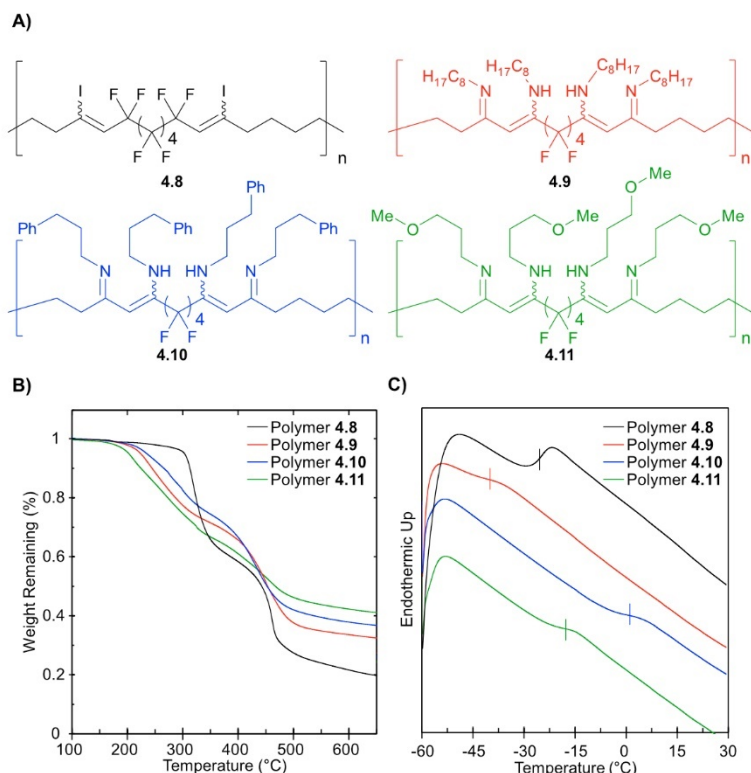


Figure 4.5: Scope of polymer derivatives and thermal properties. **A)** Structures of polymers synthesized through the optimized vinylogous amidine forming conditions. **B)** Stacked TGA traces of polymers **4.8-11** demonstrating thermal stability. **C)** Stacked DSC traces of polymers **4.8-11** demonstrating glass transition temperatures under room temperature.

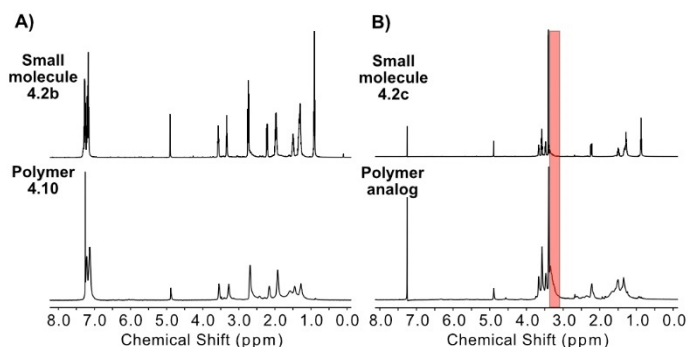


Figure 4.6: ¹H-NMR analysis of small molecule analogs and polymers **A)** Stacked ¹H-NMR analysis of phenyl containing small molecule **4.2b** and polymer **4.10**. **B)** Stacked ¹H-NMR analysis of ether containing polymer **4.2c** and its polymeric analog. Polymer impurity not observed in the small molecule model highlighted in red.

To determine if degradation of the polymer backbone was occurring, the end-group protons of the polymer **4.8** and **4.9** terminal alkynes were integrated and compared to the vinyl proton integrations (Figure 4.2, 4.7A). Similar end-group values were calculated for the starting and modified polymers (Figure 4.7B, 4.7C). Size exclusion chromatography (SEC) was also performed. In all cases, SEC indicated a decrease in polymer size, but dispersity remained consistent across modified polymers (Figure

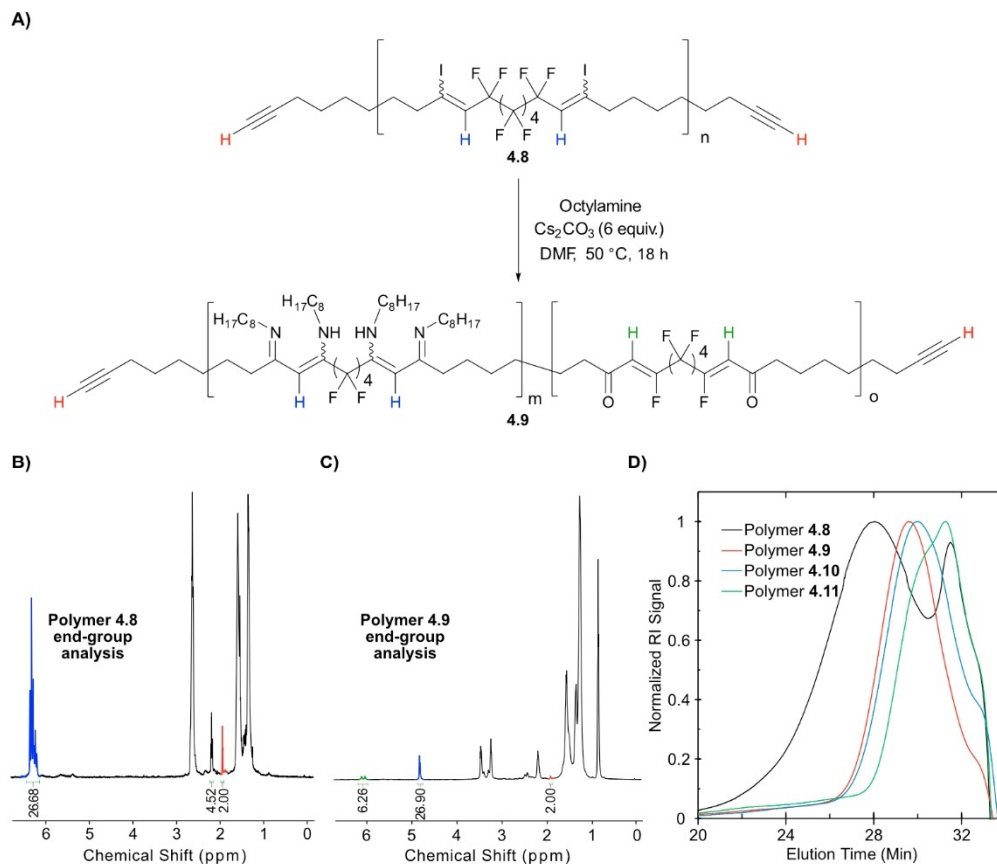


Figure 4.7: Molecular weight determination of vinylogous amidine containing polymers. **A)** Reaction scheme of the vinylogous amidine forming reaction. Terminal alkyne hydrogens highlighted in red and vinyl protons integrated for end-group analysis highlighted in blue and green. **B)** End-group analysis of polymer **4.8**. **C)** End-group analysis of polymer **4.9** demonstrating a consistent repeat unit when compared to polymer **4.8**. **D)** SEC traces of polymers **4.8-11**. Lower molecular weights observed by integration of RI signal in polymers **4.9-11** when compared to polymer **4.8**.

4.7D) The end-group analysis suggests a lack of polymer scission, while change in hydrodynamic radius could be the cause for lowered molecular weight values as measured by SEC.

Looking to further probe the stability of vinylogous amidine containing polymers, thermal gravimetric analysis (TGA) was performed on all polymer derivatives (Figure 4.5B). We found significantly lower degradation temperature for polymers **4.9-4.11** when compared to the parent polymer **4.8**, with 10% mass degradation occurring between 220 °C and 260 °C (See table 4.2 for thermal properties of all polymers). Static TGA demonstrated a slow, but consistent loss of mass at the degradation onset temperature of 120 °C (Figure 4.8). We also observed low levels of polymer degradation occurring under prolonged storage of polymers **4.9-4.11** at 0 °C for 1 week (Figure 4.9). We

Table 4.2: Summary of polymer properties.

Polymer	M_n (kDa, SEC)	M_n (kDa, NMR)	\bar{D} (SEC)	T_d ($^{\circ}\text{C}$, 10% mass loss)	T_g ($^{\circ}\text{C}$)
6	5.85	8.8	1.87	312	-26
7	2.47	12.5	1.39	244	-41
8	1.97	N/A	1.43	264	1
9	1.67	N/A	1.31	224	-20
11	N/A	N/A	N/A	250	-6

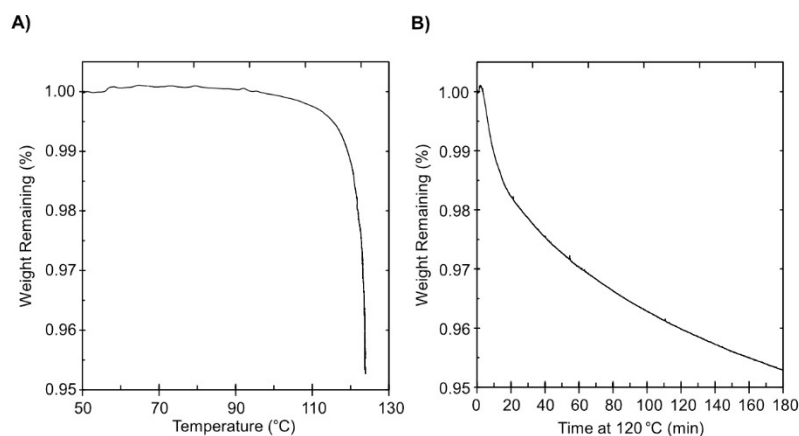


Figure 4.8: Static thermal gravimetric analysis (TGA) of polymer **4.9** with a temperature set at 120 $^{\circ}\text{C}$. **A)** TGA trace of polymer **4.9** with sample weight remaining (%) plotted against temperature. **B)** TGA trace of polymer **4.9** with sample weight remaining (%) plotted against time.

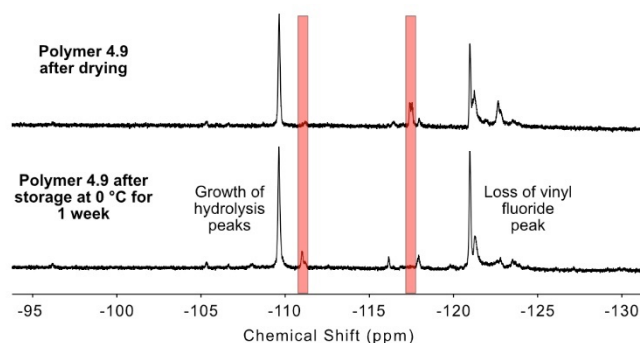


Figure 4.9: Stability of polymer **7** while stored at 0 $^{\circ}\text{C}$ as measured by ^{19}F -NMR analysis. ^{19}F -NMR of polymer **4.9** immediately after purification and drying (top) and after being stored at 0 $^{\circ}\text{C}$ for 1 week. Loss of the vinyl fluoride peaks and growth of hydrolysis peaks highlighted in red.

then probed the effect of the vinylogous amidine functionality on the thermal transitions of the polymer, via differential scanning calorimetry (DSC) (Figure 4.5C). We found that vinylogous amidine polymers **4.9-4.11** all have a glass transition (T_g) temperature under room temperature, although the T_g was increased from parent polymer **4.8** with the addition of amines containing a phenyl or ether group (Polymers **4.10** and **4.11**, Figure 4.5C, blue and green traces, respectively). Alternatively, the addition of the long octyl chain in polymer **4.9** decreased the T_g (Figure 4.5C, red trace).

With the intent of the polymers to be implemented for biological purposes, we probed the aqueous stability of the vinylogous amidine functionality. We chose phenyl containing polymer **4.10** for stability experiments, as it had the highest thermal stability of the derivatives synthesized. Furthermore, the aromatic scaffold provides potential stabilization and solubilization factors for cargo containing aromatic rings such as dyes or pharmaceutical compounds. We assayed the stability of polymer **4.10** to a 1:1 solution of DMF/PBS buffer over 1 week, at both pH 7.4 and 5.6 (Figure 4.10). Although hydrolysis occurred in both solutions, we found higher rates of hydrolysis in the pH 5.6 PBS buffer as compared to pH 7.4 buffer. When the same polymer was stirred in a DMF/1M HCl solution, complete hydrolysis was observed in 24 hours (Figure 4.11). Notably, in contrast to the small molecule analog, 1M HCl generated a mixture of vinylogous amide regioisomers as well as further hydrolysis to the vinylogous acid.

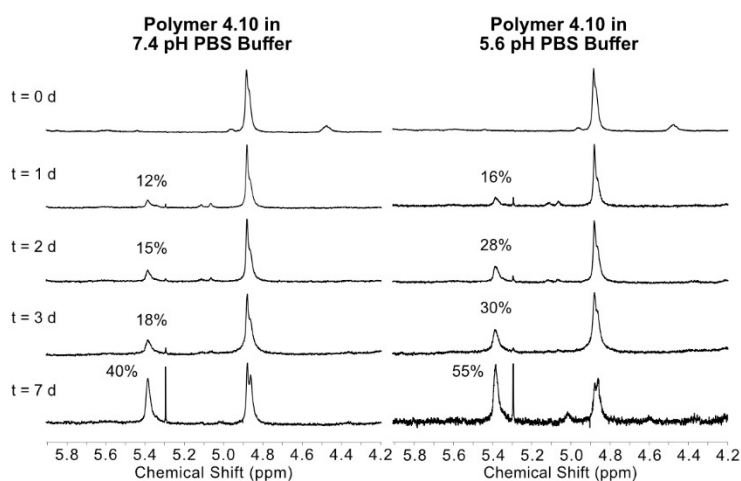


Figure 4.10: Stability of phenyl containing polymer **4.10** to PBS buffer at pH 7.4 (left) and pH 5.6 (right) over a 7-day period.

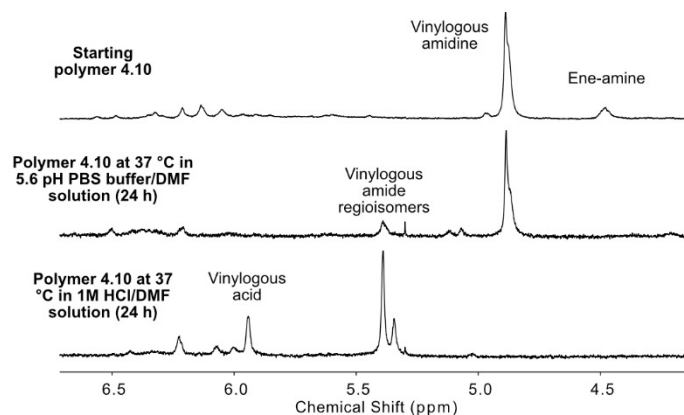


Figure 4.11: Hydrolysis of polymer **4.10** over 24 hours in aqueous DMF at different acidities at 37 °C, as measured by ^1H -NMR analysis (Starting polymer **4.10** (top trace), polymer **4.10** in a 5.6 pH PBS buffer/DMF solution (middle trace), and polymer **4.10** in a 1M HCl/DMF solution (bottom trace)).

With the post-polymerization modification established, we became intrigued at the possibility of increasing the fluorine content of the vinylogous amidine functionality. Increased weight percent fluorine could provide the means as a route towards hydrophilic-fluorophilic copolymers. Increased fluorination of polymer side chains have been studied to tune self-assembly, vehicle stability, and cargo delivery for amphiphilic copolymers.^{16,35–37} For example, block copolymers produced from the living polymerizations of fluorinated acrylate^{2,3}, oxazoline^{38–41}, and lactide⁴² monomers have all been demonstrated to self-assemble. There are other benefits of increased side chain fluorination as well. One such benefit is improved fluorinated solvent solubility, an important factor in the delivery of fluorinated payloads.⁴³ Increased fluorination of side chains also leads to increased repulsion of water on thin films in the form of increased contact angles, providing the polymer's degree of hydrophobicity.^{44–46} We found that fluorinated chains could easily be appended on to the polymer backbone through the optimized vinylogous amidine forming conditions of polymer **4.8** with fluorinated amine **4.12** to give a dually fluorinated polymer **4.13** (Figure 4.12A). Fluorinated vinylogous amidine polymer **4.13** retained similar thermal properties as the vinylogous amidine containing polymers **4.9–4.11** (Figure 4.13).

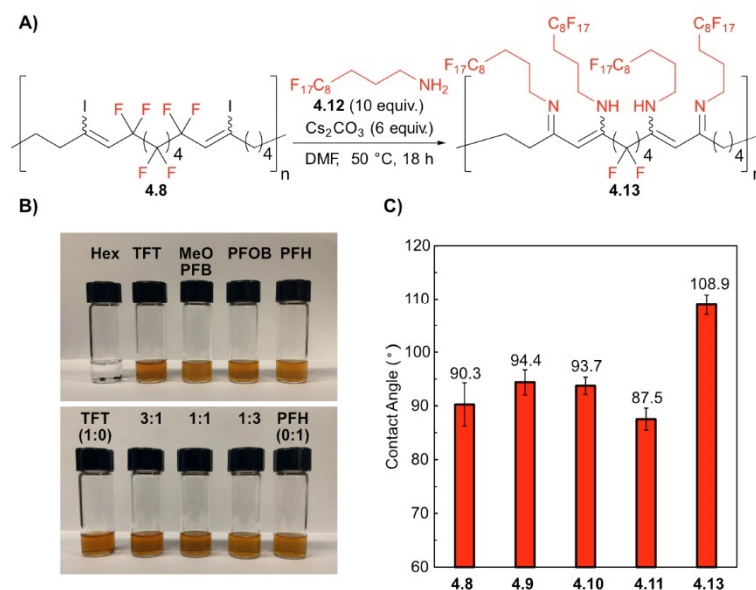


Figure 4.12: Synthesis of fluorinated vinylogous amidine containing polymer. **A)** Reaction scheme of the synthesis of fluorinated polymer **4.13**. **B)** Dissolution of polymer **4.13** in various fluorinated solvents and hexanes (top). Dissolution of polymer **4.13** in mixtures of trifluorotoluene (TFT) and perfluorohexanes (PFH) (bottom). **C)** Contact angles of water on polymers **4.8–11** and **4.13**.

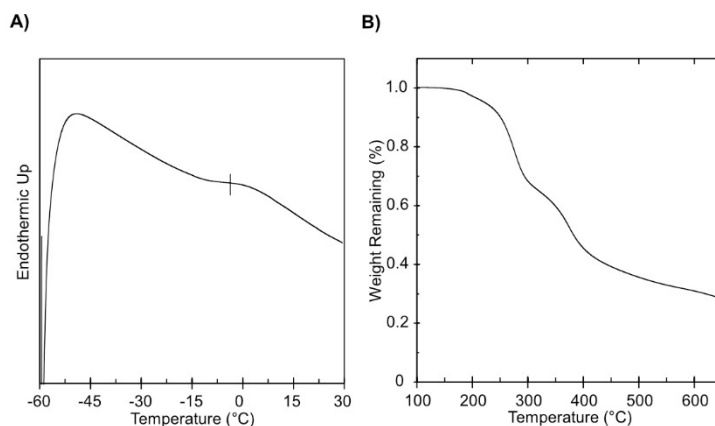


Figure 4.13: Thermal properties of fluorinated polymer **4.13**. **A)** Differential scanning calorimetry (DSC) trace of polymer **4.13**. **B)** TGA trace of polymer **4.13**. See table 4.2 for thermal properties of all polymers.

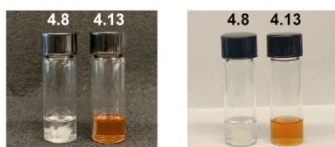


Figure 4.14: Solubility of polymer **4.8** and polymer **4.13** in 20 mg/mL solution of hexafluorobenzene. Vials with a black background (left) and white background (right) demonstrating full solubility of polymer **4.13** in hexafluorobenzene, with only minor swelling of polymer **4.8**.

Furthermore, polymer **4.13** was soluble at 20 mg/mL in hexafluorobenzene, while starting vinyl iodide polymer **4.8** slightly swelled (Figure 4.14). This comparison serves to demonstrate how increasing fluorine content through side chains improves fluorine character. This finding encouraged an analysis of solubility in other fluorine solvents. Fluoropolymer **4.13** retained solubility in trifluorotoluene (TFT) and perfluorooctyl bromide (PFOB). Decreased solubility was observed in methyl perfluorobutyl ether (MeOPFB), or perfluorohexanes (PFH) (Figure 4.12B, top). The solubility of polymer **4.13** in perfluorohexanes could be increased through mixtures with trifluorotoluene (Figure 4.12B, bottom). Complete solubility was observed in up to a 3:1 mixture of perfluorohexanes and trifluorotoluene. The fluorine solubility of polymer **4.13** prompted an investigation into the contact angles of vinylidene containing polymers (Figure 4.12C). Although there was little change in the contact angle of water against polymers **4.9-4.11** in comparison to starting vinyl iodide polymer **4.8**, increased water repulsion on dually fluorine polymer **4.13** was observed, with an increase from 90 ° to 109 °. Combined, the improved fluorine solubility and increased contact angle of water on thin films suggest this polymer scaffold could be applied towards block copolymer self-assembly and fluorine payload delivery.

4.4 Conclusion

In conclusion, we have developed a novel and facile post-polymerization modification of fluorinated iodo-yne polymers. Requiring only mild conditions, we have prepared the first known vinylogous amidine containing polymer. Although having low thermal and aqueous stability, this new polymer scaffold allows the placement of various functionalities across a fluorinated backbone, with four different amines being appended per repeating unit. We have also demonstrated that the addition of fluorous amines on the polymer greatly increases fluorous solubility and water repulsion. Furthermore, this scaffold is primed towards the synthesis of block copolymers with alkynes located on both termini. We believe addition of hydrophilic blocks will allow for polymer self-assembly, providing a delivery agent for both organic and fluorous payloads. With this development being a first step towards an unexplored functionality in polymer chemistry, further work must be done to expand substrate scope and improve polymer stability.

4.5 Experimental procedures

4.5.1 General experimental procedures:

Chemical reagents were purchased from Sigma-Aldrich, Alfa Aesar, Fisher Scientific, or Acros Organics and used without purification unless noted otherwise. No unexpected or unusually high safety hazards were encountered. Anhydrous and deoxygenated solvents toluene (PhMe), tetrahydrofuran (THF), dichloromethane (DCM), acetonitrile (MeCN), and dimethylformamide (DMF) were dispensed from a Grubb's-type Phoenix Solvent Drying System.⁴⁷ Thin layer chromatography was performed using Silica Gel 60 F254 (EMD Millipore) plates. Flash chromatography was executed with technical grade silica gel with 60 Å pores and 40–63 µm mesh particle size (Sorbtech Technologies). Solvent was removed under reduced pressure with a Büchi Rotovapor with a Welch self-cleaning dry vacuum pump and further dried with a Welch DuoSeal pump. Nuclear magnetic resonance (¹H-NMR, ¹³C-NMR, and ¹⁹F-NMR) spectra were taken on Bruker Avance 500 (¹H-NMR and ¹³C-NMR) or AV-400 (¹⁹F-NMR) instruments and

processed with MestReNova software. All ^1H , ^{13}C , and ^{19}F NMR spectra are reported in ppm and relative to residual solvent signals (^1H , ^{13}C). ^{19}F NMR were reported with trifluoroacetic acid as the reference peak at -76.0 ppm as an external standard. High resolution mass spectra were collected on an Agilent 7890B-7520 Quadrupole Time-of-Flight GC-MS (Electron Impact (EI)) or via DART-MS spectra collected on a Thermo Exactive Plus MSD (Thermo Scientific) equipped with an ID-CUBE ion source and a Vapor Interface (IonSense Inc.) (Atmospheric pressure chemical ionization (APCI)). Low resolution mass spectra (Electron impact) were collected on an Agilent 6890N-5975 Quadrupole GC-MS. Photochemical reactions were performed in a photochemical reactor with a Hanovia 450 W medium pressure mercury vapor UV lamp. Size exclusion chromatography (SEC), unless otherwise noted, was conducted on a Shimadzu prominence-I LC-2030C high performance liquid chromatography (HPLC) system with a UV detector and connected to a Wyatt Dawn Heleos-II light scattering detector and Wyatt Optilab T-rEX refractive index detector, one MZ Analysentechnik GPC-Precolumn 50 x 8.0 mm MZ-Gel SDplus Linear LS 5 μm pore, and two MZ Analysentechnik GPC-column 300 x 8.0 mm MZ-Gel SDplus Linear LS 5 μm pore. Eluent was THF at 50 °C (flow rate: 0.70 mL/ min). Calibration was performed using near monodisperse polystyrene PS standards from Polymer Laboratories. Differential scanning calorimetry measurements were taken on a PerkinElmer DSC. Thermal gravimetric analysis was performed on a PerkinElmer Pyris Diamond TG/DTA Thermogravimetric/Differential Thermal Analyzer.

Abbreviations: AIBN = azoisobutyronitrile; DBU = 1,8-Diazabicyclo[5.4.0]undec-7-ene; DCM = dichloromethane; DMF = dimethylformamide; DMSO = dimethylsulfoxide; DSC = differential scanning calorimetry; Et₂O = diethyl ether; MeCN = acetonitrile ; MeOH = methanol; PhMe = toluene; SEC = size exclusion chromatography; TGA = thermal gravimetric analysis; THF = tetrahydrofuran; TMG = tetramethylguanidine

SEC prep/procedures: Size exclusion chromatography (SEC) was conducted on a Shimadzu prominence-I LC-2030C high performance liquid chromatography (HPLC) system with a UV detector and connected to a Wyatt Dawn Heleos-II light scattering detector and Wyatt Optilab T-rEX refractive

index detector. Calibration was performed using near monodisperse polystyrene standards from Polymer Laboratories. Polymer samples were dissolved in THF (5 mg/mL) and stirred at room temperature for 1 hour. Polymer solutions were filtered through 0.2 micron PTFE filter and 100 μ L were then run through one MZ Analysentechnik GPC-Precolumn 50 x 8.0 mm MZ-Gel SDplus Linear LS 5 μ m pore, and two MZ Analysentechnik GPC-column 300 x 8.0 mm MZ-Gel SDplus Linear LS 5 μ m pore columns at 50 °C with an eluent rate of 0.7mL/min. Unless otherwise noted, dRI signal was used for molecular weight determination.

TGA prep/procedures: Polymer samples (10 mg) were placed in a calibrated ceramic container and the temperature was raised to 50 °C. After a delay of 1 minute to remove residual solvent, the weight of the sample was re-recorded, and the temperature was raised to 650 °C at a rate of 10 °C/min. The resulting data were then normalized to % weight loss of sample. Unless otherwise noted all samples were run under nitrogen atmosphere.

DSC prep/procedures: Polymer sample (10–20 mg) were placed in an aluminum pan and cooled to -60 °C and equilibrated for 2 minutes. The samples were then heated to 30 °C at a rate of 20 °C/min with a 2-minute pause at 30 °C. Samples were then cooled back down to -60 °C at a rate of 15 °C/min with a 2-minute pause at -60 °C. This cycle was then repeated two additional times.

Thin film preparation: Polymer (10 mg) was dissolved in solvent (1mL THF or hexafluorobenzene). The polymer solution (0.3 mL) was then dropped onto a glass slide to completely coat the surface and then spun at 1100 RPM for 30 seconds. The resulting films were further dried under a stream of N₂.

Contact angle measurements: Thin films were prepared in the same manner as previously described. Contact angles were measured with a slowly dispensed drop of water at a height where the drop immediately contacts film. Contact angles were measured with a 5 second delay from initial contact of water with the polymer surface. The reported values are the average of 3 films, with 4 droplets being measured on each, for a total of 12 droplets per polymer.

Figure procedures:

Buffer stability: Polymer **4.10** (10 mg) was dissolved in DMF (1 mL), at which point PBS buffer at pH 7.4 or 5.6 (1 mL) was then added. The following suspension was stirred at 37 °C between 1 and 7 days and then washed with water (4 x 2 mL), followed by methanol (4 x 2 mL). The remaining polymer was then dried on high vacuum and analyzed by ¹H-NMR.

Fluorous solubility: Polymer **4.13** (10 mg) was dissolved or dispersed in fluorinated or organic solvent (1 mL). The suspensions were shaken until dissolved (~5 minutes) and then photographed.

4.5.2 Small molecule experimental procedures:

1,1,1,2,2,3,3,4,4,5,5,6,6-tridecafluoro-8-iodotetradec-7-ene (**4.1**) was prepared as previously described.²¹

(6Z)-1,1,1,2,2,3,3,4,4,5,5-undecafluoro-N-pentyl-8-(pentylimino)tetradec-6-en-6-amine (**4.2a**):

Vinyl iodide **4.1** (0.10 g, 0.18 mmol, 1.0 equiv.) was dissolved in DMF (0.5 mL). Amylamine (0.078 g, 0.90 mmol, 5.0 equiv.) was then added, followed by cesium carbonate (0.18 g, 0.54 mmol, 3.0 equiv.). The resulting solution was stirred at 50 °C for 18 hours. The reaction was then quenched with a saturated solution of ammonium chloride (3 mL). The organic layer was then extracted with hexanes (4 x 1 mL) to give the product as an orange oil (0.056 g, 0.10 mmol, 55%). ¹H NMR (500 MHz, Chloroform-*d*) δ 11.18 (bs, 1H), 4.83 (s, 1H), 3.47 (t, *J* = 6.9 Hz, 2H), 3.27 (t, *J* = 7.0 Hz, 2H), 2.42 – 2.04 (m, 2H), 1.67 – 1.56 (m, 4H), 1.55 – 1.46 (m, 2H), 1.41 – 1.21 (m, 14H), 0.99 – 0.65 (m, 9H). ¹³C NMR (126 MHz, Chloroform-*d*) δ 163.87, 148.41 (t, *J* = 20.3 Hz), 120.59 – 106.94 (m, 5C), 90.14 (t, *J* = 7.8 Hz), 48.61, 44.91, 32.99, 31.89, 31.58, 30.44, 29.52, 29.48, 29.22, 28.10, 22.58, 22.55, 22.52, 14.06, 14.00 (2C). ¹⁹F NMR (376 MHz, Chloroform-*d*) δ -80.65 (t, *J* = 9.9 Hz, 3F), -109.54 (t, *J* = 14.3 Hz, 3F), -121.29 (m, 2F), -122.09 (m, 2F), -125.25 (m, 2F). HRMS (EI): *m/z* [M]⁺ calcd for C₂₄H₃₇F₁₁N₂: 562.2781, found: 562.2763. FT-IR: 2933 (C-H str) (s), 1621 (C=N str) Imine (s), 1569 (C=C str) Enamine (s), 1100-1200 (C-F str) (vs).

(6Z)-1,1,1,2,2,3,3,4,4,5,5-undecafluoro-N-(3-phenylpropyl)-8-((3-phenylpropyl)imino)tetradec-6-en-6-amine (**4.2b**):

Vinyl iodide **4.1** (0.10 g, 0.18 mmol, 1.0 equiv.) was dissolved in DMF (0.5 mL). 3-phenyl-1-propylamine (0.120 g, 0.90 mmol, 5.0 equiv.) was then added, followed by cesium carbonate (0.18 g, 0.54 mmol, 3.0 equiv.). The resulting solution was stirred at 50 °C for 18 hours. The reaction was then quenched with a saturated solution of ammonium chloride (3 mL). The organic layer was then extracted with hexanes (4 x 1 mL) to give the product as an orange oil (0.071 g, 0.11 mmol, 60%). ¹H NMR (500 MHz, Chloroform-*d*) δ 11.29 (s, 1H), 7.80 – 6.32 (m, 10H), 4.90 (s, 1H), 3.57 (t, *J* = 6.7 Hz, 2H), 3.33 (t, *J* = 6.9 Hz, 2H), 2.74 (t, *J* = 7.8 Hz, 4H), 2.22 (t, *J* = 8.2 Hz, 2H), 2.08 – 1.90 (m, 4H), 1.55 – 1.45 (m, 2H), 1.39 – 1.25

(m, 6H), 0.91 (t, $J = 7.0$ Hz, 3H). ^{13}C NMR (126 MHz, Chloroform-*d*) δ 164.40, 148.57 (t, $J = 20.3$ Hz), 142.03, 141.44, 128.43, 128.37, 128.35, 128.33, 125.95, 125.76, 90.77 (t, $J = 6.3$ Hz), 48.16, 44.41, 33.82, 33.58, 33.37, 33.08, 32.33, 31.57, 29.20, 28.10, 22.57, 14.03. ^{19}F NMR (376 MHz, Chloroform-*d*) δ -80.64 (t, $J = 9.9$ Hz, 3F), -109.52 (t, $J = 14.2$ Hz, 2F), -121.27 (m, 2F), -122.59 (m, 2F), -125.97 (m, 2F). HRMS (APCI): m/z $[\text{M}+\text{H}]^+$ calcd for $\text{C}_{32}\text{H}_{37}\text{F}_{11}\text{N}_2$: 659.2854, found: 659.2922. FT-IR: 3029 ($\text{C}_{\text{sp}2}\text{-H}$ str) (w) 2929 ($\text{C}_{\text{sp}3}\text{-H}$ str) (s), 1620 (C=N str) Imine (s), 1560 (C=C str) Enamine (s), 1498 (C=C str) Aromatic (s), 1100-1200 (C-F str) (vs).

(6Z)-1,1,1,2,2,3,3,4,4,5,5-undecafluoro-N-(2-methoxyethyl)-8-((2-methoxyethyl)imino)tetradec-6-en-6-amine (**4.2c**):

Vinyl iodide **4.1** (0.10 g, 0.18 mmol, 1.0 equiv.) was dissolved in DMF (0.5 mL). 3-phenyl-1-propylamine (0.120 g, 0.90 mmol, 5.0 equiv.) was then added, followed by cesium carbonate (0.18 g, 0.54 mmol, 3.0 equiv.). The resulting solution was stirred at 50 °C for 18 hours. The reaction was then quenched with a saturated solution of ammonium chloride (3 mL). The organic layer was then extracted with DCM (4 x 1 mL), and washed with perfluorohexanes (3 x 1 mL) to give the product as an orange oil (0.064 g, 0.12 mmol, 65%). ^1H NMR (500 MHz, Chloroform-*d*) δ 11.31 (s, 1H), 4.90 (s, 1H), 3.67 (t, $J = 5.7$ Hz, 2H), 3.62 – 3.56 (m, 4H), 3.48 (t, $J = 5.8$ Hz, 2H), 3.42 – 3.39 (m, 6H), 2.24 (t, $J = 8.3$ Hz, 2H), 1.50 (p, $J = 7.9, 7.4$ Hz, 2H), 1.38 – 1.24 (m, 6H), 0.88 (t, $J = 6.8$ Hz, 3H). ^{13}C NMR (126 MHz, Chloroform-*d*) δ 165.03, 148.63 (t, $J = 21.4$ Hz), 119.38 – 107.85 (m), 91.59 (t, $J = 7.0$ Hz), 73.47, 72.45, 59.05, 58.84, 47.90, 45.17, 33.34, 31.71, 29.35, 28.09, 22.69, 14.16. ^{19}F NMR (376 MHz, Chloroform-*d*) δ -80.58 (t, $J = 10.0$ Hz, 3F), -110.90 (t, $J = 14.3$ Hz, 2F), -121.24 (m, 2F), -122.37 (m, 2F), -125.93 (m, 2F). HRMS (APCI): m/z $[\text{M}+\text{H}]^+$ calcd for $\text{C}_{20}\text{H}_{29}\text{F}_{11}\text{N}_2\text{O}_2$: 539.2126, found: 539.2182. FT-IR: 2927 (C-H str) (s), 1616 (C=N str) Imine (s), 1569 (C=C str) Enamine (s), 1100-1200 (C-F str) (vs).

(Z)-10,10,11,11,12,12,13,13,14,14,14-undecafluoro-9-(pentylamino)tetradec-8-en-7-one (**4.3**):

(6Z)-1,1,1,2,2,3,3,4,4,5,5-undecafluoro-N-pentyl-8-(pentylimino)tetradec-6-en-6-amine (**4.2a**) (0.02 g, 0.039 mmol, 1.0 equiv.) was dissolved in DMF (0.2 mL). A solution of 1M HCl (0.4 mL) was then slowly

added dropwise. The resulting solution was stirred at 50 °C for 2 hours. The organic layer was extracted with hexanes (4 x 1 mL) to give the product as a yellow oil (0.013 g, 0.026 mmol, 73%). ¹H NMR (500 MHz, Chloroform-*d*) δ 10.64 (s, 1H), 5.39 (s, 1H), 3.30 (q, *J* = 6.6 Hz, 2H), 2.38 (t, *J* = 7.8 Hz, 2H), 1.68 – 1.53 (m, 4H), 1.44 – 1.17 (m, 10H), 0.97 – 0.83 (m, 6H). ¹³C NMR (126 MHz, Chloroform-*d*) δ 201.09, 148.51 (t, *J* = 22.9 Hz), 121.31 – 108.08 (m, 5C), 95.07 (t, *J* = 7.8 Hz), 45.14, 43.19, 31.79, 30.38, 29.17, 28.87, 25.62, 22.66, 22.42, 14.18, 14.02. ¹⁹F NMR (376 MHz, Chloroform-*d*) δ -80.93 (m, 3F), -111.24 (m, 2F), -121.60 (m, 2F), -122.76 (m, 2F), -126.31 (m, 2F). HRMS (EI): *m/z* [M]⁺ calcd for C₁₉H₂₆F₁₁NO: 493.1839, found: 493.1826

(*Z*)-10,10,11,11,12,12,13,13,14,14,14-undecafluoro-9-hydroxytetradec-8-en-7-one (**4.6**):

(*Z*)-10,10,11,11,12,12,13,13,14,14,14-undecafluoro-9-(pentylamino)tetradec-8-en-7-one (**4.3**) (.028 g, 0.057 mmol, 1.0 equiv.) was dispersed in a solution of 5M H₂SO₄ and vigorously stirred at 65 °C for 18 hours. The organic layer was extracted with hexanes (4 x 1 mL) to give the product as a yellow oil (0.022 g, 0.053 mmol, 93%). ¹H NMR (500 MHz, Chloroform-*d*) δ 14.60 (s, 1H), 5.96 (s, 1H), 2.44 (t, *J* = 7.6 Hz, 2H), 1.66 (p, *J* = 7.5 Hz, 2H), 1.47 – 1.27 (m, 6H), 0.89 (t, *J* = 6.6 Hz, 3H). ¹³C NMR (126 MHz, Chloroform-*d*) δ 196.88, 177.89 (t, *J* = 26.4 Hz), 119.86 – 104.32 (m, 5C), 97.35 (t, *J* = 3.2 Hz), 38.37, 31.54, 28.87, 25.71, 22.57, 14.11. ¹⁹F NMR (376 MHz, Chloroform-*d*) δ -80.64 (t, *J* = 9.8 Hz, 3F), -120.80 (t, *J* = 13.1 Hz, 2F), -122.34 (m, 2F), -122.53 (m, 2F), -126.04 (m, 2F). HRMS (EI): *m/z* [M]⁺ calcd for C₁₄H₁₅F₁₁O₂: 424.0896, found: 424.0881

(*Z*)-1,1,1,2,2,3,3,4,4,5,5-undecafluoro-8-(pentylamino)tetradec-7-en-6-one (**4.7**):

(*Z*)-10,10,11,11,12,12,13,13,14,14,14-undecafluoro-9-hydroxytetradec-8-en-7-one (**4.6**) (0.013 g, 0.031 mmol, 1.0 equiv.) and amylamine (0.013 g, 0.153 mmol, 5.0 equiv.) were stirred at 70 °C for 2 hours. The solution was then placed under high vacuum to remove remaining amine and water to give the product as an orange oil (0.014 g, 0.027 mmol, 88%). ¹H NMR (500 MHz, Chloroform-*d*) δ 11.31 (s, 1H), 5.35 (s, 1H), 3.34 (q, *J* = 6.8 Hz, 2H), 2.31 (t, *J* = 8.0 Hz, 2H), 1.66 (p, *J* = 7.2 Hz, 2H), 1.57 (p, *J* = 7.6 Hz, 2H), 1.43 – 1.27 (m, 10H), 0.97 – 0.87 (m, 6H). ¹³C NMR (126 MHz, Chloroform-*d*) δ 176.06 (t, *J* = 23.6 Hz),

173.09, 123.85 – 105.19 (m, 5C), 90.08, 43.67, 32.45, 31.55, 29.50, 29.17, 29.01, 27.73, 22.60, 22.42, 14.10, 13.99. ^{19}F NMR (376 MHz, Chloroform-*d*) δ -80.65 (t, J = 9.4 Hz, 3F), -119.71 (t, J = 12.7 Hz, 2F), -122.49 (m, 4F), -126.03 (m, 2F). HRMS (EI): m/z $[\text{M}]^+$ calcd for $\text{C}_{19}\text{H}_{26}\text{F}_{11}\text{NO}$: 493.1839, found: 493.1822

4.5.3 Polymer experimental procedures:

1-perfluorohexyl-2,9-diiodo-1,9-decadiene block polymer, Polymer 4.8:

Decadiyne (1.33 g, 9.94 mmol, 1.10 equiv.) and diiodoperfluorohexane (5.00 g, 9.00 mmol, 1.0 equiv.) were dissolved in acetonitrile (36 mL) and water (27 mL). Sodium bicarbonate (1.74 g, 20.7 mmol, 2.30 equiv.) was then added, followed by sodium dithionite (3.60 g, 20.7 mmol, 2.30 equiv.) at which point the solution was vigorously stirred for 2 hours. The reaction was quenched with water (100 mL) and centrifuged for at 5000 X *G* for 5 minutes. The resulting polymer was washed with methanol (3 x 100 mL) and then dried under high vacuum to give a yellow solid (5.68 g, 8.33 mmol, 93%) which matched literature compound by NMR analysis.²¹

Post-polymerization modification procedure:

Polymer **4.8** (0.10 g, 0.145 mmol repeat unit, 1.0 equiv.) was dissolved in DMF (1 mL). Amine coupling partner (1.45 mmol, 10.0 equiv.) was then added, followed by cesium carbonate (0.283 g, 0.870 mmol, 6.0 equiv.). The resulting solution was then stirred at 50 °C for 18 hours, at which point it was precipitated from water (25 mL) and centrifuged at 5000 X *g* for 5 minutes. The polymer was then washed with methanol (4 x 50 mL) and then dried under high vacuum to give the desired polymers as orange solids.

4.9, formation of octylamine vinyllogous amidine from polymer 4.8:

^1H NMR (500 MHz, Chloroform-*d*) δ 11.18 (bs, 2H), 4.91 – 4.71 (m, 2H), 3.55 – 3.38 (m, 4H), 3.25 (t, J = 7.0 Hz, 4H), 2.21 (t, J = 7.9 Hz, 4H), 1.66 – 1.47 (m, 12H), 1.32 (d, J = 41.3 Hz, 44H), 0.92 – 0.76 (m, 12H). ^{19}F NMR (376 MHz, Chloroform-*d*) δ -109.52 (m, 4F), -120.31 – -121.68 (m, 4F). FT-IR: 2927 (C-

H str) (s), 1625 (C=N str) Imine (s), 1563 (C=C str) Enamine (s), 1100-1200 (C-F str) (vs). TGA: 10% mass loss at 244 °C. T_g (DSC): -41 °C

4.10, formation of 3-phenyl-1-propylamine vinylogous amidine from polymer **4.8**:

^1H NMR (500 MHz, Chloroform-*d*) δ 11.28 (bs, 1H), 7.25 – 6.96 (m, 10H), 5.00 – 4.78 (m, 22H), 3.65 – 3.46 (m, 4H), 3.33 – 3.13 (m, 4H), 2.80 – 2.56 (m, 8H), 2.24 – 2.03 (m, 4H), 2.03 – 1.81 (m, 8H), 1.52 – 1.41 (m, 4H), 1.31 – 1.10 (m, 4H). ^{19}F NMR (376 MHz, Chloroform-*d*) δ -110.00 (m, 4F), -120.44 – -122.23 (m, 4F). FT-IR: 3024 (C_{sp2}-H str) (w) 2938 (C_{sp3}-H str) (s), 1613 (C=N str) Imine (s), 1564 (C=C str) Enamine (s), 1499 (C=C str) Aromatic (s), 1100-1200 (C-F str) (vs). TGA: 10% mass loss at 264 °C. T_g (DSC): 1 °C

4.11, formation of 3-methoxy-1-propylamine vinylogous amidine from polymer **4.8**:

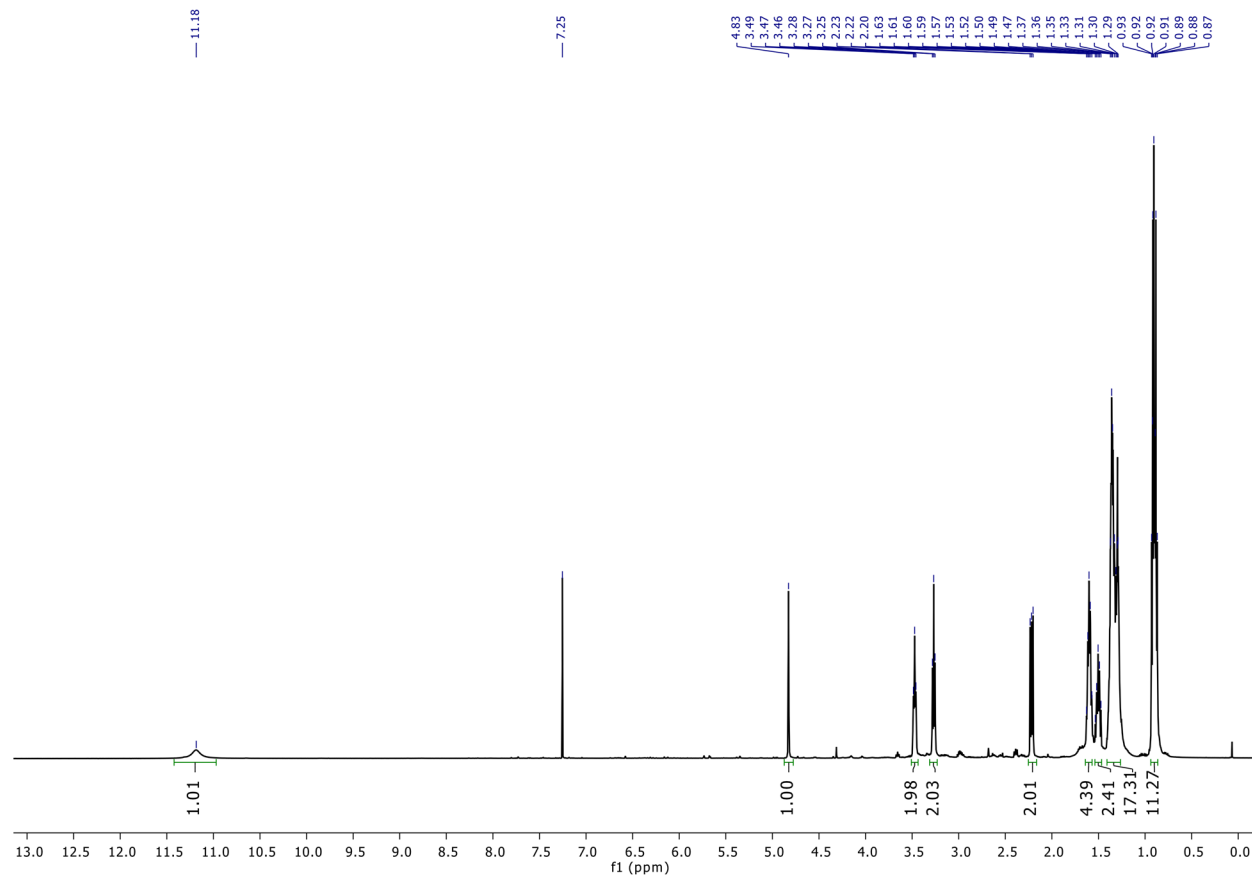
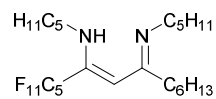
^1H NMR (500 MHz, Chloroform-*d*) δ 11.11 (bs, 2H), 4.92 – 4.70 (m, 2H), 3.58 – 3.52 (m, 4H), 3.50 – 3.43 (m, 8H), 3.40 – 3.35 (m, 4H), 3.35 – 3.14 (m, 12H), 2.28 – 2.12 (m, 4H), 1.91 – 1.74 (m, 8H), 1.62 – 1.48 (m, 4H), 1.40 – 1.31 (m, 4H). ^{19}F NMR (376 MHz, Chloroform-*d*) δ -109.63 (m, 4F), -120.41 – -121.57 (m, 4F). FT-IR: 2930 (C-H str) (s), 1613 (C=N str) Imine (s), 1563 (C=C str) Enamine (s), 1100-1200 (C-F str) (vs). TGA: 10% mass loss at 224 °C. T_g (DSC): -20 °C

4.13, formation of 3-perfluorooctyl-1-propylamine vinylogous amidine from polymer **4.8**:

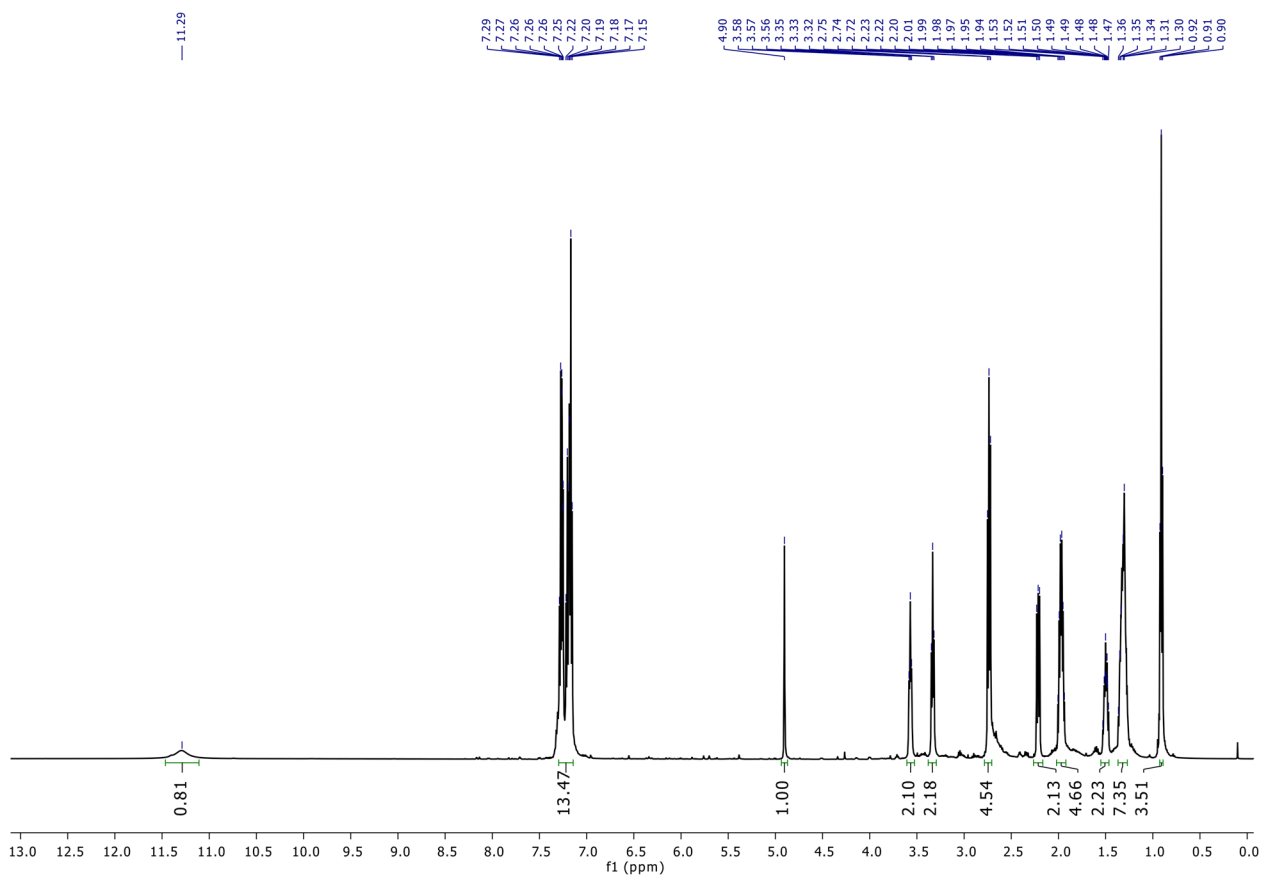
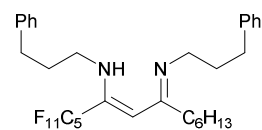
^1H NMR (500 MHz, Benzene-*d*₆/HFB (2:5)) δ 11.28 (bs, 2H), 5.05 – 4.81 (m, 2H), 3.86 – 3.59 (m, 4H), 3.52 – 3.22 (m, 4H), 2.54 – 2.15 (m, 12H), 2.12 – 1.87 (m, 8H), 1.78 – 1.60 (m, 4H), 1.60 – 1.36 (m, 4H). ^{19}F NMR (376 MHz, Benzene-*d*₆/HFB (2:5)) δ -80.74 – -85.37 (m, 12F), -110.33 – -111.61 (m, 4F), -114.89 – -116.64 (m, 8F), -121.65 – -123.33 (m, 24F), -123.57 – -125.69 (m, 20F), -127.61 (m, 8F). FT-IR: 2948 (C-H str) (w), 1627 (C=N str) Imine (w), 1566 (C=C str) Enamine (s), 1100-1200 (C-F str) (vs). TGA: 10% mass loss at 250 °C. T_g (DSC): -6 °C

4.5.4 $^1\text{H-NMR}$ spectra:

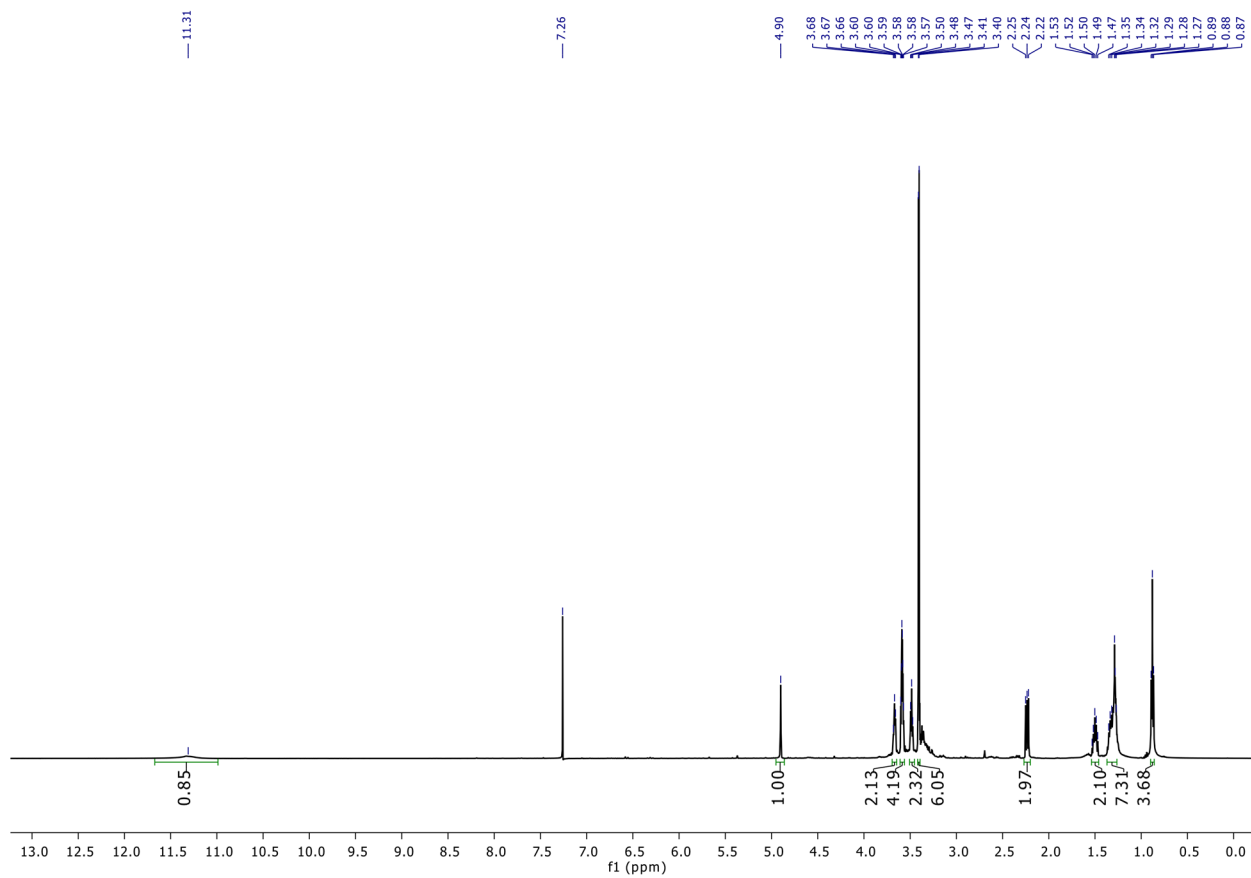
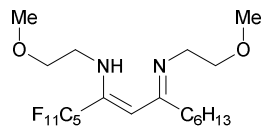
(6Z)-1,1,1,2,2,3,3,4,4,5,5-undecafluoro-N-pentyl-8-(pentylimino)tetradec-6-en-6-amine (**4.2a**):



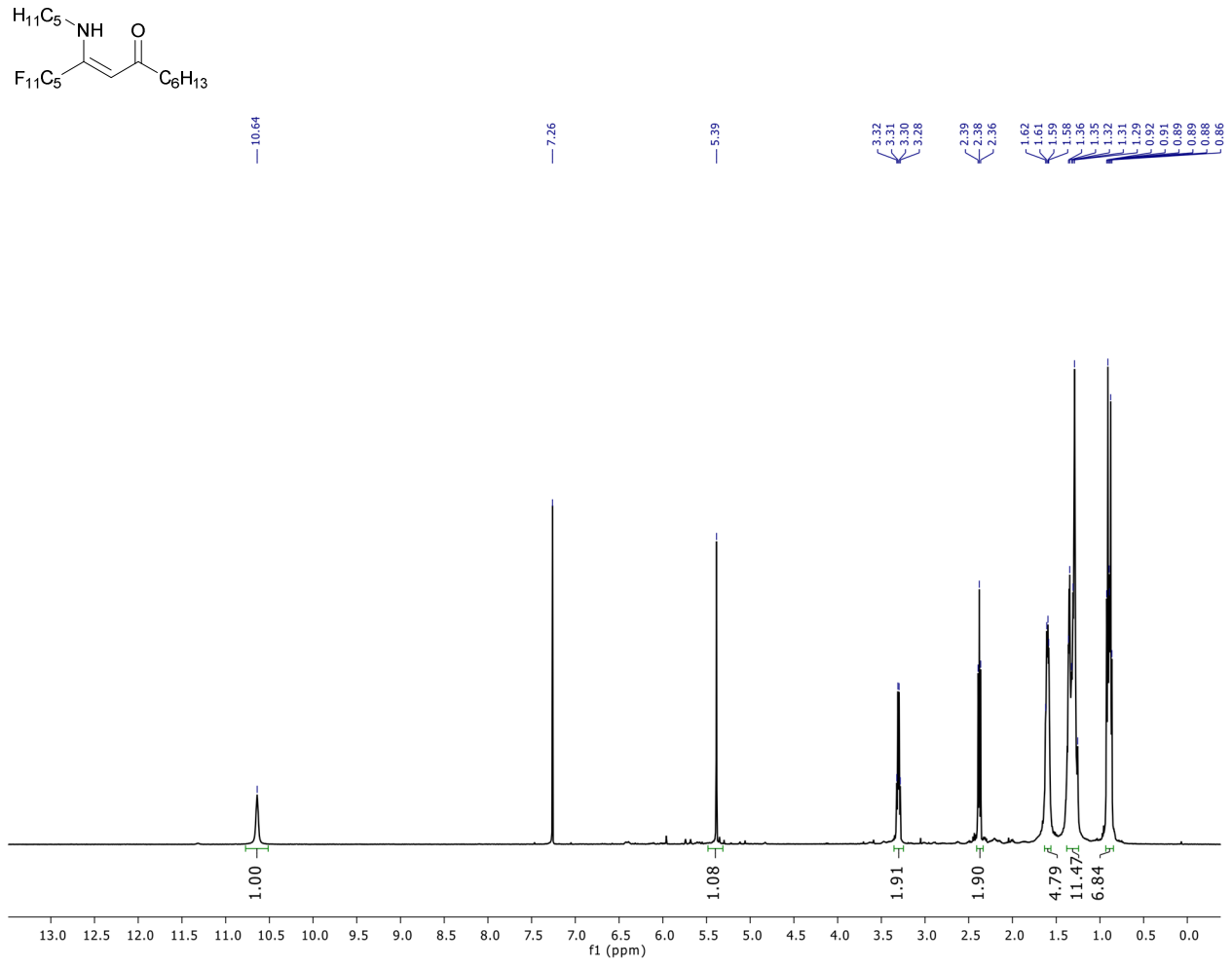
(6Z)-1,1,1,2,3,3,4,4,5,5-undecafluoro-N-(3-phenylpropyl)-8-((3-phenylpropyl)imino)tetradec-6-en-6-amine (**4.2b**):



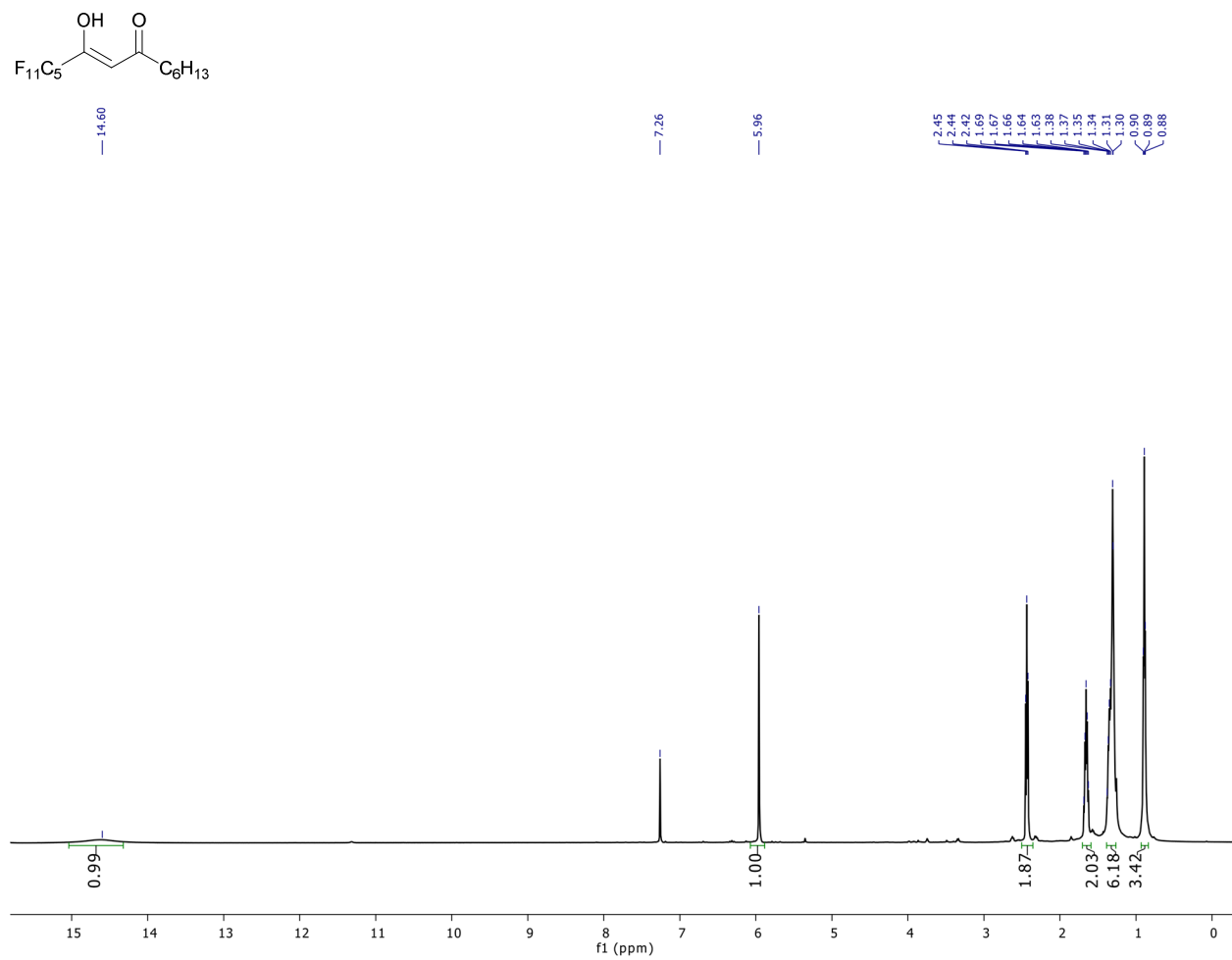
(6Z)-1,1,1,2,3,3,4,4,5,5-undecafluoro-N-(2-methoxyethyl)-8-((2-methoxyethyl)imino)tetradec-6-en-6-amine (**4.2c**):



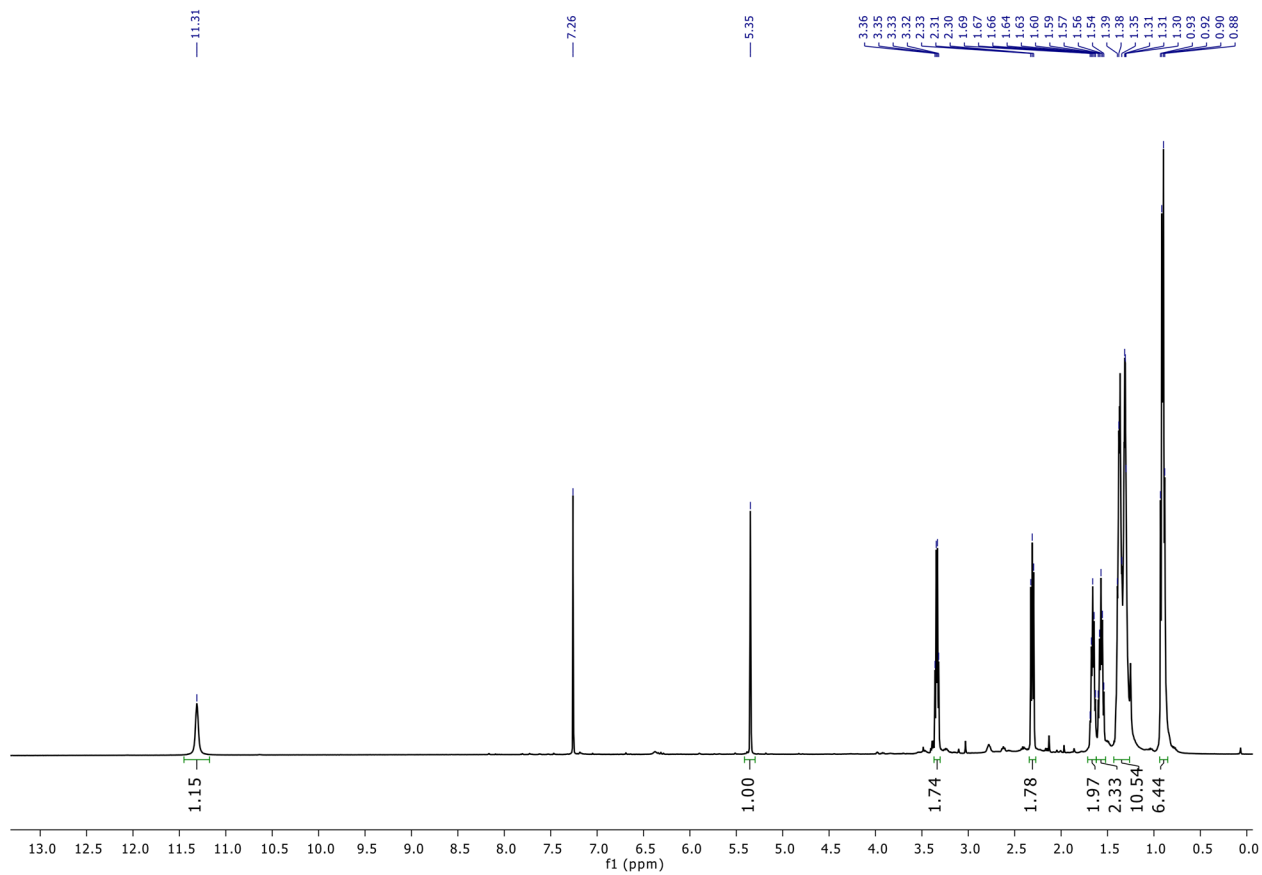
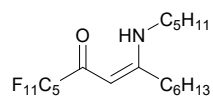
(Z)-10,10,11,11,12,12,13,13,14,14,14-undecafluoro-9-(pentylamino)tetradec-8-en-7-one (**4.3**):



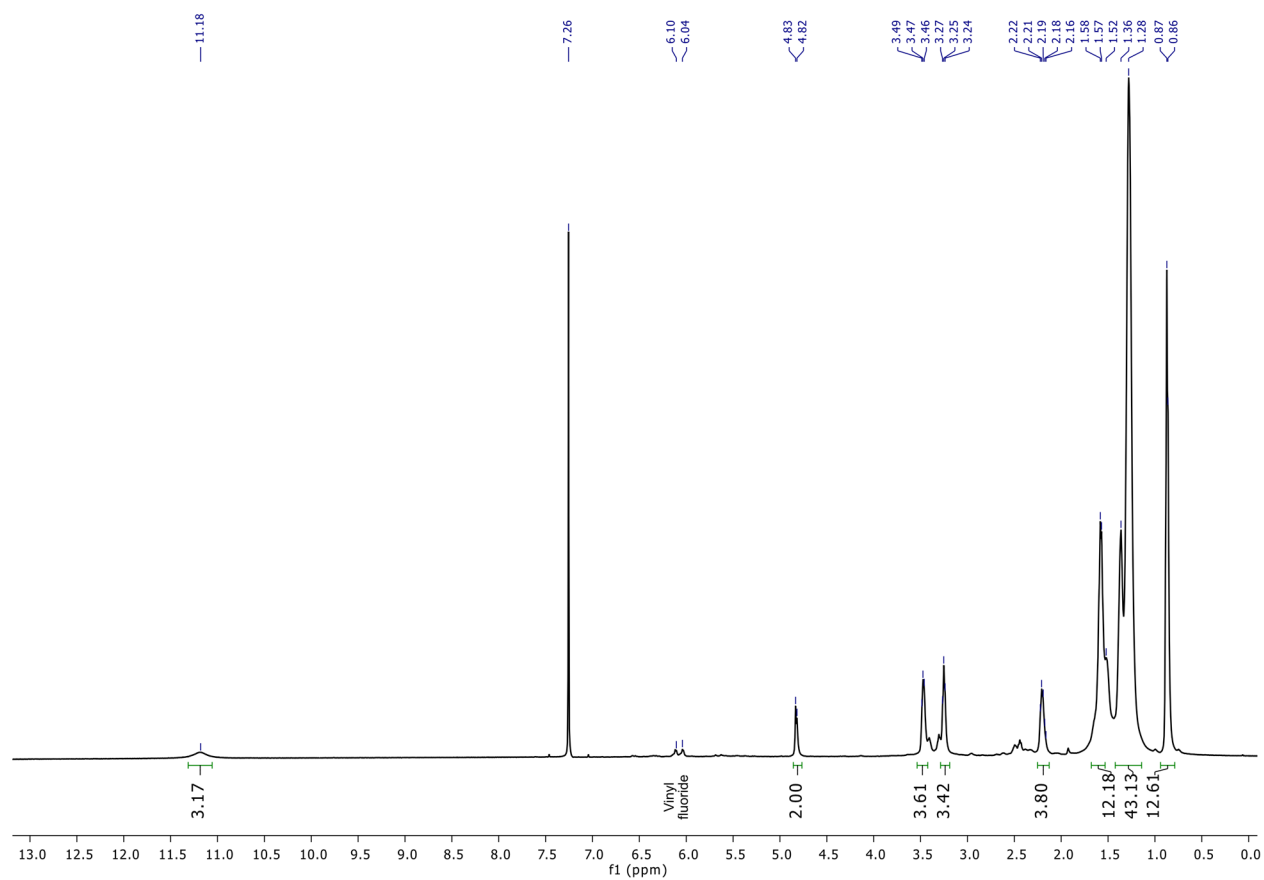
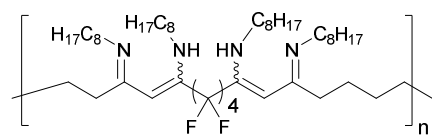
(Z)-10,10,11,11,12,12,13,13,14,14,14-undecafluoro-9-hydroxytetradec-8-en-7-one (**4.6**):



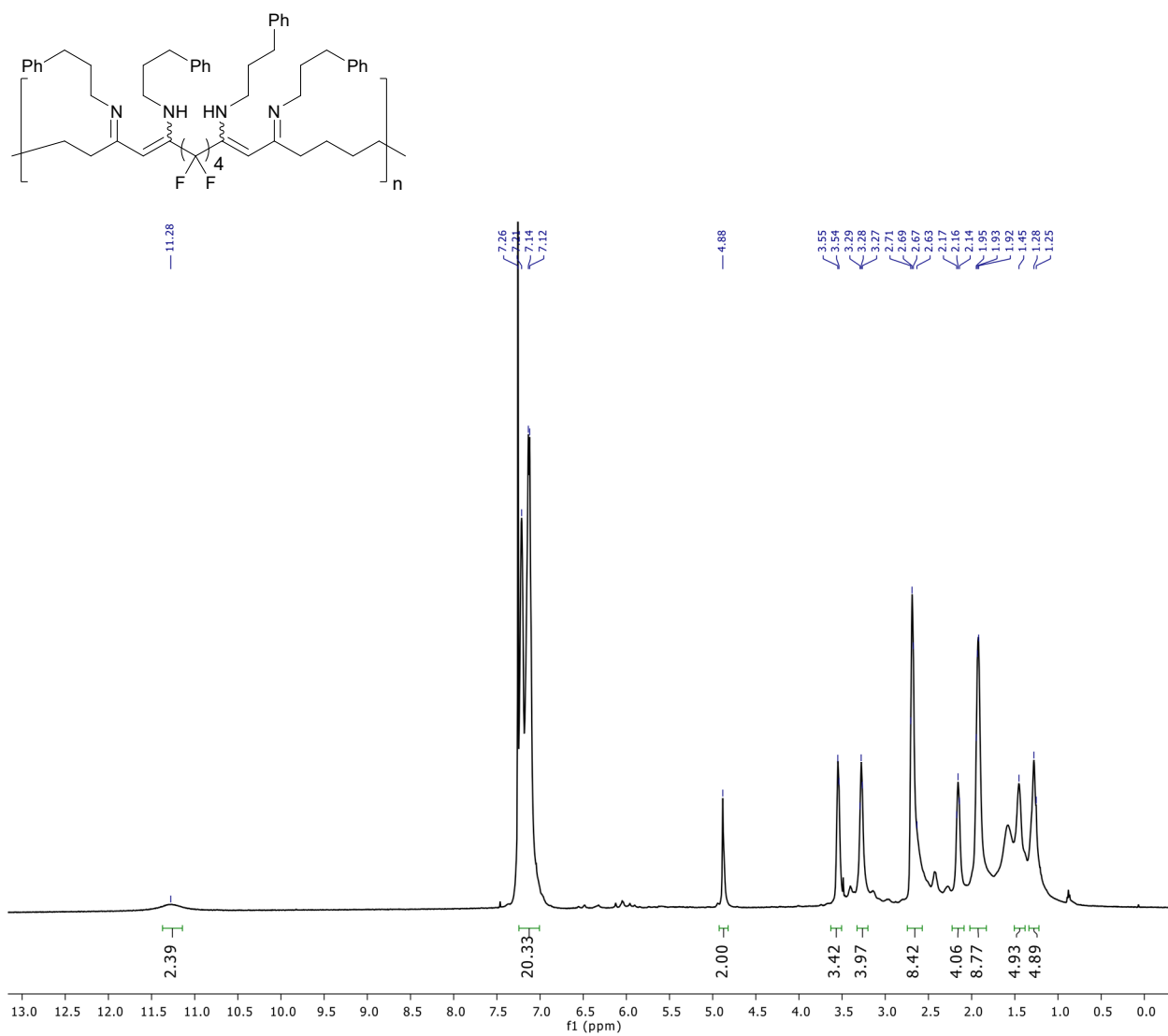
(Z)-1,1,1,2,2,3,3,4,4,5,5-undecafluoro-8-(pentylamino)tetradec-7-en-6-one (**4.7**):



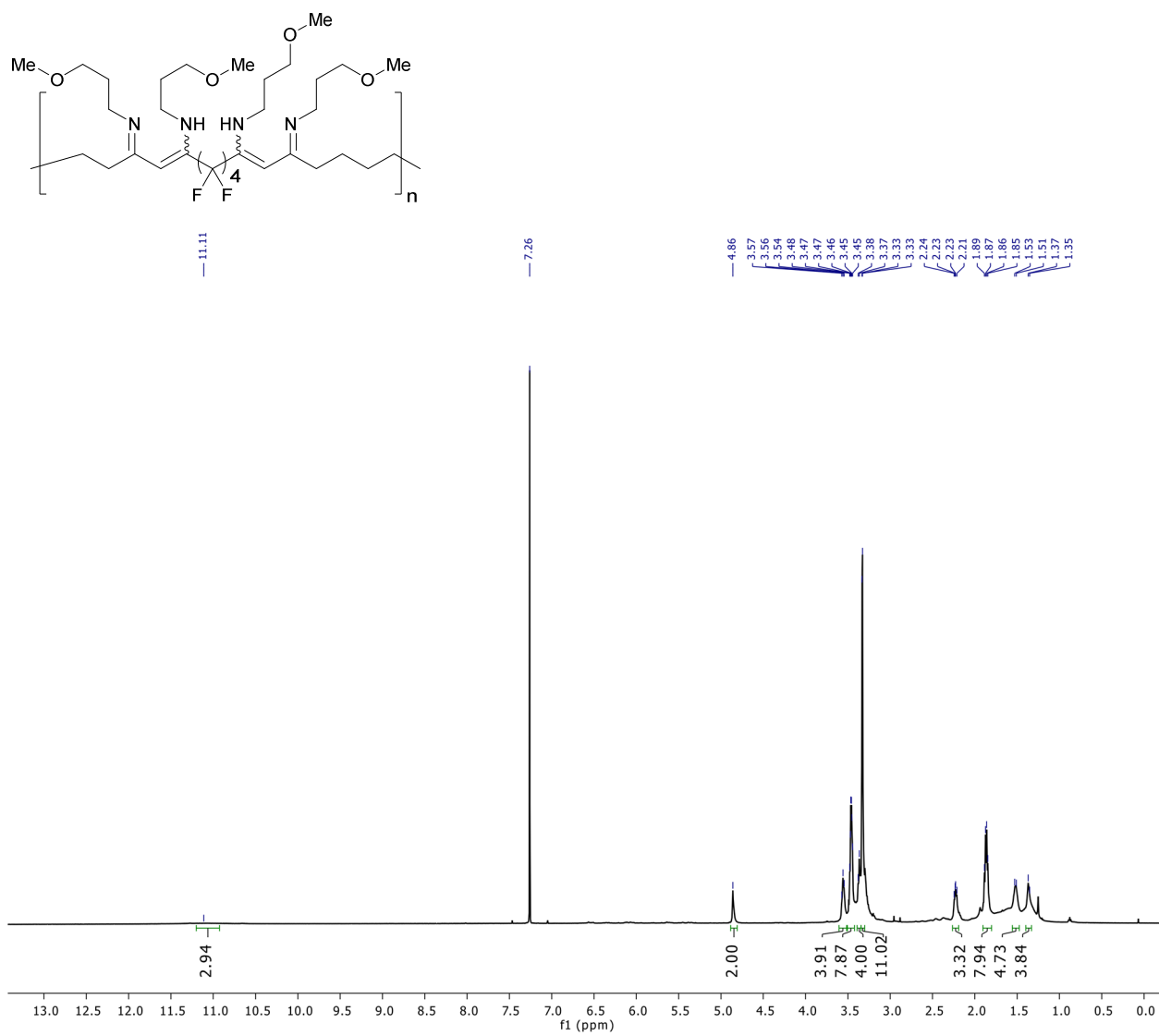
4.9, formation of octylamine vinyllogous amidine from polymer 4.8:



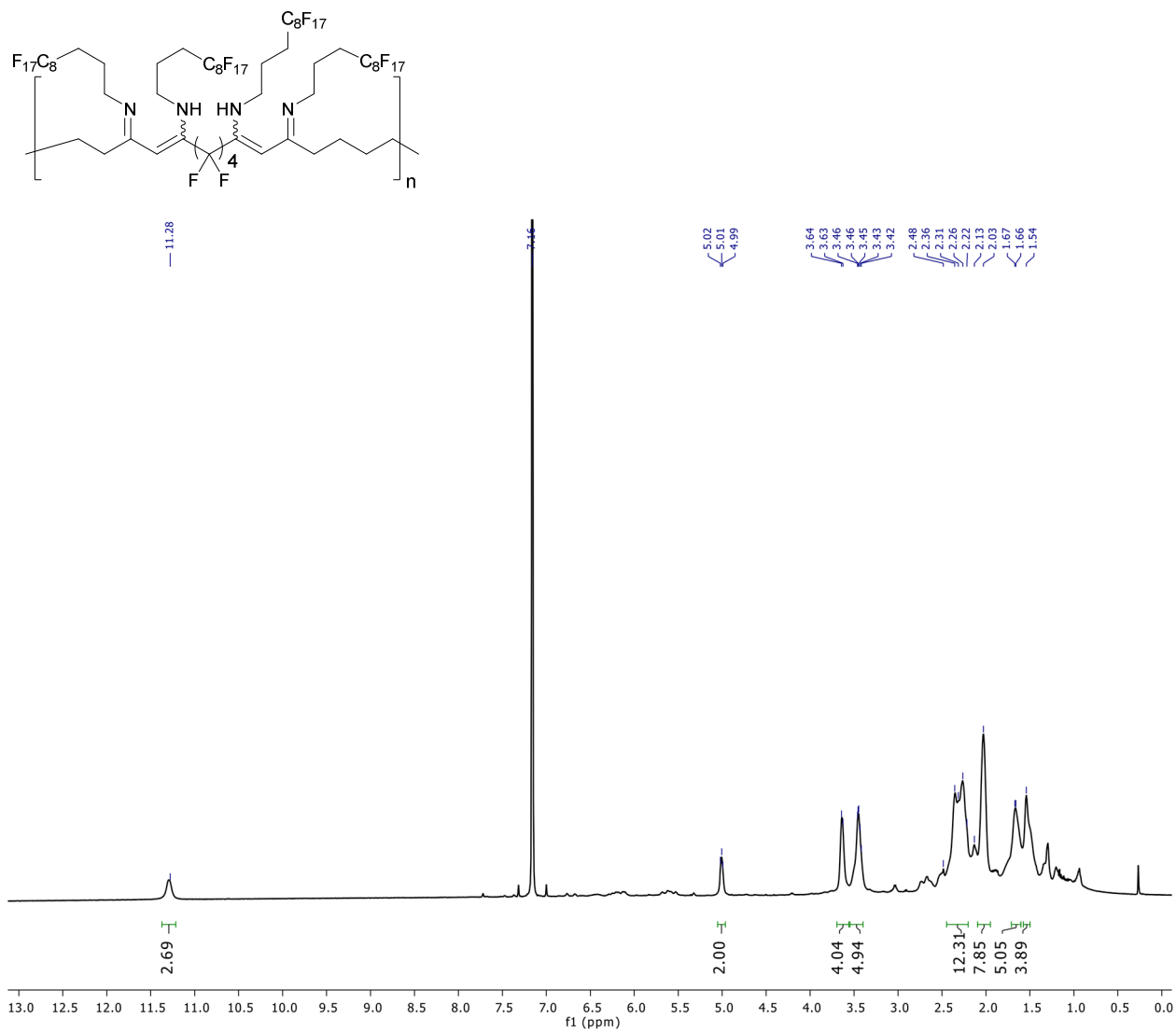
4.10, formation of 3-phenyl-1-propylamine vinyllogous amidine from polymer 4.8:



4.11, formation of 3-methoxy-1-propylamine vinyllogous amidine from polymer 4.8:

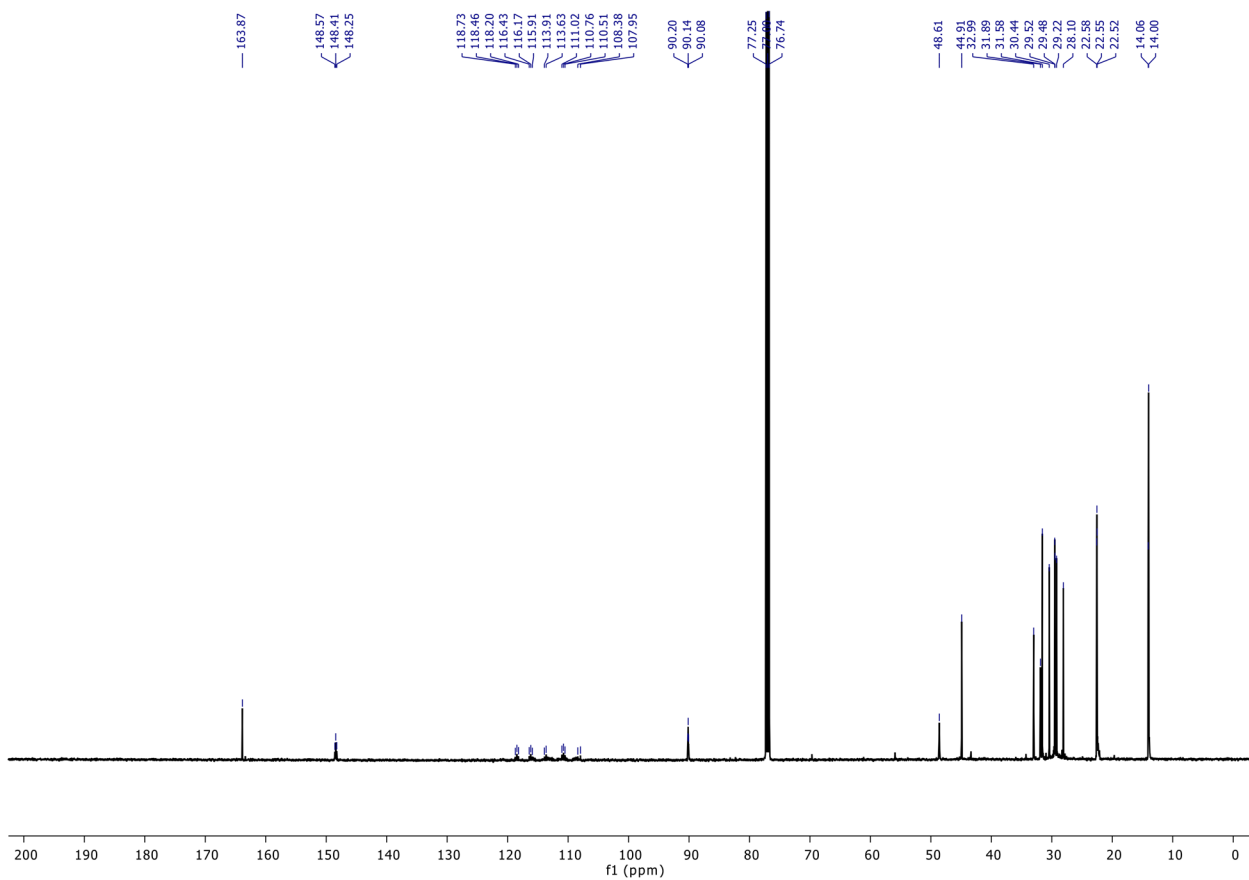
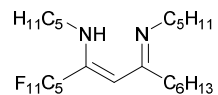


4.13, formation of 3-perfluorooctyl-1-propylamine vinylogous amidine from polymer 4.8:

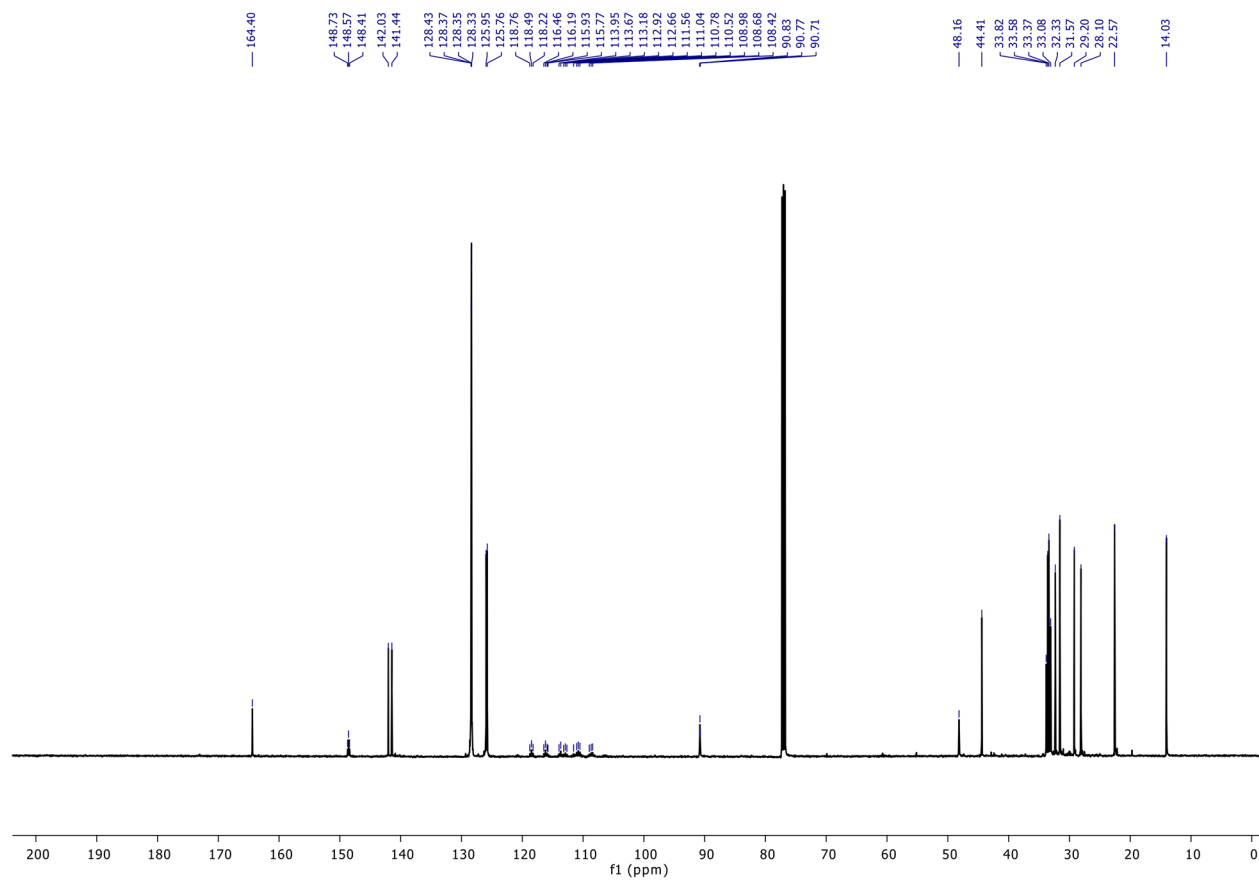
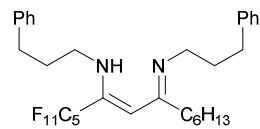


4.5.5 ^{13}C -NMR spectra:

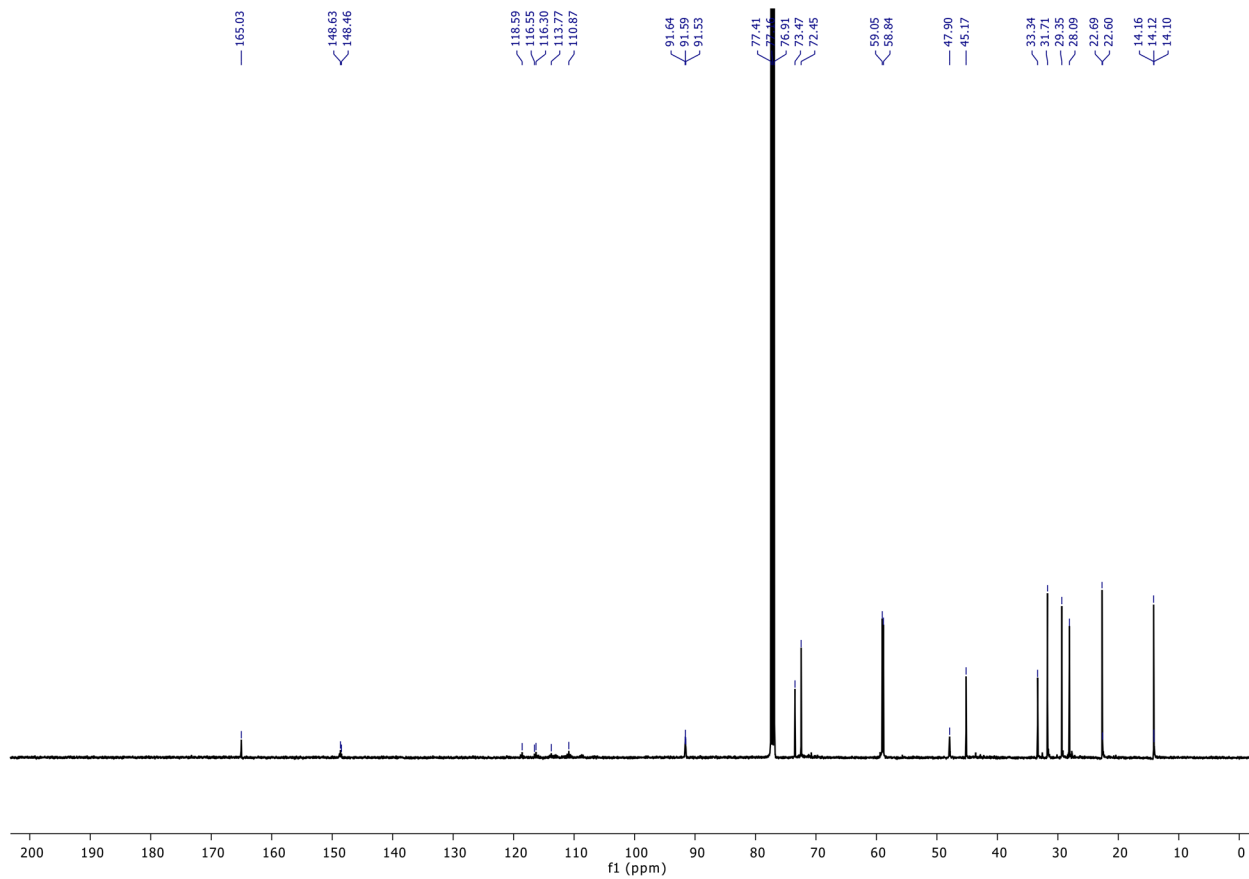
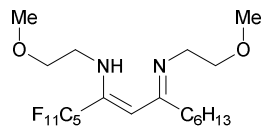
(6Z)-1,1,1,2,2,3,3,4,4,5,5-undecafluoro-N-pentyl-8-(pentylimino)tetradec-6-en-6-amine (**4.2a**):



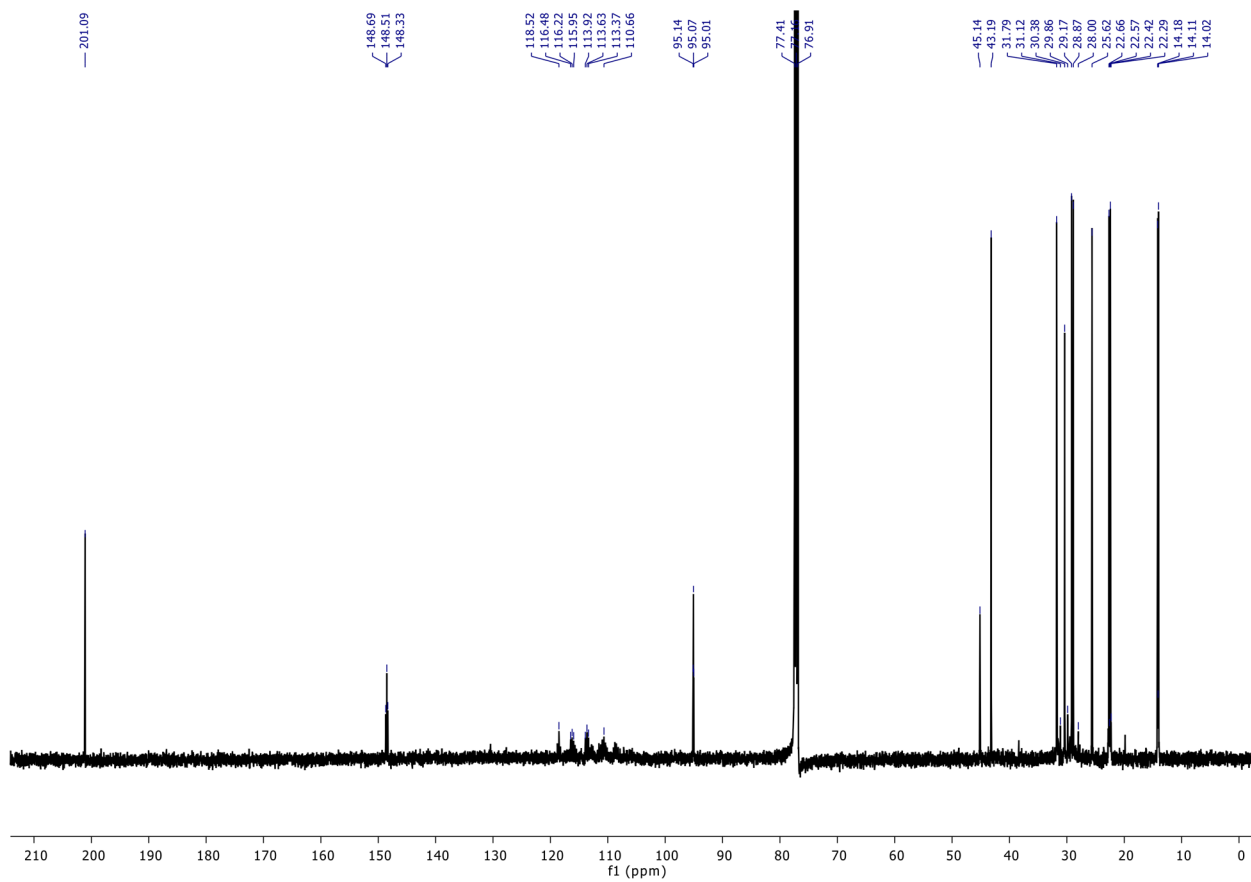
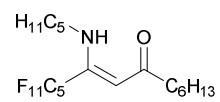
(6Z)-1,1,1,2,2,3,3,4,4,5,5-undecafluoro-N-(3-phenylpropyl)-8-((3-phenylpropyl)imino)tetradec-6-en-6-amine (**4.2b**):



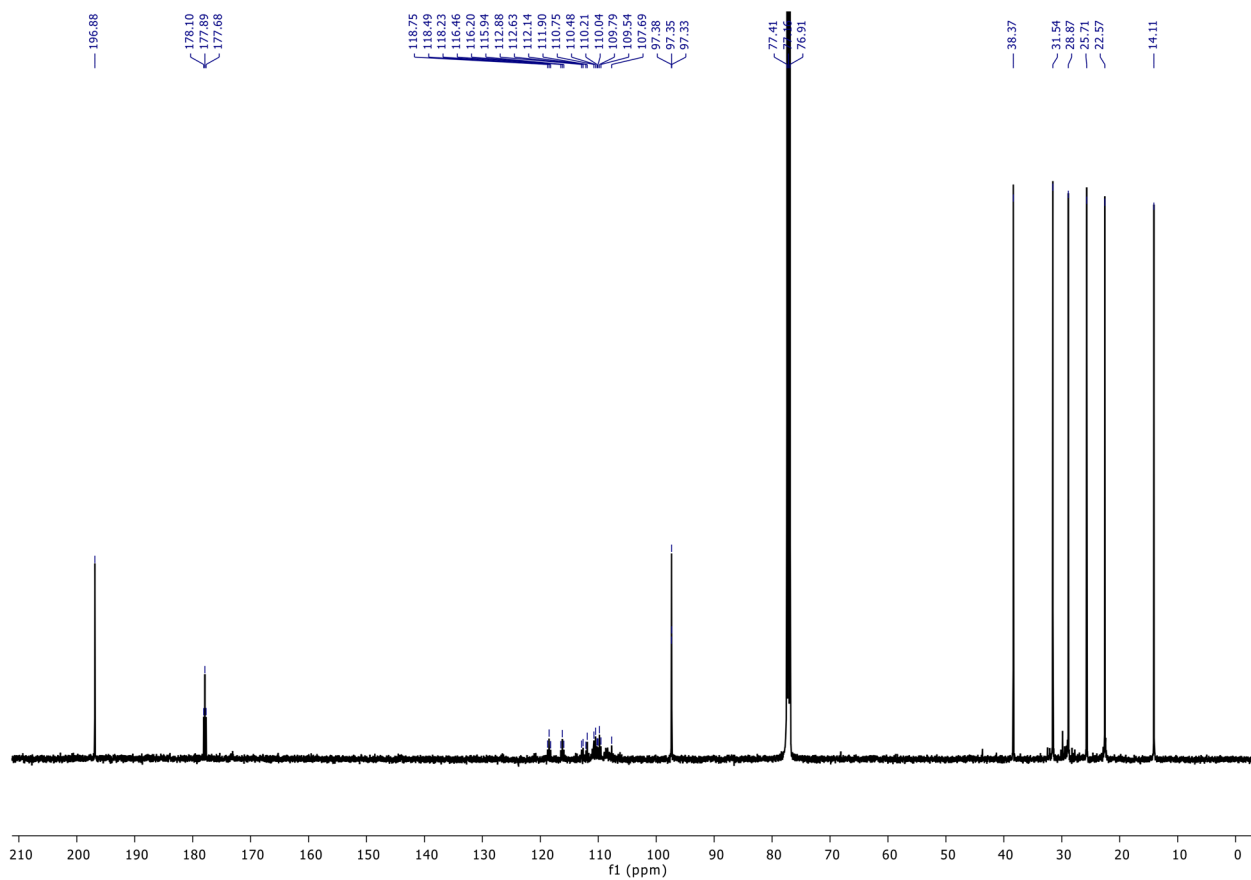
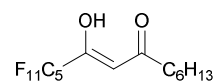
(6Z)-1,1,1,2,2,3,3,4,4,5,5-undecafluoro-N-(2-methoxyethyl)-8-((2-methoxyethyl)imino)tetradec-6-en-6-amine (**4.2c**):



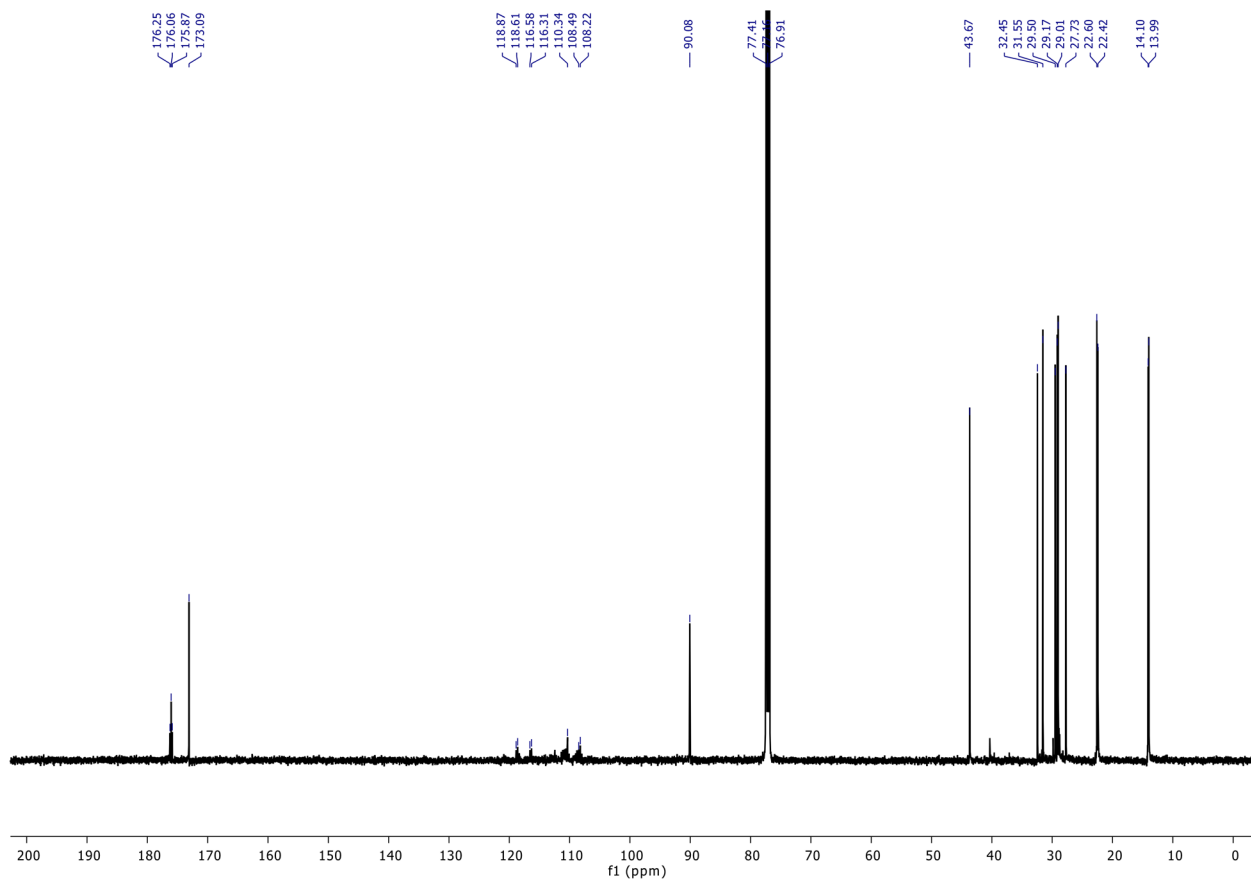
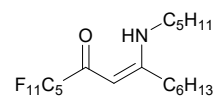
(Z)-10,10,11,11,12,12,13,13,14,14,14-undecafluoro-9-(pentylamino)tetradec-8-en-7-one (**4.3**):



(Z)-10,10,11,11,12,12,13,13,14,14,14-undecafluoro-9-hydroxytetradec-8-en-7-one (**4.6**):

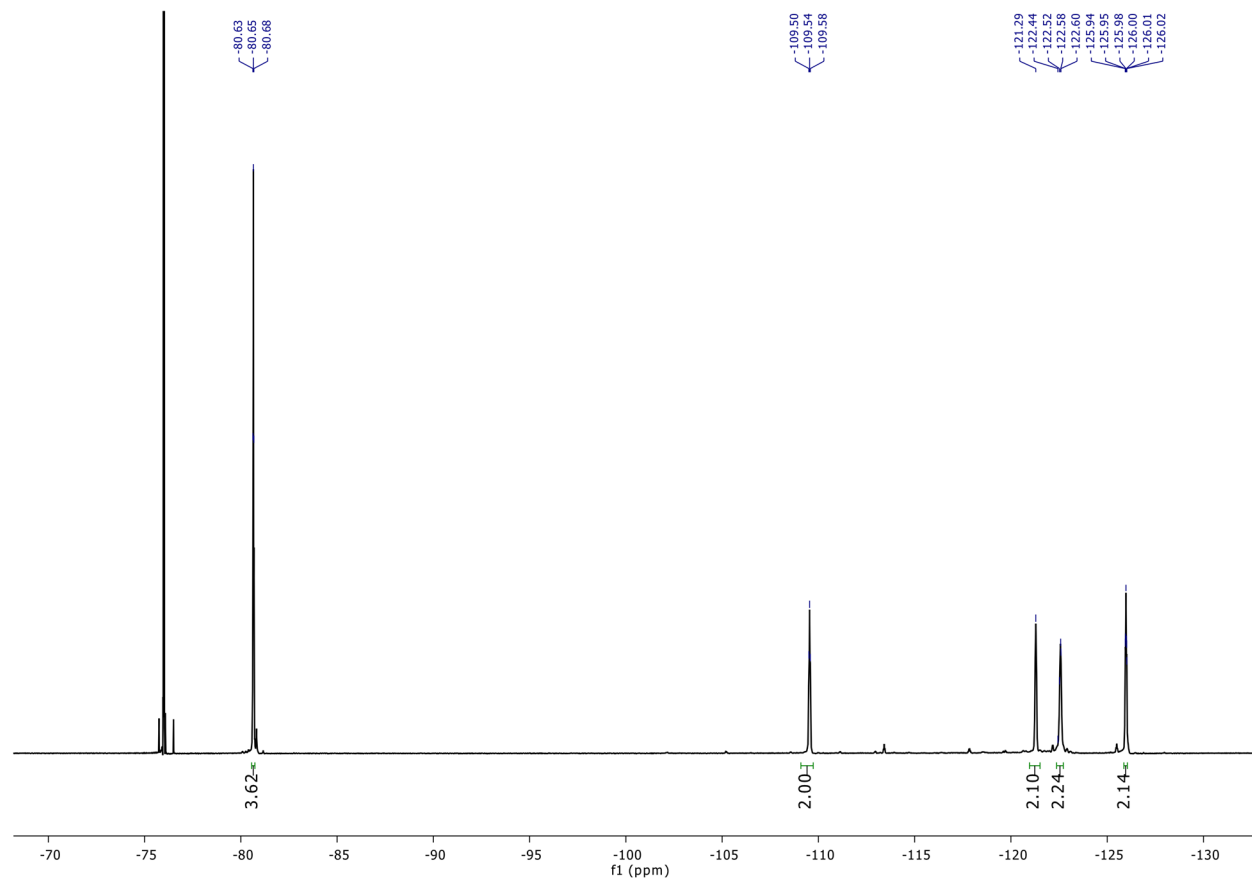
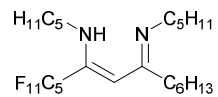


(Z)-1,1,1,2,2,3,3,4,4,5,5-undecafluoro-8-(pentylamino)tetradec-7-en-6-one (**4.7**):

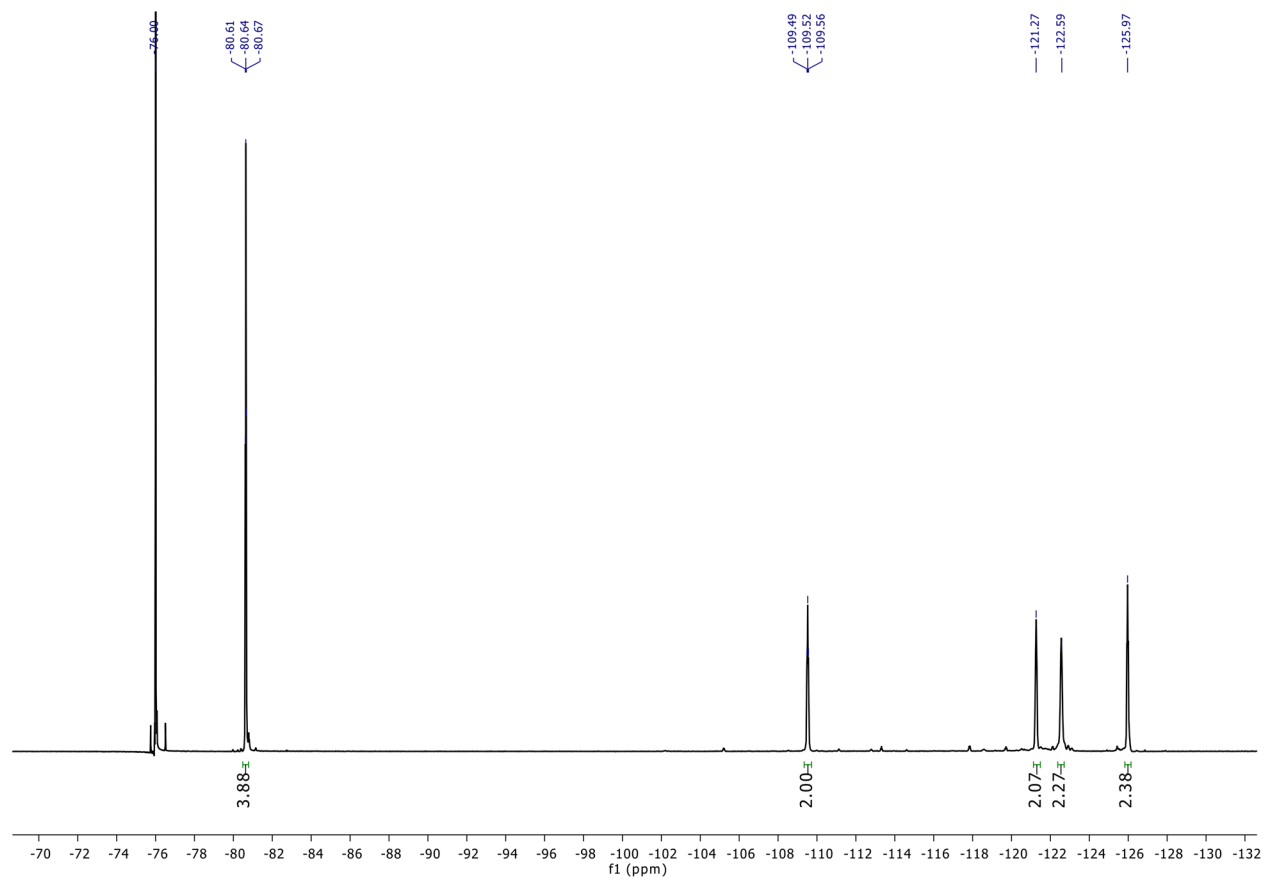
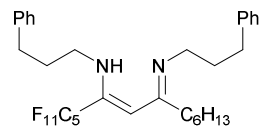


4.5.6 ^{19}F -NMR spectra

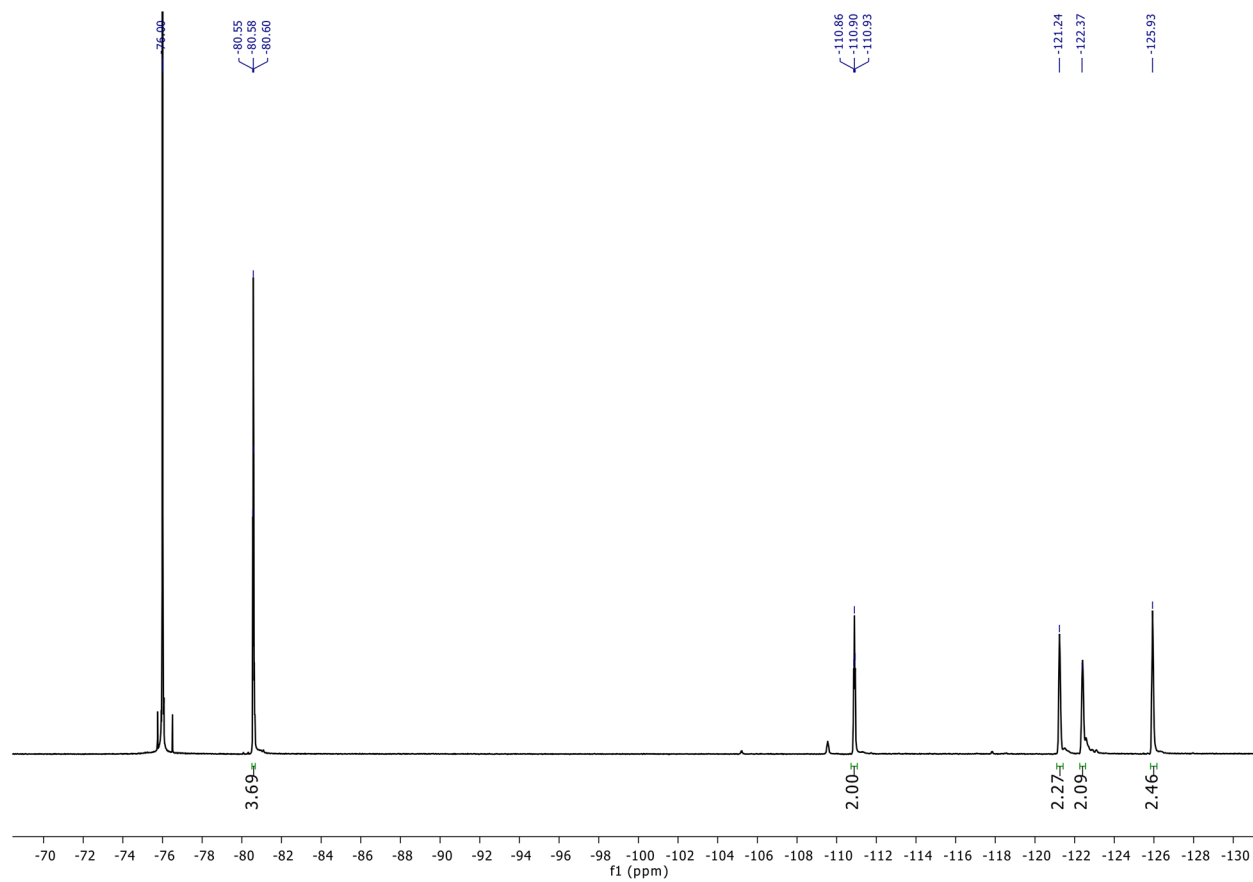
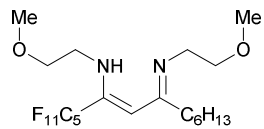
(6Z)-1,1,1,2,2,3,3,4,4,5,5-undecafluoro-N-pentyl-8-(pentylimino)tetradec-6-en-6-amine (**4.2a**):



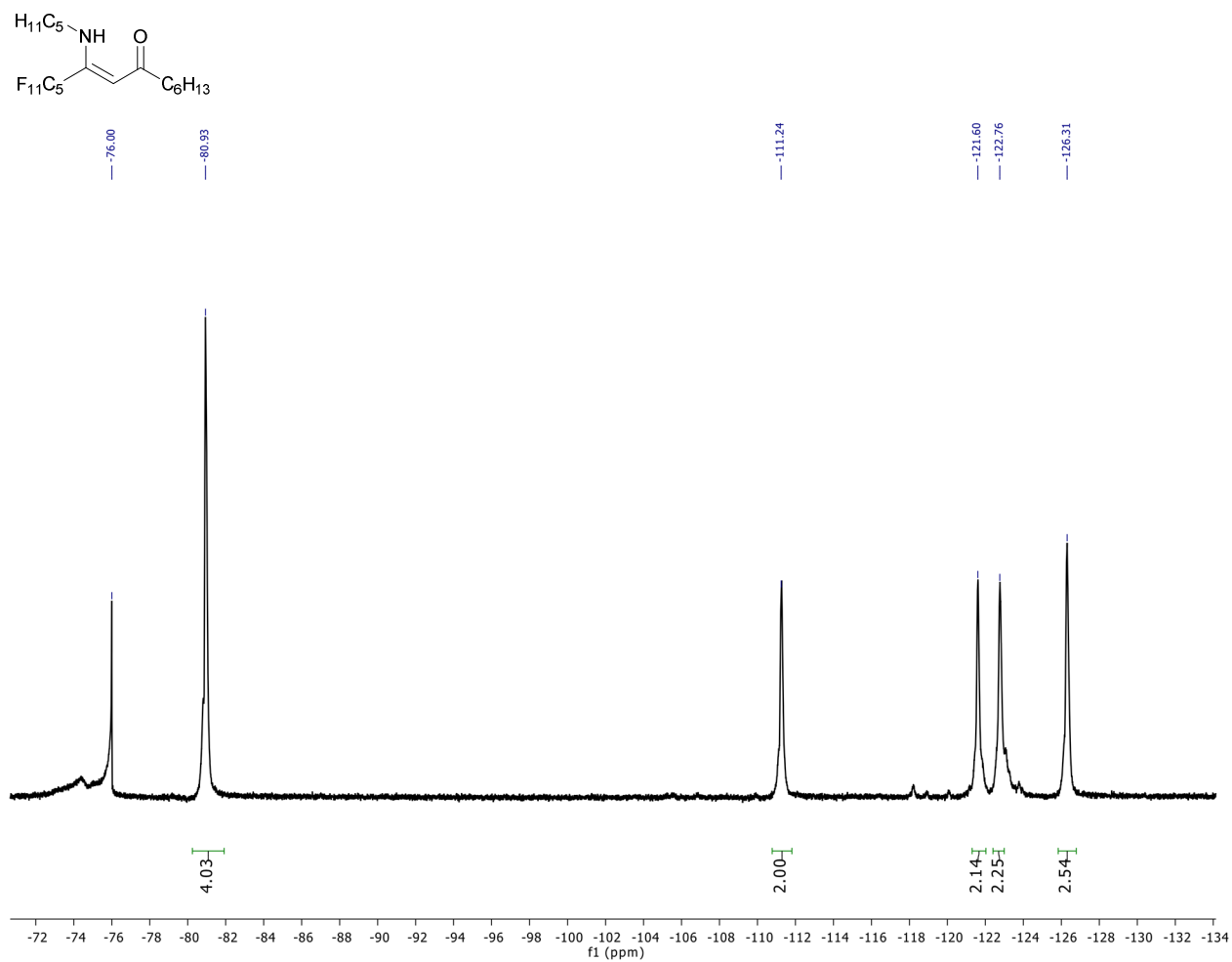
(6Z)-1,1,1,2,2,3,3,4,4,5,5-undecafluoro-N-(3-phenylpropyl)-8-((3-phenylpropyl)imino)tetradec-6-en-6-amine (**4.2b**):



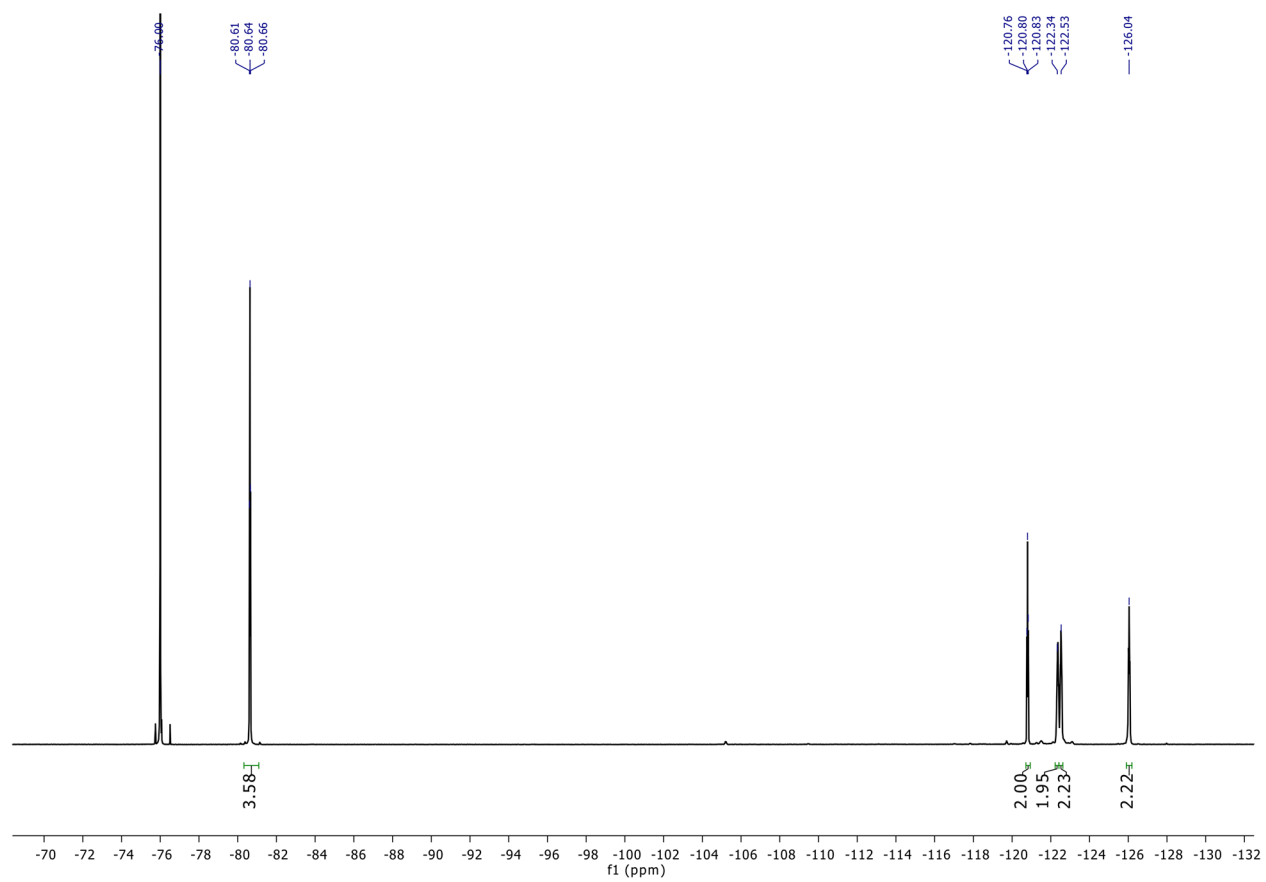
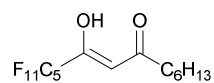
(6Z)-1,1,1,2,3,3,4,4,5,5-undecafluoro-N-(2-methoxyethyl)-8-((2-methoxyethyl)imino)tetradec-6-en-6-amine (**4.2c**):



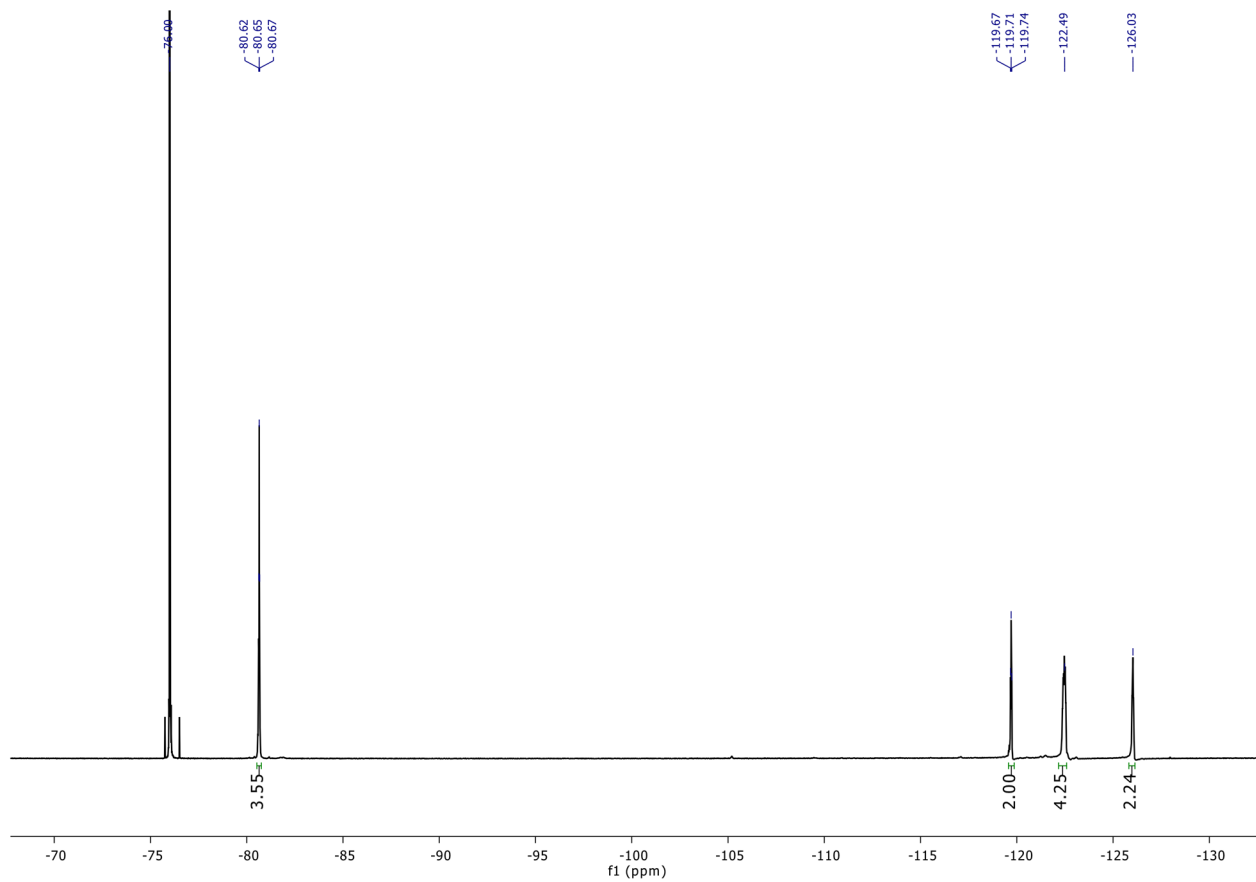
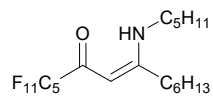
(Z)-10,10,11,11,12,12,13,13,14,14,14-undecafluoro-9-(pentylamino)tetradec-8-en-7-one (**4.3**):



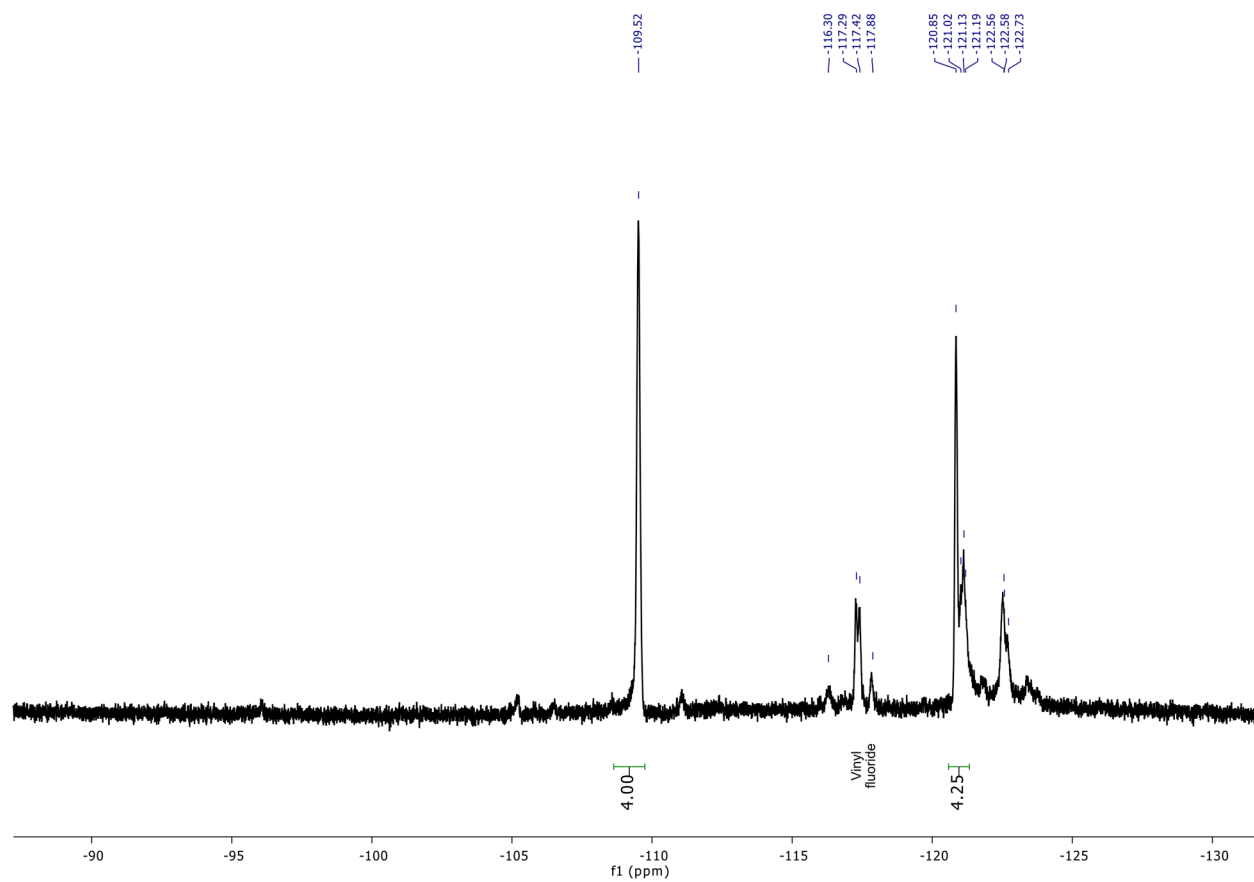
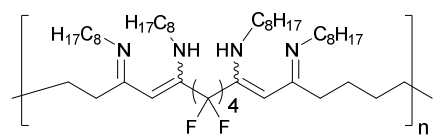
(Z)-10,10,11,11,12,12,13,13,14,14,14-undecafluoro-9-hydroxytetradec-8-en-7-one (**4.6**):



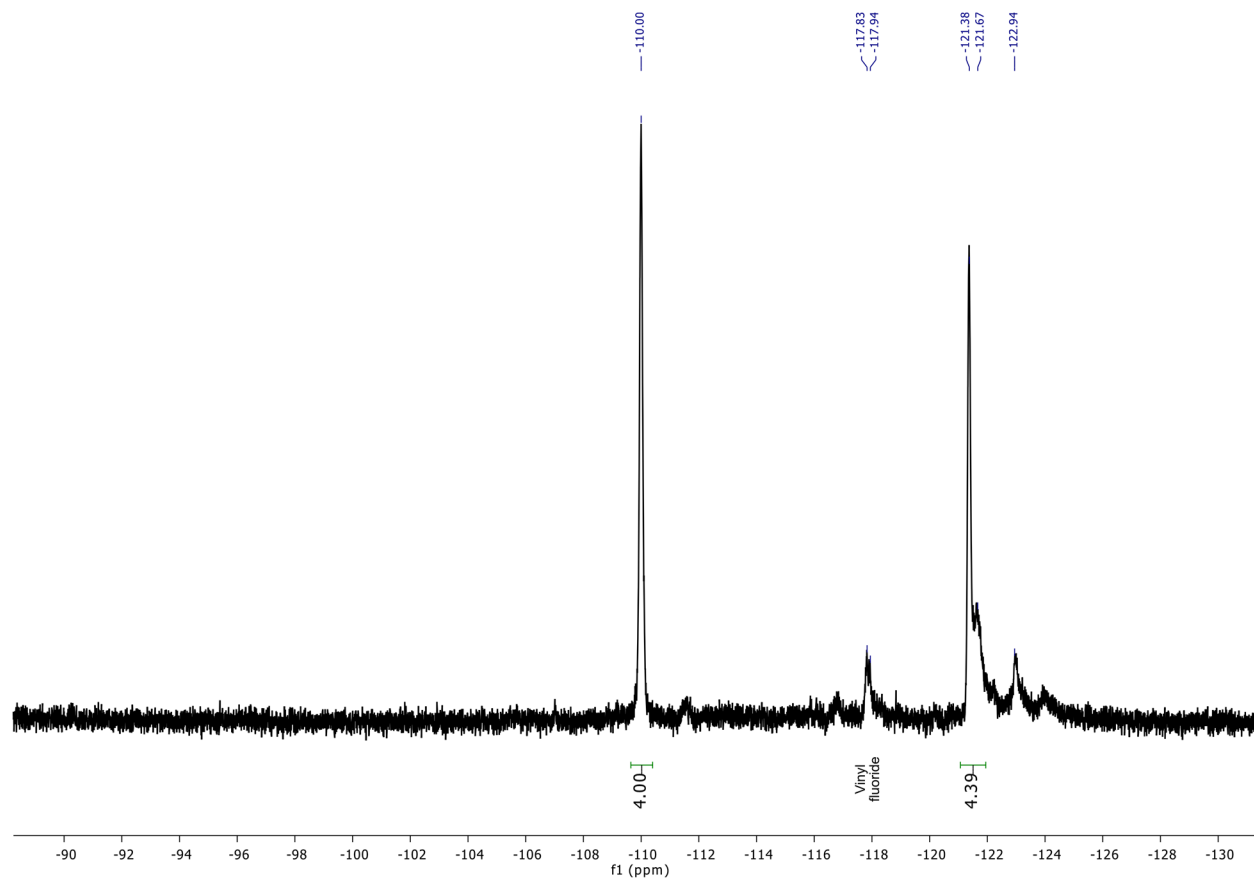
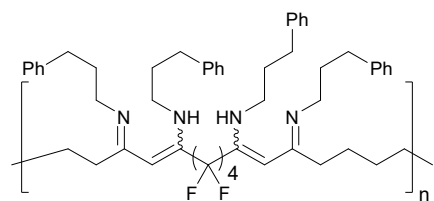
(Z)-1,1,1,2,2,3,3,4,4,5,5-undecafluoro-8-(pentylamino)tetradec-7-en-6-one (**4.7**):



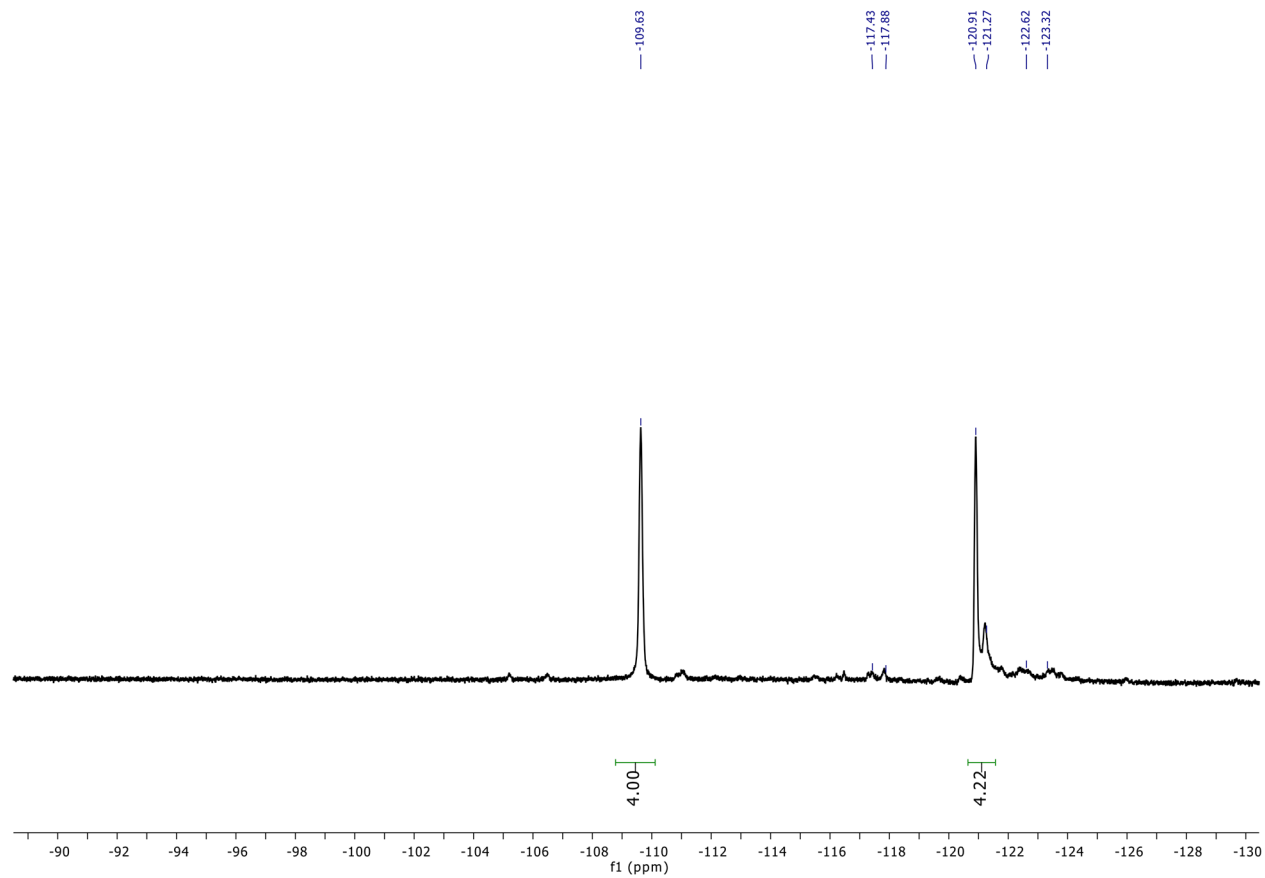
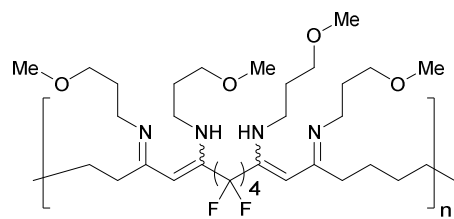
4.9, formation of octylamine vinyllogous amidine from polymer 4.8:



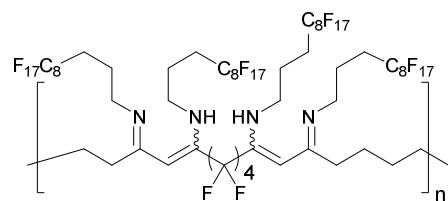
4.10, formation of 3-phenyl-1-propylamine vinylogous amidine from polymer **4.8**:



4.11, formation of 3-methoxy-1-propylamine vinyllogous amidine from polymer 4.8:



4.13, formation of 3-perfluorocetyl-1-propylamine vinylogous amidine from polymer 4.8:

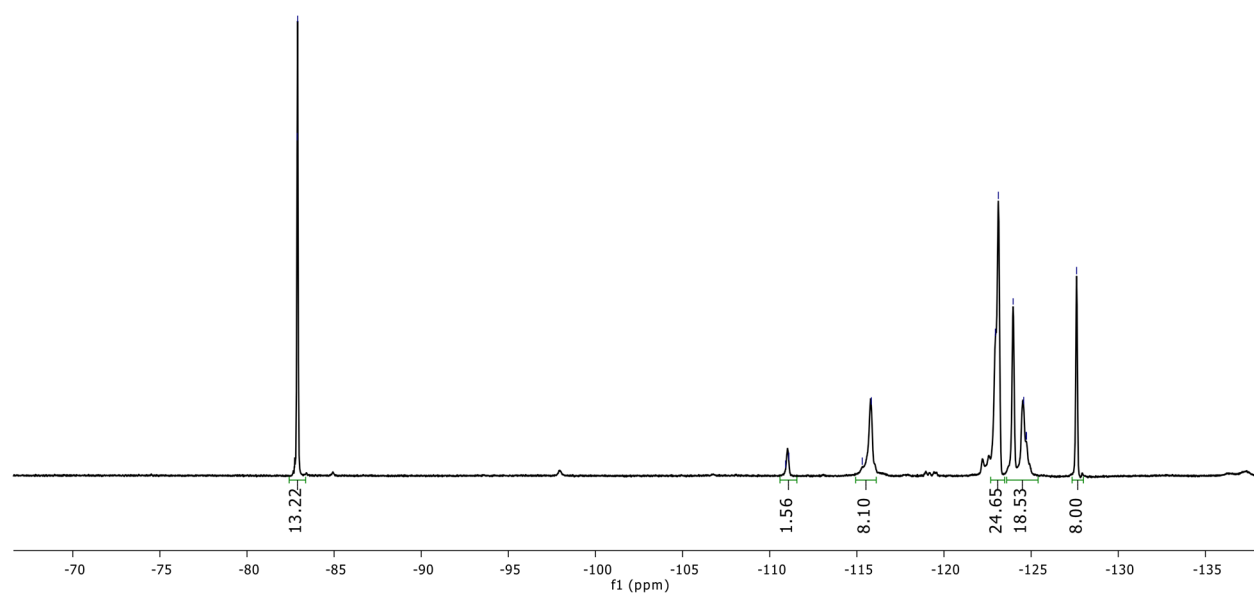


-82.88
-82.91

-110.90
-111.10

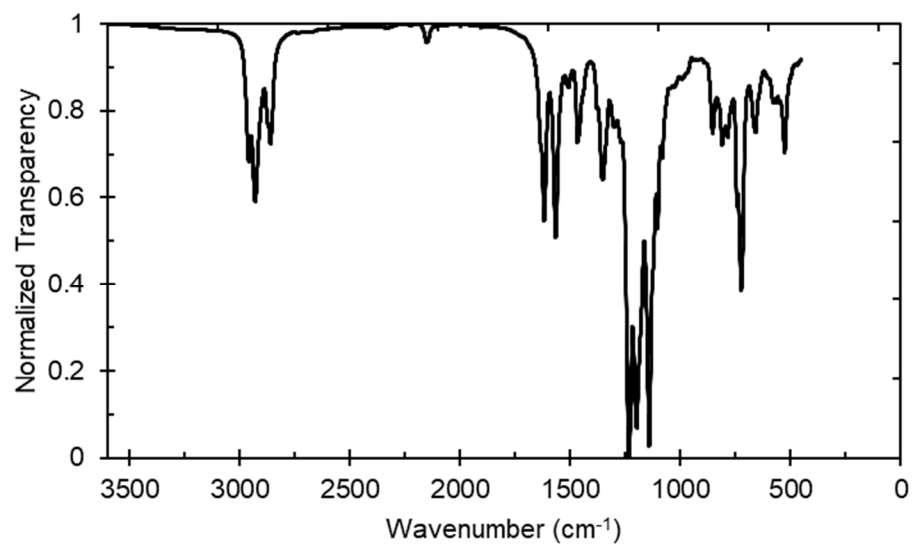
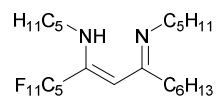
-115.31
-115.83

-122.95
-123.12
-123.97
-124.58
-124.72
-124.74
-127.61

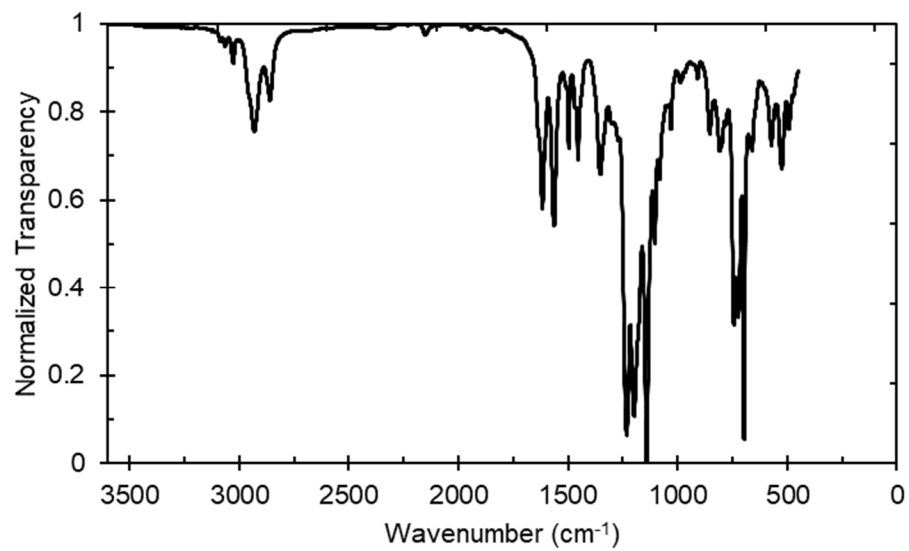
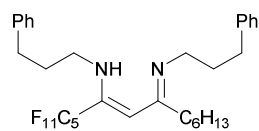


4.5.7 IR spectra

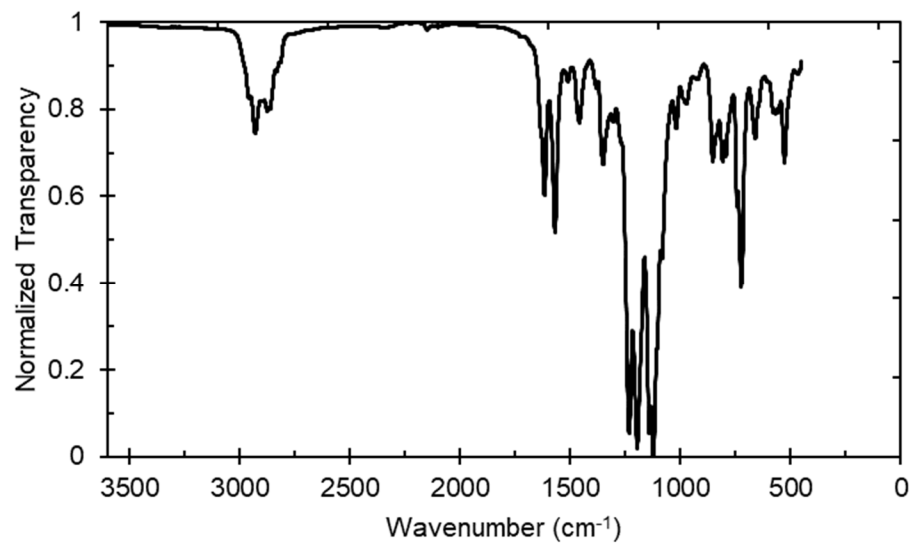
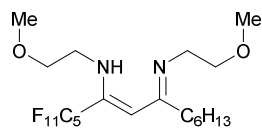
(6Z)-1,1,1,2,2,3,3,4,4,5,5-undecafluoro-N-pentyl-8-(pentylimino)tetradec-6-en-6-amine (**4.2a**):



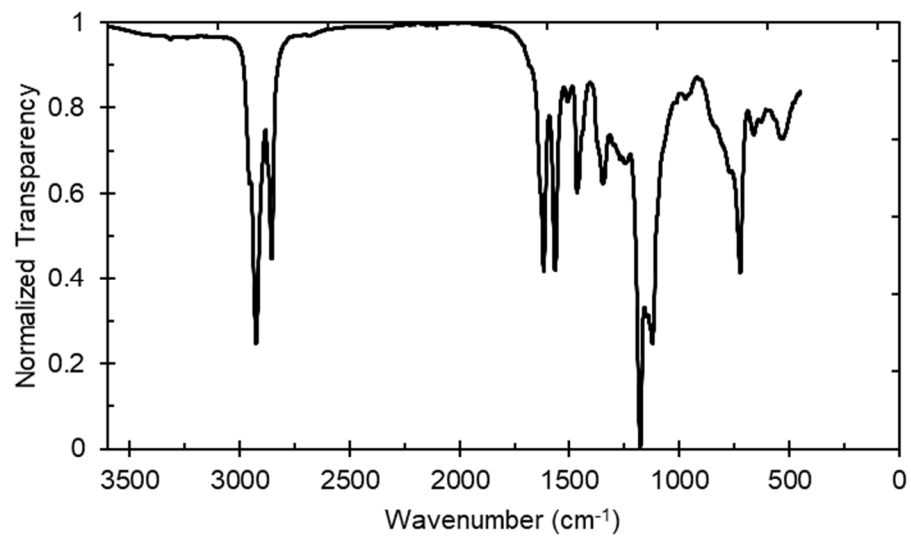
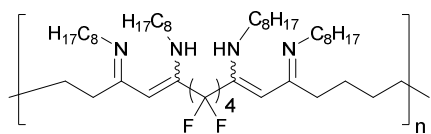
(6Z)-1,1,1,2,2,3,3,4,4,5,5-undecafluoro-N-(3-phenylpropyl)-8-((3-phenylpropyl)imino)tetradec-6-en-6-amine (**4.2b**):



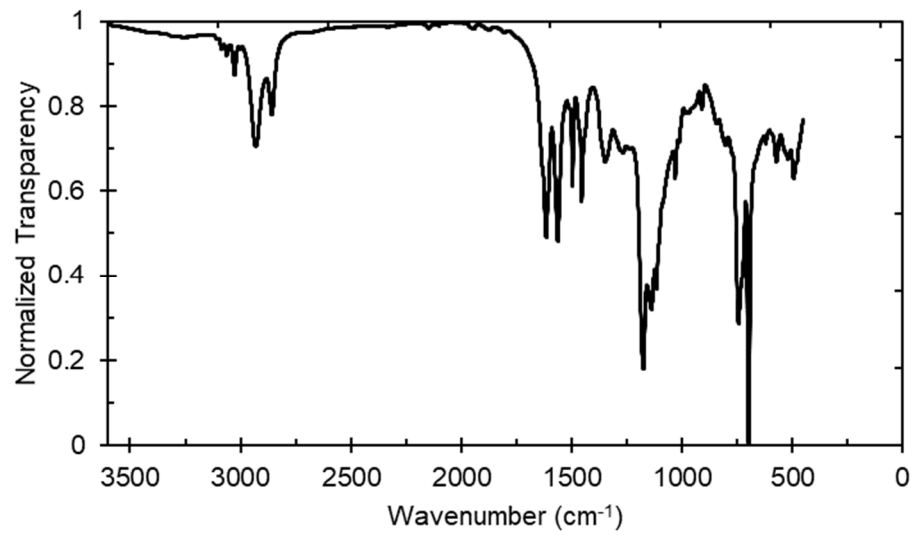
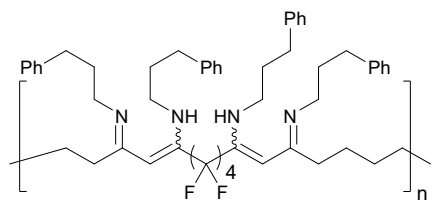
(6Z)-1,1,1,2,2,3,3,3,4,4,5,5-undecafluoro-N-(2-methoxyethyl)-8-((2-methoxyethyl)imino)tetradec-6-en-6-amine (**4.2c**):



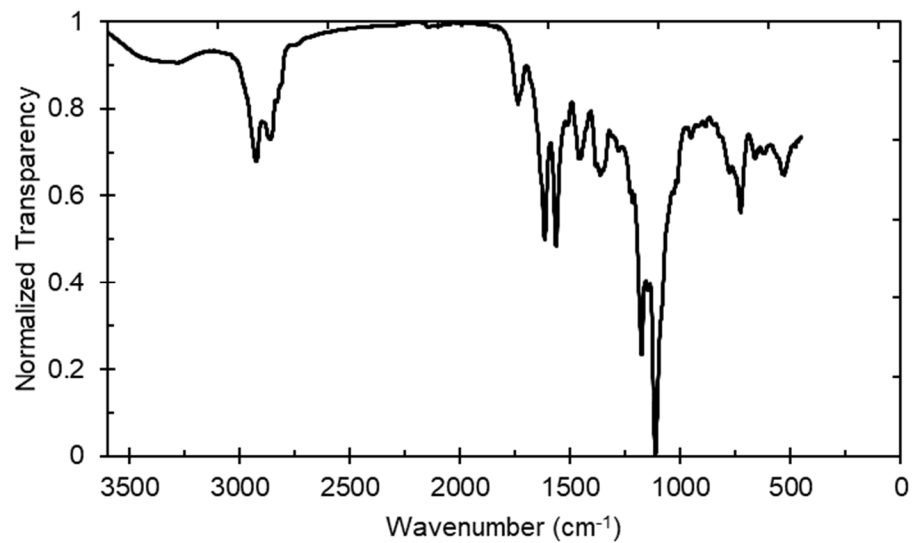
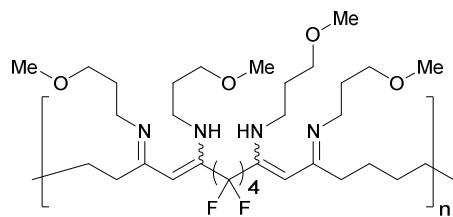
4.9, formation of octylamine vinylogous amidine from polymer 4.8:



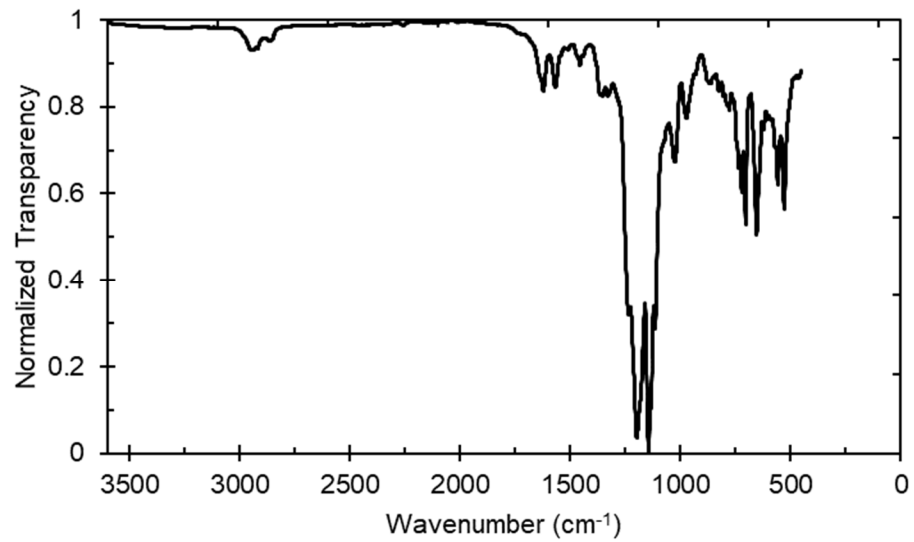
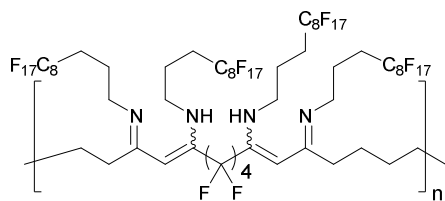
4.10, formation of 3-phenyl-1-propylamine vinylogous amidine from polymer **4.8**:



4.11, formation of 3-methoxy-1-propylamine vinylogous amidine from polymer **4.8**:



4.13, formation of 3-perfluorooctyl-1-propylamine vinylogous amidine from polymer **4.8**:



4.6 References and notes

- (1) Teng, H. Overview of the Development of the Fluoropolymer Industry. *Appl. Sci.* **2012**, *2*, 496–512.
- (2) Yao, W.; Li, Y.; Huang, X. Fluorinated Poly(Meth)Acrylate: Synthesis and Properties. *Polymer* **2014**, *55*, 6197–6211.
- (3) Gong, H.; Gu, Y.; Chen, M. Controlled/Living Radical Polymerization of Semifluorinated (Meth)Acrylates. *Synlett* **2018**, *29*, 1543–1551.
- (4) Borkar S.; Jankova, K.; Siesler, H. W.; Hvilsted, S. New Highly Fluorinated Styrene-Based Materials with Low Surface Energy Prepared by ATRP. *Macromolecules* **2004**, *37*, 788–794.
- (5) Wadekar, M. N.; Jager, W. F.; Sudhölter, E. J. R.; Picken, S. J. Synthesis of a Polymerizable Fluorosurfactant for the Construction of Stable Nanostructured Proton-Conducting Membranes. *J. Org. Chem.* **2010**, *75*, 6814–6819.
- (6) Améduri, B. The Promising Future of Fluoropolymers. *Macromol. Chem. Phys.* **2020**, *221*, 1900573.
- (7) Mohammad, S. A.; Shingdilwar, S.; Banerjee, S.; Ameduri, B. Macromolecular Engineering Approach for the Preparation of New Architectures from Fluorinated Olefins and Their Applications. *Prog. Polym. Sci.* **2020**, *106*, 101255.
- (8) Ameduri, B. Fluoropolymers: The Right Material for the Right Applications. *Chem. - A Eur. J.* **2018**, *24*, 18830–18841.
- (9) Cardoso, V. F.; Correia, D. M.; Ribeiro, C.; Fernandes, M. M.; Lanceros-Méndez, S. Fluorinated Polymers as Smart Materials for Advanced Biomedical Applications. *Polymers*, **2018**, *10*, 161–187.
- (10) Hercules, D. A.; Parrish, C. A.; Sayler, T. S.; Tice, K. T.; Williams, S. M.; Lowery, L. E.; Brady, M. E.; Coward, R. B.; Murphy, J. A.; Hey, T. A.; et al. Preparation of Tetrafluoroethylene from

the Pyrolysis of Pentafluoropropionate Salts. *J. Fluor. Chem.* **2017**, *196*, 107–116.

- (11) De Rademaeker, E.; Fabiano, B.; Buratti, S. S.; Ferrero, F.; Zeps, R.; Kluge, M.; Schröder, V.; Spoomaker, T. The Explosive Decomposition of Tetrafluoroethylene: Large Scale Tests and Simulations. *Chem. Eng. Trans.* **2013**, *13*, 817–822.
- (12) Hercules, D. A.; DesMarteau, D. D.; Fernandez, R. E.; Clark, J. L.; Thrasher, J. S. Evolution of Academic Barricades for the Use of Tetrafluoroethylene (TFE) in the Preparation of Fluoropolymers. In *Handbook of Fluoropolymer Science and Technology*; John Wiley & Sons, Inc.: Hoboken, NJ, USA, 2014; pp 413–431.
- (13) Krafft, M. P.; Riess, J. G. Per- and Polyfluorinated Substances (PFASs): Environmental Challenges. *Curr. Opin. Colloid Interface Sci.* **2015**, *20*, 192–212.
- (14) Wang, P.; Lu, Y.; Wang, T.; Meng, J.; Li, Q.; Zhu, Z.; Sun, Y.; Wang, R.; Giesy, J. P. Shifts in Production of Perfluoroalkyl Acids Affect Emissions and Concentrations in the Environment of the Xiaoqing River Basin, China. *J. Hazard. Mater.* **2016**, *307*, 55–63.
- (15) Lau, C.; Butenhoff, J. L.; Rogers, J. M. The Developmental Toxicity of Perfluoroalkyl Acids and Their Derivatives. *Toxicol. Appl. Pharmacol.* **2004**, *198*, 231–241.
- (16) Kyremateng, S. O.; Busse, K.; Kohlbrecher, J.; Kressler, J. Synthesis and Self-Organization of Poly(Propylene Oxide)-Based Amphiphilic and Tripilic Block Copolymers. *Macromolecules* **2011**, *44*, 583–593.
- (17) Mera, A. E.; Griffith, J. R. Melt Condensation and Solution Polymerization of Highly Fluorinated Aliphatic Polyesters. *J. Fluor. Chem.* **1994**, *69*, 151–155.
- (18) Lopez, G.; Ameduri, B.; Habas, J. P. A Versatile Strategy to Synthesize Perfluoropolyether-Based Thermoplastic Fluoropolymers by Alkyne-Azide Step-Growth Polymerization. *Macromol. Rapid Commun.* **2016**, *37*, 711–717.

- (19) Friesen, C. M.; Améduri, B. Outstanding Telechelic Perfluoropolyalkylethers and Applications Therefrom. *Progress in Polymer Science*, **2018**, *81*, 238–280.
- (20) Jaye, J. A.; Sletten, E. M. Modular and Processable Fluoropolymers Prepared via a Safe, Mild, Iodo–Ene Polymerization. *ACS Cent. Sci.* **2019**, *5*, 982–991.
- (21) Jaye, J. A.; Sletten, E. M. Vinyl iodide containing polymers directly prepared via an iodo-yne polymerization. *ACS Macro Lett.* **2020**, *9*, 410–415.
- (22) Xu, T.; Yin, H.; Li, X.; Zhang, L.; Cheng, Z.; Zhu, X. Step Transfer-Addition and Radical-Termination (START) Polymerization of α,ω -Unconjugated Dienes under Irradiation of Blue LED Light. *Macromol. Rapid Commun.* **2017**, *38*, 1600587.
- (23) Sinha, J.; Fairbanks, B. D.; Song, H. B.; Bowman, C. N. Phosphate-Based Cross-Linked Polymers from Iodo-Ene Photopolymerization: Tuning Surface Wettability through Thiol-Ene Chemistry. *ACS Macro Lett.* **2019**, *8*, 213–217.
- (24) Scott, T. F.; Furgal, J. C.; Kloxin, C. J. Expanding the Alternating Propagation-Chain Transfer-Based Polymerization Toolkit: The Iodo-Ene Reaction. *ACS Macro Lett.* **2015**, *4*, 1404–1409.
- (25) Wilson, L. M.; Griffin, A. C. Liquid-Crystalline Fluorocarbon—Hydrocarbon Microblock Polymers. *Macromolecules* **1993**, *26*, 6312–6314.
- (26) Konkolewicz, D.; Gray-Weale, A.; Perrier, S. Hyperbranched Polymers by Thiol-Yne Chemistry: From Small Molecules to Functional Polymers. *J. Am. Chem. Soc.* **2009**, *131*, 18075–18077.
- (27) Huang, B.; Chen, M.; Zhou, S.; Wu, L. Synthesis and Properties of Clickable A(B-b-C)₂₀ Miktoarm Star-Shaped Block Copolymers with a Terminal Alkyne Group. *Polym. Chem.* **2015**, *6*, 3913–3917.
- (28) Opsteen, J. A.; Van Hest, J. C. M. Modular Synthesis of Block Copolymers via Cycloaddition of Terminal Azide and Alkyne Functionalized Polymers. *Chem. Commun.* **2005**, *1*, 57–59.

- (29) Liu, J. T.; Zhao, F. L. A Novel Synthesis of 5-Perfluoroalkyl-2,3-Dihydro-1,4-Diazepines from 1-Perfluoroalkyl-2-Iodoethylenes. *Synthesis*. **2003**, *15*, 2307–2310.
- (30) Zhao, F.; Yang, X.; Liu, J. The Reaction of 2-Fluoroalkyl-1-Iodoethylenes with Arylamines: A Facile Method for the Synthesis of Fluoroalkylated Quinolines and Enaminoketones. *Tetrahedron* **2004**, *60*, 9945–9951.
- (31) Tellers, J.; Pinalli, R.; Soliman, M.; Vachon, J.; Dalcanale, E. Reprocessable Vinylogous Urethane Cross-Linked Polyethylene: Via Reactive Extrusion. *Polym. Chem.* **2019**, *10*, 5534–5542.
- (32) Denissen, W.; Driesbeke, M.; Nicola, R.; Leibler, L.; Winne, J. M.; Du Prez, F. E. Chemical Control of the Viscoelastic Properties of Vinylogous Urethane Vitrimers. *Nat. Commun.* **2017**, *8*, 1–7.
- (33) Lessard, J. J.; Scheutz, G. M.; Sung, S. H.; Lantz, K. A.; Epps, T. H.; Sumerlin, B. S. Block Copolymer Vitrimers. *J. Am. Chem. Soc.* **2020**, *142*, 283–289.
- (34) Denissen, W.; De Baere, I.; Van Paepegem, W.; Leibler, L.; Winne, J.; Du Prez, F. E. Vinylogous Urea Vitrimers and Their Application in Fiber Reinforced Composites. *Macromolecules* **2018**, *51*, 2054–2064.
- (35) Lv, J.; Cheng, Y. Fluoropolymers in Biomedical Applications: State-of-the-Art and Future Perspectives. *Chem. Soc. Rev.* **2021**, *50*, 5435–5467.
- (36) Marsat, J. N.; Heydenreich, M.; Kleinpeter, E.; Berlepsch, H. V.; Böttcher, C.; Laschewsky, A. Self-Assembly into Multicompartment Micelles and Selective Solubilization by Hydrophilic-Lipophilic-Fluorophilic Block Copolymers. *Macromolecules* **2011**, *44*, 2092–2105.
- (37) Li, X.; Yang, Y.; Li, G.; Lin, S. Synthesis and Self-Assembly of a Novel Fluorinated Triphilic Block Copolymer *Polym. Chem.* **2014**, *5*, 4553–4560.

- (38) Estabrook, D. A.; Ennis, A. F.; Day, R. A.; Sletten, E. M. Controlling Nanoemulsion Surface Chemistry with Poly(2-Oxazoline) Amphiphiles. *Chem. Sci.* **2019**, *10*, 3994–4003.
- (39) Kaberov, L. I.; Verbraeken, B.; Riabtseva, A.; Brus, J.; Radulescu, A.; Talmon, Y.; Stepanek, P.; Hoogenboom, R.; Filippov, S. K. Fluorophilic-Lipophilic-Hydrophilic Poly(2-Oxazoline) Block Copolymers as MRI Contrast Agents: From Synthesis to Self-Assembly. *Macromolecules* **2018**, *51*, 6047–6056.
- (40) Kaberov, L. I.; Verbraeken, B.; Riabtseva, A.; Brus, J.; Talmon, Y.; Stepanek, P.; Hoogenboom, R.; Filippov, S. K. Fluorinated 2-Alkyl-2-Oxazolines of High Reactivity: Spacer-Length-Induced Acceleration for Cationic Ring-Opening Polymerization As a Basis for Triphilic Block Copolymer Synthesis. *ACS Macro. Lett.* **2018**, *7*, 7–10.
- (41) Glassner, M.; Vergaelen, M.; Hoogenboom, R. Poly(2-Oxazoline)s: A Comprehensive Overview of Polymer Structures and Their Physical Properties. *Polym. Int.* **2018**, *67*, 32–45.
- (42) Lee, C. U.; Khalifehzadeh, R.; Ratner, B.; Boydston, A. J. Facile Synthesis of Fluorine-Substituted Polylactides and Their Amphiphilic Block Copolymers. *Macromolecules* **2018**, *51*, 1280–1289.
- (43) Lim, I.; Vian, A.; Van De Wouw, H. L.; Day, R. A.; Gomez, C.; Liu, Y.; Rheingold, A. L.; Campàs, O.; Sletten, E. M. Fluorous Soluble Cyanine Dyes for Visualizing Perfluorocarbons in Living Systems. *J. Am. Chem. Soc.* **2020**, *142*, 16072–16081.
- (44) Kimura, T.; Kasuya, M. C.; Hatanaka, K.; Matsuoka, K. Synthesis of Fluorinated Polymers and Evaluation of Wettability. *Molecules* **2016**, *21*, 358–364.
- (45) Katano, Y.; Tomono, H.; Nakajima, T. Surface Property of Polymer Films with Fluoroalkyl Side Chains. *Macromolecules* **1994**, *27*, 2342–2344.
- (46) Schneider, J.; Erdelen, C.; Ringsdorf, H.; Rabolt, J. F. Structural Studies of Polymers with Hydrophilic Spacer Groups. 2. Infrared Spectroscopy of Langmuir-Blodgett Multilayers of

Polymers with Fluorocarbon Side Chains at Ambient and Elevated Temperatures.

Macromolecules **1989**, *22*, 3475–3480.

- (47) Pangborn, A. B.; Giardello, M. A.; Grubbs, R. H.; Rosen, R. K.; Timmers, F. J. Safe and Convenient Procedure for Solvent Purification. *Organometallics* **1996**, *15*, 1518–1520.

Simple synthesis of fluorinated ene-yne via *in-situ* generation of allenes

Adapted from Joseph A. Jaye and Ellen M. Sletten.* Simple synthesis of fluorinated ene-yne via *in-situ* generation of allenes. *Synthesis* **2021**, DOI: 10.1055/s-0037-1610774

5.1 Abstract

Fluorination of small molecules is a key route toward modulating reactivity and bioactivity. The 1,3 ene-yne functionality is an important synthon towards complex products, as well as a common functionality in biologically active molecules. Here, we present a new synthetic route towards fluorinated ene-yne through simple starting materials. We employ gas chromatography-mass spectrometry analysis to probe the sequential eliminations necessary for this transformation and observe an allene intermediate. The ene-yne products are sufficiently fluorinated to enable purification via fluorinated extraction. This methodology will allow facile access to functional, fluorinated ene-yne.

5.2 Introduction

Since the incorporation of a single fluorine atom in uracil to make Fluorouracil **5.1** (Figure 5.1A) in 1957, fluorination has been a valuable strategy for the medicinal chemistry community.^{1,2} The unique combination of electronic and steric properties imparted by fluorine provide opportunities to tune stability, pharmacokinetics, and binding affinities of small molecule therapeutics. Methods to introduce a single fluorine^{3,4}, trifluoromethyl groups (as seen in Fluoxetine **5.2**)⁵⁻⁸, and even longer perfluoroalkyl chains have been extensively pursued.^{9,10}

As methodology has progressed, access to more advanced fluorinated motifs has been granted. In particular, non-aromatic sp^2 hybridized fluoride containing compounds are of growing interest based on their prevalence in bioactive compounds and function as non-hydrolyzable mimics of amide bonds.^{11,12} For example, monofluoro dipeptide mimic **5.3** (Figure 5.1A) was incorporated into an analog of

neuropeptide Substance P (SP), and found to have similar binding affinities as natural SP for its receptor. Pheromones have also been synthesized to contain vinyl fluoride functionality.¹³

Conjugation of a vinyl fluoride to an alkyne gives a new class of compounds– 1,3 ene-yne. Vitamins, prostaglandins, pheromones and unsaturated fatty acids containing fluorinated ene-yne have been prepared.^{14–16} Notably, monofluoro ene-yne **5.4** (Figure 5.1A) was found to have improved antipheromone properties when compared to its hydrogen analog.¹⁷ Not only are ene-yne present in biologically active compounds¹⁸, but they are also useful synthetic intermediates.¹⁹ Conjugated fluorinated ene-yne have been utilized as Michael acceptors or as intermediates towards fluorinated diynes.^{20,21} Additionally, the conjugated vinyl fluoride can be displaced via acetylides to give ene-diyne inhibitors.²² Finally, fluorinated ene-yne can serve as a starting material for fluorinated allenes (Figure 5.1B), another fluorinated functional group with rising popularity.^{23–27}

Previous work to access vinyl-fluoride containing ene-yne has largely involved palladium catalyzed Sonogashira-type couplings of functionalized olefins (Figure 5.1C, middle).^{14,21,22,28–31} Metal-free approaches to fluorinated ene-yne include couplings with fluorinated sulfonates or phosphonates via Julia or Horner-Wadsworth-Emmons olefination, respectively.^{18,32} These methods are often limited via the multi-step syntheses required to reach the requisite vinyl fluoride coupling partners. Currently, there is only a single reported method to incorporate a fluorinated chain onto 1-fluoro ene-yne without use of a metal catalyst (Figure 5.1C, left).²⁰ This approach involves allene starting materials, which limit the scope of ene-yne that are able to be prepared. Here, we report a new, simple, metal-free approach to fluorinated ene-yne preparation from readily available terminal alkynes and perfluoroalkyl iodide starting materials (Figure 5.1C, right). We envisioned that the simplicity of these starting materials would enable a larger scope of ene-yne products to be accessed when compared to existing methods.

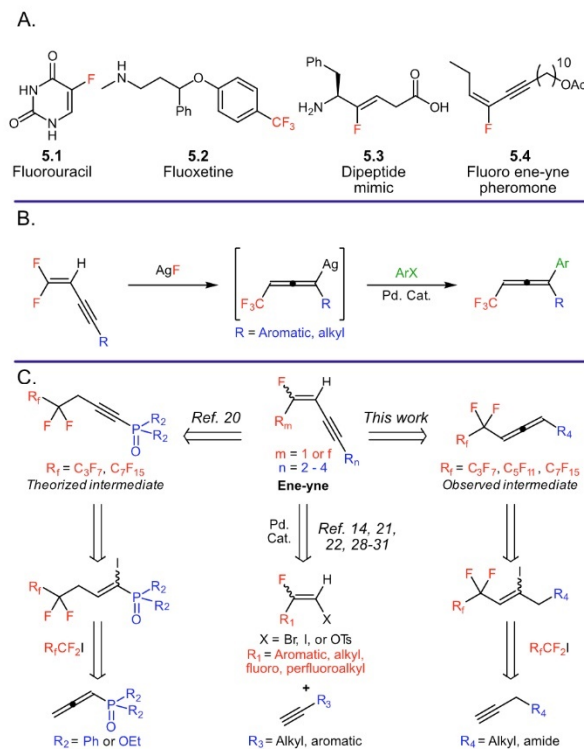


Figure 5.1 Selected examples of fluorinated bioactive compounds and chemistries related to vinyl fluorides and fluorinated ene-ynes. **A.** Bioactive fluorinated compounds. **B.** Synthesis of fluorinated allenes via difluoro ene-ynes. **C.** Retrosynthetic analysis of different pathways to reach fluorinated ene-ynes.

5.3 Results and discussion

It is well-established that perfluoroalkyl iodide addition into terminal alkynes generates 1,2-disubstituted vinyl iodides as a mixture of E and Z isomers.^{33–36} Previously, we had found that the reaction of fluorinated vinyl iodides with phenols and catalytic copper in basic conditions gave a mixture of an Ullmann coupled vinyl ether and a fluorinated ene-yne (Chapter 2).³⁷ Looking to better understand the mechanism of ene-yne formation and determine optimized conditions for this unique transformation, we built from the Ullmann conditions (Table 5.1, Entry 1), employing vinyl iodide **5.5** as a model substrate and monitoring conversion by gas chromatography mass spectrometry (GC-MS). The Ullmann conditions produced desired ene-yne **5.6** in 55% yield, measured by integration of GC peaks.

Scheme 5.1 Transformation of vinyl iodide **5.5** to ene-yne **5.6**

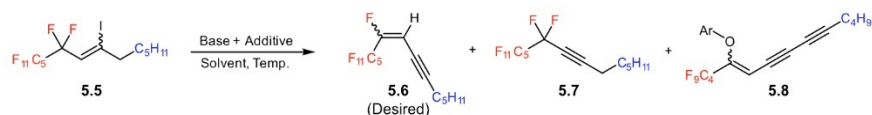


Table 5.1 Optimization of reaction conditions for the formation of fluorinated ene-yne **5.6** from vinyl iodide **5.5**.

Trial	Solvent	Base	Additives	Time (Hours)	Temp (°C)	5.5 ^a	5.6 ^a	5.7 ^a	5.8 ^a
1	Dioxane	Cs ₂ CO ₃ (2.0 equiv.)	CuI (10 mol%), <i>N,N</i> -Dimethyl glycine (30 mol%), 2,5-Dimethylphenol (4.0 equiv.),	18	85	0	55 ^b	0	0
2	Dioxane	Cs ₂ CO ₃ (2.0 equiv.)	None	18	85	47	5	48	N/A
3	Dioxane	Cs ₂ CO ₃ (2.0 equiv.)	2,5-Dimethylphenol (4.0 equiv.)	18	85	49	38	13	0
4	Dioxane	Potassium 2,5-dimethylphenolate (4.0 equiv.)	None	18	85	22	53	11	13
5	Dioxane	Cs ₂ CO ₃ (2.0 equiv.)	2,4,6-Trimethylphenol (4.0 equiv.)	18	85	45	45	9	2
6 ^c	Dioxane	Cs ₂ CO ₃ (3.0 equiv.)	2,5-Dimethylphenol (4.0 equiv.)	18	85	15	83	1	1
7 ^c	Dioxane	Cs ₂ CO ₃ (3.0 equiv.)	2,5-Dimethylphenol (4.0 equiv.)	18	105	10	89	1	1
8 ^c	Dioxane	Cs ₂ CO ₃ (4.5 equiv.)	2,5-Dimethylphenol (4.5 equiv.)	18	85	0	93	0	7
9	Dioxane	Cs ₂ CO ₃ (4.0 equiv.)	18-C-6 (4.0 equiv.)	18	85	0	39	51	N/A
10	Dioxane	Cs ₂ CO ₃ (4.0 equiv.)	18-C-6 (4.0 equiv.)	18	105	0	60	40	N/A
11	Dioxane/Silicone oil (19:1)	Cs ₂ CO ₃ (4.0 equiv.)	18-C-6 (4.0 equiv.)	18	105	4	82	13	N/A
12	DMF	Cs ₂ CO ₃ (5.0 equiv.)	18-C-6 (1.0 equiv.)	18	85	0	96 (47) 13:87 E/Z ^d	0	N/A
13	DMF	Cs ₂ CO ₃ (5.0 equiv.)	None	18	85	0	35	65	N/A
14 ^c	DMF	Cs ₂ CO ₃ (4.5 equiv.)	2,4,6-Trimethylphenol (4.5 equiv.)	18	85	0	35	0	65
15 ^c	DMF	Cs ₂ CO ₃ (4.5 equiv.)	2,5-Dimethylphenol (4.5 equiv.)	18	85	0	100	0	0
16	DMF	TMG (3.0 equiv.)	None	2	50	0	32	57	N/A
17	DMF	DBU (3.0 equiv.)	None	2	50	0	84 (46) 10:90 E/Z ^d	0	N/A
18	DMF	MTBD (3.0 equiv.)	None	2	50	0	94	1	N/A
19	MeCN	MTBD (3.0 equiv.)	None	2	50	0	73	27	N/A
20	THF	MTBD (3.0 equiv.)	None	2	50	0	37	50	N/A
21	DMF	MTBD (4.0 equiv.)	None	2	50	0	99 (64) 15:85 E/Z ^d	1	N/A

^a Conversion determined via peak integration of gas chromatography (GC) trace. Number in parentheses corresponds to isolated yield. ^b Phenol coupled product accounts for the remaining yield. ^c Products were observed by NMR that were not visible by GC-MS. ^d Determined through integration of ¹H-NMR Spectra.

Removing both the copper and phenol required for the Ullmann coupling decreased the desired ene-yne product conversion by 50%, providing a mixture of equivalent amounts of starting material **5.5** and alkyne

5.7 (Table 5.1, Entry 2). Although only trace amounts of **5.6** were observed, this result suggested that copper-catalysis was not necessary for ene-yne formation. The yield of **5.6** was significantly improved when 2,5-dimethylphenol was introduced as an additive (Table 5.1, Entry 3). Pre-forming the phenol salt improved conversion to **5.6**, but introduced phenoxide addition impurity **5.8** (Table 5.1, Entry 4). 2,4,6-trimethylphenol proved to be superior to 2,5-dimethylphenol, yielding 45% **5.6** but the increased electron density of the aromatic system increased nucleophilicity of the phenol and byproduct **5.8** was also observed (Table 5.1, Entry 5). Increasing the base loading and temperature improved conversion to **5.6** (Table 5.1, Entry 6-8) but significant amounts of **5.8** were detected via GC-MS and other addition products not visible by GC-MS were apparent via nuclear magnetic resonance (NMR) spectra.

We further probed the role of the phenol, considering two hypotheses: 1) phenol aided in solubilizing the carbonate base and 2) phenol facilitated fluoride elimination. To probe the first hypothesis, 18-crown-6 ether (18-C-6) was added in place of the phenol (Table 5.1, Entries 9 and 10). Significant differences in the production of **5.6** with 2,5-dimethylphenol and 18-C-6 as additives were observed, with 18-C-6 producing poorer conversion to **5.6** (Table 5.1, entries 9 vs 8). To test the second hypothesis, a silane additive was employed to further sequester the fluoride. A silicon oil/dioxane mixture was utilized as the solvent with the 18-C-6 coadditive. Here, we found a significant increase in preparation of **5.6**, with an 82% yield via GC-MS analysis (Table 5.1, Entry 11). These data suggested that stabilization of fluoride was important and prompted a change to the more polar dimethylformamide (DMF), yielding almost full conversion to **5.6** (Table 5.1, Entry 12). Unfortunately, our isolated yield was rather modest (47%) which we believe to be due to polymeric byproducts not observed in the GC-MS analysis. Although the solubility of Cs_2CO_3 is increased in DMF, we found that 18-C-6 was still necessary to achieve high conversions (Table 5.1, Entry 13). From these data, we believe that the major role of phenol was aiding fluoride elimination, with the solubilization of Cs_2CO_3 being a secondary factor. Further reactions with phenol additives were then attempted with the use of DMF as a solvent (Table 5.1, Entries 14 and 15). 2,4,6-trimethylphenol gave addition product **5.8** as the main product, and 2,5-dimethylphenol provided excellent conversion to **5.6** via GC analysis. In both cases, significant phenol

addition products not observable by GC were found with NMR analysis. Moving forward, we retained the polar solvents for fluoride stabilization and looked to remove any necessary additive by increasing the strength of a non-nucleophilic base. Tetramethylguanidine (TMG) provided **5.6** in modest conversion (Table 5.1, Entry 16), while 1,8-diazabicyclo[5.4.0]undec-7-ene (DBU) gave rapid conversion to **5.6**, although isolated yields remained modest (Table 1, Entry 17). 7-methyl-1,5,7-triazabicyclo[4.4.0]dec-5-ene (MTBD) was the most successful of the bases, with 94% conversion to **5.6** in only 2 hours (Table 5.1, Entry 18). Even with strong base, we confirmed that polar solvent was necessary for rapid reaction times (Table 5.1, Entries 18-20). Increasing the loading of MTBD to 4 equivalents increased conversion to 99% with an acceptable 64% isolated yield (Table 5.1, Entry 21).

With the knowledge gained from the reaction optimization, we looked to better understand the mechanism of ene-yne formation (Figure 5.2). As multiple eliminations are necessary to convert **5.5** to **5.6**, we envisioned that sequential additions of MTBD and careful GC-MS analysis would enable intermediate identification (Figure 5.2A). Addition of 1 equivalent of MTBD gave primarily alkyne **5.7**

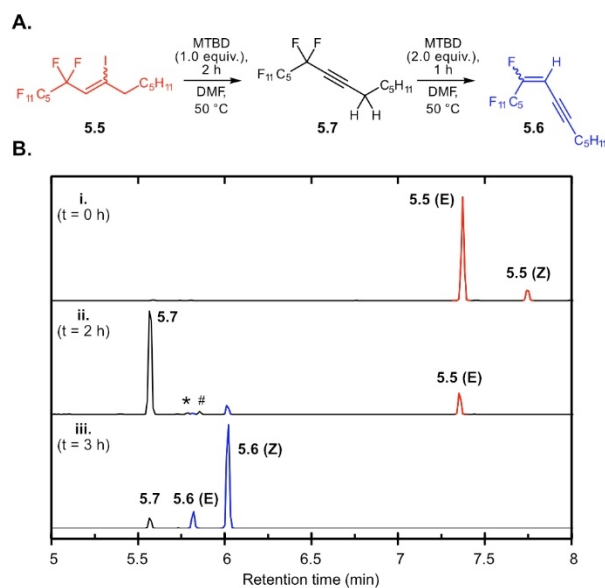


Figure 5.2 GC-MS analysis of the transformation of vinyl iodide **5.5** to ene-yne **5.6**. **A.** Reaction scheme of sequential additions of MTBD to vinyl iodide **5.5**. **B.** GC-MS traces of reaction progress in each phase of the reaction. **i.** Aliquot prior to addition of MTBD. **ii.** An aliquot from the reaction mixture 2 h after **5.5** was combined with 1 equiv. of MTBD and heated to 50 °C. **iii.** An aliquot from the reaction mixture taken 1 h after an additional 2 equivalents of MTBD were added (total reaction time = 3 h). All traces: Vinyl iodide (**5.5**) isomer peaks highlighted in red, Alkyne (**5.7**) peak highlighted in black, and ene-yne (**5.6**) isomer peaks highlighted in blue. A GC-MS standard of **5.6** can be found in Figure 5.3.

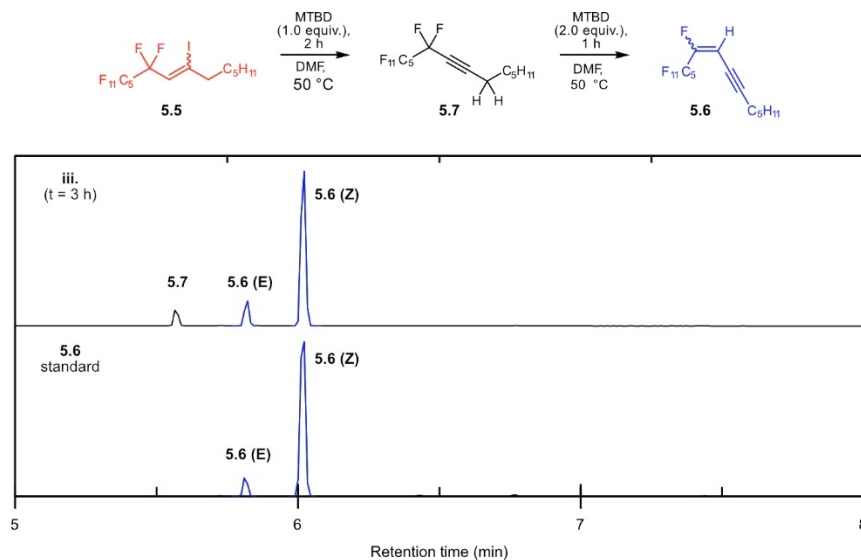
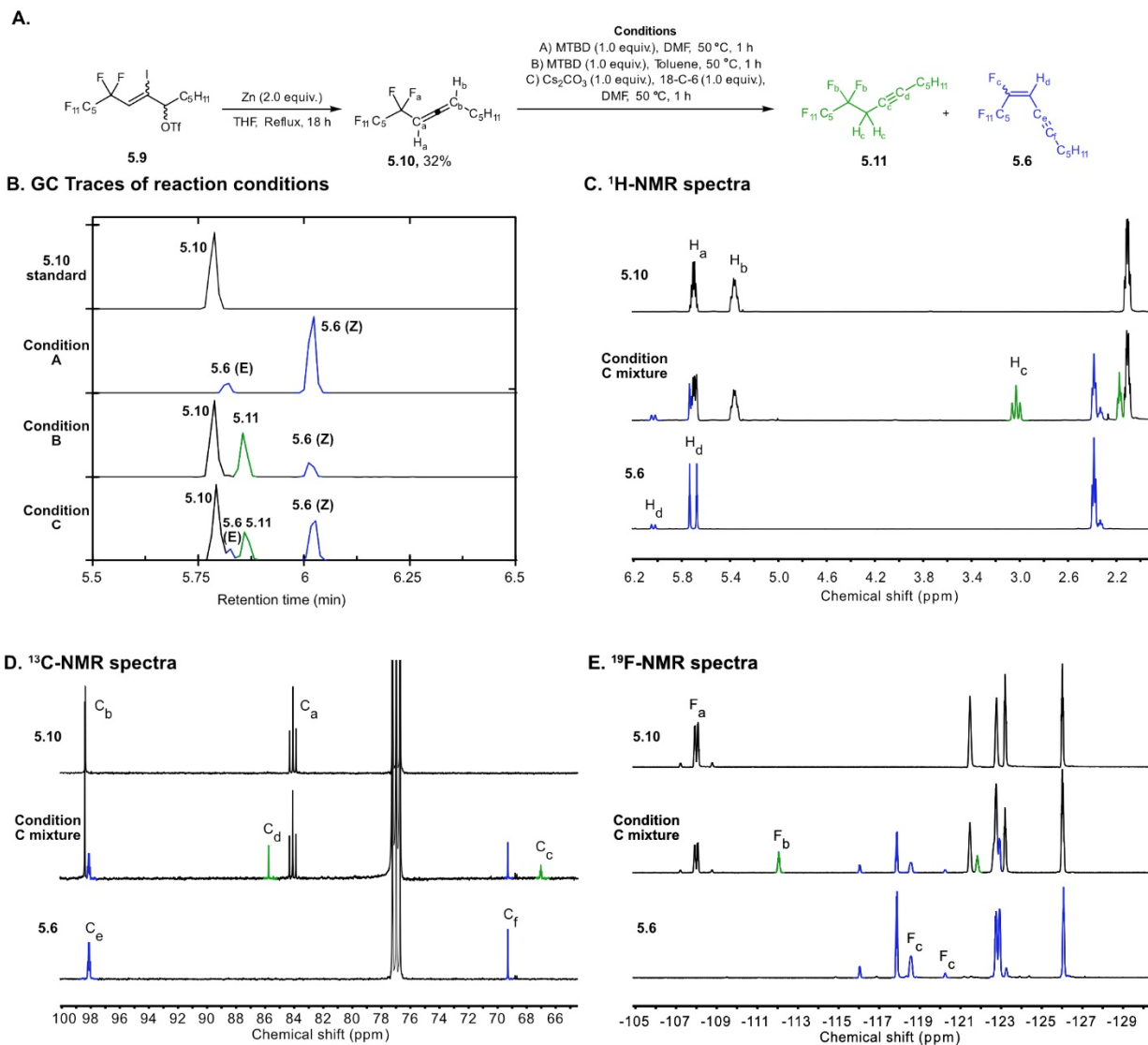


Figure 5.3: Stacked GC-MS traces comparing the sequential elimination of halides from vinyl iodide **5.5** with MTBD (top trace, 3 h aliquot) and pure ene-yne **5.6** (bottom trace).

after 2 hours, with about 10% of starting material and ene-yne product also present in the reaction mixture (Figure 5.2B, **ii** trace). Addition of 2 more equivalents of MTBD and further reaction for an hour showed nearly full conversion to **5.6** (Figure 5.2B, **iii** trace, Figure 5.3). These data suggest that alkyne **5.7** is an intermediate in the transformation of vinyl iodide **5.5** to ene-yne **5.6**. Looking closer at these data, in the 2 h trace, in addition to **5.6** there were two small peaks at 5.8 and 5.85 minutes (designated with asterisk and pound, respectively, in Figure 5.2B, **ii** trace) both with an isomeric mass to alkyne **5.7**. Our first proposal for the identity of one of these intermediates was an allene intermediate (**5.10**, Figure 5.4A).

We independently synthesized the hypothesized allene intermediate **5.10** from activated triflate **5.9** (Figure 5.4A). With **5.10** in hand as a standard, we were able to confirm that the previously observed GC-MS peak at 5.80 minutes (Figure 5.2B, asterisk) was an allene intermediate (Figure 5.5). Next, we employed isolated allene **5.10** as a starting material to probe for ene-yne conversion and attempted to identify the isomeric peak at 5.85 minutes (Figure 5.2A). We found that 1 equivalent of MTBD in DMF at 50 °C gave clean and rapid isomerization from



Figure

5.4: Exploration of allene **5.10** as an intermediate in ene-yne synthesis. **A.** Preparation of allene **5.10** and conversion to the ene-yne product **5.6** and proposed reaction intermediate **5.11**. **B.** GC-MS traces of allene (**5.10**) standard and reaction conditions A-C. **C.** ¹H-NMR spectra of **5.10** (top trace), mixture of products isolated from reaction mixture C (middle trace), and ene-yne (**5.6**) standard (bottom trace). **D.** ¹³C-NMR of **5.10** (top trace), reaction mixture C (middle trace), and **5.6** (bottom trace). **E.** ¹⁹F-NMR of **5.10** (top trace), reaction mixture C (middle trace), and **5.6** (bottom trace). All traces: All peak labels represented with the following color representation: Allene (**5.10**) highlighted in black, proposed alkyne intermediate (**5.11**) highlighted in green, and ene-yne (**5.6**) highlighted in blue.

allene **5.10** to ene-yne **5.6** in 1 hour (Figure 5.4B, Condition A). Switching the solvent from polar DMF to non-polar toluene, greatly slowed conversion to ene-yne **5.6** and enabled the peak at 5.85 minutes to be observed (Figure 5.4B, Condition B, green peak). The species eluting at 5.85 minutes was also present when using a weaker base, Cs₂CO₃, with 18-C-6 as an additive, in DMF (Figure 5.4A, Condition C). Notably, in none of the given conditions did we observe alkyne **5.7** generated from allene **5.10**, suggesting that in basic conditions alkyne **5.7** irreversibly isomerizes to allene **5.10**. Similar isomerization patterns have been observed from aryl substituted trifluoromethyl allenes.³⁸

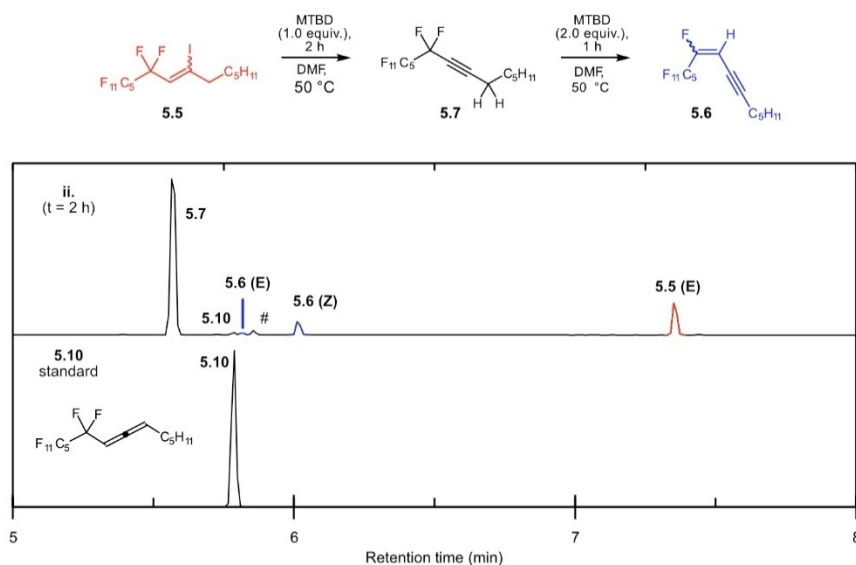


Figure 5.5: Stacked GC-MS traces comparing the sequential elimination of halides from vinyl iodide **5.5** with MTBD (top trace, 2 h aliquot) and pure allene **5.10** (bottom trace).

Upon further GC-MS and NMR spectra analysis (Figure 5.4C) we proposed the compound with a 5.85 min retention (Figure 5.2B, pound) to be the activated alkyne **5.11**. Unfortunately, we were unable to obtain an analytical standard of **5.11** as there are no facile methods that selectively produce internal alkynes beta to a perfluorinated chain, likely due to synergistic activation of the methylene protons being both propargylic and adjacent to a fluororous chain. Separation challenges prevented the isolation of **5.11** from **5.10**. We moved forward to confirm the identity of **5.11** on the mixture obtained after purification of the condition C reaction on a silica gel column eluting with hexanes. The isolated mixture of compounds was compared to standards of allene (**5.10**) and ene-yne (**5.6**). Analysis of the $^1\text{H-NMR}$ spectra showed a new triplet centered at 3.03 ppm not consistent with **5.10** or **5.6** (Figure 5.4C, green peaks, middle trace) with a J coupling of 16.2 Hz and integration of 2 (assigned H_c), suggesting a methylene group coupled to a CF_2 . This peak matches a similar fluororous acetylenic compound found in the literature.³⁹ Additionally, there is a secondary peak centered at 2.18 ppm, split into a triplet of triplets with J couplings of 7.2 and 2.5 Hz, respectively. These couplings are consistent with long-range interactions across a C-C triple bond. Further analysis of the $^{13}\text{C-NMR}$ spectra indicated two new signals in the 65-90 ppm range not consistent with allene **5.10** or ene-yne **5.6** (Figure 5.4D, green peaks, middle trace). Additionally, the carbon labeled C_c of alkyne **5.11** is split into a triplet with a J coupling of 6.0 Hz, consistent with a carbon that is beta to a CF_2 group. Finally, the $^{19}\text{F-NMR}$ spectra of the purified reaction

C mixture was analyzed in comparison to allene **5.10** and ene-yne **5.6**. As with the previous spectra, there are two new notable peaks that are not consistent with either standards (Figure 5.4E, green peaks, middle trace): a multiplet centered at -112.1 ppm and a broad singlet centered at -121.8 ppm are a close match to the previously mentioned acetylenic literature compound.³⁹

To better observe these key intermediates starting from vinyl iodides, the reaction of vinyl iodide **5.5** with Cs₂CO₃ and 18-C-6 as an additive (Table 5.1, Entry 13) was monitored over an extended reaction period of 18 hours (Figure 5.6). In contrast to trials with use of MTBD as a base, allene intermediate **5.10** is prominently observed within an hour of reaction, with ene-yne **5.6** and alkyne **5.11** being found in lesser amounts throughout the reaction.

Collectively, our studies and observations have led us to propose the mechanism in Scheme 5.2. The strong electron withdrawing nature of the perfluoroalkyl group provides fast elimination of the vinyl iodide from starting material **5.5** to yield internal alkyne **5.7**. From the internal alkyne, irreversible isomerization to allene **5.10** occurs giving the active intermediate. This key isomerization step is likely aided by the electron withdrawing perfluoroalkyl group stabilizing the anionic intermediate alpha to the fluororous chain. From **5.10**, the mechanism is dependent on reaction conditions. In a non-polar solvent, where fluoride release is disfavored, or in a polar solvent with a weak base, the dominant pathway proceeds through further isomerization from allene **5.10** to internal alkyne **5.11**. From **5.11**, HF is eliminated to give ene-yne **5.6**. Alternatively, if MTBD is used with a polar solvent, direct elimination of HF from allene **5.10** is observed as the dominant pathway to give **5.6**. A similar one-step elimination has previously been reported via cyclic allenyl halides;⁴⁰ however, we cannot rule out that MTBD acts as an efficient proton shuttle and rapidly passes through internal alkyne **5.11**. The small amount of **5.11** observed in Figure 5.2B suggest that the two pathways compete with each other.

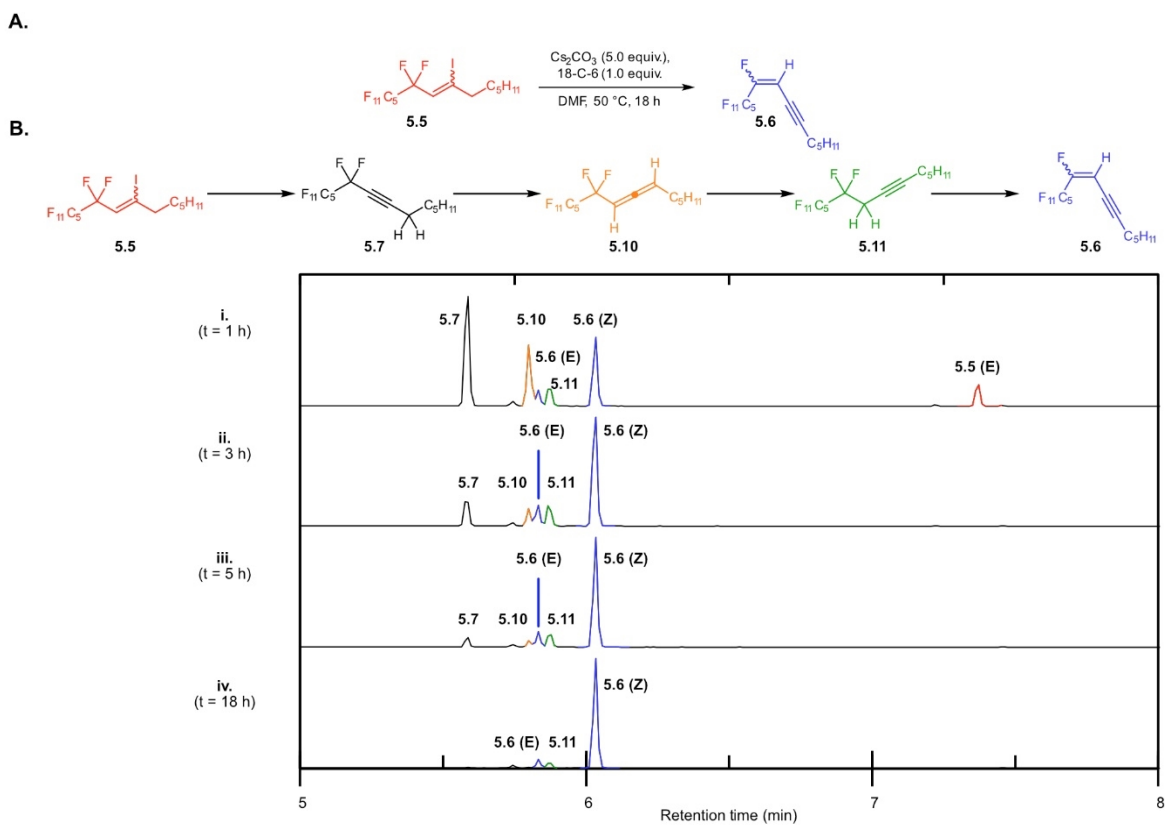
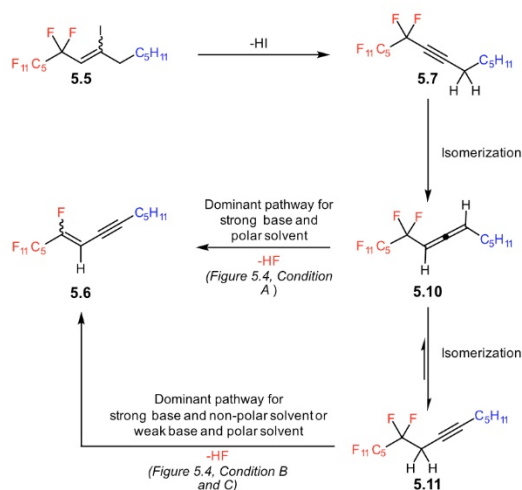
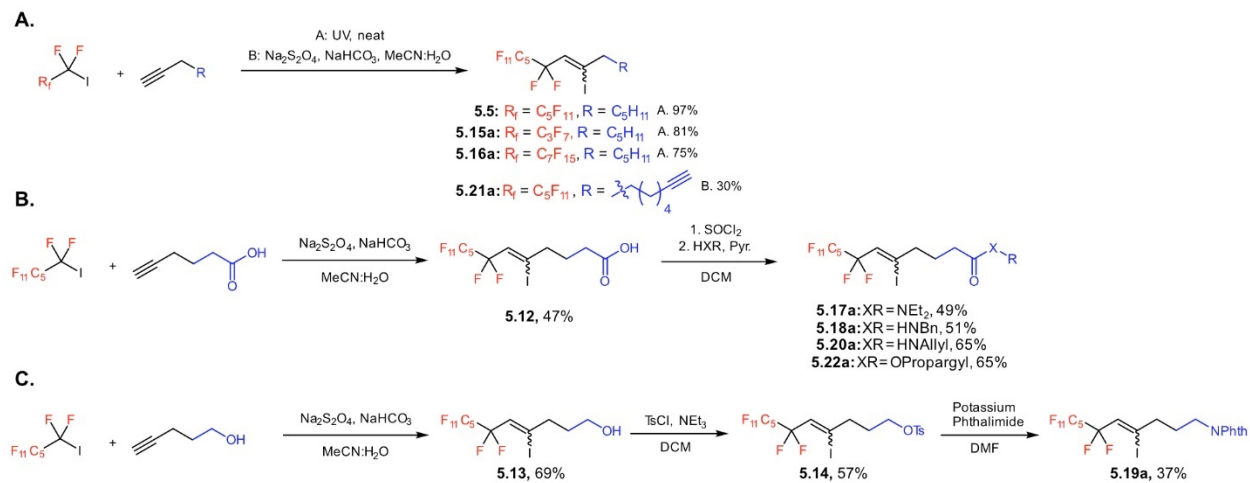


Figure 5.6: Reaction of vinyl iodide **5.5** with a Cs_2CO_3 in DMF. **A.** Reaction scheme of the transformation of vinyl iodide **5.5** to ene-yne **5.6**. **B.** General reaction pathway (see Scheme 5.2 for full proposed mechanism) and stacked GC-MS traces monitoring the reaction of vinyl iodide **5.5** with excess Cs_2CO_3 and 18-C-6. Loss of vinyl iodide **5.5** and alkyne **5.7** peak over time, with growth of ene-yne peak **5.6** (E and Z isomers) throughout reaction. All traces: Vinyl iodide (**5.5**) highlighted in red, Alkyne (**5.7**) highlighted in black, Allene (**5.10**) highlighted in orange, Alkyne (**5.11**) highlighted in green, ene-yne (**5.6**) highlighted in blue.



Scheme 5.2 Proposed mechanism for the transformation of vinyl iodide **5.5** to fluorous ene-yne **5.6**.



Scheme 5.3: Synthesis of intermediate vinyl iodide compounds used towards synthesis of ene-yne. **A.** Synthesis of vinyl iodides directly from terminal alkynes. **B.** Synthesis of vinyl iodides through acid chloride coupling, produced from acid **5.12**. **C.** Synthesis of vinyl iodide **5.19a** through tosylate **5.14**.

Finally, we looked to explore the substrate scope of this newly developed sequential elimination reaction. In some cases, the starting vinyl iodides were easily prepared in one step through perfluoroalkyl addition to terminal alkynes to give the desired products (**5.6**, **5.15a**, **5.16a**, **5.21a**, Table 5.2). In other cases, perfluoroalkylation of terminal alkynes gave an intermediate carboxylic acid (**5.12**) or tosylate (**5.14**) for further derivatization (Scheme 5.3). Higher complexity was added to the vinyl iodide substrates through an acid chloride coupling or tosylate substitution to give substrates **5.17a-5.20a**, **5.22a** (Scheme 5.4, Table 5.2).

We began our substrate exploration through shortening and lengthening the fluororous chain. Perfluorobutyl derivative **5.15b** was readily synthesized from **5.15a**, with full conversion observed via GC-MS. Variable isolated yields (from 41-84%) were obtained due to its volatile nature. Unexpectedly, the perfluorooctyl substrate **5.16a** required longer reaction times than necessary for **5.5** or **5.15a** to convert to ene-yne product. After 18 h, **5.16b** conversion was nearly complete and **5.16b** was isolated in 62% yield via fluorous extraction. While generally purification via partitioning into the fluorous phase requires an eight carbon perfluoroalkyl chain as found in **5.16b**,⁴¹ we were also able to purify shorter-chain containing ene-yne **5.6** and **5.15b** by fluorous extraction.

Scheme 5.4 Substrate scope of the reaction of vinyl iodides to fluorous ene-yne.**Table 5.2** Substrate scope of the reaction of vinyl iodides to fluorous ene-yne.

Compound #	MTBD equiv.	Temp. (°C)	Time (h)	Yield (%)	E/Z ratio ^d	Product ratio (b:c) ^e
5.15	4.0	50	2	41-84 ^{a,c}	13:87	100:0
5.16	4.0	50	18	62 ^a	17:83	99:1
5.17	3.0	rt	18	73 ^a	21:79	100:0
5.18	3.0	rt	18	60 ^b	15:85	96:4
5.19	4.0	rt	18	56 ^b	15:85	96:4
5.20	3.0	rt	18	64 ^a	20:80	96:4
5.21	3.0	rt	18	73 ^a	17:83	98:2

a. Purified via fluorous extraction. **b.** Purified via column chromatography. **c.** Range in yield due to volatility of product. **d.** Determined by integration of ¹H-NMR. **e.** Determined by integration of ¹⁹F-NMR

Next, we looked to expand the ene-yne able to be accessed to include alcohols, acids, esters, amides, and amines as these are important functional groups in bioactive molecules. To increase the compatibility with these polar functional groups, base loading was lowered from 4 to 3 equivalents. In the case of alcohols and carboxylic acid derivatives, complex mixtures of oligomers, cyclized products, and ene-yne were observed, owing to the basic reaction conditions and available acidic protons. Although conversion to ene-yne derivatives containing esters was well tolerated, we noted additional isomerization occurred to give a complex mixture of isomeric products after loss of fluoride (Figure 5.7). We believe this pathway could be blocked in the future through lengthening of the alkyl chain spacer between vinyl iodide and ester group. In comparison, amides proceeded readily at room temperature with elongated reaction times. Disubstituted amide **5.17b** was isolated via extraction from methoxy perfluorobutyl ether with no remaining alkyne in 73% yield and monosubstituted benzyl amide **5.18b** was isolated in 60% yield with small amounts of alkyne **5.18c**. While direct implementation of amino-groups was

unsuccessful, phthalimide-protected amine **5.19b** could be isolated in 56% yield, again with low amounts of alkyne **5.19c**. Notably, we returned to 4 equivalents of MTBD in this trial due to the unreactive nature of the phthalimide and decreased concerns for degradation. It has been observed that when aromatic groups are present, extraction into the fluorous phase is reduced due to the polarizable π system⁴² and column chromatography was required for purification of both **5.18b** and **5.19b**.

We also designed substrates with terminal alkene and alkyne functionality that would allow for further modification by click chemistries.⁴³ The installation of click functional handles was first demonstrated through monosubstituted amide **5.20b** containing an allyl group, which could be synthesized in a modest yield of 64%, with low amounts of alkynes **5.20c** in the mixture. Similar to disubstituted amide **5.17b**, allyl containing substrate **5.20b** could be purified via extraction with methoxy perfluorobutyl ether. The terminal alkene of **5.20b** provides a handle for thiol-ene chemistries or olefin metathesis.^{44,45} Continuing in our pursuit towards functionalizable ene-yne, terminal alkyne **5.21b** was readily synthesized in 73% yield and purified via extraction with perfluorohexanes. The terminal alkyne of **5.21b** provides opportunities for further click chemistry derivatization or bioconjugation.^{46,47}

5.4 Conclusion

To conclude, we have explored the preparation of fluorous ene-yne from fluorinated vinyl iodide starting materials. Notably, this reaction proceeded through a distinguishable allene intermediate, in contrast to previously established methods. The fluorinated ene-yne were produced in modest to good yields. In addition, a variety of functional groups could be appended to the starting materials including terminal alkynes and alkenes, aromatic groups, amides, and phthalimides. In general, this route provides a simplistic approach to fluorous ene-yne as the requisite vinyl iodides are readily synthesized from widely available starting materials, the reaction proceeds under mild conditions with no exclusion of air or water, and in most cases the products can be purified through facile fluorous extraction. Furthermore, formation of an electrophilic allene as a key intermediate could lead to nucleophilic trapping to form

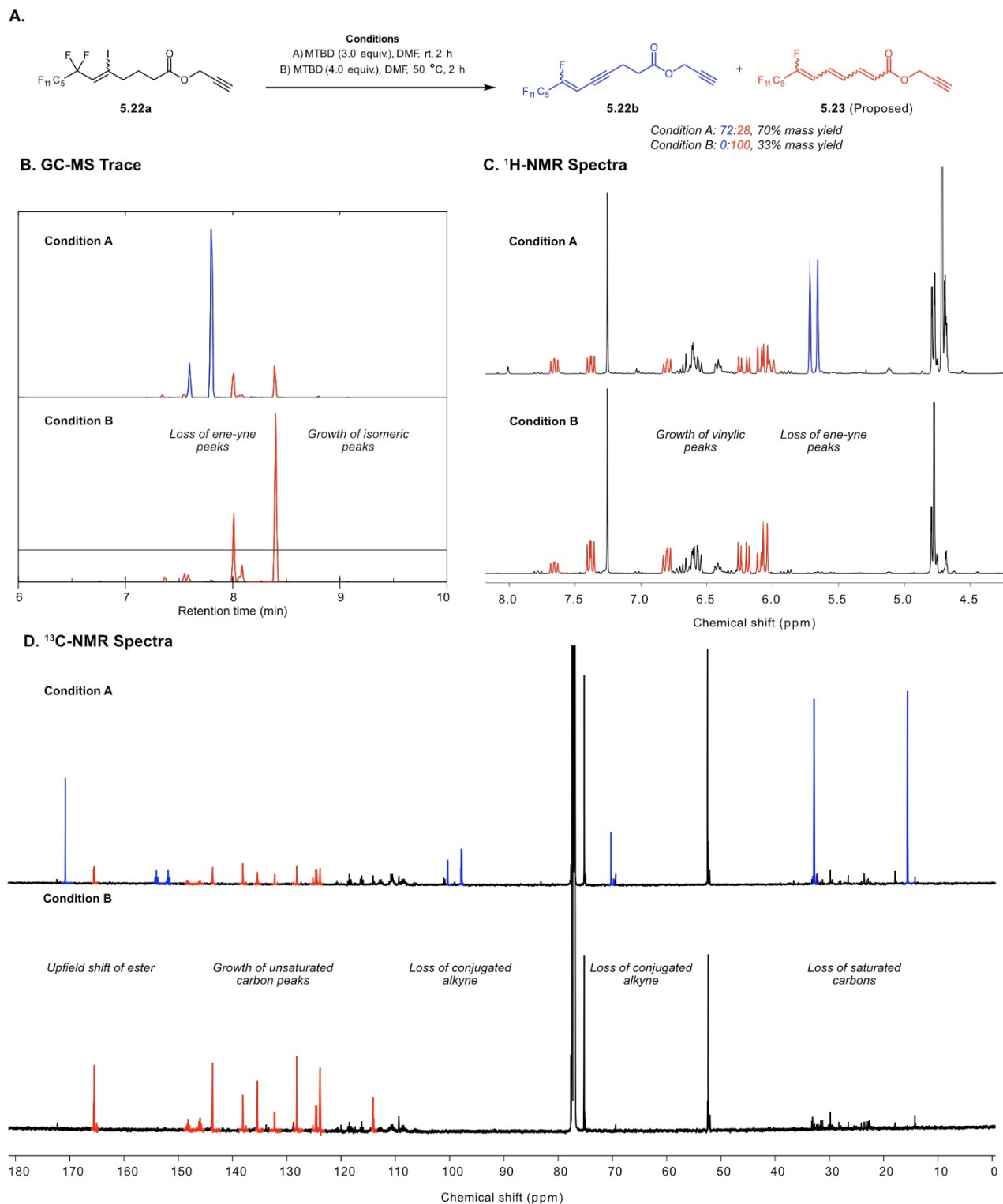


Figure 5.7: Comparison of conditions towards the synthesis of ene-yne **5.22b** and the following isomerization to proposed triene **5.23**, with and without excess base. **A.** Reaction scheme of the formation of mixtures of ester containing ene-yne **5.22b** and proposed triene **5.23** in different conditions. Excess base (condition B) consumes any remaining **5.22b** towards **5.23** (proposed). **B.** GC-MS trace indicating loss of **5.22b** and growth of isomeric compounds. **C.** ¹H-NMR spectra showing loss of vinylic ene-yne signals and growth of new vinylic protons. **D.** ¹³C-NMR spectra demonstrating loss of saturated carbon and conjugated alkyne signals, with simultaneous growth of unsaturated carbon signals. Upfield shift from 171 ppm to 165 ppm of ester C=O carbon, could be a result of conjugation.

complex fluorinated small molecules. We envision this method to allow access to a range of ene-ynes previously unavailable in as little as two steps.

5.5 Experimental procedures

5.5.1 General experimental procedures

Chemical reagents were purchased from Sigma-Aldrich, Alfa Aesar, Fisher Scientific, or Acros Organics and used without purification unless noted otherwise. No unexpected or unusually high safety hazards were encountered. Anhydrous and deoxygenated solvents toluene (PhMe), tetrahydrofuran (THF), dichloromethane (DCM), acetonitrile (MeCN), and dimethylformamide (DMF) were dispensed from a Grubb's-type Phoenix Solvent Drying System.⁴⁸ Thin layer chromatography was performed using Silica Gel 60 F254 (EMD Millipore) plates. Flash chromatography was executed with technical grade silica gel with 60 Å pores and 40–63 µm mesh particle size (Sorbtech Technologies). Solvent was removed under reduced pressure with a Büchi Rotovapor with a Welch self-cleaning dry vacuum pump and further dried with a Welch DuoSeal pump. Nuclear magnetic resonance (¹H-NMR, ¹³C-NMR, and ¹⁹F-NMR) spectra were taken on Bruker Avance 500 (¹H-NMR and ¹³C-NMR) or AV-400 (¹⁹F-NMR) instruments and processed with MestReNova software. All ¹H, ¹³C, and ¹⁹F NMR spectra are reported in ppm and relative to residual solvent signals (¹H, ¹³C). ¹⁹F NMR were reported with trifluoroacetic acid as the reference peak at -76.0 ppm as an external standard. High resolution mass spectra were collected on an Agilent 7890B-7520 Quadrupole Time-of-Flight GC-MS (Electron Impact (EI)) or via DART-MS spectra collected on a Thermo Exactive Plus MSD (Thermo Scientific) equipped with an ID-CUBE ion source and a Vapur Interface (IonSense Inc.) (Atmospheric pressure chemical ionization (APCI)). Low resolution mass spectra (Electron impact) were collected on an Agilent 6890N-5975 Quadrupole GC-MS. Photochemical reactions were performed in a photochemical reactor with a Hanovia 450 W medium pressure mercury vapor UV lamp.

5.5.2 Synthesis of starting materials and ene-yne

Starting materials **5.5**, **5.15a**, and **5.16a** were prepared from a modified procedure from Mallouk et al.⁴⁹

Starting materials **5.17a**, **5.18a**, **5.20a** and **5.22a** were prepared from the following procedure using synthesized 7,7,8,8,9,9,10,10,11,11,12,12,12-tridecafluoro-5-iodododec-5-enoic acid (**5.12**) as a starting acid:

7,7,8,8,9,9,10,10,11,11,12,12,12-tridecafluoro-5-iodododec-5-enoic acid (**5.12**) (0.880 g, 1.58 mmol, 1.0 equiv.) and thionyl chloride were (0.426 g, 3.60 mmol, 2.28 equiv.) were stirred at reflux for 2 hours and cooled to room temperature. Excess thionyl chloride was then removed via vacuum. The resulting acid chloride was used without further purification and dissolved in DCM (5 mL, anhydrous). Pyridine (0.214 g, 2.70 mmol, 1.5 equiv., anhydrous) and coupling amine (2.7 mmol, 1.5 equiv.) were added and stirred 18 hours at room temperature. The resulting mixture was quenched with a saturated solution of NH₄Cl (5 mL) and extracted with DCM (3 X 5 mL). The organic layer was dried with Na₂SO₄, decanted, and concentrated to give crude oil which was purified via flash chromatography.

Ene-yne containing products **5.6**, **5.15b-5.22b** were synthesized via the following method:

Starting vinyl iodide (0.100 mmol, 1.0 eq) was dissolved in DMF (0.25 mL) after which MTBD (0.046 g- 0.061 g, 0.30-0.40 mmol, 3.0 eq – 4.0 eq) was added and stirred at the desired temperature and time (See scheme 3). The resulting solution was quenched with a saturated solution of NH₄Cl (5 mL) and extracted against either fluoruous solvent or DCM (3 x 1 mL). Removal of solvent either gave pure product or was further purified via flash chromatography to give a mixture of stereoisomers (ratio calculated through integration of ¹H-NMR) and small amounts of remaining alkyne (remainder calculated through integration of ¹⁹F-NMR, see Table 2 for ratios and purification).

1,1,1,2,2,3,3,4,4,5,5,6,6-tridecafluoro-8-iodotetradec-7-ene (**5.5**):

To a quartz tube, 1-octyne (1.65 g, 15.0 mmol, 1.0 equiv.) was added, followed by iodoperfluorohexane (7.36 g, 16.5 mmol, 1.1 equiv.). The reaction mixture was illuminated under 254 nm light for 1 hour. The reaction mixture was placed on high vacuum to remove starting materials to give **5.5** as a pink oil and a mixture of E and Z isomers (87:13 E/Z, 8.14 g, 14.6 mmol, 97%). Spectra matched literature compound.³⁶

1,1,1,2,2,3,3,4,4,5,5,6-dodecafluorotetradec-6-en-8-yne (**5.6**):

Extracted from perfluorohexanes as a yellow oil (15:85 E/Z). Yield: 0.026 g, 0.064 mmol, 64%. ¹H NMR (500 MHz, Chloroform-*d*) δ 6.04 (E, ddt, *J* = 15.5, 4.3, 2.3 Hz, 0.15H), 5.71 (Z, dt, *J* = 29.3, 2.3 Hz, 0.85H), 2.39 (Z, t, *J* = 7.1 Hz, 1.7H), 2.34 (E, t, *J* = 8.2 Hz, 0.3H), 1.65 – 1.49 (m, 2H), 1.45 – 1.26 (m, 4H), 0.91 (t, *J* = 7.2 Hz, 3H). ¹³C NMR (126 MHz, Chloroform-*d*) δ 152.4 (Z, dt, *J* = 272.0, 28.5 Hz), 118.9 – 107.4 (5C, m), 103.5 (Z, d, *J* = 6.7 Hz), 98.3 (Z, q, *J* = 6.2 Hz), 69.4, 31.1, 28.0, 22.3, 19.9, 14.1. ¹⁹F NMR (376 MHz, Chloroform-*d*) δ -80.65 (t, *J* = 9.7 Hz, 3F), -116.04 (E, q, *J* = 12.7 Hz, 0.2F), -117.86 (Z, q, *J* = 13.6 Hz, 1.8F), -118.59 (Z, q, 0.9F), -120.23 (E, m, 0.1F), -122.36 – -123.45 (m, 4F), -126.07 (m, 2F). HRMS (EI): *m/z* [M]⁺ calcd for C₁₄H₁₂F₁₂: 408.0747, found: 408.0739

1,1,1,2,2,3,3,4,4,5,5,6,6-tridecafluorotetradec-7-yne (**5.7**):

Vinyl iodide **5.5** (0.50 g, 0.90 mmol, 1.0 equiv.) was dissolved in toluene (2.5 mL). MTBD (0.41 g, 2.7 mmol, 3.0 equiv.) was added dropwise and the solution was stirred for 5 hours at room temperature. The reaction mixture was diluted with water (5 mL) and extracted with hexanes (3 x 5 mL). The organic layer was dried with Na₂SO₄, decanted, and concentrated to give the crude oil which was further purified via a short silica plug with hexanes as the eluent to give compound **5.7** as a clear oil (0.31 g, 0.71 mmol, 79%) in 90% purity with 5% remaining **5.5** and 5% ene-yne **5.6** as determined by ¹⁹F-NMR. Spectra matched literature compound.⁵⁰

1,3,5-trimethyl-2-((1,1,1,2,2,3,3,4,4-nonafluorotetradeca-5-en-7,9-diyn-5-yl)oxy)benzene (**5.8**):

Vinyl iodide **5.5** (0.200 g, 0.360 mmol, 1.0 equiv.) and 2,4,6-trimethylphenol (0.220 g, 1.62 mmol, 4.50 equiv.) were dissolved in DMF (2 mL). Cesium carbonate (0.527 g, 1.62 mmol, 4.50 equiv.) was then added and stirred at 85 °C for 18 hours. The resulting slurry was cooled to room temperature and diluted with diethyl ether (5 mL) which was then extracted against water (4 x 5 mL). The organic layer was dried with Na₂SO₄, decanted, and concentrated to give the crude oil. The crude oil was purified further by flash chromatography with pentane as the eluent (*R_f* = 0.5) to give the enriched product **5.8** (0.029 g, 0.060 mmol, 17%) as a yellow oil. The enriched product was further purified by preparative thin layer

chromatography for analysis and structural determination. E and Z assignments match the ^{13}C -NMR J coupling values reported in literature⁵¹ and confirmed by NOESY NMR analysis.

^1H NMR (500 MHz, Chloroform-*d*) δ 6.88 (E, s, 0.6H), 6.80 (Z, s, 1.4H), 5.34 (Z, s, 0.7H), 5.00 (E, s, 0.3H), 2.44 – 1.98 (m, 11H), 1.53 – 1.34 (m, 4H), 0.94 – 0.86 (m, 3H). ^{13}C NMR (126 MHz, Chloroform-*d*) δ 150.3 (Z, t, $J = 24.1$ Hz), 148.4, 136.4, 130.4, 128.7, 120.3 – 106.2 (m, 4C), 88.3 (Z, t, $J = 8.0$ Hz), 87.3, 82.1, 64.7, 63.9, 30.4, 21.9, 20.8, 19.3, 15.8, 13.5. ^{19}F NMR (376 MHz, Chloroform-*d*) δ -80.95 (m, 3F), -113.93 (E, t, $J = 12.9$ Hz, 0.7F), -115.74 (Z, t, $J = 13.5$ Hz, 1.4F), -121.93 – -122.39 (m, 2F), -125.40 – -126.12 (m, 2F). MS (EI): m/z $[\text{M}]^+$ calcd for $\text{C}_{23}\text{H}_{11}\text{F}_9\text{O}$: 484.1, found: 484.1. HRMS (APCI): m/z $[\text{M}+\text{H}]^+$ calcd for $\text{C}_{23}\text{H}_{11}\text{F}_9\text{O}$: 485.1521, found: 485.1522

9,9,10,10,11,11,12,12,13,13,14,14,14-tridecafluorotetradeca-6,7-diene (**5.10**) was synthesized from a modified procedure from Ichihara and coworkers.⁵²

1-Octyn-3-ol (6.31 g, 5.00 mmol, 1 equiv.) and iodoperfluorohexane (2.45 g, 5.50 mmol, 1.1 equiv.) were dissolved in a MeCN/water mixture (10 mL:7.5 mL). Sodium bicarbonate (0.532 g, 6.33 mmol, 1.15 equiv.) was added followed by sodium dithionite (1.10 g, 6.33 mmol, 1.15 equiv.) and the solution was stirred for 2 hours at room temperature. The reaction mixture was then diluted with water (30 mL) and extracted with EtOAc (3 x 15 mL). The organic layer was dried with Na_2SO_4 , decanted, and concentrated to give crude oil which was used without purification in the next step. The resulting crude fluorous alcohol (2.26 g, ~4.00 mmol, 1.00 equiv.) was dissolved in DCM (10 mL, anhydrous). Triethylamine (0.481 g, 11.8 mmol, 1.2 equiv.) was added and then cooled to 0 °C. Trifluoroacetic acid (1.34 g, 4.76 mmol, 1.2 equiv.) was then added dropwise and allowed to warm to room temperature overnight. The reaction was quenched with a saturated solution of NH_4Cl (10 mL) and organic layer then extracted with DCM (3 x 15 mL). The organic layer was dried with Na_2SO_4 , decanted, and concentrated to give crude oil (**5.9**, 2.00 g, 2.84 mmol, 1.0 equiv.) which was used without purification in the next step. Previously synthesized 9,9,10,10,11,11,12,12,13,13,14,14,14-tridecafluoro-7-iodotetradec-7-en-6-yl trifluoromethanesulfonate, **5.9**, (2.00 g, 2.84 mmol, 1.0 equiv.) was dissolved in THF (3 mL, anhydrous). Activated zinc (0.371 g,

5.68 mmol, 2.0 equiv.) was then added and stirred at reflux for 18 hours. The resulting slurry was filtered and washed with dichloromethane (10 mL). This solution was concentrated and purified via flash chromatography with hexanes as the eluent ($R_f = 0.9$) to give the product as a clear oil (0.386 g, 0.90 mmol, 32%). ^1H NMR (500 MHz, Chloroform-*d*) δ 5.75 – 5.65 (m, 1H), 5.36 (tdd, $J = 11.2, 6.4, 3.2$ Hz, 1H), 2.12 (dtd, $J = 8.1, 6.9, 3.1$ Hz, 2H), 1.45 (tt, $J = 7.2, 5.4$ Hz, 2H), 1.36 – 1.28 (m, 4H), 0.89 (t, $J = 6.9$ Hz, 3H). ^{13}C NMR (126 MHz, Chloroform-*d*) δ 206.9, 126.1 – 104.4 (m, 6C), 98.6, 84.3 (t, $J = 28.3$ Hz), 31.3, 28.3, 27.7, 22.5, 14.0. ^{19}F NMR (376 MHz, Chloroform-*d*) δ -80.66 (t, $J = 9.9$ Hz, 3F), -106.20 – -109.43 (m, 2F), -121.44 (m, 2F), -122.78 (m, 2F), -123.19 (m, 2F), -126.00 (m, 2F). MS (EI): m/z [$\text{M}-\text{H}$] $^+$ calcd for $\text{C}_{14}\text{H}_{13}\text{F}_{13}$: 427.1, found: 427.1. HRMS (EI): m/z [$\text{M}-\text{C}_2\text{H}_5$] $^+$ calcd for $\text{C}_{14}\text{H}_{13}\text{F}_{13}$: 399.0418, found: 399.0413.

9,9,10,10,11,11,12,12,13,13,14,14,14-tridecafluorotetradec-6-yne (**5.11**):

Allene **5.10** (0.038 g, 0.09 mmol, 1.0 equiv.) and 18-crown-6 (0.024 g, 0.09 mmol, 1.0 equiv.) were dissolved in DMF. Cesium carbonate (0.029 g, 0.09 mmol, 1.0 equiv.) was then added and temperature raised to 50 °C for 1 hour. The resulting slurry was run through a silica plug with hexanes as the eluent to give a mixture of ene-yne **5.6**, allene **5.10**, and proposed alkyne **5.11** (0.025 g, 33:49:17 molar ratio as determined by ^{19}F -NMR).

7,7,8,8,9,9,10,10,11,11,12,12,12-tridecafluoro-5-iodododec-5-enoic acid (**5.12**):

To a quartz tube, 5-hexynoic acid (0.752 g, 6.70 mmol, 1.50 equiv.) was added, followed by iodoperfluorohexane (2.00 g, 4.50 mmol, 1.00 equiv.). The reaction mixture was illuminated under 254 nm light for 2 hours, at which point it was placed on high vacuum to remove any remaining fluororous by-products and then purified via flash chromatography (40% EtOAc in hexanes) to give title compound as a pink oil and a mixture of E and Z isomers ($R_f = 0.43$, 89:11 E/Z, 1.17 g, 2.12 mmol, 47%). ^1H NMR (500 MHz, Chloroform-*d*) δ 10.98 (bs, 1H), 6.39 (E, t, $J = 14.3$ Hz, 0.89H), 6.30 (Z, t, $J = 13.3$ Hz, 0.22H), 2.76 (Z, t, $J = 7.0$ Hz, 0.2H), 2.72 (E, t, $J = 7.0$ Hz, 1.8H), 2.41 (t, $J = 7.3$ Hz, 2H), 2.00 – 1.90 (m, 2H). ^{13}C NMR (126 MHz, Chloroform-*d*) δ 178.2, 127.8 (E, t, $J = 23.8$ Hz), 120.9 (E, t, $J = 6.3$ Hz), 118.7 – 107.7

(6C, m), 40.0 (E, t, $J = 2.1$ Hz), 32.2, 24.9. ^{19}F NMR (376 MHz, Chloroform-*d*) δ -80.76 (m, 3F), -105.31 (E, m, 1.8F), -108.73 (Z, m, 0.2F), -121.65 (m, 2F), -122.80 (m, 2F), -123.18 (m, 2F), -126.10 (m, 2F). HRMS (EI): m/z [M-I] $^+$ calcd for $\text{C}_{12}\text{H}_8\text{F}_{13}\text{IO}_2$: 431.0317, found: 431.0278.

6,6,7,7,8,8,9,9,10,10,11,11,11-tridecafluoro-4-iodoundec-4-en-1-ol (**5.13**):

4-pentyn-1-ol (1.00 g, 11.9 mmol, 1.00 equiv.) and iodoperfluorohexane (5.80 g, 13.0 mmol, 1.10 equiv.) were dissolved in a MeCN/water mixture (24 mL:18 mL). Sodium bicarbonate (1.29 g, 15.4 mmol, 1.30 equiv.) was added followed by sodium dithionite (2.68 g, 15.4 mmol, 1.30 equiv.) and the solution was stirred for 2 hours at room temperature. The reaction mixture was then diluted with water (30 mL) and extracted with EtOAc (3 x 20 mL). The organic layer was dried with Na_2SO_4 , decanted, and concentrated to give spectroscopically pure product as a yellow oil (4.33 g, 8.16 mmol, 69%) which matched the literature.⁵³

6,6,7,7,8,8,9,9,10,10,11,11,11-tridecafluoro-4-iodoundec-4-en-1-yl 4-methylbenzenesulfonate (**5.14**):

The previously synthesized fluoruous alcohol (**5.13**) (3.50 g, 6.60 mmol, 1.00 equiv.) was dissolved in anhydrous THF (10 mL). Pyridine (0.574 g, 7.26 mmol, 1.10 equiv.) was added, followed by tosyl chloride (1.38 g, 7.26 mmol, 1.10 equiv.). The reaction was stirred for 18 hours and then quenched with a saturated solution of NH_4Cl (15 mL) and extracted with EtOAc (3 x 20 mL). The organic layer was dried with Na_2SO_4 , decanted, and concentrated to give crude oil. Purification via flash chromatography (5% EtOAc in hexanes) gave the product as a white solid ($R_f = 0.5$, 72:28 E/Z, 2.58 g, 3.77 mmol, 57%) ^1H NMR (500 MHz, Chloroform-*d*) δ 7.86 – 7.59 (m, 2H), 7.51 – 7.32 (m, 2H), 6.34 (E, t, $J = 14.3$ Hz, 0.72H), 6.24 (Z, t, $J = 12.9$ Hz, 0.28H), 4.08 (E, t, $J = 6.2$ Hz, 1.4H), 4.04 (Z, t, $J = 5.9$ Hz, 0.6H), 2.80 – 2.73 (E, t, $J = 7.2$ Hz, 1.4H), 2.69 (Z, t, $J = 7.8$ Hz, 0.6H), 2.45 (s, 3H), 2.01 – 1.88 (m, 2H). ^{13}C NMR (126 MHz, Chloroform-*d*) δ 145.1, 133.0, 130.0, 128.0, 127.9 (E, t, $J = 23.9$ Hz), 119.68 (E, t, $J = 6.3$ Hz), 119.08 – 107.99 (m, 6C), 68.5, 37.6 (E, t, $J = 2.7$ Hz), 29.5, 21.8. ^{19}F NMR (376 MHz, Chloroform-*d*) δ -81.44 (t, $J = 9.7$ Hz, 3F), -106.38 (E, 1.4F), -109.54 (Z, 0.6F), -122.35 (m, 2F), -123.10 – -124.80 (m, 4F), -126.81 (m, 2F). HRMS (EI): m/z [M-I] $^+$ calcd for $\text{C}_{18}\text{H}_{14}\text{F}_{13}\text{IO}_3\text{S}$: 557.0456, found: 557.0451.

1,1,1,2,2,3,3,4,4-nonafluoro-6-iodododec-5-ene (**5.15a**):

To a quartz tube, 1-octyne (0.186 g, 1.69 mmol, 1.0 equiv.) was added, followed by iodoperfluorobutane (0.700g, 2.02 mmol, 1.2 equiv.). The reaction mixture was illuminated under 254 nm light for 1 hour. The reaction mixture was placed on high vacuum to remove starting materials to give **5.15a** as a clear oil and a mixture of E and Z isomers (89:11 E/Z, 0.62 g, 1.37 mmol, 81%). Spectra matched literature compound.⁵⁴

1,1,1,2,2,3,3,4-octafluorododec-4-en-6-yne (**5.15b**):

Extracted from perfluorohexanes as a yellow oil (13:87 E/Z). Yield: 0.013 g - .026 g, 0.041-.084 mmol, (41-84%). ¹H NMR (400 MHz, Chloroform-*d*) δ 6.04 (E, ddt, *J* = 15.9, 4.4, 2.1 Hz, 0.13H), 5.71 (Z, dt, *J* = 28.5, 2.1 Hz, 0.87H), 2.39 (Z, t, *J* = 6.7 Hz, 1.8H), 2.34 (E, t, *J* = 6.8 Hz, 0.2H), 1.59 (dd, *J* = 14.6, 7.3 Hz, 2H), 1.43 – 1.29 (m, 4H), 0.91 (t, *J* = 7.0 Hz, 3H). ¹³C NMR (126 MHz, Chloroform-*d*) δ 152.2 (Z, dt, *J* = 273.6, 29.6 Hz), 120.3 – 107.8 (m, 3C), 103.5 (Z, d, *J* = 6.1 Hz), 98.2 (Z, q, *J* = 6.9 Hz), 69.4, 31.1, 28.0, 22.3, 19.8, 14.1. ¹⁹F NMR (376 MHz, Chloroform-*d*) δ -80.59 (m, 3F), -117.02 (E, m, 0.2F), -118.83 (m, 2.8F), -127.10 (m, 2F). MS (EI): *m/z* [M]⁺ calcd for C₁₂H₁₂F₈: 308.1, found: 308.1

9,9,10,10,11,11,12,12,13,13,14,14,15,15,16,16,16-heptaecafluoro-7-iodohexadec-7-ene (**5.16a**):

To a quartz tube, 1-octyne (0.186 g, 1.69 mmol, 1.0 equiv.) was added, followed by iodoperfluorooctane (1.10 g, 2.02 mmol, 1.2 equiv.). The reaction mixture was illuminated under 254 nm light for 1 hour. The reaction mixture was placed on high vacuum to remove starting materials to give **5.16a** as a pink oil and a mixture of E and Z isomers (86:14 E/Z, 0.830 g, 1.26 mmol, 75%). Spectra matched literature compound.⁵⁴

9,10,10,11,11,12,12,13,13,14,14,15,15,16,16,16-hexadecafluorohexadec-8-en-6-yne (**5.16b**):

Extracted from perfluorohexanes as a yellow oil (17:83 E/Z). Yield: 0.031 g, 0.061 mmol, (61%). ¹H NMR (500 MHz, Chloroform-*d*) δ 6.04 (E, ddt, *J* = 15.5, 4.3, 2.3 Hz, 0.17H), 5.71 (Z, dt, *J* = 29.3, 2.3 Hz, 0.83H), 2.39 (Z, t, *J* = 7.1 Hz, 1.6H), 2.34 (E, t, *J* = 7.6 Hz, 0.4H), 1.70 – 1.51 (m, 2H), 1.47 – 1.25

(m, 4H), 0.91 (t, $J = 7.2$ Hz, 3H). ^{13}C NMR (126 MHz, Chloroform-*d*) δ 152.4 (dt, $J = 272.2, 28.5$ Hz), 121.3 – 107.4 (m, 7C), 103.5 (Z, d, $J = 6.7$ Hz), 98.3 (Z, q, $J = 6.2$ Hz), 69.5, 31.1, 28.0, 22.3, 19.9, 14.1. ^{19}F NMR (376 MHz, Chloroform-*d*) δ -80.59 (t, $J = 9.8$ Hz, 3F), -115.96 (E, q, $J = 11.7$ Hz, 0.2F), -117.78 (Z, q, $J = 13.4$ Hz, 1.8F), -118.55 (z, 0.9F), -120.16 (E, m, 0.1F), -121.83 (m, 4F), -122.67 (m, 4F) -125.94 (m, 2F). MS (EI): m/z [M] $^+$ calcd for $\text{C}_{16}\text{H}_{12}\text{F}_{16}$: 508.1, found: 508.1

N,N-diethyl-7,7,8,8,9,9,10,10,11,11,12,12,12-tridecafluoro-5-iodododec-5-enamide (**5.17a**):

Yellow oil, $R_f = 0.30$ (20% EtOAc/Hexanes), E isomer only, Yield: 0.476 g, 0.78 mmol, 49%; ^1H NMR (500 MHz, Chloroform-*d*) δ 6.37 (t, $J = 14.4$ Hz, 1H), 3.37 (q, $J = 7.0$ Hz, 2H), 3.28 (q, $J = 7.0$ Hz, 2H), 2.73 (t, $J = 7.1$ Hz, 2H), 2.31 (t, $J = 7.5$ Hz, 2H), 1.97 (p, $J = 7.4$ Hz, 2H), 1.16 (t, $J = 7.1$ Hz, 3H), 1.11 (t, $J = 7.1$ Hz, 3H). ^{13}C NMR (126 MHz, Chloroform-*d*) δ 170.8, 127.3 (t, $J = 23.7$ Hz), 122.4 (t, $J = 6.1$ Hz), 119.9 – 107.2 (m, 6C), 42.0, 40.5 (E, t, $J = 2.4$ Hz), 40.3, 31.3, 25.5, 14.3, 13.2. ^{19}F NMR (376 MHz, Chloroform-*d*) δ -80.74 (m, 3F), -105.16 (m, 2F), -121.62 (m, 2F), -122.82 (m, 2F), -123.20 (m, 2F), -126.13 (m, 2F). HRMS (EI): m/z [M-I] $^+$ calcd for $\text{C}_{16}\text{H}_{17}\text{F}_{13}\text{INO}$: 486.1103, found: 486.1122

N,N-diethyl-7,8,8,9,9,10,10,11,11,12,12,12-dodecafluorododec-6-en-4-ynamide (**5.17b**):

Extracted from methoxy perfluorobutyl ether as a yellow oil (21:79 E/Z). Yield: 0.034 g, 0.073 mmol, 73%. ^1H NMR (500 MHz, Chloroform-*d*) δ 6.03 (E, ddt, $J = 15.4, 4.2, 1.9$ Hz, 0.2H), 5.70 (dt, $J = 28.2, 2.2$ Hz, 1.8H), 3.39 (q, $J = 7.0$ Hz, 2H), 3.32 (q, $J = 7.1$ Hz, 2H), 2.77 (Z, t, $J = 7.3$ Hz, 1.6H), 2.71 (E, t, $J = 7.1$ Hz, 0.4H), 2.59 (Z, t, $J = 7.5$ Hz, 1.6H), 2.53 (E, t, $J = 7.9$ Hz, 0.4H), 1.19 (t, $J = 7.2$ Hz, 3H), 1.11 (t, $J = 7.1$ Hz, 3H). ^{13}C NMR (126 MHz, Chloroform-*d*) δ 169.5, 152.4 (Z, dt, $J = 274.1, 29.5$ Hz), 128.1 – 107.4 (m, 5C), 102.1 (Z, d, $J = 6.2$ Hz), 98.0 (Z, q, $J = 6.9$ Hz), 69.6, 41.9, 40.3, 31.6, 15.9, 14.3, 13.0. ^{19}F NMR (376 MHz, Chloroform-*d*) δ -80.63 (t, $J = 9.8$ Hz, 3F), -115.97 (E, q, $J = 12.5$ Hz, 0.2F), -117.90 (Z, m, 2.7F), -119.45 (E, 0.10F), -122.36 – -123.70 (m, 4F), -126.07 (m, 2F). HRMS (EI): m/z [M] $^+$ calcd for $\text{C}_{16}\text{H}_{15}\text{F}_{12}\text{NO}$: 465.0962, found: 465.0964

N-benzyl-7,7,8,8,9,9,10,10,11,11,12,12,12-tridecafluoro-5-iodododec-5-enamide (**5.18a**):

Yellow solid, $R_f = 0.20$ (20% EtOAc/Hexanes), 71:29 E/Z. Yield: 0.518 g, 0.80 mmol, 51% ^1H NMR (500 MHz, Chloroform- d) δ 7.39 – 7.26 (m, 5H), 6.38 (E, t, $J = 14.4$ Hz, 0.7H), 6.27 (Z, t, $J = 13.0$ Hz, 0.3H), 4.44 (d, $J = 5.6$ Hz, 2H), 2.75 (Z, t, $J = 6.9$ Hz, 0.6H), 2.71 (E, t, $J = 7.3$ Hz, 1.4H), 2.22 (dt, $J = 11.8, 7.3$ Hz, 2H), 1.98 (p, $J = 7.6, 7.1$ Hz, 2H). ^{13}C NMR (126 MHz, Chloroform- d) δ 171.4, 138.1, 128.8, 127.9, 127.6, 127.4 (E, t, $J = 23.8$ Hz), 121.5 (E, t, $J = 6.1$ Hz), 119.5 – 107.0 (6C, m), 43.7, 40.2 (E, t, $J = 2.5$ Hz), 34.7, 25.7. ^{19}F NMR (376 MHz, Chloroform- d) δ -82.11 (m, 3F), -106.53 (E, m, 1.4F), -109.94 (Z, m, 0.6F), -122.99 (m, 2F), -124.15 (m, 2F), -124.57 (m, 2F), -127.47 (m, 2F). MS (EI): m/z $[\text{M}]^+$ calcd for $\text{C}_{19}\text{H}_{15}\text{F}_{13}\text{INO}$: 647.0, found: 647.0

N-benzyl-7,8,8,9,9,10,10,11,11,12,12,12-dodecafluorododec-6-en-4-ynamide (**5.18b**):

Purified via flash chromatography with a gradient from 15-50% EtOAc in hexanes. $R_f = 0.5$ (50% EtOAc/Hexanes). Yellow solid (15:85 E/Z). Yield: 0.030 g, 0.06 mmol, 60%. ^1H NMR (400 MHz, Chloroform- d) δ 7.37 – 7.26 (m, 5H), 5.98 (E, dt, $J = 15.4, 2.6$ Hz, 0.15H), 5.88 (bs, 1H), 5.64 (Z, dt, $J = 29.0, 2.2$ Hz, 0.85H), 4.53 – 4.41 (m, 2H), 2.78 (Z, t, $J = 6.9$ Hz, 1.7H), 2.72 (E, t, $J = 7.2$ Hz, 0.3H), 2.47 (Z, t, $J = 7.1$ Hz, 1.7H), 2.43 (E, t, $J = 7.5$ Hz, 0.3H). ^{13}C NMR (126 MHz, Chloroform- d) δ 170.4, 152.7 (Z, dt, $J = 272.4, 28.1$ Hz), 138.0, 128.7, 127.8, 127.6, 119.4 – 105.7 (m, 5C), 101.1 (Z, d, $J = 6.8$ Hz), 97.7 (Z, q, $J = 6.3$ Hz), 70.2, 43.8, 34.9, 16.2. ^{19}F NMR (376 MHz, Chloroform- d) δ -80.61 (t, $J = 9.6$ Hz, 3F), -115.98 (E, q, $J = 12.7$ Hz, 0.2F), -117.21 (Z, m, 0.9F), -117.89 (Z, q, $J = 13.6$ Hz, 1.8F), -118.72 (E, m, 0.1F), -122.16 – -123.46 (m, 4F), -126.05 (m, 2F). MS (EI): m/z $[\text{M}]^+$ calcd for $\text{C}_{19}\text{H}_{13}\text{F}_{12}\text{NO}$: 499.1, found: 499.1

2-(6,6,7,7,8,8,9,9,10,10,11,11,11-tridecafluoro-4-iodoundec-4-en-1-yl)isoindoline-1,3-dione (**5.19a**):

Previously synthesized 6,6,7,7,8,8,9,9,10,10,11,11,11-tridecafluoro-4-iodoundec-4-en-1-yl 4-methylbenzenesulfonate (**5.14**) (0.680 g, 1.00 mmol, 1.0 equiv.) was dissolved in DMF (5 mL, anhydrous) and potassium phthalimide (0.661 g, 5.00 mmol, 5 equiv.) was added. The resulting solution was stirred at room temperature for 18 hours at which point the solution was diluted with a saturated solution of NaHCO_3 (10 mL) and extracted with EtOAc (4 x 5 mL). The organic layer was dried with Na_2SO_4 ,

decanted, and concentrated to give crude oil. Purification via flash chromatography (10% EtOAc in hexanes) to give the product as a white solid with 10% tosylate remaining ($R_f = 0.25$, E isomer only, 0.249 g, 0.37 mmol, 37%). ^1H NMR (500 MHz, Chloroform-*d*) δ 7.85 (dd, $J = 5.5, 3.0$ Hz, 2H), 7.72 (dd, $J = 5.4, 3.0$ Hz, 2H), 6.34 (t, $J = 14.3$ Hz, 1H), 3.73 (t, $J = 7.1$ Hz, 2H), 2.73 (t, $J = 7.7$ Hz, 2H), 1.98 (p, $J = 7.5$ Hz, 2H). ^{13}C NMR (126 MHz, Chloroform-*d*) δ 168.4, 134.2, 132.1, 127.5 (t, $J = 24.1$ Hz), 123.4, 120.4 (t, $J = 6.1$ Hz), 38.8 (t, $J = 2.8$ Hz), 36.7, 29.1. ^{19}F NMR (376 MHz, Chloroform-*d*) δ -80.75 (m, 3F), -105.53 (m, 2F), -121.75 (m, 2F), -122.87 (m, 2F), -123.21 (m, 2F), -126.14 (m, 2F). HRMS (EI): m/z [M-I] $^+$ calcd for $\text{C}_{15}\text{H}_{13}\text{F}_{13}\text{INO}$: 532.0582, found: 532.0600

2-(6,7,7,8,8,9,9,10,10,11,11,11-dodecafluoroundec-5-en-3-yn-1-yl)isoindoline-1,3-dione (**5.19b**):

Purified via flash chromatography (25% EtOAc in hexanes). $R_f = 0.67$ Yellow solid (15:85 E/Z). Yield: 0.029 g, 0.056 mmol, 56%. ^1H NMR (500 MHz, Chloroform-*d*) δ 7.86 (td, $J = 5.4, 2.9$ Hz, 2H), 7.73 (dd, $J = 5.5, 3.1$ Hz, 2H), 5.99 (E, ddt, $J = 15.5, 4.6, 2.5$ Hz, 0.15H), 5.65 (Z, dt, $J = 29.1, 2.3$ Hz, 0.85H), 3.93 (Z, t, $J = 7.0$ Hz, 1.7H), 3.88 (E, t, $J = 7.0$ Hz, 0.3H), 2.83 (Z, t, $J = 7.4$ Hz, 0.17H), 2.79 (E, t, $J = 7.5$ Hz, 0.4H). ^{13}C NMR (126 MHz, Chloroform-*d*) δ 168.1, 153.0 (Z, dt, $J = 274.3, 28.8$ Hz), 134.3, 132.1, 123.5, 121.5 – 107.7 (m, 5C), 98.5 (Z, d, $J = 7.0$ Hz), 97.6 (Z, q, $J = 6.8$ Hz), 71.2, 36.2, 19.8. ^{19}F NMR (376 MHz, Chloroform-*d*) δ -80.62 (t, $J = 9.7$ Hz, 3F), -116.09 (E, q, $J = 11.9$ Hz, 0.2F), -116.62 (Z, 0.9F), -117.99 (Z, q, $J = 13.9$ Hz (1.8F), -118.27 (E, m, 0.1F), -122.15 – -123.67 (m, 4F), -126.07 (m, 2F). MS (EI): m/z [M] $^+$ calcd for $\text{C}_{19}\text{H}_{13}\text{F}_{12}\text{NO}$: 511.0, found: 511.0

N-allyl-7,7,8,8,9,9,10,10,11,11,12,12,12-tridecafluoro-5-iodododec-5-enamide (**5.20a**):

Yellow oil, $R_f = 0.16$ (20% EtOAc/Hexanes), 81:19 E/Z, Yield: 0.461 g, 0.77 mmol, 49%, ^1H NMR (500 MHz, Chloroform-*d*) δ 6.37 (E, $J = 14.4$ Hz, 0.8H), 6.30 (Z, t, $J = 13.0$ Hz, 0.2H), 5.92 – 5.77 (m, 1H), 5.52 (bs, 1H), 5.26 – 5.10 (m, 2H), 3.89 (t, $J = 5.7$ Hz, 2H), 2.75 (Z, t, $J = 7.2$ Hz, 0.4H), 2.70 (E, t, $J = 7.3$ Hz, 1.6H), 2.27 – 2.17 (m, 2H), 1.96 (p, $J = 7.5$ Hz, 2H). ^{13}C NMR (126 MHz, Chloroform-*d*) δ 171.5, 134.2, 127.5 (E, t, $J = 23.7$ Hz), 121.7 (E, t, $J = 6.1$ Hz), 116.8, 116.5 – 107.9 (6C, m), 42.2, 40.3 (E, t, $J = 2.2$ Hz), 34.8, 25.9. ^{19}F NMR (376 MHz, Chloroform-*d*) δ -81.32 (m, 3F), -105.71 (E, m, 1.6F), -109.14

(Z, S, 0.4F), -122.19 (m, 2F), -123.37 (m, 2F), -123.76 (m, 2F), -126.67 (m, 2F). MS (EI): m/z [M]⁺ calcd for C₁₅H₁₃F₁₃INO: 597.0, found: 597.0

N-allyl-7,8,8,9,9,10,10,11,11,12,12,12-dodecafluorododec-6-en-4-ynamide (**5.20b**):

Extracted from methoxy perfluorobutyl ether as a yellow oil (20:80 E/Z). Yield: 0.028 g, 0.064 mmol, 64%. ¹H NMR (500 MHz, Chloroform-*d*) δ 6.02 (E, ddt, *J* = 15.5, 4.3, 2.3 Hz, 0.2H), 5.90 – 5.77 (m, 1H), 5.70 (Z, dt, *J* = 29.2, 2.3 Hz, 0.8H), 5.65 (bs, 1H), 5.24 – 5.10 (m, 2H), 3.91 (tt, *J* = 5.8, 1.5 Hz, 2H), 2.77 (Z, t, *J* = 7.1 Hz, 1.6H), 2.71 (E, t, *J* = 7.2 Hz, 0.4H), 2.46 (Z, t, *J* = 7.2 Hz, 1.6H), 2.41 (E, t, *J* = 7.3 Hz, 0.4H). ¹³C NMR (126 MHz, Chloroform-*d*) δ 170.3, 152.7 (Z, dt, *J* = 272.9, 28.4 Hz), 133.9, 116.6, 122.8 – 106.8 (m, 5C), 101.1 (Z, d, *J* = 6.9 Hz), 97.74 (Z, q, *J* = 6.4 Hz), 70.2, 42.1, 35.0, 16.1. ¹⁹F NMR (376 MHz, Chloroform-*d*) δ -80.62 (t, *J* = 9.7 Hz, 3F), -115.97 (E, q, *J* = 11.4 Hz, 0.2F), -117.25 (m, 0.9F), -117.93 (Z, q, *J* = 13.5 Hz, 1.8F), -118.75 (m, 0.1F), -122.82 (m, 4F), -126.06 (m, 2F). MS (EI): m/z [M]⁺ calcd for C₁₅H₁₁F₁₂NO: 449.1, found: 449.0

11,11,12,12,13,13,14,14,15,15,16,16,16-tridecafluoro-9-iodohexadec-9-en-1-yne (**5.21a**):

Iodoperfluorohexane (0.446 g, 1.00 mmol, 1.0 equiv.) and 1,9-decadiyne (0.402 g, 3.00 mmol, 3.0 equiv.) were dissolved in a MeCN/water mixture (2.0 mL:1.5 mL). Sodium bicarbonate (0.0960 g, 1.15 mmol, 1.15 equiv.) was added, followed by sodium dithionite (0.200 g, 1.15 mmol, 1.15 equiv.) and the solution was stirred for 2 hours at room temperature. The reaction mixture was then diluted with water (5 mL) and extracted with hexanes (3 x 2 mL). The organic layer was dried with Na₂SO₄, decanted, and concentrated to give crude oil. Purification through flash chromatography with hexanes as the eluent yielded the product as a clear oil and mixture of E and Z isomers (*R_f* = 0.50 (hexanes), 88:12 E/Z, 0.172 g, 0.300 mmol, 30%). ¹H NMR (500 MHz, Chloroform-*d*) δ 6.32 (E, t, *J* = 14.5 Hz, 0.94H), 6.24 (Z, t, *J* = 13.0 Hz, 0.06H), 2.67 (Z, t, *J* = 7.4 Hz, 0.12H), 2.63 (E, t, *J* = 7.5 Hz, 1.88H), 2.19 (td, *J* = 7.0, 2.6 Hz, 2H), 1.94 (t, *J* = 2.7 Hz, 1H), 1.63 – 1.30 (m, 8H). ¹³C NMR (126 MHz, Chloroform-*d*) δ 126.5 (E, t, *J* = 23.8 Hz), 122.8 (E, t, *J* = 6.0 Hz), 118.8 – 107.6 (6C), 84.4, 68.2, 41.0 (E, t, *J* = 2.4 Hz), 29.9, 28.3, 28.2, 27.9, 18.3. ¹⁹F NMR (376 MHz, Chloroform-*d*) δ -80.80 (m, 3F), -105.36 (E, m, 1.88F), -108.55 (Z, m, 0.12F),

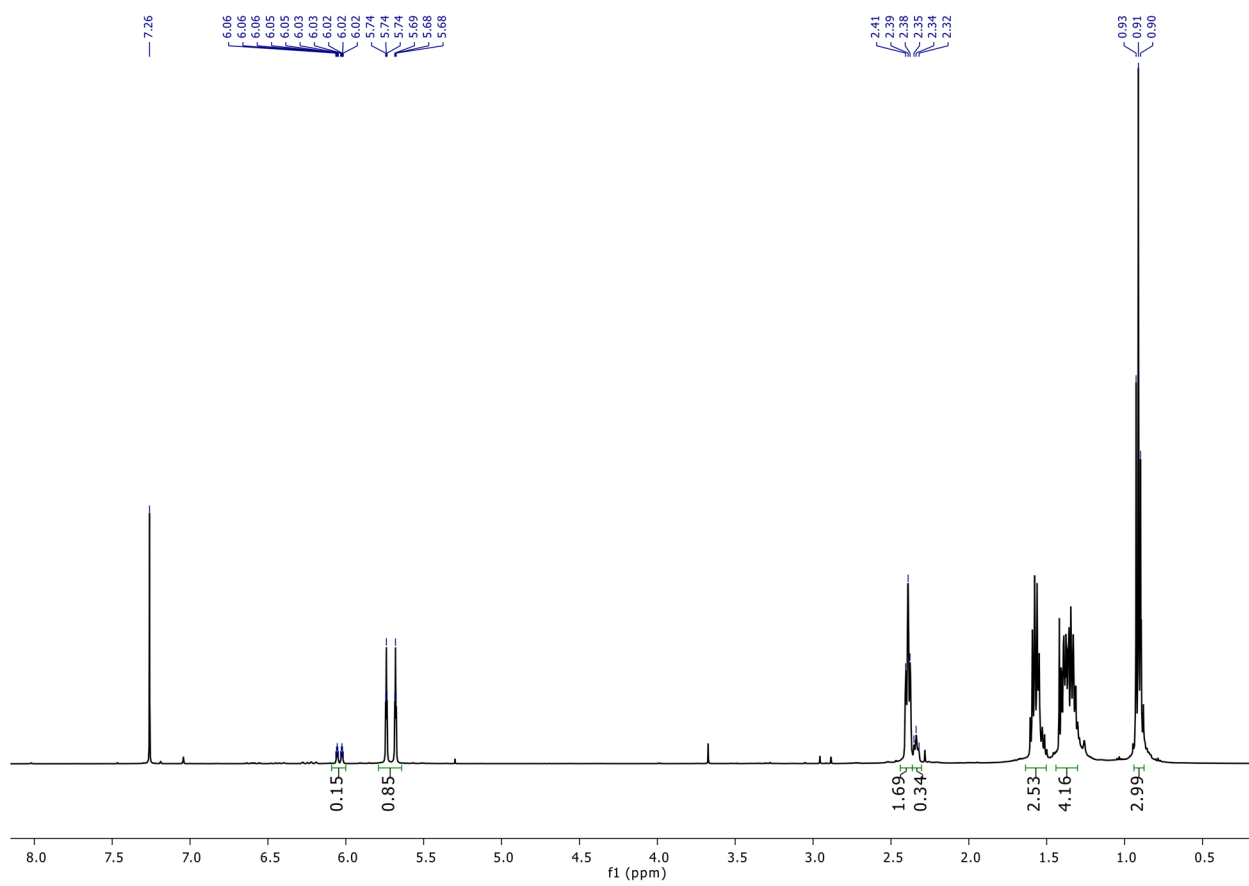
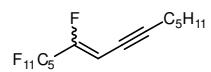
-121.69 (m, 2F), -122.85 (m, 2F), -123.28 (m, 2F), -126.15 (m, 2F). HRMS (EI): m/z [M-I]⁺ calcd for C₁₆H₁₄F₁₃I: 453.0888, found: 453.0881

11,12,12,13,13,14,14,15,15,16,16,16-dodecafluorohexadeca-10-en-1,8-diyne (**5.21b**):

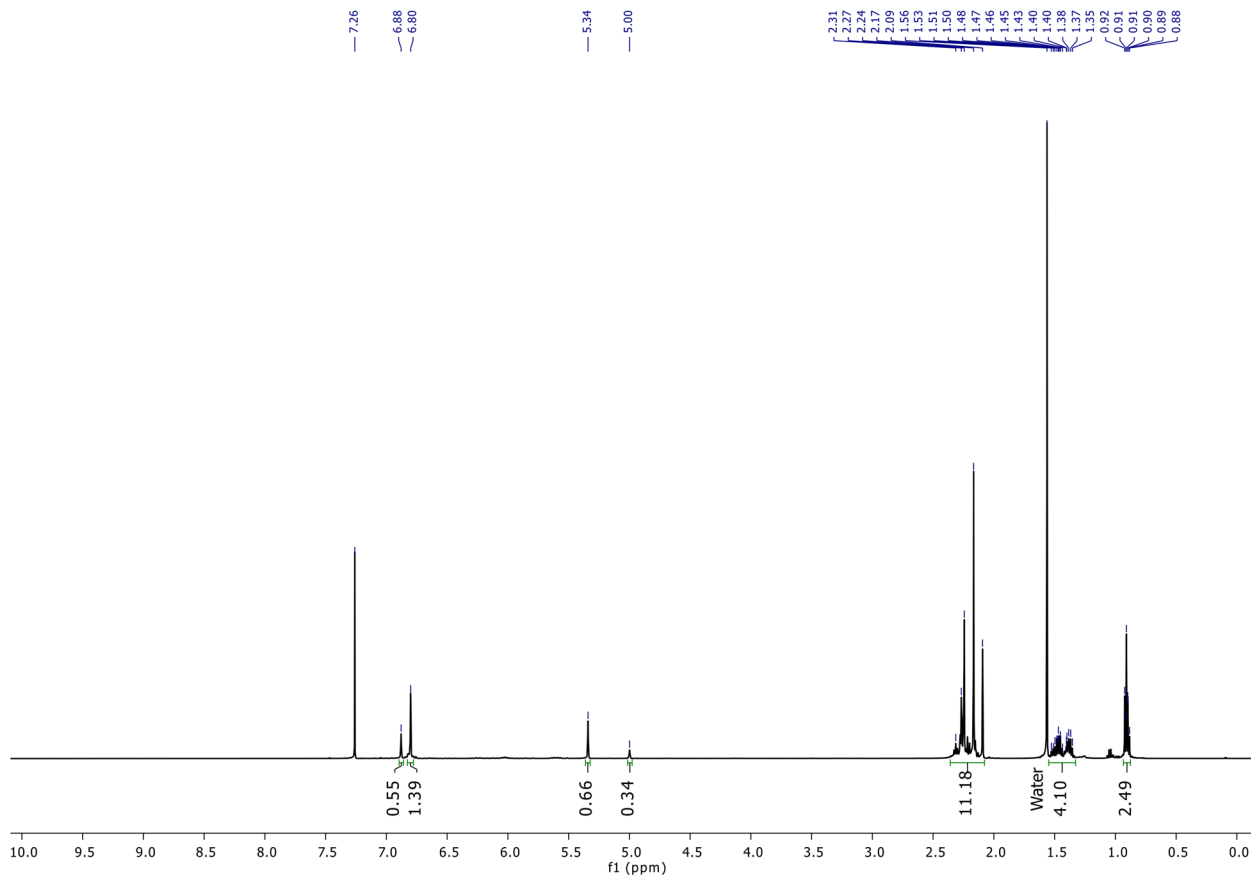
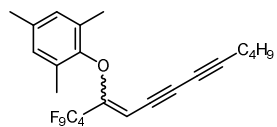
Extracted from perfluorohexanes as a yellow oil (17:83 E/Z). Yield: 0.031 g, 0.073 mmol, 73%. ¹H NMR (500 MHz, Chloroform-*d*) δ 6.04 (E, ddt, $J = 15.5, 4.3, 2.2$ Hz, 0.17H), 5.71 (Z, dt, $J = 29.2, 2.3$ Hz, 0.83H), 2.41 (Z, t, $J = 6.4$ Hz, 1.6H), 2.36 (Z, t, $J = 7.3$ Hz, 0.4H), 2.24 – 2.15 (m, 2H), 1.94 (t, $J = 2.6$ Hz, 1H), 1.64 – 1.50 (m, 6H). ¹³C NMR (126 MHz, Chloroform-*d*) δ 152.5 (Z, dt, $J = 271.3, 28.0$ Hz), 122.3 – 106.2 (m, 5C), 103.0 (Z, d, $J = 6.7$ Hz), 98.2 (Z, q, $J = 6.3$ Hz), 84.4, 69.7, 68.5, 28.1, 28.0, 27.8, 19.8, 18.4. ¹⁹F NMR (376 MHz, Chloroform-*d*) δ -80.68 (t, $J = 8.8$ Hz, 3F), -116.04 (E, q, $J = 12.1$ Hz, 0.2F), -117.91 (Z, q, $J = 13.3$ Hz, 1.8F), -118.15 (Z, m, 0.9F), -120.02 (E, m, 0.1F), -122.77 – -123.72 (m, 4F), -126.11 (m, 2F). MS (EI): m/z [M-H]⁺ calcd for C₁₆H₁₂F₁₂: 431.1, found: 431.1

5.5.3 $^1\text{H-NMR}$ Spectra

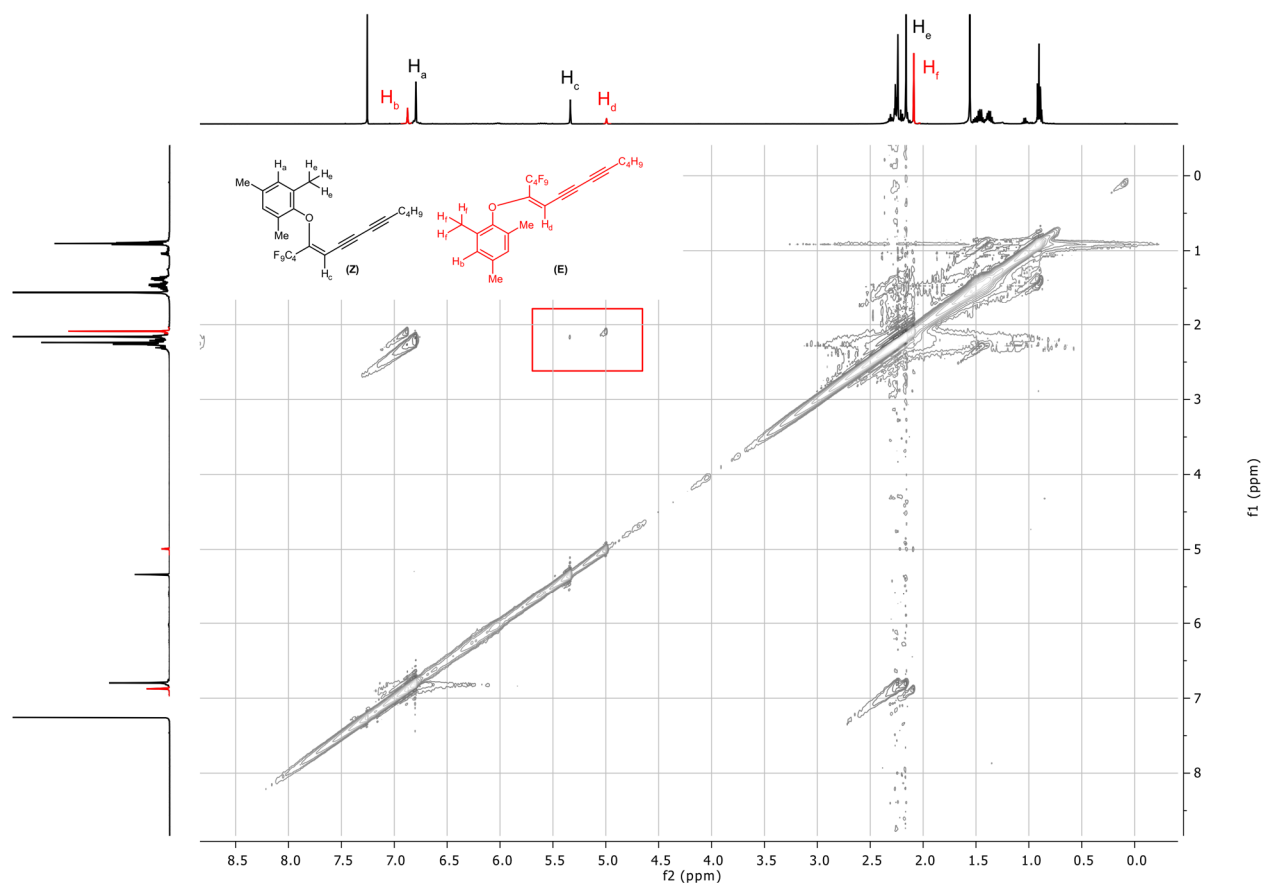
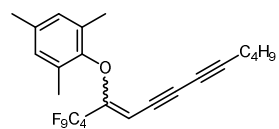
1,1,1,2,2,3,3,4,4,5,5,6-dodecafluorotetradec-6-en-8-yne (**5.6**):



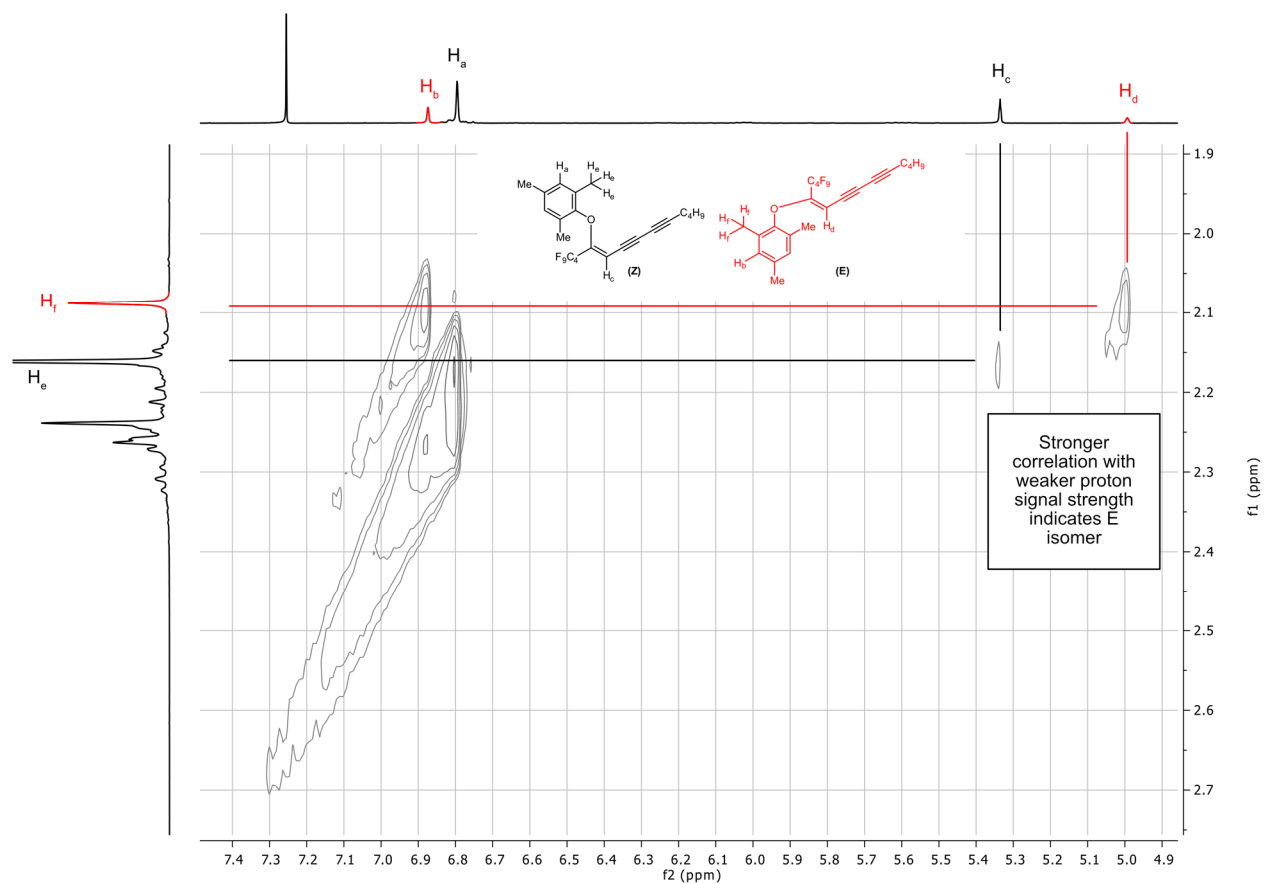
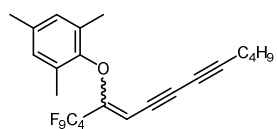
1,3,5-trimethyl-2-((1,1,1,2,2,3,3,4,4-nonafluorotetradeca-5-en-7,9-diyn-5-yl)oxy)benzene (**5.8**):



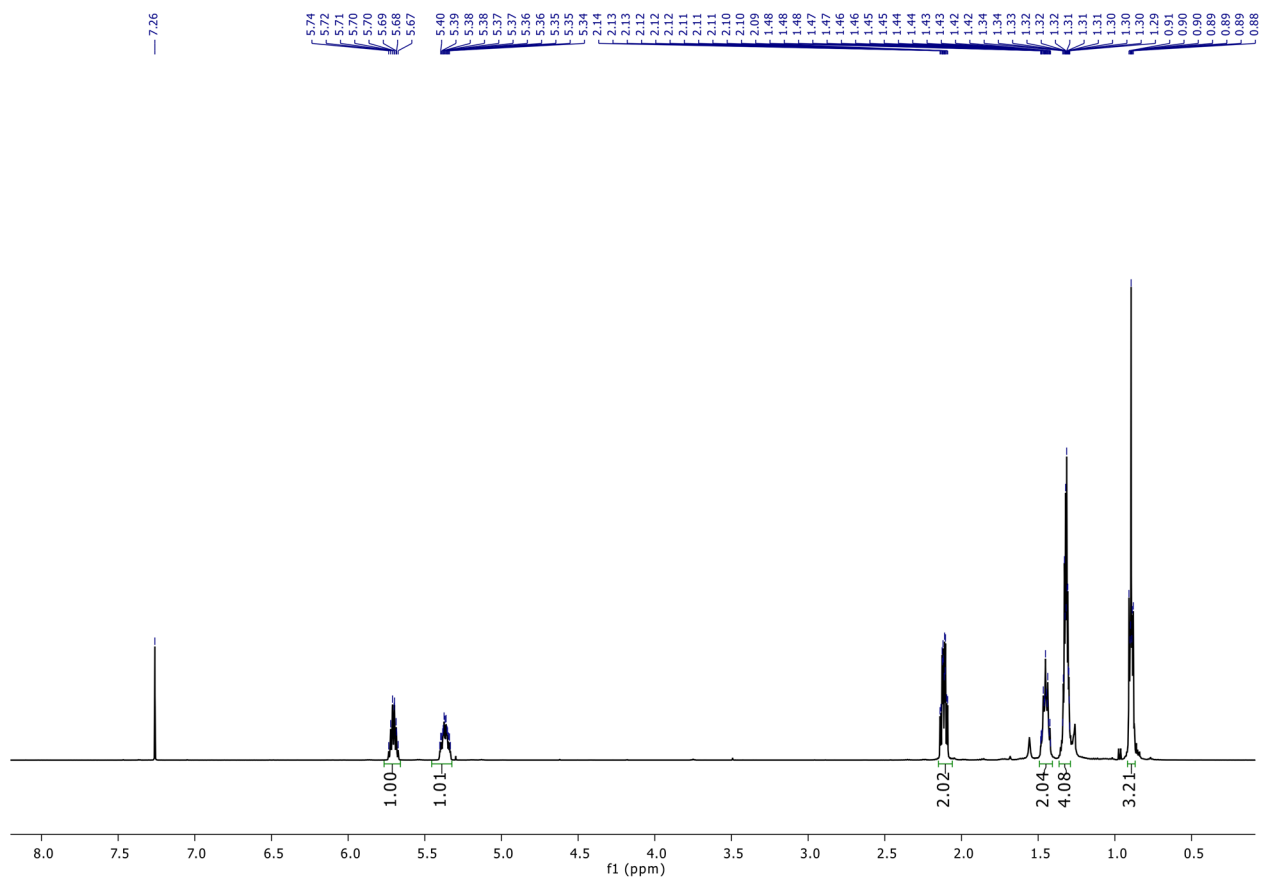
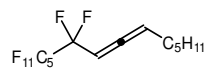
1,3,5-trimethyl-2-((1,1,1,2,2,3,3,4,4-nonafluorotetradeca-5-en-7,9-diyn-5-yl)oxy)benzene (**5.8**): NOESY NMR with box around the vinyl proton and aromatic methyl proton interactions.



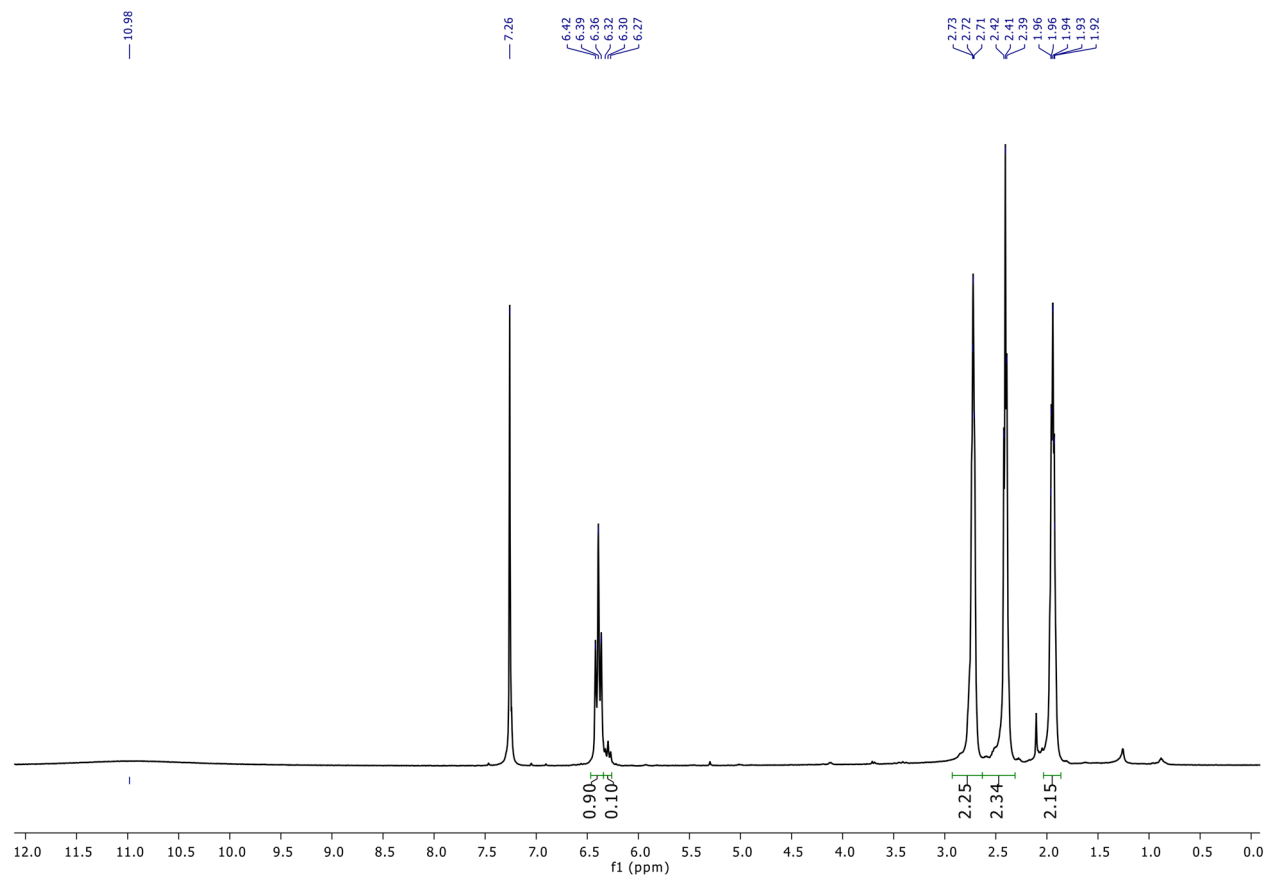
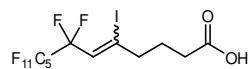
1,3,5-trimethyl-2-((1,1,1,2,2,3,3,4,4-nonafluorotetradeca-5-en-7,9-diyn-5-yl)oxy)benzene (5.8):
 Enhanced region NOESY NMR demonstrating vinyl proton and aromatic methyl group interactions. E and Z assignments match the ^{13}C -NMR J coupling values reported in literature.⁵¹



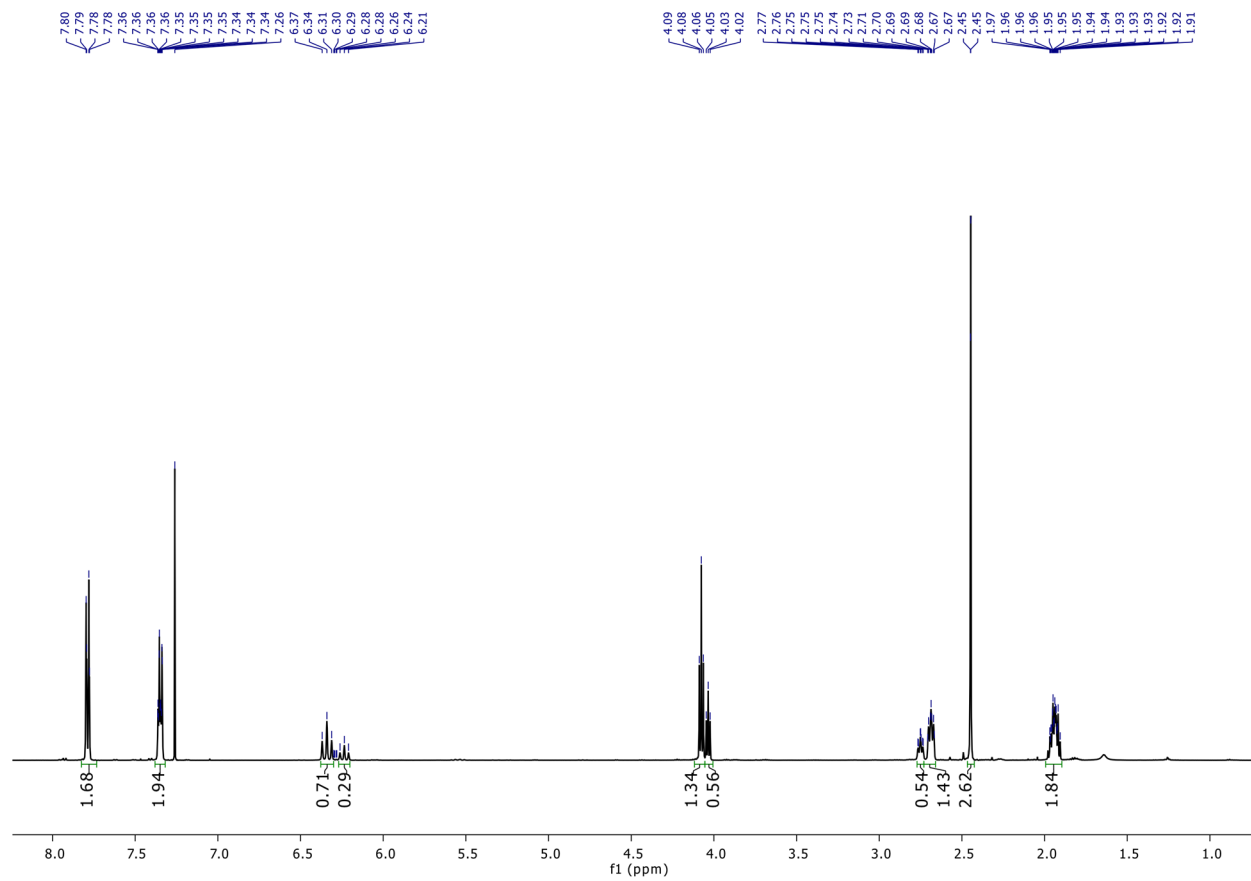
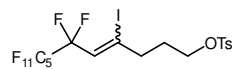
9,9,10,10,11,11,12,12,13,13,14,14,14-tridecafluorotetradeca-6,7-diene (**5.10**):



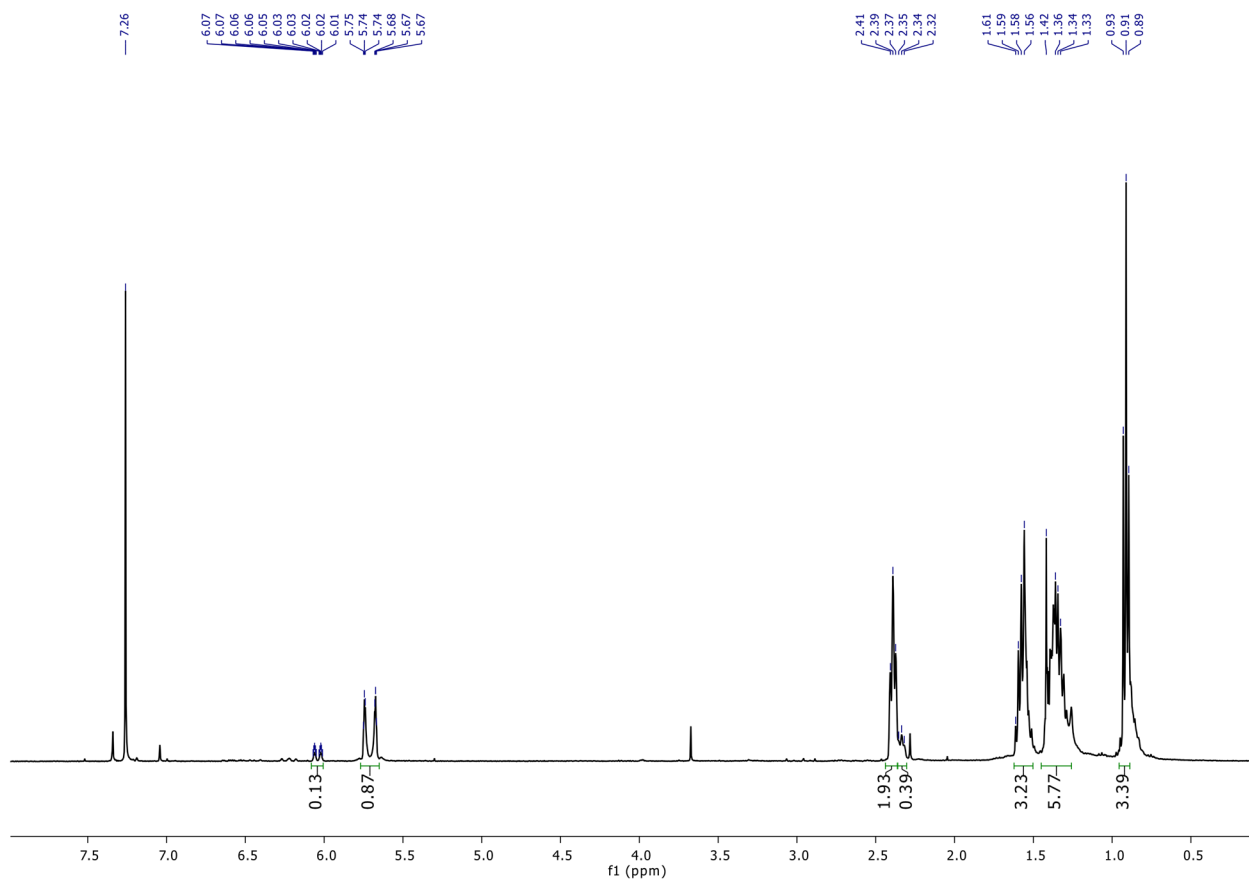
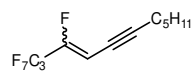
7,7,8,8,9,9,10,10,11,11,12,12,12-tridecafluoro-5-iodododec-5-enoic acid (**5.12**):



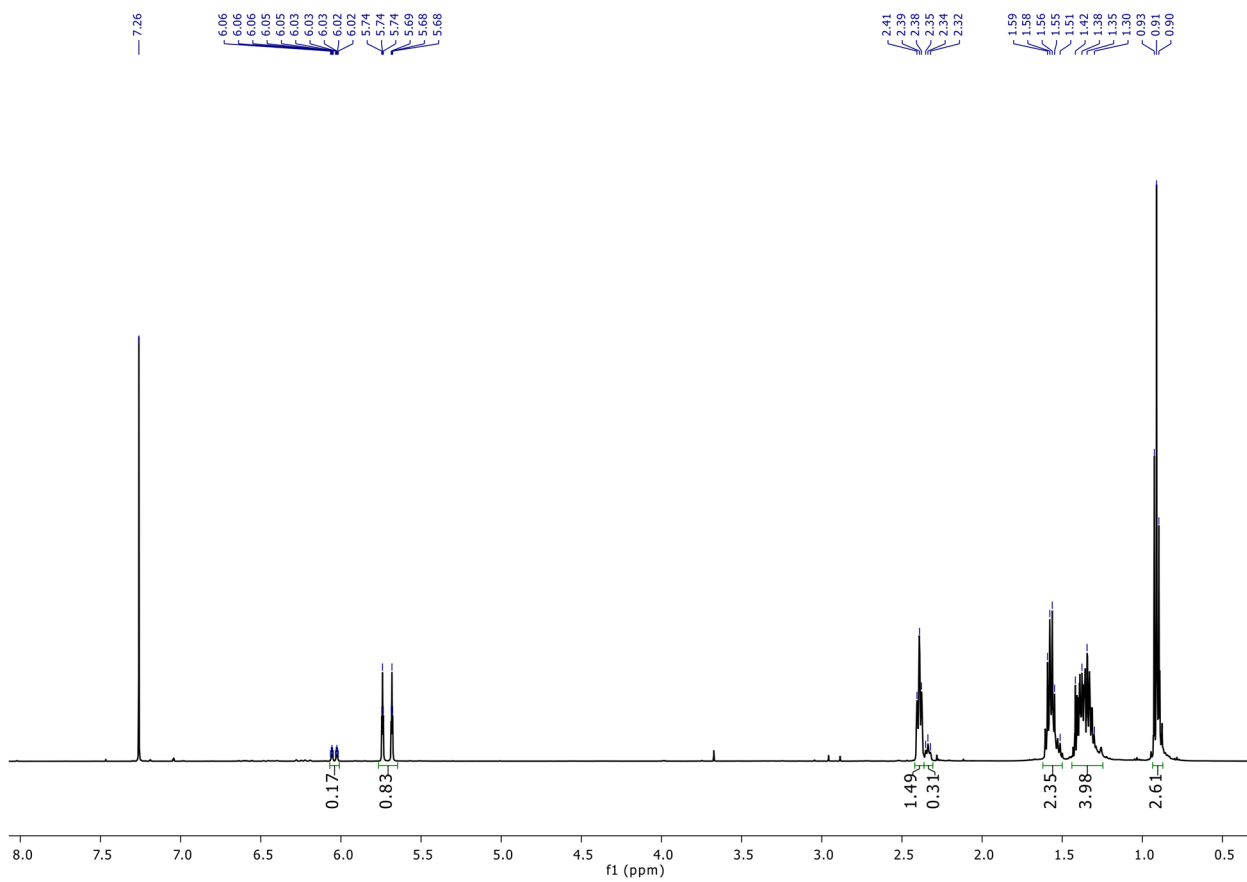
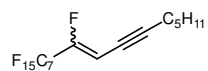
6,6,7,7,8,8,9,9,10,10,11,11,11-tridecafluoro-4-iodoundec-4-en-1-yl 4-methylbenzenesulfonate (**5.14**):



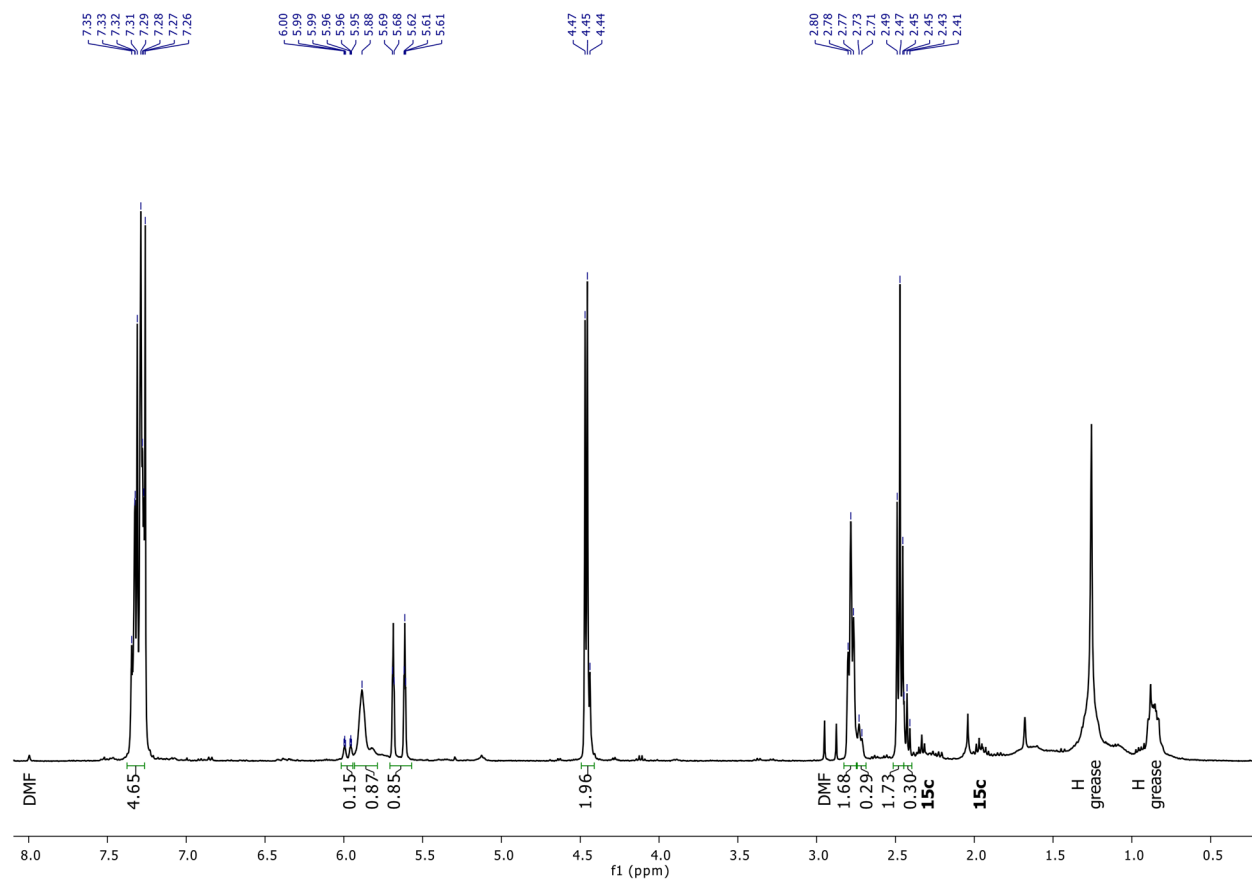
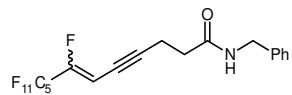
1,1,1,2,2,3,3,4-octafluorododec-4-en-6-yne (**5.15b**):



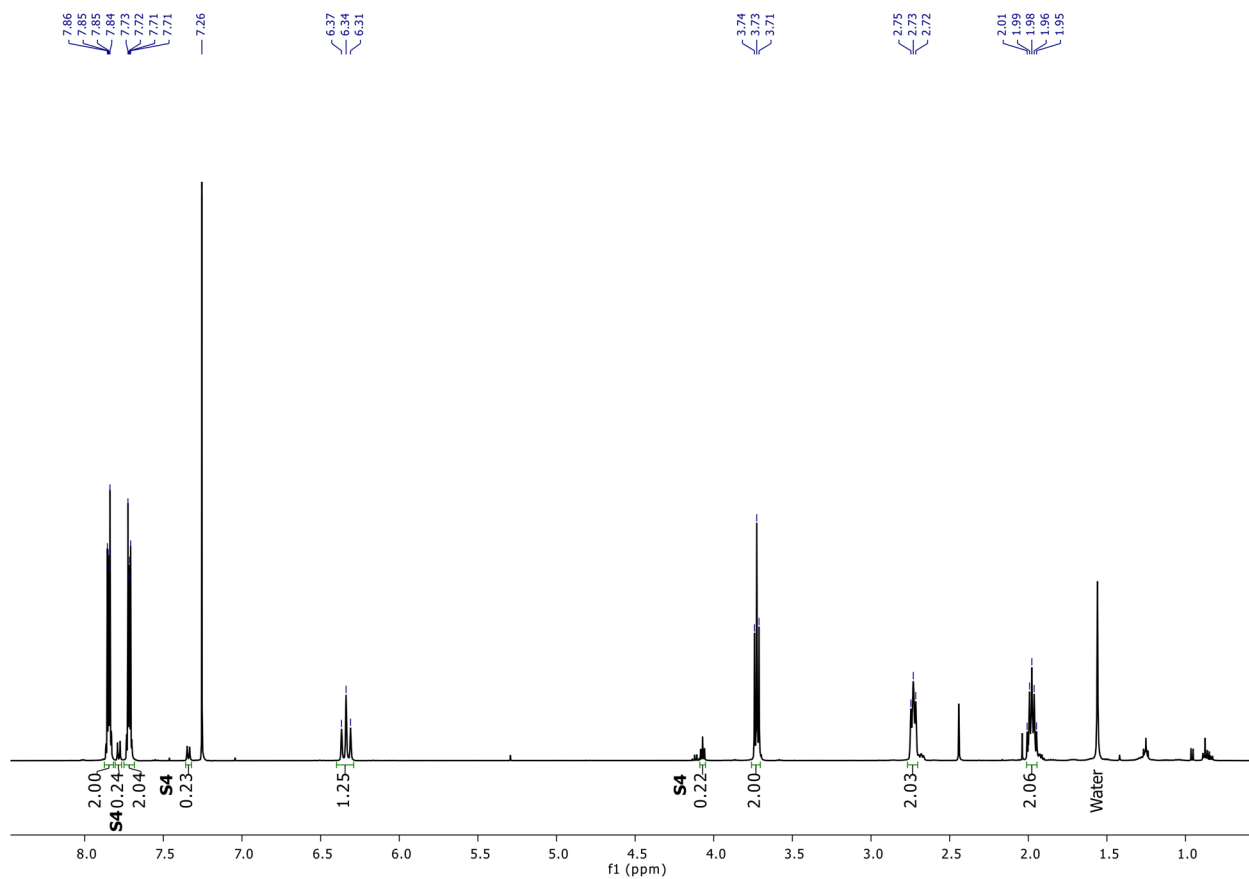
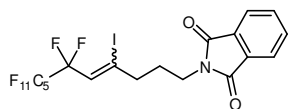
9,10,10,11,11,12,12,13,13,14,14,15,15,16,16,16-hexadecafluorohexadec-8-en-6-yne (**5.16b**):



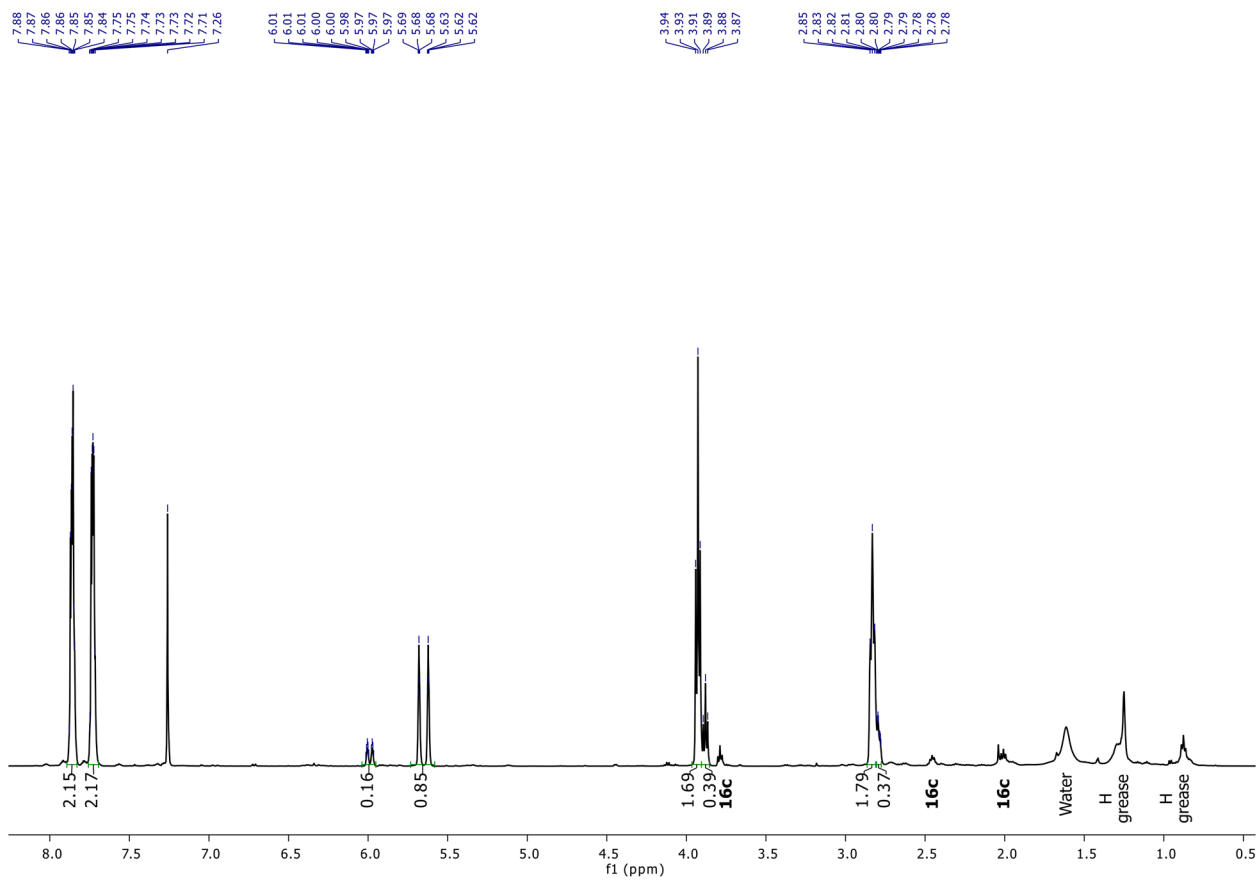
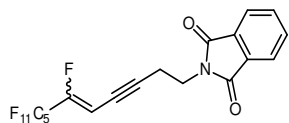
N-benzyl-7,8,8,9,10,10,11,11,12,12,12-dodecafluorododec-6-en-4-ynamide (**5.18b**):



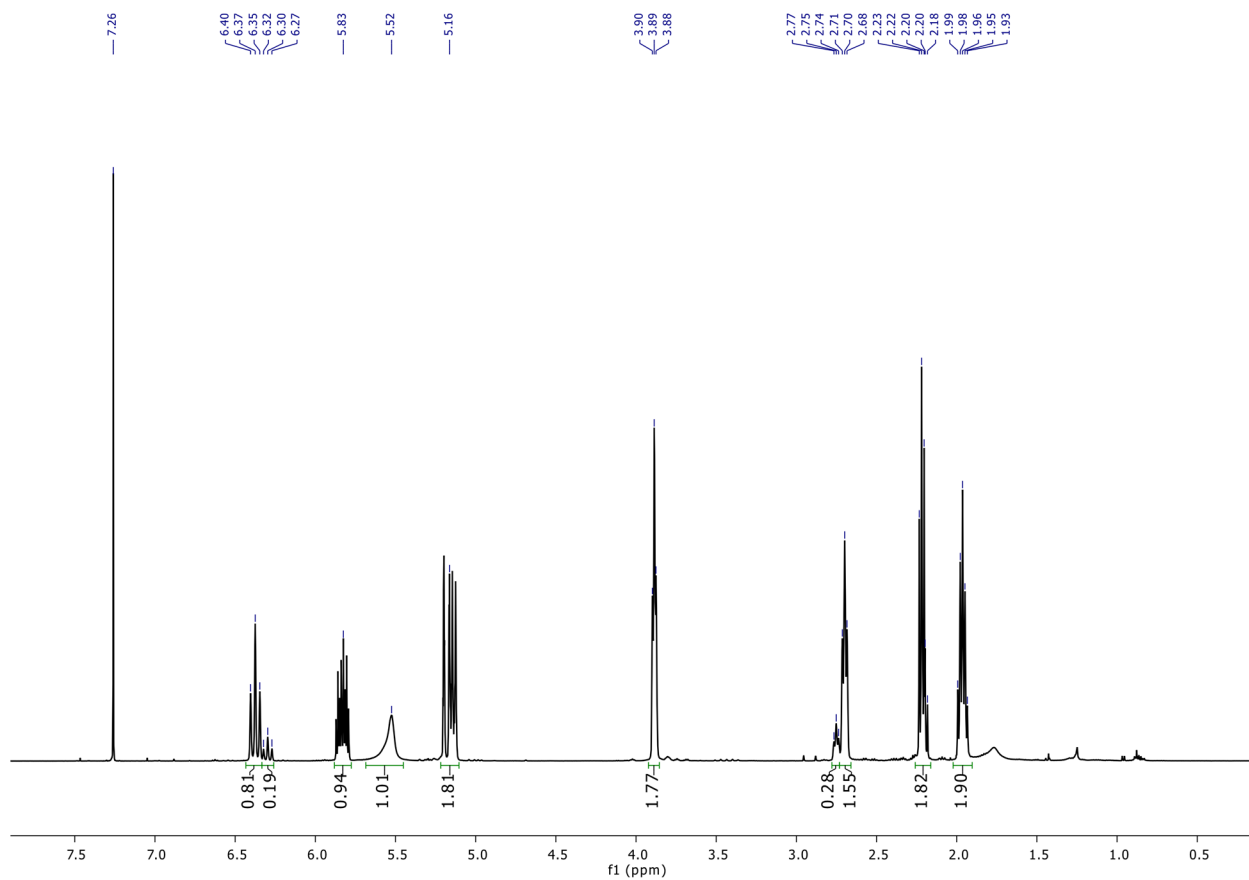
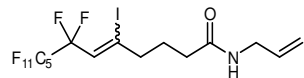
2-(6,6,7,7,8,8,9,9,10,10,11,11,11-tridecafluoro-4-iodoundec-4-en-1-yl)isoindoline-1,3-dione (**5.19a**):



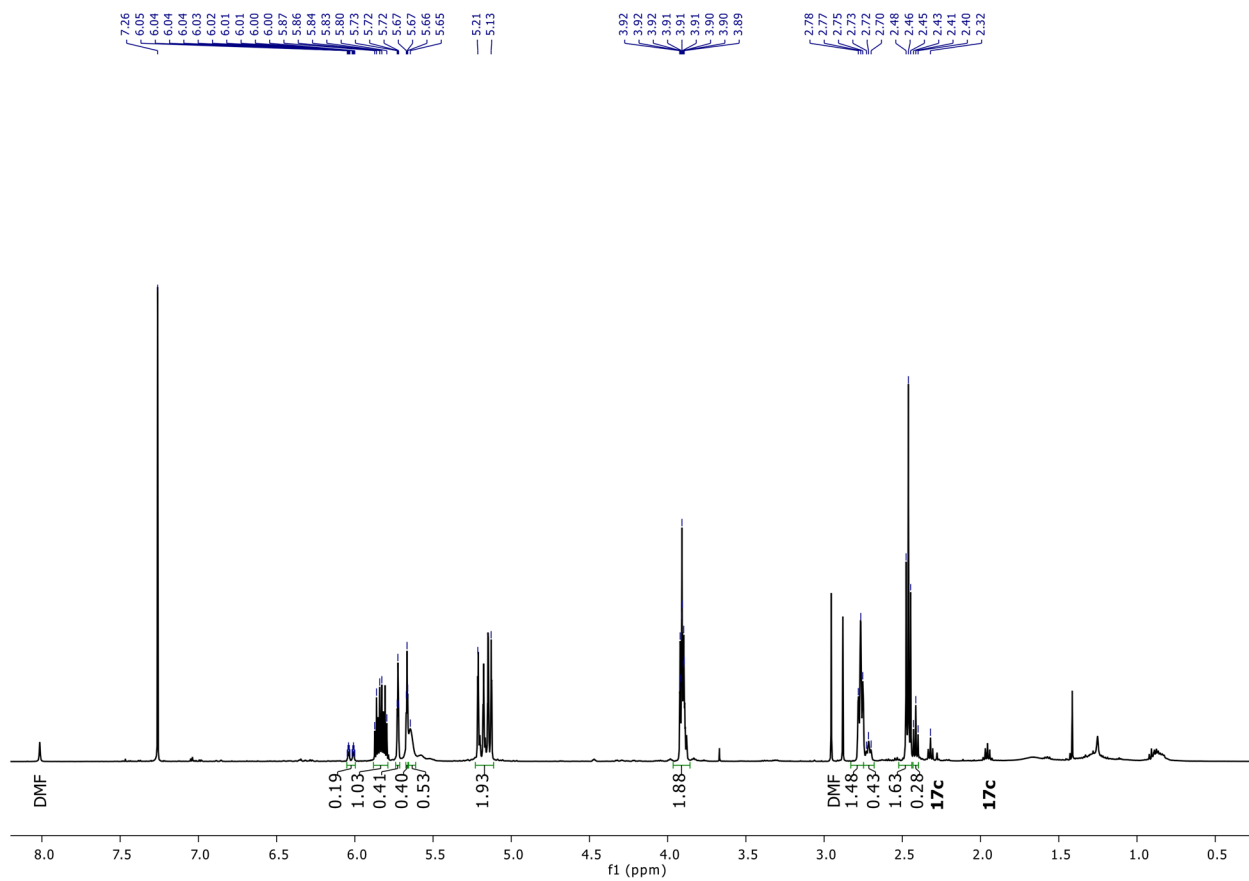
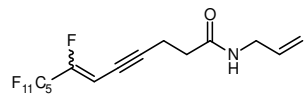
2-(6,7,7,8,8,9,9,10,10,11,11,11-dodecafluoroundec-5-en-3-yn-1-yl)isoindoline-1,3-dione (**5.19b**):



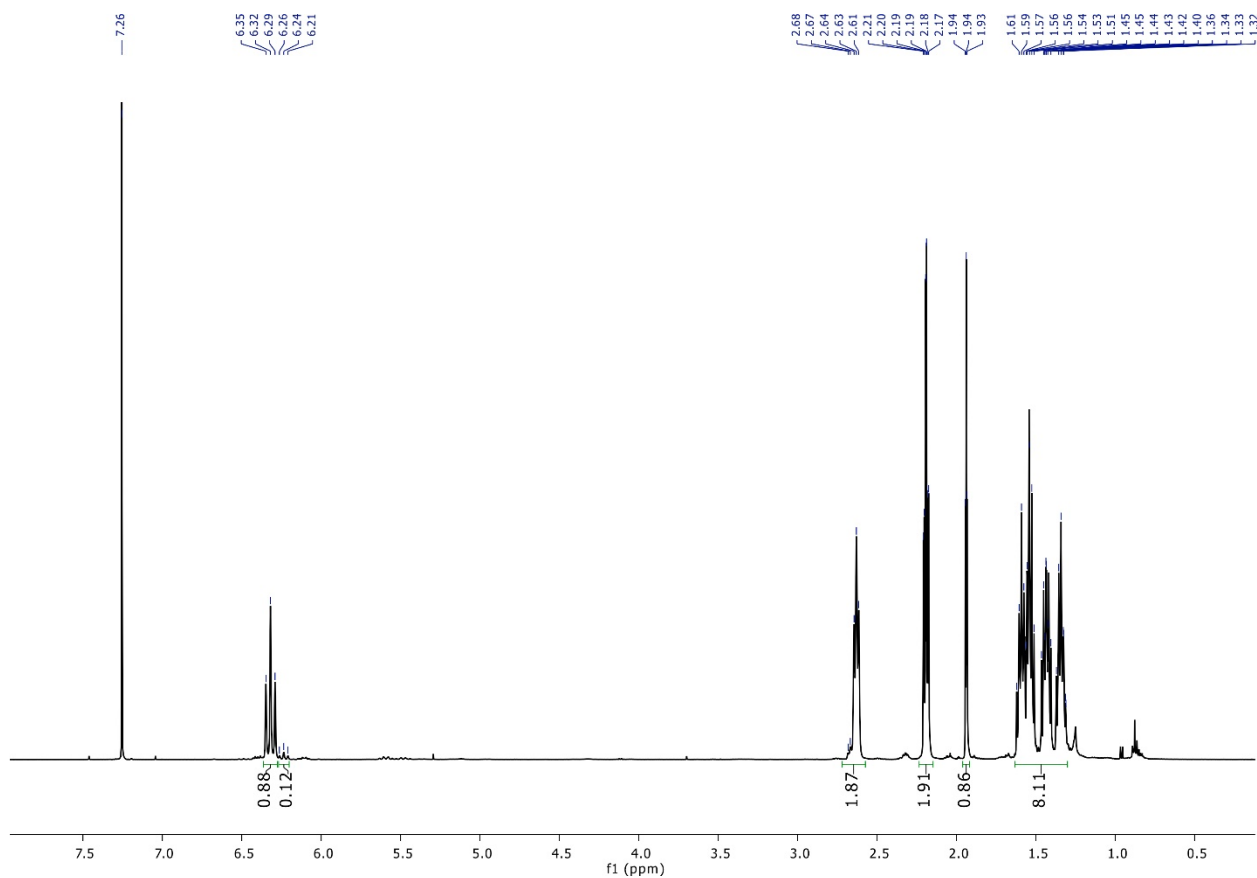
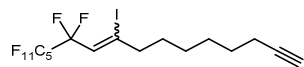
N-allyl-7,7,8,8,9,9,10,10,11,11,12,12,12-tridecafluoro-5-iodododec-5-enamide (**5.20a**):



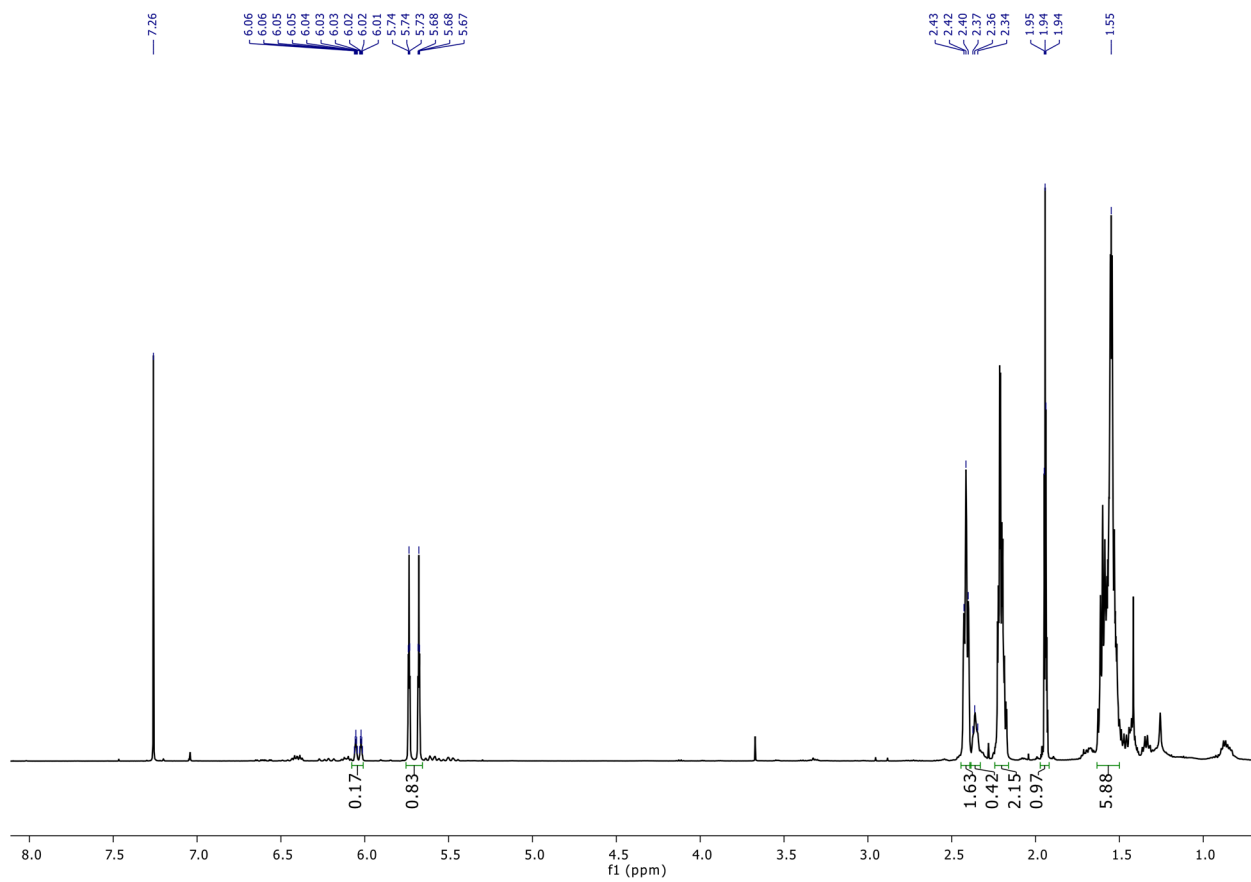
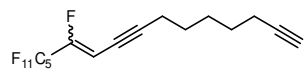
N-allyl-7,8,8,9,9,10,10,11,11,12,12,12-dodecafluorododec-6-en-4-ynamide (**5.20b**):



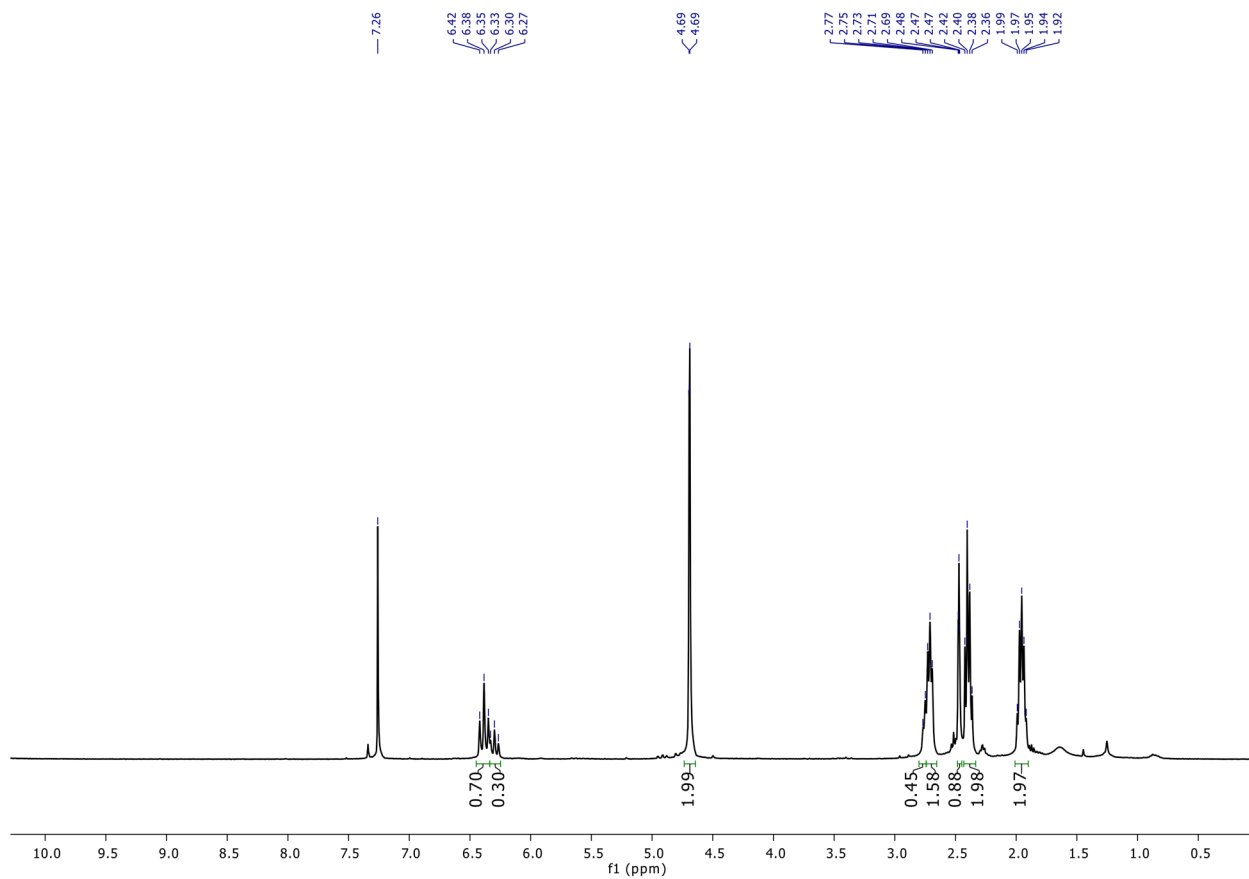
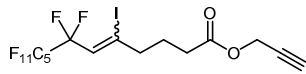
11,11,12,12,13,13,14,14,15,15,16,16,16-tridecafluoro-9-iodohexadec-9-en-1-yne (5.21a):



11,12,12,13,13,14,14,15,15,16,16,16-dodecafluorohexadeca-10-en-1,8-diyne (**5.21b**):

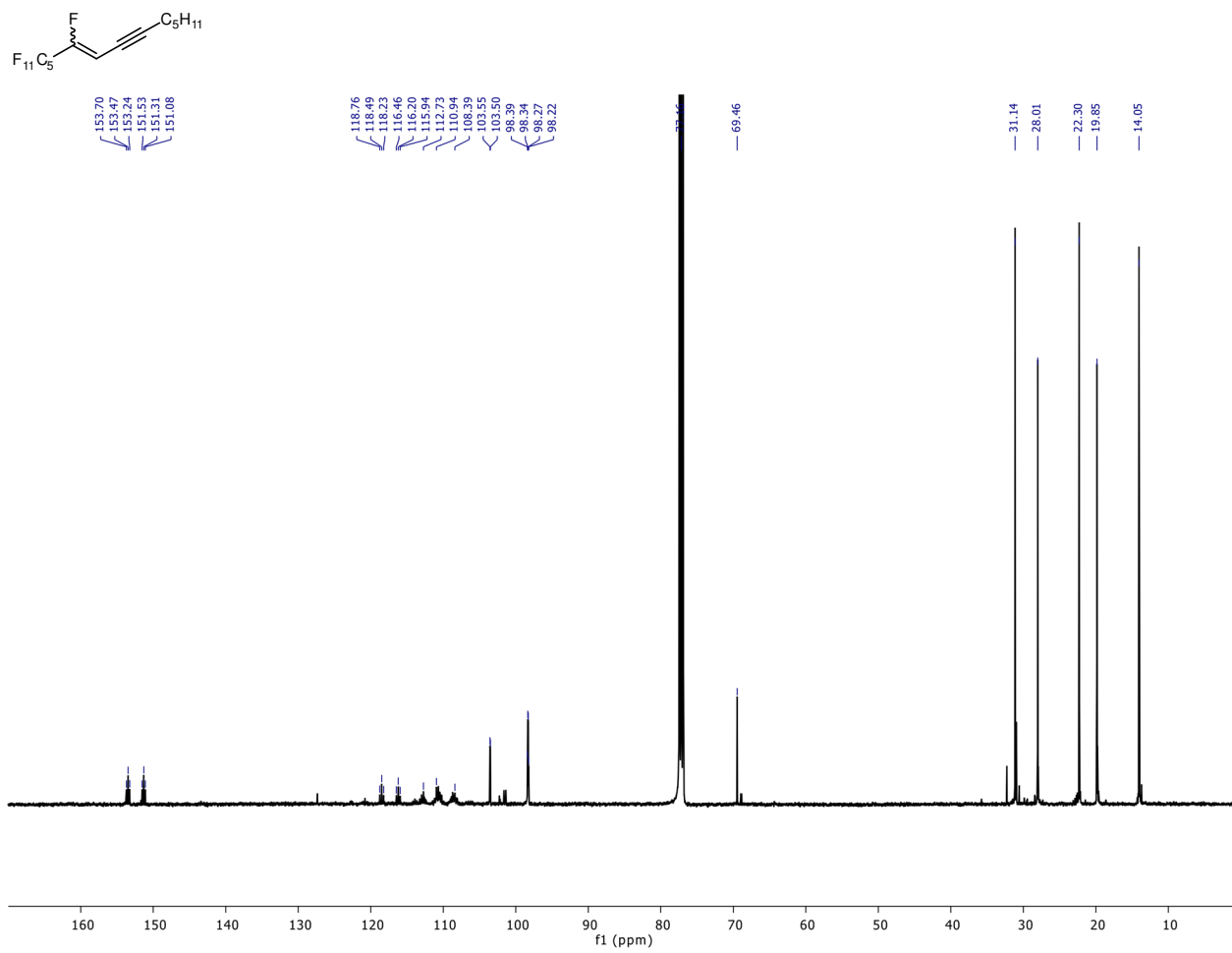


prop-2-yn-1-yl 7,7,8,8,9,9,10,10,11,11,12,12,12-tridecafluoro-5-iodododec-5-enoate (**5.22a**):

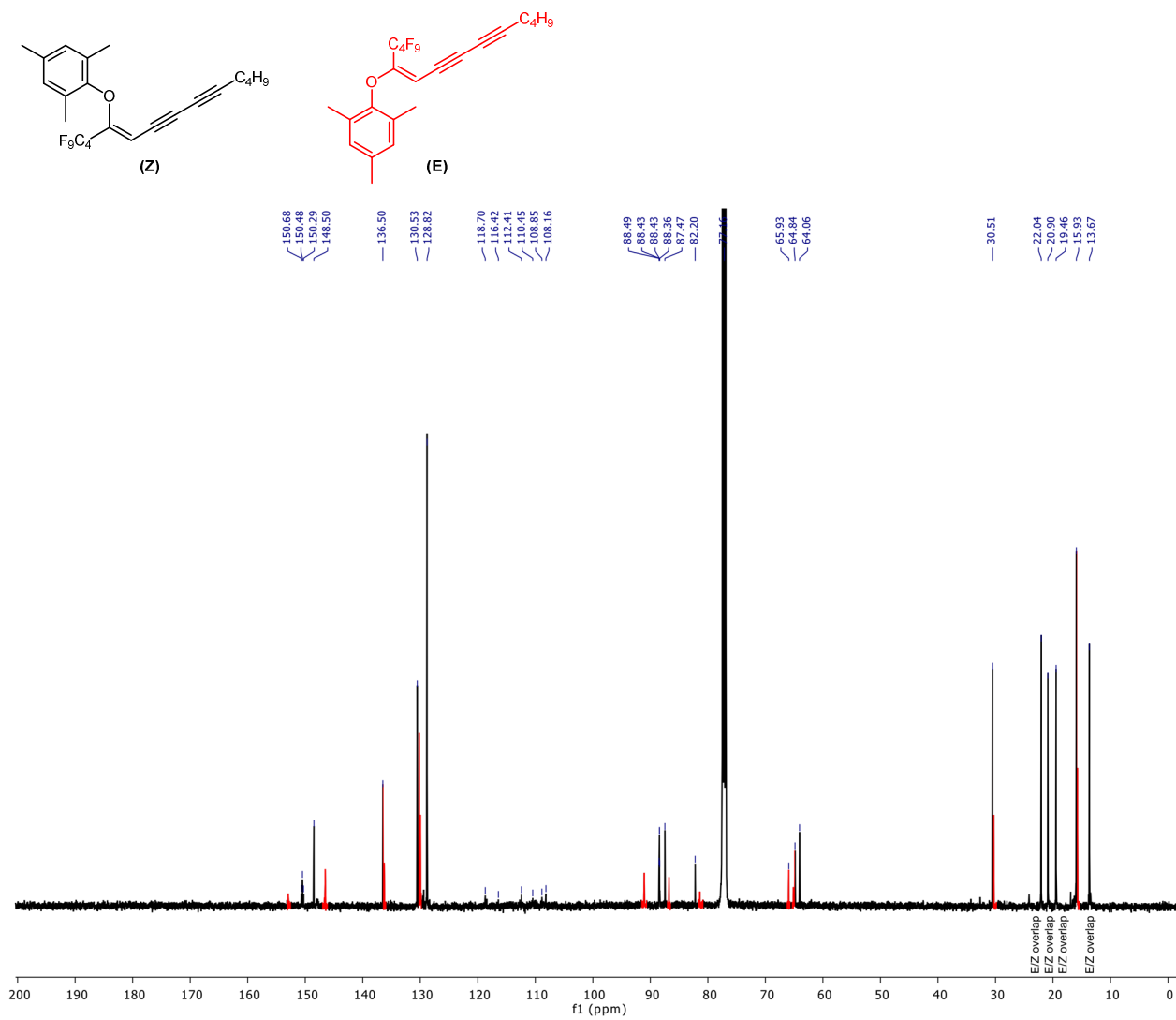


5.5.4 ^{13}C -NMR Spectra:

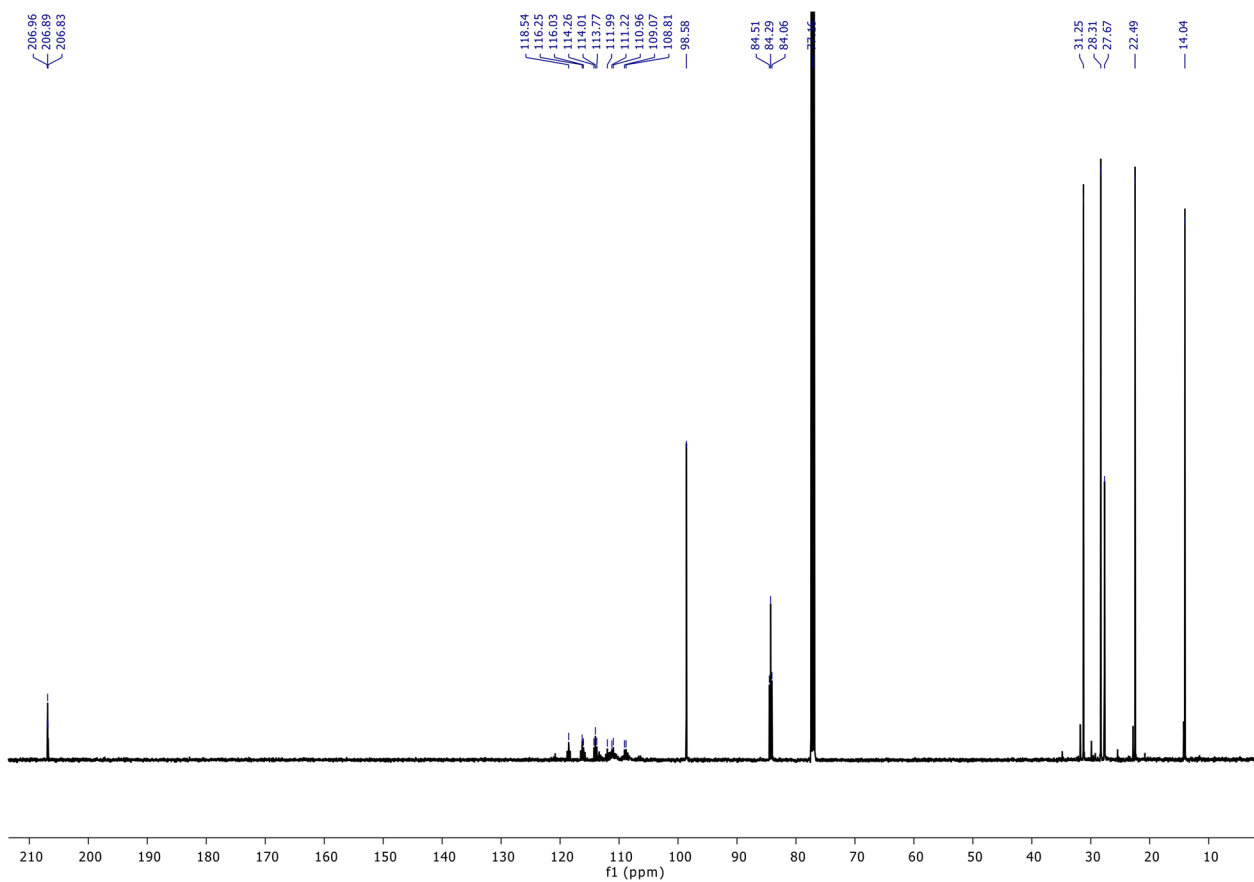
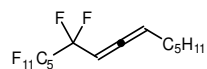
1,1,1,2,2,3,3,4,4,5,5,6-dodecafluorotetradec-6-en-8-yne (**5.6**):



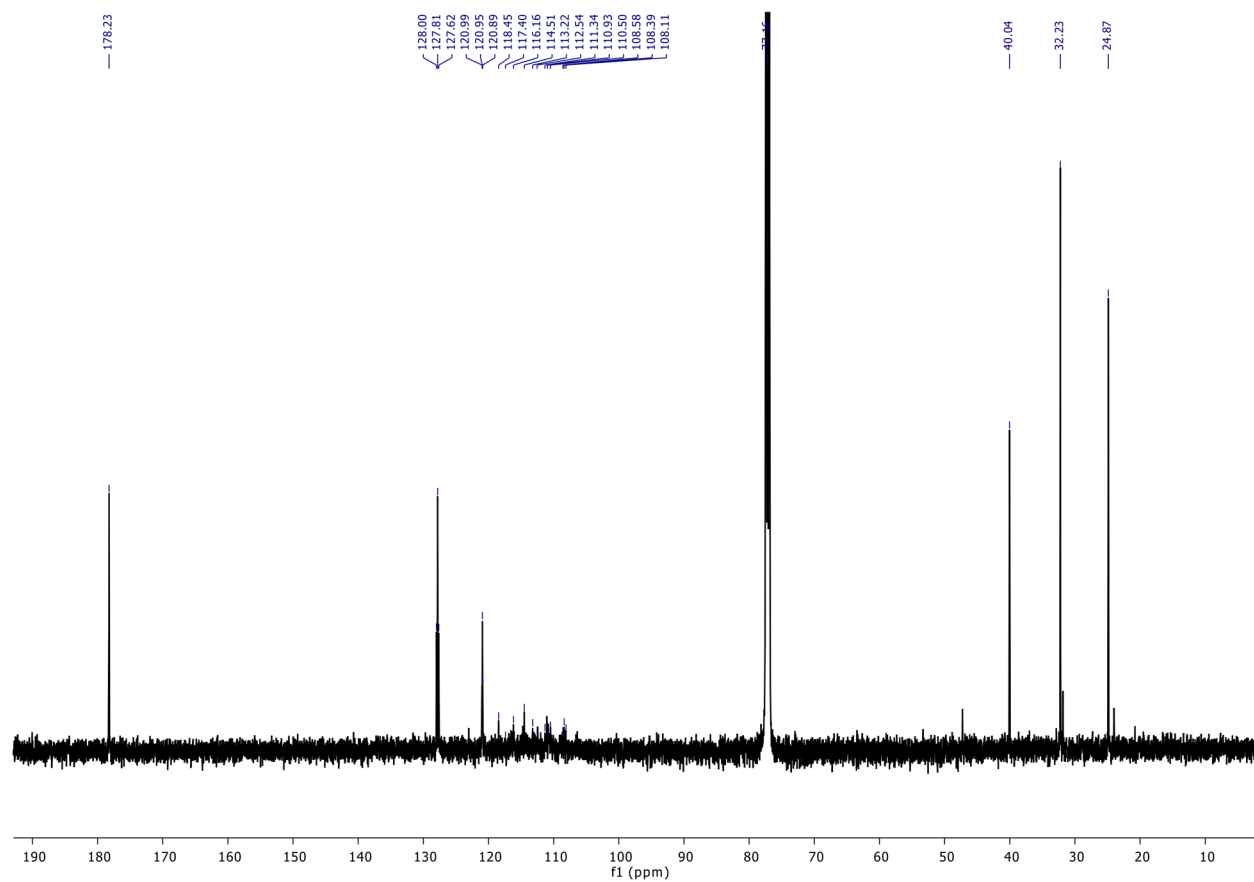
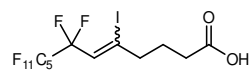
1,3,5-trimethyl-2-((1,1,1,2,2,3,3,4,4-nonafluorotetradeca-5-en-7,9-diyn-5-yl)oxy)benzene (**5.8**):



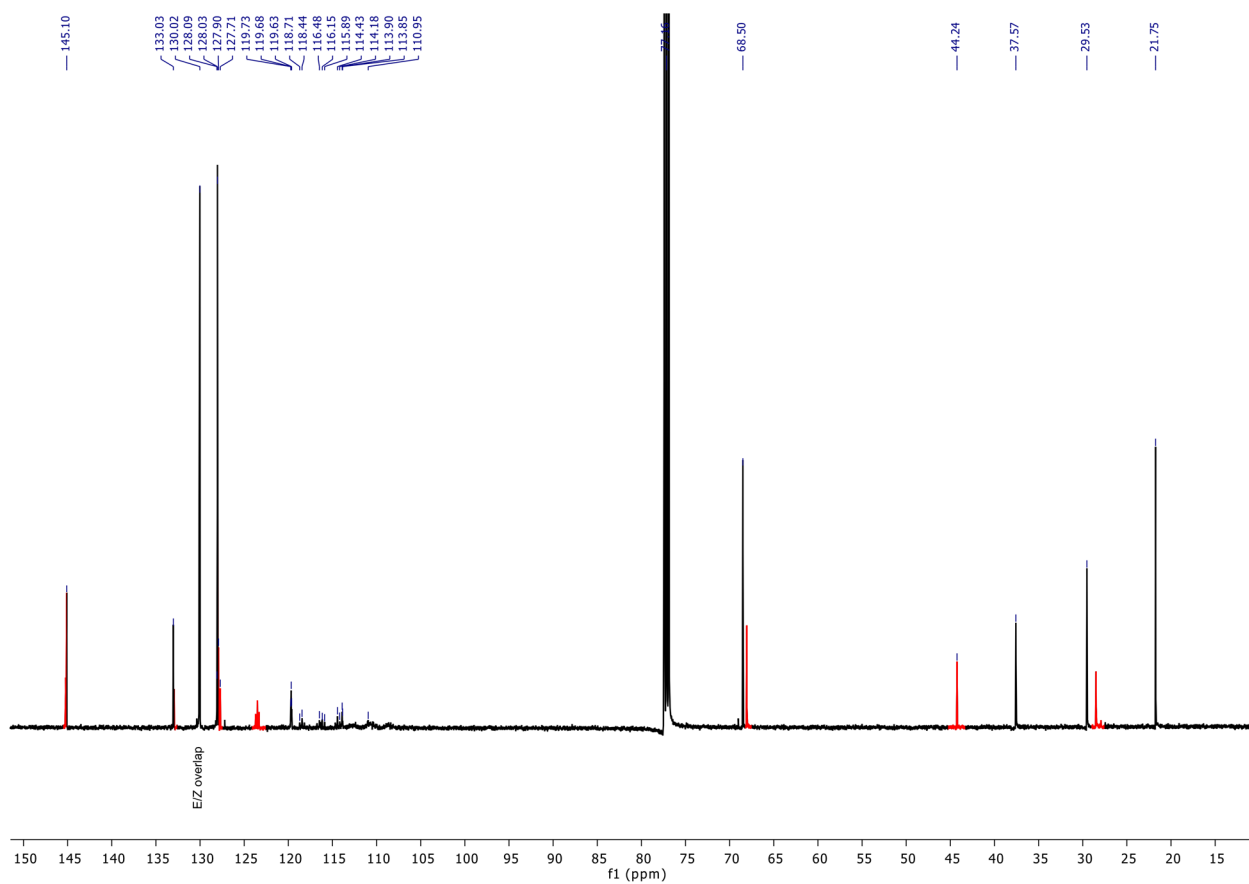
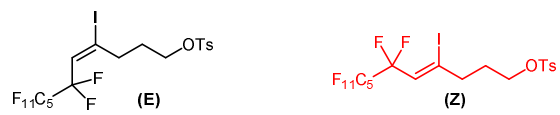
9,9,10,10,11,11,12,12,13,13,14,14,14-tridecafluorotetradeca-6,7-diene (5.10):



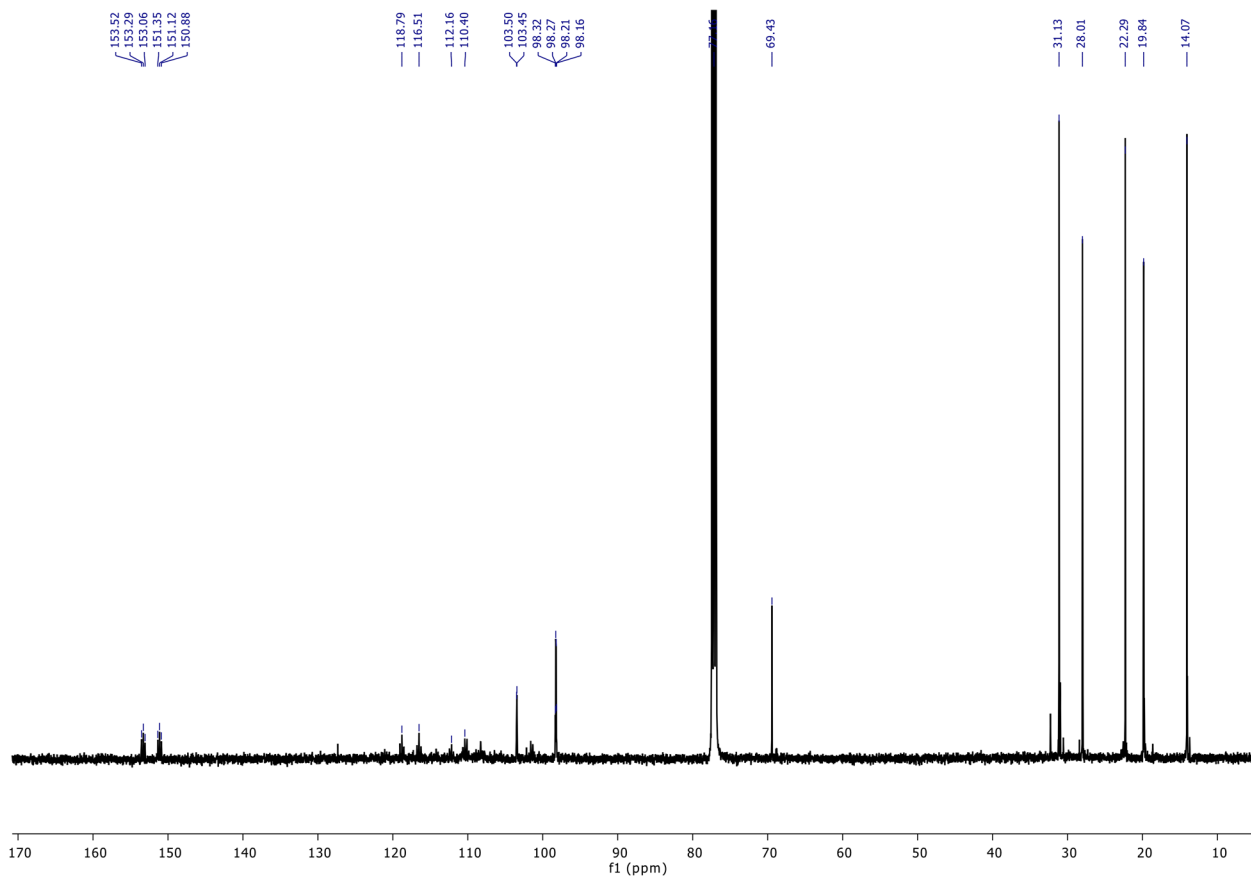
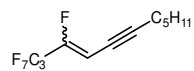
7,7,8,8,9,9,10,10,11,11,12,12,12-tridecafluoro-5-iodododec-5-enoic acid (**5.12**):



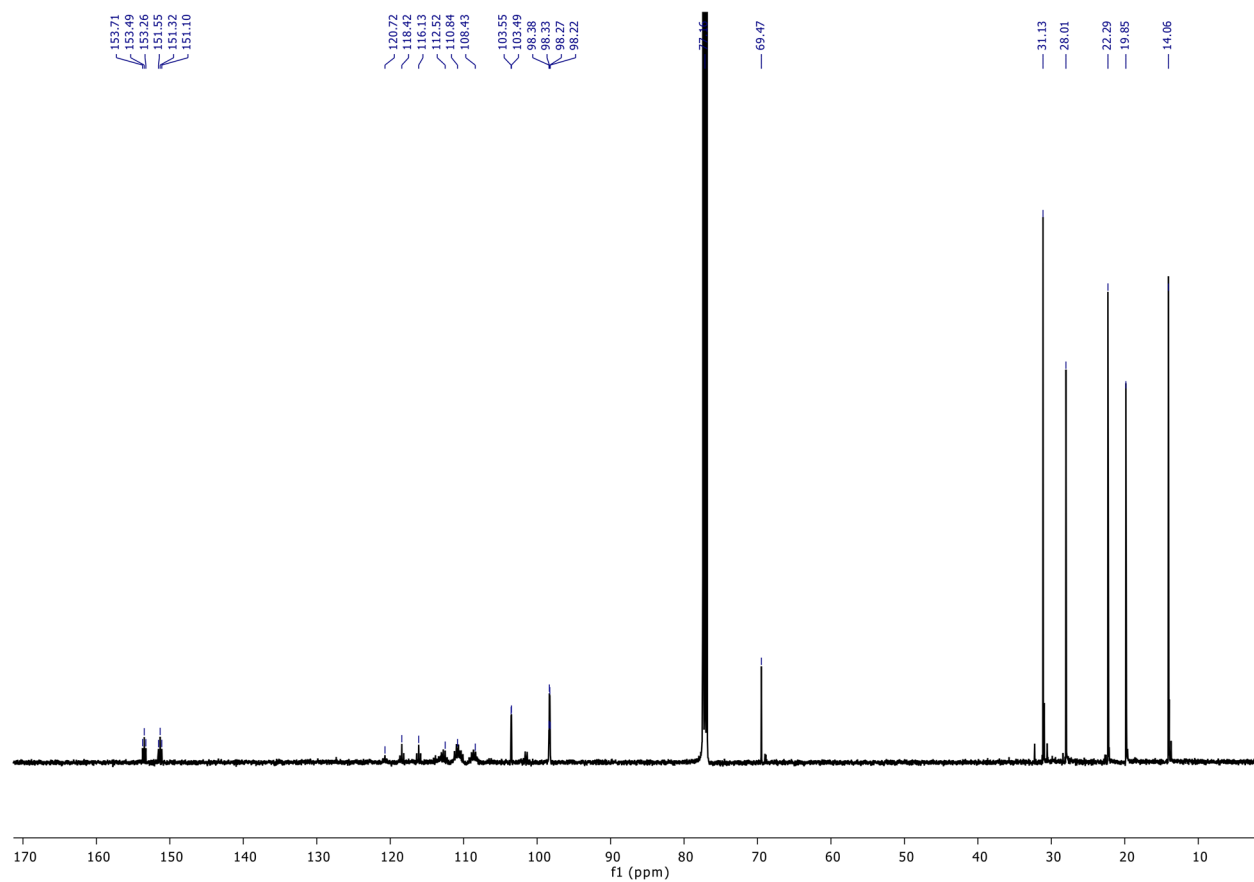
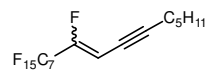
6,6,7,7,8,8,9,9,10,10,11,11,11-tridecafluoro-4-iodoundec-4-en-1-yl 4-methylbenzenesulfonate (**5.14**):



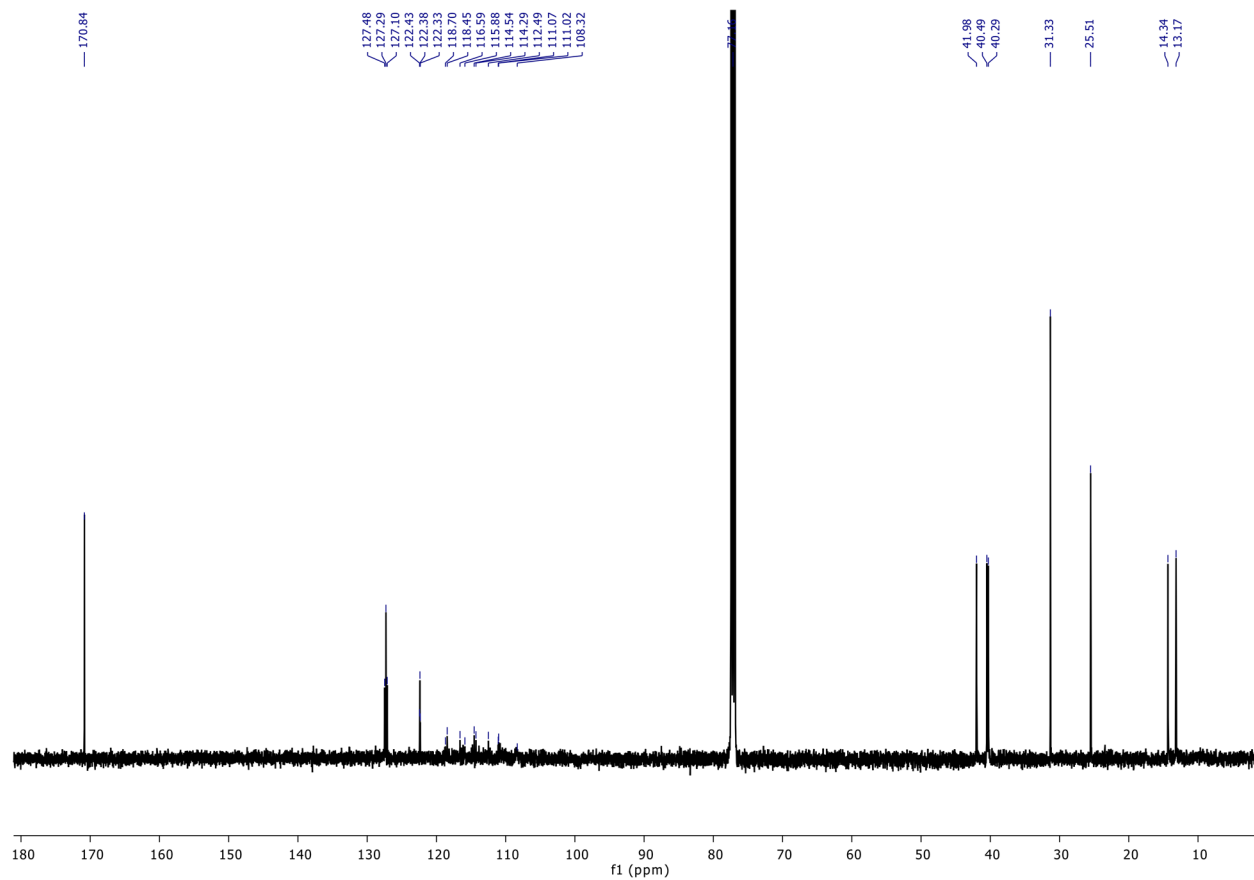
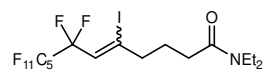
1,1,1,2,2,3,3,4-octafluorododec-4-en-6-yne (**5.15b**):



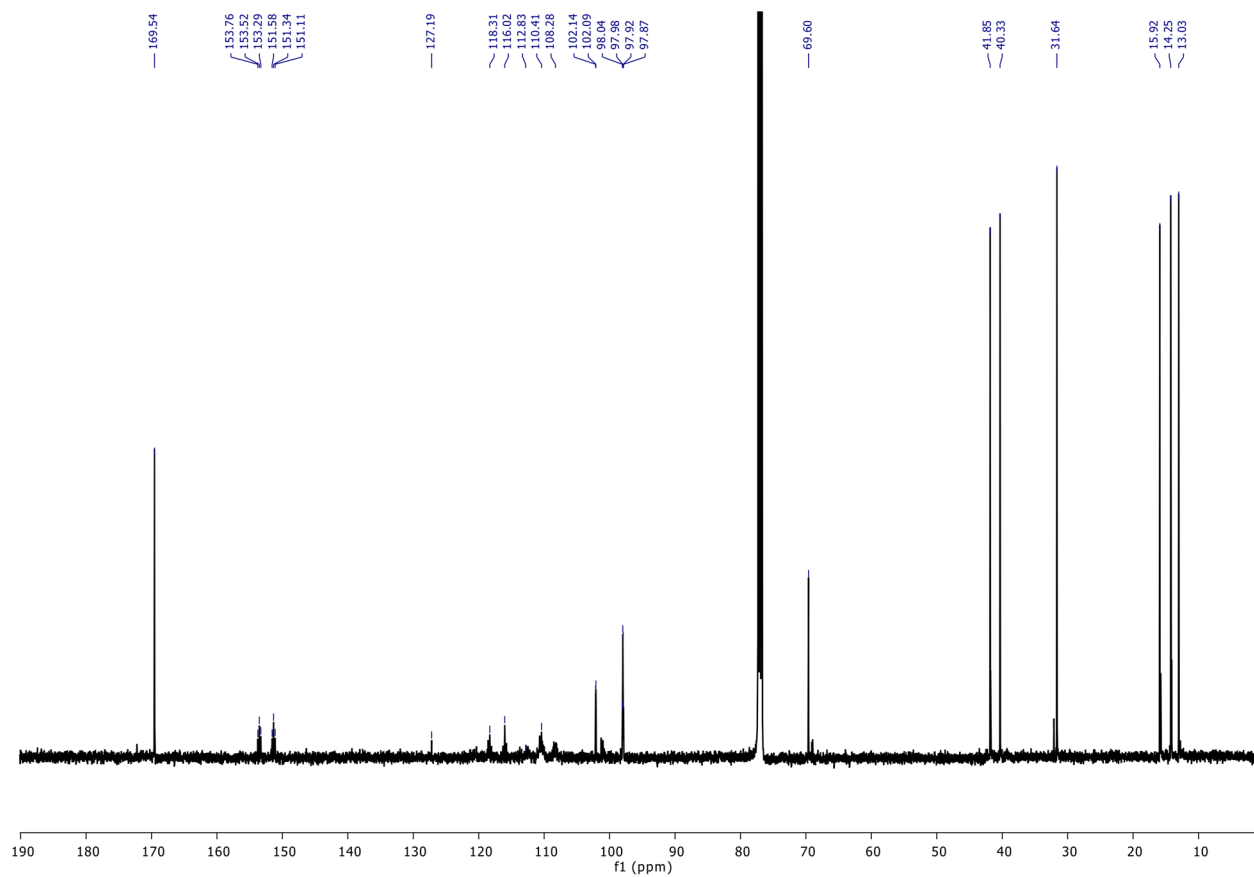
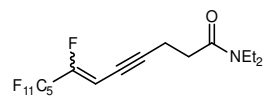
9,10,10,11,11,12,12,13,13,14,14,15,15,16,16,16-hexadecafluorohexadec-8-en-6-yne (**5.16b**):



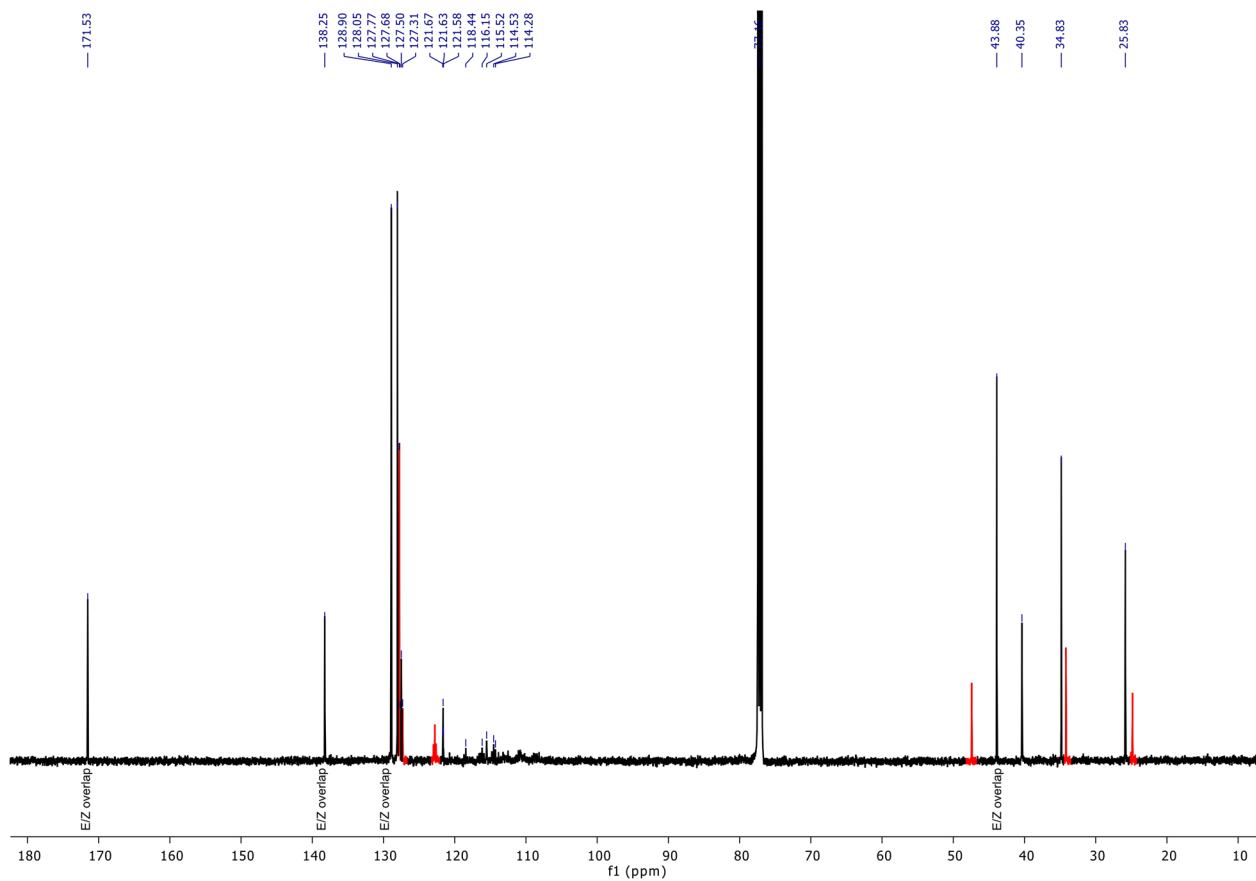
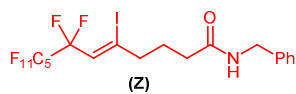
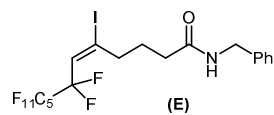
N,N-diethyl-7,7,8,8,9,9,10,10,11,11,12,12,12-tridecafluoro-5-iodododec-5-enamide (**5.17a**):



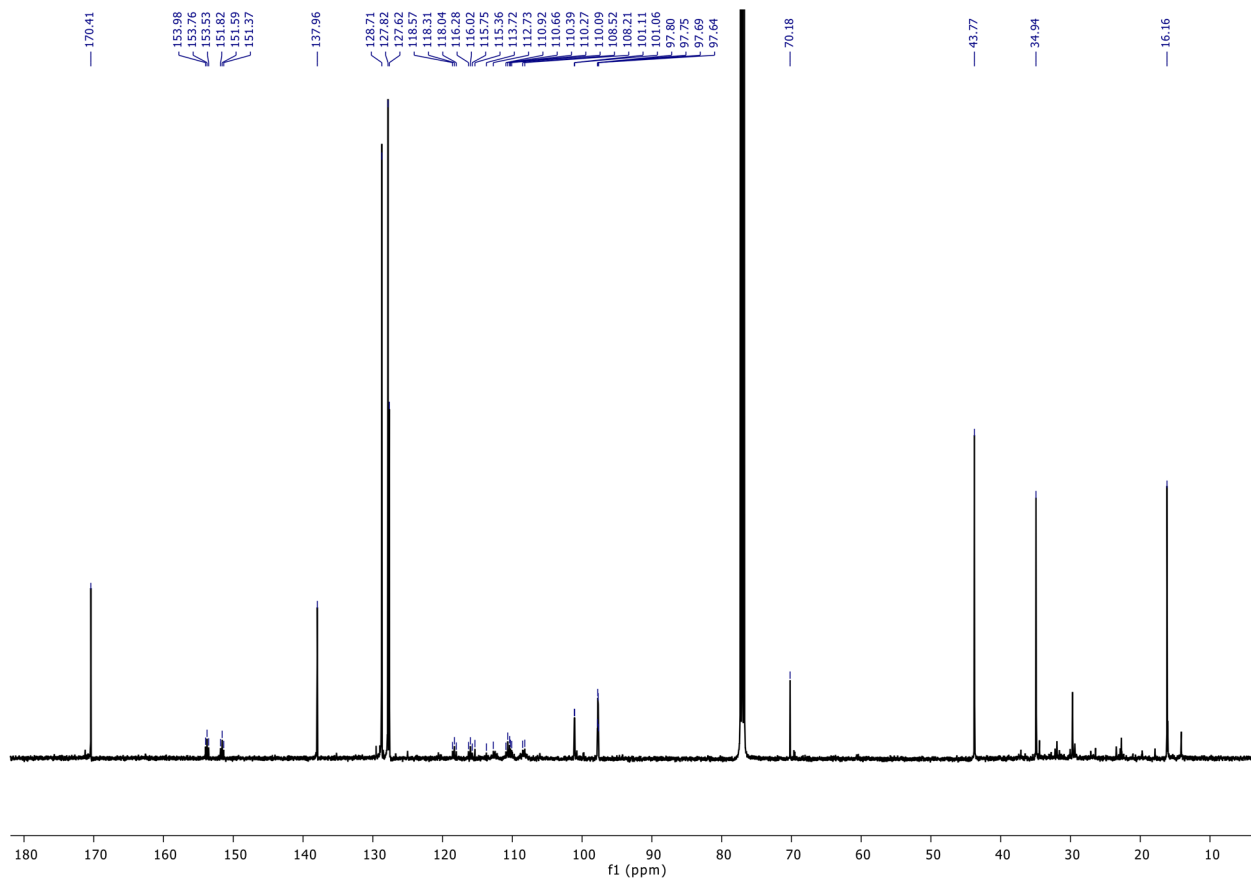
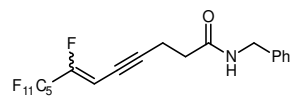
N,N-diethyl-7,8,8,9,9,10,10,11,11,12,12,12-dodecafluorododec-6-en-4-ynamide (**5.17b**):



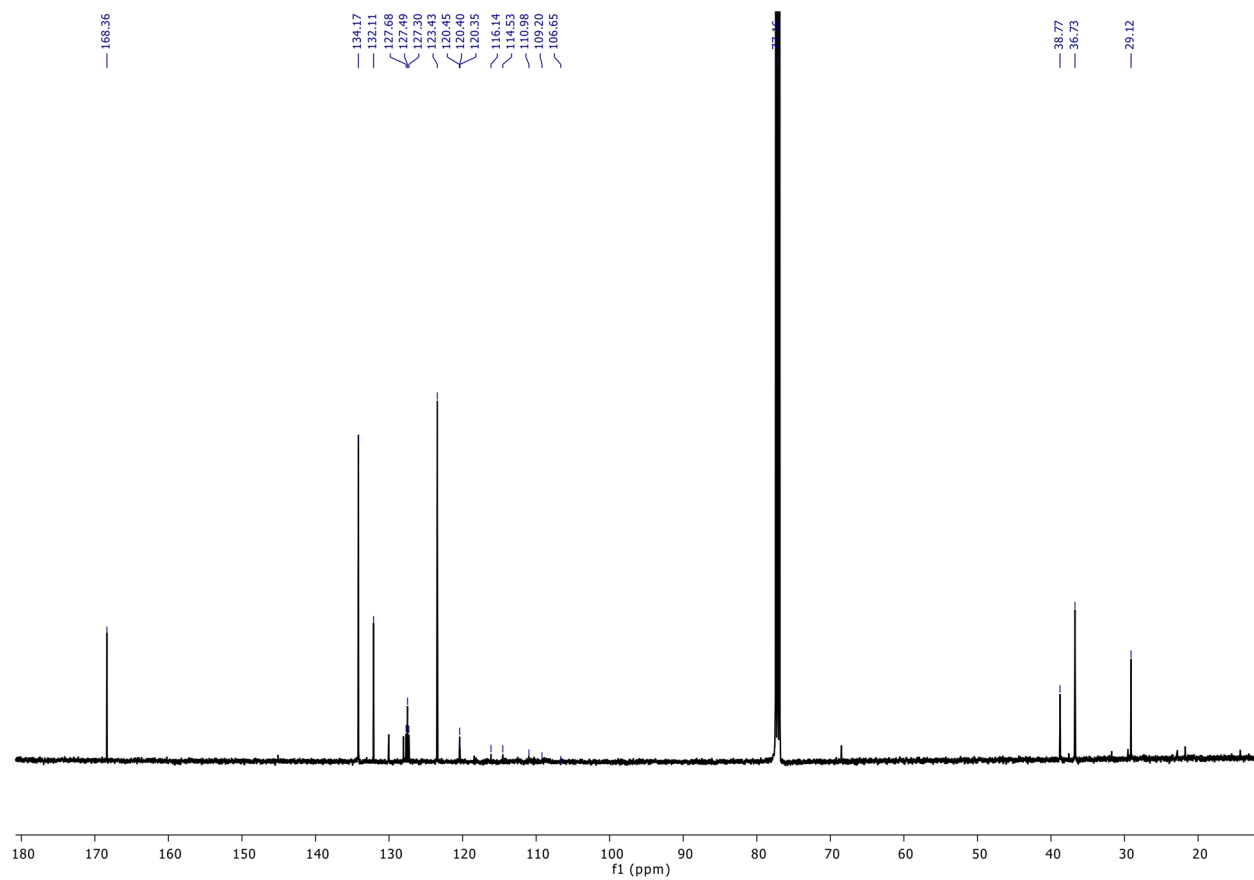
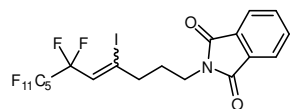
N-benzyl-7,7,8,8,9,9,10,10,11,11,12,12,12-tridecafluoro-5-iodododec-5-enamide (**5.18a**):



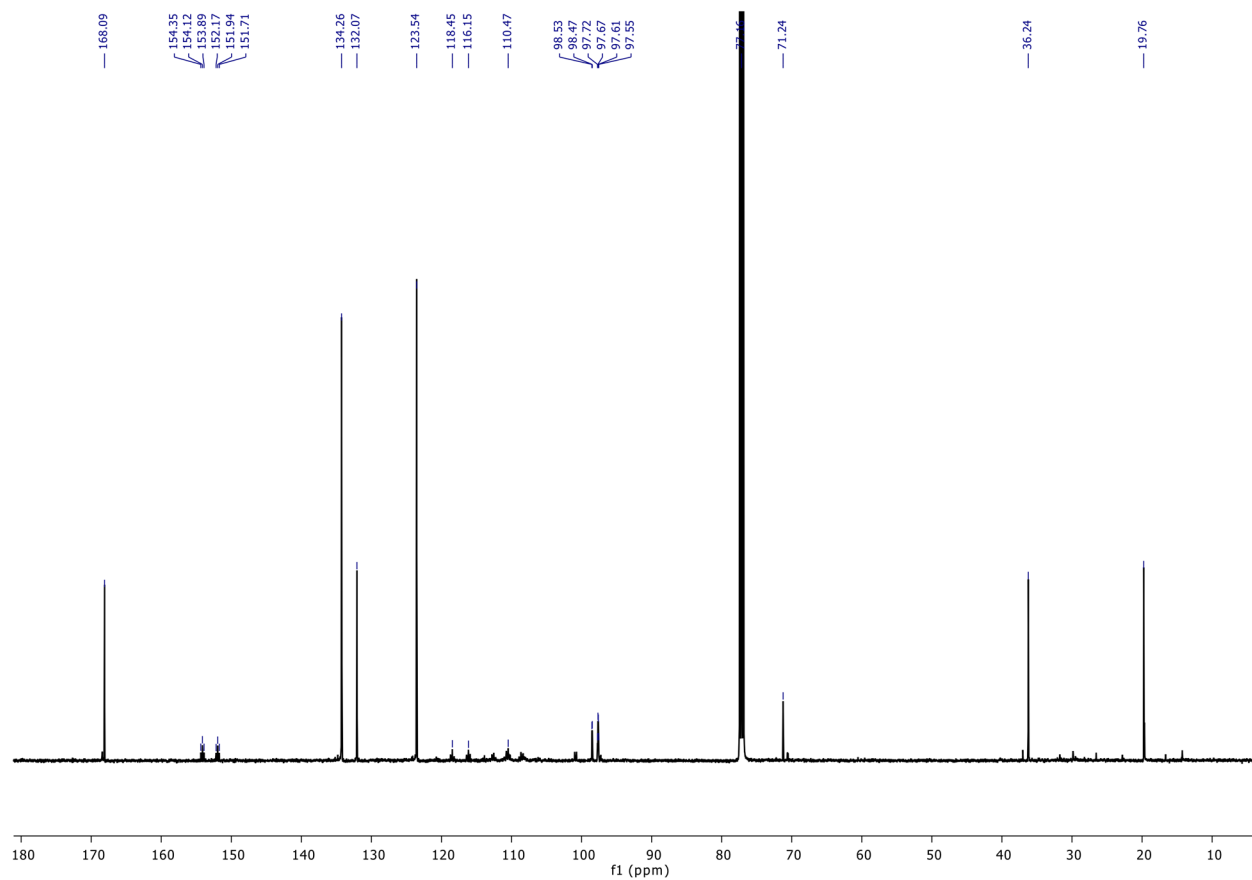
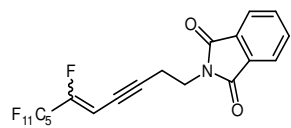
N-benzyl-7,8,8,9,9,10,10,11,11,12,12,12-dodecafluorododec-6-en-4-ynamide (**5.18b**):



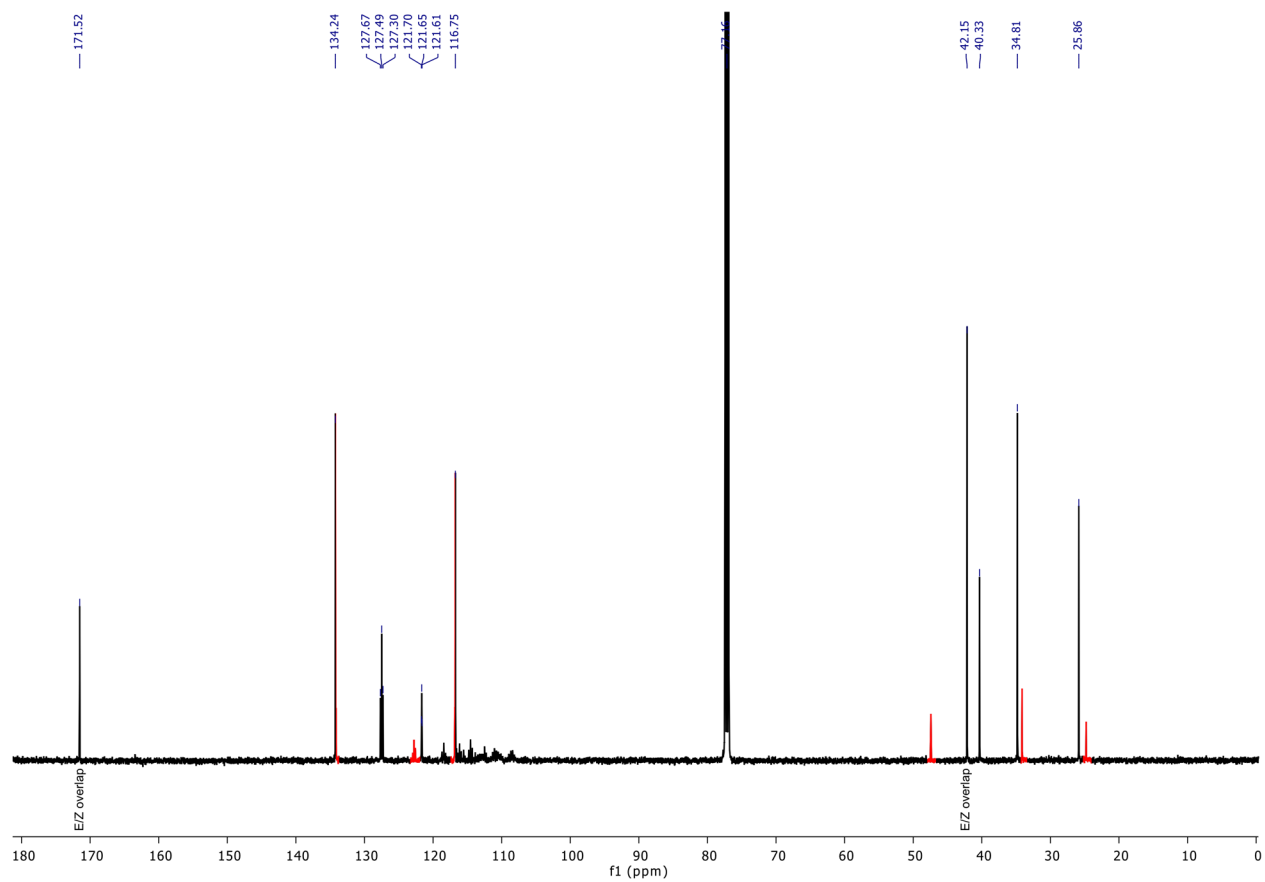
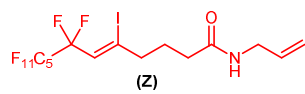
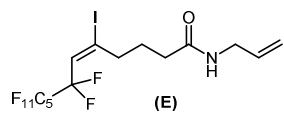
2-(6,6,7,7,8,8,9,9,10,10,11,11,11-tridecafluoro-4-iodoundec-4-en-1-yl)isoindoline-1,3-dione (**5.19a**):



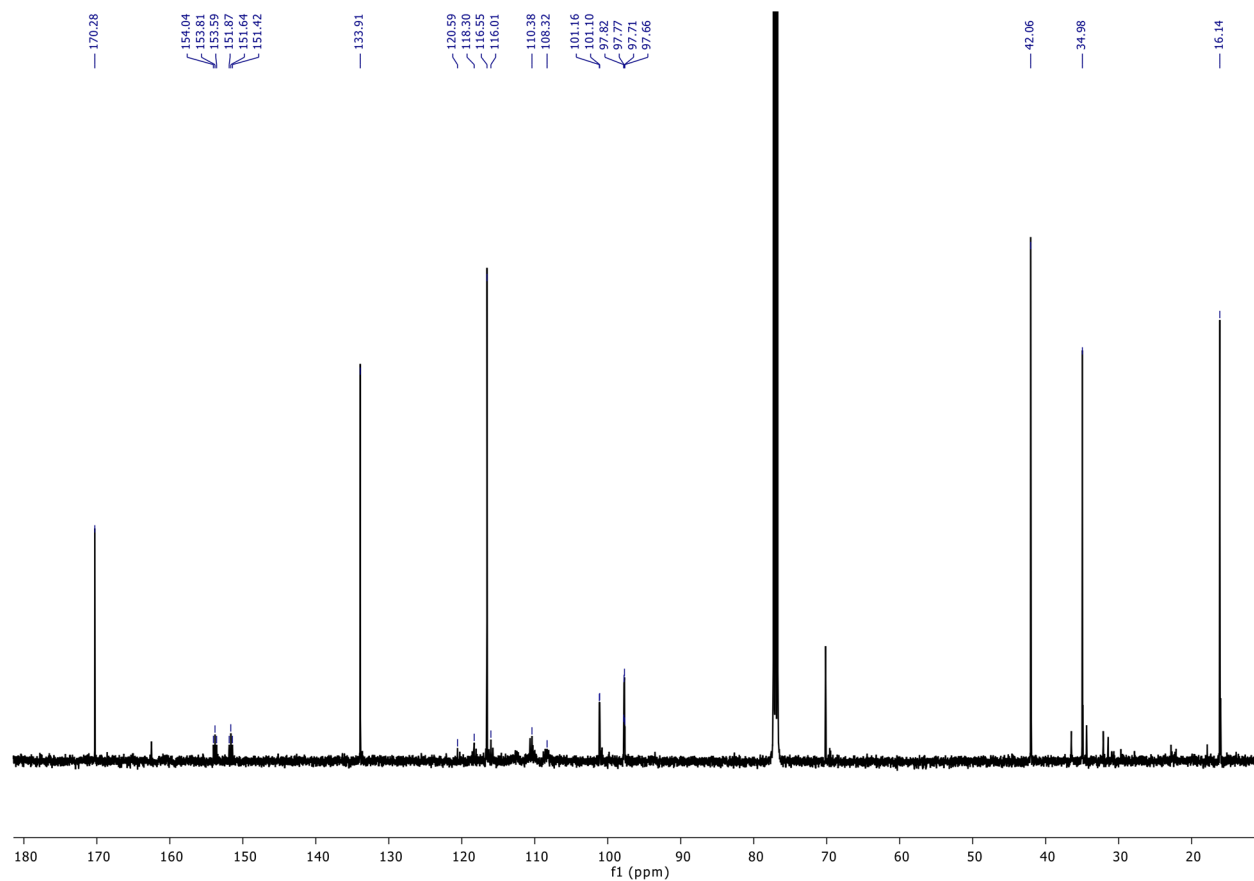
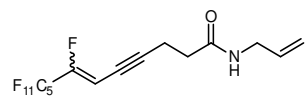
2-(6,7,7,8,8,9,9,10,10,11,11,11-dodecafluoroundec-5-en-3-yn-1-yl)isoindoline-1,3-dione (**5.19b**):



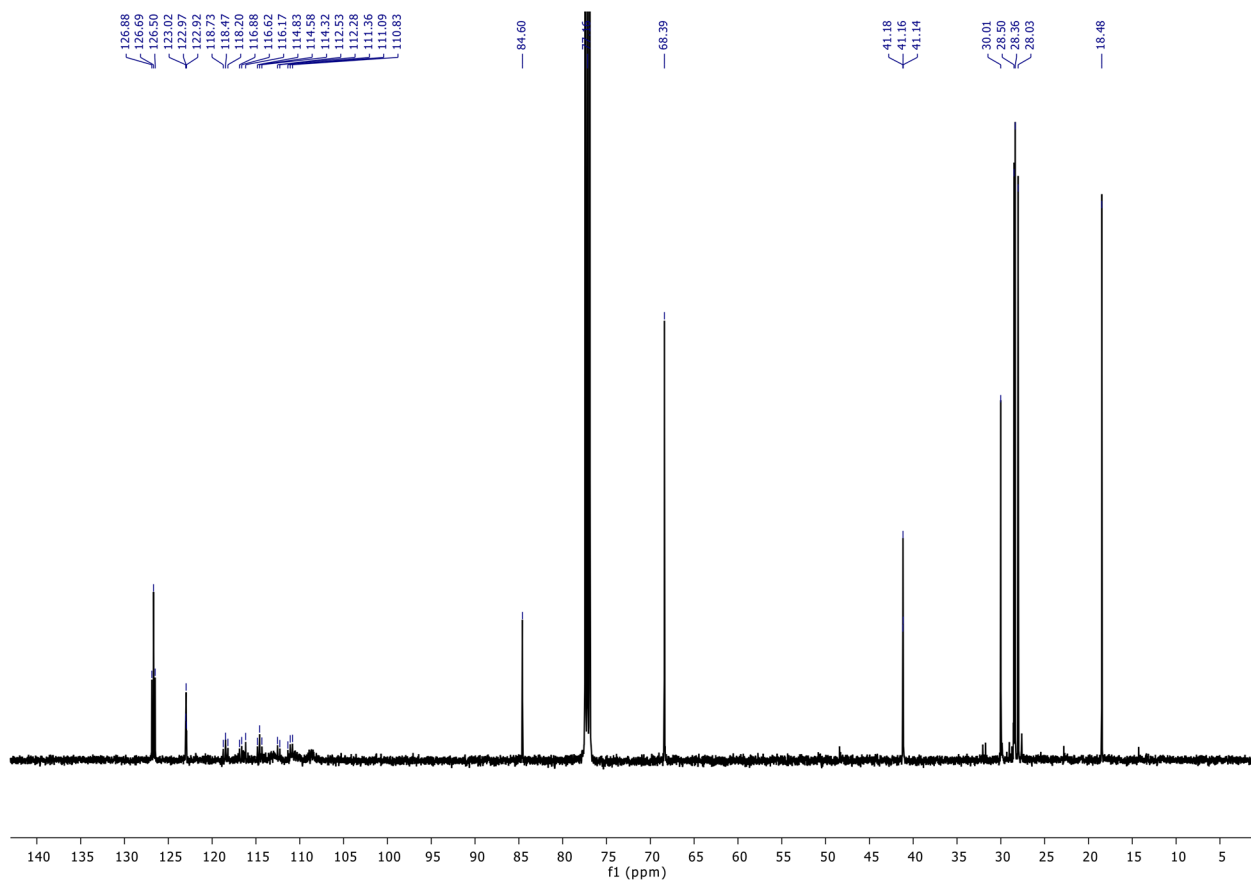
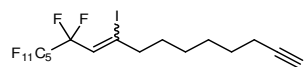
N-allyl-7,7,8,8,9,9,10,10,11,11,12,12,12-tridecafluoro-5-iodododec-5-enamide (**5.20a**):



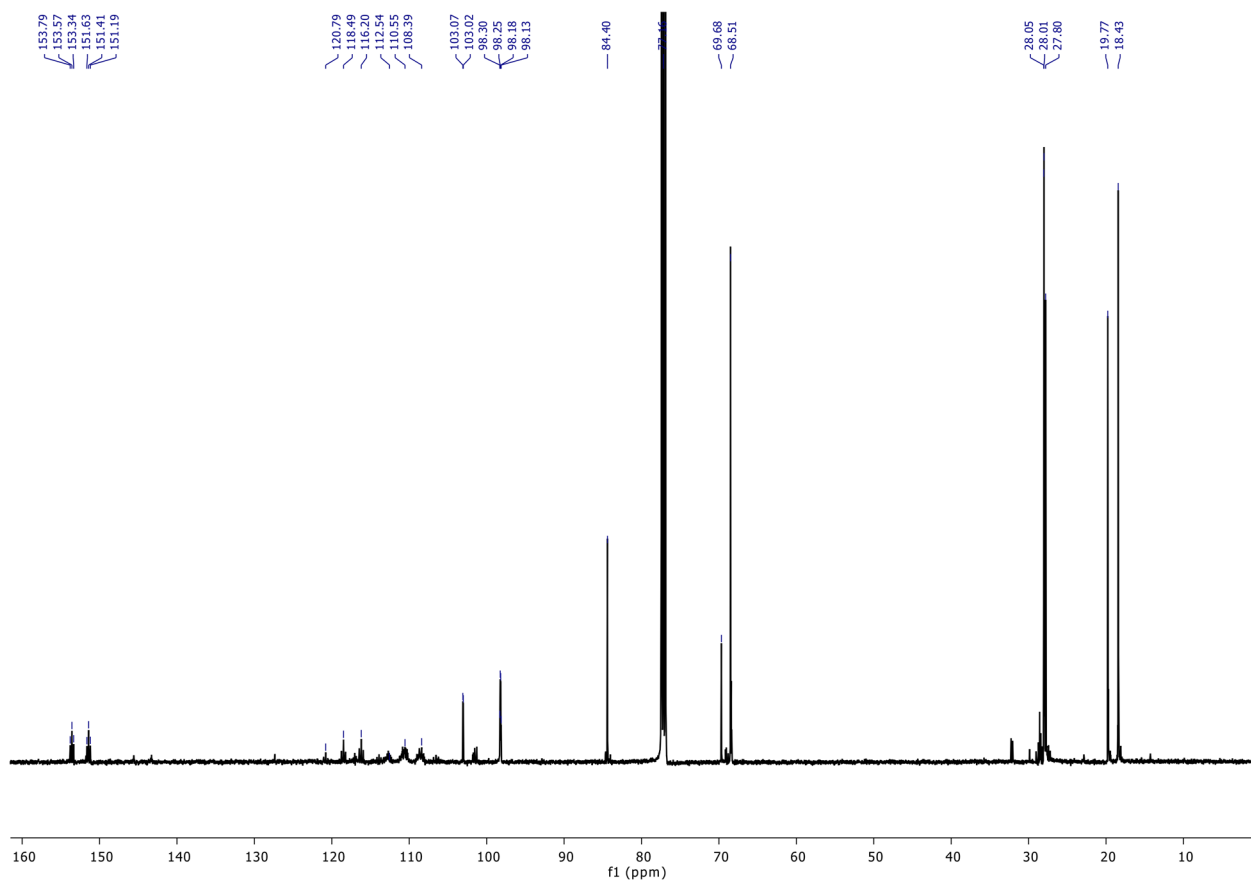
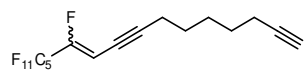
N-allyl-7,8,8,9,9,10,10,11,11,12,12,12-dodecafluorododec-6-en-4-ynamide (**5.20b**):



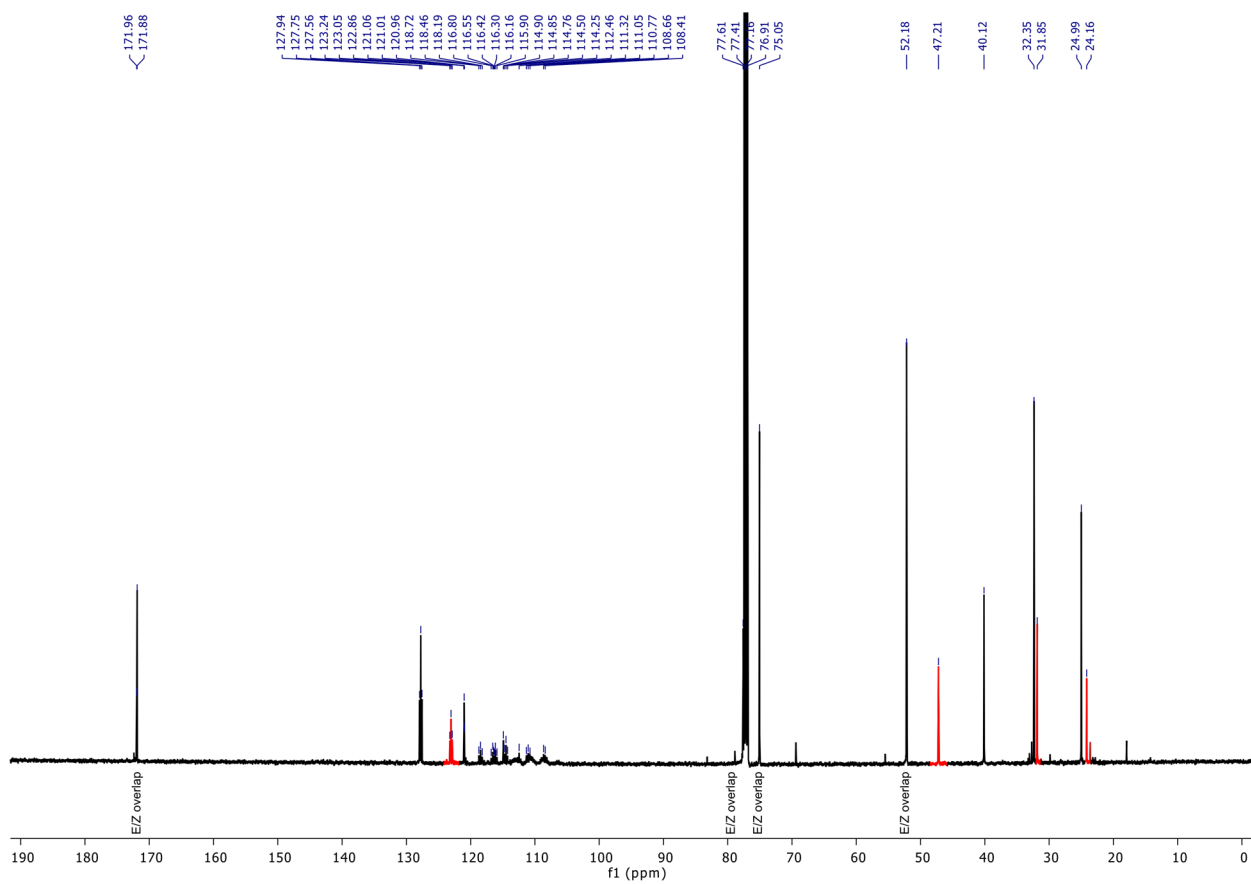
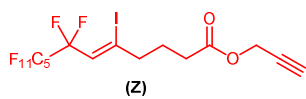
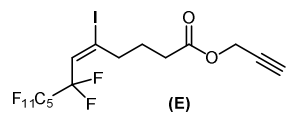
11,11,12,12,13,13,14,14,15,15,16,16,16-tridecafluoro-9-iodohexadec-9-en-1-yne (5.21a):



11,12,12,13,13,14,14,15,15,16,16,16-dodecafluorohexadeca-10-en-1,8-diyne (**5.21b**):

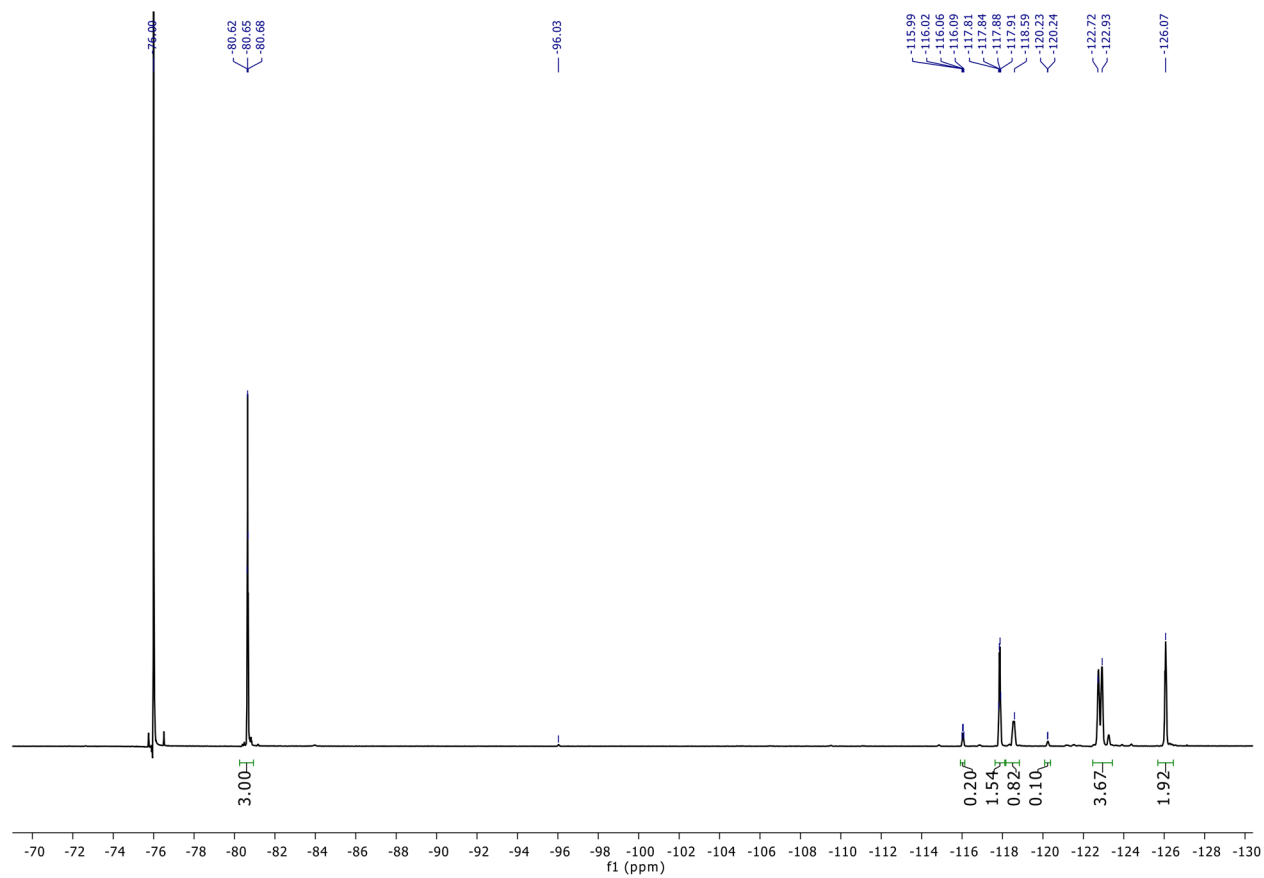
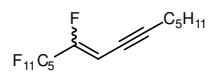


prop-2-yn-1-yl 7,7,8,8,9,9,10,10,11,11,12,12,12-tridecafluoro-5-iodododec-5-enoate (**5.22a**):

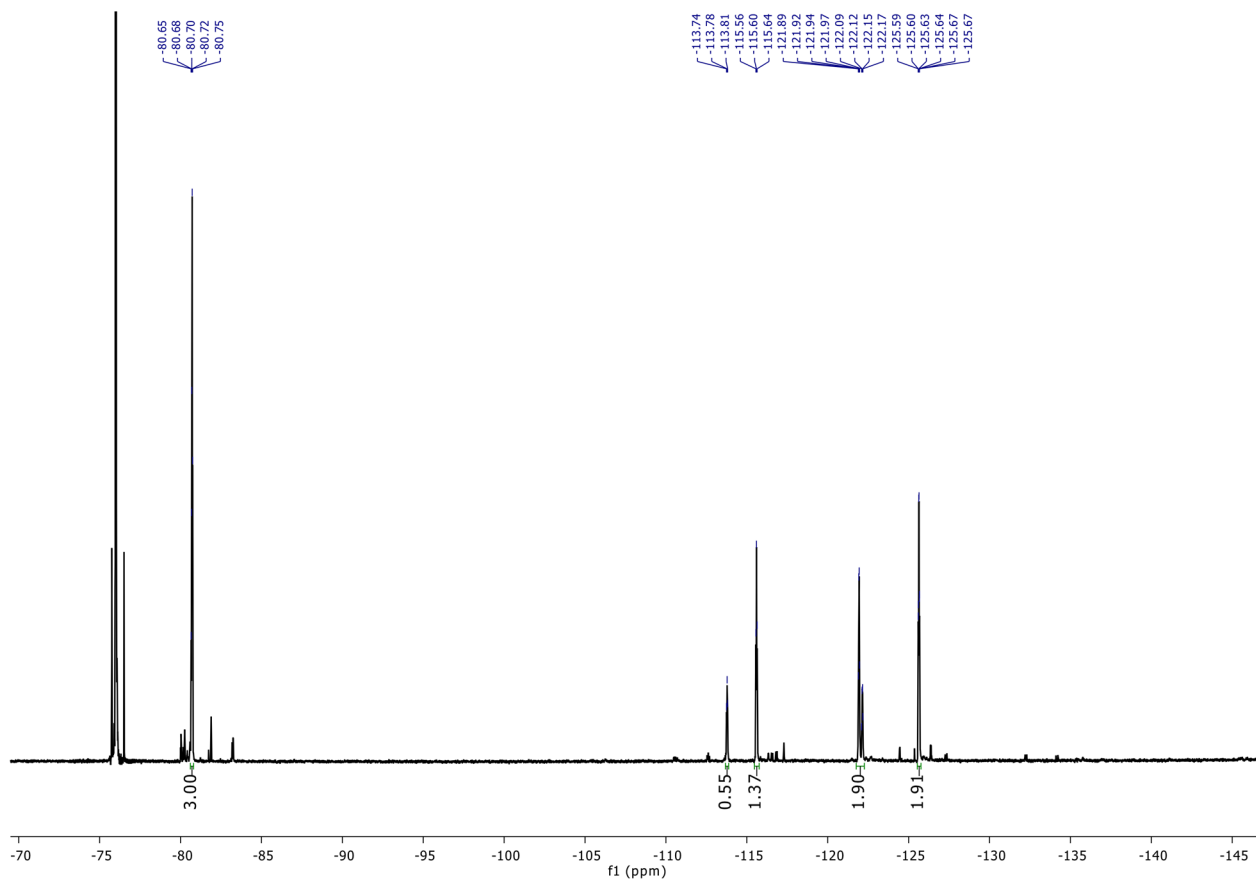
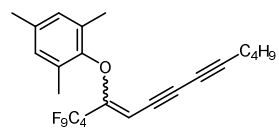


5.5.5 ^{19}F -NMR Spectra:

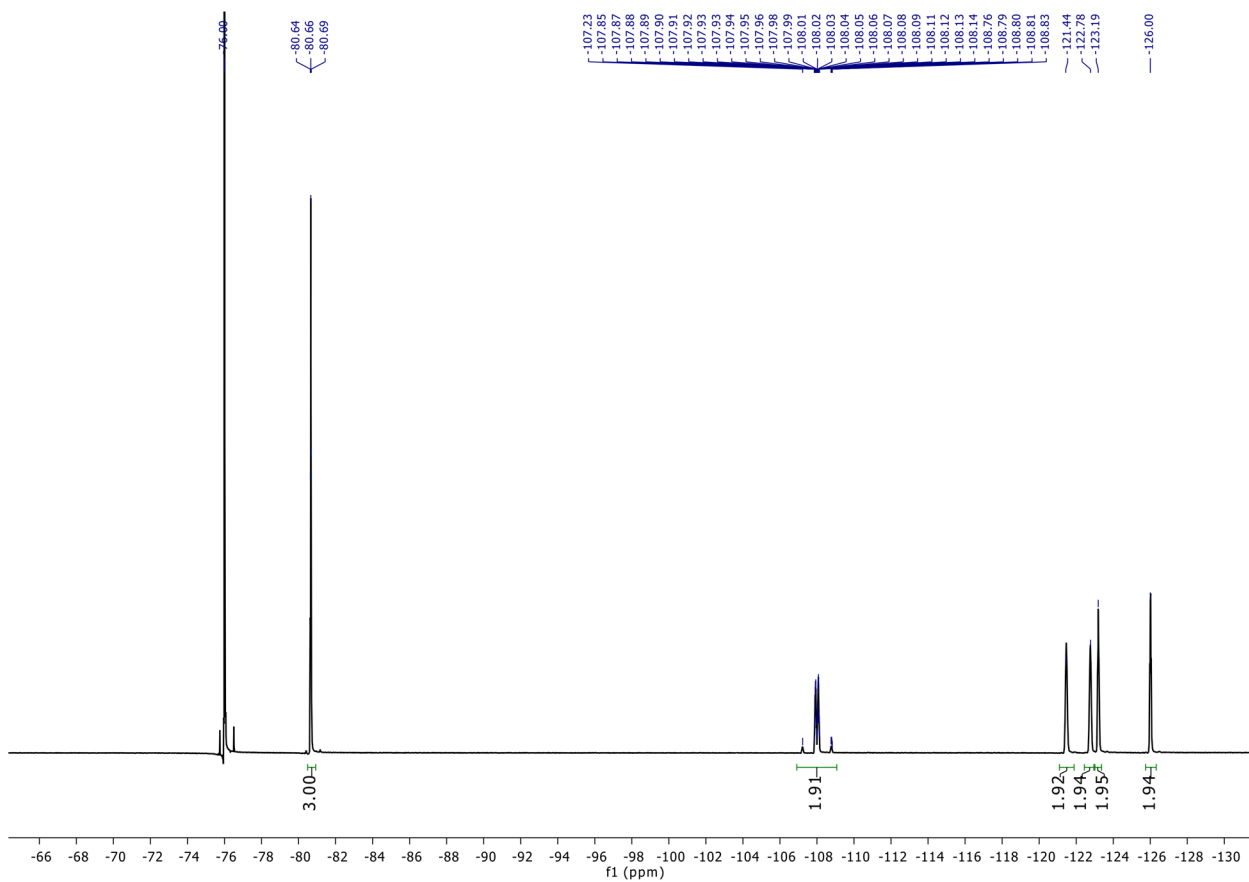
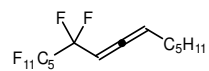
1,1,1,2,2,3,3,4,4,5,5,6-dodecafluorotetradec-6-en-8-yne (**5.6**):



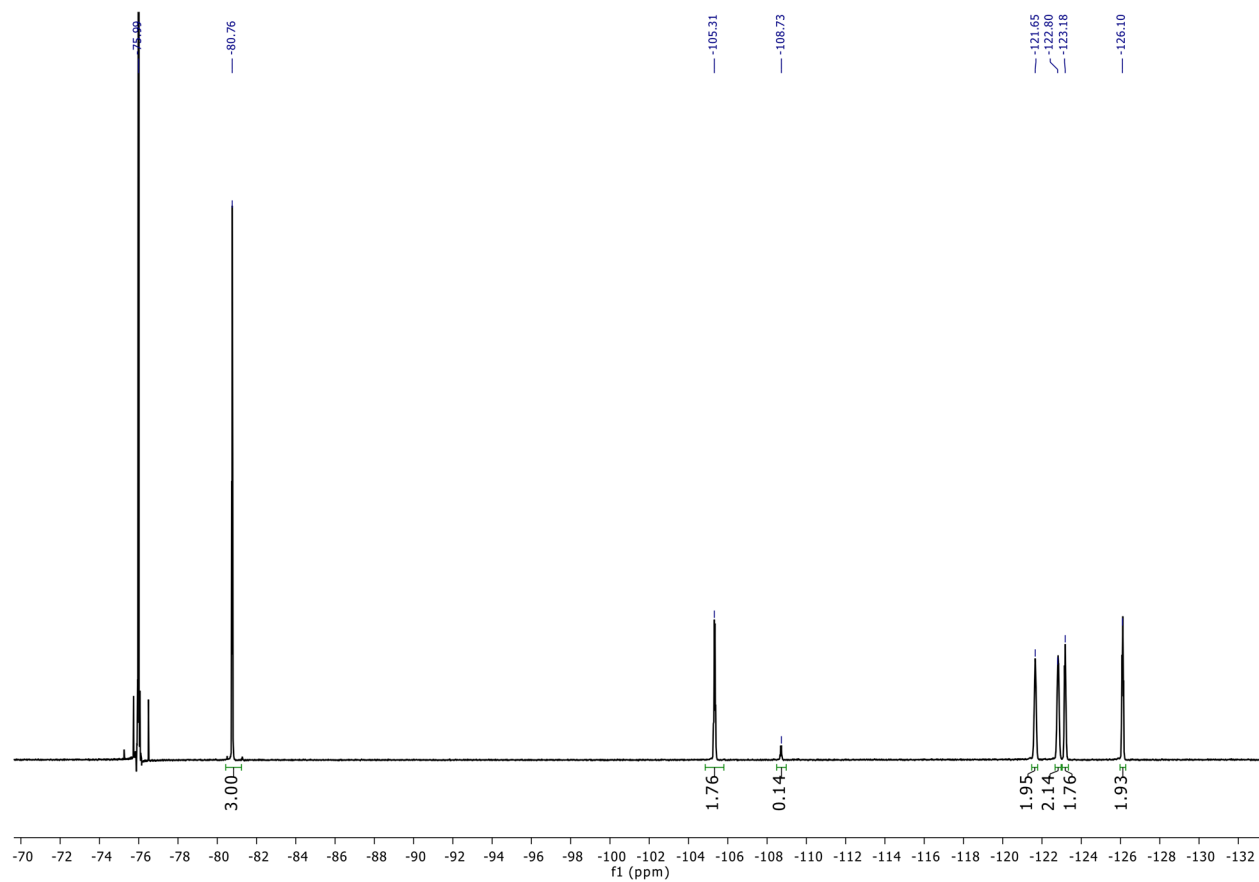
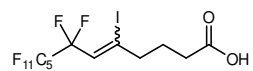
1,3,5-trimethyl-2-((1,1,1,2,2,3,3,4,4-nonafluorotetradeca-5-en-7,9-diyn-5-yl)oxy)benzene (**5.8**):



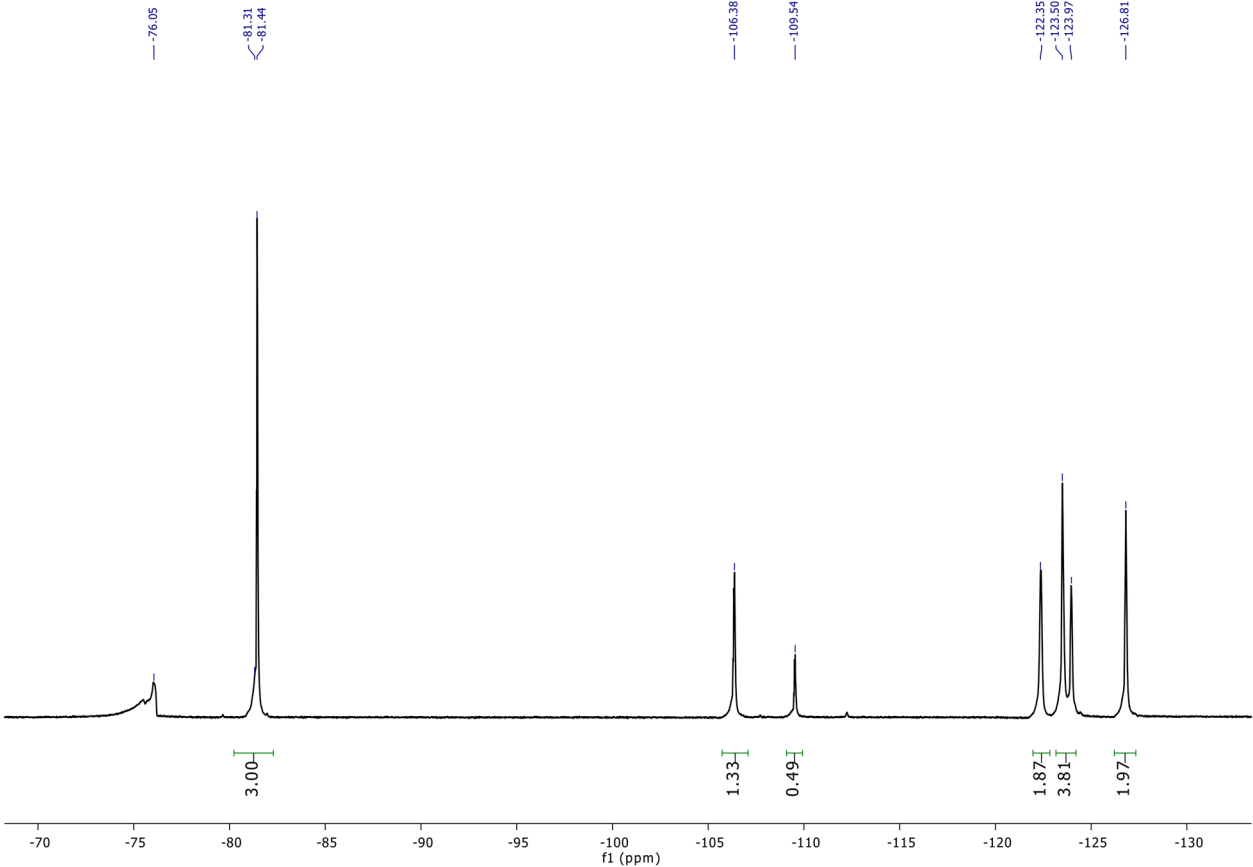
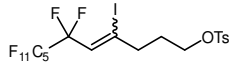
9,9,10,10,11,11,12,12,13,13,14,14,14-tridecafluorotetradeca-6,7-diene (**5.10**):



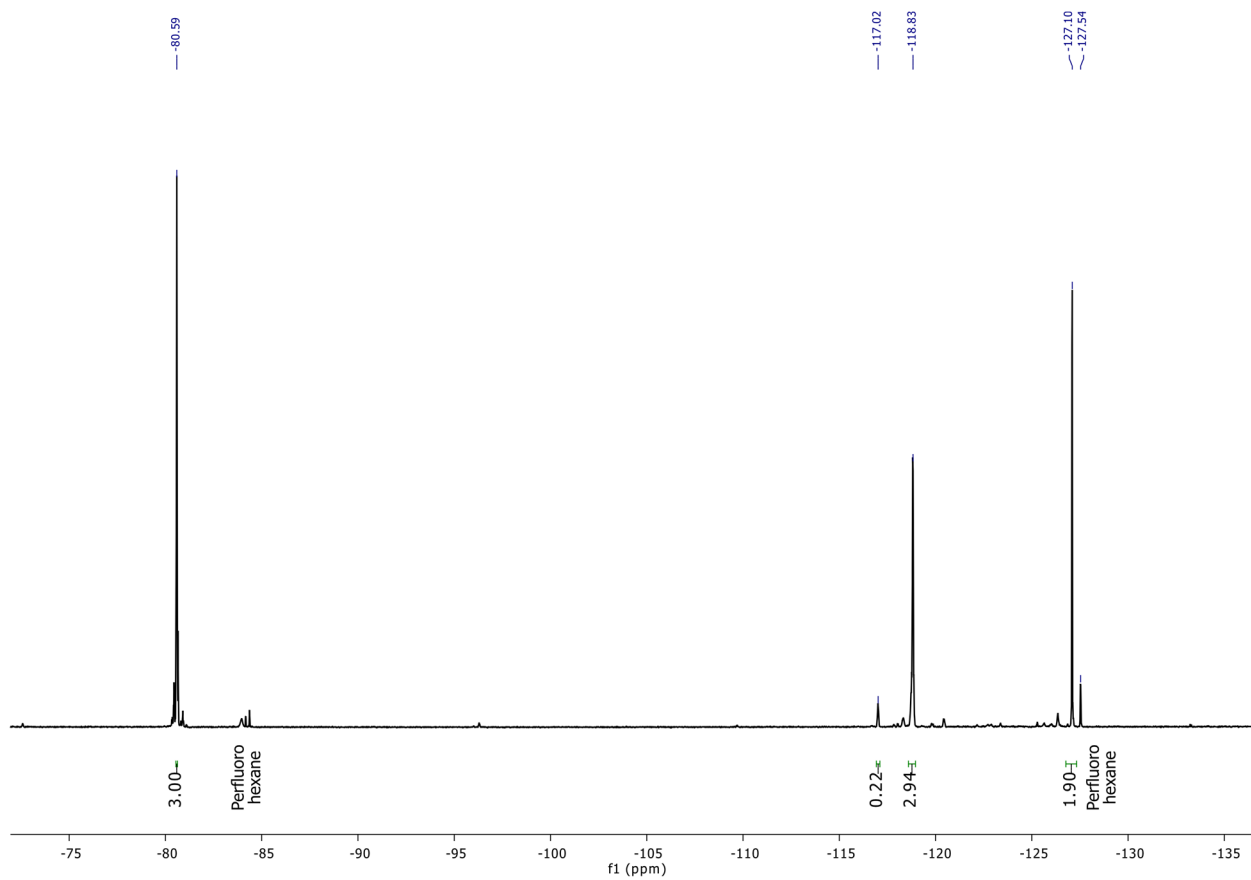
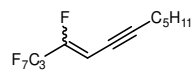
7,7,8,8,9,9,10,10,11,11,12,12,12-tridecafluoro-5-iodododec-5-enoic acid (**5.12**):



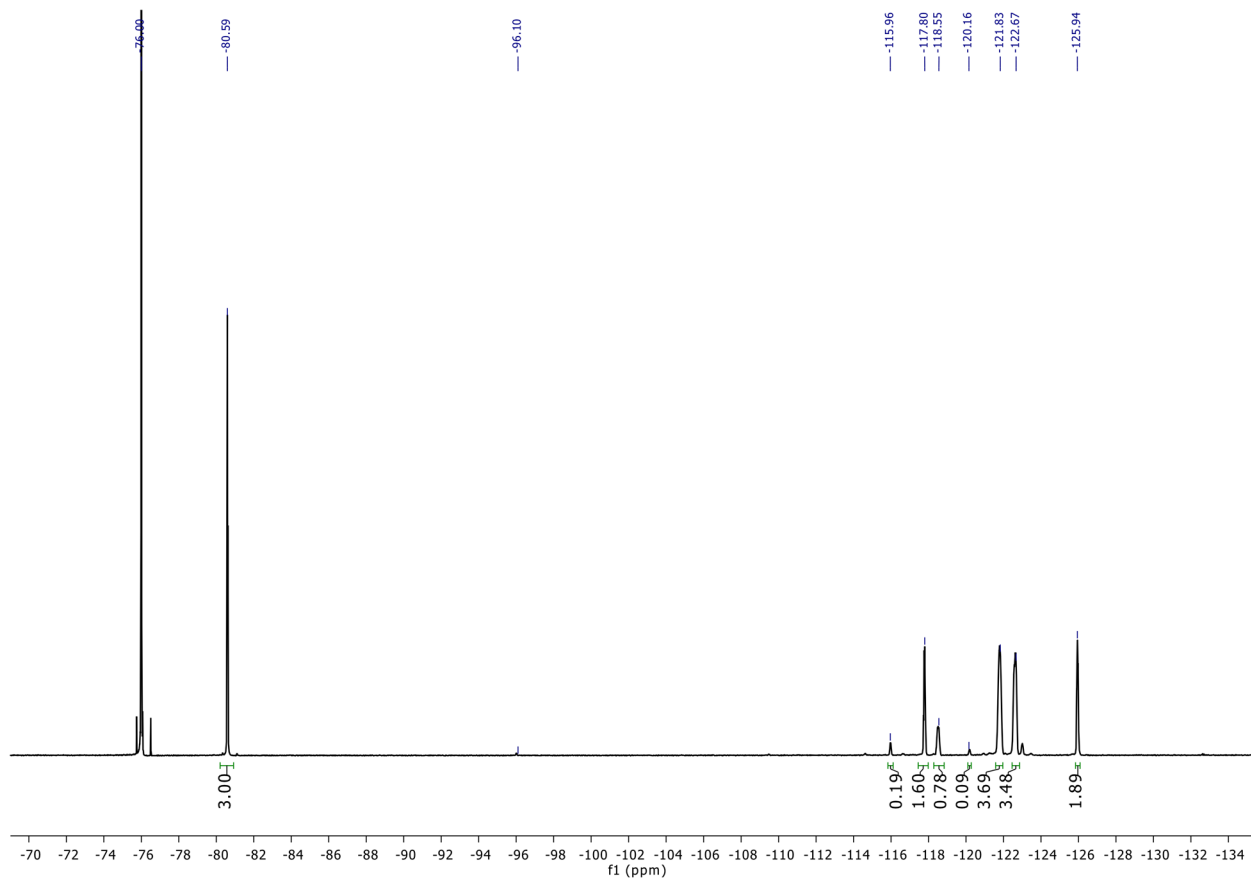
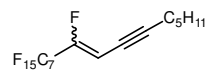
6,6,7,7,8,8,9,9,10,10,11,11,11-tridecafluoro-4-iodoundec-4-en-1-yl 4-methylbenzenesulfonate (**5.14**):



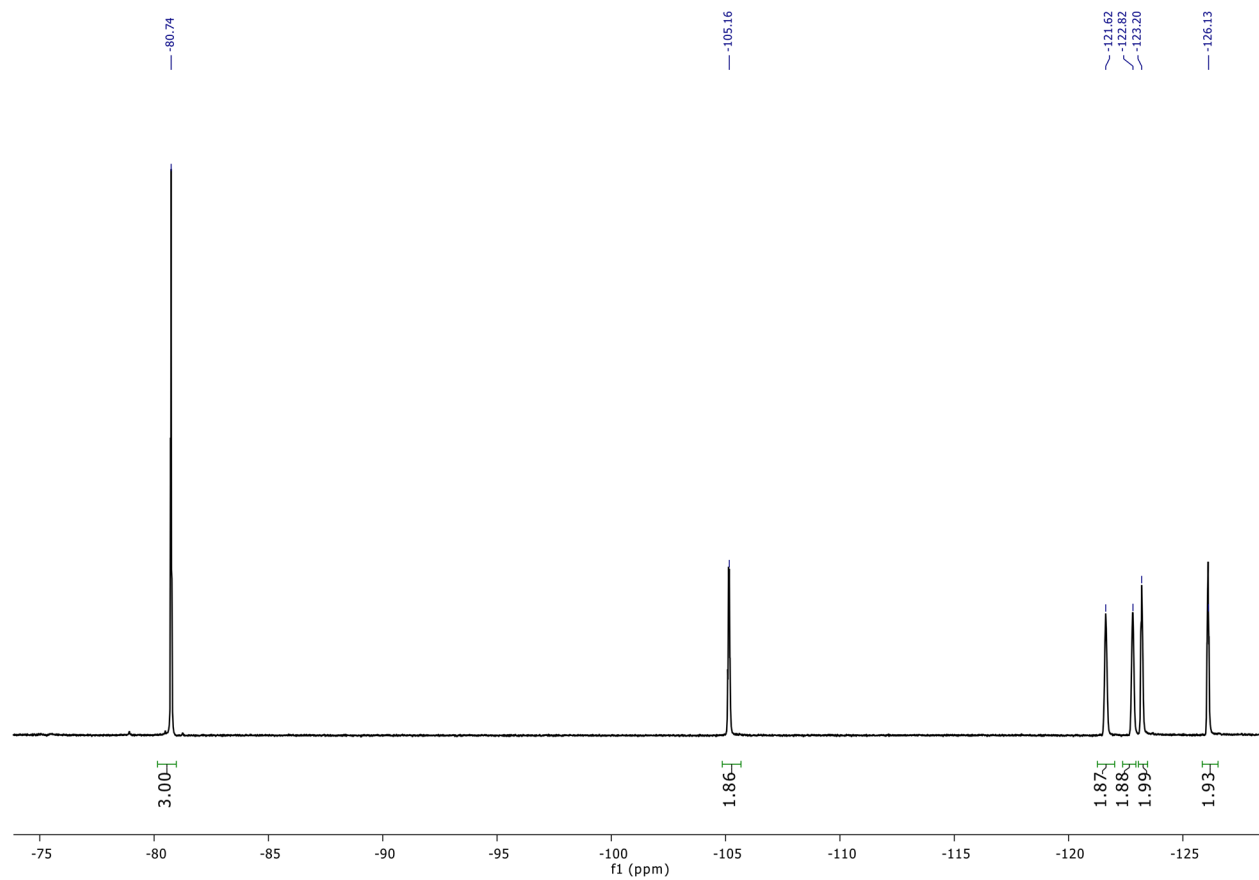
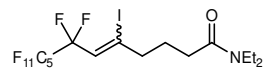
1,1,1,2,2,3,3,4-octafluorododec-4-en-6-yne (**5.15b**):



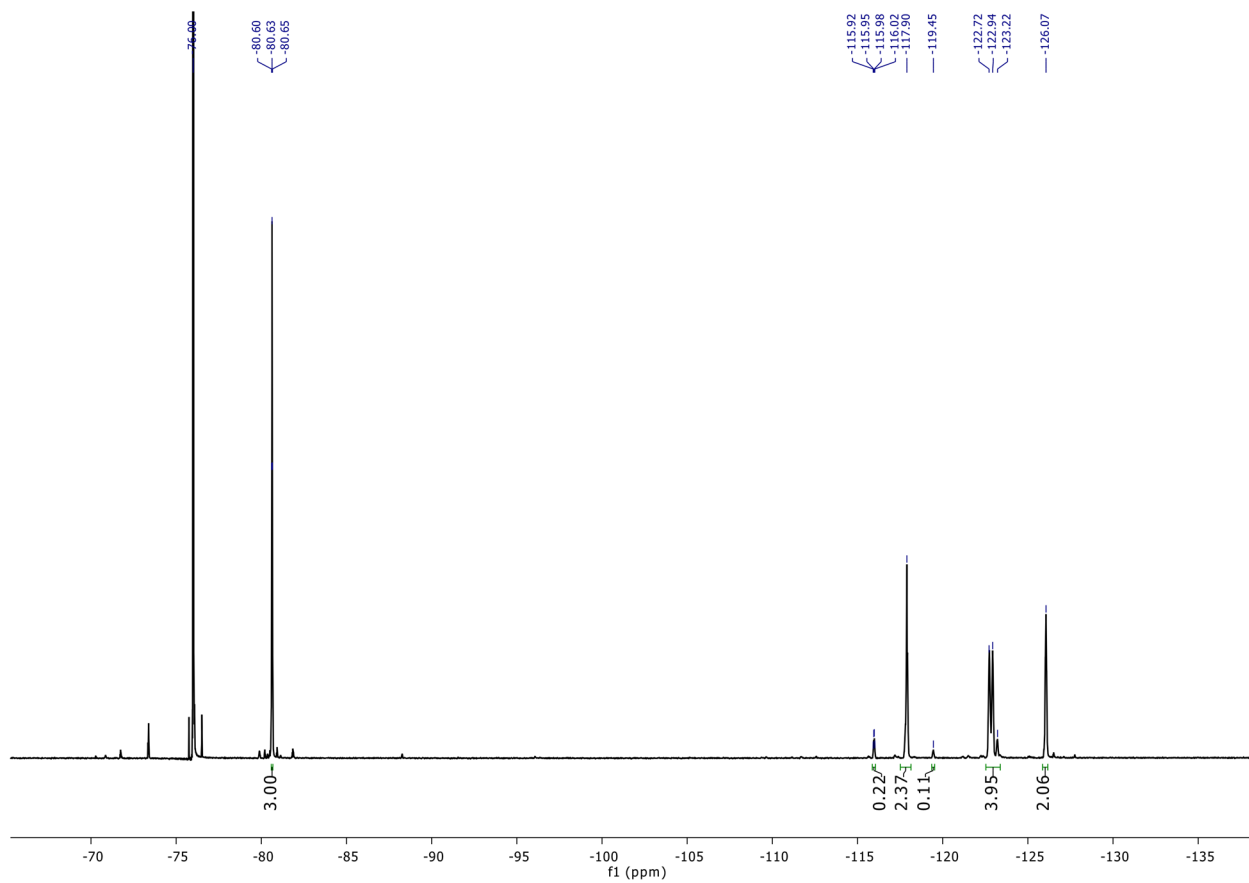
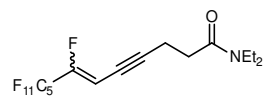
9,10,10,11,11,12,12,13,13,14,14,15,15,16,16,16-hexadecafluorohexadec-8-en-6-yne (**5.16b**):



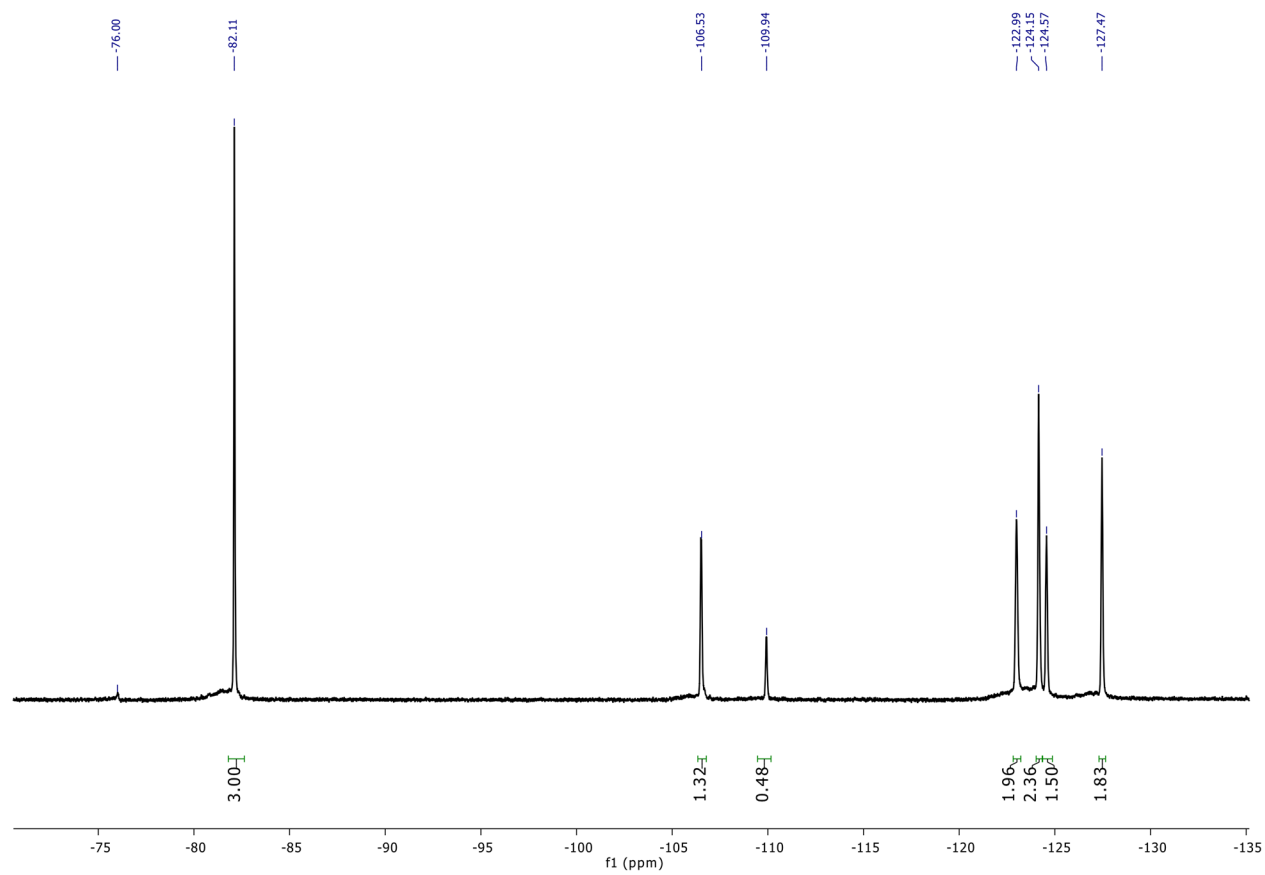
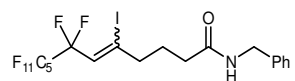
N,N-diethyl-7,7,8,8,9,9,10,10,11,11,12,12,12-tridecafluoro-5-iodododec-5-enamide (**5.17a**):



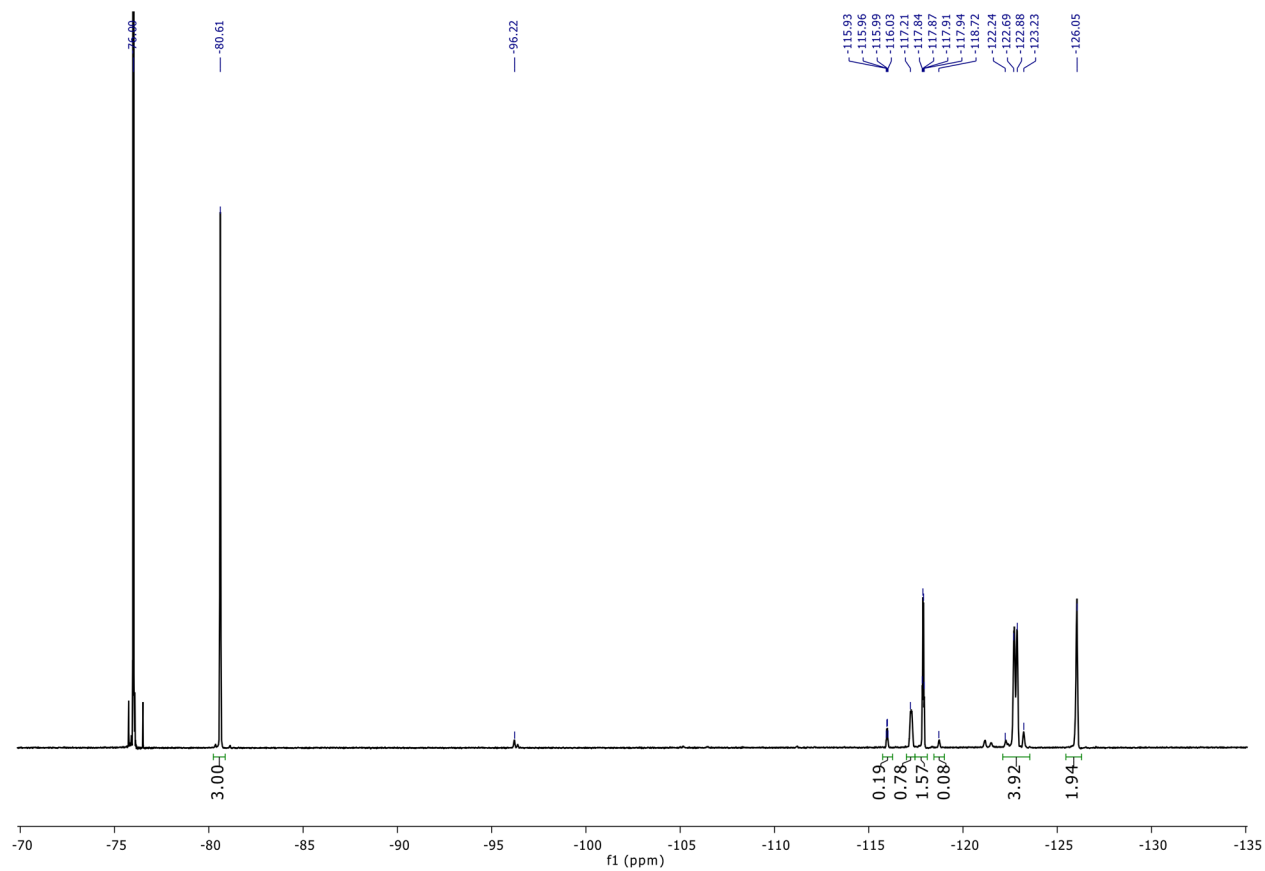
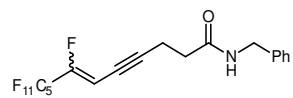
N,N-diethyl-7,8,8,9,10,10,11,11,12,12,12-dodecafluorododec-6-en-4-ynamide (**5.17b**):



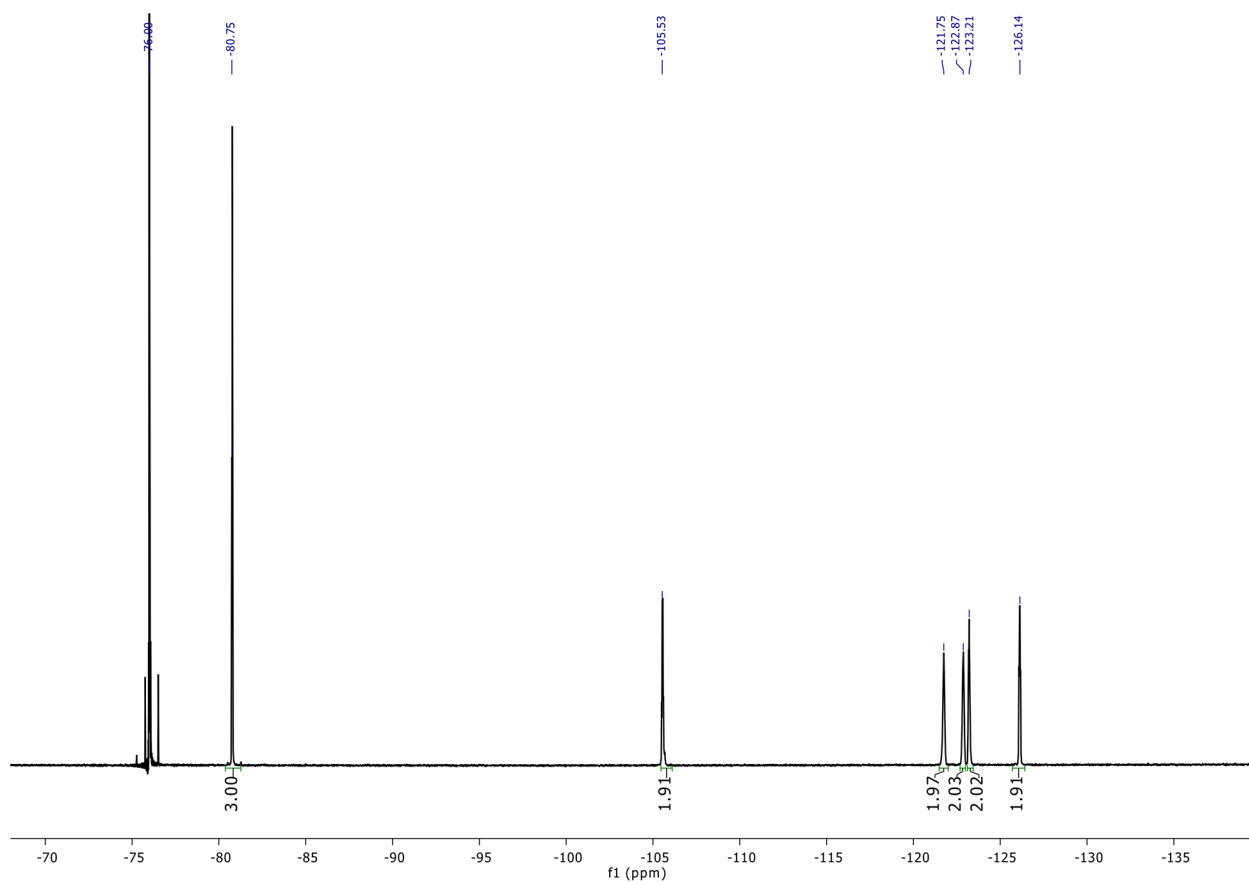
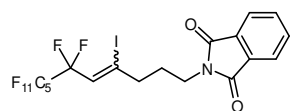
N-benzyl-7,7,8,8,9,9,10,10,11,11,12,12,12-tridecafluoro-5-iodododec-5-enamide (**5.18a**):



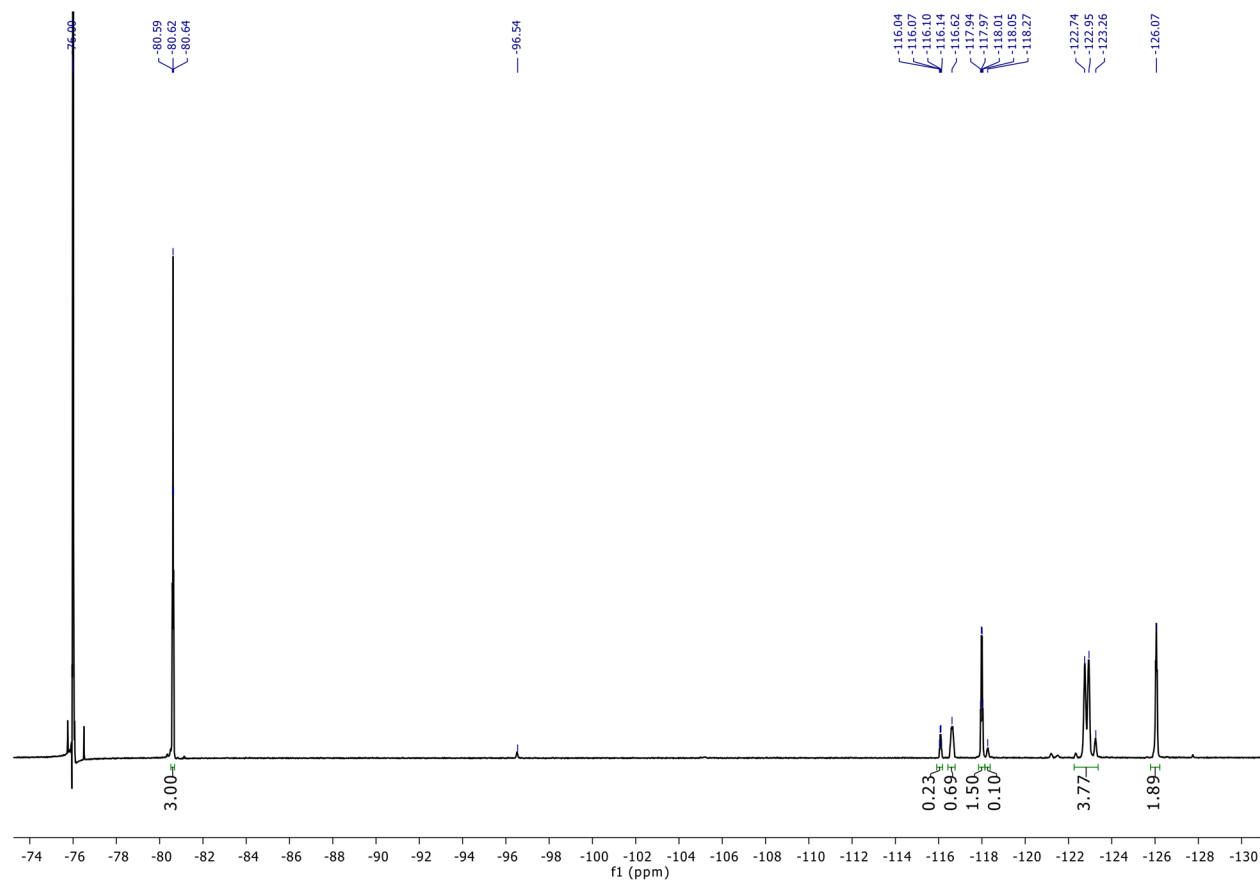
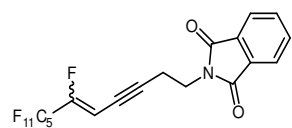
N-benzyl-7,8,8,9,9,10,10,11,11,12,12,12-dodecafluorododec-6-en-4-ynamide (**5.18b**):



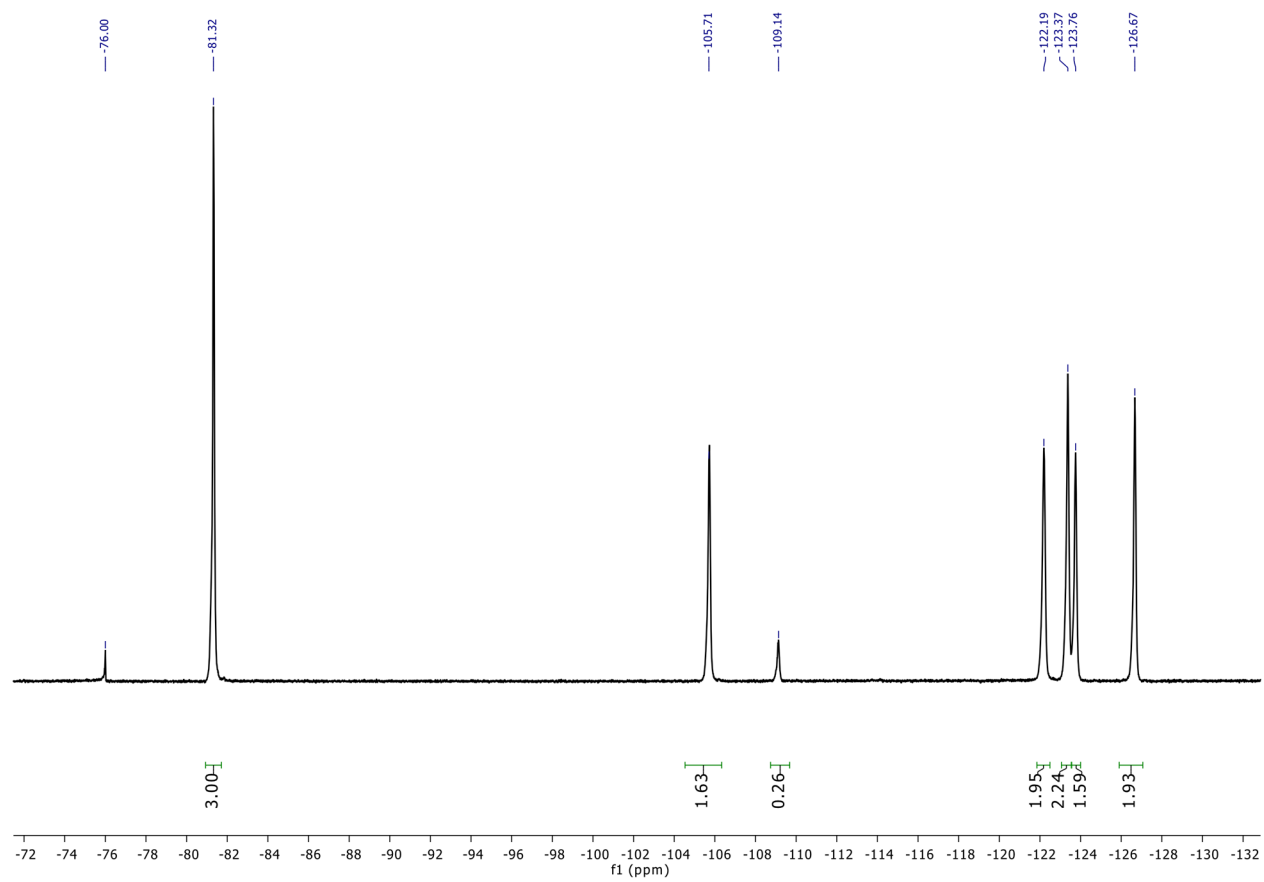
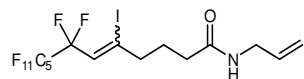
2-(6,6,7,7,8,8,9,9,10,10,11,11,11-tridecafluoro-4-iodoundec-4-en-1-yl)isoindoline-1,3-dione (**5.19a**):



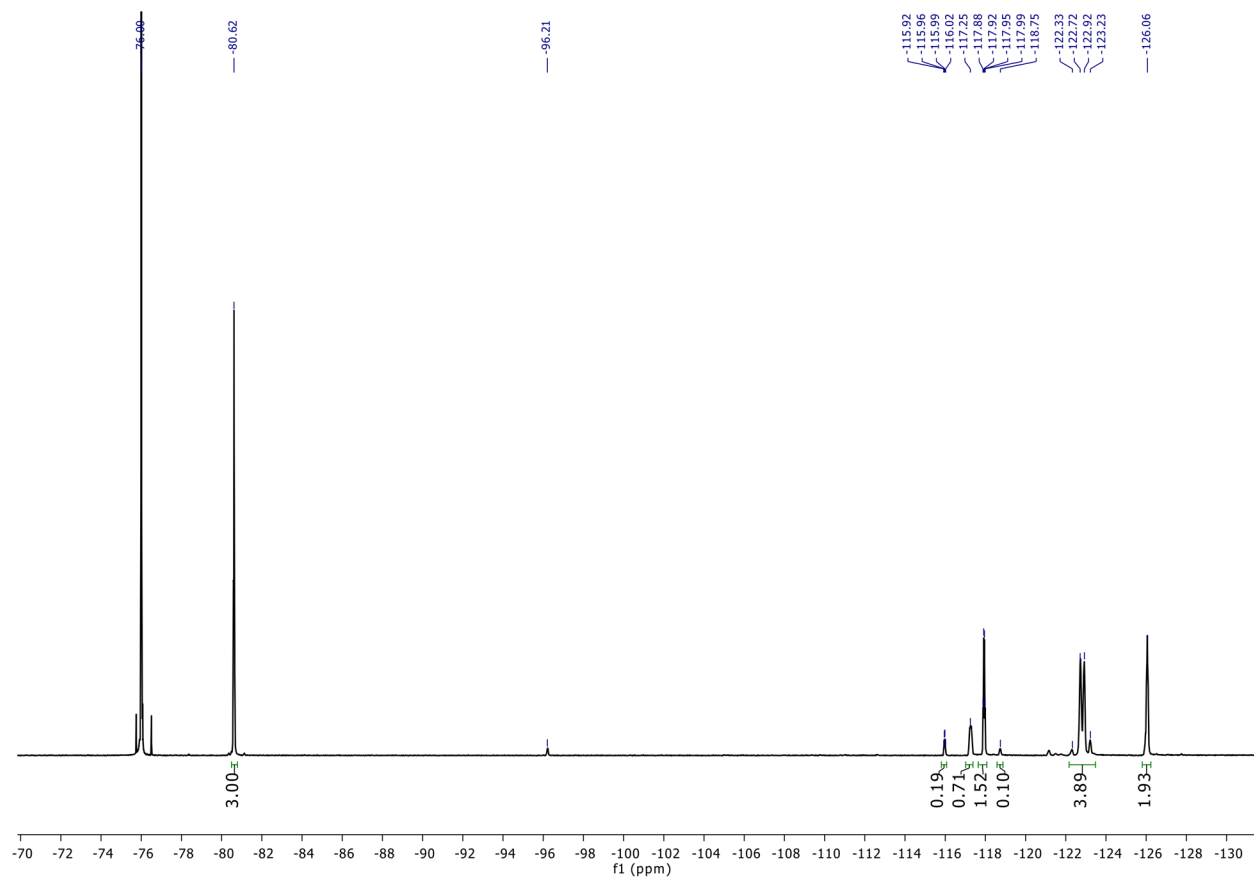
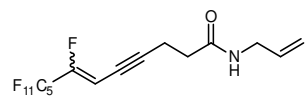
2-(6,7,7,8,8,9,9,10,10,11,11,11-dodecafluoroundec-5-en-3-yn-1-yl)isoindoline-1,3-dione (**5.19b**):



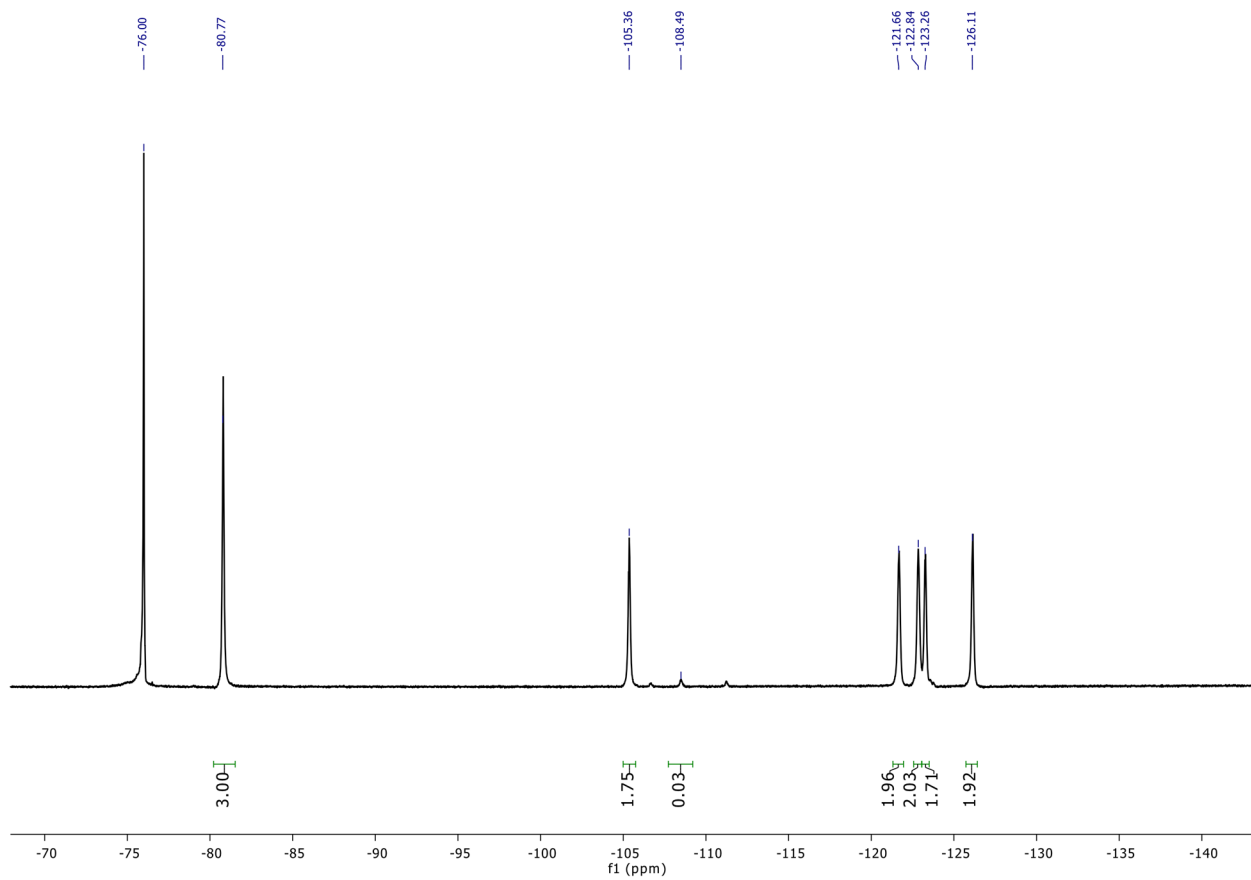
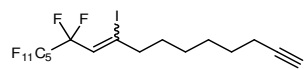
N-allyl-7,7,8,8,9,9,10,10,11,11,12,12,12-tridecafluoro-5-iodododec-5-enamide (**5.20a**):



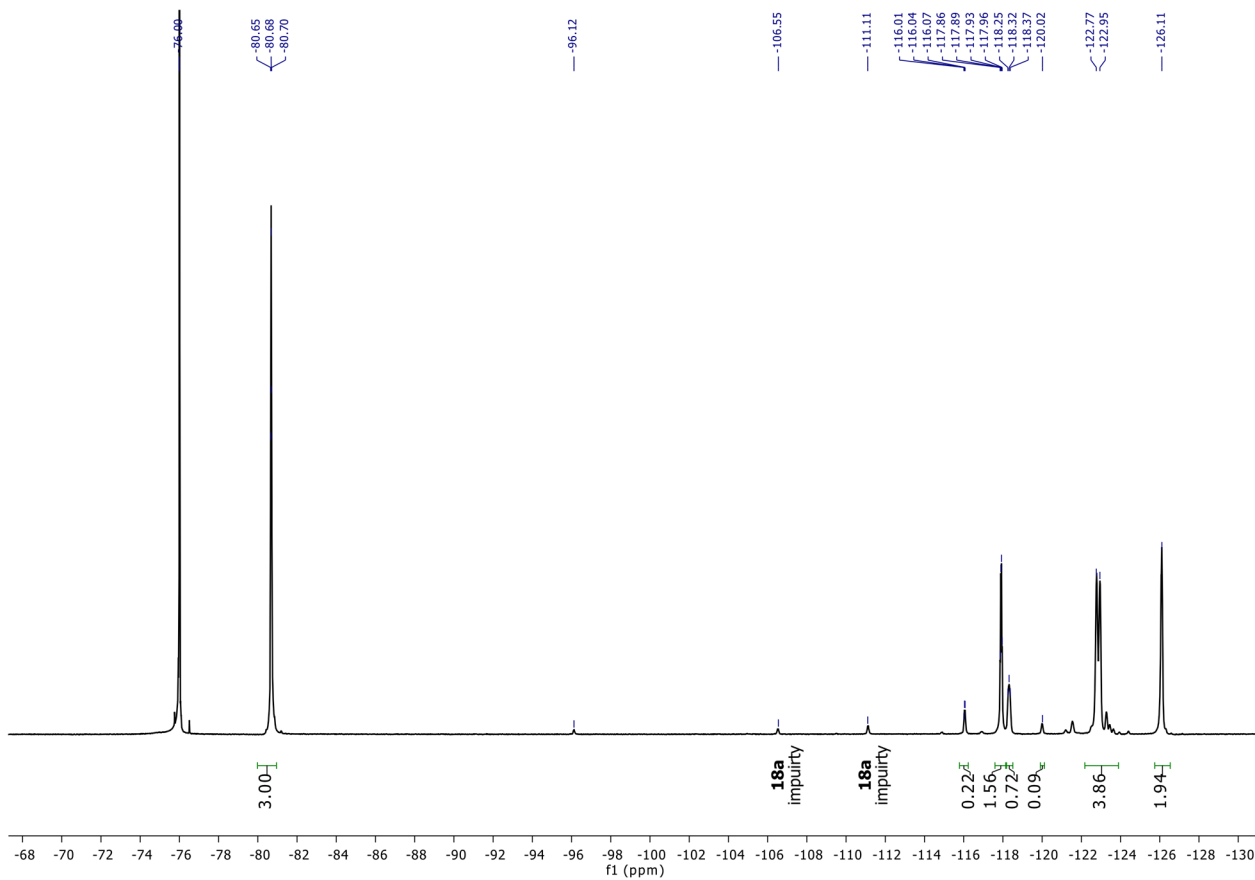
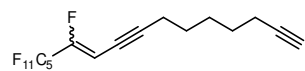
N-allyl-7,8,8,9,9,10,10,11,11,12,12,12-dodecafluorododec-6-en-4-ynamide (**5.20b**):



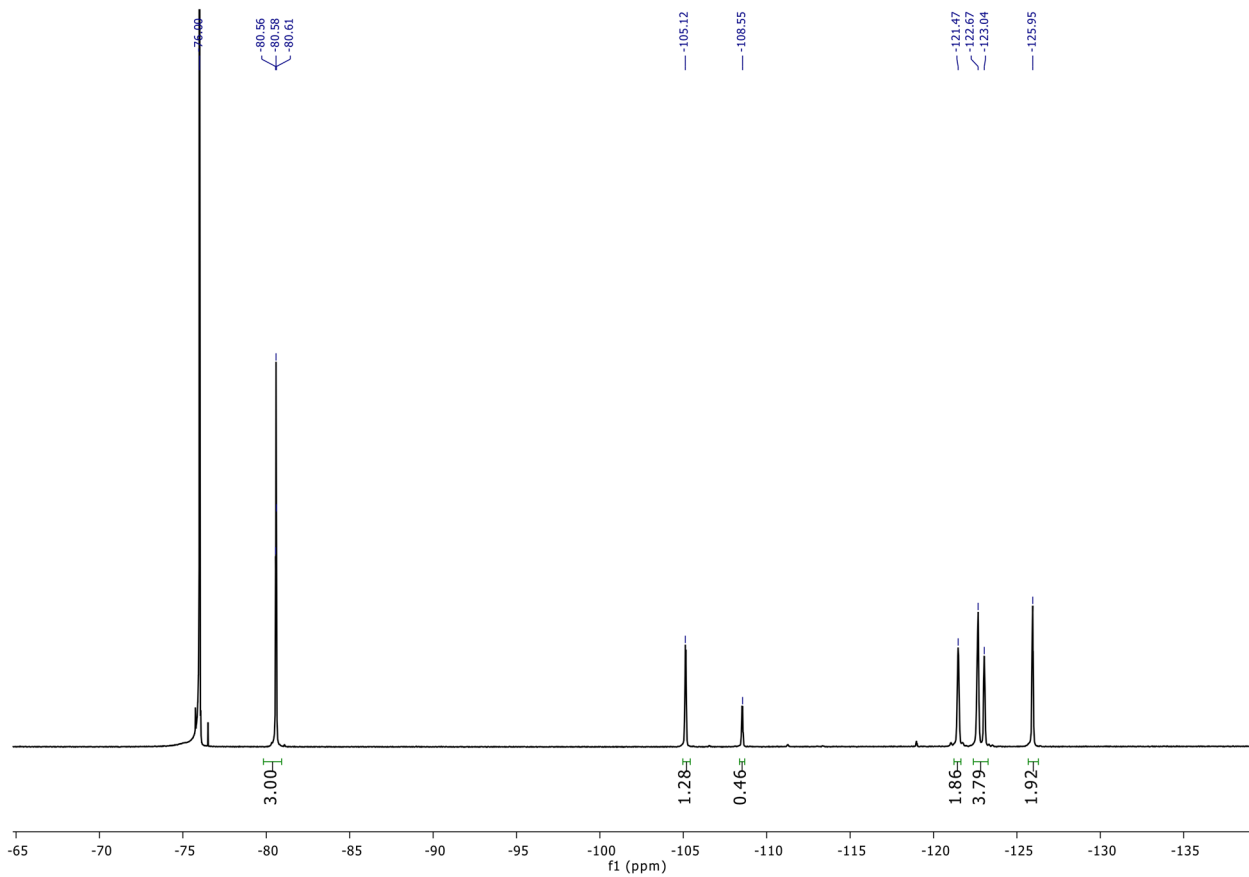
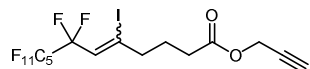
11,11,12,12,13,13,14,14,15,15,16,16,16-tridecafluoro-9-iodohexadec-9-en-1-yne (**5.21a**):



11,12,12,13,13,14,14,15,15,16,16,16-dodecafluorohexadeca-10-en-1,8-diyne (**5.21b**):

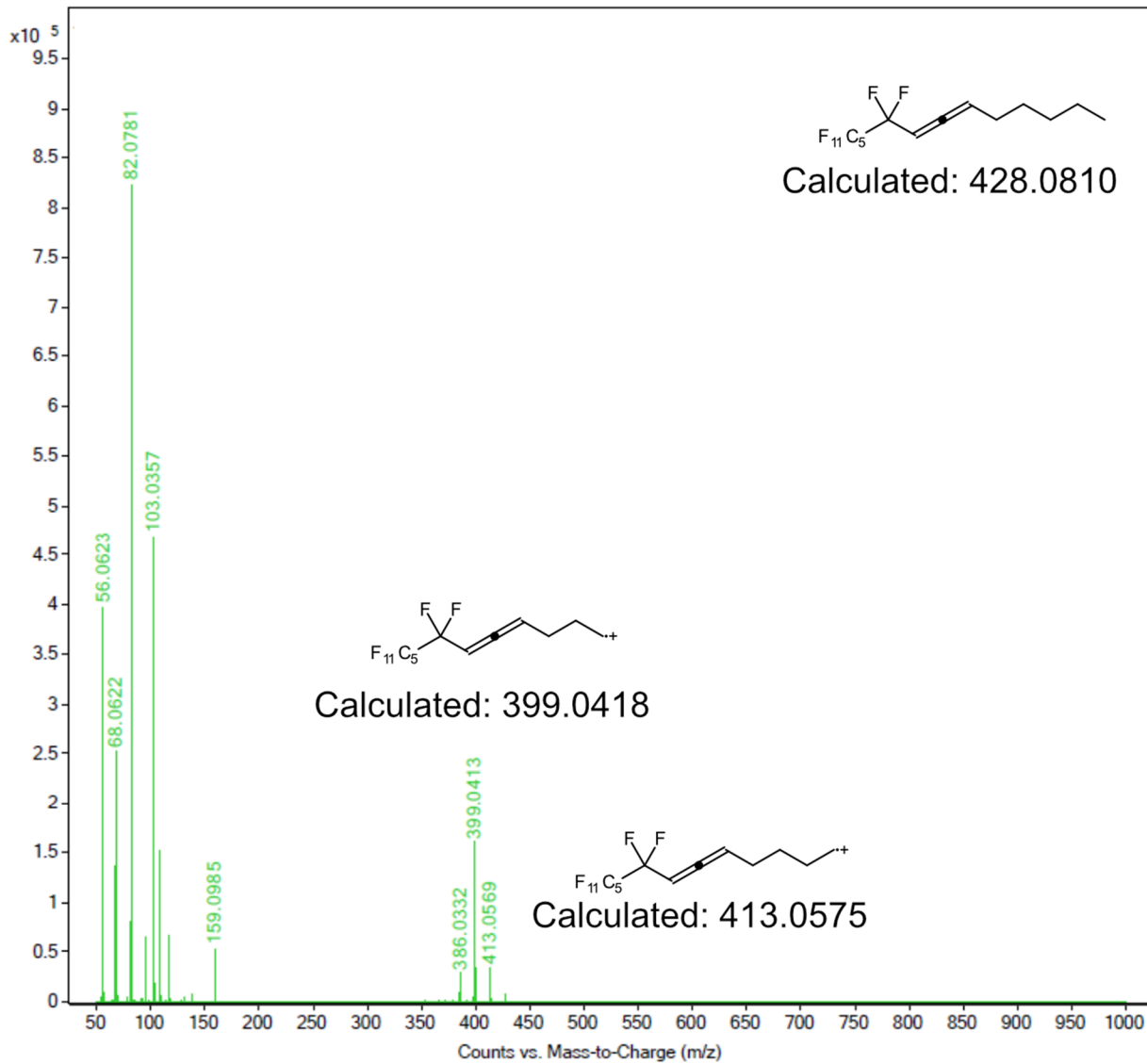
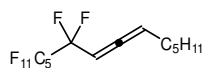


prop-2-yn-1-yl 7,7,8,8,9,9,10,10,11,11,12,12,12-tridecafluoro-5-iodododec-5-enoate (**5.22a**):

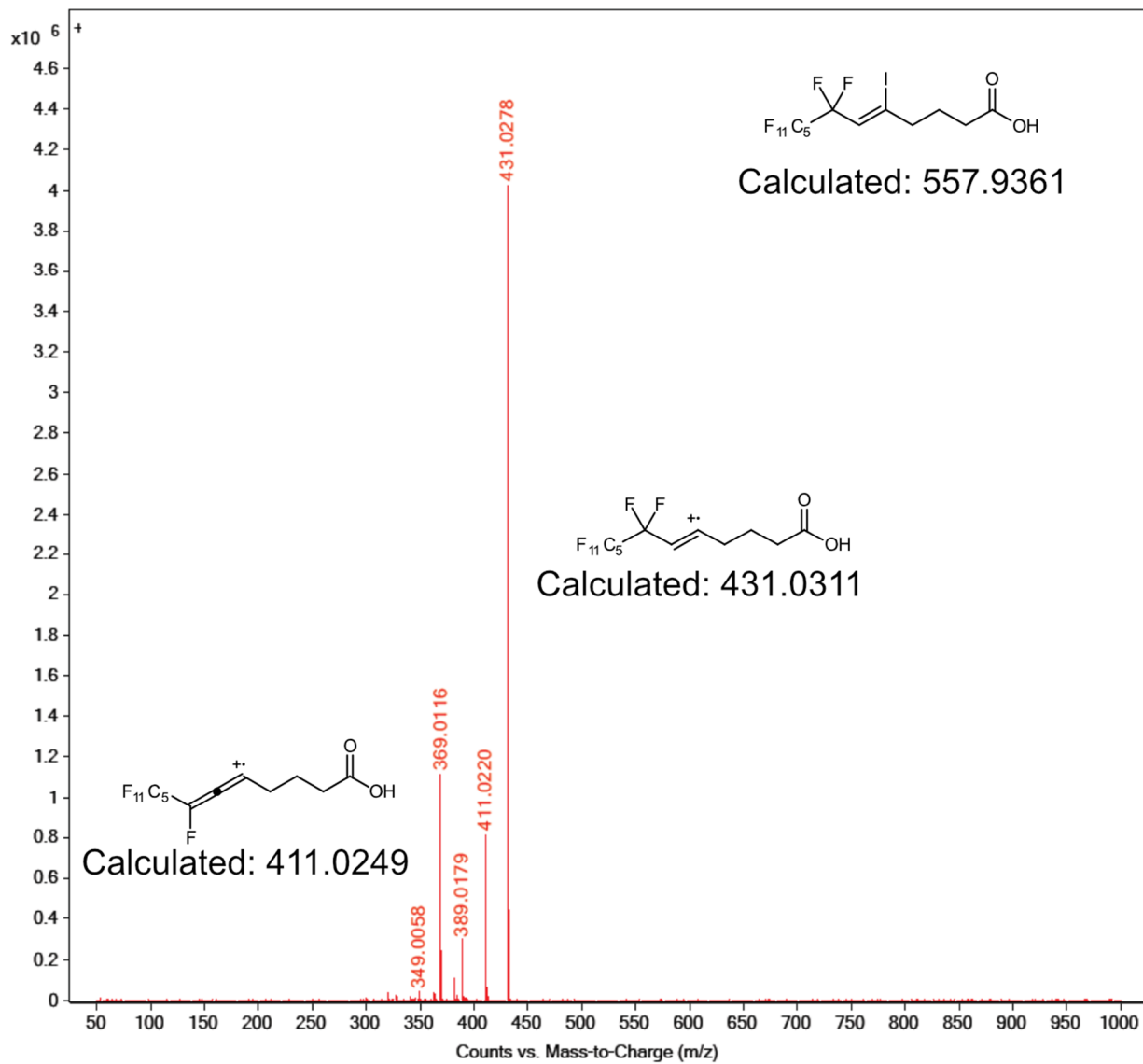
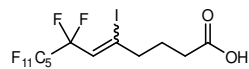


5.5.6 HRMS Spectra

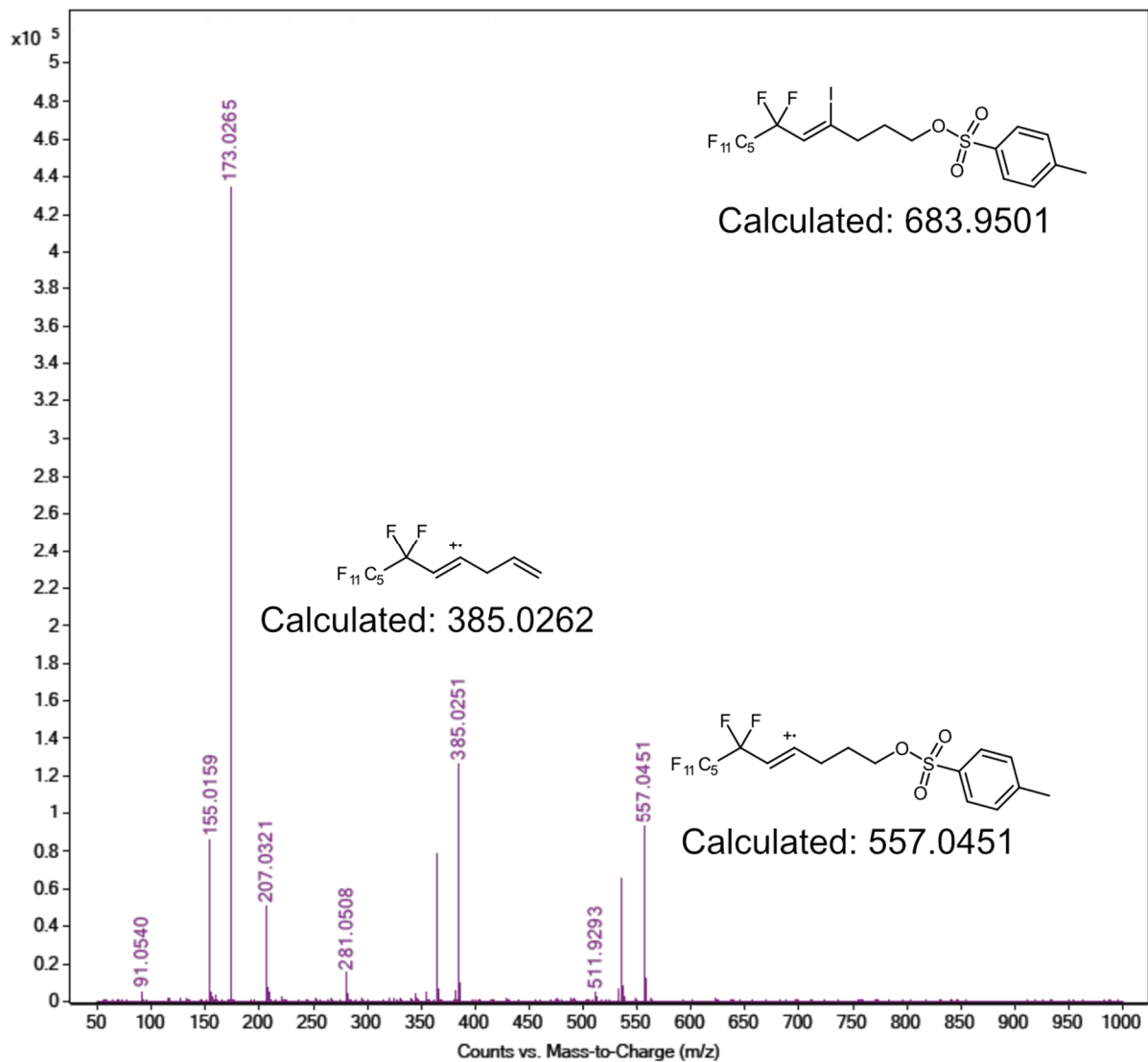
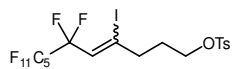
9,9,10,10,11,11,12,12,13,13,14,14,14-tridecafluorotetradeca-6,7-diene (**5.10**):



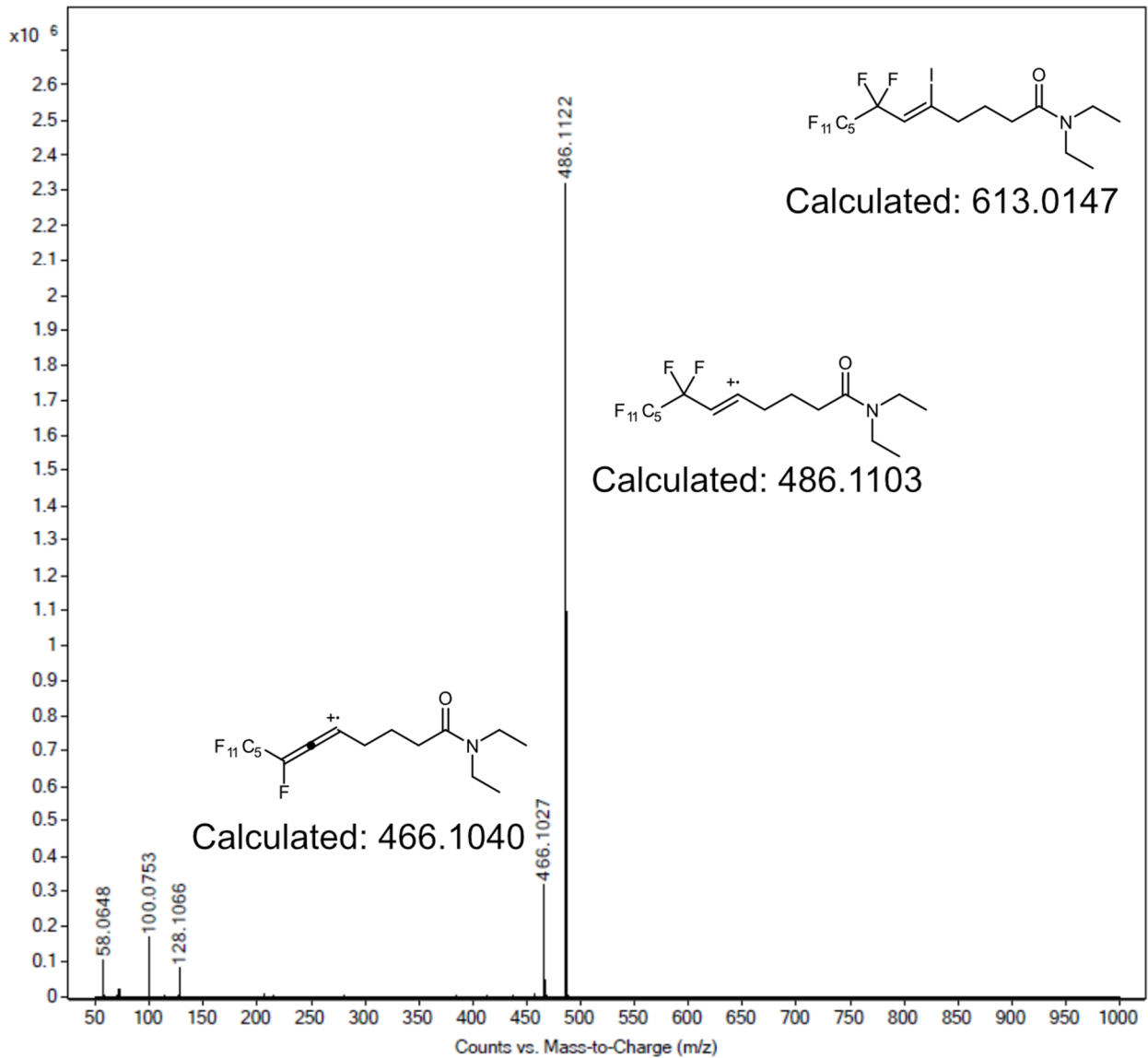
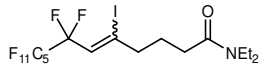
7,7,8,8,9,9,10,10,11,11,12,12,12-tridecafluoro-5-iodododec-5-enoic acid (**5.12**):



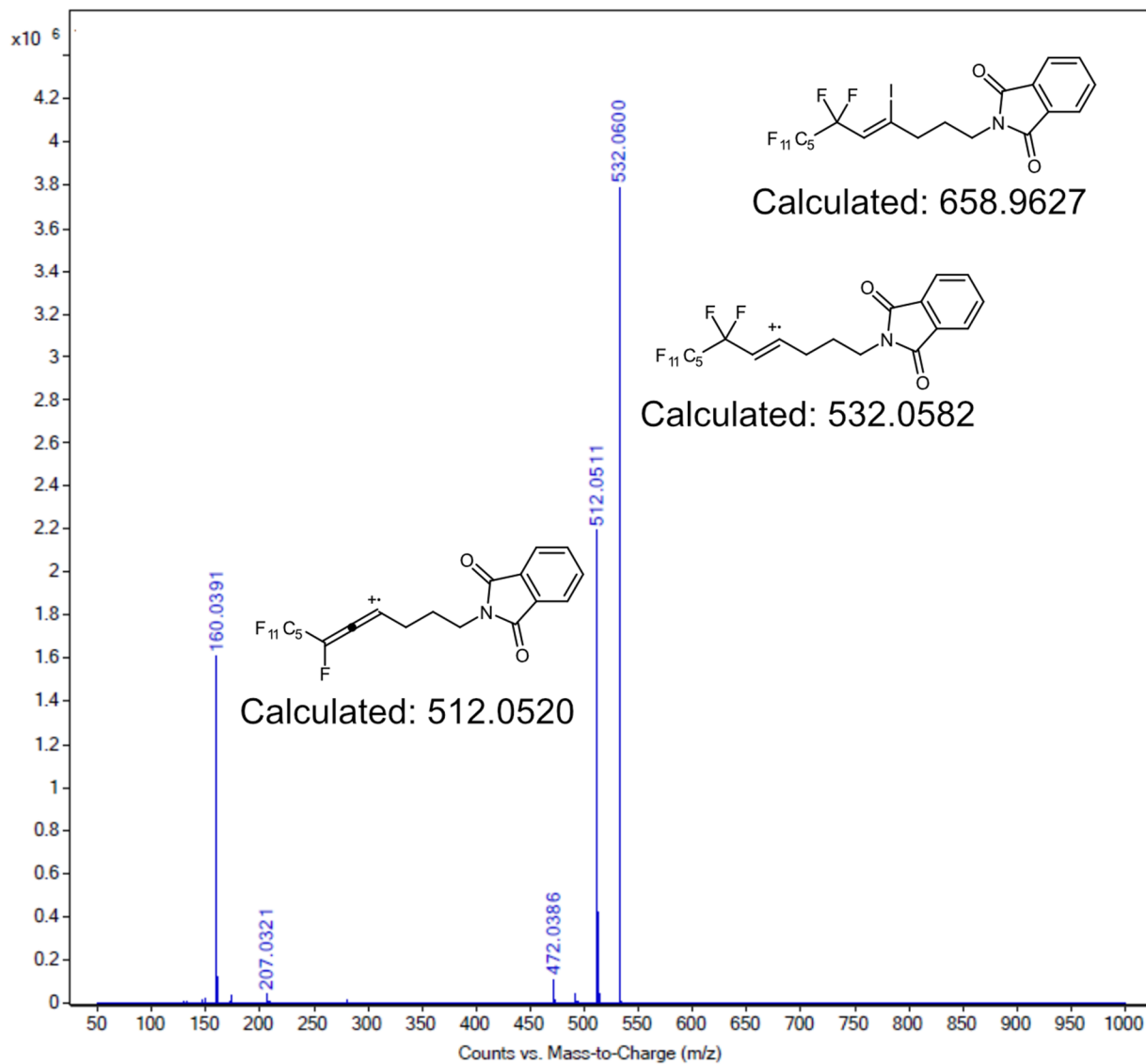
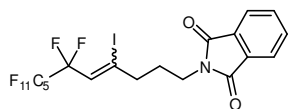
6,6,7,7,8,8,9,9,10,10,11,11,11-tridecafluoro-4-iodoundec-4-en-1-yl 4-methylbenzenesulfonate (**5.14**):



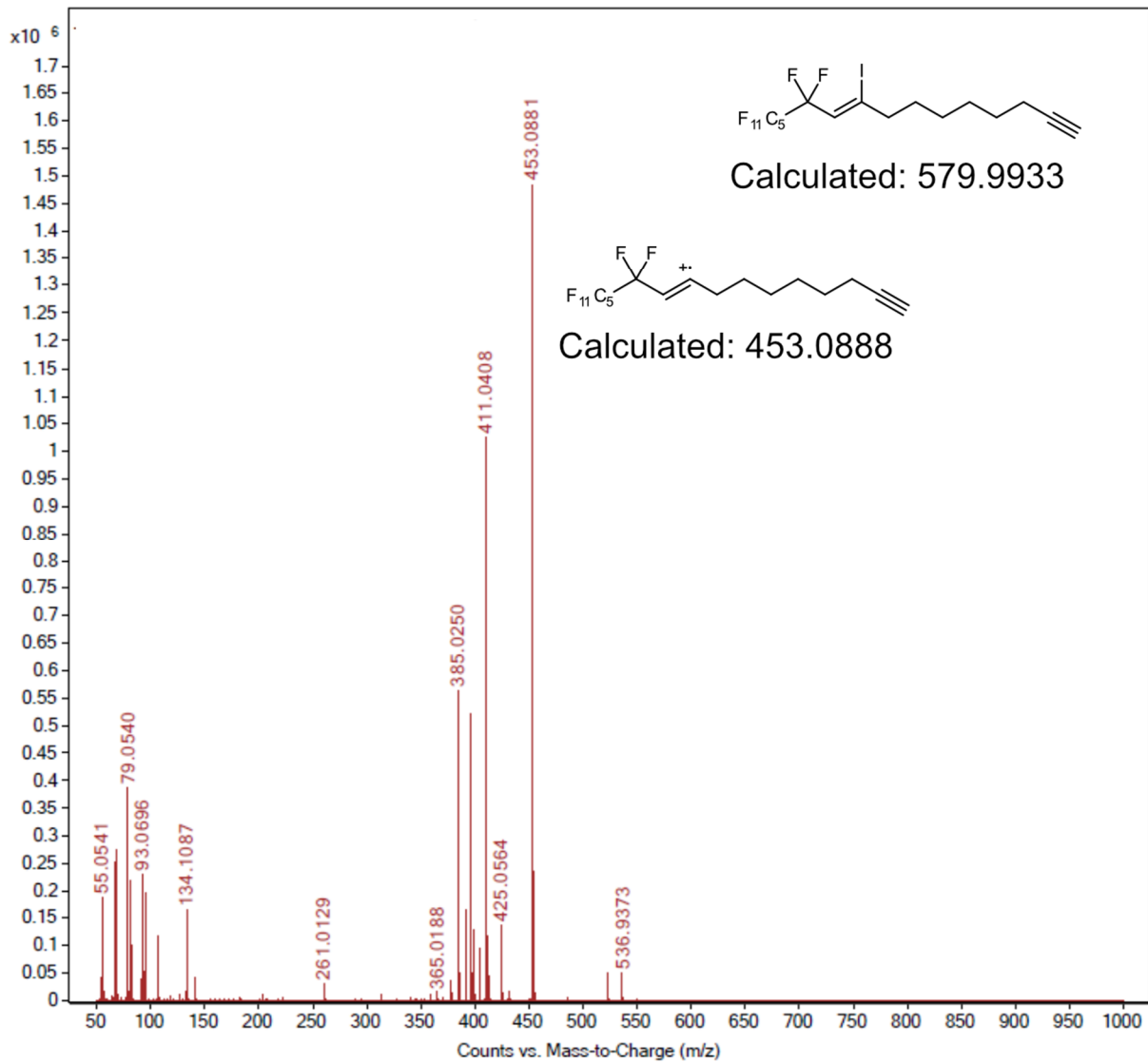
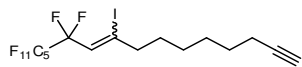
N,N-diethyl-7,7,8,8,9,9,10,10,11,11,12,12,12-tridecafluoro-5-iodododec-5-enamide (**5.17a**):



2-(6,6,7,7,8,8,9,9,10,10,11,11,11-tridecafluoro-4-iodoundec-4-en-1-yl)isoindoline-1,3-dione (**5.19a**):



11,11,12,12,13,13,14,14,15,15,16,16,16-tridecafluoro-9-iodohexadec-9-en-1-yne (**5.21a**):



5.6 References and notes

- (1) Wang, J.; Sánchez-Roselló, M.; Aceña, J. L.; Del Pozo, C.; Sorochinsky, A. E.; Fustero, S.; Soloshonok, V. A.; Liu, H. Fluorine in pharmaceutical industry: Fluorine-containing drugs introduced to the market in the last decade (2001-2011). *Chem. Rev.* **2014**, *114*, 2432.
- (2) Gillis, E. P.; Eastman, K. J.; Hill, M. D.; Donnelly, D. J.; Meanwell, N. A. Applications of fluorine in medicinal chemistry. *J. Med. Chem.* **2015**, *58*, 8315.
- (3) Nyffeler, P. T.; Durón, S. G.; Burkart, M. D.; Vincent, S. P.; Wong, C.-H. S. Selectfluor: mechanistic insight and applications. *Angew. Chem. Int. Ed.* **2005**, *44*, 192.
- (4) Meyer, D.; Jangra, H.; Walther, F.; Zipse, H.; Renaud, P. A. A third generation of radical fluorinating agents base on *N*-fluoro-*N*-arylsulfonamides. *Nat. Commun.* **2018**, *9*, 1.
- (5) Ma, J. A.; Cahard, D. Strategies for nucleophilic, electrophilic, and radical trifluoromethylations. *J. Fluor. Chem.* **2007**, *128*, 975.
- (6) Alonso, C.; Martínez De Marigorta, E.; Rubiales, G.; Palacios, F. Carbon trifluoromethylation reactions of hydrocarbon derivatives and heteroarenes. *Chem. Rev.* **2015**, *115*, 1847.
- (7) Charpentier, J.; Früh, N.; Togni, A. Electrophilic trifluoromethylation by use of hypervalent iodine reagents. *Chem. Rev.* **2015**, *115*, 650.
- (8) Liu, X.; Xu, C.; Wang, M.; Liu, Q. Trifluoromethyltrimethylsilane: Nucleophilic trifluoromethylation and beyond. *Chem. Rev.* **2015**, *115*, 683.
- (9) Dolbier, W. R. *Chem. Rev.* Structure, reactivity, and chemistry of fluoroalkyl radicals. **1996**, *96*, 1557.
- (10) Zhang, C.-P.; Chen, Q.-Y.; Guo, Y.; Xiao, J.-C.; Gu, Y.-C. Progress in fluoroalkylation of organic compounds *via* sulfinatodehalogenation initiation system. *Chem. Soc. Rev.* **2012**, *41*, 4536.

- (11) Zhang, W.; Huang, W.; Hu, J. Highly stereoselective synthesis of monofluoroalkenes from α -fluorosulfoximines and nitrones. *Angew. Chem. Int. Ed.* **2009**, *48*, 9858.
- (12) Couve-Bonnaire, S.; Cahard, D.; Pannecoucke, X. Chiral dipeptide mimics possessing a fluoroolefin moiety: A relevant tool for conformational and medicinal studies. *Org. Biomol. Chem.* **2007**, *5*, 1151.
- (13) Tellier, F.; Sauvêtre, R.; Normant, J. F. Synthèse de fluorodecolemones. *J. Organomet. Chem.* **1989**, *364*, 17.
- (14) Yoshida, M.; Yoshikawa, S.; Fukuhara, T.; Yoneda, N.; Hara, S. Stereoselective synthesis of (E)-1-fluoro-3-enynes. *Tetrahedron* **2001**, *57*, 7143.
- (15) Camps, F.; Fabrias, G.; Guerrero, A. Synthesis of a fluorinated analog of the sex pheromone of the processionary moth *Thaumetopea pityocampa*. *Tetrahedron*. **1986**, *42*, 3623.
- (16) Welch, J. T. Advances in the preparation of biologically active organofluorine compounds. *Tetrahedron* **1987**, *43*, 3123.
- (17) Camps, F.; Fabrias, G.; Gasol, V.; Guerrero, A.; Hern, R. Analogs of sex pheromone of processionary moth *Thaumetopoea pityocampa*: Synthesis and biological activity. *J. Chem. Ecol.* **1988**, *14*, 1331.
- (18) Kumar, R.; Zajc, B. Stereoselective synthesis of conjugated fluoro enynes *J. Org. Chem.* **2012**, *77*, 8417.
- (19) Jeanne-Julien, L.; Masson, G.; Kouoi, R.; Regazzetti, A.; Genta-Jouve, G.; Gandon, V.; Roulland, E. Stereoselective access to (E)-1,3-enynes through Pd/Cu-catalyzed alkyne hydrocarbation of allenes. *Org. Lett.* **2019**, *21*, 3136.
- (20) Mei, Y. Q.; Liu, J. T. Synthesis and selective carbocupration reaction of fluorine-containing enynic esters, enynylphosphine oxides, and enynylphosphates. *Tetrahedron* **2008**, *64*, 8801.

- (21) Konno, T.; Kishi, M.; Ishihara, T.; Yamada, S. Stereoselective synthesis of CF₃-substituted trans- and cis-enediynes via carbocupration or hydrostannation reactions of CF₃-containing diyne *Tetrahedron* **2014**, *70*, 2455.
- (22) Konno, T.; Kishi, M.; Ishihara, T.; Yamada, S. Highly stereoselective approach to 3-fluoroalkylated (E)-hex-3-ene-1,5-diyne derivatives via an addition–elimination reaction. *J. Fluor. Chem.* **2013**, *156*, 144.
- (23) Dai, D.-T.; Xu, J.-L.; Chen, Z.-Y.; Wang, Z.-L.; Xu, Y.-H. Synthesis of enynic and allenic orthoesters via defluoromethoxylation of 2-trifluoromethyl-1,3-enynes. *Org. Lett.* **2021**, *23*, 1898.
- (24) Yang, C.; Liu, Z. L.; Dai, D. T.; Li, Q.; Ma, W. W.; Zhao, M.; Xu, Y. H. Catalytic asymmetric conjugate protosilylation and protoborylation of 2-trifluoromethyl enynes for synthesis of functionalized allenes. *Org. Lett.* **2020**, *22*, 1360.
- (25) Qi, S.; Gao, S.; Xie, X.; Yang, J.; Zhang, Palladium-catalyzed fluoroarylation of *gem*-difluoroenynes to access trisubstituted trifluoromethyl allenes. *J. Org. Lett.* **2020**, *22*, 5229.
- (26) Shen, H.; Xiao, H.; Zhu, L.; Li, C. Copper-catalyzed radical bis(trifluoromethylation) of alkynes and 1,3-enynes. *Synlett* **2020**, *31*, 41.
- (27) Huang, J.; Jia, Y.; Li, X.; Duan, J.; Jiang, Z.-X.; Yang, Z. Halotrifluoromethylation of 1,3-enynes: Access to tetrasubstituted allenes. *Org. Lett.* **2021**, *ASAP*
- (28) Fujino, T.; Hinoue, T.; Usuki, Y.; Satoh, T. Synthesis of difluorinated enynes through Sonogashira-type coupling. *Org. Lett.* **2016**, *18*, 5688.
- (29) Jayaraman, A.; Lee, S. Selective mono- and dialkynylation of 1-fluoro-2,2-diiodovinylarenes using Pd-catalyzed decarboxylative coupling reactions. *Org. Lett.* **2019**, *21*, 7923.
- (30) Eddarir, S.; Mestdagh, H.; Rolando, C. Synthesis of fluorinated enynes and dienes via 1-bromo 2-fluoro alkenes. *Tet. Lett.* **1991**, *32*, 69.

- (31) Wang, Y.; Xu, J.; Burton, D. J. A simple, two-step, site-specific preparation of fluorinated naphthalene and phenanthrene derivatives from fluorobromo-substituted alkenes. *J. Org. Chem.* **2006**, *71*, 7780.
- (32) Zapata, A. J.; Gu, Y.; Hammond, G. B. The first α -fluoroallenylphosphonate, the synthesis of conjugated fluoroenynes, and the stereoselective synthesis of vinylfluorophosphonates using a new multifunctional fluorine-containing building block. *J. Org. Chem.* **2000**, *65*, 227.
- (33) Jennings, M. P.; Cork, E. A.; Ramachandran, P. V. A facile synthesis of perfluoroalkyl vinyl iodides and their palladium-mediated cross-coupling reactions. *J. Org. Chem.* **2000**, *65*, 8763.
- (34) Slodowicz, M.; Barata-Vallejo, S.; Vázquez, A.; Nudelman, N. S.; Postigo, A. Light-induced iodoperfluoroalkylation reactions of carbon-carbon multiple bonds in water. *J. Fluor. Chem.* **2012**, *135*, 137.
- (35) Rong, G.; Keese, R. The addition of perfluorobutyl iodide to carbon-carbon multiple bonds and the preparation of perfluorobutylalkenes. *Tetrahedron Lett.* **1990**, *31*, 5615.
- (36) Xu, T.; Cheung, C. W.; Hu, X. Iron-catalyzed 1,2-addition of perfluoroalkyl iodides to alkynes and alkenes. *Angew. Chem. Int. Ed.* **2014**, *53*, 4910.
- (37) Jaye, J. A.; Sletten, E. M. Vinyl iodide containing polymers directly prepared via an iodo-yne polymerization. *ACS Macro Lett.* **2020**, *9*, 410.
- (38) Ji, Y.-L.; Luo, J.-J.; Lin, J.-H.; Xiao, J.-C.; Gu, Y.-C. Cu-catalyzed C-H trifluoromethylation of 3-arylprop-1-ynes for the selective construction of allenic Csp²-CF₃ and propargyl Csp³-CF₃ bonds. *Org. Lett.* **2016**, *18*, 1000.
- (39) Hung, M. H. Fluorinated allenes and alkynes. *Tetrahedron Lett.* **1990**, *31*, 3703.
- (40) Perscheid, M.; Schollmeyer, D.; Nubbemeyer, U. First synthesis of medium-sized ring allenyl lactams. *European J. Org. Chem.* **2011**, *27*, 5250.

- (41) Rocaboy, C.; Hampel, F.; Gladysz, J. A. Syntheses and reactivities of disubstituted and trisubstituted fluorinated pyridines with high fluorinated phase affinities: Solid state, liquid crystal, and ionic liquid-phase properties. *J. Org. Chem.* **2002**, *67*, 6863.
- (42) Yang, L.; Adam, C.; Cockroft, S. L. Quantifying solvophobic effects in nonpolar cohesive interactions. *J. Am. Chem. Soc.* **2015**, *137*, 10084.
- (43) Kolb, H.; Finn, M. G.; Sharpless, B. K. Click chemistry: Diverse chemical function from a few good reactions. *Angew. Chem. Int. Ed.* **2001**, *40*, 2004.
- (44) Sinha, A. K.; Equbal, D. Thiol–ene reaction: Synthetic aspects and mechanistic studies of an anti-markovnikov-selective hydrothiolation of olefins. *Asian J. Org. Chem.* **2019**, *8*, 32.
- (45) Ogba, O. M.; Warner, N. C.; O’Leary, D. J.; Grubbs, R. H. Recent advances in ruthenium-based olefin metathesis. *Chem. Soc. Rev.* **2018**, *12*, 4510.
- (46) Pickens, C. J.; Johnson, S. N.; Pressnall, M. M.; Leon, M. A.; Berkland, C. J. Practical considerations challenges, and limitations of bioconjugation via azide-alkyne cycloaddition. *Bioconj. Chem.* **2018**, *29*, 686.
- (47) Meldal, M.; Tomøe, C. W. Cu-catalyzed azide-alkyne cycloaddition. *Chem. Rev.* **2008**, *108*, 2952.
- (48) Pangborn, A. B.; Giardello, M. A.; Grubbs, R. H.; Rosen, R. K.; Timmers, F. J. Safe and convenient procedure for solvent purification. *Organometallics* **1996**, *15*, 1518
- (49) Habib, M. H.; Mallouk, T. E. Photochemical addition of perfluoro-n-butyl iodide to alkynes and olefins *J. Fluor. Chem.* **1991**, *53*, 53.
- (50) Umemoto, T.; Gotoh, Y. Perfluoroalkylations of carbanions with (Perfluoroalkyl)phenyliodonium triflates (FITS Reagents). *Bull. Chem. Soc. Jpn.* **1986**, *59*, 439.

- (51) Kharrat, S.; Laurent, P.; Blancou, H. Novel synthesis, reactivity, and stereochemistry of substituted 3-trifluoromethyl- and 3-perfluoroalkyl-3-phenoxyprop-2-enal *J. Org. Chem.* 2006, *71*, 6742.
- (52) Yamazaki, T.; Yamamoto, T.; Ichihara, R. Preparation of CF₃-containing 1,3-di- and 1,1,3-trisubstituted allenes. *J. Org. Chem.* **2006**, *71*, 6251.
- (53) Takeyama, Y.; Ichinose, Y.; Oshima, K.; Utimoto, K. Triethylborane-induced stereoselective radical addition of perfluoroalkyl iodides to acetylenes *Tet. Lett.* **1989**, *30*, 3159.
- (54) Konno, T.; Chae, J.; Kanda, M.; Nagai, G.; Tamura, K.; Ishihara, T.; Yamanaka, H. Facile syntheses of various per- or polyfluoroalkylated internal acetylene derivatives *Tetrahedron* **2003**, *59*, 7571.